THE DEFORMATION BEHAVIOUR OF THE COLLAPSING AND DESTRUCTURED SOILS OF THE SANA'A AREA AND THEIR RESPONSE TO FIELD TREATMENT

KHALED ABDALLAH AL-GASOUS
Doctor of Philosophy

ASTON UNIVERSITY
August 1995

THESIS SUMMARY

Aston University.
The Deformation Behaviour of the Collapsing and Destructured Soils of the Sana'a Area and Their Response to Field Treatment.
Khaled Abdallah Al-Gasous.
PhD.
1995.

Previous work has indicated the presence of collapsing and structured soils in the surface layers underlying Sana'a, the capital of Yemen Republic. This study set out initially to define and, ultimately, to alleviate the problem by investigating the deformation behaviour of these soils through both field and laboratory programmes. The field programme was carried out in Sana'a while the laboratory work consisted of two parts, an initial phase at Sana'a University carried out in parallel with the field programme on natural and treated soils and the major phase at Aston University carried out on natural, destructured and selected treated soils.

After an initial assessment, four sites were selected for the field programme and four major treatments - ponding, preloading, roller compaction and deep compaction - were applied at 28 locations within these sites which were subjected to standard penetration and dry density testing. Disturbed and undisturbed (block) samples were obtained from all the soil layers at these locations for the laboratory programme.

The initial phase of the laboratory programme included classification, permeability, and single (collapsing) and double oedometer tests while the major phase, at Aston, was extended to also include extensive single and double oedometer tests, Scanning Electron Microscopy and Energy Dispersive Spectrum analysis. The mechanical tests were carried out on natural and destructured samples at both the in situ and soaked moisture conditions.

The engineering characteristics of the natural intact, field-treated and laboratory destructured soils are reported, including their collapsing potentials which show them to be weakly bonded with nil to severe collapsing susceptibility. Flooding had no beneficial effect, with limited to moderate improvement being achieved by preloading and roller compaction, while major benefits were achieved from deep compaction. From these results a comparison between the soil response to the different treatments and general field remarks were presented.

Laboratory destructuring reduced the stiffness of the soils while their compressibility was increased. Their collapsing and destructuring mechanisms have been examined by studying the changes in structure accompanying these phenomena. Based on the test results for the intact and the laboratory destructured soils, a simplified framework has been developed to represent the collapsing and deformation behaviour at both the partially saturated and soaked states, and comments are given on its general applicability and limitations. It has been used to evaluate all the locations subjected to field treatment. It provided satisfactory results for the deformation behaviour of the soils destructured by field treatment. Finally attention is drawn to the design considerations together with the recommendations for the selection of potential improvement techniques to be used for foundation construction on the particular soils of the Sana'a region.

Key words:- Collapsing Soil, Destructuring, Soil Structure, Soil Improvement, Deep Compaction.

TO MY WIFE AND PARENTS

TO MY CHILDREN

AMIRA, AHMED, ANAS, ALLA, ISRRA AND AFFNAN

TO MY PEOPLE IN YEMEN

ACKNOWLEDGEMENTS

I am most grateful to almighty ALLAH for providing me an opportunity and capability to complete this thesis .

TABLE OF CONTENTS

LIST OF FIGURES

LIST OF TABLES

LIST OF PLATES

LIST OF SYMBOLS

A	=	Activity
C_c	=	Compression index
CDFW	=	Collapsing - destructuring laboratory framework
CMC	=	Compacted moisture content
C_p	=	Collapsing potential after (Jennings and Knight, 1975)
C_s	=	Swelling index
C.S.	=	Compacted surface level
C_v	=	Coefficient of consolidation
Δc	=	Deformation in the field due to wetting at specific stress
Δc_{dn}	=	Collapsing deformation of the D/C soil upon loading alone at CMC state
Δc_{ds}	=	Collapsing deformation of the D/C soil upon wetting
Δe_c	=	Collapsing deformation of the intact soil due to wetting
Δe_{cn}	=	Collapsing deformation of the intact soil due to loading alone at NMC state.
Δe_d	=	Destructuring deformation at the SMC state
Δe_{dn}	=	Destructuring deformation at the NMC state
Δi	=	Immediate deformation
Δt	=	Deformation with time
δv	=	Vertical displacement
D	=	Depth of improvement
D/C	=	Destructured/Compacted soil
DC	=	Deep Compaction, Deformation curve of the partially saturated D/C soil
Ds	=	Destructured sample
DS	=	Deformation curve of the destructured soil at SMC state
e_o	=	Initial void ratio
e_1	=	Void ratio at soaking stress before wetting
e_2	=	Void ratio at soaking stress after wetting
e_L	=	Void ratio at liquid limit
EDS	=	Energy Despersive Spectrum
E_a	=	Stiffness after wetting
E_b	=	Stiffness before wetting
γ_d	=	Dry unit weight
γ_n	=	In-situ unit weight or wet unit weight
G_s	=	Specific gravity
G.S.	=	Original ground surface
h	=	Height of impact
I_c	=	Collapse potential due to wetting, in this study
I_d	=	Destructuring potential
I_L	=	Collapse potential due to loading only at NMC state
I_T	=	Total collapse potential due to both wetting and loading
IC	=	Isotropic Compression Test
I.D.	=	Influenced depth
K	=	Coefficient of permeability
K_{af}	=	The inndicator of field deformation resistance after wetting
K_{bf}	=	The inndicator of field deformation resistance before wetting
KF1, KF2, KF3, KF4	=	SPT and log bores of the flooded location at site IV

K_h	=	Coefficient of permeability for horizontal direction
K_v	=	Coefficient of permeability for vertical direction
K_c	=	Collapsing subsidence
L.I	=	Liquidity index
LL	=	Liquid limit
MF1, MF2, MF3, MF4	=	Log bores of the flooded location at site III
m_v	=	Coefficient of volume change
N	=	Natural sample
NN	=	Deformation curve of the natural soil at the NMC state
NS	=	Deformation curve of the natural soil at the SMC state
NMC	=	Natural moisture content (state)
N_s	=	Standard penetration test value
p	=	Applied pressure
Pc	=	Overconsolidation stress
Pcc	=	Critical collaping stress, at I_c max
PI	=	Plasticity index
PL	=	Plastic limit
RI	=	Relative increase in dry density
RC	=	Roller Compaction
ρ_n	=	Wet density
ρ_d	=	Dry density
$\Sigma\Delta$	=	Summation of deformation under specific stress
σ_{vo}	=	Overburden pressure
σ_y	=	Yield stress at soaked moisture state
σ_{yn}	=	Yield stress at natural moisture state
S_o	=	Initial degree of saturation
SEM	=	Scanning Electronic Microscope
S_f	=	Final degree of saturation (at the end of the test)
SMC	=	Soaked moisture content
SPT	=	Standard Penetration Test
SUM Δ	=	Accumulative deformation throughout the test
TMC	=	Treated moisture content
$\Sigma \Delta e$	=	Total deformation due to both collapse and destructurig
Σe_c	=	Total collapse due to both loading and wetting
W	=	Dropping load
Wc	=	Moisture content at the testing time of the D/C soil
W_n	=	Natural moisture content
Wcom	=	Moisture content at the time of compaction
Wopt	=	Optimum moisture content
W_s	=	Moisture content at saturation
YSR	=	Yield stress ratio

CHAPTER 1

INTRODUCTION

1.1 THE STUDY AREA

The Yemen Republic (Y.R.) lies along the south western part of the Arabian Peninsula, and the study area of this research is Sana'a, the capital of the Yemen Republic (Figure 1.1). It is located in the central high mountains of the Sana'a Basin at an elevation of 2300 metres above the sea level with the surrounding mountains rising a further 750 metres above the Basin. Sana'a is an arid to semi arid region, in which the evaporation rate is considerably in excess of the precipitation rate. The mountains bound the study area from the west, east and partially from the south. These steeply sloping mountains coupled with the arid climate have greatly influenced the processes of the soil formation.

Major developments have taken place in the region since 1962 leading to a great expansion in construction. This urban development has been restricted by the surrounding mountains forcing new works to concentrate in a limited area. This has lead to the construction of multistorey buildings to provide the essential number of housing units. In the Yemen Republic, much of this development has involved combinations of different structural systems, often through additions to existing structures. Consequently, masonry, bricks and/ or stonewalls are often deployed with reinforced concrete in the same structure; either side by side or on top of one another. In addition, different materials are used within the same structure. These practices require extreme care in both design and construction to safeguard against differential settlement which could jeopardize the safety of individual structures.

1.2 THE BACKGROUND AND THE PROBLEM

The recent upsurge in construction activities, coupled with shortage of local design experience, has placed high demands on the engineering community in the Yemen Republic, particularly those involved with building construction. Foremost of these demands is the need to establish geotechnical guide-lines and a code of practice to guide the selection of appropriate geotechnical parameters for the safe and economic design of individual structures.

The initial phase of this task was commenced in the 1986. The geotechnical properties of the surface soils of Sana'a were studied as a first step in identifying all the soils in the Yemen Republic (Al-Gasous, 1988). Unfortunately, these initial investigations indicated considerable variations in the soil types. Of particular concern was the presence of some soils that seemed to be sensitive to water. Such soils were characterized by having an open, micro-fabric structure of silt and quartz, with calcite as a cementing agent. These soils, characterised by a tendency to collapse upon wetting, are defined as collapsing soils and, as such, resemble Loess soils. In common with Loess soils, they have high shear strength when dry so, under such conditions, can safely carry superstructures resting on shallow foundations. However, when wetted or the moisture content raised, this can produce both a considerable drop in shear strength and an excessive settlement or, even, collapse. Under such conditions, structures resting on shallow foundations are not safeguarded against differential settlement which may jeopardize their safety.

The initial investigation (Al-Gasous, 1988) indicated that many structures have been damaged by settlement movements. Although over 95% of the buildings in Sana'a are light structures of one to three floor storeys, a great number have exhibited moderate to severe cracks in their finishes, bearing walls and even the structural skeleton. Roads have also been repeatedly damaged by collapse within the subgrade, necessitating repair and repaving. With all these failures, changes in the moisture content within the bearing soil were found to be the principal trigger causing such failures. This breakdown within the surfacial soil structure, due to the wetting, has been termed as collapse, subsidence, hydrocompaction or hydroconsolidation. Throughout this study the terms collapse and collapsing soil will be used.

As an arid to semi arid region the water table within Sana'a is also very low. The current damage to structures due to collapsing in the underlying soil arises primarily as a result of the rapid urban development in the capital. As an example, 30 years ago the use of water was limited both in and around buildings and large-scale irrigation was almost non-existent. Furthermore sewage was treated in its dry state and so only limited liquor discharges were produced. However, when such an arid area is opened up to industrial and urban development, the opportunities are provided for spillages of large quantities of water, not only through irrigation but also from the discharge of waste sewage into septic tanks. Typically individual septic tanks are constructed for each structure so that they extend below the foundation level. This enables water to reach the bearing soil layers, leading to an extensive collapse in the adjacent super-structures. Indeed, during the construction of the main sewer lines in Sana'a, the temporary increase in moisture content of these soils produced by the construction processes led to unbelievable cases of failure in the existing structures and roads. These became so severe that the insurance company cancelled its policy with the main

contractor. The scale of these problems can be seen from Plate 1.1. Some cases of failures were investigated by the author and these are summarized in Table 1.1.

1.3 THE OBJECTIVES

The problems associated with the collapsing potential of Sana'a soil are the subject of this thesis. The research has both investigated the mechanisms of collapse and considered solutions to these problems. The main aims of this research may be summarized as follows:

1) To study the mechanical properties and behaviour of the various collapsing soils, in the Sana'a area, and to classify and identify their degree of collapsibility.

2) To study the collapsing potential in the field and to investigate the effects of different compaction techniques - steel roller compaction, dynamic compaction and preloading - and flooding with water, including the combined effects of flooding with the individual compaction processes on Sana'a soils. The effectiveness of these treatments to be assessed both by laboratory (collapse potential, water infiltration, deformation characteristics) and field testing (SPT and dry density).

3) To establish a laboratory framework to evaluate the response of the soils to the various field treatments, including both the mechanism(s) of collapse and the role of soil structure, and destructuring, on the observed deformations.

4) To analyse both the field and laboratory data to provide the most appropriate techniques to minimise the collapsing potential within the Sana'a soils. In addition, it is intended to produce recommendations for the design and construction of both safe and economic foundations on the collapsing soils of Sana'a.

Generally, the deformation of collapsing soils has been studied and evaluated by defining the collapsing potential following wetting, with or without static loading. However, the influence of destructuring on the collapsing behaviour has not been considered previously. Consequently, a further aim of this study is to investigate the relationship between the collapsing and destructuring phenomena of these soils.

1.4 THE LAYOUT OF THE THESIS

The main aim of this thesis is to study the mechanical behaviour and collapsing mechanism of Sana'a soils and their response to field treatment. Previous work on these Sana'a soils is described in Chapter 2, and is followed by a literature view dealing with collapsing soils, the effect of structure on the behaviour of natural cemented soil and techniques that have been used to improve such soils. The scope of investigation, in both the field and the laboratory, is described in Chapter 3. Chapter 4 gives a general description of the soil formations, selected sites and engineering properties, while the mechanical behaviour (collapsing and deformation) of the soils are given in Chapter 5. The field study and the associated data are presented in Chapter 6 together with the analysis of this data. The mechanical behaviour, collapsing and deformation of the laboratory destructured soils are given in Chapter 7 together with the analysis and correlation of these results with those of the natural soils. The laboratory framework of the collapsing and deformation behaviour is presented in Chapter 8 which includes the interpretation, evaluation and correlation of the data from both the field and laboratory investigation. Finally, the general conclusion, recommendations and suggestions for further work are presented in Chapter 9. This final Chapter, is followed by the references and the Appendices A2- B4, C5, D6, E7, F8 and G9 corresponding to the Chapters 2, 4, 5, 6,7, 8 and 9.

Table 1.1 : Representative cases of failure in different structures due to increased moisture content (1983 - 1990).

STATION	DESCRIPTION	TYPE OF THE STRUCTURE	SOURCE OF WETTING	FAILURE REMARKS
Ammar Al Zoomer	Al Harazi house	3 storeys of mixed materials	water pipe at 1.0m depth	Severe cracks all over
Ammar Al Zoomer	Al Khamisy house	4 storeys of mixed materials	water pipe at 1.0m depth	Moderate cracks in stairs
Ammar Al Zoomer	In front of Al Harazi house	2 storeys of mixed materials	water pipe at 1.0m depth	Minor cracks within the front bearing wall
Sooq Al Baqer	Sha'areh house	3 storeys of mixed materials	water pipe at 1.2m depth	Severe cracks in the front bearing wall
Sooq Al Baqer	South of Sha'areh house	2 storeys of mixed materials	water pipe at 1.2m depth	Moderate cracks within the front bearing wall
Sooq Al Baqer	Eastern of Sha'areh house	3 storeys of mixed materials	water pipe at 1.2m depth	Moderate cracks within the front bearing wall
Al Qasemi	Abdul Qadder house	3 storeys of mixed materials	Sewage excavation	Severe cracks in the back bearing walls
Al Saffiah Al Janobiah	Al Kohali office	1 floor of bearing blocks	Irrigation	Moderate cracks all over
Al Saffiah Al Janobiah	Al Thari house	1 floor of mixed materials	Plants and irrigation	Moderate cracks all over
Al Saffiah Al Janobiah	Al Aossta Jameh school	1 floor of mixed materials	Rain	Severe cracks all over
Al kuwait Hospital	Street of Blood Bank	Paved road	Sewage line	Severe cracks in the pavent
Al Saddi	Augbah house	Bearing layer and vertical cut	Flooding of open excavation from broken pipe	Total faliure in the vertical cut reached the foundation
Beer Kairan	Al Gasous house	1 floor of mixed materials	Plants and irrigation	Moderate cracks in the bearing walls
Beer Kairan	Al Talabi house	2 floors of mixed material	Dump due to sealing the adjacent yard surface	Moderate cracks in the bearing wall above the wetted area
Al Giraf	Mareb Hotel	9 storeys of reinforced concrete	Accumulation of water in the back due to depresion in ground level	Moderate cracks in the bearing wall of the bacement above the wetted area
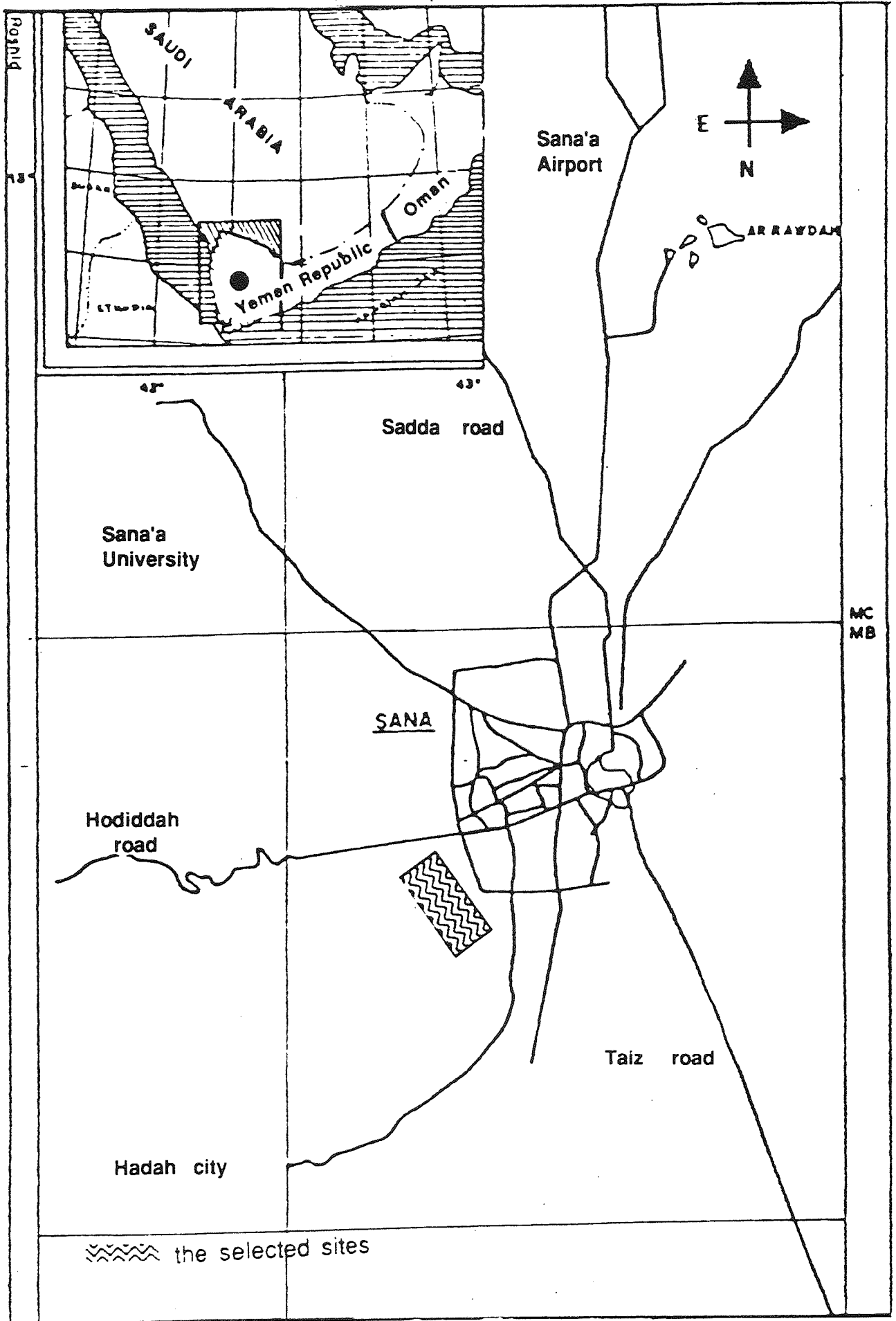
Fig. 1.1: The map of the study area, the Sana'a Region.
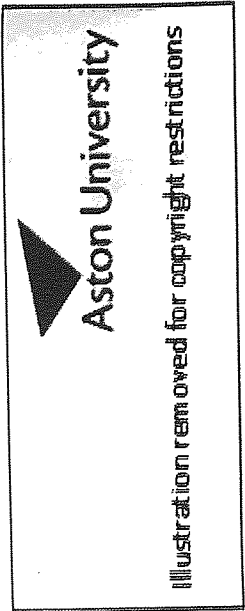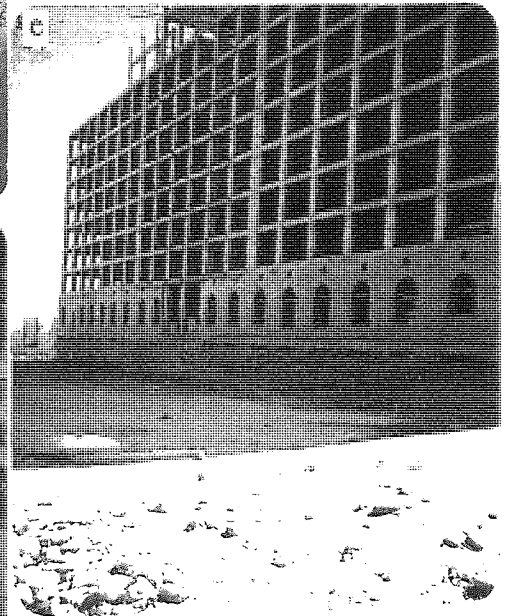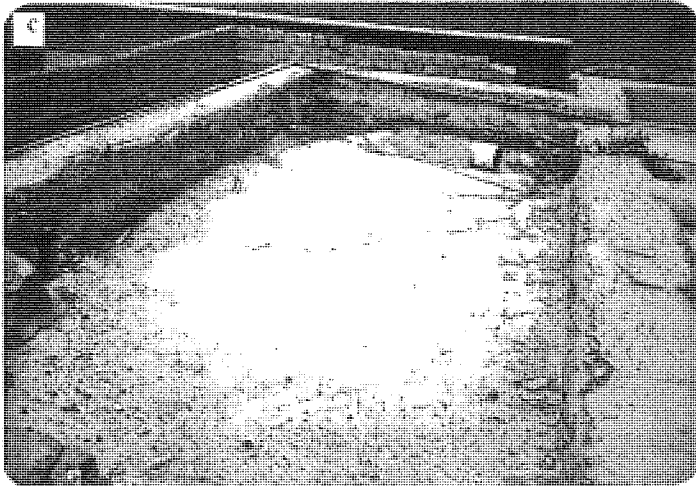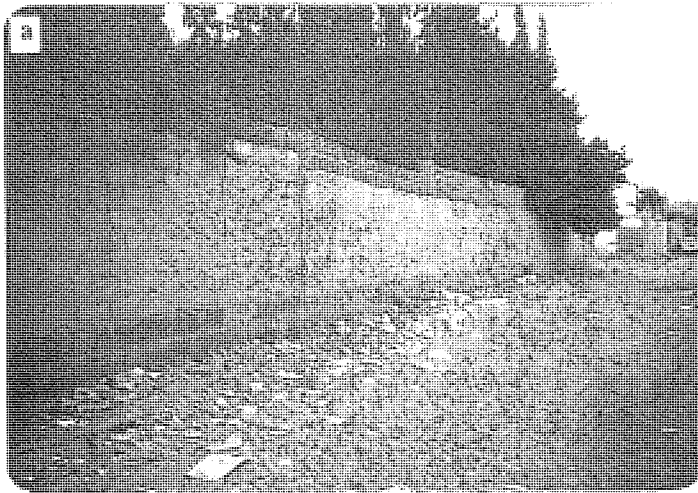
Plate 1.1 : Various inspected failures and cracks due to wetting in;

a) fences,   b) subgrade and pavement,

c) and d) light masonry and reinforced concrete structures, and

e) tilting in nine storeys of a reinforced concrete structure.

CHAPTER 2

THE LITERATURE REVIEW

To cover the field of this study the literature survey is divided into four sections. The first section, 2.1, deals with previous work on the soils of Yemen and, more specifically, the Sana'a soils. The general review of the collapsing phenomenon and collapsing soil and their characteristics are considered in section 2.2. Section 2.3 describes the properties of naturally cemented soils including their structure and the consequences of destructuring. The final section considers the field improvement of the collapsing soils by compaction, flooding, hydroconsolidation, preloading, pounding and roller compaction.

2.1 THE SOIL IN SANA'A AREA

Information on the geotechnical properties and soil characteristics for the soils of the Yemen Republic are almost nonexistent. Most of the available information is in the form of geological profiles, maps and water-well data, and cannot be labelled as geotechnical per se. Documented information on the Yemen in general and, more specifically, on the Sana'a area in terms of published reports and books covers only the surface geology, the physiography and the hydrology of the region (Italconsult, 1973). The exception being recent work undertaken at King Fahd University, KFUPM, (Abduljauwad, Al-Mana and Al-Gasous, 1991). Additionally, construction and geotechnical reports on projects executed in Sana'a and nearby areas are available and have provided preliminary information on the geotechnical setting of the Sana'a region (Ministry of Public Work, 1985).

The physiography of the Yemen Republic (North) can be divided into five regions, which, from west to east, are the Western Plain (Tihama), the Western Slope, the Highlands, the Eastern Slope and finally the Eastern Plain as shown in Fig. 2.1 (Al-Gasous, 1988; Mustafa, 1985).

The Highlands lie in the central part of the country with an elevation varying from 1500 to 3000 metres. The Sana'a area lies within this region some 2200 to 2300 m above sea level. A great variation exists in the types of rock within this region, for example Precambrian rocks, marine Jurassic rocks and Quaternary volcanic rocks. A series of highland plains (basins) separates the discontinuous mountains in the Highlands region. These are the

Dhamar, Yerim, Sana'a, Amran and Sadah plains and they are filled with alluvium and alluvial deposits derived from volcanic debris (El-Anbaawy, 1985).

The morphology of the Sana'a Basin is typified by flat tabular forms with a deeply entrenched valley and the morphogensis is quite recent, primarily of the Quaternary period. These rocks are of two types: Quaternary basalt volcanic rocks, with a thickness that varies from 0.0 to 300 m, and Quaternary sediments (Italconsult, 1973). The Quaternary sediments are divided, according to the transportation mode, into aeolian (wind-laid) and fluvial (water-laid). Within the Sana'a region these alternate as coarse (water-laid) and fine (mostly wind-laid) horizons. The former is composed of silty-sandy gravel with boulders that range upward to 50 centimetres in diameter and are light brown to light greenish-white in colour. The layer thickness of individual coarse material can be 10-15 metres. The fine horizons from the inter bedding - light brown silt or sandy silt - being only a few metres thick. Indeed, beds of clean sand and gravel are quite rare. Instead, a clayey-silty matrix is almost always present (Italconsult, 1973).

The geological map of Sana'a which was developed by W. Kruck in 1983 shows that the area under study is covered by washplain sand and basin alluvium deposits. Fig. 2.2 shows the different geological formations, surrounding the Sana'a area (Al-Gasous, 1988; Kruck, 1983). Grolier and Overstreet (1983) published a geological map of Yemen Republic which indicated that alluvial (gravel, sand and silt) deposits covered the flood plains at stream levels, while fluvial deposits covered the base of the hills. The studies which were carried out by Italconsult, for the Sam Wan Company as part of the project for the Sana'a water supply, and by the Ministry of Public Works (Sam Wan, 1982) describe the surface soils of Sana'a as silty-sandy soil, silty-clayey with sharp pebbles and some as gravelly sand with a matrix of clayey silt.

The work by the author while at KFUPM (Al-Gasous, 1988) indicated the existence of the wind deposits which are dominated by aeolian silt accumulation and evaporated deposits with some sand accumulations. These sediments are of well-sorted particles and most of the grains are quartz. The fine cementing agent is primarily calcite. The general features and the engineering characteristics of this deposit are mostly recognized as a loess deposit. They exist within the middle of three strips of the study area extending from south to north (Wadi area, as will be indicated in detail in Chapter 4). This loess soil was deposited by the wind forming the primary loess soil-sandy silt. The primary loess soil may have been reworked and deposited by water forming a secondary loess soil, consisting of sandy-clayey silt with gravel (Al-Gasous, 1988).

The identification of both sandy silt and sandy-clayey silt with gravel from both the engineering properties and scanning electronic microscopy, indicated that those two types of soil are similar to loess soils. In addition, laboratory tests showed that these soils exhibited

excessive settlement when wetted. This is termed a collapse within the structure domain of the soil and is a major characteristic of loess soil (Abduljauwad and Al-Gasous, 1991).

2.2 COLLAPSING SOIL

2.2.1 General

Collapsing soils are widely distributed throughout the world, in the United States, Russia, Europe, South Africa, China and other parts of Asia. These deposits exist extensively in the form of wind-borne and/or water-borne deposits. In addition, residual soils and volcanic tuffs may produce collapsing soils, as may also some man-made formations such as fills. All these soils are deposited so that they exist in a metastable form at both a relatively low density and in an unsaturated condition, so that wetting leads to a great reduction in volume. This collapse mechanism may also be produced by the application of stress, particularly during compaction, and further accentuated when accompanied by an increase in water content. Indeed, this generalization of the definition is sufficient to include all the variety of surface subsidence and soil structure collapse that may be caused by means other than soaking. The collapsing soil, in it's natural state, is characterised by low moisture content, low dry density, high shear strength and a loose structure of bulky shaped grains, often in the silt to fine sand size range.

2.2.2 Soil Formation

2.2.2.1 Aeolian Formations

These deposits consist of materials transported by wind and produce features such as sand dunes, loess, loessial-type deposits, aeolic sand beaches and large volcanic dust deposits (Clemence and Finbarr, 1981). Loess deposits are widespread throughout the midwestern and western United States, China and other parts of Asia, South Africa, Europe, Russia and Siberia (Clemence and Finbarr, 1981).

The loess particles are predominantly of silt-size and composed of quartz and feldspar. A small amount of clay, usually not more than 15 %, may be present. Loess may be identified by its colour and particle size. Loess is tan to light brown in colour, crumbly, and essentially devoid of stratification. Its open fabric structure and ability to stand in vertical cuts, at natural moisture state, are also distinguishing characteristics (Sheeler, 1968). The density of undisturbed soil may be as low as 1.2 Mg/m^3, although the specific gravity of loess

varies between 2.59 and 2.79, and the natural water content is low of the order of 10%. Most loess plot near the A-line in the plasticity chart (Gibbs et al, 1960; Sheeler, 1968; Mitchell, 1976). Loess is also characterised by the existence of the vertical root holes, produced by the gradual burial of grassy plains, so that the vertical coefficient of permeability is appreciably greater than that for horizontal flow. Along the sides of these root holes and between the particles, calcite precipitates and acts as a weak cement so that both clay and calcite can serve as the cementing agent within loess deposits, with the calcite content reaching 30% (Gibbs et al, 1960; Terzaghi and Peck, 1967; Das, 1984).

Typical of these formations are the Aeolian sands that occur widely in South Africa (Jennings and Knight, 1957) and which are composed of quartz and feldspar with small amounts of heavier minerals, the predominant clay mineral being kaolinite. As a consequence of drying during the deposition of these grains, in arid to semi-arid regions, clay and some colloidal clumps have formed at the contact between sand grains. These clusters acted as bridges or buttresses to support the sand grains in their position (Dudley, 1970) so that the soil structure was at equilibrium under the natural overburden pressure and in situ degree of saturation. For such soil the range of the dry density is 1.09 - 1.68 Mg/m^3, with a liquid limit range of 21- 25% and the plasticity index between 9-12%. However, the addition of water and more load resulted in a collapse (Jennings and Knight, 1957). The observed settlement within such soil reached 150mm (6in) (Dudley, 1970).

2.2.2.2 Water-laid Deposits

Water-laid deposits are primarily alluvial fans, flowslides and sheet flows. Such deposits consist of loose sediments, laid down suddenly and locally forming a loose, metastable structure with stream deposits, in particular, producing a loose, poorly graded material. Clay present in these materials can act as a binder, while additional cementation may develop from the upward movement of water which, in arid regions, evaporates and so precipitates the dissolved salts. The resulting structure is susceptible to collapse if wetted, and collapses of up to 4.3m have been reported in such deposits (Clemence and Finbarr, 1981; Dudley, 1970).

The collapse phenomena in such deposits are influenced by the clay content. When the clay content of the soil is below 5 per cent, the soil is unlikely to exhibit collapse. The risk of collapse increases as the clay content increases above this figure and when it reaches some 12 per cent of the soil, the risk of collapse is high. When the clay content exceeds 30 %, the soil becomes susceptible to swelling. However, at clay contents between 12 and 30 per cent, the void ratio becomes the predominant factor controlling the collapsing potential so that the risk of collapse is directly related to the void ratio. The role of the moisture content is linked to the deposition process since the deposits dry as they are laid down so the soil is typically at

low moisture content. This rises rapidly following flooding and so, in general terms, the drier the soil is before flooding, the greater the collapse (Dudley, 1970).

2.2.2.3 Residual Deposits

The deposits produced by the in situ weathering of crystalline rocks are known as residual soils. While the texture of these soils may be similar to that of the parent rock, the sediments vary in size from large fragments to gravel, sand, silt, clay, colloidal and, in some cases, organic matter. The intense weathering and leaching, coupled with an abundance of colloidal silts, result in fabrics and textures ranging from open metastable structures at the top horizons to denser fabric structures lower in the horizon. The weathering processes is more pronounced within the upper horizon than the lower horizon. The resulting high void ratio and low dry density make this top horizon more prone to collapse while, in the lower horizon, the structure is denser with a higher clay content due to leaching from top horizon. Concretion, crumbing and nodules are common in residual soil (Barden, 1973 and Smart, 1975). Such residual collapsing soil occurs in South Africa, and Rhodesia (Clemence and Finbarr, 1981).

2.2.2.4 Other Collapsing Soils

Man made fill is another formation that may exhibit collapse upon wetting. Compacted embankments for roads and earth dams are those that may collapse. Any compacted clay soil or clayey sand can collapse significantly under both loading and wetting and, especially, if they are compacted dry of the (Proctor) optimum water content (Barden et al, 1973; Hausmann, 1990; Bell, 1992). The collapsing potential in compacted fill has been primarily related to both the initial structure and the negative pore water pressure (Barden et al, 1973).

Other soil types which exhibit collapse upon soaking are those derived from cemented loose sand, dispersive clays, volcanic tuff, gypsum soil and sodium-rich montmorillonite clays (Clemence and Finbarr, 1981).

2.2.3 Criteria for Recognizing Susceptibility to Collapse

The susceptibility to collapse and its magnitude are related to many factors such as the natural moisture content, density, soil structure, applied stress, testing method and the weathering effect. Peck et al (1974) classified the loess deposits with respect to the soil formation as primary loess, upper horizon, and secondary loess, lower horizon. The collapsing tendency is known to be more prevalent in the primary loess than in the secondary loess. Al-Gasous (1988) and Gao (1988), indicated that leaching and fines migration effect

both the formation of loess and collapsing soils and their collapsing tendency. The loss of fine particles and cementation from the upper horizon, due to leaching, increased its tendency to collapse resulting in a primary collapsing horizon, while deposition of these materials within the lower horizon increased its stability and minimized its tendency to collapse resulting in a secondary collapsing soil. Therefore, some of the soil deposits described in section 2.2.2 may not exhibit a primary collapse being considered to only exhibit secondary collapse. Several methods are available for the identification and evaluation of the collapsibility of soil and they are based on a number of factors such as void ratio, moisture content and density. In addition, experimental techniques have become powerful methods for defining such criteria. Some of these qualitative and quantitative methods are described in the following sections.

2.2.3.1 Qualitative Methods

Qualitative Methods Based on Void Ratios: Denisov (1951) defined a coefficient of subsidence as K_c :-

$$K_c = e_L \div e_o \quad\quad\quad\quad\quad (2.1)$$

where, e_L = void ratio at the liquid limit, and

e_o = in situ void ratio.

K_c = 0.5 - 0.75 : Highly collapsible soil.

K_c = 1.0 : Non-collapsible loam.

K_c = 1.5 - 2.0 : Non-collapsible soils.

The USSR Building Code (Northey, 1969) also employs a relationship based on the void ratio. For soils with a degree of saturation, S_o, below 60% and

$$(e_o - e_L) / (1 + e_o) > -0.1 \quad\quad\quad\quad\quad (2.2)$$

the soil is susceptible to collapse, where

e_o = in situ void ratio, and

e_L = void ratio at liquid limit.

Denisov (1951) used relationships to evaluate the magnitude of collapse due to loading only, and due to the combination of both loading and soaking, as :-

$$R_p = (e_o - e_p) / (1 + e_o) \quad\quad\quad\quad\quad (2.3)$$

where, R_p is the coefficient of subsidence or collapse due to loading only, and

      e_p = void ratio in oedometer under pressure p, before wetting, similarly

$$R_t = (e_o - e_w) / (1 + e_o) \quad \dots\dots\dots\dots\dots\dots\dots\dots\dots\dots\dots\dots \quad (2.4)$$

where, R_t is the coefficient of the total collapse, and

      e_w = void ratio after wetting under the same pressure p.

The difference between R_p and R_t is the collapse due to wetting.

Feda, 1964, stated the possibility of collapse in terms of the porosity of the soil, n_o, rather than the void ratio. He stated that, if the initial porosity, n_o, is greater than 40 per cent the soil is susceptible to collapse.

<u>Qualitative Methods Based on Moisture Content:</u> Priklonski (1952) suggested a relationship between moisture content, Atterberg Limits and an indicator factor K_d as follows:-

$$K_d = (W_L - W_o) / I_p \quad \dots\dots\dots\dots\dots\dots\dots\dots\dots\dots \quad (2.5)$$

where, W_L = Liquid limit,

        W_o = Natural moisture content, and

        I_p = Plasticity index.

    $K_d < 0$ Highly collapsing soil.

    $K_d \geq 0.5$ Non-collapsing soil.

    $K_d > 1.0$ Swelling soil.

Feda (1964) developed Priklonski's relationship by including the initial degree of saturation, thus :-

$$K_1 = (W_o/S_o) - (W_p / I_p) \quad \dots\dots\dots\dots\dots\dots\dots\dots\dots \quad (2.6)$$

where, W_o : Natural moisture content,

        S_o : Natural degree of saturation,

        W_p : Plastic limit, and

I_p : Plasticity index.

Partially saturated soils with K_1 values greater than 0.85 are classified as collapsing soil, Feda used the term "Subsident Soils". For the other soils, collapse should be expected upon wetting when $S_o \leq 0.6$.

<u>Qualitative Methods Based on Density:</u>   If the density of a soil is sufficiently low to produce a void space larger than that required to hold the liquid limit water content, collapse problems are likely (Gibbs and Bara, 1962). However, if the void space is less than that required to accommodate the liquid limit water content upon saturation, W_s, collapse is not likely, N.L., unless the soil is also loaded. On the basis of these observations, a relationship has been developed to predict collapse by plotting dry unit weight against liquid limit for different values of the specific gravity, G_s, as shown in Fig. 2.3, where Gibbs and Bara (1962) used the unit weight in kN/m^3 rather than the more usual density in Mg/m^3. Clevenger, 1956, related the collapsing potential, in terms of the expected settlement, directly to the dry density. He stated that, if the dry density is less than 1.28 Mg/m^3, the settlement will be large, while it will be limited if the dry density is greater than 1.44 Mg/m^3.

In addition to these methods, others have been presented which combine physical properties with the soil texture. Anderson (1968) developed a relationship to define a collapsing ratio, R, in term of the Atterberg Limits, uniformity coefficient, the grain diameters corresponding to specific percentages of the soil and the the fraction passing No. 10 and 200 sieves as indicated in Table 2.1. Use of the soil texture to define the collapsing criteria was also reported by Handy, 1973, who related the collapse probability of an Iowa Loess solely to the clay content as follows:-

Clay contents   < 16 % = high probability of collapse

16 to 24 % = probably collapsible.

24 to 32 % = less than 50% probability.

> 32 % = usually safe from collapse.

<u>Qualitative Experimental Methods:</u>   A lot of experimental methods have been presented to indicate the susceptibility to collapse. Among these Benites (1968) suggested a simple dispersion test which consists of dropping 2 grams of natural soil, in its bulky form, into a cup containing 125 cc of distilled water, and recording the time required for the sample to disperse. The dispersion time for collapsing soil is 20 to 30 seconds (Northey, 1969). Table 2.1 summarises the criteria for collapsing identification, methods mentioned above, described by Lutenegger and Saber (1988).

The following approach, as a field identification, was suggested (Kantey, 1967):

(1)   Most collapsing soils, when removed in the form of small lumps, will break down readily between the fingers.

(2)   If an auger hole is excavated and refilled with the soil removed from the hole, collapse is likely if the returned soil does not fill the hole.

(3) A very simple test, referred to as the sausage test (Clemence and Finbarr, 1981), is similar to (2) above, and can be readily carried out in the field. A hand-size sample of the test soil is broken into two pieces, and each is trimmed until they are of equal volume. One is moulded and wetted in the hands to form a damp ball. The two volumes are compared again and collapse can be expected if the wetted soil is obviously smaller in volume (Clemence and Finbarr, 1981).

Audric and Bouquier (1976) distinguished between collapsible and non-collapsible soils by performing a series of consolidated undrained triaxial tests. They noted that when collapsible loess was tested, the deviator stress reached a peak at a rather small value of axial strain and decreased with further straining, although the pore water pressure continued to increase after the peak deviator stress had been reached. With the non-collapsible soils, the deviator stress continued to increase with strain although the accompanying increase in pore pressure was small

The most powerful experimental method for identifying the collapsing susceptibility is the oedometer test suggested by Knight (1963). A natural sample of the tested soil is trimmed to fit in the oedometer ring, and stresses are applied progressively to approximately 200 kPa. At this stage the specimen is soaked by water and left for a day when the test is resumed and taken to the maximum loading limit. A typical curve resulting for this procedure is shown in Fig. 2.4, from which the collapsing potential, C_p, can be defined as:-

$$C_p = \Delta e_c \,/\, (1+e_0) \qquad \text{...} \qquad (2.7)$$

where, Δe_c = difference in void ratios upon soaking; (e_1-e_2) and $e_1>e_2$

e_0 = natural void ratio.

This collapsing potential C_p may also be defined as:

$$C_p = \Delta H_c \,/\, H_0 \qquad \text{...} \qquad (2.8)$$

in which, ΔH_c = change in height upon soaking; and

H_0 = initial height of the sample.

Jennings and Knight (1975) have suggested values for this collapsing potential, C_p, to indicate the severity of the collapsing problem and these are given in Table 2.2.

2.2.3.2 Quantitative Methods

Jennings and Knight (1975) have developed a method to give not only a qualitative determination of the susceptibility to collapse, but also quantitative measures to predict the magnitude of the collapse. It consists of concurrently running two oedometer tests on natural, undisturbed samples of the soil, preferably obtained from block samples trimmed by hand. One sample is tested at its natural moisture content while the other is inundated with water. An initial load of 1.0 kPa is used as the setting load for each test, and this load is doubled each 24 h throughout the normal oedometer test, with the results expressed graphically as a consolidation curve with void ratio, e, plotted against the pressure, p, on semi-logarithmic paper as shown in Appendix A2-1. The magnitude of the settlement, due to either loading at natural moisture (Δ_{en}) or loading and wetting (Δ_{ec}), can be estimated by superimposing the consolidation curves for the two tests. The method of calculation depends on whether the soil is normally consolidated or overconsolidated as shown in A2-1 (Jennings and Knight, 1975). However, for the investigated soils as slightly overconsolidated soils, the setting pressure was used instead of the overburden pressure, p_o, in A2-1 after Houston et al (1988). In fact, since 1975 this quantitative method has been used widely to predict and classify the collapsing potential and has recently been published as a standard method by ASTM (1992). According to ASTM (1992), a single oedometer tests is employed to define the value of the collapsing potential, I_c, under any pressure while that occurring under a pressure of 200 kPa is defined as the Collapsing Index, I_{cx}. There are some differences between these parameters and the C_p, employed by Jennings and Knight, and these are related to variations in the classification ranges and the corresponding degree of collapse identification. Both of these methods have been employed in this study and the particular testing procedures and classification systems are presented in Chapter 5.

2.2.4 Effect of Inundation on Soil Structure

The infiltration of water into the soil mass leads to an increase in the moisture content. Extensive study has indicated that there are four main types of inundation that can trigger the collapse of soils (Goldshtein, 1969) and these are as follows:-

a) Local, shallow wetting caused by water from pipelines and/or septic tanks and the uncontrolled drainage of surface water during construction. In addition, extensive irrigation adjacent to the construction can be another source of local wetting. This does not usually penetrate to great depths, so that rises in the ground water level are not normally expected with settlement primarily occurring in the upper layer of soil below the inundated zone. As a consequence of this local wetting, differential settlement can be expected which may jeopardize the safety of structures in the immediate surroundings.

b) Intense, deep, local inundation caused by the discharge of industrial effluents or irrigation. If the flow rate is sufficient to cause a continuous and considerable rise in the ground water level, the entire zone of collapsible soil can be rapidly saturated. This can produce dangerous and extremely uneven settlements which may involve the whole thickness of the soil layer. Such collapse may be initiated by either the load from existing structures or even the weight of the overlying soil.

c) Slow and relatively uniform rise in the ground-water level from water flow from a source outside the collapsible area. In this case, the settlement is normally uniform and gradual.

d) Gradual, slow increase in the moisture content of a thick layer of soil resulting from the condensation of water vapour caused by changes in the evaporation conditions, such a case occurs when the ground is covered by asphalt or concrete. The weakness within the internal bond of the affected soil is partial so settlement is incomplete, and increases slowly with the wetness of the soil. Collapse may occur due to water alone, or due to the combined action of soaking and loading.

2.2.5 The Mechanism of Collapse and its Requirements

Investigations have indicated that the collapsing mechanism of these partially saturated soils is due to local shear failure between the soil grains or peds, so it is compatible with the principle of effective stresses (Barden, 1973; Maswoswe, 1985). This collapse mechanism is best considered in terms of two separate components of effective stress, namely the applied stress and the suction, as demonstrated by Bishop and Blight (1963). Both these components develop intergranular stresses by different mechanisms. The applied stress causes shear stresses leading to instability at intergranular contacts, while the suction is a normal stress and hence increases the stability of the intergranular contacts.

Holtz and Hilf (1961) explained collapse on the basis that soaking reduces suction to zero, thereby causing the effective stress path to be translated (at constant shear stress, q) across the Mohr-Coulomb failure envelope by an amount equal to the presoaking suction. Intersection of the effective stress path with the failure line would result in the sample undergoing general shear failure and additional settlement . They also obtained compression curves showing that collapse occurs in soils compacted to high densities when dry of optimum water content.

A similar approach has been used by other researchers to explain the collapse mechanism. Jennings and Burland (1962) described the increase in effective stress in a partially saturated soil, due to water menisci at the grain contact points, as a form of

"bonding" that offers considerable resistance to local shear forces. If, however, the partially saturated, granular soil is wetted while under load, these interparticle "bonds" are removed and the soil collapses as indicated in Fig. 2.5. Barden, Madedor, and Sides (1969) postulated that the soil suction in a partially saturated soil provides the structure with a temporary rigidity which is removed by wetting, thereby leading to collapse.

The bonding or rigidity in a soil, which is reduced during collapse, is not necessarily due to capillary suction. A similar effect can be produced by chemical cementing agents such as iron oxide and calcium carbonate (Barden, McGown, and Collins,1973). Whatever the basis of the bonding strength, all types are weakened by the addition of water, thereby allowing locally large shear stresses to collapse the structure. In the case of capillary suction the drop in strength will be immediate, whereas in the case of chemical cementing, it is usually slow.

Another approach for analysing the collapsing mechanism is to consider the soil structure and its effect on this phenomenon. The arrangement of the soil particles has an important role in determining the extent of the collapse that occurs when the soil is wetted under a given set of conditions. Generally, appreciable collapse requires satisfaction of the three following conditions:-

1)   An open, potentially unstable, partially saturated structure,

2)   An appropriate level of applied stress to produce a metastable condition,

3)   A soil sufficiently bonded, by suction or cementing action, to hold the intergranular contacts in position but which, upon soaking, will collapse.

The individual contribution of each of these factors can greatly affect both the magnitude and the rate of collapse (Barden et al, 1973).

2.2.5.1 Unstable Soil Structure

The term "structure" is broadly applied to cover the combined effects of particle arrangement and interparticle forces. The metastable structure of the collapsing soil is characterised by having an open fabric structure of bulky shaped grains individually held in place by some bonding materials or forces. This open fabric has been termed a honeycombed structure by Casagrande (1932) and typically consists of highly compressed, bonding clay trapped between silt and fine sand grains as shown schematically in Fig. 2.6 (Mitchell, 1976). The arrangement of the grains and the bonding agent within the collapsing soil domain can take different structural forms as shown in Fig. 2.7 with bonding, attributed to capillary tension (Fig. 2.7(a)) and fine material, such as silt or clay, supporting the (collapsing) soil structure. These materials and/or forces are susceptible to reduction or elimination by

increasing the moisture content, so the support is reduced and the grains are able to slide on one another and into the vacant space (Dudley, 1970). In fact, the bulky metastable structure of the silt particles is a key element leading to the collapsing criteria.

2.2.5.2 Metastable Stress Condition

Collapsing soils have the ability of carrying very high loads with only limited deformation at low moisture contents for, under these conditions, the bonding materials and/or forces provide the necessary shear strength to support the applied pressures. Therefore, under dry conditions, the structure remains highly voided and the potential for collapse exists (Houston et al, 1988). When the moisture content of the collapsible silt starts to rise, for whatever reason, the supporting system will weaken. Ultimately, as the moisture content continues to rise, the bonding reaches a limit where it can no longer resist the existing applied stress and hence the soil collapses. This collapse will be accelerated if the applied load also increased and this could be due to an increase in the overburden pressure, produced by the deposition process, or an increase in the external load as a consequence of construction.

2.2.5.3 Bonding Strength

The interparticle bonding strength is greatly affected by the depositional system and the climate. Water-borne fine deposits, after deposition, or the wind-borne deposits subjected to rainfall exist in a wetted condition, although rainfall affects only soils near the exposed surface. As the wetted soil starts to dry by evaporation, capillary tension pulls the remaining water into the spaces at the soil grain interface and this water may contain soluble salts, clay colloids, and silt particles. As the soil continues to dry, the dissolved salts, clays, and silts come out of solution and bond or weld the larger soil particles together at their interface through capillary tension, clay bonding and cementation. These processes produce significant interparticle forces (Mitchell, 1976; Houston et al, 1988; Ismael, 1993). In arid climates, where the rate of evaporation exceeds the rate of precipitation, most deposited soils are primarily silty sands, sandy silts, and clayey sands of low plasticity, typical of this study. As a consequence, these soils possess bonding forces in the form of capillary tension, clay bonding and cementation (Gibbs et al, 1960; Mitchell, 1976).

Capillary Tension: When a collapsing soil consists primarily of sand with a fine silt binder, the capillary tension forces are considered to provide the silt-silt and silt-sand bonds as shown in Fig. 2.7. When the moisture content of the soil falls below the shrinkage limit, the remaining water is attracted to the soil particles by surface tension, and so withdraws into the narrow spaces close to the junctions between the soil grains (Fig. 2.7(a)). The curved air-water interface produces a pore water tension which, in turn, generates an effective compressive stress between particles. In effect the soil is internally prestressed so that an apparent increase is produced in the effective stress due to the bonding mobilised by capillary

tension (Burden, 1973 ; Derbyshire and Mellors, 1988). However with the arrival of water, the surface tension is released, and as the strength is reduced, the risk of collapse is increased which can lead to a rapid decrease in the volume.

Aitchison and Donald (1956) demonstrated that, for uniform spherical grains in an open or cubical packing, the maximum added pressure due to capillary effect occurs at a moisture content of about 32%. For the densest packing of uniform spherical grains, the maximum tension force occurs at moisture content of 10%. In fact, due to the inherent variation in grain sizes and shapes, the peak effective stress values of the various collapsing soils occur at moisture contents above 10% and below saturation (Dudley, 1970; Clemence and Finbarr, 1981). The maximum effective intergranular stress due to moisture films was calculated to be of order of 13.7 kPa (Dudley, 1970). In contrast, for unsaturated silts, with particle sizes from 0.02 to 0.002 mm, the effective stresses may be in the range of, 34.3 to 343 kPa.

Clay Bond: Clay particles represent the predominant bonding agent when they exist among the bulky sand and silt grains of the collapsing soil. A number of different structural arrangements of the clay particles, either within their domains or with respect to the silt and sand grains, are possible depending on the geological origins and history of the soil. When the clay is formed in place by authogenesis, changes in surface texture, conversion of minerals and the formation of interparticle bonds may take place as a result of temperature, pressure and time. Under such effects, the formation of a parallel plates around the quartz particles can lead to the aggregated clay grains form (Fig. 2.7(c)). When the soil begins to dry by evaporation, the capillary tension causes the clay particles to withdraw with water into the junctions of the larger grains forming a random, flocculated arrangement leading to a buttress support as shown in Fig. 2.7(d). The subsequent addition of water causes the clay grains to separate, thereby producing a collapse in the soil structure (Knight, 1963; Dudley 1970).

The bond due to clay action can result from capillary and/or electrochemical effects. The interference between these two phenomena makes it complex to separate these two components (Clemence and Finbarr, 1981) for, when water is added, the capillary tension would be relieved while the ion concentration in the fluid would also be reduced. Both would increase the repulsive forces existing between particles as shown in Fig. 2.8. In the flocculated structure, the ion concentration affects the amount and type of forces between particles. In the same structure any two grains would have portions at various distances of separation. At the high ion concentration all parts would be attracted while at the low concentration a portion could be at a distance that produces a net repulsion. Thus, with this type of clay bond, adding water would change the ion concentration which in turn would produce a change in the supportive and cohesive effects of the clay buttresses (Dudley, 1970). It has been generally observed that the lower the water content, the greater the bond strength.

This flocculated structure is not the only possible arrangement in the clay. Among the clay particles, aggregations can be formed and each aggregation acts as a grain in a flocculated structure thereby producing their own capillary tensions as the silt grains. The amount of clay within the soil structure has an important effect on the collapsing behaviour. Bull (1964) has shown for maximum collapse the clay should comprise about 12% of the total solids. Above 30% the clay swells, while below 5% there is a little collapse. In between, there are cases in which soil with larger pore spaces collapse more than those at the same void ratio, but with smaller pores.

Cementation Bond: Many collapsing soils contain cementation agents such as calcite, iron oxide, silica, and alumina (Mitchell,1976; Bell, 1992). Calcite is the predominant cementing agent in loess soil while alumina and iron oxide are the predominant bonding agents in residual soil. The cementation action is the prime source of bonding in loessial soil. Upon saturation the soil loses its bond strength and a noticeable volume decrease accompanies this weakening from wetting. In contrast, the cohesion is higher and the deformation is much lower for a similar unsaturated sample so, for these collapsing soils, the lower the water content the higher the bond strength (Clemence and Finbarr, 1981). The loss of the cementing action is directly related to the degree of wetting and the presence of contamination in the water, together with the applied load. Generally the higher the level of saturation and the higher the applied stress, the greater the loss of cementation (Gillott, 1987).

However, irrespective of the basis of the bond strength, all collapsing soils are weakened by the addition of water. Collapse is fastest when the grains are hold together by capillary suction, and slower when cementing agents provide the bonding, and slowest in the case of clay buttresses. In all cases, the addition of water to the soil is the triggering action.

2.3   DESTRUCTURING OF THE CEMENTED SOIL STRUCTURE

2.3.1   Introduction

The conventional soil mechanics concepts, which rely upon the stress history and initial porosity, still provide the guidelines for describing the behaviour of engineering soils. In the recent years, some investigators have expressed reservations concerning the continuous use of these concepts with such soils as residual soil, soft clays, stiff clays, and sands. Among these are Mitchell and Sitra, 1982; Vaughan, 1985; Leroueil and Vaughan, 1990; Wesley,1990.

Vaughan (1985) stated that the use of the conventional concepts of soil mechanics, based on sedimentary soils, is "universally inapplicable to the behaviour of residual soil, and

misleading if inadvertently applied". Wesley (1990) has shown that "residual soils can be wrongly evaluated as problem soils simply because some aspects of their behaviour do not confirm to that of sedimentary soil". Mitchell and Sitra (1982) found that caution was necessary before applying the classic concepts of soil mechanics to the behaviour of residual soils. In fact, all these investigators drew attention to variations in the weathering and deposition processes which primarily account for the variations in soil structure and bonding. It has been suggested that the structural effects should be introduced into the general concepts of soil mechanics, together with the initial void ratio and stress history, as they are considered to be of similar importance in describing soil behaviour (Vaughan,1985; Leroueil and Vaughan, 1990; Wesley, 1990).

The behaviour of collapsing soil is primarily characterized and described by the soil structure. The effect of wetting on the soil structure has been investigated and identified as the collapsing phenomenon. This collapse, as indicated earlier, is attributed to a release of the capillary tension and/or a weakening process of the bonding or cementation agents. In fact, such effects do not represent complete destructuring, since part of the structure will remain even after collapse has taken place as will be considered subsequently. The relation between the soil structure, collapsing and destructuring of the collapsing soils has not been studied in the manner that it has been for residual soils. It is, therefore, encouraging to investigate this relation, particularly when some of the collapsible soils are also residual soils. Moreover, there is similarity between collapsing and residual soils with respect to the existence of the open structure and the bonding forces, although the bond is weaker in the collapsing soils. To study the collapsing and the destructuring of collapsing soils on the basis of the soil structure, it is important to review the importance of structure on the behaviour of naturally cemented soils.

2.3.2 Importance of Structure

The term structure reflects the effects of particle arrangement within the fabric and the interparticle forces that provide the bond strength or cementation. Leroueil and Vaughan (1990) have considered different types of soils - soft clay, residual soils, volcanic tuff, and artificially bonded soils - that possess bonding forces and they have been defined as structured soils. These structured soils exhibited the same soil behaviour but, when their structure is destroied by destructuring through the loss of bonding and the accompanying changes in the particle arrangements, they exhibited different behaviour. They concluded that the effects of structure in widely different soils are essentially similar, and these can be formulated in a general way, similar to the description of the effects of stress-history and overconsolidation in the plasticity models and the concepts of yield developed for sedimentary clays. This indicates that it may be possible to adapt these models to include the effects of structure.

Collapsing soils are characterized by their open fabric structure and internal bonding which are common with residual soils and, as indicated earlier, some residual soils are also collapsing soils. In spite of the similarity, there are some differences between collapsing and residual soils. Such differences are the variations in the degree of bond and the initial degree of saturation due to differences in the local climate, arid and humid. Collapsing soils, which are mostly found in arid climates, exist at low moisture content while residual soils occur in tropical regions where intensive rainfall is common. The leaching processes and cycles of wetting and drying within collapsing soils, in arid region, are less marked than in residual soils so the amount of cementation in collapsing soils is less than that in residual soils. The most common cementation agent in collapsing soil is calcite while iron oxide and aluminum oxide perform this role in residual soils. Such differences may account for some of the variation in the soil behaviour of each soil type. This may also explain why residual soils exhibit higher apparent preconsolidation pressures and so act as overconsolidated soils, while the collapsing soils with lower apparent preconsolidation pressures act as a slightly overconsolidated soils. Some of the secondary collapsing loess soils, that occur in the lower formations, can exhibit the same behaviour as residual soils due to their high bonding strength. The concepts proposed by Vaughan (1985) to include structure along with the stress history and pore voids, appear to provide not only a basis for understanding the behaviour of residual soils but also provide a link between residual and sedimentary soil behaviour patterns (Wesley 1990).

2.3.3 Natural Cemented Soils

Natural cemented soils occur widely in many formations, albeit with different degrees of cementation. These range from sensitive clays, like Leda clay, to varved clay and deep marine clays (Sangrey, 1972), through porous volcanic soils, like those from Canary Island (Uriel and Serrano, 1973), to natural cemented sands (Saxena and Lastrico, 1978; Clough et al, 1981). Such a broad classification includes both residual soils and collapsing soils. Studies of natural cementation or bonding have led to the development of a number of explanations. These have included calcium carbonate precipitation from supersaturated solution (Houston and Mitchell, 1969), aluminium and iron hydroxide precipitation (Quigley and Thompson, 1966), and amorphous manganese oxides and organic compounds (Mitchell and Solymar, 1984).

Cementation has important effects on the properties, stability, and behaviour of many soils. It is not always easily identified, nor are its effects always readily determined quantitatively, although it is well known to contribute to soil sensitivity (Mitchell, 1976) and to the development of an apparent preconsolidation pressure (Kenney, Moum and Berre, 1967; Bjerrum and Wu, 1960). The sensitivity of Leda clay has been found to range from 45

to 780 (Sangrey, 1972) while the apparent preconsolidation stress, p_c, has been found to be larger than any past stress history of the soil. Similar behaviour has been exhibited by a late glacial plastic clay from Sweden. It has a sensitivity of 30 to 70 and an apparent preconsolidation pressure much greater than the maximum past overburden pressure (Bjerrum and Wu, 1960). Bjerrum (1967) indicated that the removal of carbonates, gypsum, and iron oxide by leaching with a disodium salt of ethylene-diamine-tetra acetic acid, EDTA, resulted in a marked reduction in the apparent preconsolidation pressure of a quick clay from Labrador. Both sensitivity and apparent preconsolidation stress, p_c, are employed to distinguish between cemented and non-cemented soils (Sangrey,1972). The value of p_c is very high, when compared with the existing overburden pressure, p_o, for highly cemented soils as shown in Fig. 2.9 (Terzaghi and Peck, 1967), a typical void ratio/ log p curve for a cemented soil. The curve is quite flat at low stresses but breaks abruptly after p_c when the soil structure collapses. When the difference is small, the soil may be slightly cemented soil, such as a lightly cemented sands (Saxena and Lastrico, 1978).

Cementation affects both the shear strength and deformation behaviour of the soils for, up to a limiting applied stress, it increases the resistance to deformation. When the cementation is broken, the magnitude and the rate of deformation are large usually leading to an engineering failure or yield, although a higher ultimate strength may be obtained with further strain beyond this yield point. This yield point has been found to be stress path independent (Maccarini, 1987) and, before destroying the bond, the cemented soil behaves elastically with the behaviour being independent of the stress ratio followed. Following the deterioration of the bonds, the soil behaved plastically and the behaviour was dependent on the stress ratio (Maccarini, 1987). At low confining stresses, the bond strength predominates over the frictional resistance while, at larger confining stresses, the opposite occurs with the bond component being less dominant.

2.3.4 Soil Destructuring

The concept of using the soil structure as a basic soil parameter has been employed over the last ten years as discussed earlier, by many investigators. Leroueil and Vaughan (1990) indicated that the behaviour of soils which possess bonding and cementation is greatly influenced by the structure. Such soils are termed structured, while those that have never possessed a definite structure or which have been strained, remoulded or highly disturbed are described as destructured.

Destructuring can result from many actions, such as remoulding the soil or straining it to a high limit. Soil sampling, handling and preparation for testing may also result in (relative) destructuring. When the natural soil is subjected to liquefaction, earthquake or compaction destructuring is produced, unusually with the degree of deterioration ranging with

depth, and such destructuring has been studied by many investigators. The influence of the soil structure and the consequences of its removal by remoulding intact samples was recognized by Vargas in 1953. He presented the results of oedometer tests carried out on both intact and remoulded samples of the same soil, shown in Fig. 2.10, which clearly show the influence of soil structure on the behaviour of the soil. The curve AB represents the intact sample while A'''B''' is the curve of the remoulded sample prepared at its natural water content. The curves A'B' and A"B" represent remoulded and compacted samples prepared at the liquid limit(A'B') and the optimum moisture content (A"B"). Vargas suggested that the curve A'''B''' would be plotted in the region between A'B' and A"B". He also suggested the existence of the virtual pre-consolidation p_c within the upper horizon of the residual soil while in the lower layers of the same soil, this virtual pre-consolidation pressure followed the concept of pre-consolidation load, introduced by Casagrande. Wesley (1974) demonstrated that the natural soil was stiffer and could sustain a higher pressure than the destructured soil for the same void ratio, as shown in Fig. 2.11.

Leroueil et al (1979) studied the behaviour of three destructured, natural clays. They indicated that destructuring a clay produced important modifications in most of the mechanical characteristics, such as the shape and position of the limit state curve, the shear and bulk moduli in the overconsolidated state, the peak and large strain strengths and the coefficient of volumetric compression in the normally consolidated state. The effect of destructuration on these characteristics is shown in Fig. 2.12. The effect of destructuring can also be recognized by comparing the oedometer test results for both natural and re-sedimented soils, reconstituted from slurry, as shown in Fig. 2.13 (Leroueil and Vaughan, 1990). These show the difference in void ratios between the natural and re-sedimented soils, the structure having been removed from the re-sedimented soil. The stress-strain behaviour of two destructured clays was studied by Tavenas and Leroueil (1985) and again showed that the removal of the soil structure decreased stiffness.

Disturbance during sampling may cause partial destructuring and the greater the degree of disturbance, the more marked will be the effect of destructuring on the soil behaviour. This relative loss of structure leads to a decrease in stiffness and strength, with reduced yield stress and modification of the limit state of yield as shown in Fig. 2.14 (Leroueil and Vaughan, 1990). Destructuring can also result from a number of experimental techniques such as the method of saturation, eccentric loading and the stress path followed prior to failure. The consequences on the strength of weakly bonded soil is shown in Fig. 2.15 (Bressani and Vaughan, 1989). The structure of the vacuum saturated samples(a-c), was not affected as much as that of the samples saturated by back pressure (d-e). These had been subjected to many small loading and unloading cycles of effective stress that may have effected the soil structure and so the yield results, while those saturated by vacuum experienced less disturbance and so developed a higher yield stress. Similar differences were also reported for

the samples (j, k, 1 and m) subjected to drained triaxial testing. Samples j, k and 1 were saturated by vacuum and then sheared, while sample m was subjected to isotropic cyclic loading, by loading to 60 kPa, unloading to zero, loading again to 60 kPa and then unloading to 25 kPa followed by loading to 60 kPa and sheared. The yield results of the first three are consistent with acceptable variation of ± 5% while the sample m exhibited a substantial reduction in the yield stress. Thus, the cycles of isotropic stress during saturation effected the soil structure (Bressani and Vaughan, 1989).

Study of the behaviour of destructured soil can assist the interpretation of the behaviour of the cemented soils. Leroueil et al (1979) used this approach to study the behaviour of natural cemented soils. The same approach has also been discussed by Vaughan et al (1988) and Leroueil and Vaughan (1990). The suggested framework involves testing both the natural and destructured samples of the bonded soil in an oedometer to identify the boundary limits. An artificial bonded material has been used to simulate the natural bonded soils (Vaughan et al, 1988; Maccarini, 1987).

Maccarini (1987) tested an artificially bonded soil in the oedometer. The same soil was destructured by rubbing between fingers and gentle use of the pestle and mortar, and re-tested with the oedometer. The results, shown in Fig. 2.16, indicate that the compression curve, line C, of the destructured soil provides a boundary or a limit state in the stress/void ratio graph. It separates the stable state on the left of the curve from the metastable state on the right of the curve. The curves for the bonded soils of the same material are located within the metastable state region according to the degree of bonding. When the structure or bond is destroyed by strain beyond the yield stress, the compression curve converges towards the destructured curve as shown in Figure 2.17 (Vaughan et al, 1988).

In fact, use of this destructuring, or remoulding, line as a limit state has also been independently suggested by Mitchell (1976). He stated that a saturated clay, at a given water content and pore fluid composition, cannot be made weaker than its thoroughly remoulded strength so, a water content-effective stress condition to the left of the remoulded line is not possible. This curve is a sensitivity contour since the sensitivity of clay at any point in this line must be unity. At any point to the right of this curve, the sensitivity is greater than one, and the maximum gradient of sensitivity increase is generally normal to the remoulded curve. In other words, to the right of this curve the metastable state increases as the bond strength increases to dominate the deformation behaviour. Generally, the further a point is located away to the right from this curve, the greater the bond strength and sensitivity of the particular soil.

Nagaraj (1990) suggested that sensitive soils possess amorphous bonds between particles, due to which the initial void ratio prevails even under stresses greater than initial overburden pressures. He stated "This state, which is not a true reflection of the external

stresses acting, as in uncemented normally consolidated soil, is termed metastable state" (Nagaraj, 1990). According to Holtz et al (1986) as illustrated in Fig. 2.18, Nagaraj assumed that the locus of yield stress σ_c, for different degrees of disturbance was a straight line perpendicular to each of the curves at their points of maximum curvature. Within this limiting condition, this line can logically be expected to be perpendicular to the remoulded curve, as shown in Fig. 2.19. As a result of this analogy, to the right of the remoulded curve is the zone in which any disturbance is possible, the metastable state, while the maximum absolute possible disturbance is on the remoulded curve (Nagaraj, 1990).

2.4. SOIL IMPROVEMENT

The collapsing potential of collapsible soil, such as loess, can cause differential settlement leading to severe cracks or great damage in the superstructure. Consequently there is a demand to improve this type of soil by using suitable techniques to prevent, or at least restrict, the possible occurrence of collapse or differential settlement.

Wilson (1960) stated that compaction is the oldest method of improving soil and it is still the most economical and practical method. Improving the soil by means of compaction can be achieved by several different techniques, such as impact compaction by allowing a certain weight to fall into the soil from a specific height, often refereed to as pounding (Lukas, 1980; Manye et al, 1984). Pounding was successfully used by Lutengger (1986), Abelev (1975), Minkov et al (1981) in densifying loess soils and other loose soils. Abelev and Minkov et al used pounding successfully in compacting loess soils in Bulgaria and U.S.S.R. respectively. Lutengger (1986) found that loess soil was improved to a depth of 4.0 metres by this method. He also suggested that this depth would be more than sufficient for most shallow foundations and a similar view has been declared by others (Lukas,1986; Evstatiev, 1988). Pounding has been extensively used, particularly for deep improvement, and in some references is termed Dynamic Deep Compaction (Abelev, 1975; Minkov et al, 1981). Another form of compaction can be achieved by (vibratory) roller techniques using a steel roller, sheep's foot roller or rubber tired roller. Improvement by this method extends to a depth of 1.5 m (ASCE, 1978).

As an alternative to compaction, flooding by water, or ponding, has been extensively used to improve collapsable soils. Prewetting the collapsable soil causes failure within the soil fabric and so modifies the soil. Flooding can reach greater depths with values of up to 10 metres being achieved. The investigation by Balaev (1967), on a stratum of Terkkum loess, indicated a slump of 110 cm after a two months period of surface flooding on a layer 17.0 m thick. He indicated that the preliminary flooding, sometimes in combination with surface

compaction, provides a convenient method of improvement, since long periods of flooding are not necessary. Skvaletskii (1967) reported that the upper 4.5 m of a sand loess layer gave a slump of 32-38 cm after 1.5-2.0 months of flooding. He considered this slump to represent appreciable compaction of the top 4.5 m of the loess layer. In addition, he stated that loading soil to a stress of 150 kPa after flooding gave no noticeable deformation. Skvaletskii declared that, "preflooding is an effective method of compacting slumping soils characterized by low cohesiveness and a predominance of previous structural bonds, not only in the lower but also in higher horizons". He also indicated that, soils which have been noticeably compacted in the upper layers by preflooding do not need to be compacted by any additional heavy tampers or other measures.

A combination of both conventional compaction and flooding with water before compaction may increase the depth of the soil benefiting from treatment. The various compaction and ponding techniques have been summarised (ASCE,1978) and this information is presented in Table 2.3. Further details are presented in Chapter 6 when describing the field work undertaken in this investigation.

Table 2.1 : Summary of criteria for identifying collapsing soils
(after Lutengger and Saber,1988).

Table 2.2 : Collapsing potential values (after Jennings and Knight, 1975).

Table 2.3 : Methods of treating collapsing foundation soils
(soil improvement, ASCE, 1978)

Fig. 2.1 : The physiography of the main regions of the Republic of Yemen (adopted from Mustafa, I.,1985).

Fig. 2.2 : The geological map of Sana'a area and surrounding areas (adopted from Kruck,W.,1983).
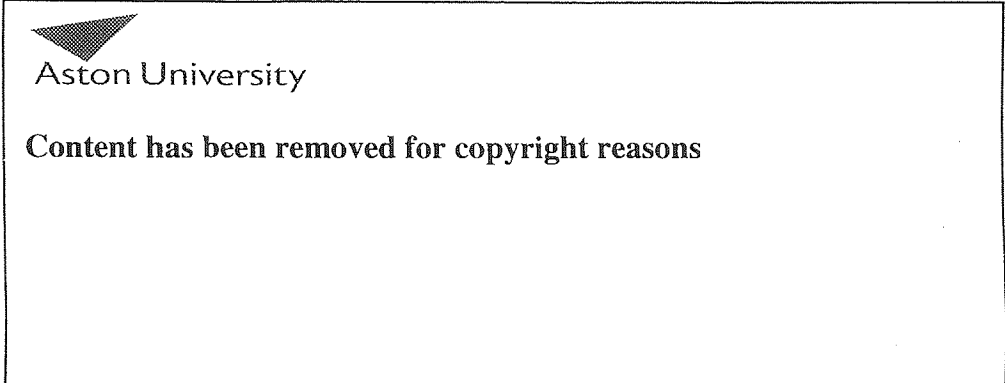
Liquid limit, %

Fig. 2.3 : Collapsing prediction (Gibbs and Bara, 1962).
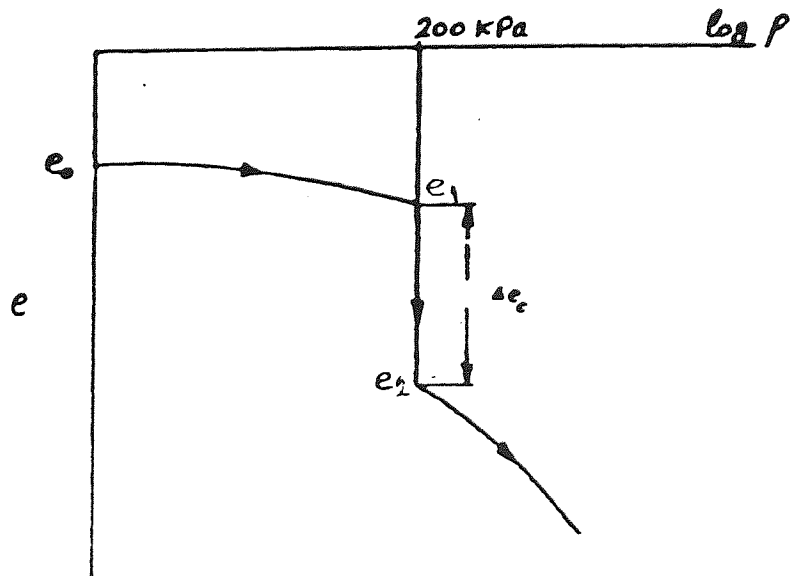
Fig. 2.4 : Typical collapsing potential result .
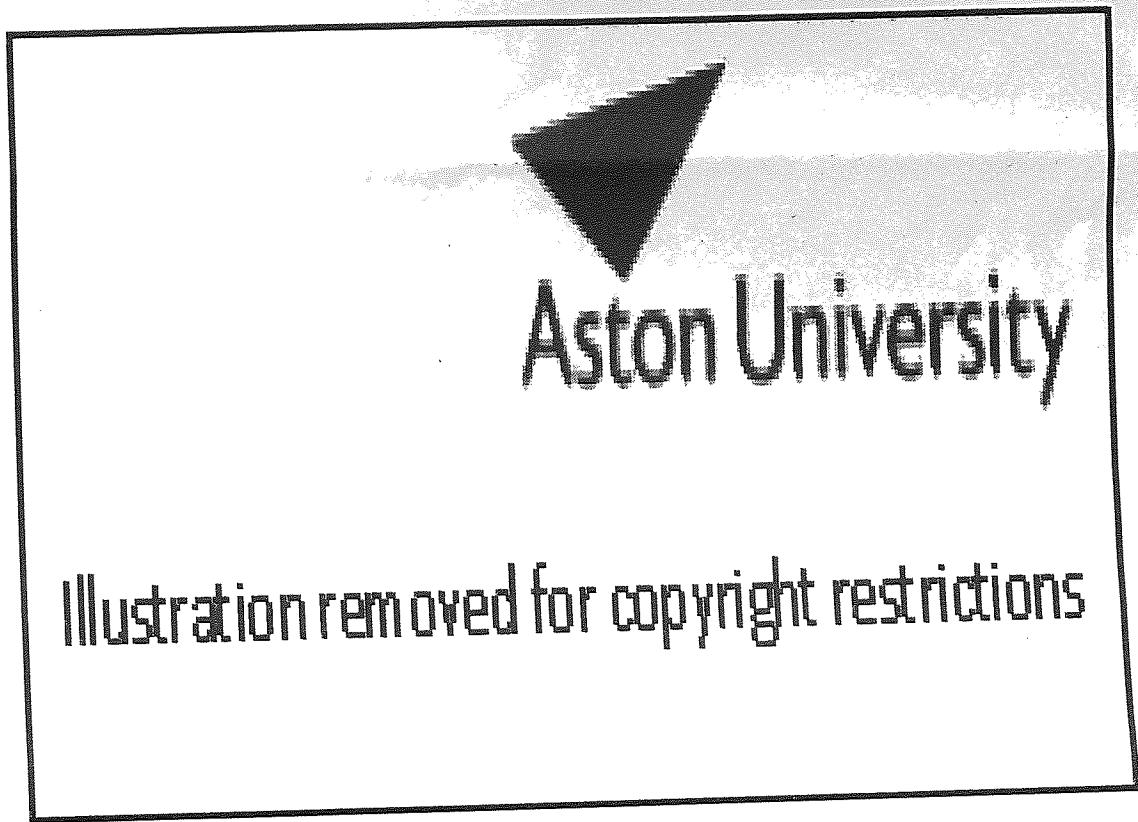
Fig. 2.5 : Forces acting at the contact points between the grains
(after Jennings and Burland, 1962).
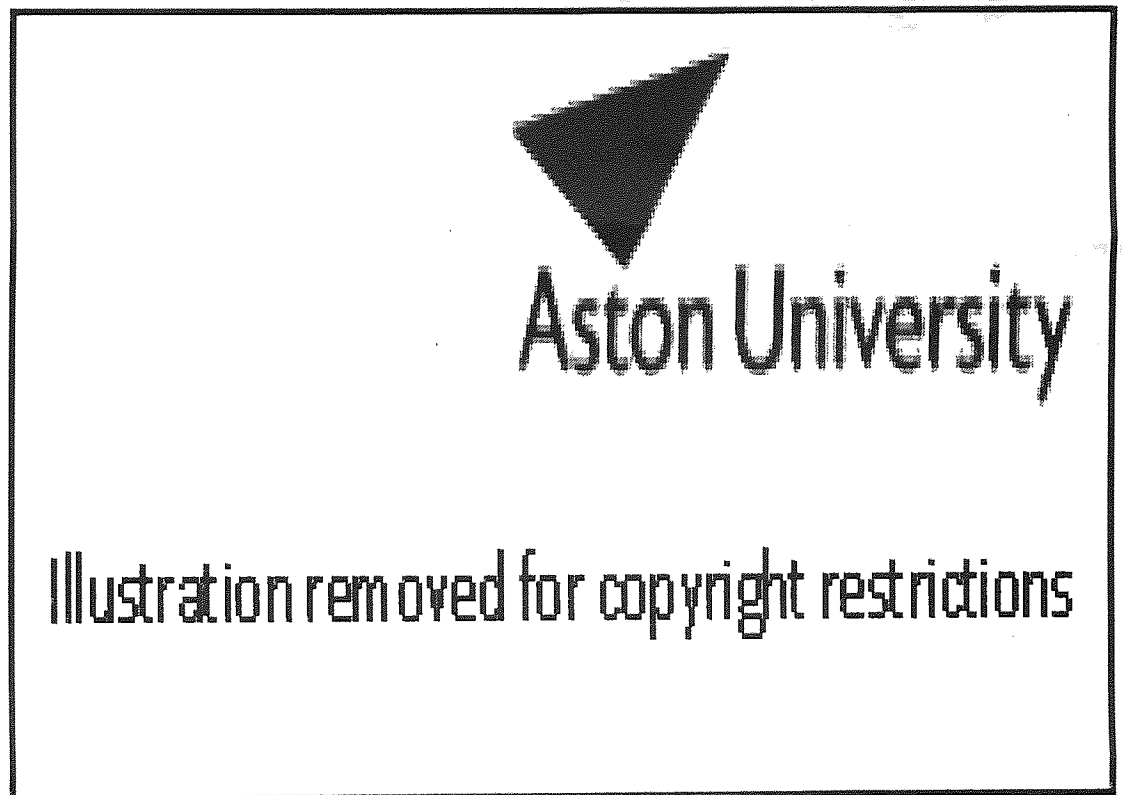
Fig. 2.6 : Structure of sensitive clay suggested by Casagrande (1932).

Fig. 2.7 : Structure and bonding within the collapsing soil (adopted after Dudley, 1970; Clemence and Finbarr, 1981).

Fig. 2.8 : Repulsion and attraction forces due to the ion concentration
in the double layer system (Dudley, 1970).

Fig. 2.9 : Typical e - log p curve for natural cemented soil (Sangrey, 1972).

Fig. 2.10 : One-dimensional test results on residual soils (Vargas, 1953).
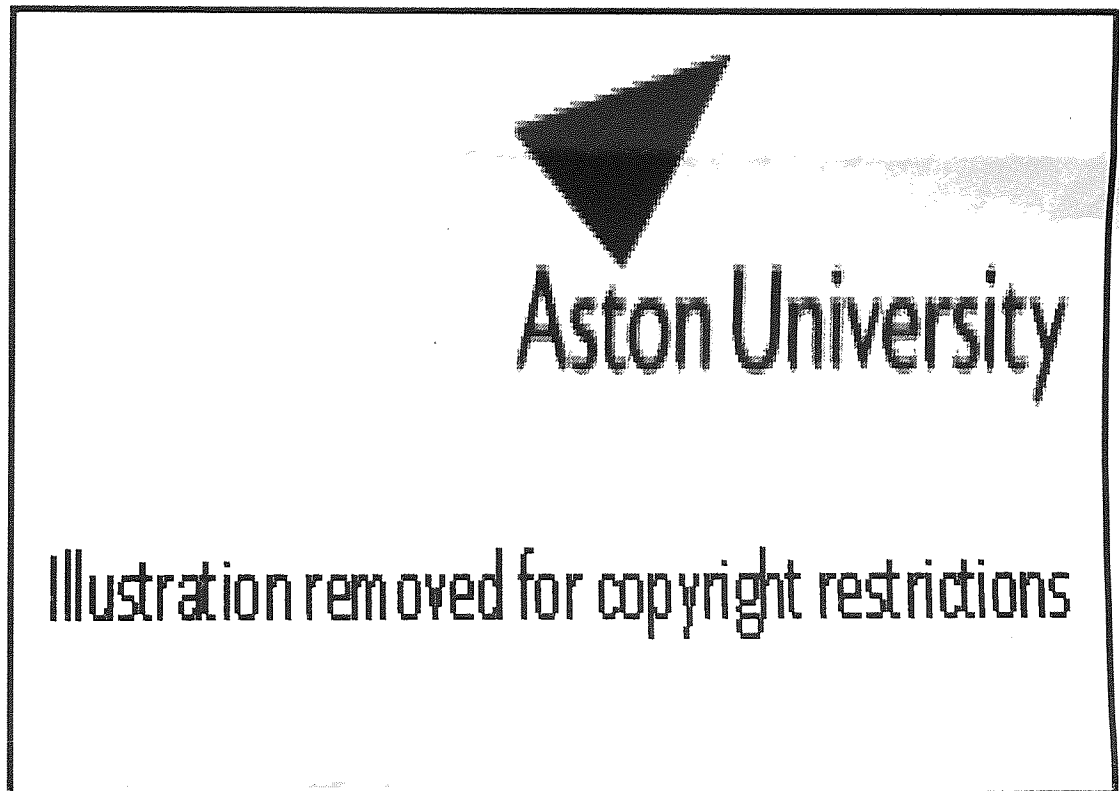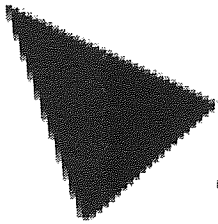
Fig. 2.11 : One-dimensional compression test on a residual soil from Java
(Wesley, 1974).

Fig. 2.12 : Intact and destructured Saint Alban clay from 3.0m depth,

a) volumetric strain v versus p' in triaxial σ_3 / σ_1 = cons.,

b) Stress-strain and pore pressure in CIU test, and

c) normalized limit state (Leroueil et al., 1979).

Aston University

Content has been removed for copyright reasons

Aston University

Content has been removed for copyright reasons
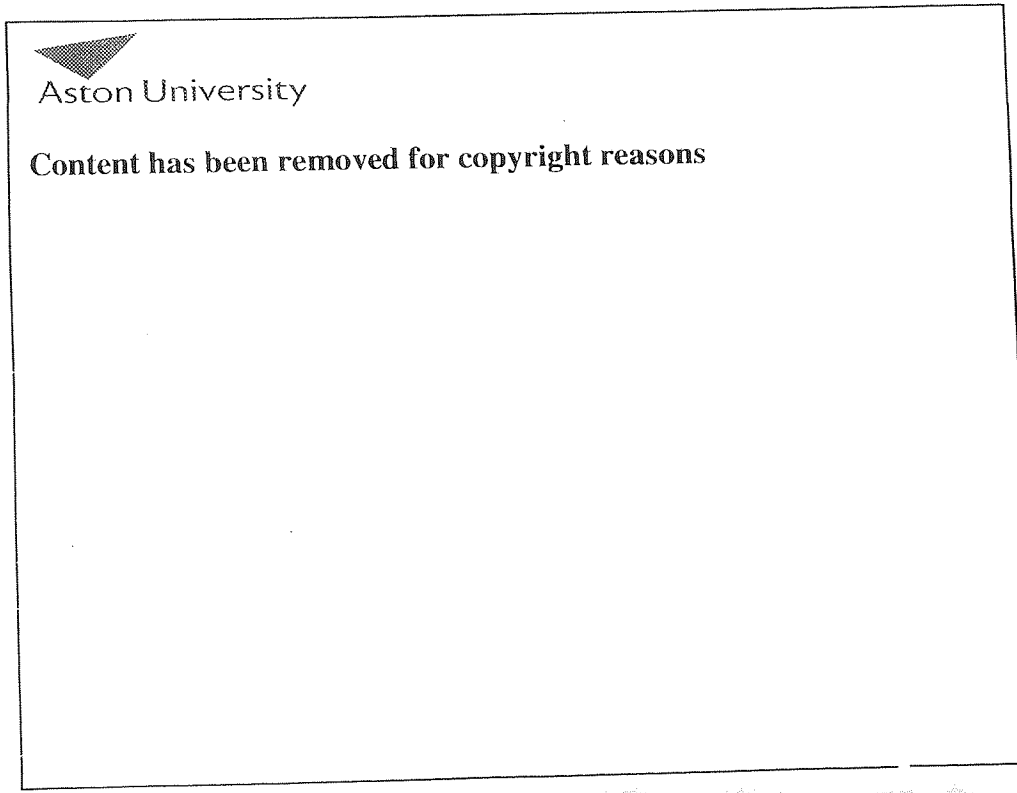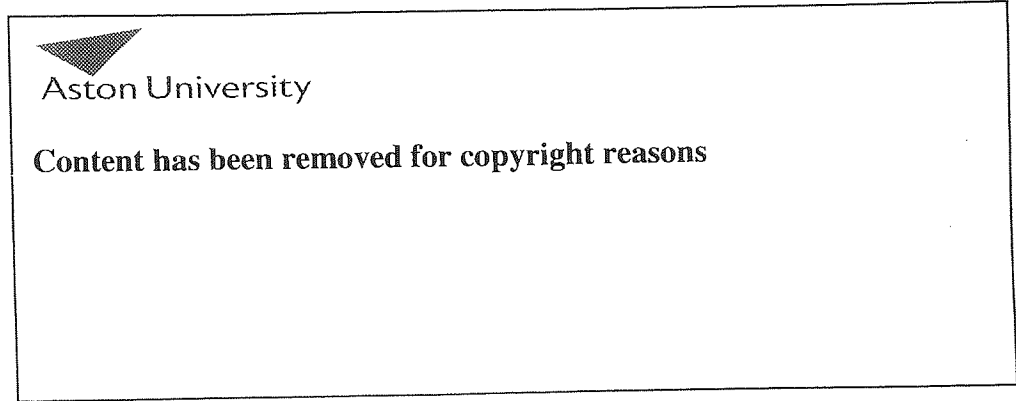
$$10^0 \qquad 10^1 \qquad 10^2 \qquad 10^3 \qquad 10^4$$

$$\sigma_v{'}, \text{kPa}$$

Fig. 2.13 : One-dimensional behaviour of two natural clays after remoulding
(Leroueil and Vaughan, 1990).

Fig. 2.14 : The effect of sampling disturbance on shear strength, on the abruptness of yield and yield stress; a) undrained triaxial test, b) oedometer test and c) limit state (Leroueil and Vaughan, 1990).

Aston University

Fig. 2.15 : The effect of saturation method on yield and failure of artificial bonded soil. Test a-i : 57%qs, 30% ks, 13% kb; tests j-m : 87% qs, 13% kb; all fired for 5 hours at 500 °C (Brassani and Vaughan, 1988).
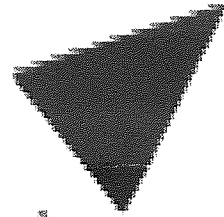
Fig. 2.16 : Yield observed in artificial bonded soil (Maccarini, 1987).
Artificial soil : 87% and 13% kaolin slurry for bonding.
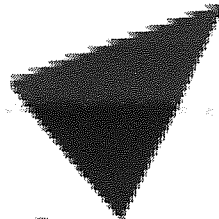
Fig. 2.17 : One-dimensional compression of soil with bonded structure
(Vaughan et al., 1988).

Fig. 2.18 : Effect of disturbance on e-log p' curves (Holtz et al., 1986).

Fig. 2.19 : Prediction of σ_{ct} and field e-logs paths using laboratory curves (Nagaraj, 1990).

CHAPTER THREE

THE SCOPE OF THE STUDY

3.1 GENERAL

This study is concerned with the behaviour of the fine soils within the Sana'a area and includes both field and the laboratory work. The field programme included exploration, site selection, field testing, field treatment and soil sampling, while the laboratory work included both general and specific tests carried out on the natural, field-treated and laboratory destructured soils. This laboratory work consisted of two parts, an initial phase carried out in parallel with the field programme on the natural and treated soils, at Sana'a University in Sana'a and the major phase carried out on the natural, destructured and some of the field treated soils, at Aston University in Birmingham. The field and laboratory routine tests are described herein, while the more specific tests, of both field and laboratory, are described in the appropriate sections in Chapters 5 and 6. A schematic diagram of the investigation is shown in Fig. 3.1.

3.2 FIELD PROGRAMME

This was primary concerned with monitoring the various soils that were subjected to the selected improvement techniques, which are described in detail in Chapter 6.

3.2.1 Field Exploration and Site Selection

An earlier investigation of 42 stations, within the Sana'a Plain, indicated the existence of troublesome, collapsing soils mainly located in the Wadi area (Al-Gasous, 1988). Within this area a further 12 boreholes were installed to aid the selection of the trial sites and, subsequently, four sites were selected for both the field and laboratory phases of this research. The exploration of the soil profile of each site was established before initiating any field tests or treatments. The different sites and their soil formation are described in Chapter 4, section 4.2.

3.2.2 Standard System for Coding the Sites, Locations and Samples

In view of the large number of sites, test locations and soil horizons, it was necessary to produce a standardised system to uniquely identify each site, location, layer and sample. The selected four sites throughout the text are referred by either Roman numbers - I, II, III and IV - or by the letters A, G, M and K respectively. The letters A, G, M and K with numbers being used to distinguish the different layers at each site, e. g. A1, A2 at site I, etc.. Similarly, the letters A, G, M and K linked with another letter and number are used to identify the different treated locations at each site, e. g. AC0, AC1, AC2 being the locations at site I treated by roller compaction and MD0, MD1, MD2 being the locations at site III treated by deep compaction, etc.. The numbers, 0, 1 and 2 are used to distinguish the different periods of the preflooding before compaction or treatment, e. g. 0; refers to the treatment at the natural moisture content without preflooding, 1; preflooding for one day and 2; preflooding for more than one day according to the treatment method as is explained in Chapter 4 (see, Table 4.3). The tested samples are coded by a key or legend, to the right of each figure, which consists of two parts separated by "/". The first part, before /, refers to the soil layer, type of test and the moisture condition during the test, while the second part, after / refers to the state of the sample if natural "N", destructured "Ds", etc., and to either the magnitude of the stress level (collapsing results) or the depth bellow the ground level. For example, the symbols on Figure 5.10(a) - A1En/N-1.0m - define the soil layer, A1, subjected to the Oedometer test (E) at the natural moisture content (n), En, while the last two terms refer to the sample condition as natural undisturbed, N, and the sample depth, 1.0m, below the ground level. For soaked tests "Es" is substituted for "En" and similarly in Figure 5.10(b) the soil is changed to A2 from A1 taken at a depth 3.0m rather than 1.0m. Similar nomenclature has been used for all the remaining tests throughout this study and whenever a different nomenclature is used, its code will be defined by then.

3.2.3 Field Tests

The field observations were augmented by data from the following field tests.

3.2.3.1 Auger Drilling

Due to limited resources, in situ testing was limited to the standard penetration test, SPT, and to carry out these tests at different levels, boreholes had to be drilled using continuous flight augers. A tractor-mounted drilling rig from either the Ministry of Construction or the Consulting Engineering Centre, was used. The flight augers had a solid stem with an outer diameter of 152mm and were used in sections of 1.5 and 3.0 metres.

To advance the hole, a cutter head was attached to the tip of the auger and, during the drilling operation, the rotary equipment applied a pressure against the cutter head which rotated at a speed of 75 revolution per minute. As the drill advanced, additional auger flights were added and the hole extended downward. In order to conduct the SPT and to obtain the disturbed samples, it was necessary to clean the bottom of the hole by maintaining the rotation of the auger while reducing the applied pressure so that the disturbed soil was brought to the surface. The auger was withdrawn at selected points in order to conduct the SPT, and the accompanying disturbed samples were inspected and used for the soil classification tests.

3.2.3.2 Standard Penetration Tests (SPT)

The limited availability of in situ test equipment and the absence of highly skilled labour in Sana'a necessitated the use of the simplest piece of available equipment, namely SPT. This equipment was suited to this research as it can be used with virtually all soil types, even soft rocks, and the procedure is simple and permits frequent tests. The existence of some gravel particles, and even boulders, restricted the use of the cone penetration test, while the layering of the soil profiles limited the value of the plate bearing test. Furthermore, the SPT results correlate with several useful properties (Terzaghi and Peck, 1967; Bowles, 1984), such as consistency, relative density, unit weight and friction angle, which could be used for classification purposes and subsequent comparisons.

These tests were performed at 24 locations which encompassed the selected sites both before and after treatment including both soil conditions, natural or treated, at either the natural moisture content (NMC) or the soaked moisture content (SMC). Testing extended to a maximum depth of 6.0m and was conducted at either half metre or one metre intervals below the treated surface. The test involved driving a split spoon sampler a distance of 46 cm (18 in) into the undisturbed or the treated soil using a 63.5 kg (140 lb) hammer falling freely from a height of 76 cm (30 in). The number of blows required to drive the split spoon the last 30.5 cm (12 in) was recorded as the Ns value (Douglas, 1983). As some of the treatments changed the moisture content of the soils, this restricted the use of the SPT data for making comparisons between the various improvement techniques as comparisons are only valid at the same moisture content, and this is considered in more detail in Chapter 6.

3.2.3.3 Field Density Tests

The core-currer method was used (BS 1377:1975) to obtain the field density of both the natural and improved soil from the various locations. A cylindrical tube, measuring 130mm by 100mm diameter, with a cutting edge at one end was used as the sampler. Each core-currer was numbered and weighed in the laboratory before placing in a sealed plastic bag. At the selected location, the top surface of the soil was carefully levelled and the soil locally trimmed in position by hand tools. The core-currer was pushed slightly and vertically

into the trimmed soil keeping the cutting edge downward. The soil surrounding the outer side of the core-currer was trimmed and the core was pushed further into the soil, under the steel rammer. This process of trimming and pushing continued until the soil extended above the tube. The top surface of the soil was levelled and the bottom of the soil block around the sharp edge was cut and levelled. The tube with the soil were tightly sealed in two plastic bags. The direction, location, depth and the sample name were written on both the outside of the core-currer and the nylon bag. During the trimming and pushing three soil samples were taken for subsequent moisture content determinations, and placed in another sealed and labelled bag. After the core had been carefully transferred to the laboratory the bulk density (ρ_n) and the natural moisture content (W_n) were computed, together with the field dry density (ρ_d). Two to four cores were taken from each soil layer. The different natural soil layers at each site and the different levels of the treated locations were detected to define the field density of the natural and treated soils.

3.2.4   In Situ Soil Destructuring and Improvement

Collapsing soil is generally characterized by its unstable, open structure. A means of improving their performance may be by densifying or, in other wards, destructuring the unstable structure in the field to form a more stable soil. The studied soils were subjected to several techniques; pre-loading, steel roller compaction, dynamic pounding or deep compaction and flooding, which was also used in combination with the other techniques. In addition, an attempt was undertaken to stabilize the soil using both cement and lime. The description of the field testing procedures are presented in the appropriate sections in Chap. 6.

3.2.5   Sampling

<u>3.2.5.1 General</u>

Undisturbed soil samples can be defined (Hvorslev, 1948) as: "Samples in which the material has been subjected to so little disturbance that it is suitable for all laboratory tests and thereby for approximate determination of the strength, consolidation and permeability characteristics and other physical properties of the in situ material. The term is to some extent misleading since it is impossible to obtain a truly undisturbed sample, but it is firmly established in the engineering terminology and therefore has been retained". Indeed, in this study the undisturbed term is used both for natural undisturbed soil samples and, relatively, for the field-treated, undisturbed soil. The relatively undisturbed term used for the treated soils means that they were obtained after treatment from field pits in the same way as the natural, undisturbed samples with minimal further disturbance following changes resulting from the particular treatment.

Field sampling was conducted in three stages to obtain both disturbed samples from the natural locations and undisturbed samples from the natural and the treated locations. The first stage was carried out during the exploration tests while the second stage was carried out during the performance of the field programme. The samples from the treated locations were used in the laboratory programme at Sana'a University concurrent with the field work. The last stage of sampling was carried out at the end of the field programme. More than 200 kg of undisturbed, block samples were obtained from Sites I and III and these were waxed and protected before being transferred to Aston University, where they were kept in a humid room for use in the second phase of the laboratory programme. One year later, further undisturbed samples were needed from the treated locations in the field and so a second trip was made to Sana'a.

The disturbed samples were obtained from both auger drilling and excavated test pits while the undisturbed samples were obtained only from the excavated pits. "The pits are open excavation, large enough for a person to enter and study the soil in its undisturbed condition. They may be dug either by hand or power equipment" (Wray, 1986). Samples of the natural soils were obtained from seven test pits, excavated by shovel and hand tools to depths of 5.0m, while a further 19 test pits were excavated to provide samples of the treated soil from depths to 4.0m as shown in Plate 3.1. This also shows the excavation for a septic tank, that extended to more than 7.0m below the ground surface, which was also used as a test pit during the exploration of the selected area (see Plate 4.2(a)). A further 11 septic tanks were similarly used in the study and these excavations, usually made by hand tools in the Sana'a area, can extend to more than 20m below the ground surface.

3.2.5.2 Disturbed Samples

These were obtained from the Auger Drilling at the locations where the SPT was carried out, from the excavated pits or from the trimmings of the undisturbed samples. Each disturbed sample was placed in a double nylon bag along with a label indicating the location name, the depth of the sample and the date of sampling. Disturbed samples, as defined after Hvorslev (1948), were used for inspection, compaction and general classification tests. A divider (riffle) was used in the preparation procedures to obtain the most appropriate representative disturbed samples for these tests (BS 1377:1975).

3.2.5.3 Undisturbed Samples

Undisturbed samples of hand carved block types were obtained from the excavated pits. They were taken from various levels corresponding to changes in the soil characteristics. Special wood and steel boxes, as well as over-coring barrel samplers, were used to obtain these samples. Oedometer rings were also used for direct sampling from the pits during the first part of the laboratory testing programme at Sana'a while, for the programme at Aston,

these specimens were obtained from undisturbed block samples, (see Plate 3.3). The undisturbed samples were mainly used for specific laboratory tests including consolidation, collapsing, permeability and scanning electronic microscope tests.

3.2.5.4 Hand-Carved Undisturbed Soil Samples

Application : Test pits and trenches are the most reliable source for undisturbed soil samples. Undisturbed block samples can be hand-carved from these excavations. According to Terzaghi and Peck (1967), "Samples obtained from such excavations are less disturbed than others", while the International Manual for the Sampling (1981) reported that, "Sampling from pits or trenches is specially valuable in obtaining high quality samples. In addition to undisturbed samples, information of the soil stratification and discontinuities can be obtained by this method. This method is often more expensive than other undisturbed sampling methods, but the greater value of the information obtained can offset the increase in cost".

Excavation and Equipment :   Both powered and hand-excavating tools were used to obtain undisturbed block samples. For the samples of natural soil, a power shovel was used to make a rough trench that would allow more than one block sample to be obtained from the same pit. Berms or terraces were formed at different levels along one side of the trench while the slope of the other side of the excavation was selected to avoid side collapse or basal heave. These terraces were located approximately at the top of each layer in the soil stratification. The power shovel was used to excavate to a depth of approximately 500 mm above the top of the intended sample and some 50-100mm in each direction around the sample.

In contrast, at the treated locations only hand tools were used and, to maximise the number of undisturbed samples, the excavation started from the perimeter of the treated location. When the level of the intended sample was reached, the excavation turned towards the centre and most undisturbed samples were obtained from the middle third of the treated location.

Samplers and Sampling Procedures : Different samplers were used according to the laboratory testing programme. For all the tests carried out in Sana'a, where no great precautions were required as transferring, handling and storage were minimised, over-coring barrel samplers, see subsection 3.2.2.3, and oedometer rings were used. Very stiff plastic tubes, each 15cm in diameter, 20cm in height and 0.6cm in thickness, were also used as over-coring barrel samplers. Two labelled plastic bags were used to seal each sample and these were handled carefully during transfer to Sana'a University. Trimming and sample preparation procedures were carried out in the laboratory to suit the type of the test and no waxing or storage was required.

In contrast, great caution was required for the undisturbed samples to be transferred to Birmingham for the second part of the laboratory programme. For these samples a wooden

box, having clear internal dimensions of 210x210x240mm and 15mm thick sides, was used as a soil protector. The top and bottom lids measured 240 x 240 x 15mm. The sides were fixed using halved joint connection system (groove and tongue jointing) with glue as a binder agent along the internal side corners of the box so it would resist the lateral movement and minimise the risk of sample disturbance during handling and transporting. Three steel boxes were designed and manufactured at Aston University to be used as samplers, each having clear internal dimensions of 210 x 210 x 210mm and 6mm thick sides. Two opposite corners of the box were welded while the other corners were extended outward and bolted so that the box could be spilt into two parts by releasing the bolts. The bottom edge was sharpened while the top edge was grooved so that a steel lid fitted into the groove could seal the top of the box. The steel box was used for direct sampling from the field, while the wooden box was used as a protector or cover for these samples, by setting the wooden box around the soil sample after removing the steel box.

Fig. 3.2 shows the hand-carving procedures commonly used for undisturbed soil samples (Krynine, 1957) which were adopted for this investigation. After the block of the soil had been trimmed to within several centimetres of the final size, the steel sampling box (or the barrel tube) was used as a template for the soil block sample. The top and sides of the block were carefully trimmed to the final dimensions using a sharp, square-mouthed shovel, sharp knifes and a trowel. The sampler was pushed down over the block, removing the excess soil from the sides with the hand-excavating tools (Plate 3.2). When the sampler reached the desirable depth, the top of the soil block was levelled (Fig.3.2a.a) and the lid fixed (Fig. 3.2a. b). The base of the soil block was then cut several inches below the bottom of the box and the block with the box was lifted out and inverted (Fig. 3.2a.c). The excess soil was removed, levelled and finally covered with the bottom wooden cover (Fig. 3.2a. d). In case of the steel sampler (Plate 3.2) and the plastic barrel sampler, two nylon bags were temporarily used to cover and seal each sample during transporting to the laboratory, before the permanent filming, waxing and sealing.

Some samples that contained both cohesive and cohesionless soil (silty clay with gravel or pebbles) were difficult to obtain with smooth sides and so the dimensions were under-sized by approximately 4mm on each side. Fine sand or fine soil from the same location was used to fill the resulting gaps between the soil block and sampler's sides (Fig. 3.2b.a). Light tapping, with a flat thin knife, was carefully performed on the filling soil in order to support the sample and prevent movement of the soil block inside the sampler during transportation and handling. The filling and sampling procedures in case of cohesive soil with gravelly material are shown in Fig. 3.2b. Specimens for the determination of the natural water content were taken during sampling.

Filming, Waxing and Labelling the Samples :   The samples were directly transferred to the laboratory at Sana'a University and the temporary top cover removed. A few millimetres

of soil were gently removed from the top of the sample. Two film layers were placed on the top surface and melted wax was poured over them until it reached the top edge of the sampler (stiff plastic tube sampler). In case of the samples obtained by the steel boxes samplers, after releasing the steel box, two film layers were wrapped all over the sample, before setting the protector wooden box. The melted wax was poured all around the sample to close any gap between the sample and the sides of the wooden box. After the wax had hardened another film layer was placed over it and the top part of the sample was sealed against the wooden lid in case of the wooden box sample or by several layers of sticky tape in case of the tube sampler. The sample was inverted and the same procedures were carried out on the bottom side. Finally, each sample was labelled and marked carefully, showing the direction of sampling, depth, location, number of sample and the date of sampling.

Storage and Handling of Block Samples :   Each six plastic barrel samples were protected by putting them in a covered wooden box. All samples were kept in a room under a wet blanket till they were transported carefully by aeroplane to Aston University where they were subsequently stored in a humid room in the Civil Engineering Department until required for re-sampling for the various laboratory tests.

3.3 LABORATORY PROGRAMME

3.3.1 Introduction

The laboratory programme was divided into two parts, the first phase being carried at Sana'a University and the second part at Aston University. Each part included preliminary, general and specific tests. The first part included tests on both the natural and field treated/destructured soils, while the second part included some tests on both the natural and field destructured soils, together with additional tests on laboratory destructured soils. All tests were carried out following the appropriate BSI and ASTM specifications, although some modifications were necessary to permit comparison with other investigations and these are indicated in the text. Indeed, it was difficult to follow a unique reference as alternative specifications are used in the study area, The Yemen Republic. Consequentely, it was preferable to use those specifications likely to achieve the most desired benefit for this research. In the following sections details are given of the laboratory sampling, specimen preparation and test procedure for some tests undertaken at both Sana'a and Aston.

3.3.2 Laboratory Sampling and Specimen Preparation

A large number of specimens were prepared and subjected to the various laboratory tests. These included specimens representing a wide range of soil conditions from undisturbed natural soils through relatively undisturbed treated soils to the laboratory destructured materials. The sampling of these different soils and the details of each specimen type -natural undisturbed, field treated undisturbed and laboratory destructured and compacted- are explained separately for each particular test.

3.3.2.1 Collapsing and Oedometer Specimens

The natural undisturbed oedometer specimens were obtained directly from the natural soil at the excavated pit in Sana'a, or from the block sample at Aston as shown in Plate 3.3(b). Oedometer rings of diameters 72.0, 71.14, and 50.0mm and respective depths of 19, 20 and 20mm were used for cutting the oedometer specimens. Five to nine specimens were obtained for each soil type. The ring was placed on the top levelled surface of the soil with the sharp edge downward and pushed slowly and steadily using a cutter holder, the surplus soil being trimmed by hand from the leading edge of the ring during this depression processes. The top and bottom faces of each specimen were levelled using a sharp blade and a flat glass plate, (Manual of Soil Laboratory Testing, 1981). A sample of the trimmed soil was used to determine the moisture content. For specimens taken directly from the pits, after pushing the ring into the soil, the lower portion of the specimen was cut so that its average thickness exceeded that of the ring by at least 15mm. The specimen was immediately placed in a labelled sealed plastic bag and carefully transferred to the laboratory where the final trimming and levelling were carried out. The moisture content was also determined from a specimen taken at the time of trimming in the field and placed in another labelled and sealed nylon bag. A total of some 90 natural undisturbed specimens were obtained from different levels (14) at the four sites (11 layers) for both the collapsing (48 specimen) and double oedometer (42) tests. The relatively undisturbed treated field specimens were all obtained directly from the treated locations using the oedometer rings in the same way. Some 168 specimens were obtained from the different levels of 19 treated locations and these were used for both collapsing and double oedometer tests.

The laboratory destructured specimens were obtained from three sources. These were specimens prepared from destructuring the intact specimens which had been subjected to double oedometer tests, those produced from the oven dry or wet disturbed soil at in situ conditions and those reconstituted specimens obtained from a slurry. For the first type, at the completion of the double oedometer test, each specimen was oven-dried and then destructured by breaking it down into fragments. These fragments were ground into individual particles by rubbing them between the hands or by gentle use of a mortar and pestle, care being taken to

minimise any damage to the soil particles and loss of material. The resulting material was weighed and distilled water was added until the original wet weight of the undisturbed specimen was achieved. The soil and the water were thoroughly mixed and placed in a sealed plastic container to allow the sample to condition. Subsequently, this soil was poured into a specially manufactured mould (Booth, 1975-b) as shown in Fig. 3.3 and Plate 3.3(d). The same oedometer ring that had been used for the natural undisturbed specimen was fitted into the mould before pouring the soil. The soil was statically compacted into the ring, by pressure applied through the upper piston, so that it occupied the same volume as the corresponding undisturbed specimen. This pressure was sustained for ten to fifteen minutes to condition the sample and so minimise expansion of the soil when the pressure was released. The mould was opened, the ring and destructured specimen were removed and weighed, to check that no loss in weight had occurred, and placed in the oedometer for testing.

The slurry specimens were prepared by mixing the oven dried soil with distilled water to a moisture content between 1.2 and 1.5 of the liquid limit, as suggested by Burland (1990). The slurry was poured into the ring which was placed over a filter paper resting on the bottom porous stone. Great care was necessary to eliminate trapped air and prevent loss of solid grains. The porous stone and the prepared slurry specimen were gently fitted into the oedometer cell for testing, (Plate 3.3). The slurry specimens were prepared to a range of dry densities to correlate and compare their compressibility behaviour with that of destructured specimens prepared at specific moisture content lower than the liquid limit.

3.3.2.2 Permeability Specimens

Undisturbed specimens for the falling head permeability test were obtained directly from the field pits using the steel tube of the cell of the permeameter. It has the same diameter and height, 100mm, and has a base with sharp edge. These samples were obtained in the same way as those for field density. At the required level, two specimens were obtained, one taken in the vertical direction and one in the horizontal direction.

3.3.2.3 Scanning Electronic Microscope (SEM) and Energy Dispersive Spectrometer (EDS) Specimens

Undisturbed natural, treated and some of the laboratory destructured material were subjected to both tests. For the natural soil, the specimens were prepared from the block samples while, for the field treated soils, some specimens were obtained from small blocks, 10x10x12cm, taken at some of the treated locations. These small blocks were sealed, labelled, packed and transferred to Aston. The destructured natural specimens were taken from the oedometer tests.

After air drying, the soil was split into two parts through a vertical section and at least four specimens were obtained and inspected to select a representative specimen. This

specimen was sectioned into 10x10x8mm and mounted on a metal plinth with a thin adhesive layer (Araldite) keeping the surface under study relatively undisturbed (Gillott, 1976). This specimen was oven-dried at 50° C and coated with a thin layer of gold (100 Å in thickness) prior to the examination. This layer acts as a conductive layer to avoid the build up of absorbed electrons on the surface which can give rise to abnormal contrast. A small trail of silver was used to earth the gold layer, in this case to the aluminium mount.

3.3.3 Laboratory Tests

Laboratory testing included both general and specific tests. The description of the apparatus, along with the setting of the specimen, and the testing procedures of the routine tests are described herein, while the more specific tests (single, collapsing, and double oedometer tests) are described in the appropriate sections in Chapter 5. For tests that were carried out according to a standard specifications, the procedures are given in the Appendices.

3.3.3.1 Inspection Tests

The soil samples were subjected to preliminary inspection in the laboratory to detect colour, smell, texture and the existence of organic material, such as plant debris. The characteristics of the boulders, gravel, and sand were identified by the naked eye. The silty sandy soil was distinguished from the silty clay soil by observing the water absorption of each sample. They could also be distinguished by pressing a wet sample between the palm and fingers and detecting the friction, in case of silty sand soil, and the susceptibility to casting of the silty clay soil. Such preliminary tests were very helpful in selecting the appropriate laboratory tests for the different soil types. The visual description of the soil is reported as recommended by ASTM (D2488-69).

3.3.3.2 Classification and General Tests

As a result of the variations in horizontal and vertical distribution many representative disturbed samples were required for classification purposes. Such tests were performed on twenty four samples, obtained from 7 locations (12 layers, including A0), and included wet sieve analysis, hydrometer analysis and Atterberg limits (plastic limits and liquid limits). The tests performed on each sample depended on the texture and cementation. When some samples were subjected to the dry sieve analysis they gave very different results to those obtained from wet sieving analysis, probably due to the effect of cementation. Due to the difficulty in breaking the fine soil into its individual particles, even with a rubber-tipped pestle, a combined sieving procedure was adopted. In this method (ASTM D2217) the cementation between the silty and granular particles was loosened by washing the soil sample through 2.12 and 0.63μm sieves into a deep container. The soil retained on the 63μm was air dried and re-sieved through five or six sieves according to ASTM D421 and BS 1377:1975 (2.7). The

silty and clayey soil samples were tested by wet sieve analysis, hydrometer analysis, Atterberg limits and specific gravity tests. In the hydrometer tests use was made of both a 152H hydrometer (ASTM D422) and a calibrated hydrometer as described by Lambe (1951) and BS 1377:1975 (2.7). The liquid limit tests were carried out using both the Casagrande apparatus and the cone penetrometer (BS 1377:1975 (2.2)). The samples were air dried as recommended by ASTM D 421, and the tests were preformed as recommended by BS 1377:1975, USCS and AASHTO soil classification after (Bowles, 1988 and Wray, 1986) and ASTM D3282-85. The specific gravity test was to BS 1377:1975 (2.6), and was performed on four specimens of each soil, the mean value being reported.

3.3.3.3 Permeability Test

The falling head test was used to determine the coefficients of permeability in both the horizontal and vertical directions. The specimen was placed in the permeability cell and tested in accordance to the procedures described by Bowles (1988). The test results and analysis are presented in Chapter 6.

3.3.3.4 Scanning Electronic Microscope and Energy Dispersive Spectrometer Tests

The SEM is widely used for the examination and analysis of the microstructure characteristics of material in a solid form. The SEM analysis performed in this study was carried out on Cambridge S 90 located in the Mechanical and Electrical Engineering Department of Aston University. The S 90 enables morphological observations to be made of the very fine structure together with a full elemental analysis from the EDS system. In the secondary image, the S 90 has 5μm resolution and the magnification ranges from 15x to 200,000x. This is very useful for EDS analysis and the spectrum can be viewed immediately on the screen.

The SEM analysis was deemed necessary to examine the structure of the fine soil and the distribution of pores within the soil. In addition, bonding between the fine particles such as clay and/or silt particles was identified. The effect of field treatment and laboratory testing on the destructuring of the bonds and the accompanying densifying of the soils were also investigated. Twenty two soil samples were used for SEM analysis.

The coated specimen, fixed on a metal-mount, was inserted into the chamber of the SEM apparatus and the air was evacuated. The analysis involved the examination of the microstructure and elemental structure by EDS at several areas of each specimen. To fully understand the formation and distribution of the pores, micrographs were taken at several locations in the transverse (horizontal) and longitudinal (vertical) sections. The EDS analysis was obtained at these respective microstructure locations. The analysis and results are discussed in Chapters 4, 6, 7 and 8.

Investigation Programme

Field Inspection 12 stations

Previous Inspection 42 stations

4 Sites

Field Programme

Laboratory Programme

Field Test
- Inspection (27)
- SPT (25)
- Field density (170)
- Hydroconsolidation and collapsing (6)

Field Improvement and destructuring
- Steel roller (5)
  - At NMC (1)
  - Flooding for one day followed by compaction (2)
  - Flooding for three to five days followed by compaction (2)
- Pounding (6)
  - At NMC (2)
  - Flooding for one day followed by pounding (2)
  - Flooding for five days followed by pounding (2)
- Flooding (2)
- Pre-loading (6)
  - Loaded at NMC then soaked (2)
  - Soaked during the test (2)
  - Pre-soaked for five days (2)
- Stablization (2)
  - By cement (1)
  - By lime (1)

Sampling
- Disturbed
- Undisturbed (7 locations, 246 samples)

Lab programme at Sana'a University

General Tests
- Liquid limit (8)
- Plastic limit (8)
- Hydrometer (5)
- Specific gravity (4)
- Wet sieve analysis (7)

Specfic Tests
- Collapse (154)
- Consolidation (78)
- Compaction (5)
- Permeability(12)

Lab programme at Aston University

General Tests
- Liquid limit (4)
- Plastic limit (4)
- Hydrometer (7)
- Specific gravity (15)
- Wet sieve analysis (5)

Specfic Tests
- Compaction (8)
- Scanning Electronic Microscope (22)
- Energy Dispersive Spectrometer (12)
- Oedometer (72)
  - Single collapse
  - Double oedometer
    - Consolidation at NMC state
    - Consolidation at SMC state

(No. of individual tests).

Fig. 3.1 : Schematic diagram of the scope of the study.
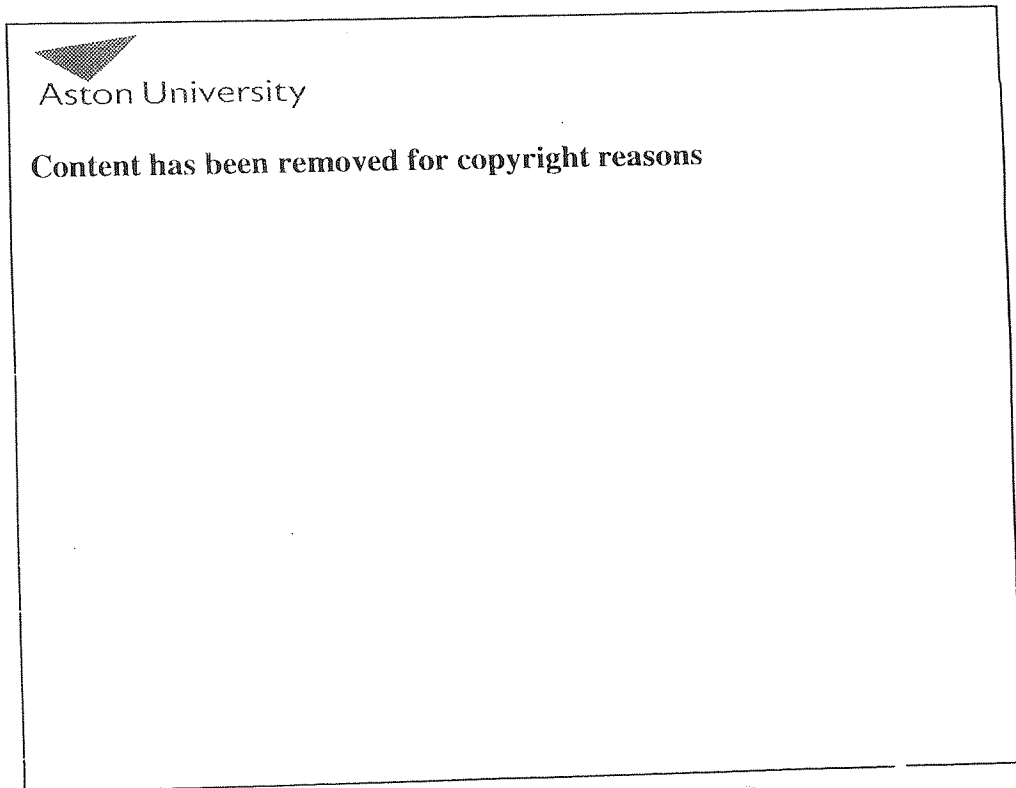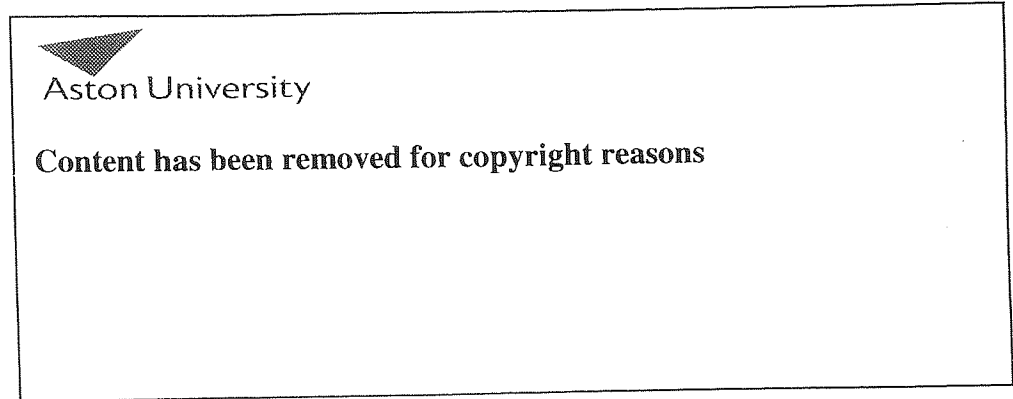
Fig. 3.2 : Hand-carved sampling (after Krynine, 1957).

(ALL DIMENSIONS IN MILLIMETRES)
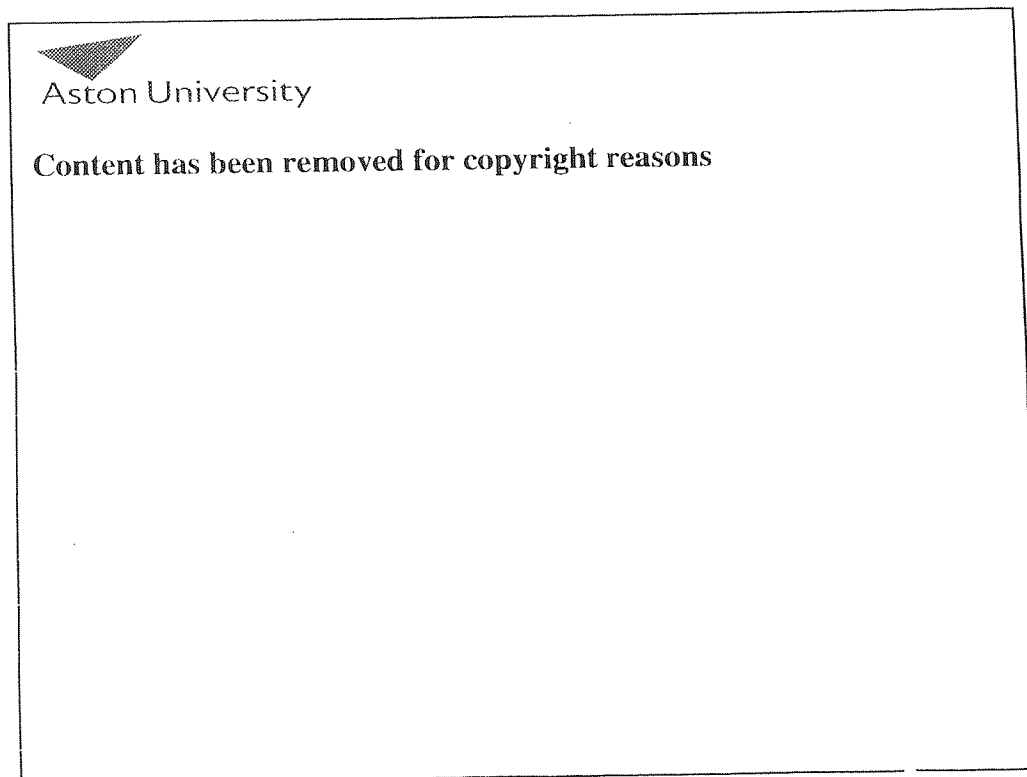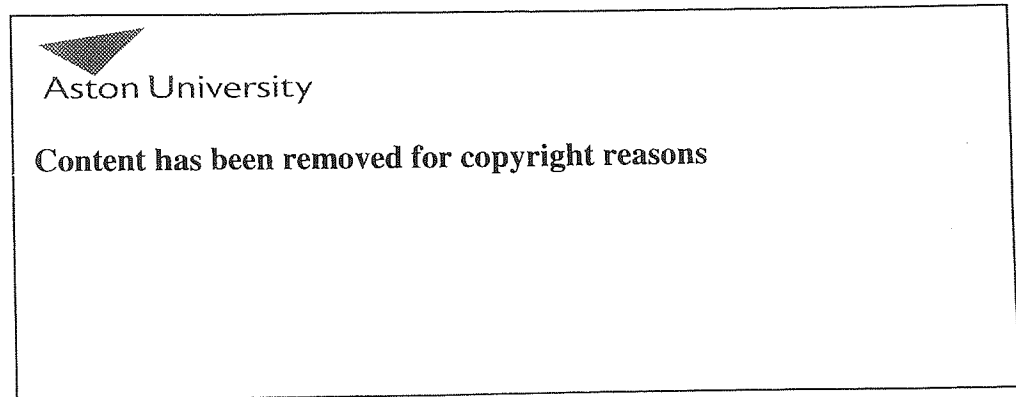
Cross-sectional plan of mould

Fig. 3.3: Manufactured mould for preparing the destructured/compacted
samples in the laboratory (after Booth, 1975-b).
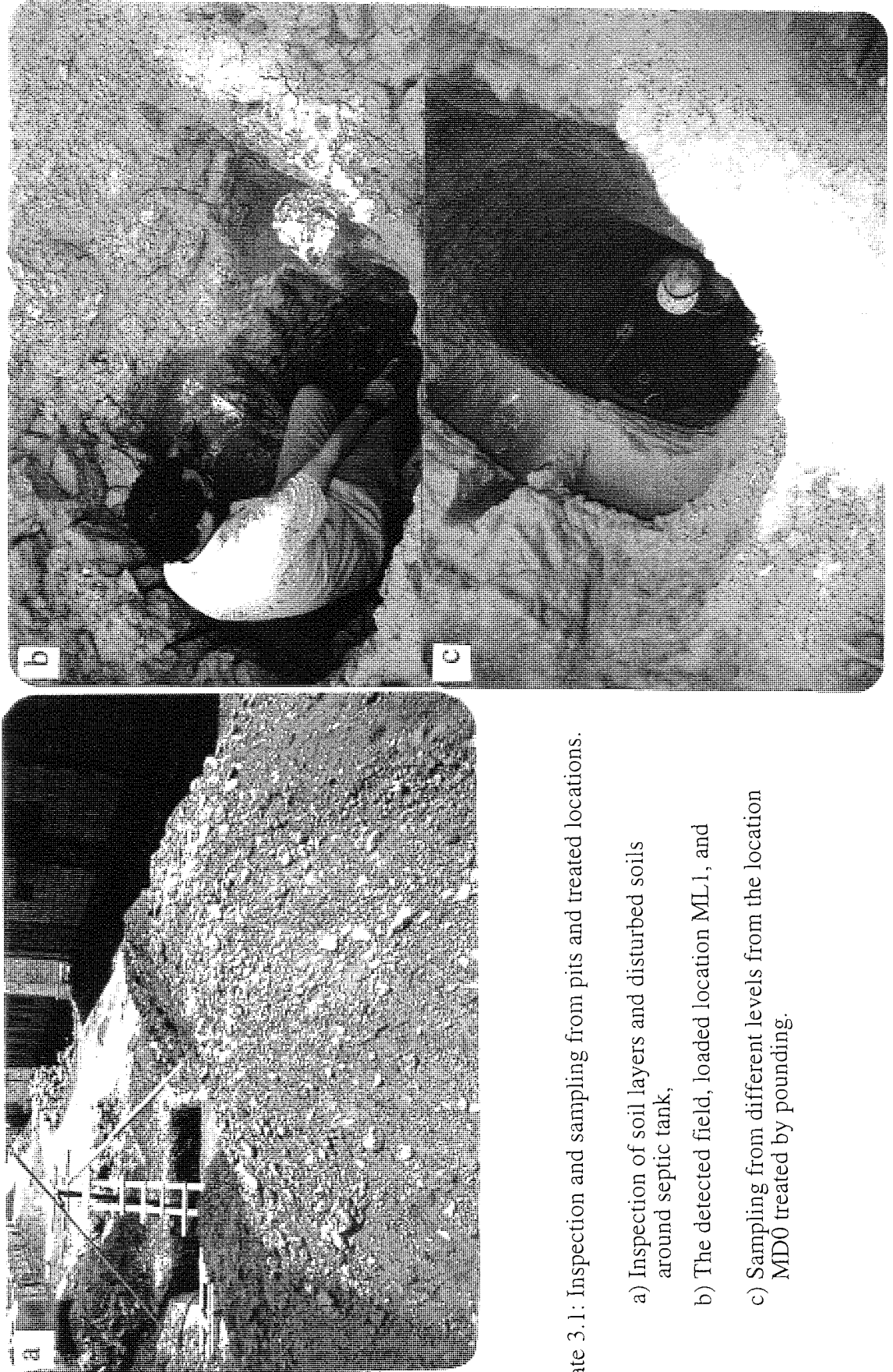
Plate 3.1: Inspection and sampling from pits and treated locations.

a) Inspection of soil layers and disturbed soils around septic tank,

b) The detected field, loaded location ML1, and

c) Sampling from different levels from the location MD0 treated by pounding.
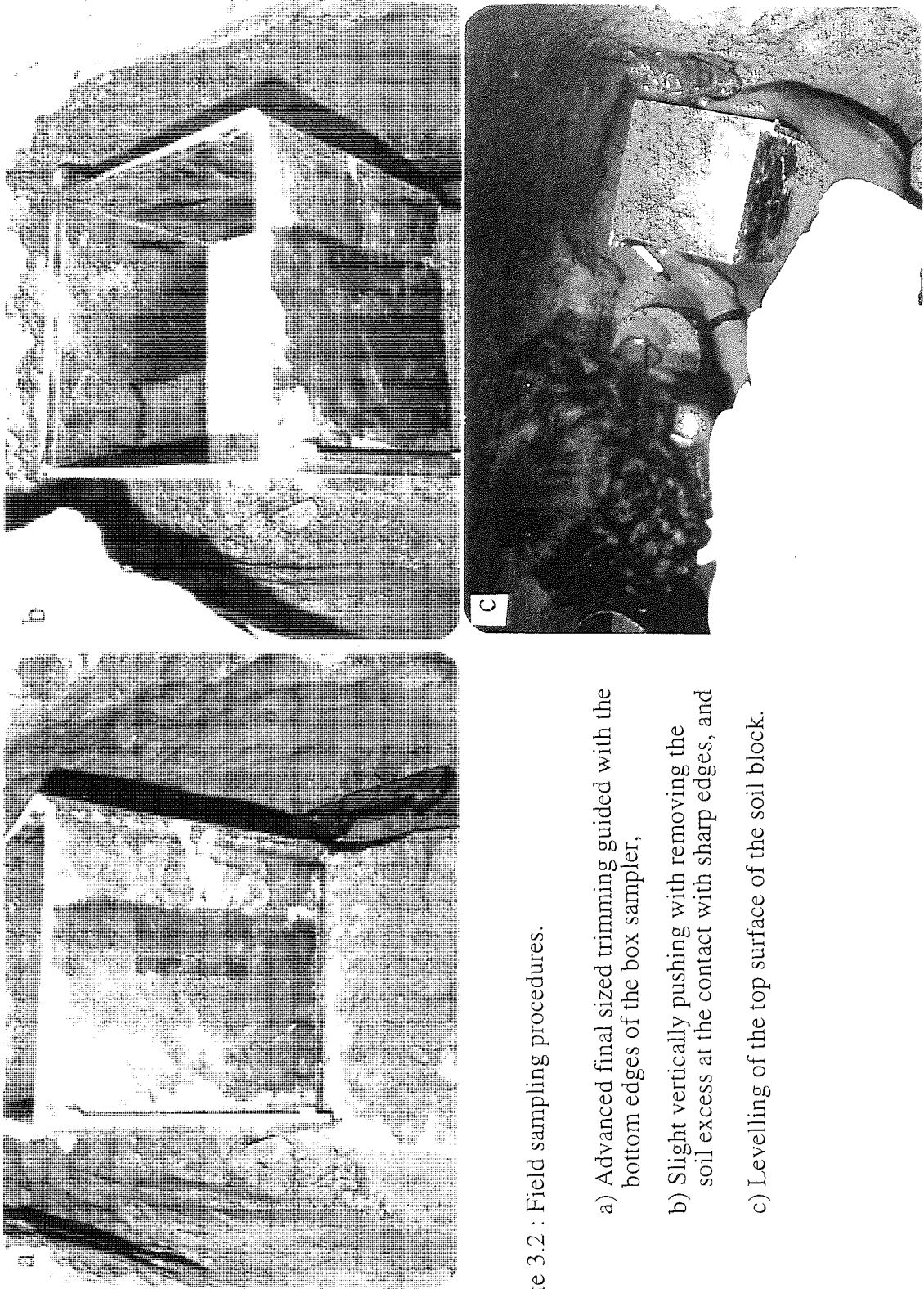
Plate 3.2 : Field sampling procedures.

a) Advanced final sized trimming guided with the bottom edges of the box sampler,

b) Slight vertically pushing with removing the soil excess at the contact with sharp edges, and

c) Levelling of the top surface of the soil block.
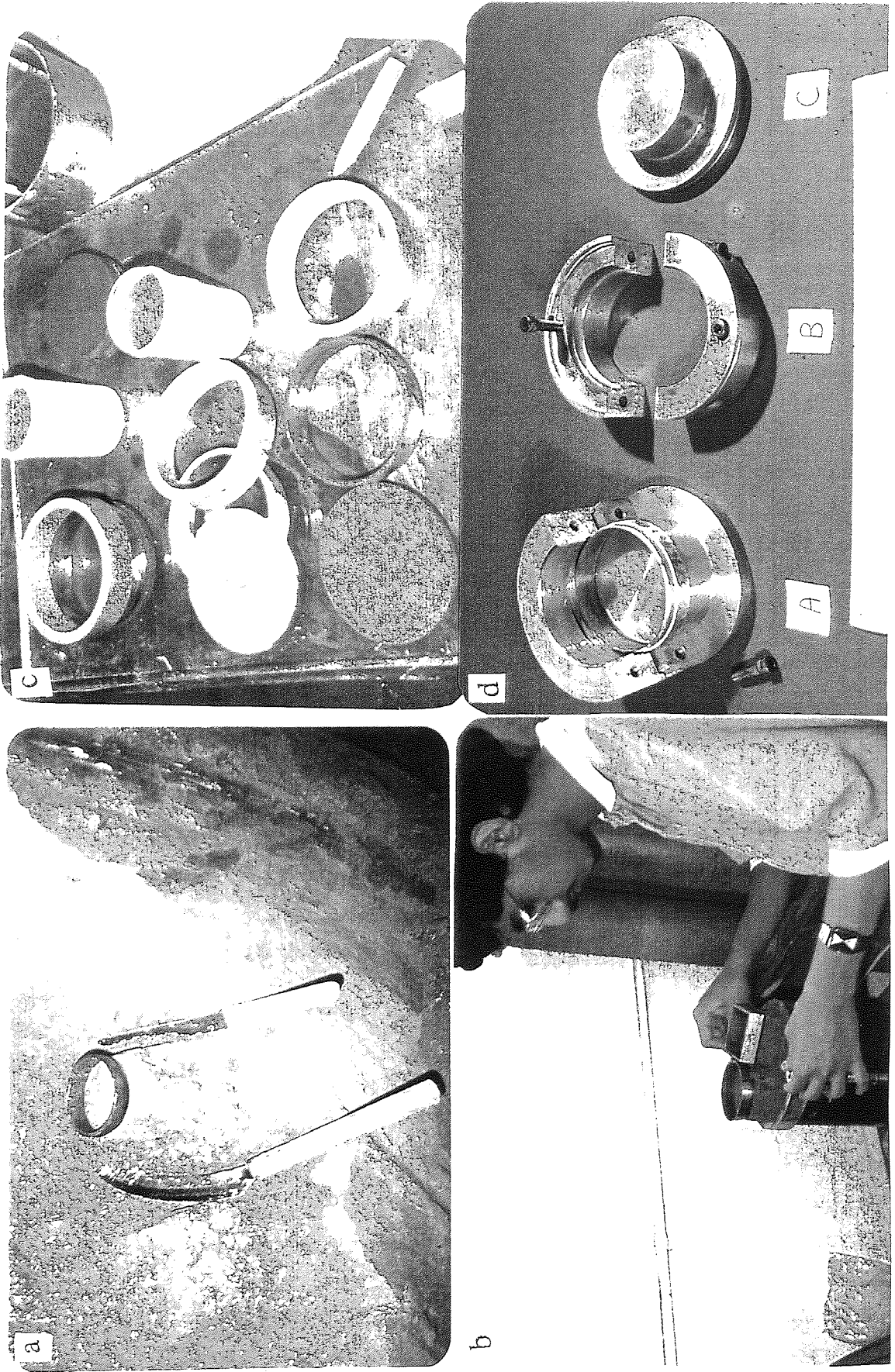
Plate 3.3 : Oedometer sampling and apparatus shown; a) Field sampling using the oedometer ring, b) Re-sampling from the block sample, c) Slurry samples preparation, and d) Manufactured mould after Booth (1975-b) used for preparing the oedometer destructured samples.

CHAPTER 4

GENERAL DESCRIPTION OF THE SOILS OF THE SANA'A AREA

4.1 SOIL FORMATION

4.1.1 Depositional Systems

The formation and deposition of soil within the study area have been markedly effected by the environmental and topographical conditions. The Sana'a area is classified as an arid to semi-arid region, where the evaporation rate is considerably in excess of that for precipitation. Mountains, which surround the study area from the west, east and partially the south, act as a barrier to the wind which blows from the north-east and north. Moreover, the steep slopes of these mountains together with the gentle slope of the plain, have had a predominant bearing on both the depositional systems and the nature of the soil formation. As a consequence of these features, the Sana'a area has been subjected to a variety of depositional systems, leading to differences in the soil formation and distribution.

At various times the Sana'a plain has been subjected to physical weathering by both alluvial and aeolian processes while chemical precipitation, as a minor weathering agent, has influenced the soil horizons both by leaching and oxidation. These systems have produced a range of soil deposits classified as water-laid, wind-laid and chemical deposits.

4.1.2 Water-laid Deposits

Within the study area these exist in the form of arid alluvial fans and Wadi deposits. Arid alluvial fans are developed as a result of the change in slope between the steep mountains and the gently sloping plain. These fans are primarily located along the western and eastern sides of the central Wadi area, near mountain bases, with some at the north (at the end of the main stream, "Al Sayelah") and south (at the bases of Al Nahdin mountains) as shown in Fig. 4.1. Such arid fans are generally subdivided into three zones: the upper-fan near the apex, the mid-fan and the lower-fan. The sediments within such fans arise from four sedimentation processes: debris flow, stream channels, sieve deposition and sheet-floods (Richard, 1983). Generally, the Sana'a Plain has been affected by all or some of these processes, depending on the flood or rainfall intensity.

For moderate rainfall with no flood, the arid fans were predominantly deposited in restricted areas at the apex between the mountains and stream channels, while no significant deposition occurred within the Wadi area. In these apices, the deposition loads were mainly boulders and coarse gravel with only limited material of sand size and they were laid down by debris flow and sieve deposition, unlike the channel deposits of gravel and sand with some graded formations. Gravel layers are typically concentrated at the base of the channels, while the formation of graded bedding with cross-stratification of sand layers with imbricated pebbles are common within the vicinity of the stream channels as shown in Plate 4.1 (Bull, 1972).

As a contrast, normal flood and normal annual rainfall conditions, commonly produced sand and silt accumulations as mid-fan deposits in the Wadi area, this being in addition to other deposits near the base of the mountains and within the channels. Extreme floods and high intensity rainfall, as recorded in 1967 and 1970 (Italconsult, 1971), produced sheet-flood deposits that extend towards the Wadi area. This deposition produces a relatively, irregular soil distribution in the vertical direction.

The floods result from high rates of precipitation occurring in the study area and/or the surrounding mountains extending in the south-east to the Khawlan Mountains producing floods along Wadi El-Ser. The resulting deposits commonly form widespread sheets of poorly sorted sand and fine gravel with some silt (Bull, 1972). These may invade the Wadi from the sides, depending on the flood source, as the floods flow smoothly across the plain towards the north as a result of the slopes of existing land forms.

The stream channels, which spread out from either the alluvial fans on the sides of the study area or the braided stream along Wadi El-Ser in the south-east, deposit sediments in the Wadi areas as a water-laid deposits. These stream channels link to form a main channel, known locally as 'Al-Sayelah', this channel having been defined by Mc Gowen and Garner (1970) as a coarse-grained meander belt. "The coarse-grained meander belt is actually somewhat of a transition between typically braided system and the classical meandering systems", (Richard, 1983). It passes through the Wadi area along the axis of the plain and extends to AR Rawdah at the northern boundary of the region. The coarse-grained meander belt displays sand and gravel with almost no mud accumulation at the southern end of the Wadi area, while sand pebbles and predominantly silt are displayed in point bars, the inside of the stream bends. Downstream from this region most of finer materials such as silt, clay and fine sand are spread out and specifically with, high floods, fines such as silt and clay are spread along the channel sides forming levees. Coarse gravel and sand with small pebbles are laid down either in the bed or the sides of the braided stream. These sediments are characterized by having smooth surfaces and being well-sorted due to the effects of long transportation. Graded bedding is common in the sand, while some imbrication may be

present in gravel as shown in Plate 4.1. Figure 4.1 shows a block diagram of the distribution of the arid alluvial fan stream and Wadi deposits while Table 4.1 summarizes the common characteristics of the water-laid deposits.

4.1.3   Wind-laid Deposits

The study area is an arid to semi arid region in which there is commonly an absence of moisture during the long period with no rainfall. Consequently there is considerable aeolian transport of sediments during these periods. These sediments are dominated by aeolian silt accumulations and evaporate deposits with some sand accumulation. These sediments consist of well sorted particles with most grains being quartz and, in some cases, even particles in the clay-size range.

The mechanism of deposition is significantly affected greatly by the topographical feature of the Sana'a area, namely a Highland Plain. As indicated earlier, the prevalent wind from the north-east and north, is faced by the mountains located to the south-east and south. These mountains present a barrier to the wind, forcing it to slow down and release its sediment load as aeolian deposits. Agha Shaher (1983) indicated that the wind deposits are mainly in the form of loess deposits, carried both from the nearby mountains and the distant deserts such as the Rub-Al-Khali (Empty Quarter) Desert. Some of the fine fraction in the water borne deposits are reworked by wind and retransported from either the bars in the channel or the downstream deposits of the floods. In contrast some loess deposits are reworked by water action or chemical decomposition to form modified loess, while true loess deposits have never been saturated (Terzaghi and Peck, 1967).

A wide spread of wind deposits is present in the Wadi area, consisting mainly of stratified loess. These deposits are of variable thicknesses with respect to the location of deposition. The intensity of the individual floods and the length of the period between successive rainfalls or floods, along with the existing slopes and man-made terraces, effect both the occurrence and thickness of these fine deposits at a given location. Wind-laid deposits, as loess, are concentrated mainly in the Wadi area, although they do exist as thin beds within, or beyond, the mountain base areas. Within the Wadi area, the loess deposits accumulate in thicker layers than the alluvial deposits, as shown in Plate 4.2, due to the long periods in which the winds have operated without interruption from water-borne deposition. Near the mountains this is reversed since only a limited amount of water is sufficient to wash the accumulated fines down to the Wadi. The recognition characteristics of the wind-borne deposits are summarized in Table 4.2.

4.1.4 Chemical Deposits

The chemical effects are restricted because of the relatively dry state of both the soil and the atmosphere for, generally, both the oxidation and leaching reactions are directly related to water availability.

Oxidation has only a minor influence on the arid fan sediments, for such minerals as calcite and iron oxide are present as precipitation products especially in the Wadi areas and the lower parts of fans (Bull, 1972). In deposits produced by high rates of rainfall or flood, oxidation is clearer in the materials near the mountain bases, particularly where terraces are available as they reduce the run-off effect and so increase the duration of the weathering processes. Oxidation of surfacial particles, such as feldspathic rock fragments, may be recognizable since such rock is easily weathered.

Leaching is clearly present in the Wadi area where it can be linked to increases in the amount of the chemical cementation agent, typically calcite. In addition leaching results in the formation of thin vertical tubes in the loess, like sink holes in fine soil. Moreover, leaching is indicated by the existence of aragonite with its needle forms, as calcium carbonate in the surface layer to a depth of 2.0m. When aragonite leaches downwards it alters to calcite having the same chemical formula with different forms, as bulky and shell forms, as shown in Fig. 4.2.

Both the leaching and oxidation processes lead to the formation of chemical deposits which act as cementation agents. These produce adhesion between the fines from the calcite precipitation, while the quartz sands are slightly cemented by the presence of hematite. Fig.4.2 indicates the chemical deposits in form of calcite, iron oxide, potassium, aluminium, etc. as indicated by Energy Despersive Spectrum (EDS), Fig. 4.2(c).

4.1.5 Soil Profile and Soil Types

The Sana'a Plain has been subjected to a variety of depositional systems leading to a considerable variation in both the soil horizons and their distribution over the Plain. Observations at more than sixty pit excavation types, hand-made, across this area have indicated the existence of seven soil types (Abduljauwad et al, 1991). A general observation is that near the mountains, the soils are gravelly with some boulders, little sand and often no fines. Moving towards the centre of the Plain the fines fraction increases with the gravelly soil decreasing until it is completely absent. Within the Wadi area, there are repetitive formations of thick, wind-laid (loess) and thinner water-laid sand as indicated in Fig.4.1 and Plate 4.2. At some locations, the depth of the aeolian deposits can be in excess of 8.0 m before the appearance of water-laid deposits, typically gravelly-sand formations. This regular

profile may be disturbed on occasions by the presence of streams or hills as well as the man-made effect (i.e. terraces, structures and other activities).

The seven soils that have been arbitrarily identified are as follows (Al-Gasous, 1988):-

1) Well to poorly graded gravel with sand 'Sayelah coarse soil'

2) Well to poorly graded sand with gravel 'Sayelah medium-coarse soil'

3) Sandy silt 'Suffrri'

4) Sandy-silty-clay with gravel 'Zanjabili'

5) Silty-clayey-sand with gravel 'Hazbah'

6) Lean clay with sand 'Kartheh'

7) Lean clay 'Merriah'

Fig. 4.3 shows the different soil profiles and soil groups at sites across the Sana'a Plain (Abduljauwad et al, 1991). The accumulations of sand and silt represent more than 60% of the total soil formations. The Wadi area is covered by most of the accumulations that are the major sources of the collapsing and subsurface settlement problems in Sana'a, and so it is convenient to study the mechanical behaviour of these particular formations to both assess the problem and provide the best reliable solution. Consequently the Wadi area was selected for this research. The description of this area, the selected sites and the soil profiles of each site are presented in the following section. The preliminary engineering properties of the selected natural soils are presented in the last section (4.3) of this Chapter, while the collapsing and deformation properties are presented in Chapter 5.

4.2 SELECTED AREA, SITES AND SOILS

4.2.1 Selected Area

The Wadi area, as a part of the Sana'a Plain, covers the middle strip of the Sana'a area, and has an average width of 3.0 Km. It extends gently from Al Nahdin in the south to AR Rawdah in the north along the Plain axis at the termini of fans as shown in Fig. 4.4. It is defined as a Wadi with no permanent channels due to the lack of water flow (Richard, 1983) and it lies at an elevation of 2230 m above sea level.

4.2.2 Selected Sites

A soil investigation of the Sana'a area was carried out by Al-Gasous (1988), this extensive field programme included subsurface exploration, sampling and in situ testing at some 42 stations. In the present study, twelve additional stations were investigated and four representative sites were chosen to study the composition and engineering behaviour of the various soils detected in the initial phase, some of which were identified as collapsing soils. In addition, based on past experience, the Wadi area contains those soils considered to be most susceptible to collapse.

In selecting sites for this study it was considered that, as well as the presence of highly collapsible soils, they also had to be located in areas that were not expected to be developed within at least one year from the start of the test programme. Ideally, there should also be variation in the soils, specifically in the sandy, silty and clayey soils, within the selected sites to ensure that a representative cover was obtained of the major fine soils present in the Sana'a Plain, including even those that do not show a tendency to collapse. From the practical standpoint it was necessary to ascertain free legal access to the sites so that trespassing would not be a problem. As it was proposed to assess the suitability of several improvement techniques, it was essential that these could be applied without causing problems to neighbouring structures. Bearing in mind all these requirements, the most convenient and appropriate sites were chosen for the field study. Four sites were finally selected to cover any unexpected variations in the soil profiles, particularly the fine soils with sand, and their locations are shown in Fig.4.4 and defined in Table 4.3. Sites I and III were investigated extensively while the other two sites II and IV were used as complementary sites. A total of 28 locations were utilised within these four sites for this research, including natural sampling (7 locations), and the following treated locations - surface compaction (5), deep compaction (6), flooding (2), preloading (6) and lime and cement stabilization (2).

Follow the standardised system produced in Chapter 3 (section 3.2.2), the four sites (I to IV), layers at each site (A1, A2, A3, etc.) and the treated locations (AC1, AD1, etc.) are all detailed in Table 4.3. Figs. 4.5 and 4.6 show the plans of sites I and III, while the plans of the other two sites are shown in Appendices B4-1 and B4-2.

4.2.3 Selected Soils

4.2.3.1 General

Detailed study of the mechanical properties of natural soils is difficult due to the wide scatter in the results caused by the normal variation in their physical properties. To minimize this effect it is, therefore, important to start with a comprehensive field investigation covering

all the Sana'a area to provide a valid representation of the natural soils, namely the 42 stations that had been extensively studied before this investigation (Al-Gasous, 1988; Abduljauwad et al, 1991). This information is summarized in following sections. Most of the fine soils exist within the Wadi area were investigated and their plasticity characteristics are plotted on the A-chart shown in Fig. 4.7. Most of these lie in the ML region and are classified as inorganic silts and very fine sands, rock flour, silty or clayey fine sands, or clayey silts with slight plasticity according to the USCS (Bowles, 1988). In fact, even those soils which lie slightly above the A-line in Fig.4.7 (with LL < 35%) were defined as silty loess and not clayey soils when using the system shown in Fig. 4.8 (Gibbs et al, 1960).

The Wadi area was selected for this study and an additional 12 stations within this area have been investigated, as a part of this research, and the same soils were identified. The four selected sites contain most of the fine soils that exist in the Sana'a Plain. Their data are also plotted in Fig. 4.7 and all are loosely classified as ML soils, although they exhibited variations in colour, structure and composition which may affect the engineering behaviour. These variations reflect the effects of the particular depositional systems and the local environment. Indeed the selection of these four sites was guided by the desire to include most of the fine soils in Sana'a and individual strata that would display these variations. Structure and composition ultimately provide clear guidance to the mechanical behaviour of these fine soils. Representative soils from these four sites were studied in detail and this information is presented in this chapter. The soil profile at each site is described briefly in the following subsections and detailed informations are given in Appendix B4-3.

4.2.3.2 Soils of Sites I and II

These two sites exhibited very similar soil profiles and Fig. 4.9 shows the bore hole plot and the Standard Penetration Test, SPT, values (Ns) for site I. A slight variation was observed with the presence of coarse gravel and sand within the deeper layer of the sandy-silty-clay being thicker at site I than at site II. In addition, there was variation between the sites in the distribution of coarse sand and gravel particles, in the form of lenses and pockets within the upper sandy silt layer. Such variation is expected with natural soils and not just between different sites but also within a given site, as was found at site I. The concentration of these pockets was greater at the location AN0 than at location AN2. Furthermore, the random distribution of gravel and sand particles in some locations - AC0 and AD2- made representative sampling very difficult to achieve. Generally, the major features at both sites are the same, apart from the above mentioned variations. The soil profile in Fig. 4.9 represents the common soil profile for both sites, with the natural moisture content, W_n, and Ns values being the average values for site I data, although this data is also representative of the soils at site II. The SPT spoon sampler was driven 45 cm in three equal sets each 15 cm. The blows of the first set were excluded to minimize the possible disturbance of the soil

caused by the auger, while the blows of the last two sets (30 cm) added together to give the Ns values , as shown in Fig. 4.9. On this soil profile, four soil horizons are shown and the grading for these four soils are shown in Figure 4.10. The description of these layers is given in Appendix B4-3 and they are classed as follows:-

A0)   The top dark stiff fissured lean clay 'Merriah'

A1)   Medium to stiff reddish to light brown sandy silt 'Suffrri'

A2)   Soft to medium brown silt with sand 'Suffrri'

A3)   Medium to stiff, light to reddish brown sandy silt to sandy silt with gravel 'Zanjabili'

4.2.3.3   Soil of Site III

This site, and site I, cover most of the soil variations that it was desirable to investigate, and so has also been investigated in detail. The gradation curves of the site III soils are shown in Fig. 4.11 while Fig. 4.12(a) indicates the soil profile of this site consisted of five layers to 6.0m below the ground surface. These layers are described briefly in Appendix B4-3, with a concentration on the variations as compared with the soils at site I. These layers are classed as follows:-

M0)   Stiff brown to mixed material fill

M1)   Medium to stiff light brown sandy silt 'Suffrri'

M2)   Soft to medium dark grey to blackish brown silty soil 'Soft Carab'

M3)   Stiff to very stiff greenish to yellowish sandy silt 'Stiff Carab'

M4)   Medium to stiff, light to reddish brown sandy silt to sandy silt with gravel 'Zanjabili'

The soils M2 and M3, known locally by Soft and Stiff Carab respectively, were not among those seven soil units identified in the previous investigation (Al-Gasous, 1988).

4.2.3.4 Soil of Site IV

The soil profile of this site is shown in Fig. 4.12(b), and consists of four main layers to 6.0m below the ground surface. The general features of these soils have already been presented and so only general remarks will be presented on each layer. The top layer, K0, is a stiff, dark, lean clay similar to A0 and with a thickness of 0.6 to 0.7m. The second layer, K1, was located 0.7 below the surface with a thickness of 1.7 to 1.8m and is a light brown,

sandy silty clay of medium stiffness similar to M1 and A1. Its gradation (clay 12%, silt 41% and sand 34%) is between that of these two layers with a larger gravel content (13%). The third layer, K2, is medium to stiff, light to reddish brown, sandy silt clay with gravel, 'Zanjabili'. It resembles A3 and M4 with two minor variations, namely its depth and higher gravel content. It was found at 2.5 to 2.7m below the surface, extending down to 5.0 to 5.3m. The existence of a soft layer was not found at this site as shown in Fig. 4.12(b). Its high gravel content resulted in high SPT values, ranging from 20 to 30 blows as shown in Fig.4.12(b). The last layer in this profile, K3, was a sand-gravel with a clay and silt matrix, although boulders were also observed in this layer. These coarse particles -sand, gravel or boulders- are similar to those of the other water-laid deposits. The gradation curve of this layer together with those of the soils A3, M4 and K2 are shown in Fig. 4.13. The Ns values for this layer are again high, 42 to 63, as shown in Fig. 4.12(b).

4.3 SOIL ENGINEERING AND SOIL PROPERTIES

The engineering properties including the physical, chemical, and mineralogical are presented in this section.

4.3.1 Soil Engineering

4.3.1.1 Physical Properties

Natural Dry Density (ρ_d):   The in situ dry density of the selected soils were determined four times using the cutter core method. The undisturbed samples for the triaxial, oedometer and direct shear tests were also used to determine the in situ dry density and all these results are summarised in Table 4.4. The dry density values for all fine soils ranged from 1.10 to 1.45 Mg/m^3. Generally these are considered to be very low values, but are typical for the fine soils found in the Sana'a Plain. They are close to the lower limit for loess soils as identified by Clevenger, 1956 (Chapter 2). Similar values have also been reported by Zur and Wiseman (1973) and Al-Alfi (1984) for the collapsing soil, and by Bressani (1990) and Maccarini (1987) for tropical residual soil. These low dry densities make the soil undesirable for foundation engineering and, without further investigation, it would certainly be suspect and would probably require treatment before being used in an engineering project. However, by investigating such highly porous soils it may be possible to provide a better understanding of the collapsing and destructuring phenomena in denser soils, and so identify possible techniques for improving such unstable soils.

The lowest average dry density of 1.10 Mg/m^3 in Table 4.4, obtained for A2 and M2 soils, is below the limit, 1.12 Mg/m^3 suggested by Clevenger and is equivalent to a void ratio (e_o) of 1.54. This void ratio indicates a very loose state, much looser than a loosely packed material. Local assemblages of particles in the soil might be much denser but, due to large voids between such densified areas, a honeycombed fabric (Casagrande,1932; Mitchell, 1976) is formed producing a lower dry density. This is characteristic of a collapsing soil where the soil particles are bonded and so initially stronger than a non-collapsing soil of similar properties. With the selected soils most of these voids are due to the nature of the formation process, subsequent leaching processes and the decay of roots or the action of termites.

Natural Water Content (W_n): The natural water contents were determined and the average values are given in Table 4.5, together with the maximum and minimum values that possibly occurred during the wet and dry seasons between 1986 and 1990. Values up to 13 % (all soils except; A2, M1, M2 and M4) are very close to those typically reported for loessial soils, and are normal for the arid climate and region. A minimum value of 4 % is expected for surfacial soils at an excavation left open for few days in the dry season. However, this value can fluctuate between 6% to 28% for these soils within a relatively short period of time and it must be recognized that this fluctuation could influence soil properties and behaviour. Soils A2 and M2 had higher average moisture contents, primarily due to their higher clay contents, while M3 had a lower moisture content, due to its higher sand content and the discontinuous pore system of tubes, despite its relatively high clay content, 21%. Generally, the lower the moisture content, the higher the collapsing potential.

Atterberg Limits: The standard procedures were used to determine the liquid limit and plastic limit and the average values, together with the plasticity index, are given in Table 4.5. The liquid limit values ranged from 26 to 46% with the plasticity index ranging from 2 to 19%, the higher values being associated with the more clayey soils. The activity index, A, for each soil, is also shown in the Table 4.5. When these values are compared with the criteria developed by Gillott (1987), the fine soils are classified as inactive to normal soil. Soils, having A values less than 0.75, are inactive and so their clay contents do not significantly influence their behaviour. In contrast, those soils which have higher values between 0.75 and 1.25, are normally active and so are significantly affected by their clay contents. Lutengger and Hallberg (1988) have reported that loess deposits in Iowa with clay contents between 16 and 32%, had an activity ratio about 1.33.

Specific Gravity (G_s): The average values of the specific gravity for the soil solids varied between 2.75 and 2.80 as indicated in Table 4.5. These are slightly higher than values associated with sandy silt and silty clay soils which range of 2.65 and 2.7. The specific

gravity of the soil depends on the predominant soil minerals, and this will be considered in section 4.3.4 with the mineralogy.

4.3.1.2 Soil Classification

The soils in the Sana'a Plain were classified according to USCS and AASHTO after Wray (1986). The soils were classified as ML to CL-M as the main groups, according to USCS, and as A-4, with group indices of 3 to 12, and A-7-6, with group indices of 13 to 20, according to AASHTO and these are summarized in Table 4.6. An exception was the top part of A1 which was classified as SM and A-2(0) according to these systems. According to AASHTO all the selected soils are considered to be silty to clayey material with the exception of the top of A1 which is termed as a silty gravel and sand. Generally, all the soils having liquid limits below 35% are identified as inorganic silt of low to medium compressibility or silty loess, while those having liquid limit above 35%, A2 and M2, are identified as inorganic clay soils with medium plasticity or clayey loess.

Similar identification of the silty and clayey loess soils have been reported by Gibbs et al (1960) which coincide with the AASHTO classifications given in Table 4.6 (A2, M2). For the selected soils, the slight difference in soil texture between aeolian silty and clayey loesses resulted in shifting of the soil from CL to ML and this is primarily attributed to differences in the climatic and depositional systems. The migration of clay particles from the upper to the lower horizons due to leaching, is an example of such effect and so a clayey loess in the upper horizon may become a silty loess and a silty loess in a lower horizon may ultimately become a clayey loess.

Despite the narrow ranges covered by the soil texture and the index properties, the selected soils exhibited a considerable variation in the consistency from soft (A2, M2) to very stiff (M3) and, as a consequence, variations in bond strength, soil structure and soil composition can be expected from soils in the same classification group (A1, M1 and M3). Thus all the selected soils were subjected to further investigation, to assess such differences so as to produce valued conclusions with respect to the behaviour of these soils.

4.3.2 Compaction Characteristics

The compaction characteristics for selected soils, according to the BS 1377:1975 and ASTM -D698, are summarized in Table 4.7 and representative compaction curves are shown in Appendix B4-4. The maximum dry densities (ρ_d) ranged from 1.51 to 1.62 Mg/m^3, while the optimum moisture contents ranged from 18% to 28%. The Relative Increase of the maximum dry density over the natural dry density (RI) was between 19% to 47% as shown in Table 4.7, and this indicates how poorly structured are the selected soils in their natural

conditions. The natural moisture content was lower than the optimum moisture content for each soil. Both A2 and M2 exhibited a better response to compaction, or a larger increase in dry density, than the other soils, and this may due to their lower natural dry densities. Further increases in dry density could have been expected by increasing the compactive effort but, at this stage, only standard compaction was used on soils. Clevenger (1956) and Sheeler (1968) reported that for loess soils the standard Proctor maximum densities vary from about 1.68 to 1.77 Mg/m^3 (105 to 110pcf). Loess soils with natural dry densities above 1.44 Mg/m^3 (90pcf) have fairly high shear resistance and settle only a relatively small amount. All the studied soils have natural dry densities below 1.44 Mg/m^3, apart from was the sandy silt, M3 having ρ_d = 1.45 Mg/m^3. When these soils were compacted in the laboratory the values of the ρ_d, 1.51 to 1.62 Mg/m^3, exceeded 1.44 Mg/m^3 (Table 4.7), but they did not reach the high values reported by Clevenger (1956) and Sheeler (1968). This indicates the scope for field treatment to further improve the soil performance.

4.3.3 Soil Chemistry

General chemical analysis has been carried out by Al-Gasous (1988) on the soils of the Sana'a Plain. In the present investigation this was undertaken using the Energy Disperesive Spectrum (EDS), attached to the Scanning Electronic Microscope (SEM). These results did not demonstrate any significant differences from the findings of the previous study and so the chemical properties of the fine soils are only summarised in this section.

The representative EDS plots presented in this Chapter show the patterns of the most common elements, Al, Ca, Fe, K, etc. within the fine soils. The different minerals detected by SEM that contain these elements are shown in the same Figures, i.e. Fig. 4.2. The height of the peaks in the EDS patterns indicates the element concentration with respect to other elements present in the same SEM image. Generally, there was a high concentration of calcium (Ca) in most of the fine samples. A second concentration was iron (Fe) although it was less than that of the calcium. Potassium (K), titanium (Ti), manganese (Mn) were also found and Table 4.8 summarises these concentrations for soils subjected to EDS. These EDS exposures were carefully chosen to reflect the most common concentrations, both overall in the soil structure and at the particle contacts.

The chemical composition of the fine soils were detected in the earlier study (Al-Gasous, 1988) using X-ray fluorescence and the results are given in Table 4.9. The general features of the element content (Table 4. 8) and the element oxide content (Table 4.9) are very similar demonstrating the reliability of the data. Comparing the chemical composition of these fine soils with the average chemical composition of the earth's crust, after Beer (1964), the following conclusions may be drawn:

- All the soils have high calcium oxide content (17%-31%) with respect to that of the typical soils (5.1%), which indicates the presence of calcium carbonate, calcite or aragonite.

- The soils contain higher values of Fe_2O_3 (6.6% - 22.7%) than the natural values (3.7%), while higher values, up to 38% of the total elemental concentrations, were detected by EDS as indicated in Table 4.8. High stability of soil aggregates and high soil porosity are usually associated with such high iron oxide contents (Bear, 1964), the iron oxide having been inherited from the parent rock.

- All the soils exhibited high values of TiO_2, averaging 4%, than is typical in soils (1%).

- Finally, all the other elements and oxides of the soils are in the expected range.

The earlier wet chemical analysis (Al-Gasous, 1988) indicated that the cation exchange capacity of the fine soils was in the range of 13 to 15 milliequivalents per 100 grams of soil. The organic matter of the soils was very low, and so the inorganic clay minerals may be considered the primary seat of cation exchange. The pH of the soils were in the range of 8.1 to 8.5 , indicating medium alkalinty. It is believed that these high values of the pH are related to the high calcium contents and lead to high values of both the cation exchange capacity and specific gravity. The maximum sulphate content of the fine soils was expressed as 18 parts of SO_3 per 10^{-5} of a 1:2 water : soil extraction. This value is less than 30 SO_3 parts per 10^{-5}, after Tomlinson (1980), and so normal portland cement, type I, could be considered for foundation construction in these soils.

4.3.4 Mineralogical Composition

The mineralogy of the soils in the Sana'a Plain were investigated by Al-Gasous (1988) using X-ray diffraction analysis for both the non-clay and clay minerals. This work has been discussed in detail elsewhere (Al-Gasous, 1988) and Table 4.10 summarises the quantitative analysis for soils from sites I and IV.

The data indicate that the predominant non-clay minerals were quartz, calcite, aragonite and albite. Augite and maghemite, as iron compounds were only found at low concentrations. The predominant clay mineral was kaolinite and there was no evidence of the presence of montmorillonite. The existence of both quartz and calcite were also detected in the clay fraction. Kaolinite is a very common clay mineral with strong bonding so it does not show swelling. Quartz is a highly stable mineral so it is able to exist in the clay fraction size. "Quartz is common in the clay size grade and is sometimes fine enough to have colloidal particles" (Gillott, 1987). The widespread limestone formations in the northern parts of Sana'a are a rich source for calcium carbonate which, as calcite, has an essential role in soil

formation, and cementation. In addition, the calcite is soluble in water, and so it contributes to the collapsing of loess soils. Chemically calcite is the same as aragonite, and so the X-ray data for calcite could refer to either, although aragonite exists primarily within the surfacial soils, top horizon, and dissolves faster than calcite.

4.3.5 Scanning Electron Microscopic Study of the Natural Soils

4.3.5.1 General

Extensive electron microscopic studies were carried out on soils from sites I, II and III, to investigate the nature of the soil structure and its possible effects on the collapsing and destructuring phenomena. This technique uniquely provides information about the metastable structure and the type and intensity of the interparticle bonding forces. An understanding of the variations in the consistency of the selected soils (soft to stiff) may also be provided by studying these phenomena. Numerous photomicrographs were taken to describe the forms of the soil structure for the natural soils, the field destructured soils and the laboratory destructured samples. Those related to the natural undisturbed soils are considered in this section, while the others will be considered in the appropriate Chapters.

4.3.5.2 The Fabric of the Natural Soils

In this thesis fabric refers to the physical arrangement of particles, particle groups and pore spaces, while structure is taken to cover both the fabric and the associated interparticle forces (Leroueil and Vaughan, 1990). Microstructure is often used to show the effect of interparticle forces as well as fabric on soil properties. The soil fabric, as a key component of the soil structure, can decisively effect the engineering properties of some soil such as sensitive clays and loess soils. The primary form of the fabric develops at deposition time, while the secondary fabric can develop subsequently due to such effects as deformation, consolidation and shear, crystal growth, moisture movements.

One of the earliest descriptions of the fabric of loess soils was given by Terzaghi (1925) who suggested that some soils were composed of individual grains of silt and flocculated clay arranged in an arch skeleton enclosing large voids, and this was termed honeycombed by Casagrande (1932). Lambe and Martin (1953) predicted the parallel type of arrangement of clay particles of fresh water deposits. In recent work it has been suggested that clay minerals are more often deposited as aggregates than as single crystals (Gillott, 1987). The microstructure of the selected soils can be described in terms of the arrangements depicted in Fig. 2.7. These identify elementary particles, particle assemblages and pore spaces within the soil matrix.

Figs. 4.14-4.17 are micrographs, taken at magnifications ranging from 10.8X to 335X, of several undisturbed soils. The Energy Dispersive Spectrum (EDS) of each soil is included on the appropriate Figure to indicate the available elements within the soil, and the Figures indicate various structural arrangements. The disperse phase of the soil is granular of sand-silt size particles with moderate to numerous chemical precipitations. The microstructure is characterized as very open with large cavities and channels which reached 2.0mm in diameter, and they can be seen with naked eye and on micrographs at low magnifications. Additional pores were found within the agglomerations and between the individual particles and agglomerations. These high pore contents give the spongy form of these soils as shown by the (a) Figures, and the accompanying low dry densities are related to the presence of these pores. Figure 4.14(b) shows the highly granular appearance of the sandy silt (A1), while a less marked appearance for the sandy silt (M3) is shown in 4.17(c). They do not show the spongy appearance of the silt with sand (A2) and the silt to silty clay (M2) shown in Figs. 4.15(b) and 4.16(b) respectively.

The variation in appearance is related to differences in the grain sizes and cementation. The EDS Figures show the existence of two binders, calcium carbonate and iron oxides. Soils with open fabrics and particle cementation, particularly when accompanied by high silt and low clay contents, are the classical conditions for metastable structures that collapse easily upon wetting. Stronger bonds produce more stable soils which have higher resistance to collapsing or destructuring. Bonding can be produced by several phenomena such as flocculated clay buttresses, capillary forces, chemical precipitation, clay bridges and particle coating by clay interaction and the resulting particle arrangements and assemblages shown in Fig. 2.7. The structure of the selected soils has been established by using SEM. The photomicrographs are provided in Appendices B4-5 to B4-7, and the main features are described in the following paragraphs.

Figs. 4.14(a,b) and B4-5 show the pores and open fabric of A1, typical of sandy silts including M1 and M3. The sand- silt grains are sub-rounded to sub-angular, with some silt grains of angular type and irregular shaped, coated by the clay. This clay coating was found in all the detected soils in this section, although it was not continuous and the thickness varied. Detailed study of the micrographs shows the sand and silt grains were separated by clay and silt particles, or clay and silt assemblages, so limiting the grain to grain contacts and leading to large void formations. This arrangement is the clothed particle interaction shown in Fig. 2.7-c. Both the sandy silts from 1.2m, A1 and M1, and 1.8m, A1, (B4-5 (a) and (b)) exhibited a high to moderate open fabric as shown in Fig.4.14(b) and B4-5. The sandy silt, M3, has many pores due to the discontinuous thin roots or channels and fewer pores in the form of micropores as shown in Fig. 4.17(a-c). This localization of pores as channels and the high clay and cementation content gave this soil the characteristics of a limited open fabric with highly clothed grain interaction.

In addition to the high clay and silt contents and the high contents of calcium carbonate and iron oxide of the silty soil with sand, A2 and the silty/clayey soil, M2, they had higher void ratios than the other soils. At low magnification, these soils showed edge to edge assemblages formed by silt and clay aggregations. Within and between these assemblages, trapped pores were found as shown in Figs. 4.15(c) and 4.16(b). The micropores and high chemical precipitation of these soils are shown in Appendix B4-6 at a higher magnification. Generally, these two soils had fewer channels but relatively more pore space within the soil matrix than M3. The trapped, pore spaces and associated assemblages with high fines and colloidal contents and cementation, of soils A2 and M2 gave them their spongy form as a primary feature.

The variation in structure can be related to the differing bonding mechanisms and connectors. In the open granular coated fabric, the connectors were limited in some of the sandy silt soils (A1, K1 and M1), but in others, M3 and K2 they were widely distributed and even coated the granular domain with cementation agents and clay particles as shown in Fig. 4.18, the accompanying EDS graph indicates a high concentration of calcite at the connectors. The assemblages within the silt with sand soil, A2, and the silty soil, M2, were connected in an interweaving bunches of clay and calcium carbonate, aragonite, with silt inclusions (Collins and McGown, 1974) as shown in B4-7.

At higher magnifications an open fabric, or honeycomb structure (Cassagrande, 1932), can be seen in Fig. 4.19(a), this being the predominant form of metastable fabric. Clay precipitation provides the connectors between sand, silt and clay assemblages, with the particles and assemblages being sustained by calcite, iron oxide and aggregated clay bonds. The soils of the upper horizon, A1, M1 and K1, exhibited a very porous and honeycomb structure which was less apparent in A2 and M2 and not present in M3. Saturation collapses the structure at the coated granular interaction as the grains slide over one another, moving into vacant spaces with the clay coating acting as a lubrication agent to reduce the grain to grain friction.

Another open fabric can be described in which the silt and sand grains are kept in position, without grain to grain contact, by supports or bridges as shown in Fig.4. 19(b). These bridges consist primarily of clay with significant amounts of calcium carbonate and iron oxide. The thickness and development of these bridges differed between the soils and even samples of the same soil. Upon wetting, the weakening of these bridges governs the collapse of the structure. Clay precipitation was seen to buttress the cusps of quartz grains, again this flocculated clay was found to be rich in calcite, the predominate cementing agent within loess soils. Such aggregation appears to wedge the quartz grains apart and have only been observed in the loess (Derbyshire and Mellors, 1988). On wetting collapse occurs both in the

cusp buttresses and the flocculated microstructure. The dissolution of the cementating agents also contributes to this collapse but at a slower rate than that due to grain sliding.

4.3.5.3 Depositional Effects on Soil Fabric

Soil fabric is influenced by the depositional processes and environmental conditions. The soil formations of Sana'a Plain have yet to be classified with respect to the effect of the depositional and environmental conditions but the general features of the selected soils are considered in detail in Appendix B4-8. The consequences of weathering can be identified by studying the chemical and mineral composition, the textural features and fabric of the soil and, based on these criteria, loess soil can be classified. Buraczynski (1988) adopted four basic groups for this lithological description of loess as shown in Table 4.11, and both this system and the description provided by Derbyshire and Mellors (1988), in Appendix B4-8, have been used to classify the selected soils. Table 4.12 summarizes the general structural and weathering features of the different soils.

Table 4.1 : Typical characteristics of Water-laid Deposits in Sana'a Plain.*

a) Great variation in bulky forms due to variation in the period of transport.

b) Sharp upward decrease in grain size (in case of graded bedding structure).

c) Common presence of imbricated pebbles and sand cross-stratification.

d) Commonly calcite - cemented, or locally cemented by gypsum or anhydrate.

e) Many grains coated with hematite.

f) Common presence of different coloured particles due to variation in their parent rocks.

g) Conglomerates may be common, and sometimes with several cycles of deposition that lack a sand-size fraction at the top of the cycles (deflation of the sand and silt).

h) Presence of mud-flow conglomerates.

i) Clayey deposits are commonly stiff with no vertical holes and so have low permeability.

* Plate 4.1 shows some examples of the Water-laid deposits within the study area.

Table 4. 2 : Recognition of Wind-laid Deposits as Aeolian soils.

a) Relative overall homogeneity of the sediment within the deposited layer, with particles generally being uniformly sorted.

b) Most grains are quartz, consisting of silt and silt-size particles with a poorly graded distribution.

c) Fine sand and clay particles are present.

d) Cementation between the silt-size particles is dependent on either the clay coating over these particles or the precipitation of chemicals leached by rain water.

e) The material is slightly or moderatly plastic.

f) The permeability in the vertical direction is greater than in its horizontal direction due to the presence of long vertical tubes in the soil fabric, of the loess.

Table 4.3 : Description and definitions of the different sites, layers and treated locations.

#	Site — Position, [Area]	Layers — Detected #	Layers — Symbol	Detected #	Detected Symbol	$Z1^*$ (m)	Location — Status of location
I	Allaw Al-Kohali land in the diplomatic area, in front of Al-Rodhi land [1800 m²]	4	A0	8	AN0	-	Natural, natural sampling for lab programme in Sana'a
					AN2	-	Natural, natural sampling for lab programme in Aston
			A1		AC0	0.6	Treated by Roller Compaction at natural moisture content
					AC1	1.0	Treated by Roller Compaction with pre-flood for one day
			A2		AC2	0.6	Treated by Roller Compaction with pre-flood for five days
					AD0	0.0	Treated by Deep Compaction at natural moisture content
			A3		AD1	0.6	Treated by Deep Compaction with pre-flood for one day
					AD2	0.6	Treated by Deep Compaction with pre-flood for five days
II	Ahmad Al Kasos land in the diplomatic area in front of Al-Kuwait Embassy [600 m²]	2	G1	4	GN	0.0	Natural, natural sampling for lab programme in Sana'a
					GL1	1.2	Field loading with 50, 100 and 150 kPa at in-situ moisture content, then flooding with water
			G2		GL2	1.2	Field loading with 50 and 100 kPa at insitu moisture content, followed by flooding and then loading up to 150 kPa
					GL3	1.5	Flooding for 5 days and then loading with 50, 100 up to 150 kPa

O.G.S. ⌐ removed ⌐ Z1 : Depth to the removed soil before treatment

* Z1 : Depth to the removed soil before treatment

(Table 4.3 : Continued.)

#	Site Position, [Area]	Layers Detected #	Layers Symbol	Detected #	Symbol	Z1* (m)	Location — Status of location
			M0		MN0	-	Natural, natural sampling for lab programme in Sana'a
					MN2	-	Natural, natural sampling for lab programme in Aston
			M1		MC1	0.6	Treated by Roller Compaction with pre-flood for one day
					MC2	0.6	Treated by Roller Compaction with pre-flood for three days
III	Mohamed Abdulrab land in the diplomatic area, in front of Abu- Baker Mosque, [2300 m²]	5	M2	13	MD0	0.34	Treated by Deep Compaction at natural moisture content
					MD1	0.34	Treated by Deep Compaction with pre-flood for one day
					MD2	0.34	Treated by Deep Compaction with pre-flood for five days
			M3		ML1	0.8	Field loading with 50, 100 and 150 kPa at in-situ moisture content, then flooding with water
					ML2	0.8	Field loading with 50 and 100 kPa at insitu moisture content, followed by flooding and then loading up to 150 kPa
					ML3	0.8	Flooding for 5 days and then loading with 50, 100 up to 150 kPa
			M4		MSC	0.4	Stablization by Cement/Water slurry with no pressure
					MSL	0.4	Stablization by Lime/Water slurry with no pressure
					MF	0.6	Flooding with water for 50 days, 0.8 m³/day
IV	Khamthan Al Kohali land on the 30 th Street, near Bn -Majed School, [600 m²]	3	K0	3	KN0	-	Natural, natural sampling for lab programme in Sana'a
			K1		N0°	-	Natural, natural sampling for previous work in Sana'a
			K2		KF	0.9	Flooding with water for 42 days, 0.8 m³/day

Table 4. 4 : Variation in dry density, ρ_d

Soil	Depth m	W_n %	CutterMethod Samples #	ρ_d min	ρ_d max	ρ_d ave	Triaxial Samples @ #	ρ_d min	ρ_d max	ρ_d ave	Oedometer and Direct[@] Shear Samples #	ρ_d min	ρ_d max	ρ_d ave	$\rho_{d_{ave}}$ * Mg/m³
A1	1.0	14	2	1.19	1.20	1.20					7	1.10	1.25	1.24	1.22
	1.8						6	1.24	1.29	1.27					
	2.2	10	4	1.19	1.29	1.24					13	1.22	1.29	1.26	1.25
A2	3.0	18	4	1.09	1.11	1.10	10	1.08	1.14	1.11	12	1.07	1.13	1.10	1.10
A3	4.5	16	2	1.22	1.30	1.26	-	-	-	-					1.26
G1	1.5	12	2	1.24	1.26	1.25	-	-	-	-	8	1.23	1.26	1.24	1.23
	2.3	11	2	1.18	1.20	1.19					8	1.19	1.22	1.21	
M1	1.0	16	3	1.23	1.25	1.24	-	-	-	-	7	1.25	1.30	1.27	1.24
M2	2.2	25	3	1.10	1.11	1.10	9	1.05	1.14	1.09	12	1.06	1.12	1.09	1.10
M3	2.8	11	2	1.44	1.47	1.46	7	1.43	1.46	1.45	9	1.43	1.51	1.45	1.45
M4	4.0	16	3	1.22	1.26	1.24	-	-	-	-	12	1.21	1.27	1.24	1.24
K1	1.2	13	2	1.25	1.27	1.26	-	-	-	-	5	1.21	1.34	1.27	1.26
	2.8	14	2	1.26	1.28	1.27	-	-	-	-	5	1.20	1.31	1.26	
K2	3.5	18	1	1.29		1.29	-	-	-	-	5	1.20	1.32	1.26	1.28
Total Number of Samples			32				32				103				

@ The strength results of both triaxial and direct shear tests are not presented in this work.

* 1.0 gm/cm³ = 9.807 kN/m³ = 62.4 lb/c ft

Table 4.5 : Index properties, and the variation in moisture content and
specific gravity of the representative studied soils.

Soil layer	Depth (m)	Moisture content (%)			Spcific gravity			Index property (%)			Clay %	Activity (A)
		min	max	ave	min	max	ave	LL	PL	PI		
A1	1.2	8	1 6	12	2.79	2.81	2.8	29	27	2	6	0.33
	2.2	8	1 4	10	2.78	2.8	2.79	33	28	5	15	0.33
A2	3.0	13	26	17	2.78	2.82	2.80	43	27	16	19	0.84
A3	4.0	12	20	15	2.75	2.75	2.75	30	27	3	17	0.176
M1	1.0	12	20	16	2.78	2.8	2.79	35	25	10	16	0.625
M2	2.2	16	28	25	2.76	2.8	2.79	46	27	19	24	0.80
M3	3.0	7	15	12	2.74	2.77	2.75	35	25	10	21	0.48
M4	4.0	14	21	17	2.79	2.8	2.79	35	27	8	6	1.33
K1	1.5	10	16	13	2.75	2.76	2.75	26	18	8	12	0.66
K2	3.5	10	18	14	2.74	2.76	2.75	35	20	15	17	0.88

Table 4.6 : Summary of the classification results of the different selected soils.

Soil layer	Depth (m)	Average thickness (m)	Soil texture Gravel %	Sand %	Silt %	Clay %	W_n %	LL %	PI %	USCS Group symbol	Group name	AASHTO
A1	1.2	2.0	4	70	20	6	12	29	2	SM	Silty sand	A-2(0)
	1.8		7	43	42	8	10	33	5	ML	Sandy silt	A-4(1)
A2	3.0	0.7	2	21	58	19	18	43	16	ML @	Silt with sand	A-7-6(13)
A3	3.8	>2.5	6	23	54	17*	15	30	3	ML	Sandy silt to sandy silt with gravel	A-4(3)
M1	1.0	0.9	6	20	58	16	16	35	10	ML	Sandy silt	A-4(7)
M2	2.2	1.4	0	10	66	24	25	46	19	ML @	Silt	A-7-6(20)
M3	3.0	0.6	7	29	43	21	12	35	10	ML	Sandy silt	A-4(12)
M4	3.9	2.2	4	34	56	6*	17	35	8	ML	Sandy silt to sandy silt with gravel	A-4(5)
K1	1.5	2.0	13	34	41	12	15	26	8	CL-M	Sandy silty clay	A-4(3)
K2	3.5	2.3	17	28	38	17	12	35	15	CL-M	Sandy silty clay with gravel	A-4(4)

* The variation in the gradation of these layers is expected due to the variation of the gravel concentration within the same layer.
@ These two soils according to Gibbs and et al., 1960 can be classified as clayey loess which coincide with AASHTO classification.

Table 4.7 : Summary of the compaction characteristics of the different soils.

Site and soil position			W_n	ρ_d	W_{opt}	$\rho_{d_{max}}$	G_s	S_o	S_{opt}	RI*
Site	Soil	Depth m	%	Mg/m^3	%	Mg/m^3		%	%	%
I	A1	1.2	10	1.24	21	1.57	2.8	31	75	27
	A2	3.0	18	1.1	23	1.62	2.79	33	89	47
III	M1	1.1	16	1.24	18	1.53	2.79	29	61	23
	M2	2.2	25	1.1	28	1.52	2.79	45	93	38
	M4	3.8	17	1.23	22	1.55	2.79	38	77	26
IV	K1	2.5	14	1.27	23	1.51	2.75	33	77	19

$$* \quad RI = \frac{\rho_{d\,max} - \rho_d}{\rho_d} \times 100 \quad , \text{where } \rho_d \text{ is the in-situ dry density, also}$$

$$RI = \frac{\gamma_{d\,max} - \gamma_d}{\gamma_d} \times 100 \quad , \text{where } \gamma_d \text{ is the in-situ dry unit weight.}$$

Table 4.8 : Chemical analysis of the soil element concentration as detected by Energy Despersive Spectrum (EDS).

Soil	Depth m	Detected area	Na	Mg	Al	Si	P	K	Ca	Ti	Mn	Fe	General observation
A1	1.8	General exposure	2.27	0.68	18.6	46.6	0.0	2.01	8.19	0.0	0.0	19.07	High concentration of Al, Si and Fe for the General View.
		at contact	1.95	0.61	19.67	29.82	0.0	0.61	6.66	0.0	0.0	32.99	
A2	3.0	At particle contact	1.15	0.77	27.1	45.3	0.0	4.64	8.22	0.00	0.0	11.92	High Al, Si and K
A3	4.2	Gravel with sharp edges	0.73	0.73	8.4	37.5	0.0	4.6	33.7	0.49	0.0	12.7	High Calcite in bulky form
M1	1.1	White needle particles	0.41	0.18	3.62	12.29	0.0	1.14	65.7	0.33	0.11	9.34	Rich with Aragonite
			5.31	1.68	8.52	37.6	0.0	3.21	11.3	2.93	0.0	25.3	High iron oxide concentra.
M2	2.2	Clothing of grains ~ General	0.0	0.0	14.07	57.6	0.0	2.66	2.06	1.42	1.0	21.2	High concentration of Al, Si and Fe.
			0.48	1.01	18.8	47.0	0.0	3.67	9.12	0.54	0.0	16.5	
		At contact (Bridge)	0.0	0.0	5.76	18.11	0.0	2.06	53.1	0.41	2.47	16.5	Very rich with Ca
M3	3.0	Clothed particle	0.31	1.07	3.46	24.0	0.0	0.94	28.8	1.61	0.0	37.7	Generaly rich in Calcite and iron oxide with less Al and Si at fine contents or at high magnification.
		At contact	0.0	0.51	3.2	6.74	2.86	0.0	58.5	0.0	2.35	24.2	
		Clay fraction	0.43	.07	0.7	5.94	1.33	0.7	82.4	0.0	0.25	7.7	
M4	3.8	Particle with sharp edges	0.0	1.1	9.6	38.2	0.0	3.8	31.8	0.55	0.0	6.7	High Calcite and Silica

Table 4.9 : Chemical composition of fine soil by X-ray Flourescence Spectrometer (adopted from Al-Gasous, 1988).

Soil type	Layer	Depth m	SiO_2 %	Al_2O_3 %	K_2O %	CaO %	TiO_2 %	V_2O_5 %	MnO %	Fe_2O_3 %	SO_3 %	Total %
Sandy silt	A1	1.9	55.88	6.26	3.63	17.59	4.11	0.08	0.68	10.51	1.26	100
	A3	4.5	47.01	5.84	3.62	24.96	4.35	0.08	0.78	11.89	1.47	100
	G1	2.5	43.64	5.97	3.02	27.68	5.06	0.08	0.73	12.22	1.60	100
Sandy silty caly	K1	2.0	49.17	5.04	3.13	31.62	2.85	0.04	0.48	6.65	1.02	100

Table 4.10-a : Non clay minerals of representative soils (Al-Gasous, 1988).

Soil layer	Soil type	Depth (m)	Quartz SiO_2 %	Alabite $NaAl Si_3O_8$ %	Calcite $CaCO_3$ %	Augite $Ca(Mg,Fe) Si_2O_6$ %	Maghemite $Mg-Fe_2O_3$ %	Other Minerals %
A0	Lean clay	0.7	71	25	4	---	---	---
A1	Sandy silt	1.8	55	15	15	4	12	4
K1	Sandy silty clay	2.0	57	14	28	---	---	---
K3	Sandy silty clay with gravel	4.5	59	12	30	---	---	---

Table 4.10-b : Clay minerals of representative soils (Al-Gasous,1988).

Soil layer	Soil type	Depth m	Quartz SiO_2 %	Calcite $CaCO_3$ %	Kaolinite $(OH)_4 Si_2 Al_2 O_5$ %
A0	Lean clay	0.7	37	23	39
A1	Sandy silt	1.8	81	--	19
K3	Sandy silt clay with gravel	4.5	22	53	25

Table 4.11 : Loess lithological classification (Adopted from J. Buraczynski, 1988).

Table 4.12 : Summary of the natural soil fabric and the depositional effects on the soil fabric of the different selected soils.

Soil layer	Depth m	Soil texture				Soil type	Soil fabric		Weathering effect
		Gravel %	Sand %	Silt %	Clay %		Description	Bonding forces	
A1	1.2	4	70	20	6	Silty sand	Highly metastable open fabric with low to fair coated grains and bridges	Mostly capillary forces, eroded aragonite and silicon increase with depth	weathered
	1.8	7	43	42	8	Sandy silt			
A2	3.0	2	21	58	19	Silt with sand	Metastable open fabric of spongy feature (coated assemblages and trapped pores)	High chemical precipitation of calcium carbonate	unweathered
A3	3.8	6	23	54	17 *	Sandy silt to sandy silt with gravel	Relative stable fabric with rich buttresses and calcareous gravel grains	Some chemical precipitation and conciderable occurrence of calcareous particles	-
M1	1.0	6	20	58	16	Sandy silt	Highly metastable open fabric of honeycombed and coated grains	Capillary forces and chemical precipitation of calcium carbonate and silicon	weathered (leaching)
M2	2.2	0	10	66	24	Silt	Metastable open fabric with trapped pores and coated assemblages, spongy.	High chemical precipitation of aragonite-calcite, iron oxide and silicon	relatively weathered (precipitation)
M3	3.0	7	29	43	21	Sandy silt	Relatively stable with visable pores and highly coated grains	High chemical precipitation of calcite and iron oxide	weathered (decomposition)
M4	3.9	4	34	56	6 *	Sandy silt to sandy silt with gravel	Relative stable fabric with richy buttresses and calcareous gravel grains	Some chemical precipitation and conciderable occurrence of calcareous particles	-
K1	1.5	13	34	41	12	Sandy silty clay	Highly metastable open fabric with fair to high coated grains and buttresses	Capillary tension with some clay and chemical bonding, traces of thin calcar. grains	weathered (leaching)
K2	3.5	17	28	38	17	Sandy silty clay with gravel	Relative stable fabric with rich clay buttresses and calcareous gravel grains	High clay and chemical precipitation with high calcareous particle contents	-

* The variation in the gradation of these layers is expected due to the variation of the gravel concentration within this layer.
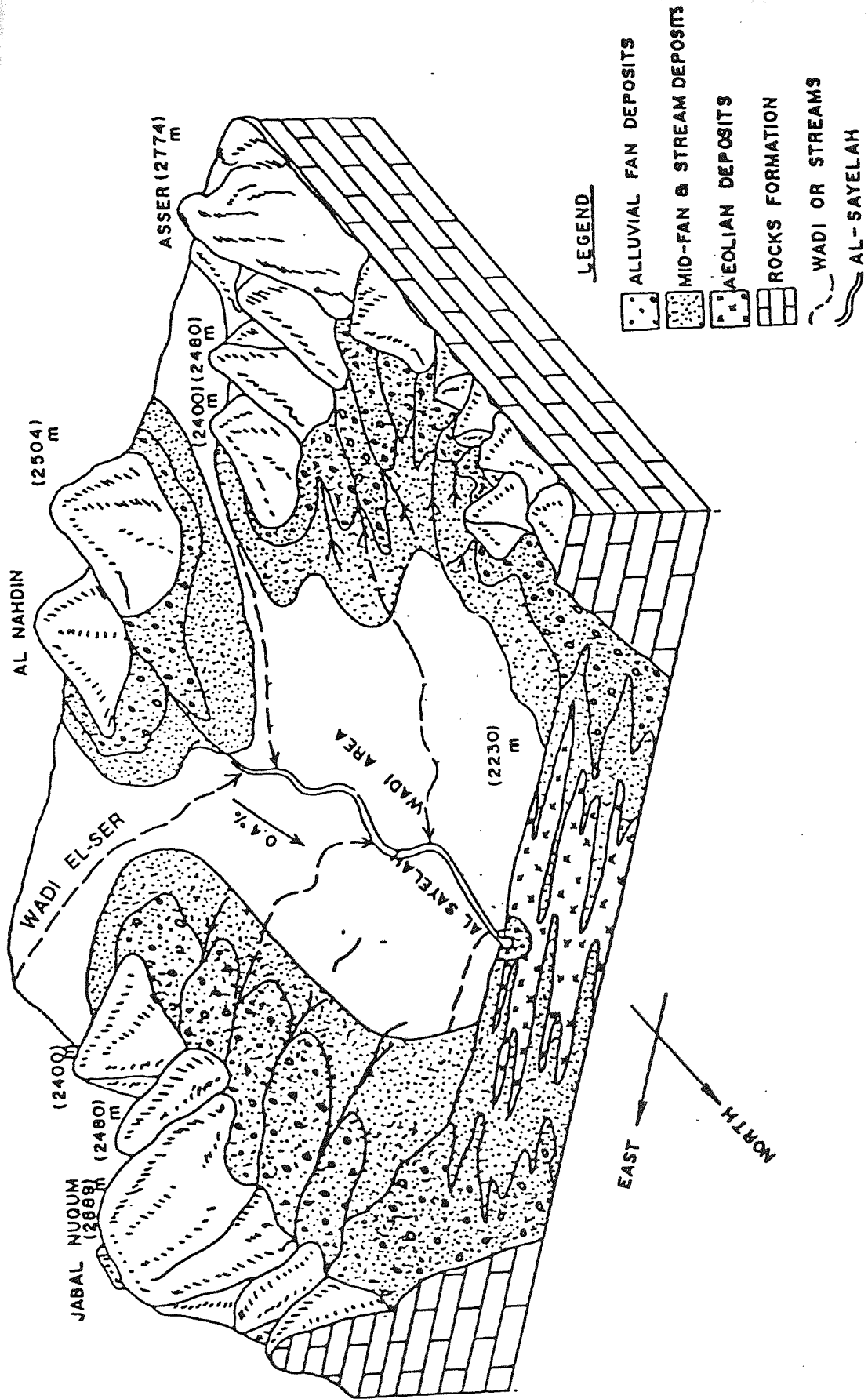
Fig. 4.1 : Block digram of the depositional systems and soil deposits.
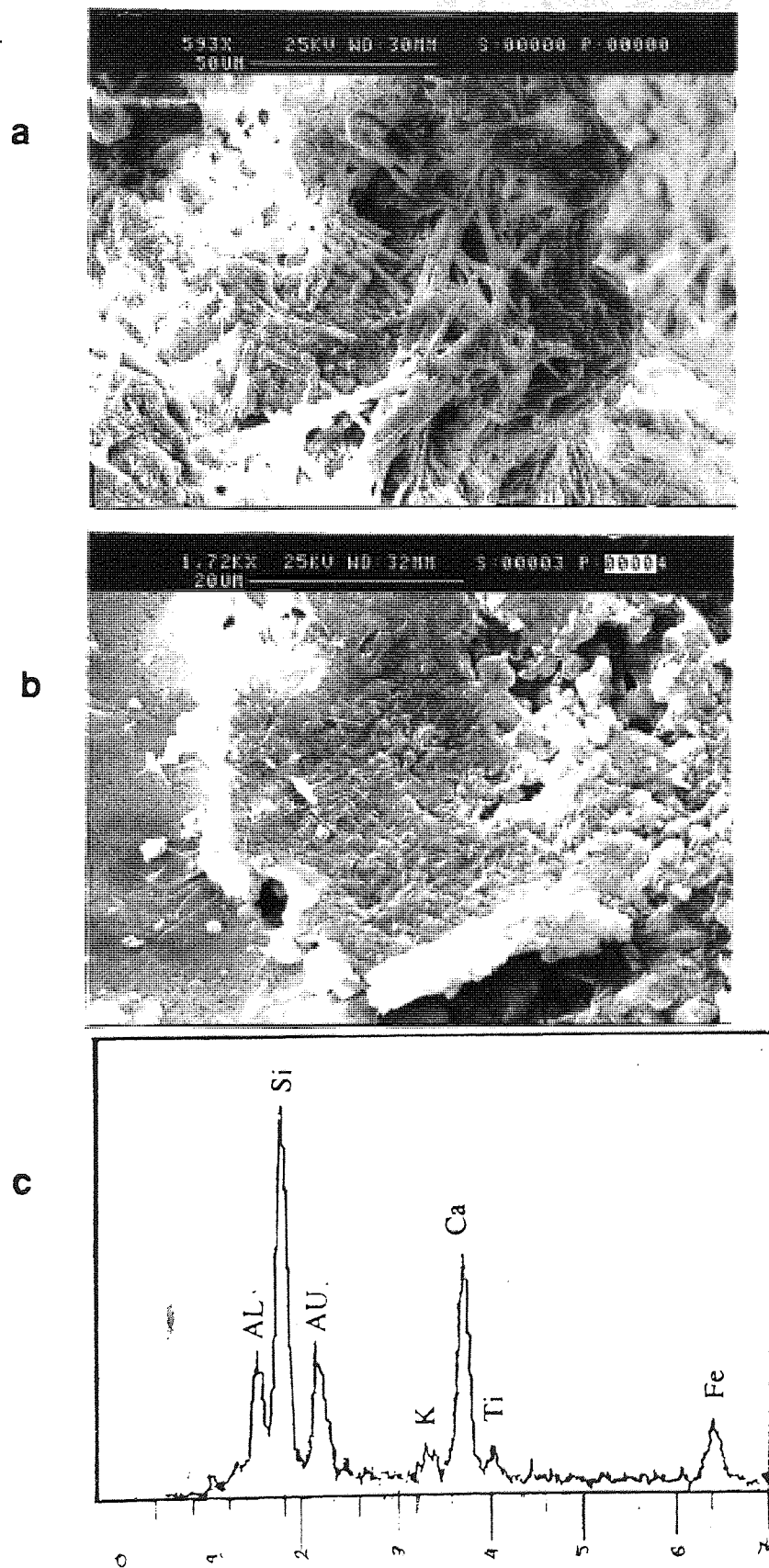
Fig. 4.2 : Aragonite and calcite resulting from leaching ;

a) Aragonite in the needle form,

b) Calcite in the shell form, and

c) EDS of the chemical precipitations shown in (a).

Aston University

Content has been removed for copyright reasons

Aston University

Content has been removed for copyright reasons
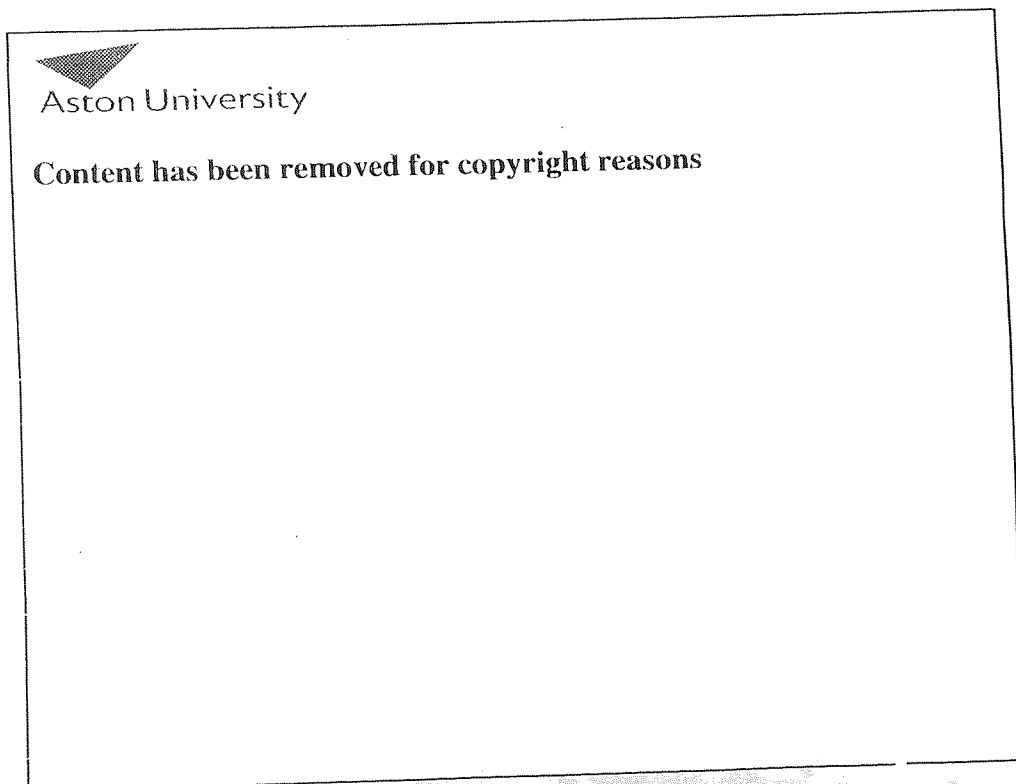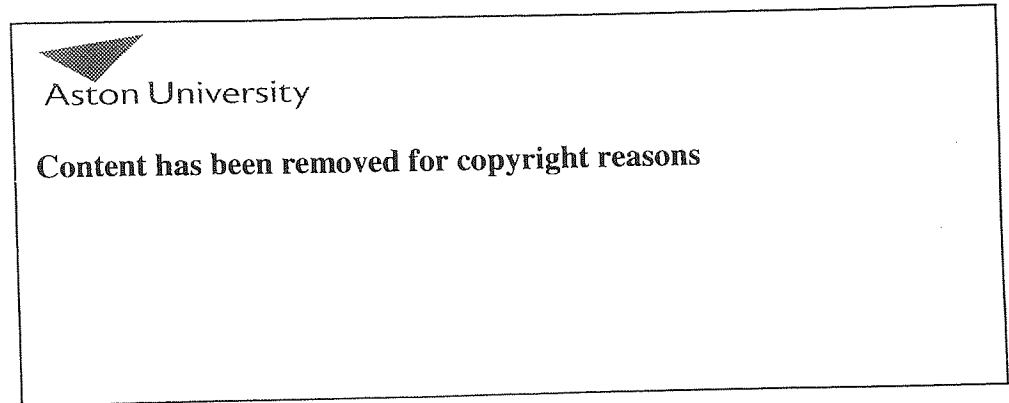
Fig. 4.3 : Soil profiles (adopted from Abduljauwad, et al.. 1991).
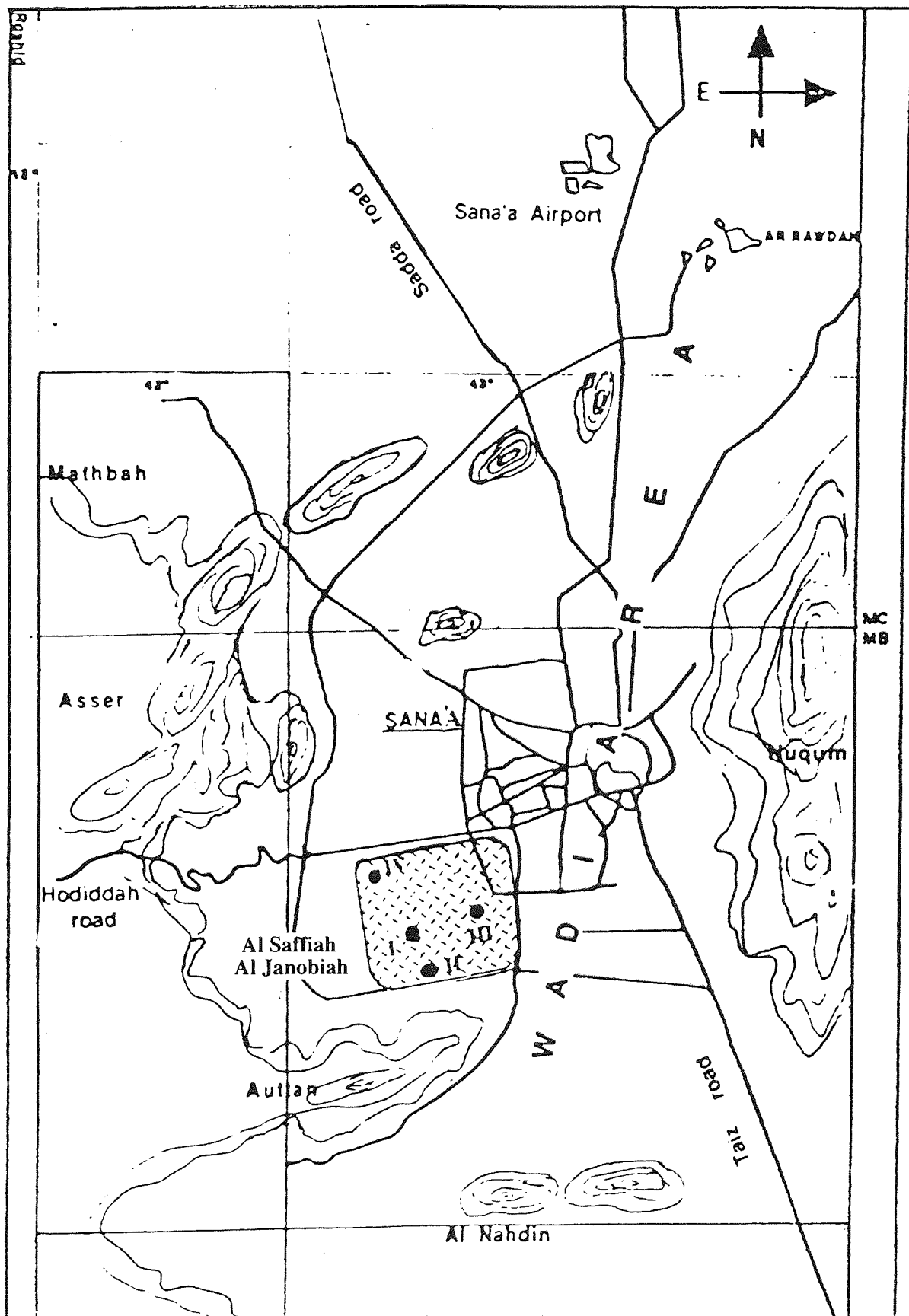
Fig. 4.4 : The Wadi area and the selected sites.
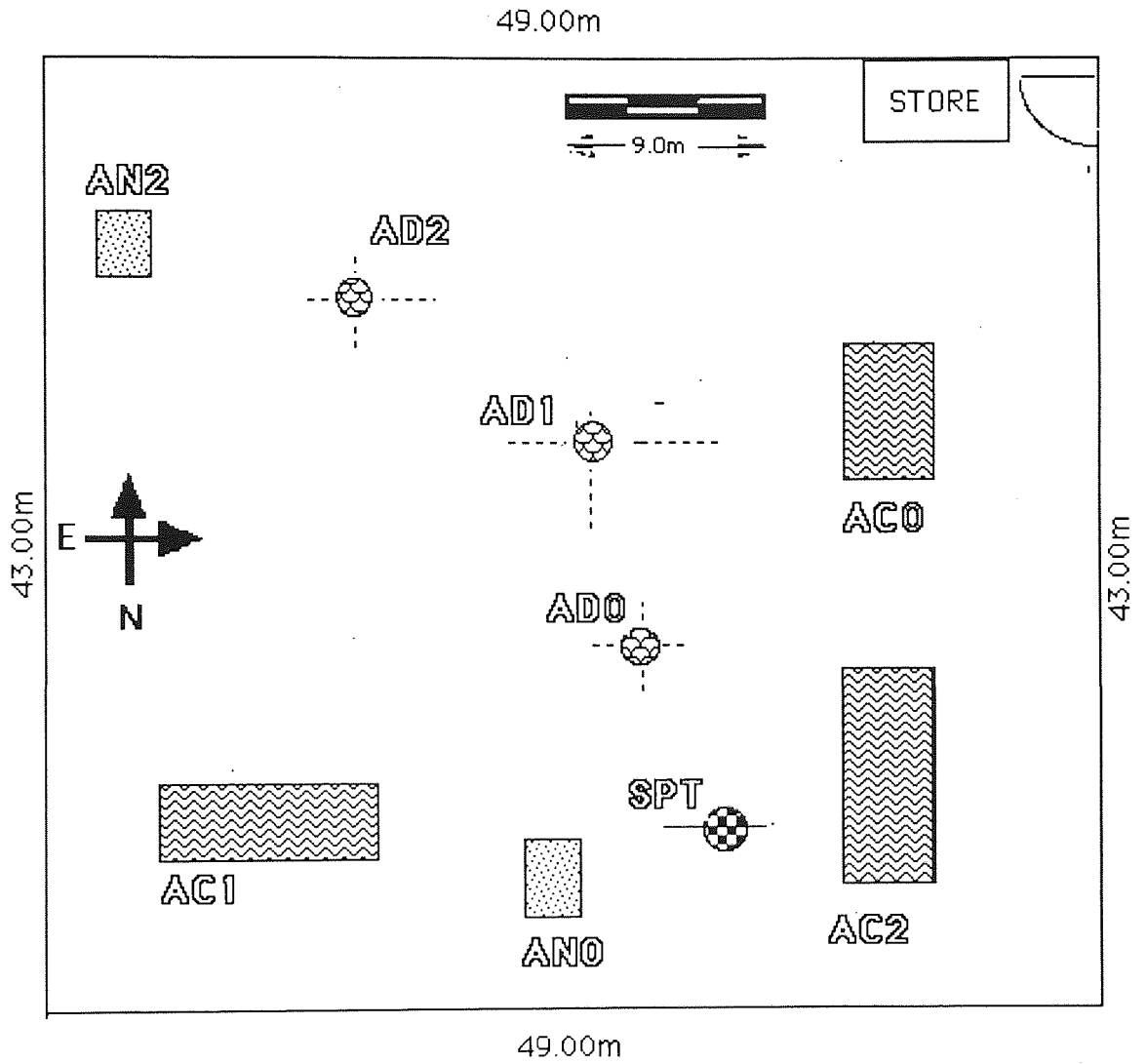
Fig. 4.5 : The layout of the different locations within Site I, Scale 1:300.
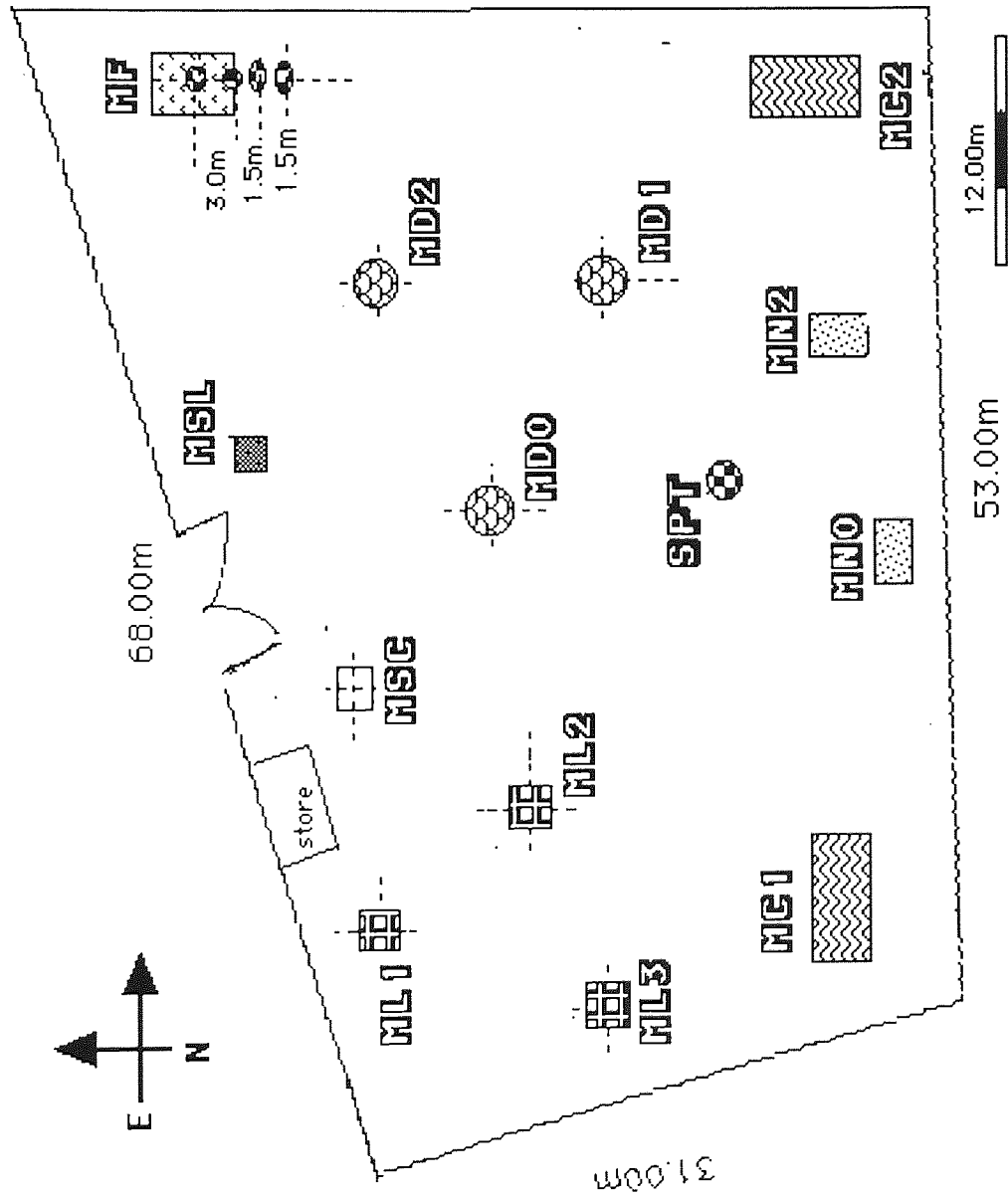
Fig. 4.6 : The layout of the different locations within site III, Scale 1 :400
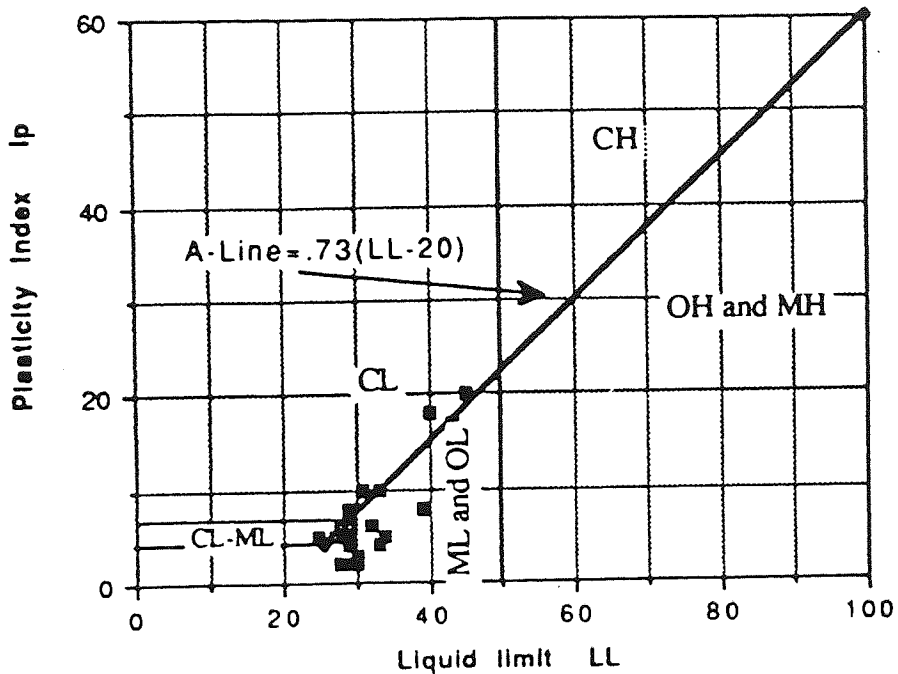
Fig. 4.7 : The plotted fine soils of the Sana'a area on A-Chart.

Fig. 4.8 : Trends pf gradation and plasticity for loess (after Gibbs et al., 1960).

Depth, m	Soil profile	Soil description	Symbol	Wn %	SPT values			
					① 15cm	② 15cm	③ 15cm	* Ns
1.0		Blackish stiff fissured lean clay with root traces.	A0	13	4	5	5	10
2.0		Yellowish to reddish brown sandy silt to silt with sand with some lenses of gravelly sand, known as "Suffrri".	A1	15	8	7	6	13
				13	4	4	4	8
3.0		Brown silt with sand with white traces and thin holes or tubes.	A2	15	4	3	5	8
		A strip of gravelly sand, 5.0-10.0cm.		12	6	23	10	33
4.0		Brown sandy silt, with some discontinuous roots, in form of sharp edge particles of highly cemented sandstones with rough surfaces, known as Zangabili".	A3	10	8	10	10	20
5.0				12	5	8	25	33
6.0				12	5	8	9	17

* Ns = ② + ③

Fig. 4.9 : Bore log from site I, Allaw Al Kohali Land (A).
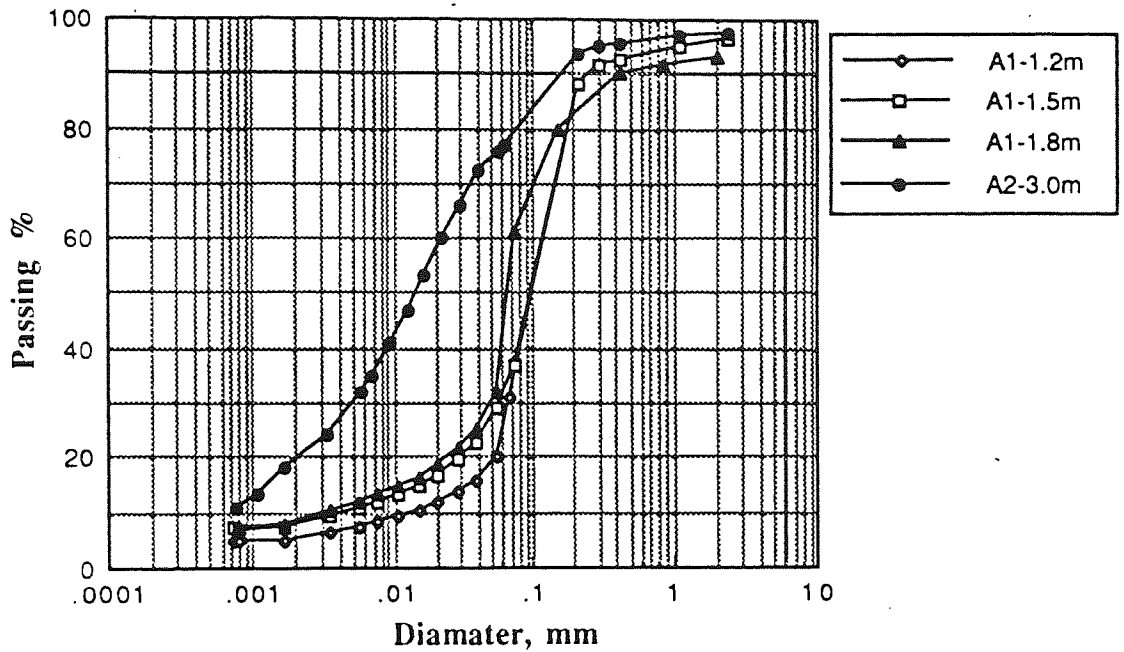
Fig. 4.10 : Gradation curves of sand to sandy silt, A1, and
silt with sand, A2, (site I).
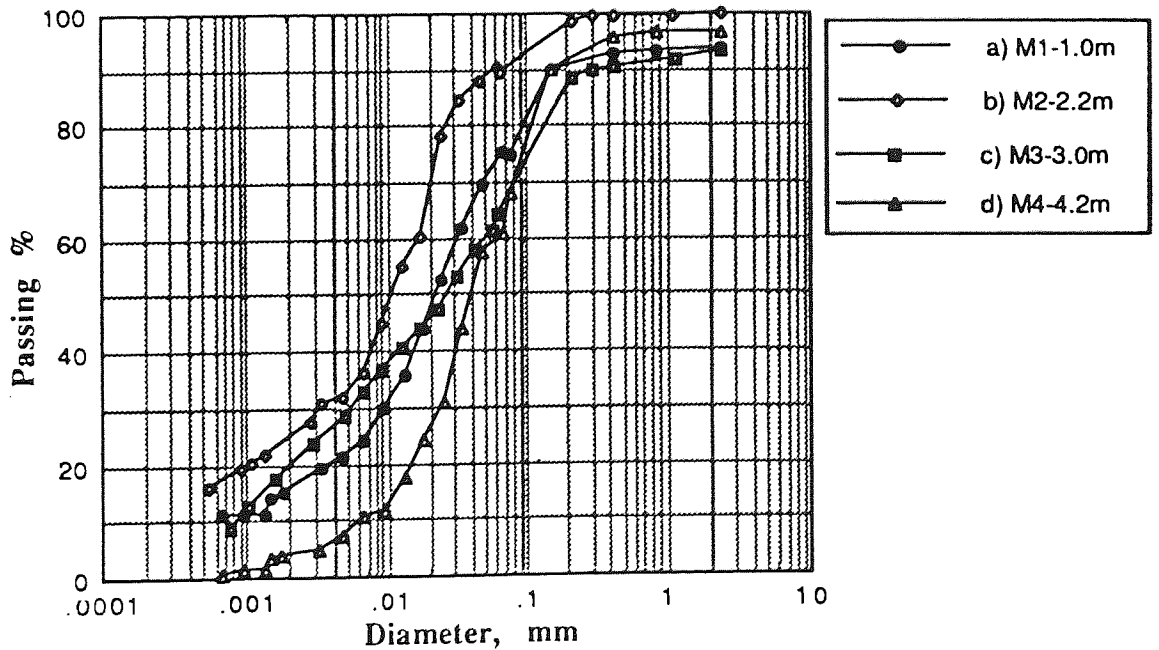
Fig. 4.11 : Gradation curves of the soils of site III including;
a) Light brown sandy silt, b) Blackish to dark brown silty soil,
c) Yellowish brown sandy silt; and d) Brown sandy silt with gravel.

Fig. 4.12(a) : Bore log from site III, Mohamed Abdulrab Land (M).

Depth, m	Soil profile	Soil describtion	Symbol	Wn %	SPT values ① 15cm	② 15cm	③ 15cm	* Ns
		Stiff brown fill.	M0	20	3	4	5	9
1.0		Light brown sandy silt, with thin tubes and white traces.	M1	20	4	4	5	9
2.0		Brown to blackish brown silt to silty clay with limited traces of calcareous gravel.	M2	28	3	3	3	6
3.0		Translation zone of fine sand 10-15cm		26	6	7	10	17
		Highly cemented, yellowish to greenish beige sandy silt	M3	12	11	12	13	25
4.0		Brown sandy silt, with some discontinuous roots, in form of sharp edge particles of highly cemented sandstones with rough surfaces, known as Zangabili".		15	15	19	16	35
				16	6	5	8	13
5.0			M4	22	7	7	9	16
				15	5	8	7	15
6.0				12	8	9	13	22

Fig. 4.12(b) : Bore log from site IV, Khamthan Al Kohali Land (K).

Depth, m	Soil profile	Soil describtion	Symbol	Wn %	SPT values ① 15cm	② 15cm	③ 15cm	* Ns
		Blackish stiff fissured lean caly soil with root traces.	K0	--				
1.0		Light brown to yellowish, medium to stiff sandy silty clay.	K1	15	3	5	7	12
2.0				12	6	6	8	14
3.0		Stiff brown sandy silt clay with calcareous gravel with sharp edges.	K2	16	12	13	17	30
4.0				17	15	16	14	30
				17	10	10	10	20
5.0								
		Sand gravel with clayey silty matrix and some boulders.	K3	8	12	16	26	42
6.0					20	30	33	63

* Ns = ② + ③

Fig. 4.12 : Bore logs from sites III and IV.

Fig. 4.12(a) : Bore log from site III, Mohamed Abdulrab Land (M).

Depth, m	Soil profile	Soil describtion	Symbol	Wn %	SPT values ① 15cm	② 15cm	③ 15cm	* Ns
		Stiff brown fill.	M0	20	3	4	5	9
1.0		Light brown sandy silt, with thin tubes and white traces.	M1	20	4	4	5	9
2.0		Brown to blackish brown silt to silty clay with limited traces of calcareous gravel.	M2	28	3	3	3	6
3.0		Translation zone of fine sand 10-15cm		26	6	7	10	17
		Highly cemented, yellowish to greenish beige sandy silt	M3	12	11	12	13	25
4.0				15	15	19	16	35
		Brown sandy silt, with some discontinuous roots, in form of sharp edge particles of highly cemented sandstones with rough surfaces, known as Zangabili".		16	6	5	8	13
5.0			M4	22	7	7	9	16
				15	5	8	7	15
6.0				12	8	9	13	22

Fig. 4.12(b) : Bore log from site IV, Khamthan Al Kohali Land (K).

Depth, m	Soil profile	Soil describtion	Symbol	Wn %	SPT values ① 15cm	② 15cm	③ 15cm	* Ns
		Blackish stiff fissured lean caly soil with root traces.	K0	--				
1.0				15	3	5	7	12
		Light brown to yellowish, medium to stiff sandy silty clay.	K1	12	6	6	8	14
2.0								
3.0				16	12	13	17	30
		Stiff brown sandy silt clay with calcareous gravel with sharp edges.	K2	17	15	16	14	30
4.0				17	10	10	10	20
5.0								
		Sand gravel with clayey silty matrix and some boulders.	K3	8	12	16	26	42
6.0					20	30	33	63

* Ns = ② + ③

Fig. 4.12 : Bore logs from sites III and IV.

Fig.4. 13 : Gradation curves of the sandy silty clayey soils with gravel.
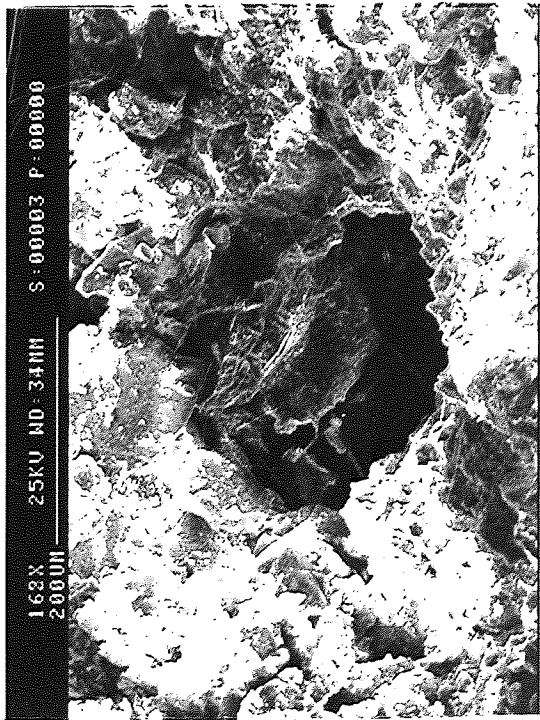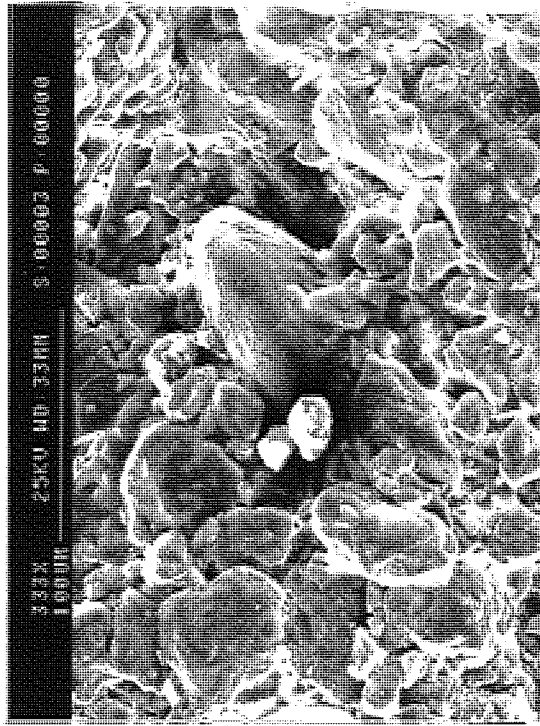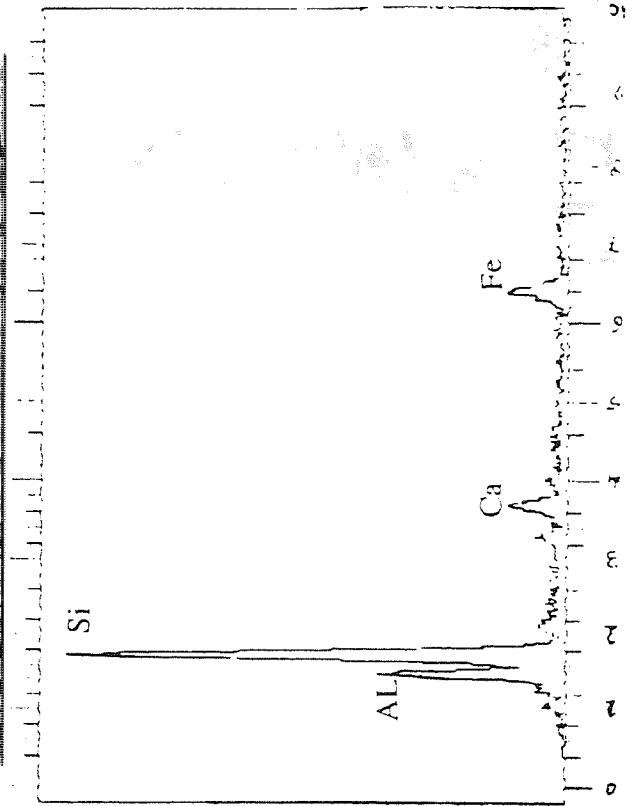
Fig.4.14 : SEM of the sandy to sandy silt soil A1, from vertical cross section indicating;

a) Pores and surrouding structure,

b) General sand and silt matrix clothed with fines; and

c) EDS of the general view in (b).
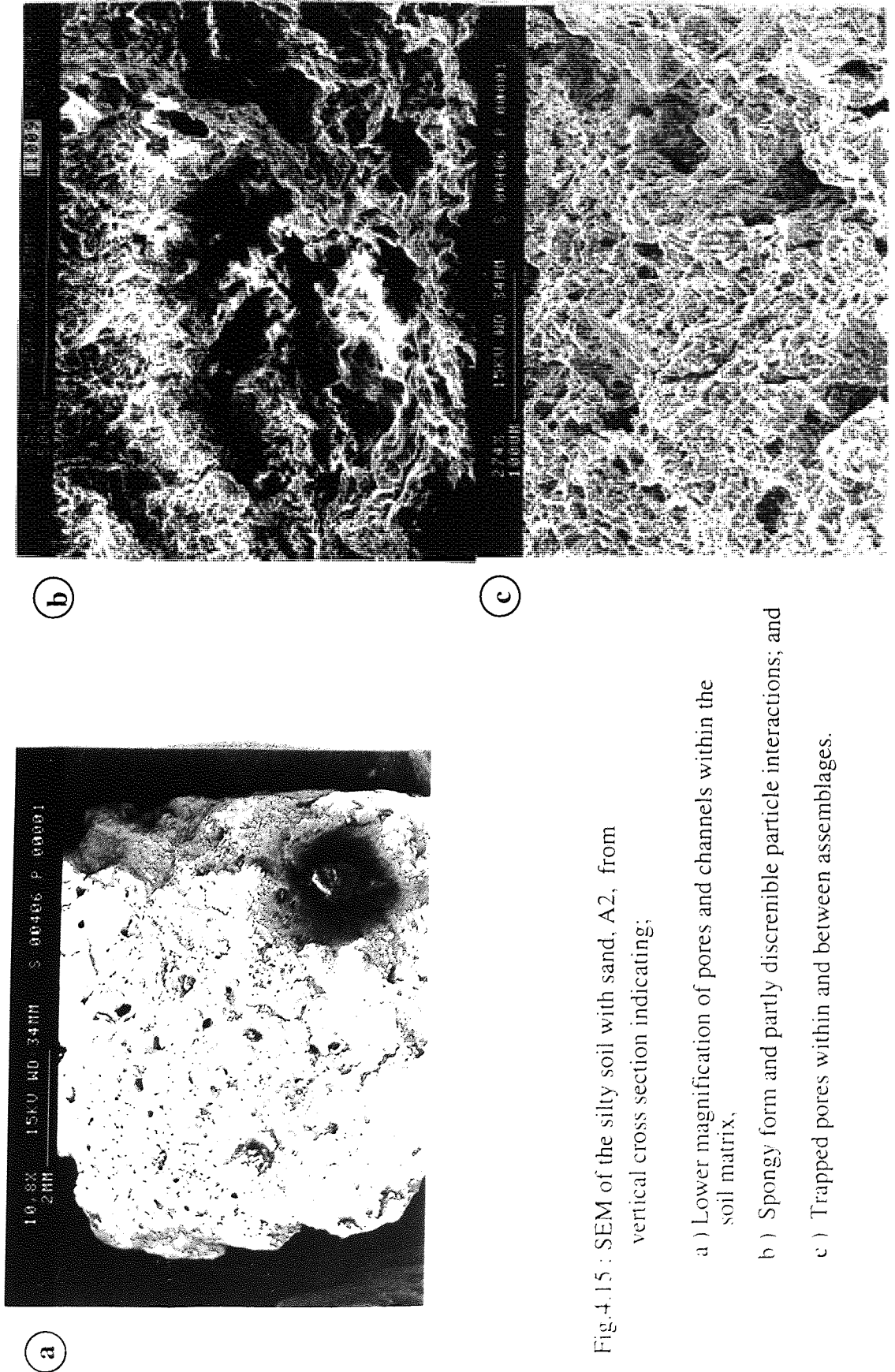
Fig.4.15 : SEM of the silty soil with sand, A2, from
vertical cross section indicating;

a) Lower magnification of pores and channels within the
soil matrix,

b) Spongy form and partly discrenible particle interactions; and

c) Trapped pores within and between assemblages.
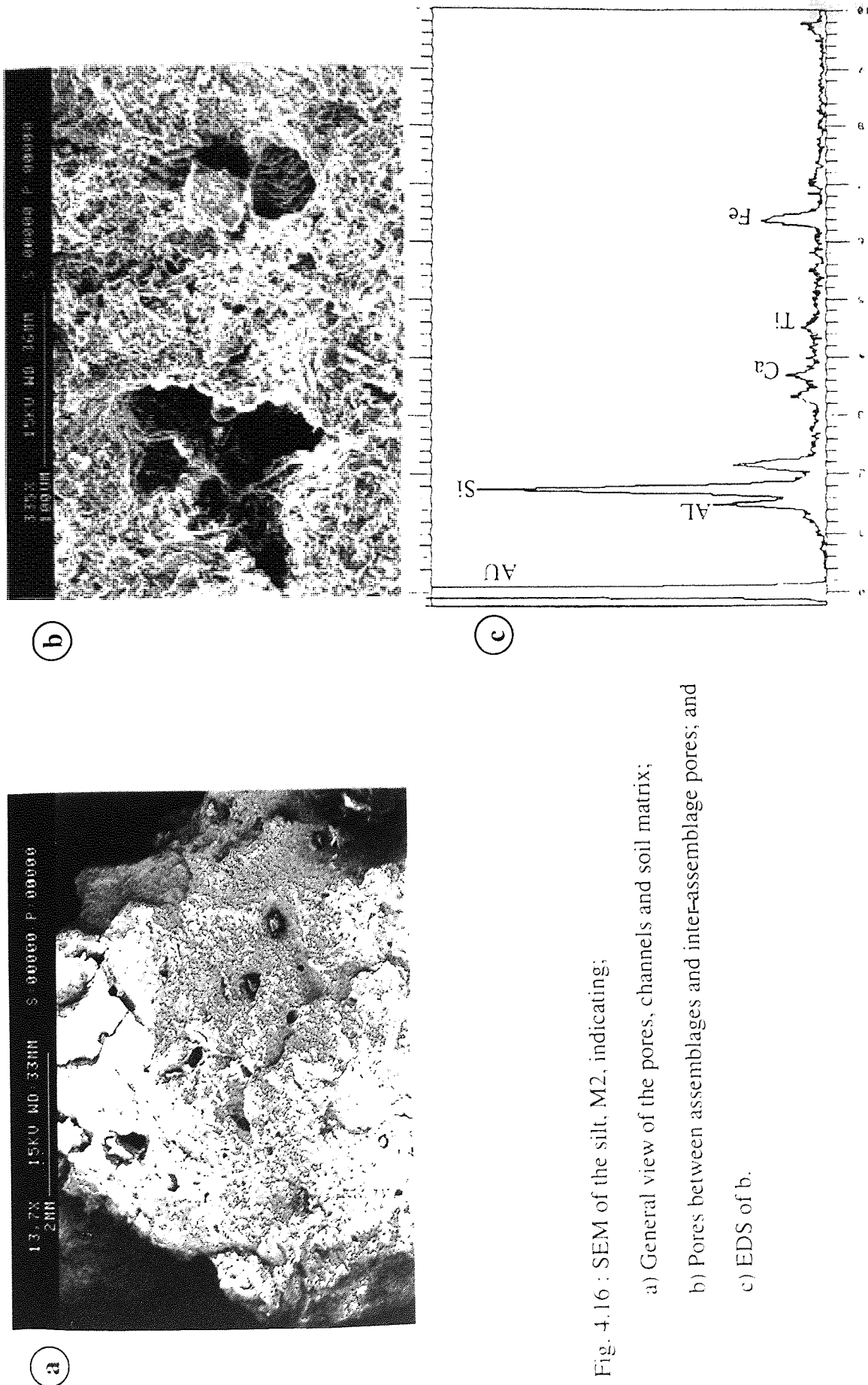
Fig. 4.16 : SEM of the silt. M2. indicating;

a) General view of the pores, channels and soil matrix;

b) Pores between assemblages and inter-assemblage pores; and

c) EDS of b.
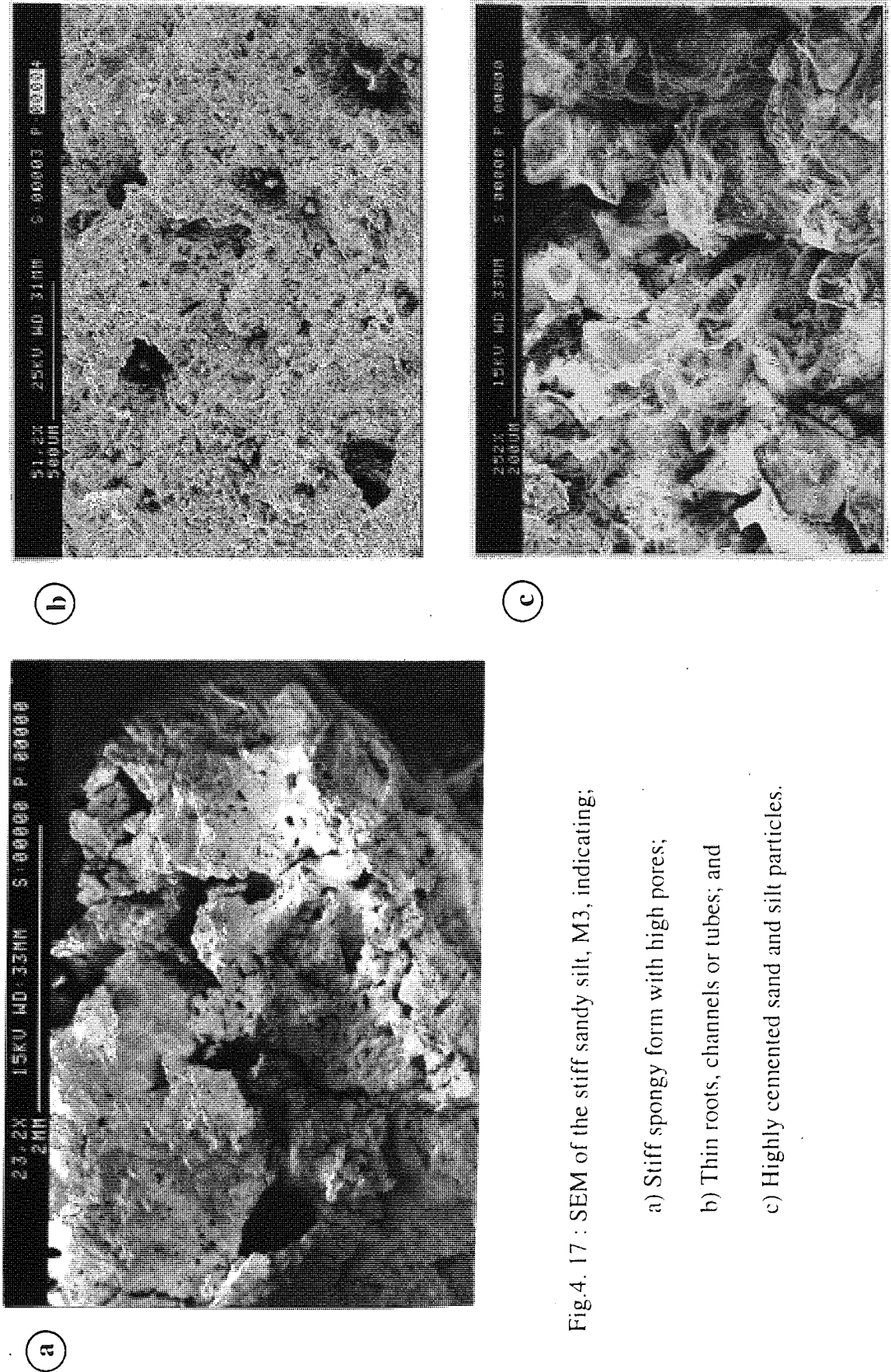
Fig.4. 17 : SEM of the stiff sandy silt, M3, indicating:

a) Stiff spongy form with high pores;

b) Thin roots, channels or tubes; and

c) Highly cemented sand and silt particles.
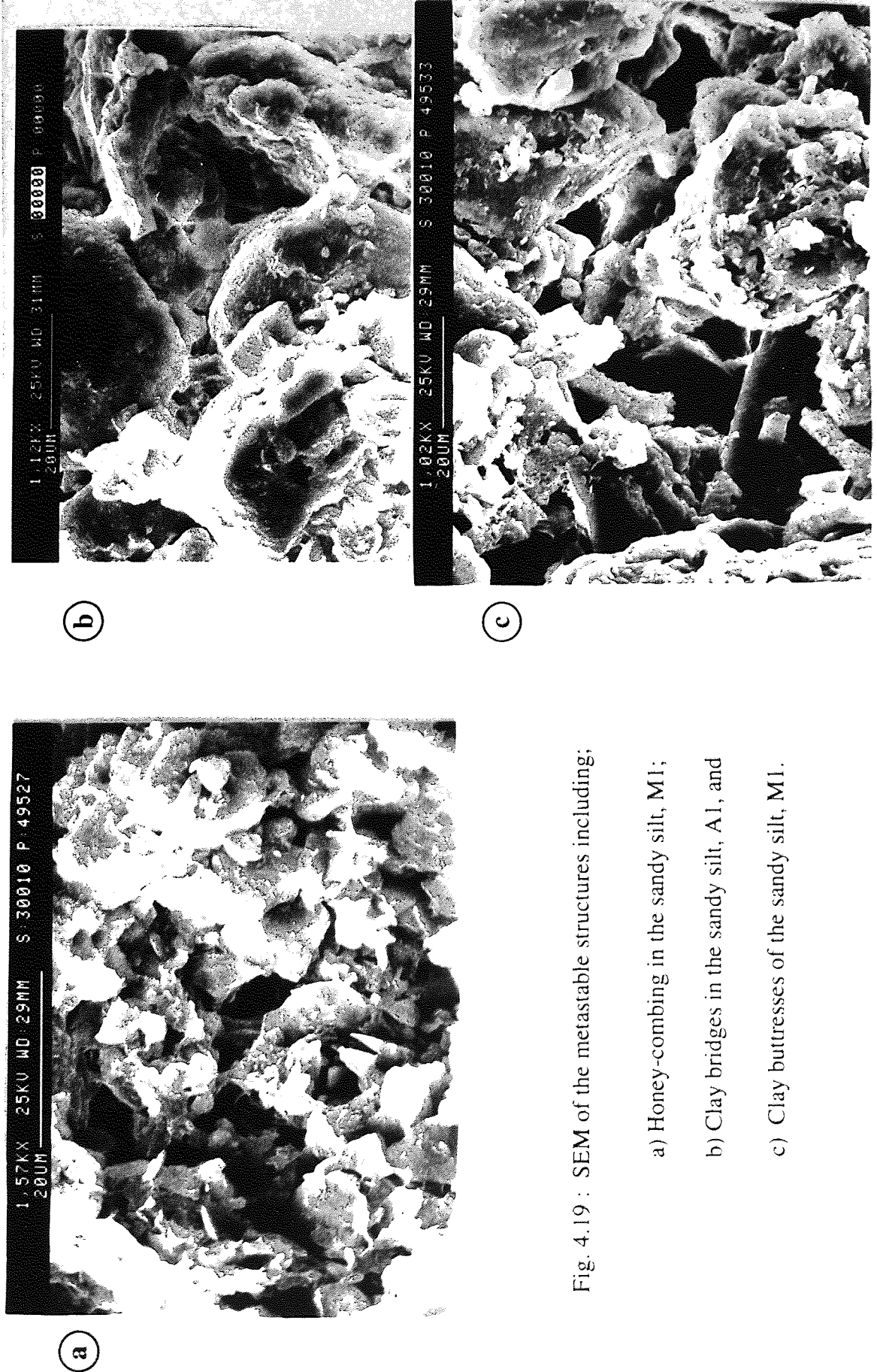
Fig. 4.19 : SEM of the metastable structures including;

a) Honey-combing in the sandy silt, M1;

b) Clay bridges in the sandy silt, A1, and

c) Clay buttresses of the sandy silt, M1.
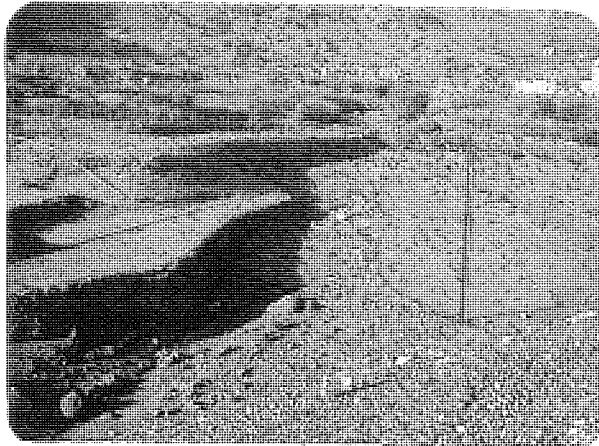
a
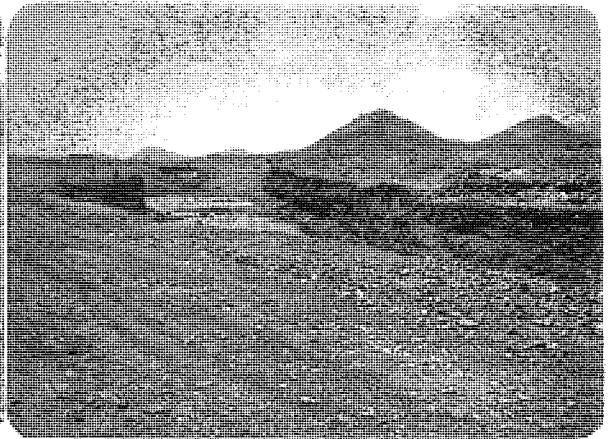
b
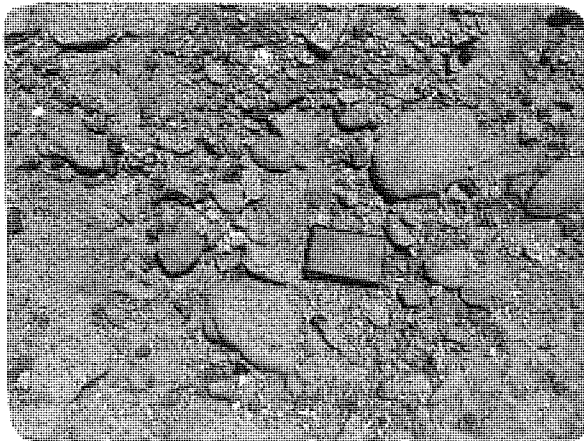
c
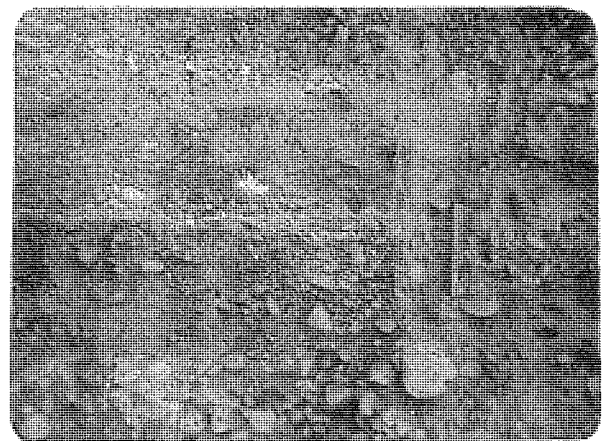
d

Plate 4.1 :

Water-laid Deposits and Formations.

   a) The deposit of the upper fan portion (apex),

   b) Coarse-grained Meander belt " Sayelah",

   c) Bed stream deposit,

   d) Granular soil of graded bedding form, indicated scale is 13 cm, and

   e) Imbricated pebbles formation in the granular soil.
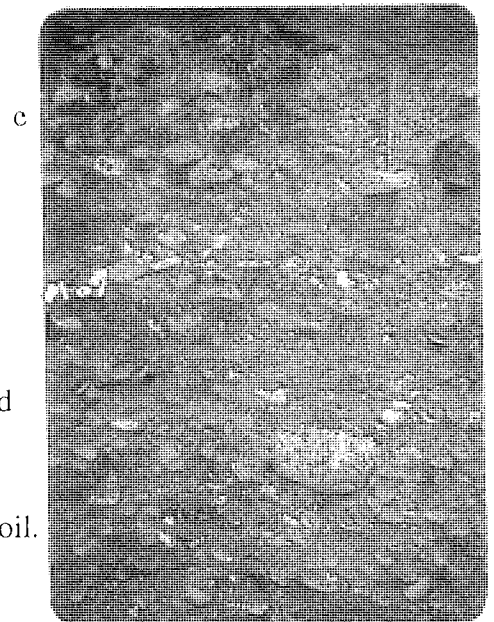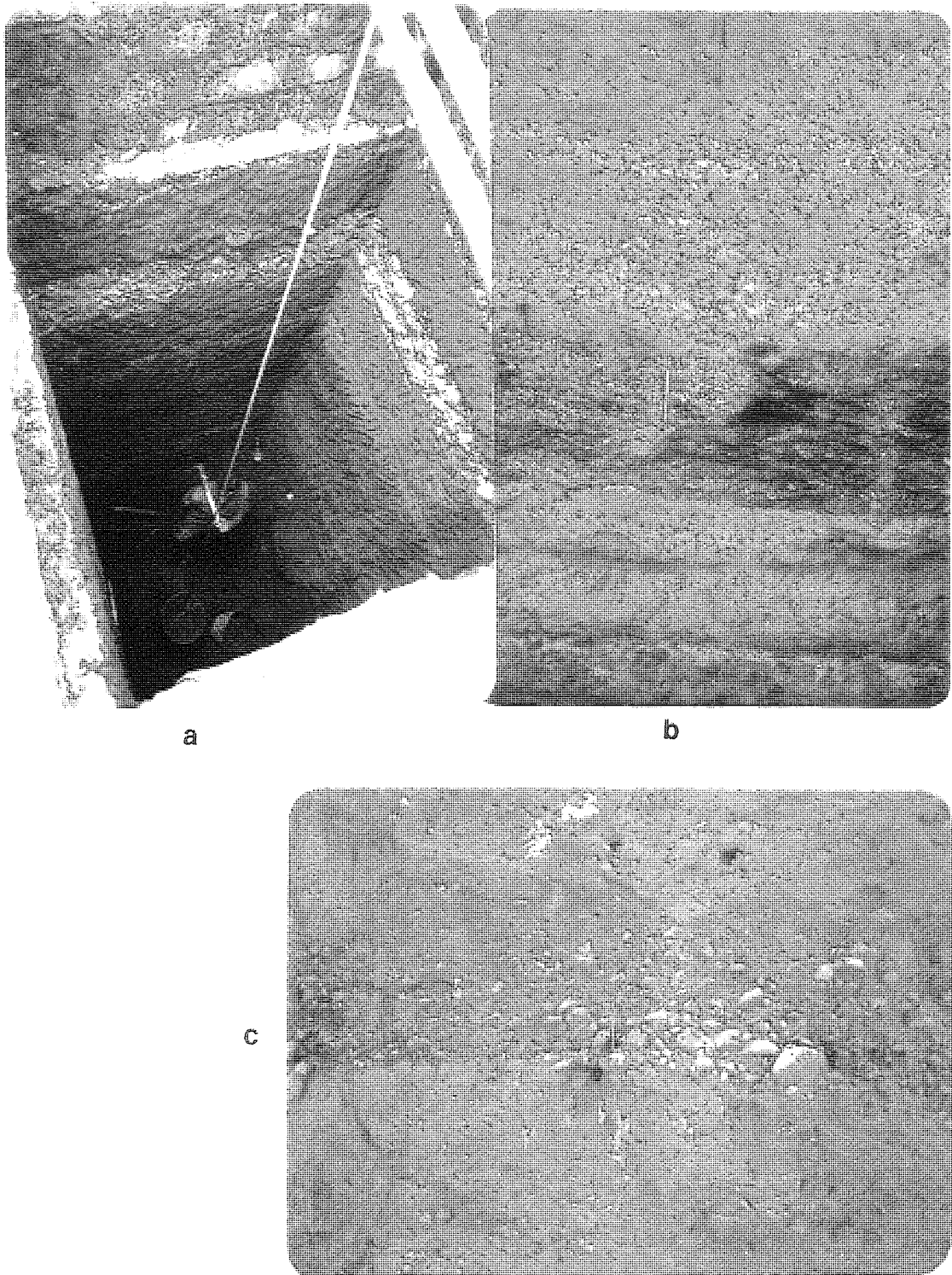
Plate 4.2 :

Wind-laid deposits in the Wadi Area.

    a) Thick layers of wind deposit (loess) as detected from a septic tank,

    b) Wind-laid (primary loess) and water-laid (sheet flood) repeated layers, and

    c) Reworked loess by water action (secondary loess deposit).

CHAPTER FIVE

THE DEFORMATION BEHAVIOUR OF THE NATURAL SOILS

5.1 INTRODUCTION

Preliminary investigation of the Sana'a soils indicated considerable variations in their characteristics, the most notable being the tendency for some to exhibit drastic volume change upon wetting, or "collapsing". In this Chapter the deformation behaviour of the natural soils, particularly those which are known to produce collapsing, are presented.

As indicated in Chapter 4, the selected soils were identified as primarily silty aeolian deposits. Such deposits have been well known to have high shear strength and low compressibility at low moisture contents (Sheeler, 1968; Peck et al, 1974; Bell, 1992). Upon wetting they exhibit a great reduction in shear strength and high compressibility. The deformation behaviour has been investigated at both the natural moisture content (NMC) and following inundation (SMC), and the data include the collapsing and consolidation characteristics. These characteristics were determined from the collapsing, the double oedometer and the isotropic compression (IC) tests.

5.2 COLLAPSE CHARACTERISTICS FROM THE SINGLE OEDOMETER

5.2.1 General

The studied soils have a wide range of properties and so they were expected to exhibit different collapsing potentials. Therefore, to identify and classify their collapsing potential, each soil must be examined and the adopted classification system should incorporate the results of such examination. The most widely used methods for predicting the collapsibility of soils were presented in Chapter 2. Most of these methods are qualitative and do not indicate the magnitude of collapse, and so there is a need to employ an alternative method that can identify the degree of collapsibility of the studied soils using comparable data. This section considers the collapsing results from the single oedometer or collapsing test, while those obtained from the double oedometer and isotropic compression tests will be presented in the following sections.

5.2.2 Collapsing Identification and Classification

Two qualitative methods, after Denisov (1951) and Gibbs and Bara (1962), were used to give a preliminary rating to the potential for collapse, and these findings are given in Table 5.1. The definition of the various terms given in the Table have been provided in Chapter 2.

The ratings in Table 5.1 do not predict the magnitude of the collapse, and so it is impossible to directly compare the extent of the collapse of different soils demonstrating the need for a quantitative approach to collapsing classification. The single oedometer collapsing test results are presented in the following subsection as a direct method to establish this collapsing potential. Double oedometer tests were also carried out, but primarily to establish the consolidation characteristics of the soils at both the natural moisture and soaked conditions, and these results are only presented to provide a comparison with the collapsing potential assessments.

The single oedometer collapsing test was first reported by Denisov (1951) and was termed a "modified inundation test". In 1963 Knight recommended that water should be added at a stress level of 200 kPa to define the collapsing potential, due to wetting, and so classify the soil as indicated in Chapter 2. Recently, this method has been adopted as a standard by ASTM, under the jurisdiction of ASTM committee D18 (ASTM,1992), whereby the collapsing potential due to wetting, I_c, is defined by the magnitude of collapse (in per cent) at any stress level as follows:

$$I_c = \{(e_1 - e_2) / (1 + e_0)\} \ X \ 100 \ \text{------------------------------------} \ (5.1)$$

where

$(e_1 - e_2)$ - Change in void ratio produced by wetting; where e_1 is the void ratio before wetting and e_2 the void ratio after wetting, and

e_0 - Initial void ratio.

In this method the magnitude of collapse determined at 200 kPa defines the Collapsing Index, I_{cx}. The classification values according to this method are slightly different from those suggested by Jennings and Knight (1975) who referred to a collapsing potential, by C_p, as shown in Table 5.2. To avoid confusion, the symbol I_c will be used to refer to the collapsing potential due to wetting (in per cent) from both the single and double oedometers at any stress level in this work. The classification values of I_c in Table 5.2 after ASTM (1992) will be used to evaluate the collapsing results and to classify the studied soils. Equation 5.1 defines the collapse due only to wetting, while the collapse due only to loading (I_L) before wetting, can be addressed in the same manner following Denisov (1951) as:

$$I_L = \{(e_0 - e_1) / (1 + e_0)\} \ X \ 100 \ \text{------------------------------------} \ (5.2)$$

where

I_L — the collapse due to loading and before wetting, and

e_0 and e_1 as defined in Eq. (5.1).

The total collapse due to both loading and wetting is defined by I_T as:

$$I_T = I_c + I_L \quad\text{--} \quad (5.3)$$

The total collapse I_T can be also identified using a similar equation as follows:

$$I_T = \{(e_0-e_2)/(1+e_0)\} \times 100 \quad\text{--} \quad (5.4)$$

5.2.3 Single Oedometer -Collapsing- Test

5.2.3.1 Test Procedures

This was carried out on undisturbed samples of both the natural and treated soil. This test has been termed a collapsing test, one-point load test, inundation test, or single oedometer test, but the term collapsing (single oedometer) is used in this study. For each collapsing test, generally three incremental loads were applied, the second load being the collapsing stress (soaking stress) at which the sample was wetted or soaked. Three soaking stress levels, 50, 100 and 200 kPa, which covered the typical range of the design stresses for residential and public structures in the Sana'a area, were selected and so the increments for each of these stress levels were (25,50,100), (50,100,200) and (100,200,400) respectively.

After setting the specimen, the first load was applied and sustained for 4 hours, by which time most of the soils had reached equilibrium. The dial was read and the second incremental load applied and left for 4 hours before taking the second gauge reading. At this sustained load (collapsing stress), water was added to the cell and it was left for 24 hours before taking the reading. The final load increment was applied and the sample was left for a further 24 hours before taking the last reading and, to complete the test, the sample was weighed, oven dried, and re-weighed to establish the final moisture content.

5.2.3.2 Test Results

Table 5.3 summarises the test results together with the initial conditions of each soil, namely moisture content (W_n), wet density (ρ_n), dry density (ρ_d), void ratio (e_0), and the degree of saturation before and after testing, S_0 and S_f respectively. In particular, the table presents, in per cent, the total collapse I_T, collapse potential due to wetting (I_c), collapse potential due to loading (I_L) and the ratio of I_c to I_L for each soil at each stress level. Finally,

the stiffness before (E_b) and after (E_a) wetting, together with the stiffness ratio are also given in the table, the stiffness values being defined as:

$$E_b = \Delta\sigma_{vb} / (\Delta H / H_o) \text{--} (5.5)$$

where

E_b = the stiffness before wetting,

$\Delta\sigma_{vb}$ = the stress increment prior to wetting,

ΔH = the change in the sample thickness under a stress increment $\Delta\sigma_{vb}$ prior to wetting (4 hrs), and

H_o = initial thickness of the sample for stress increment $\Delta\sigma_{vb}$.

$$E_a = \Delta\sigma_{va} / (\Delta H / H_w) \text{--} (5.6)$$

where

E_a = the stiffness after wetting,

$\Delta\sigma_{va}$ = the stress increment after wetting,

ΔH = the change in the sample thickness under a stress increment $\Delta\sigma_{va}$ just after wetting (24 hrs), and

H_w = initial thickness of the sample for stress increment $\Delta\sigma_{va}$.

The results were graphically expressed and typical behaviour is shown in Figs. 5.1 - 5.6 for selected samples, detailed graphs for all the soils are presented in Appendices C5-1 to C5-6. Figs. 5.1 - 5.3 illustrate the collapsing behaviour for layers A1 (at 1.2 and 2.2) and A3 from site I, while Figs. 5.4 and 5.5 show the behaviour of the upper (M1) and the lower (M4) detected layers of site III, and Fig. 5.6 refers to soil layer K2 of site IV. Each Figure presents the behaviour at the three soaking stress levels, 50, 100 and 200 kPa, with the point at which the water was added being indicated by an arrow ↓. On the right side of the Figure 5.1 the expression " A1COL/N-50" defines the test in terms of the soil layer "A1", subjected to a collapsing test "COL/", in the undisturbed state "N" either at a wetting stress of "-50" or for a sample from a depth of "-3.0m". This key, uniquely defines the tested sample and this method of nomenclature is used in all the other Figures, both in the text and Appendix C5.

5.2.3.3 Results Analysis and Interpretation

The initial identification of the collapsibility is given in Table 5.1 using the qualitative methods of both Denisov (1951), and Gibbs and Bara (1962) and virtually all the soils were shown to have the tendency to collapse upon wetting, the sole exception being the hard

yellowish sandy silt, M3, which was classed as a non-collapsing soil. According to the Gibbs and Bara criteria, all the soils were identified as being mostly likely collapsing soil (M.L.C.), except M3. The Denisov criteria state that soils with K_c above 1.0 are non-collapsing while those with K_c below 0.75 are highly collapsing soils, but no guidance is given for soils with intermediate values, i.e. 0.75-1.0. However, a number of the tested soils had K_c values only marginally above 0.75, namely 0.78 to 0.83 and these have been arbitrary classed as likely collapsing soils. On this basis it is clear that the two methods provide very similar indications of the risk of collapse in the various soils.

Further clarification of the quantitative risk of collapsing can be obtained from the various potentials I_c, I_L and I_T given in Table 5.3 from the collapsing tests. The degree of collapse and hence the classification as a collapsing soil depends on which of these factors is used as a criterion, so great importance is placed on the selection of the appropriate collapsing potential factor. Investigation of the various collapsing potentials, affecting the degree of collapsibility and the soil classification, is presented in the following paragraphs by analysing the collapsing test results in Table 5.3 in terms of the standardized method (ASTM, 1992).

The results in Table 5.3 indicate that overall I_c varied from -0.16 to 2.6%, 0.0 to 5.4% and 0.6 to 17.8% under the respective wetting stresses of 50, 100 and 200 kPa and this variation indicates that the soils display a wide range of collapsing characteristics. The values of I_L (Table 5.3) similarly varied from 0.5 to 1.9%, 0.32 to 2.8% and 1.3 to 3.3% under the same respective stresses, without wetting, apart from the values of the sandy silt, A1 at 2.2m, which gave the highest I_L values of 3.6, 7.6 and 10.3% under the respective stresses as indicated in Table 5.3. The limited variation in the values of I_L at each stress indicates that the soils have a narrow range of collapsing due solely to loading, apart from was A1 at 2.2m. Its behaviour may be due to the slight increase in the initial degree of saturation, S_o, (25 to 29%) at 2.2m compared with that at 1.1m of the same soil (18 to 24%) as shown in Table 5.3. At low stress levels, 50 and 100 kPa, the values of I_c and I_L are almost in the same range, while at the highest stress level, 200 kPa, the values of I_c are greater than those of I_L for all soils, apart from A1 at 2.2m. At 200 kPa, the ratio of I_c over I_L varied from 1.25 to 10.6 for all soils, apart from A1 at 2.2m, M3 and K2. Generally, the results indicate that the collapse potential, I_c, due to wetting under loading is responsible to the effect of wetting and so provides a better indicator of the extent of collapse than I_L. Increasing the stress level from 50 to 200 kPa significantly increased I_c from 1.0 to 10.8%, 0.14 to 7.6% and 2.6 to 10.5% for the soils A1 at 1.2m, M1 and K1 respectively while, in comparison, the corresponding I_L values only show limited increase in Table 5.3, from 1.7 to 2.7%, 1.0 to 3.3% and 1.1 to 2.4%. This indicates that the collapsing potential I_c is a function of the level of loading and, again, reflects the effect of stress level more significantly than I_L.

Indeed the collapsing soils, particularly Loess, have been characterised by such low deformation when loaded at the natural moisture, almost dry, state (Peck et al, 1974; Mitchell,

1976; Bell, 1992). Furthermore the collapsing identification and classification have generally been established on the basis of the collapse due to wetting, I_c, under loading rather than the collapse due only to loading, I_L, (Jennings and Knight, 1975; ASTM, 1992). There is concern that classification of the susceptibility to collapse in terms of their I_L, may give a false indication of the risk of collapse since the role of wetting is excluded. It is clear that the value of I_L is inappropriate as a criterion for predicting collapse and so I_c or I_T must be considered. However as I_L is involved in the summation to produce I_T, it is considered that I_c is the most reliable indicator of collapse potential.

As I_c provides the most reliable collapse potential indicator, this term will be used in classifying and analysing the collapsing behaviour of the investigated soils. Bearing in mind that, throughout the rest of the thesis when ever the collapse potential is mentioned it refers to the collapse due to wetting, I_c, while the total collapse I_T and the collapse due to loading I_L will be considered separately.

The collapsing potential (I_c) under the lowest stress, 50 kPa, was generally in the range of 0.12 to 1.01%, with a minimum value of -0.16 % for soil, M2, and the maximum value of 2.6% for soil K1. For values between 0.0 and 1.0%, the soil is classified (Table 5.2, ASTM, 1992) as non to slightly collapsing and would be expected to perform satisfactorily under this low stress, however the design of structures to be erected on the soil with a value of 2.6% would require some care. Indeed, a light structure at this site, IV, resting on soil K1, exhibited moderate cracks in the load bearing walls and finishes. In contrast is the expansive behaviour, indicated by the negative I_c value, of soil M2. Most of the silts, when wetted under no load exhibited free swell so an initial light stress (0.5 to 25 kPa) was applied to restrict this behaviour, although this was not effective with M2. In fact, such a behaviour may be expected due to its high clay content, 24%. Indeed, using the system developed by Mitchell (1976), this soil is shown in Figure 5.7 to have a swell potential of approximately 4%. Furthermore, this soil was tested at low moisture content of 18.5% which, although in range of the natural moisture content of 16 to 28%, it was significantly below the optimum value of 28%. Indeed the swelling under low loads of collapsing soils with high clay contents and low moisture content has been observed by others, (Burland, 1965; Jennings and Knight, 1975; Lawton et al, 1992). The role of montmorillonite can be discounted for earlier work (Al-Gasous, 1988) did not find it present in any of the soils of the Sana'a Plain.

The collapsing potential (I_c) under the moderate stress of 100 kPa ranged from 0.0 to 5.4% with the minimum I_c value being recorded with the hard stiff sandy silt, M3, and the maximum I_c value for the sandy silty clay, K1. Under this stress, the top horizon of the sandy silt and sandy silty clay, A1, M1 and K1, exhibited moderate collapse, with respective I_c values of 5.1, 2.1 and 5.4%, while the remaining soils had I_c values below 1.0%. Furthermore, no expansion was measured under the moderate loading.

At 200 kPa the collapsing potential (I_c) ranged from 0.6 to 13.8% for the soils. These values produced a wide range of collapsing classifications, ranging from slight to severe collapse. The stiff sandy silty clay, K2 and the hard stiff sandy silt, M3, were the only soils that exhibited a slight degree of collapse, with values below 2%, while the remainder were classified as having moderate to severe degrees of collapse. To investigate the collapsing behaviour at stress levels greater than 200 kPa, double oedometer and double isotropic compression (IC) tests were performed and the results from these tests are presented subsequently.

Figure 5.8 shows the variation in the collapse potential, I_c, with depth for sites, I, III, and IV from the single oedometer test. This potential varied under the different wetting stresses, both within the same layer and between layers. For all sites, it decreased with increasing depth for wetting stresses of 50 and 100 kPa. At the highest wetting stress, 200 kPa, the potential decreased for site IV but the trend was more varied at sites I and III. At this highest wetting stress, the variation can be related to individual variation in each soil profile. Although there was variation in the collapsing potential within a given layer under the different wetting stresses, in broad terms the value in each layer increased with the wetting stress. This increase was gradual for wetting stress up to 200 kPa in the top layers of sandy silt and sandy silty clay (A1, M1 and K1). Within the lower layers, the increase in I_c was marginal between 50 and 100 kPa but significantly larger increases were recorded with further increase in the wetting stress to 200 kPa, except for the sandy silty clay with gravel, K2, from site IV. The low increase in I_c of this particular layer can be attributed to the presence of highly cemented calcareous particles. Generally, the top horizons of the studied soils were susceptible to collapse when wetted at low stresses, 50 to 100 kPa, while the lower horizons only became susceptible when the wetting stress exceeded 100 kPa.

Figure 5.9 shows the variation in the total collapse potential, I_T, and the collapse potential due to loading only, I_L, for sites, I, III, and IV. The variations of I_T (dot lines) are very similar to those of I_c for all sites at the different stress levels, due to the large contribution of the high values of I_c to the values of I_T. In contrast, I_L (solid lines) varied slightly with depth over a limited range, apart from that within layer A1 at 2.2m, as indicated earlier.

The consequence of wetting in reducing the soil stiffness is apparent from the large difference in the stiffness values before (E_b) and after (E_a) wetting as shown in Table 5.3. The stiffness ratio may be used to compare the effect on collapsing behaviour of wetting under stress with that of loading before wetting. This can and also be used to distinguish between the bonding forces attributed to suction and those derived from cementing through chemical and clay bonds. Generally high stiffness ratios suggest the predominant role of the suction bond so that wetting has the major role on the collapsing, as shown from Figs. 5.1, 5.4 and 5.5 for the soils A1 at 1.2m, M1 and M4 respectively which were characterized by having low

cementation and open fabrics. In contrast, low stiffness ratios suggest either the presence of significant cementation bonds which minimize collapse under moderate stresses, as shown in Table 5.3 by M3 which had a medium, dense structure with considerable cementation agents, or a high initial degree of saturation and so that loading produced considerable deformation before wetting with only limited collapse after wetting as shown in Fig. 5.2 for the soil A1 at 2.2m and indicated in Table 5.3.

5.3 CONSOLIDATION CHARACTERISTICS

These include the consolidation behaviour from the double oedometer and isotropic compression tests for the soils at both the SMC and NMC states, with the appropriate collapsing potential being identified at any stage of loading during these tests.

5.3.1 Double Oedometer Test

5.3.1.1 Test Procedures

By employing the double oedometer test (Jennings and Knight, 1975), two nominally identical specimens can be tested at two different moisture states. Prior to each test the loading frame was levelled, the prepared sample was weighed and placed on the flat porous stone in the oedometer cell. Another porous stone was placed over the sample and a dial gauge, sensitive to 0.01mm, was mounted and adjusted under a setting load, equivalent to 0.5 to 1.0 kPa, to give the initial reading.

One specimen was kept at its natural moisture content throughout the test (NMC state), the top of the cell being wrapped in a damp cloth to minimize the moisture loss. The specimen was loaded incrementally starting typically from 6.25 kPa up to 800 or 1660 kPa, followed by unloading to either 100 or 200 kPa then reloading to 1660 kPa. The loading period for each increment was 24 hours for stresses between 200 and 1660 kPa both during the unloading and reloading stages, while a shorter period of 8 hours was used at the lower stresses. The dial gauge was read at the end of each period before applying the next load. Finally, after reloading at 1660 kPa for 24 hours, the damp cloth was removed and water was poured into the cell leaving the sample to collapse for another 24 hours before terminating the test, and removing the specimen to determine the final moisture content.

The second specimen was seated in the oedometer and soaked with water before loading. The remainder of the test procedure followed that of the consolidation test, in

accordance to method D 2435 of ASTM (1985) and the procedures are detailed in appendix C5-7.

The double oedometer test is still considered the most useful method for giving quantitative estimation of the magnitude of collapse, as indicated earlier in Chapter 2. Generally, it has been observed that the two compression curves, of the samples tested at both the NMC and SMC conditions, deviate from each other through out the test. Collapse is given by the difference between the two curves. Two forms of adjustment have been proposed by Jennings and Knight (1975) as presented in Chapter 2 (Sec. 2.2.3) and shown in Appendix A2-1. As the deformation trend of the studied soils exhibited slightly overconsolidated behaviour, the justification A2-1(b) was adopted. The soils are recent deposits with the apparent preconsolidation probably being due to cementation so the setting pressure was used instead of the overburden pressure, p_o, in A2-1(b) after Houston et al (1988). This adjustment was applied on the natural samples when there was variations in e_o.

Although these tests were carried out on the natural undisturbed, natural treated and laboratory destructured samples, this section only considers the results for the natural undisturbed soils, while those of the natural treated and laboratory destructured soils are presented in Chapters 6 and 7 respectively.

5.3.1.2 Test Results

Figs. 5.10 - 5.12 show typical consolidation curves for the soils, with a complete set of the curves being given in Appendices C5-8 to C5-11. As an illustration Fig. 5.10(a) shows the two curves obtained from tests carried out on two undisturbed samples of A1. One was tested at its natural moisture and soaked at the end of the test while the other was soaked before loading commenced. Similarly Fig. 5.10(b) shows the results for the same two tests performed on soil A2. The symbols on Figure 5.10(a) - A1En/N-1.0m - define the soil layer, A1, subjected to the Oedometer test (E) at the natural moisture content (n), En, while the last two terms refer to the sample condition as natural undisturbed, N, and the sample depth, 1.0m, below the ground level. For soaked tests "Es" is substituted for "En" and similarly in Figure 5.10(b) the soil is changed to A2 from A1 taken at a depth 3.0m rather than 1.0m. Similar nomenclature has been used for the remaining tests.

The initial condition of the specimens and results of the tests at the soaked condition are shown in Table 5.4 in terms of selected key parameters. The overburden pressure, σ_{vo}, was calculated from the in situ state, while the yield stress σ_y was determined by Casagrande's method, as illustrated in C5-11 (Wray, 1986). Throughout this study the traditional terms 'pre-consolidation pressure' and 'overconsolidation ratio' are replaced respectively by the yield stress, σ_y, and the yield stress ratio (YSR), σ_y/σ_{vo}, as defined by Burland, 1990. The compression index C_c was determined from the slope of the linear portion of the soaked consolidation curve. The swelling index C_s was determined from the

average slope of the unloading-reloading values. The coefficient of volume compressibility, m_v, was taken as the average value of the changes in void ratio corresponding to the changes in pressure from 50 to 100 and 100 to 200 kPa. The values of the coefficient of consolidation C_v were determined by the square root of time method (Wray, 1986). The average values of C_v, presented in Table 5.4, were based on the individual values at the following stress increments - 50, 100, 200, 400 kPa.

Table 5.5 summarises the initial properties and the results from samples tested at their natural moisture content, NMC, (partially saturated condition). These were obtained in the same way as those for the soaked condition, except that C_v values were not obtained for the NMC condition as they do not reflect the coefficient of consolidation at saturation, since the theoretical assumption of saturation was not satisfied at NMC.

5.3.1.3 Results Analysis and Interpretation

The climatic and geological history of the study area has conditioned the composition and structure of the soils and, thereby, has influenced their deformation characteristics. The data in Table 5.4 shows that the ratio of the yield stress to the overburden pressure ranged from 1.2 to 5.3 indicating that these soils were slightly over consolidated. Indeed, the soils within the Sana'a Plain are recent Quaternary deposits and they have not been subjected to any preloading (Kruck, 1983; Abduljauwad and Al-Gasous, 1991), although environmental and chemical effects have had a predominant effect on the apparent preconsolidation. These phenomena include drying and wetting, leaching, oxidation and the precipitation of chemical, clay, calcite and colloidal materials resulting in a cemented soil. The cementation acts as an apparent preconsolidation pressure (Mitchell, 1976) and, with all the soils being recent deposits, it is this cementation rather than the stress history that have produced the yield ratios shown in Table 5.4.

The double oedometer results, Figs. 5.10-5.12 and Tables 5.4 and 5.5, show typical patterns of behaviour that are compatible with those from the single oedometer test. In general, from Figs. 5.10-5.12, the curves at the natural moisture content are not steep under light to moderate stresses, from 200 to 400 kPa, but become steeper under larger stresses, with the exception of the sandy silt, G1, (Fig. 5.11(a)) due to its very low moisture content (9%) shown in Table 5.5. This indicates that the bonding forces of these soils contribute considerably to their deformation resistance under moderate loads, with the subsequent steepening indicating a partial breakdown of the bond between the particles. The load at which this occurs defines the yield stress, σ_{yn}, at the natural moisture state as shown in Table 5.5, and is dependent on the moisture content and the strength of the bond. In contrast, the deformation curves for the soaked soils display significant consolidation under even low stresses, 35 - 85 kPa. This deformation was considerably greater than that for similar soils tested at natural moisture state as shown in Figs. 5.10 - 5.12, apart from the stiff sandy silt,

M3, (Fig. 5.12(b)) and the sandy silt with calcareous gravels, A3 and K2 (C5-8 to C5-10 and Table 5.4)). These soils exhibited a tendency to resist consolidation (Figs. 5.10 - 5.12) until the applied stress exceeded the yield stress at the soaked condition, σ_y, beyond which excessive consolidation took place with increasing the stresses.

In Fig. 5.13 the oedometer results, for the soils from sites I and III, are replotted on a linear void ratio-pressure graph to illustrate the deformation trends at both the natural and soaked moisture conditions. Although this figure indicates that the deformation of these soils at the NMC condition was much less than at the SMC condition, the yield stress cannot be easily determined from such linear plots. However, the deformation curves for the soaked soils, which display significant consolidation under low stresses, indicate that the amount of consolidation depended on the initial density as shown in Fig. 5.13. The shape of these curves for the saturated soils is concave upward with the exception for the limited portion for stresses below the yield value. At higher stress levels, the curves converge to a narrow range of the void ratio.

When the soils at natural moisture content were wetted, at the end of the test, they collapsed to produce the same void ratio as that of each of their corresponding soaked samples (Sheeler, 1968; Burland, 1965; Ismael, 1993). For all these soils, the yield stress, σ_y, was greater than the overburden pressure σ_{vo} probably indicating the existence of some degree of cementation. The soils are characterized (Gibbs et al, 1960; Sheeler, 1968) by low natural dry densities, 1.07 to 1.28 Mg/m^3, apart from the stiff sandy silt, M3, with a medium density of 1.45 Mg/m^3 as shown in Fig. 5.13. Indeed, the increase in the dry density of this soil can be attributed to its high level of chemical precipitations and so it exhibited less deformation than the other soils due both to its higher cementation and dry density. Generally, the deformation of the soils at the NMC was affected by the initial moisture content, the applied stress and the extent of bonding while that of the saturated soils was affected by the initial density, the applied stress and the degree of cementation. At their natural moisture content the soils exhibited less compressibility and a higher yield stress than when tested at the soaked condition. Generally, the higher the water content, the lower the yield stress and the higher the volume change.

Figs. 5.14 and 5.15 show the variations in yield stresses, σ_y and σ_{yn}, and the yield stress ratio, YSR, with depth for sites I and III as obtained from the oedometer tests. All the values of yield stress exceed the corresponding overburden stress, with the soaked values being much lower than those at the natural moisture content. These results indicate the existence of bonding forces both from suction, as indicated by the rapid collapse as soon as the water was added, and cementation agents. Potential collapse due to wetting is demonstrated by $\sigma_{yn} > \sigma_y$ and potential destructuring by load is implied by $\sigma_y > \sigma_{vo}$. At stresses above yield, drastic volume change took place due to the breakdown of the remaining bonds.

The reduction in the yield stress following soaking is significally affected by the initial degree of saturation. Holtz and Gibbs (1951) stated that the void ratio-pressure relationships at different moisture contents demonstrate the structural properties of loess soil and the influence of cementation on the deformation characteristics of such soil. Reginatto and Ferrero (1973) defined the yield stress of the soaked soil, σ_y as the collapse pressure, p_{cs}, beyond which deformation increased considerably as shown in Fig. 5.16. They stated that this pressure cannot be defined as a preconsolidation pressure, as it varies with the degree of saturation. A similar limiting pressure is the yield stress at the natural moisture content, σ_{yn}, and this was defined as the collapsing pressure p_{cn} for a soil at its natural moisture content, so for collapsing deformation $p_{cn} > p_{cs}$. Under the effect of wetting and loading, collapsing soil can be identified as either truly or conditionally collapsing soil. Truly, collapsing soils are defined as those for which $p_{cs} < p_o$, where p_o is the overburden vertical pressure. When saturated, those soils will not support the stresses produced by the overburden and so large volume reduction takes place upon saturation without any external loading. This did not occur with the studied soils. In contrast, when $p_{cs} > p_o$ the soils are classed as conditionally collapsing and they are able to support a certain level of stress upon soaking or saturation. Under any applied pressure $p < p_{cs}$ no collapse occurs with soaking (Reginatto and Ferrero, 1973; Popescu, 1986). As a conclusion, all the investigated soils are conditionally collapsing soils and such identification is consistent with the reported results that σ_y exceeded σ_{vo}.

Increasing the moisture content to saturation produces a minimum yield stress and minimizes the yield stress ratio as indicated on Figures 5.14(c) and 5.15(c). The values of the YSR range from 1.2 to 5.3 for the SMC state and 2.5 to 30 for the NMC state. This reduction in the YSR between the NMC and SMC states reflects the high collapsibility due to wetting, while the residual YSR after wetting reflects the residual bonding forces (due to cementation) of the soil in the SMC state. At the soaked condition it is suggested that the soils are weakly bonded with an average yield stress ratio of 2.8. Some soils in the upper horizon exhibited greater values which may reflect the effect of drying and wetting and the effects of surface loading or sampling disturbance. The hard stiff sandy silt, M3, exhibited a high YSR, 3.9, again demonstrating its highly cemented structure. In general the YSR decreased with increasing depth, and this trend was more pronounced at the NMC than at SMC state as shown in Figs. 5.14(c) and 5.15(c).

The average compression index, C_c, at the steepest slope on the consolidation curves ranged from 0.282 to 0.639 and 0.113 to 0.994 respectively at the soaked and natural moisture contents. For loess soils, Holtz and Gibbs (1951) reported values of 0.27 for samples at the natural moisture and 0.33 for saturated samples, similar values being reported by Bradford and Norton (1983). The values for the studied soils are higher and this illustrates the effect of cementation in resisting consolidation. The data in Tables 5.4 and 5.5 show for some soils that the C_c values obtained at the NMC were greater than those from soaked samples, which reflects the sharp change in compressibility due to the failure of the bonding

forces at higher loads. At high values of C_c the slope of the consolidation curve becomes more pronounced due to the deterioration of the bonding materials, leading to excessive compressibility.

The swelling index, C_s of the soils ranged from 0.021 to 0.052 and 0.021 to 0.062 respectively for the soaked and natural conditions. All these values are very low, with both the maximum values, 0.052 and 0.062, being exhibited by the silt to silty clay, M2. Mitchell (1976) reported that the compressibility of saturated soils was dependent on the clay mineralogy and typical values for C_c, C_s and the coefficient of consolidation, C_v, for the major clay minerals are shown in Appendix C5-12, after Mitchell (1976). The reported values of C_s are in the range for kaolinite while those for C_c at the soaked condition given in Table 5.4, span the range for kaolinite and montmorillonite. However, no montmorillonite has been detected in the soils of the Sana'a region (Abduljauwad and Al-Gasous, 1991) and so the high values of C_c probably reflect the effects of oxidation and cementation. Furthermore, the C_c values from the isotropic compression (next Section) are below the lower limit for montmorillonite, 0.5, with the exception of the soil M2 which has a value of 0.554, as shown in Table 5.6(b). The reported values of C_v are typical of the kaolinite, as shown in C5-12, again suggesting the existence of cementation rather than the presence of montmorillonite.

The coefficient of the volume compressibility, m_v, ranged from 0.26 to 0.56 m^2/MN and 0.06 to 0.4 m^2/MN respectively for the soaked and natural moisture conditions. Using the criteria presented by Tomlinson (1980), soil M3 is of medium compressibility ($m_v = 0.1$-0.3 m^2/MN), while for all the other soils in Table 5.4 are classified as highly compressible ($m_v = 0.3$-1.5 m^2/MN). These highly compressible soils having already been classified as moderate to severe collapsing soils, while M3 was the only one classified as a slightly collapsing soil. These results suggest that the collapsing potential would appear to be related to the compressibility of the soaked soils, the higher the compressibility the higher the possible collapsing potential.

Figure 5.17 shows the variation in the collapsing potential (I_c) for stresses up to 1660 kPa from the double oedometer test for all the soils from sites I, III and IV. The behaviour shown in Fig. 5.17 is similar to that reported earlier with all the soils exhibiting only a limited collapse potential below a stress of 50 kPa. At stresses between 50 and 100 kPa, two types of behaviour are apparent, with the top sandy silt soils exhibiting a rapid increase in I_c values to reach the moderate collapsing stage, ($I_c = 2$ to 6%), while the soils from below 1.5m exhibit only a slight risk of collapse with limited increases in I_c. Two soils the silt with sand, A2, and the silt, M2, did not follow this trend and this may be due to slight variations in their initial properties, as seen by comparison of the data in Tables 5.3, 5.4, and 5.5. This is compatible with the variation apparent in Tables 4.4 and 4.5 and is attributed to seasonal variations within the Sana'a Plain, which can influence the collapsing potential of all soils. The variation in the initial moisture content (W_n) of the soil M2 is an example of such effect as

shown in Fig. 5.17(b). Increasing it from 22% to 28% reduced the collapse potential under all the applied loads. Increasing the stress from 100 to 200 kPa produced rapid increases in the collapsing potential of all the soils, apart from the stiff sandy silt, M3, and the sandy silty clay with gravel, K2, which displayed only a slight risk of collapse as was also indicated in the single oedometer test.

Beyond 200 kPa the soils exhibited a rapid increases in the collapsing potential with the exceptions of the stiff sandy silt, M3, with only a moderate increase and the M2 soil, at the high initial moisture content of 28%, where I_c decreased. For all the soils from sites I and III, apart from M1 and M3, the maximum collapsing potential was reached at an applied stress of 400 kPa, while those from site IV exhibited increases for pressures up to 800 kPa. Indeed, the stress at which the maximum collapsing potential is reached defines the critical collapsing stress (P_{cc}), beyond that the collapsing potential either remained constant or decreased. This change in the collapsing potential is related to the significant change in the deformation of the NMC sample, due to the considerable breakdown of the bonding forces beyond the P_{cc} stress. The values of P_{cc} can be estimated from Fig. 5.17 as shown for soil A1 (5.17(b)). These values ranged between 400 and 800 kPa, apart from the silt M2 with a P_{cc} values of 100 and 300 kPa corresponding initial moisture content of 28% and 22% respectively. The value of P_{cc} is affected by the initial moisture content as shown by these results from soil, M2, interesting that the higher the moisture content the lower the collapsing potential and the lower the critical collapsing stress. This should be carefully considered in selecting the design stress where the shear strength established at the in situ moisture content may be used for design.

Fig. 5.18 shows the trends of the total collapse (I_T) and the loading collapse (I_L) potentials from the double oedometer test for representative soils. Both I_T and I_L increased progressively with increase in the applied stresses and no rapid changes are shown unlike the collapse due to wetting, I_c, that markedly changed. The figure also indicates that, at stresses up to 200 kPa, the values of I_L varied over a narrow range, similar to the results from the single oedometer test, while beyond this stress level significant increases are apparent with values of 16 to 22% at a stress of 1660 kPa. In contrast the values of I_T increased rapidly at the stress increased up to 200 kPa, again as shown by the results from the single oedometer test, while beyond this stress level the rate of increase started to decrease, reaching values of 27 to 33% at 1660 kPa.

5.3.2 Isotropic Compression (IC) Test

This test was carried out, as a complementary test, on representative soils (A1, A2 M2, and M3) to compare and correlate their collapsing and deformation behaviour under the isotropic compression with that obtained from the single and double oedometer tests.

5.3.2.1 Test Procedures

This test was carried out on 8 specimens of the undisturbed natural soils. Four representative soils - A1, A2, M2 and M3 - were selected and subjected to the double isotropic compression test (IC), on the same basis as the double oedometer test. Two specimens of each soil were isotropically compressed with incremental stresses of 25, 50, 100, 200 and 400 kPa, this last value being the maximum that could be achieved with the test equipment. One specimen was tested at its natural moisture content, the other being saturated before applying the isotropic stress. The specimens were obtained from undisturbed block samples by trimming, each to a height of 76mm and a diameter of 38mm. The specimen setting up and saturation procedures were similar to those of the consolidated drained triaxial test, without the shearing stage, described by Wrey (1986) and Bowels (1988). The effect of saturation on the volume change of the specimens tested at the SMC state was monitored. The test procedures are described herein.

1- After saturation, the specimen was isotropically consolidated to equilibrium under the first applied confining pressure, 25 kPa, and the volume change was measured.

2- The second isotropic consolidation at 50 kPa was undertaken and the specimen was similarly allowed to consolidate to equilibrium. The volume change was also measured and these procedures were repeated under confining pressures of 100, 200 and 400 kPa.

3- When the equilibrium was reached at 400 kPa, the apparatus was dismantled and the specimen was removed to determine the final moisture content.

5.3.2.2 Test Results

The relationships between the void ratio and applied pressure (cell pressure) for these representative soils are given in Figs. 5.19 and C5-13 (dark lines). The key for each graph is similar to that used for the oedometer tests, except that the symbol "I" (isotropic compression) replaces the "E" which denoted the oedometer test. The initial conditions and the individual results are shown in Table 5.6 for both testing conditions.

5.3.2.3 Results Analysis and Interpretation

These results, Figs. 5.19 and C5-13 and Table 5.6, show similar patterns of behaviour to those obtained from the oedometer tests. However, the deformation curves lie slightly above those obtained from the oedometer tests (dot lines), particularly for samples tested at the SMC state (dark symbol) as shown in Figs. 5.20 and C5-13, where the respective consolidation curves for each soil are superimposed in the e-log p space. Furthermore, Table 5.7 provides comparison of the yield stress ratios obtained from these tests at both the NMC and SMC states and, although there are small variations in the results,

in general they are compatible. These small variations can be attributed to variations in the sample dimensions, the confining strains and the method of loading.

The relationship between collapsing potential (I_c) and applied stress obtained from the isotropic compression test for soils from sites I and III, are shown in Fig. 5.21. The effect of variations in the initial dry density of saturated samples of A1 and M2 soils, and the moisture content of the NMC samples of A2, are included in the figure (3 extra samples). The effects on the I_c values were limited, apart from soil M2 (Fig. 5.21-b), which exhibited a considerable decrease in I_c due to the increase in the initial dry density. The general trend for A1, A2 and M2 is broadly similar to that from the oedometer tests with the collapsing potential increasing with increased applied stress, although the greatest values of the collapsing potential ($I_{c\ max}$) for these samples were reached at a lower applied stress (P_{cc}), 200 kPa, apart from M2 with ρ =1.17 Mg/m^2. These values are slightly lower than those obtained in the oedometer test for the same soil, as can be seen from the comparable data in Table 5.8, and this may be attributed to differences in the dimensions of the test specimen and the type of loading. Crawford (1964) and Holtz et al. (1986) indicated that the rate of loading and the type and manner of testing can affect the configuration of the consolidation curve and the characteristics of deformation, such as the yield stress and the compression index. Rizkallah (1989) reported that the collapsing potential decreased with increased specimen height. Furthermore, Feda (1988) compared the collapsibility coefficients, $\iota_c = \Delta\varepsilon_a/(1-\varepsilon_a)$ where $\Delta\varepsilon_a$ is the additional axial strain due to wetting and ε_a is axial strain at the same stress before wetting, determined from both triaxial and oedometer samples, for the particular loess soils. The oedometer gave a mean ι_c value of 9.5% (ranges 8.4 to 11.1%) whereas the triaxial apparatus yielded a mean value of 8.2% (ranging from 5.8 to 10.2%) and he considered that these were compatible given the differences between the tests. Similar variation in the I_c and the corresponding collapsing classification of the different soils can be seen in Table 5.8 where this data is presented with the maximum values of the collapsing potential ($I_{c\ max}$) and the corresponding values of the critical collapsing stress (P_{cc}) from the various tests.

5.4 SUMMARY AND GENERAL COMMENTS

From the previous discussion, the following main remarks are drawn:

1) By applying the qualitative criteria of Denisov (1951) and Gibbs and Bara (1962) for identifying collapsing soils, the studied soils were identified as likely to most likely collapsing soils, apart from the stiff sandy silt, M3.

2) The results of the oedometer, single and double, and IC results have enable the collapsing characteristics for the studied soils to be summarized as follows:

- The collapsing potential upon wetting under loading, I_C, is significantly greater than the collapsing potential due to loading, I_L, only. At stresses up to 200 kPa, the values of I_C varied over a wide range while I_L only varied over a narrow range. Beyond 100 kPa, the I_C values increased rapidly with increase in the stress until a maximum collapsing potential was reached at the critical collapsing stress, beyond which it either decreased or remained constant. In contrast, the I_L values increased only slightly with increase in stress up to 200 kPa, but beyond that limit it increased considerably with further stress increase. The trend of the total collapsing potential, I_T, is similar to that of I_C at stresses up to 200 kPa, beyond which it exhibited increase with further stress increase.

- Soil collapsibility cannot be classified in terms of either the collapsing potential due to loading, I_L, or the total collapse potential, I_T, the collapsing potential upon wetting, I_C, represents the most appropriate term for a collapsing classification system.

- Based on the values of I_C at 200 kPa, the studied soils were classified as non to severe collapsing soils, with those from the upper horizon (A1, M1, G1 and K1) being more susceptible to collapse than those at depth (M3, M4, A3 and K2). At stresses up to 100 kPa, only the soils of the upper horizons were susceptible to collapse when wetted, while the lower horizons only became susceptible when the wetting stress exceeded 100 kPa. Therefore, the removal of the top horizon, 1.0 to 1.5m, is recommended to provide a foundation base with reduced collapsing potential.

- For the same soil the values of the collapsing potential (I_C) from the IC test were slightly lower than those obtained in the oedometer test.

- For all the soils, the maximum collapsing potentials ($I_{C\ max}$), obtained from the oedometer, were reached at critical collapsing stresses (P_{CC}) of 400 to 800 kPa, apart from M2 (at 300 kPa) and K2 (at 1660 kPa).

3) The results of the double oedometer and isotropic compression tests have been used to summarise the consolidation behaviour, at both the SMC and NMC states, as follows:

- For all the soils, the yield stress, σ_y, was greater than the overburden pressure σ_{vo}, with all the soils being recent deposits, this probably indicates the existence of some degree of cementation. This cementation acts as an apparent preconsolidation pressure, consequently the soils were identified as slightly overconsolidated.

- Generally, the deformation of the soils at the NMC and SMC states was affected by the initial moisture content, dry density, the applied stress and the magnitude of bonding forces. At their natural moisture content the soils exhibited less compressibility and a higher yield stress than at the soaked condition.

- At the NMC state the bonding forces contributed considerably to the deformation resistance under moderate stresses while, at the soaked state, the soils displayed significant consolidation under low stresses, 35 - 85 kPa, apart from the stiff sandy silt, M3, and the sandy silt with calcareous gravels, A3, K2 and M4.

- As the yield stress exceeded the corresponding overburden stress, all the soils were rated as conditionally collapsing.

- At the soaked condition (SMC), the soils were identified as being weakly bonded with an average yield stress ratio of 2.8, while at the NMC the soils were considered to be weakly to strongly bonded with a yield stress ratio range from 2.5 to 30. This indicates the effectiveness of the suction or capillary bonds at the NMC state and so the susceptibility to collapse upon wetting. In general the YSR decreased with increasing depth, and this trend was more pronounced at the NMC than at SMC state.

- The values of C_C, C_S and C_V were in the range for Kaolinite and these results are consistent with the mineralogical identification.

- The collapse and consolidation results from the oedometer and IC tests, in general, were compatible, despite small variations which were attributed to variations in the sample dimensions and the type of loading. Such variations produced slightly lower values of both the I_c and the P_{cc} from IC test compared to those from the oedometer test for the same soil.

Table 5.1 : The collapsing criteria for the studied soils.

Soil layer	Soil type and description	Depth m	Denisov's (1951) method				Gibbs and Bara (1962) method				
			e_o	e_L	K_c (e_L/e_o)	Status *	G_s	γ_d kN/m³	LL %	W_s ¥ %	Status ®
A1	Light brown sandy silt	1.5	1.253	0.812	0.65	H.C.	2.8	12.2	29	44	M.L.C.
A2	Reddish brown silt with sand	3.0	1.536	1.2	0.78	L.C.	2.79	10.8	43	55	M.L.C.
G1	Light brown sandy silt	1.2	1.23	0.77	0.63	H.C.	2.75	12.1	28	44	M.L.C.
G2	Reddish brown silt with sand	2.5	1.5	1.127	0.75	H.C.	2.75	10.8	41	55	M.L.C.
M1	Brown sandy silt	1.0	1.253	0.977	0.78	L.C.	2.79	12.2	35	45	M.L.C.
M2	Blackish brown silt to silty clay	2.2	1.536	1.283	0.83	L.C.	2.79	10.8	46	55	M.L.C.
M3	Yellowish to greyish brown sandy silt	3.0	0.9	0.935	1.04	N.C.	2.75	14.2	34	32	N.C.
M4	Reddish brown sandy silt with calcareous gravel	4.0	1.26	0.963	0.76	L.C.	2.79	12.1	35	45	M.L.C.
K1	Light brown sandy silty clay	1.5	1.196	0.715	0.6	H.C.	2.75	12.3	26	43	M.L.C.
K2	Brown sandy silty clay with calcareous gravel	3.0	1.178	0.963	0.812	L.C.	2.75	12.4	35	43	M.L.C.

* L. C. : Likely collapsing soil
H. C. : Highly collapsing soil

® N. C. : Non-collapsing soil, if $W_s <$ LL
M. L. C. : Most likely collapsing soil, if $W_s \geq$ LL

¥ $W_s = \dfrac{(\gamma_w\, G_s - \gamma_d)}{G_s * \gamma_d}$

Table 5.2 : Classification system for assessing collapsing soils.
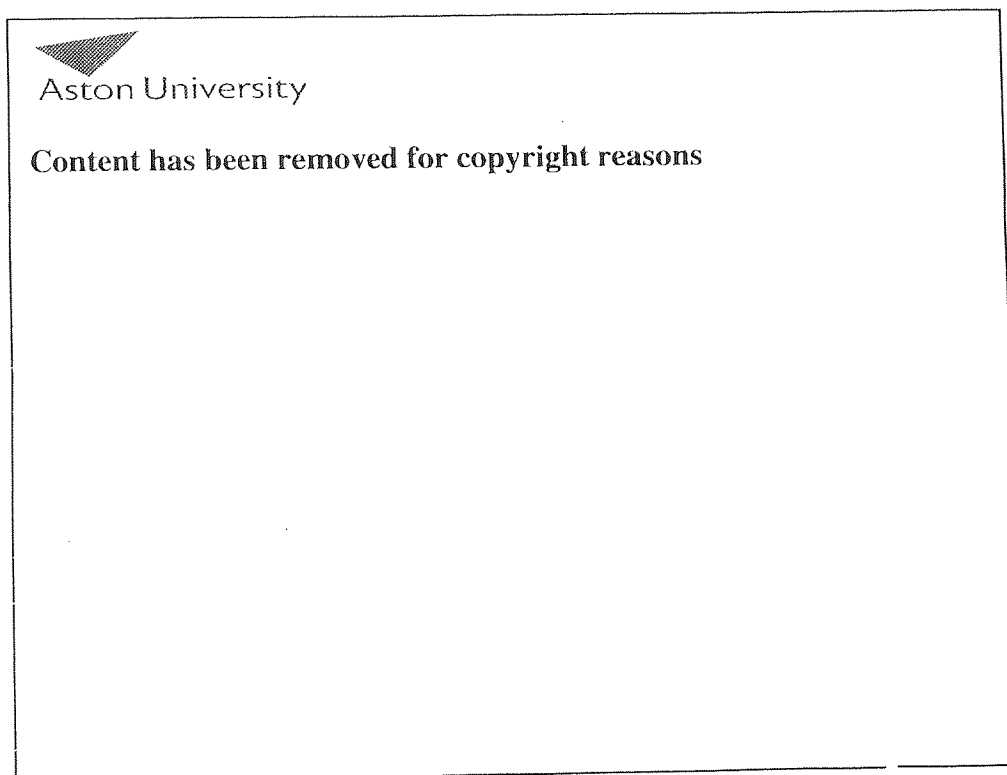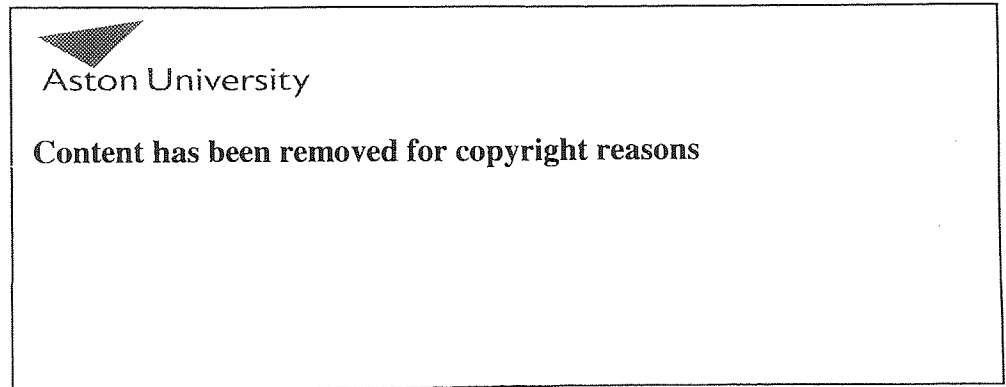
Table 5.3 : Summary of the collapsing data obtained from the single oedometer test.

Site	Layer and sample name	Depth m	Natural moisture W_n %	Wet density ρ_n Mg/m³	Dry density ρ_d Mg/m³	Natural void ratio e_o	Degree of saturation S_o %	S_f %	Wetting stress σ_w kPa	I_c %	I_L %	I_T %	ratio I_c/I_L	before wetting E_b kPa	after wetting E_a kPa	ratio E_b/E_a
I	A1COL/N-50	1.2	7.7	1.356	1.264	1.22	18	78	50	1.0	1.7	2.7	0.59	2172	1081	2.01
	A1COL/N-100	1.2	10.3	1.379	1.275	1.2	24	92	100	5.1	2.0	7.1	2.55	7588	1367	5.6
	A1COL/N-200	1.2	9.0	1.397	1.275	1.19	21	92	200	10.8	2.7	13.5	3.8	9855	2930	3.87
	A1COL/N-50	2.2	12.6	1.407	1.254	1.236	29	94	50	0.9	2.7	3.6	0.33	6973	1461	4.77
	A1COL/N-100	2.2	12.1	1.417	1.244	1.244	27	100	100	2.2	5.4	7.6	0.41	1674	1606	1.04
	A1COL/N-200	2.2	10.1	1.428	1.417	1.154	25	100	200	3.0	7.3	10.3	0.41	3817	2748	1.39
	A2COL/N-50	3.0	19.1	1.315	1.111	1.482	35	95	50	0.25	1.0	1.25	0.25	5013	1051	4.77
	A2COL/N-100	3.0	25.5	1.275	1.020	1.74	41	99	100	1.15	1.9	3.05	0.61	6590	1095	6.0
	A2COL/N-200	3.0	22.2	1.438	1.173	1.372	45	97	200	4.8	3.9	8.7	1.23	4565	2174	2.1
	A3COL/N-50	3.8	18.0	1.479	1.253	1.187	42	85	50	0.2	0.8	1.0	0.25	7107	5497	1.29
	A3COL/N-100	3.8	17.7	1.479	1.255	1.19	42	94	100	0.7	1.5	2.2	0.47	11011	1633	6.74
	A3COL/N-200	3.8	17.7	1.458	1.244	1.218	41	100	200	8.5	2.2	10.7	3.86	9879	2305	4.28
II	G1E(s,n)/N-200^f	1.2	11.3	1.377	1.244	1.231	25	--	200	13.8	1.3	15.1	10.6	27612	3126	8.8
	G1COL/N-200	1.7	11.6	1.366	1.224	1.261	26	98	200	5.1	1.4	6.5	3.64	1684	1644	1.02
	G2COL/N-200	2.5	11.8	1.230	1.101	1.518	22	99	200	17.8	2.7	20.5	6.6	7266	3037	2.44

(Table 5.3 : Continued)

Site	Layer and sample name	Depth m	W_n %	ρ_n Mg/m³	ρ_d Mg/m³	e_o	S_o %	S_f %	σ_w kPa	I_c %	I_L %	I_T %	I_c/I_L	E_b kPa	E_a kPa	E_b/E_a
	M1COL/N-50	1.0	11.2	1.468	1.326	1.11	28	97	50	0.14	1.0	1.14	0.14	6164	3721	1.7
	M1COL/N-100	1.0	14.4	1.489	1.305	1.138	35	91	100	2.1	2.8	4.9	0.75	5000	2390	2.1
	M1COL/N-200	1.0	14.4	1.438	1.264	1.218	32	99	200	7.6	3.3	10.9	2.3	9855	2930	3.36
	M2COL/N-50	2.2	18.5	1.346	1.136	1.455	35	89	50	-0.16	1.2	1.04	--	5538	4050	1.37
	M2COL/N-100	2.2	19.6	1.407	1.175	1.374	40	99	100	0.63	0.32	0.99	2.0	6894	1819	3.79
III	M2COL/N-200	2.2	22.8	1.374	1.118	1.496	42	99	200	7.5	2.4	9.9	3.1	8735	2276	3.84
	M3E(s,n)/N-50[f]	2.8	15.0	1.624	1.417	0.955	43	100	50	0.12	1.7	1.82	0.07	4560	4559	1.0
	M3E(s,n)/N-100[f]	2.8	15.0	1.624	1.417	0.955	43	100	100	0.0	2.7	2.7	0.0	5193	4559	1.13
	M3COL/N-200	2.8	11.4	1.645	1.477	0.862	36	97	200	1.3	1.8	3.1	0.72	14146	5700	2.6
	M4COL/N0-50	3.8	18.2	1.458	1.234	1.257	40	90	50	0.13	0.85	0.98	0.15	6241	6208	~1
	M4COL/N0-100	3.8	19.7	1.458	1.213	1.296	42	90	100	0.1	1.1	1.2	0.09	12661	5640	2.24
	M4COL/NO-200	3.8	18.2	1.458	1.234	1.252	41	95	200	5.6	2.3	7.9	2.43	12326	2853	4.32

(Table 5.3 : continued)...

Site	Layer and sample name	Depth m	W_n %	ρ_n Mg/m³	ρ_d Mg/m³	e_o	S_o %	S_f %	σ_w kPa	I_c %	I_L %	I_T %	I_c/I_L	E_b kPa	E_a kPa	E_b/E_a
	K1COL/N-50	1.0	12.0	1.397	1.244	1.204	27	100	50	2.6	1.1	3.7	2.36	3834	996	3.85
	K1COL/N-100	1.0	14.0	1.384	1.213	1.266	30	100	100	5.4	2.6	8.0	2.08	4945	1083	4.56
	K1COL/N-200	1.0	12.0	1.458	1.300	1.154	30	100	200	10.5	2.4	12.9	4.4	12993	2808	4.63
IV	K1COL/N-50	2.0	13.1	1.495	1.322	1.081	33	97	50	0.32	1.9	2.22	0.17	2152	5440	0.4
	K1COL/N-100	2.0	18.7	1.498	1.261	1.180	43	100	100	0.75	2.1	2.85	0.36	5939	.2660	2.23
	K1COL/N-200	2.0	15.5	1.502	13.01	1.113	38	100	200	3.0	2.4	5.4	1.25	11617	2454	4.63
	K2COL/N-50	3.5	19.1	1.430	1.200	1.289	41	88	50	0.15	0.5	.65	0.3	24782	9170	2.7
	K2COL/N-100	3.5	11.1	1.470	1.324	1.08	28	84	100	0.48	1.5	1.98	0.32	6081	5159	1.18
	K2COL/N-200	3.5	18.9	1.467	1.234	1.229	42	100	200	0.6	2.3	2.9	0.26	8988	2556	3.52

f The values are obtained from the double oedometer tests.

Table 5.4 : Summary of the oedometer test results of the soaked natural soils.

Soil layer	Depth m	Natural moisture W_n %	Wet density ρ_n Mg/m³	Natural void ratio e_o	Initial saturation S_o %	Overburden pressure σ_{vo} kPa	Yield stress σ_y kPa	YSR σ_y / σ_{vo}	C_c	C_s	$m_v \times 10^{-4}$ m²/kN	$C_v \times 10^{-7}$ m²/sec
A1	1.0	10.1	1.446	1.124	25	14.2	35	2.5	0.282	0.021	3.02	1.46
	2.0	10.9	1.347	1.304	23	26.4	50	1.9	0.344	—	3.3	1.0
A2	3.0	17.3	1.305	1.508	32	38.4	69	1.8	0.624	0.036	5.56	1.29
A3	3.8	17.0	1.479	1.207	39	48.1	130	2.7	0.551	—	5.57	—
G1	1.2	13.7	1.407	1.232	31	16.6	50	3.01	0.418	—	4.04	—
	1.7	12.5	1.397	1.229	28	23.2	57	2.44	0.30	—	5.15	—
G2	2.8	15.5	1.264	1.523	28	34.8	43	1.2	0.578	—	5.3	—
M1	1.0	14	1.346	1.366	29	13.2	70.0	5.3	0.512	0.032	4.8	1.4
M2	2.2	25	1.346	1.569	44	29.0	82.0	2.8	0.639	0.053	5.6	1.0
M3	3.0	12.7	1.631	0.905	41	41.0	160.0	3.9	0.390	0.025	2.55	0.98
M4	3.9	19.4	1.397	1.382	39	53.5	130	2.43	0.595	0.022	4.55	0.8
	4.0	16.8	1.479	1.207	39	58.0	170	2.93	0.616	—	3.04	—
K1	1.2	14.2	1.540	1.035	38	18.1	82	4.5	0.466	0.026	5.2	2.7
	2.3	20	1.489	1.227	45	35.6	170	4.8	0.566	0.023	4.47	2.75
K2	3.5	14.7	1.438	1.201	34	49.3	140	2.83	0.566	0.028	3.71	3.2

Table 5.5 : Summary of the oedometer test results of the soils at the natural moisture state.

Soil layer	Depth m	W_n %	ρ_n Mg/m³	e_o	σ_{vo} kPa	σ_{yn} kPa	σ_{yn}/σ_{vo}	C_c	C_s	$m_v \times 10^{-4}$ m²/kN
A1	1.2	8.9	1.407	1.16	16.6	320	19.3	0.368	0.053	3.85
A1	2.0	8.6	1.356	1.244	26.6	>400	>15	0.116	—	3.74
A2	3.0	17.0	1.315	1.481	38.7	700	18.1	0.994	0.043	0.61
A2		16.6	1.337	1.433	39.3	500	12.7	0.847	0.034	0.56
A3	3.8	17.1	1.490	1.192	49.0	>400	>8	0.176	—	1.23
G1	1.2	9.0	1.356	1.231	15.9	400	2.5	0.153	—	4.04
M1	1.2	14.3	1.458	1.234	15.0	450	30	—	—	1.03
M2	2.2	28.4	1.377	1.589	30.3	270	8.9	0.654	0.062	2.91
M2		21.2	1.336	1.514	28.8	620	21.5	0.979	0.021	0.9
M3	3.0	12.0	1.621	0.9	47.7	600	12.6	0.468	0.026	1.13
M4	3.9	17.8	1.489	1.206	61.2	450	7.35	0.624	—	0.86
K1	1.0	12.2	1.509	1.05	14.8	180	12.2	0.744	—	0.744
K1	2.0	17.7	1.407	1.293	27.7	350	12.6	0.233	—	1.13
K2	3.0	16.1	1.316	1.42	38.7	800	20.6	0.342	—	0.753
K2		15.0	1.479	1.138	43.5	>800	>18.4	0.113	—	0.783

Table 5.6 (a) : Summary of the isotropic compression test results for natural soils at the natural moisture.

Soil layer	Depth m	Natural moisture W_n %	Wet density ρ_n Mg/m³	Natural void ratio e_o	Overburden pressure σ_{vo} kPa	Yield stress σ_{yn} kPa	YSR σ_{yn}/σ_{vo}	C_c	C_s	m_v X 10⁻⁴ m²/kN	C_v X 10⁻⁷ m²/sec
A1	1.0	12.0	1.224	1.19	24.8	>200	>81	0.342	—	1.37	—
A2	3.0	17.8	1.290	1.545	38.0	>200	>5.3	0.585	—	1.18	—
M2	2.2	26.0	1.386	1.536	29.9	>200	>6.7	0.399	—	1.46	—
M3	2.8	11.4	1.613	0.902	44.3	>400	>9	0.056	—	0.74	—

Table 5.6 (b) : Summary of the isotropic compression test results for natural soils at the saturated conditions.

Soil layer	Depth m	W_n %	ρ_n Mg/m³	e_o	σ_{vo} kPa	σ_y kPa	YSR σ_y/σ_{vo}	C_c	C_s	m_v X 10⁻⁴ m²/kN	C_v X 10⁻⁷ m²/sec
A1	1.0	10.7	1.387	1.2	24.5	85	3.5	0.388	—	4.75	—
A2	3.0	17.0	1.285	1.536	37.9	120	3.20	0.482	—	4.18	—
M2	2.2	27.1	1.397	1.536	30.1	80.0	2.7	0.554	—	5.70	—
M3	2.8	12.0	1.632	0.89	44.8	>400	>8.9	0.103	—	0.79	—

Table 5.7 : Yield stress ratio of the representative soils from the oedometer and isotropic compression tests.

Soil layer	Soil type	Depth	σ_{vo}	Yield stress ratio (YSR)			
				Double oedometer		Istropic compression	
		m	kN/m^2	Natural $\sigma_{yn} / \sigma_{vo}$	Soaked σ_y / σ_{vo}	Natural $\sigma_{yn} / \sigma_{vo}$	Saturated σ_y / σ_{vo}
A1	Sandy silt	1.8	24.5	17.5	2.2	>8.1	3.5
A2	Silt with sand	3.0	38.5	15.4	1.8	>5.3	3.2
M2	Silt/silty clay	2.2	29.4	15.2	2.8	>6.7	2.7
M3	Sandy silt	2.8	44.4	12.6	3.9	>9.0	8.9

Table 5.8 : Summary of the collapsing characteristics and the collapsing classification of the different soils.

Soil layer	Soil type	Depth m	Collapsing potential at 200 kPa (I_c) (%)*			Collapsing soil classification	$I_{c\ max}$ %	P_{cc} @ kPa
			Single oedometer	Double oedometer	Isotropic comp.			
A1	Sandy silt	1.8	3.0 - 10.0	2.0 - 5.0	6.6	moderate to moderately severe	9.0	400
A2	Silt with sand	3.0	5.0 - 17.0	10.0 - 12.2	4.9 - 5.5	moderate to severe	19.8	800
A3	Sandy silt with gravel	3.9	8.5	5.2	--	moderate to moderately severe	10.2	400
M1	Sandy silt	1.0	7.6	6.0	--	moderatly severe	16.6	800
M2	Silt/silty clay	2.2	7.5	1.7 - 7.9	2.6 - 10.6	slight to moderately severe	9.8	300
M3	Sandy silt	2.8	1.3	1.3	0.4	slight	6.2	800
M4	Sandy silty clay with gravel	3.8	5.6	3.7	--	moderate	10.4	400
K1	Sany silty clay	1.5	3.0 - 10.5	2.7 - 10.0	--	moderate to moderately severe	19.2	800
K2	Sany silty clay with gravel	3.5	0.6	0.2 - 3.3	--	slight to moderate	13.0	1660

* : The collapsing potential at 200 kPa is defined as the Collapse Index, I_{cx}, after ASTM (1992).   @ : From the double oedometer test.
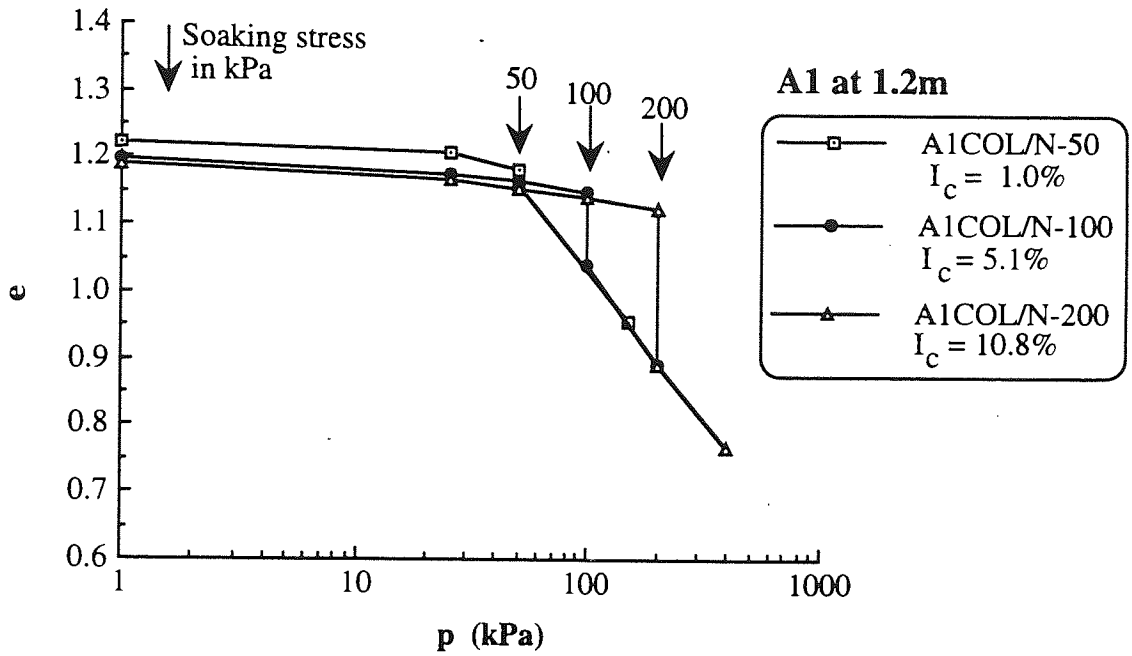
Fig. 5.1 : Collapsing potential of A1 from 1.2m below the surface.
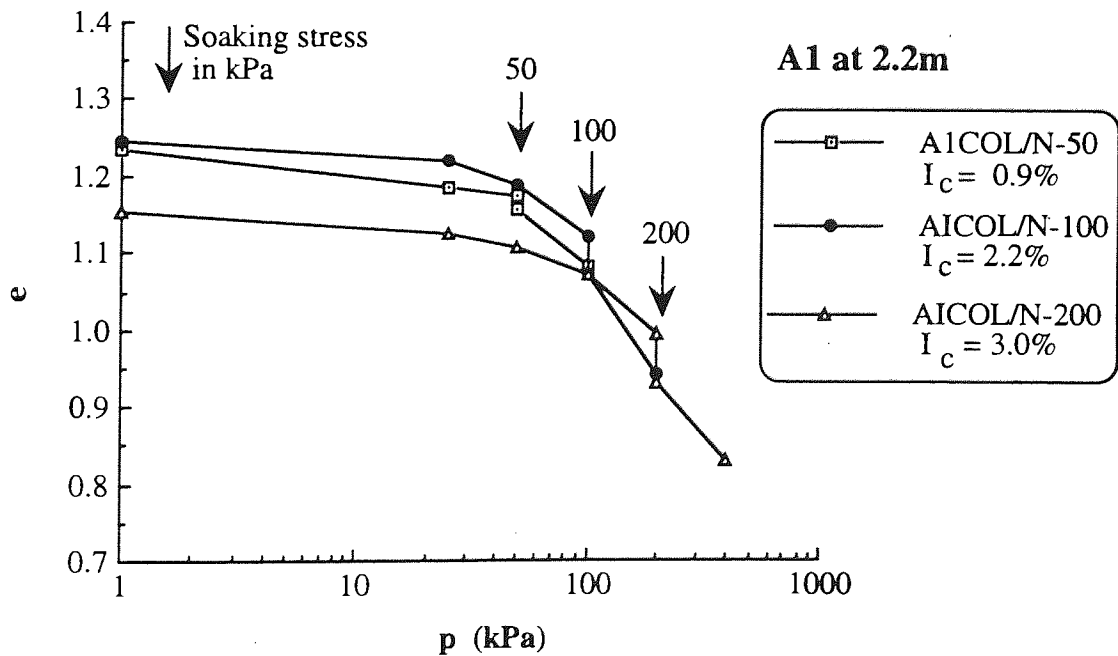
Fig. 5.2 : Collapsing potential of A1 from 2.2m below the surface.
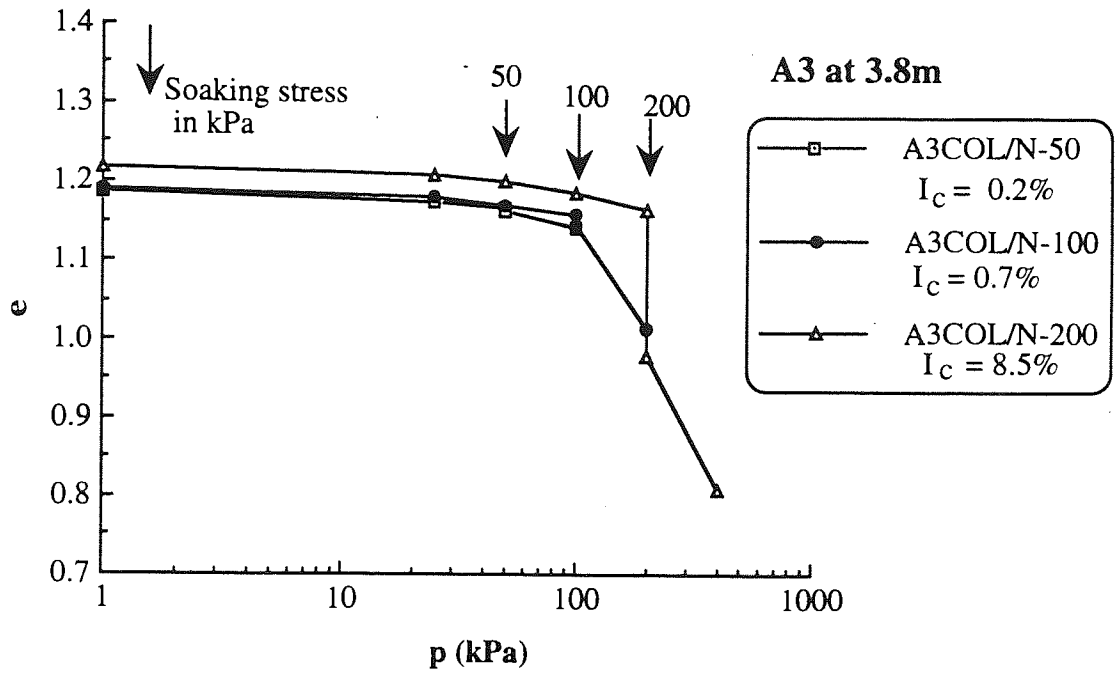
Fig. 5.3 : Collapsing potential of A3 from 3.8m below the surface.
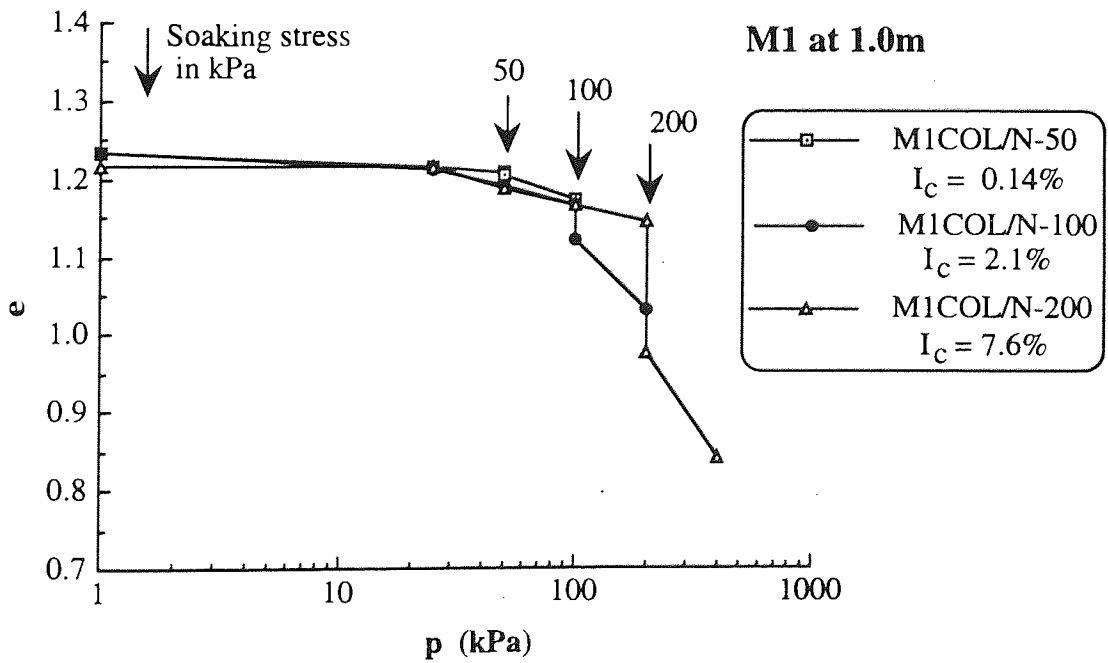
Fig. 5.4 : Collapsing potential of M1 from 1.0m below the surface.
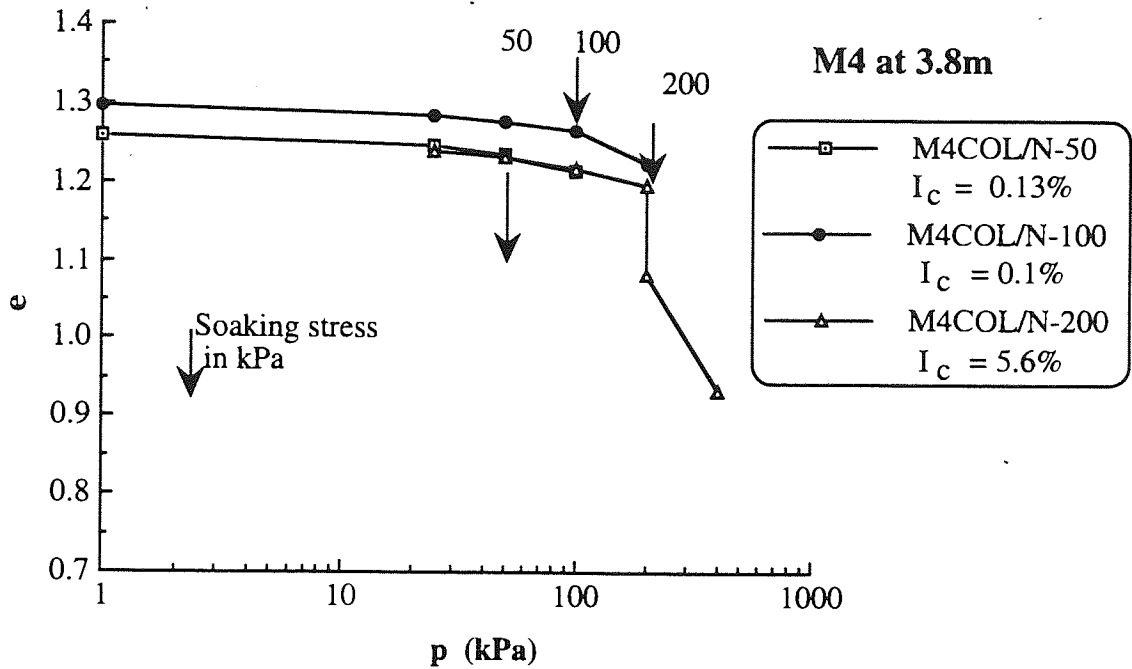
Fig. 5.5 : Collapsing potential of M4 from 3.8m below the surface.
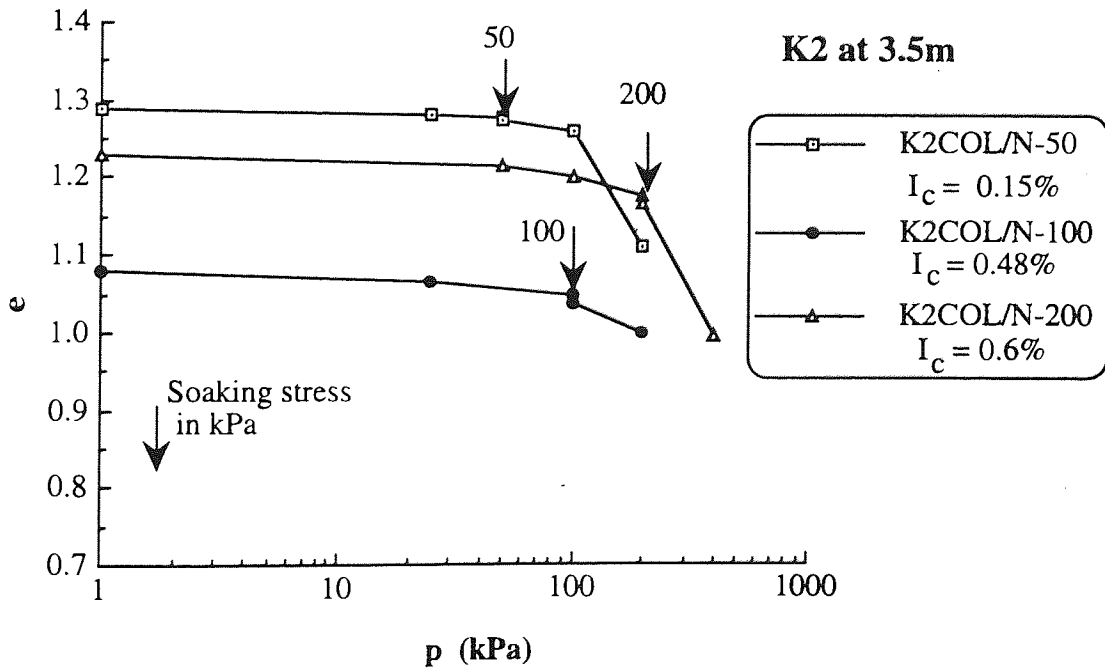
Fig. 5.6 : Collapsing potential of K2 from 3.5m below the surface.

Fig. 5.7 : Classification chart for swelling pressure
(adopted from Mitchell, 1976).
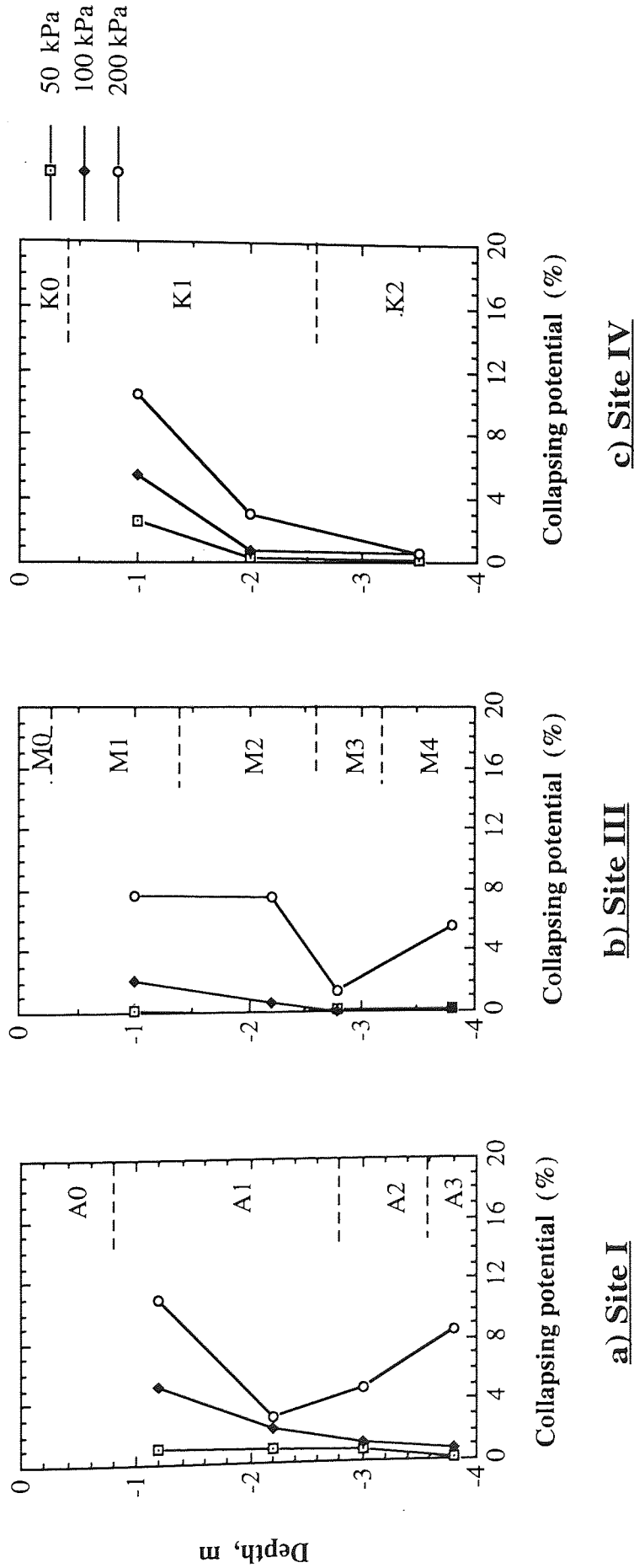
Fig. 5.8 : Variation in collapsing potential (I_c) with depth for the different sites due to wetting under various stress levels, 50, 100 and 200 kPa.
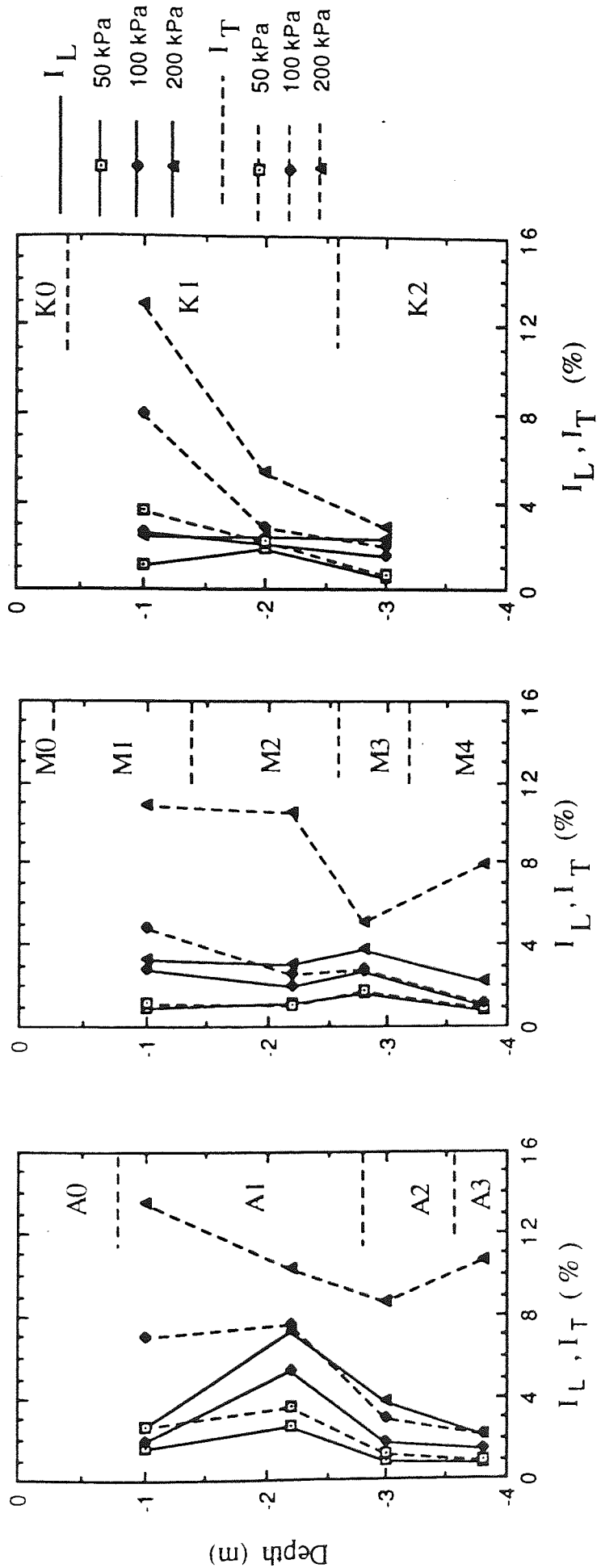
Fig. 5.9 : Variation in collapsing potentials, I_L and I_T with depth for the different sites under various stress levels, 50, 100 and 200 kPa.
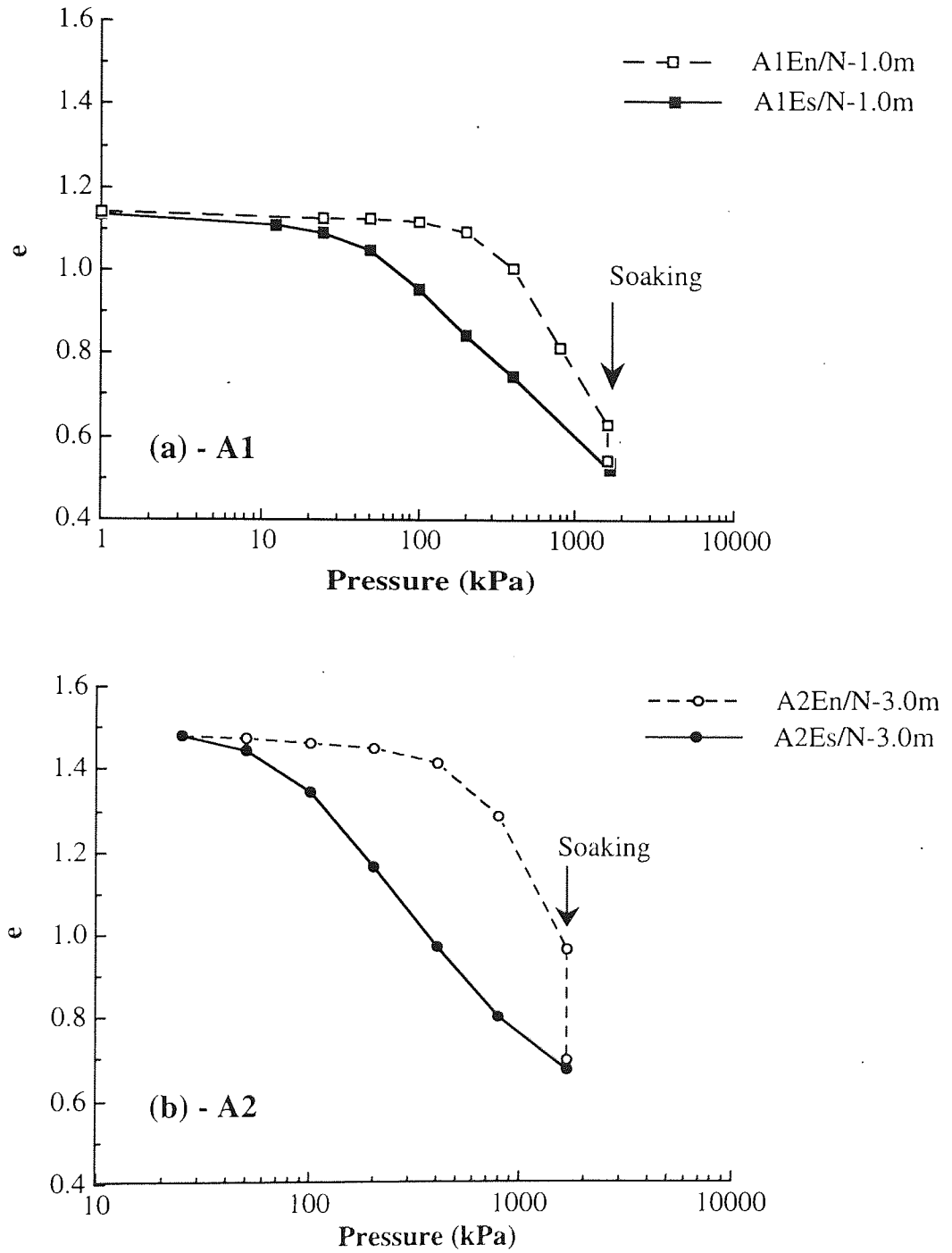
Fig. 5.10 : Oedometer test results of the natural samples of A1 and A2
soils, tested at the natural and soaked moisture conditions.
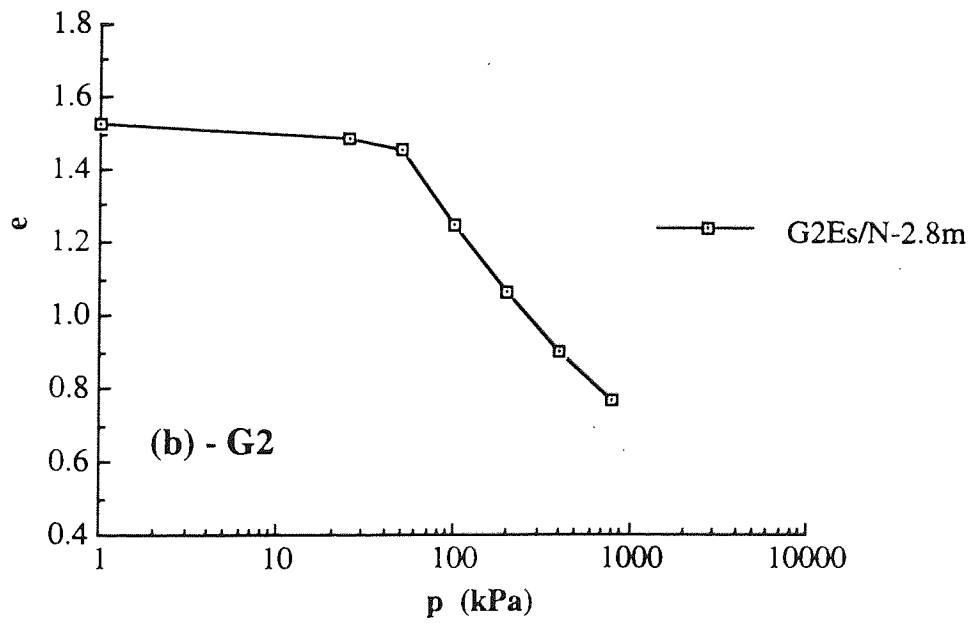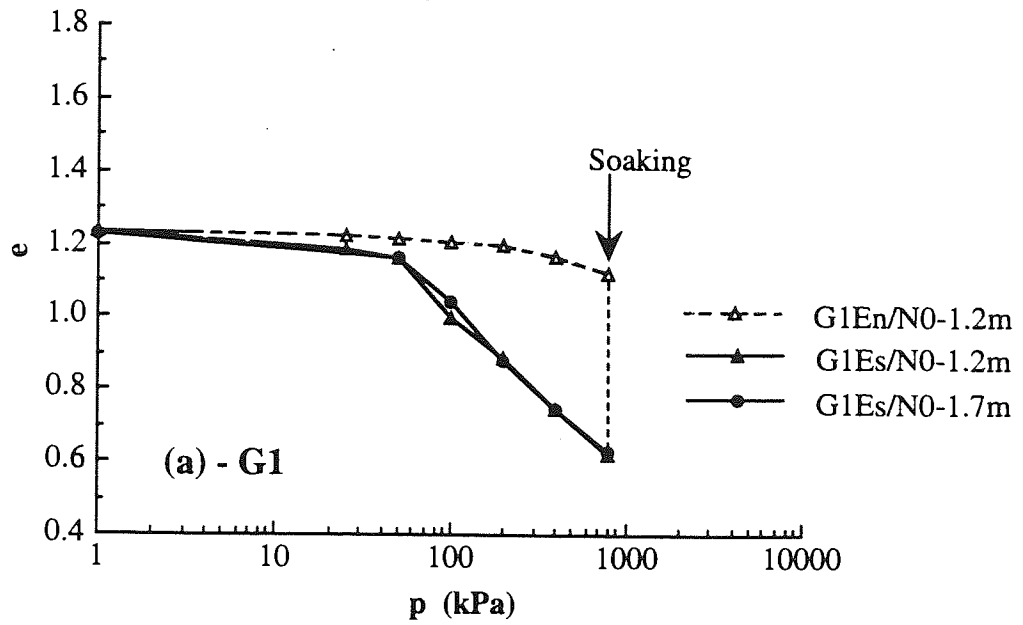
Fig. 5.11 : Oedometer test results of the natural samples of G1 and G2
soils, tested at the natural and soaked moisture conditions.
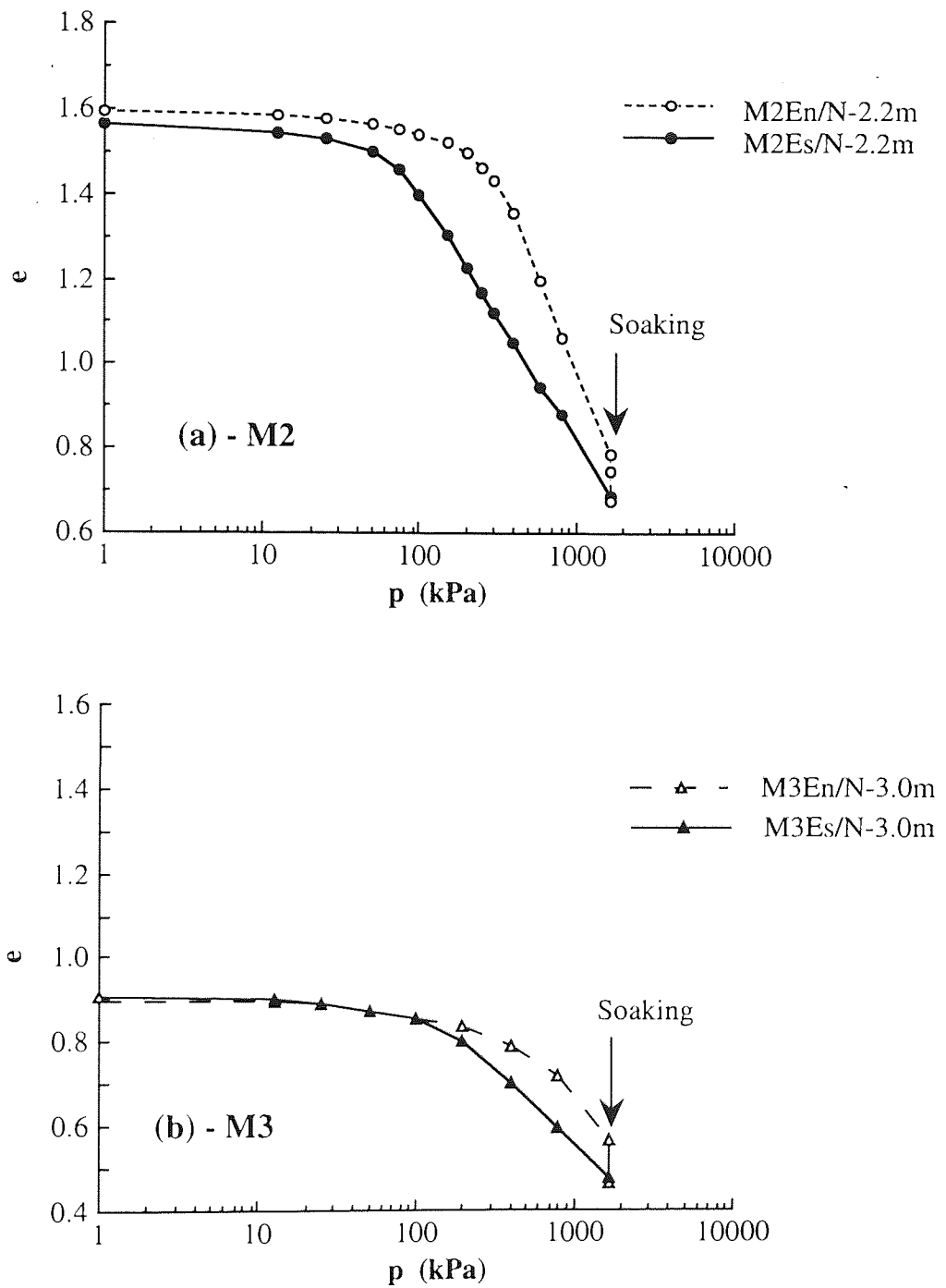
Fig. 5.12 : Oedometer test results of the natural samples of M2 and M3 tested at the natural and soaked moisture conditions.
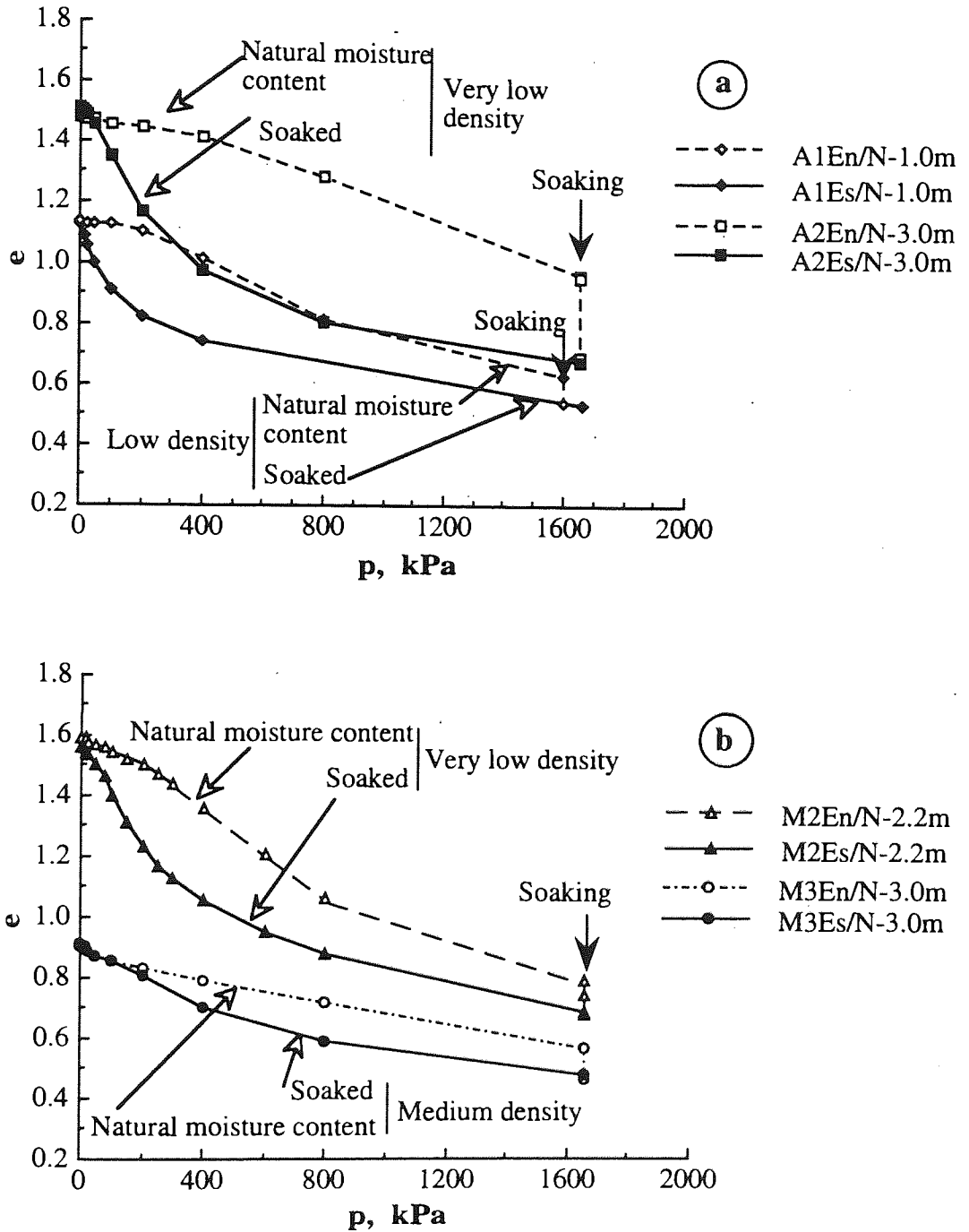
Fig. 5.13 : Typical consolidation curves of the natural soaked and partial saturated soils of: a) site I and b) site III.
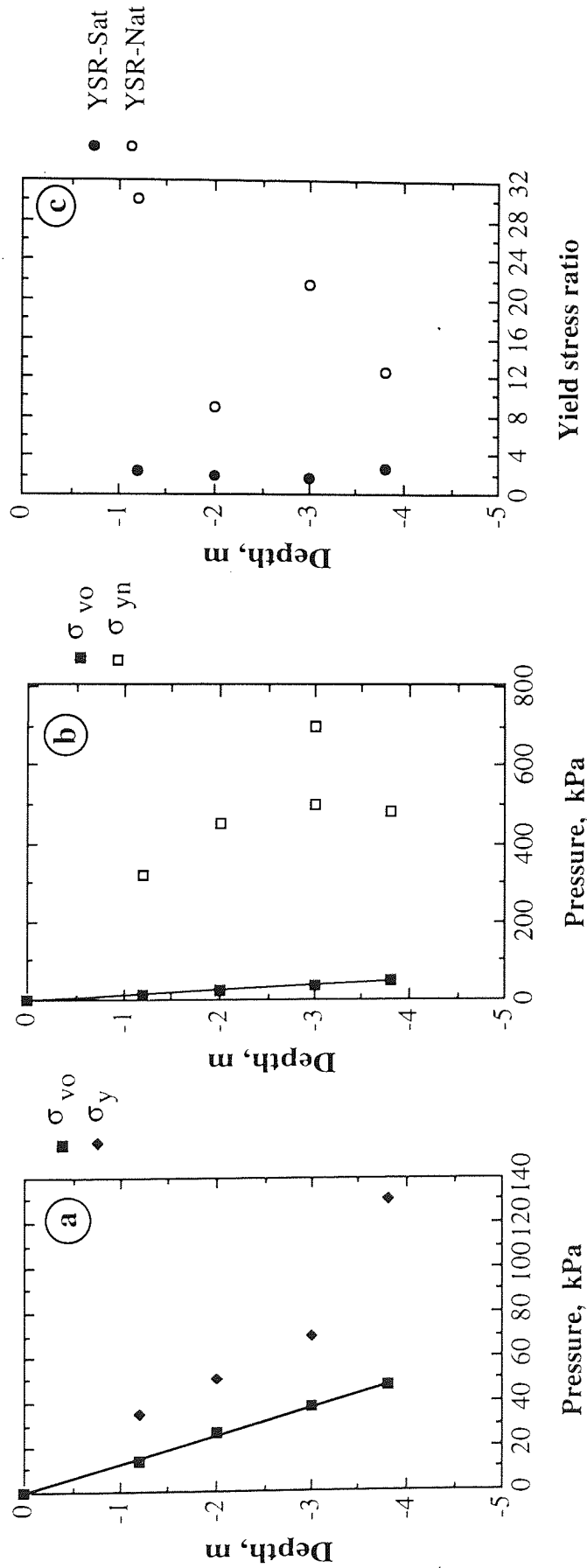
Fig. 5.14 : Variations in yield stress and yield stress ratio with depth for site I;
   a) Yield stress for soaked soils,
   b) Yield stress for soils tested at NMC state, and
   c) Yield stress ratio for soils tested at both moisture states.
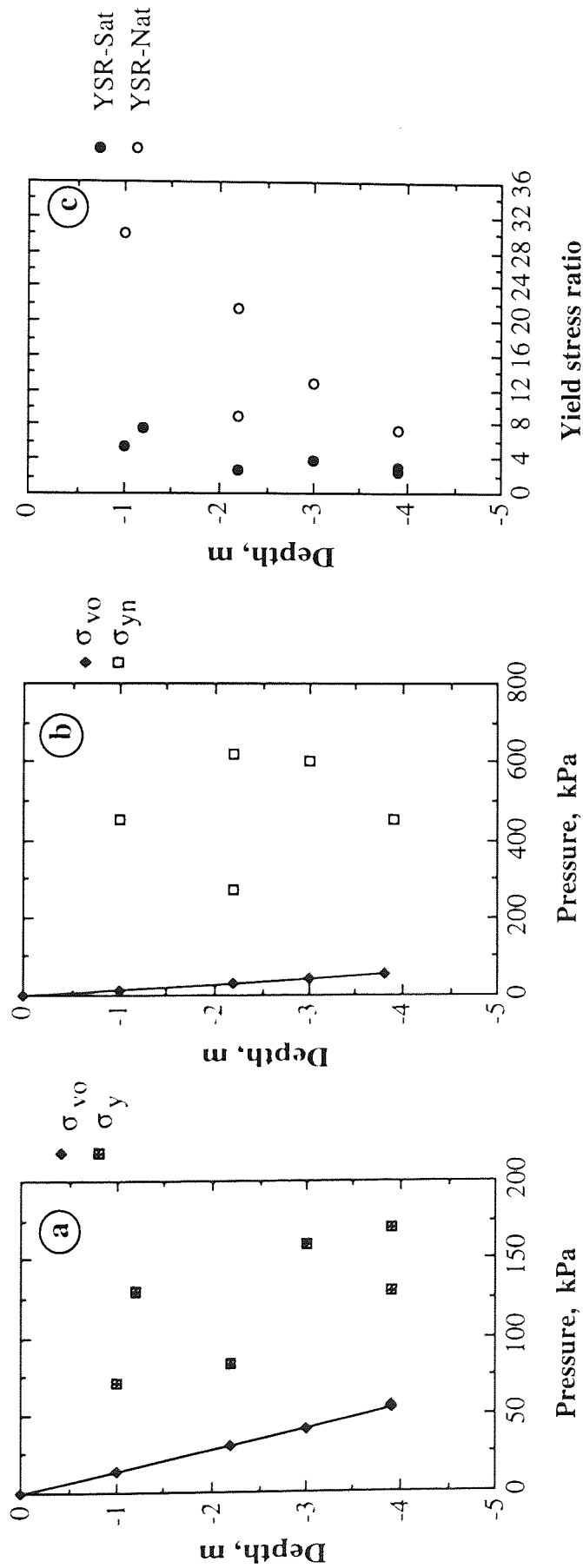
Fig. 5.15 : Variations in yield stress and yield stress ratio with depth for site III;
    a) Yield stress for soaked soils,
    b) Yield stress for soils tested at NMC state, and
    c) Yield stress ratio for soils tested at both moisture states.

Fig. 5.16 : Collapsing pressure definition (after Reginatto and Ferrero, 1973).
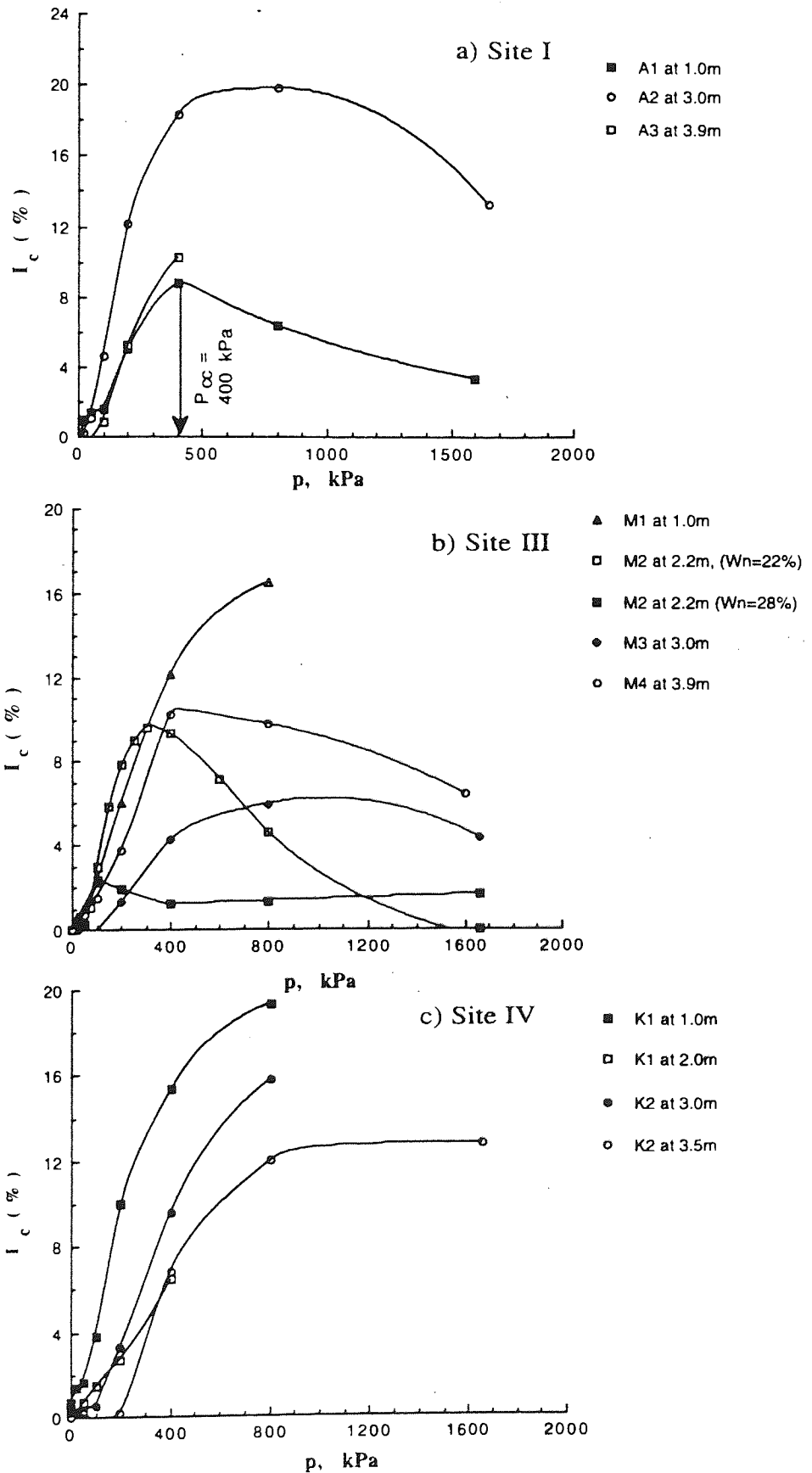
Fig. 5.17 : Collapsing potential from the double oedometer
tests on the soils from sites I, III and IV.
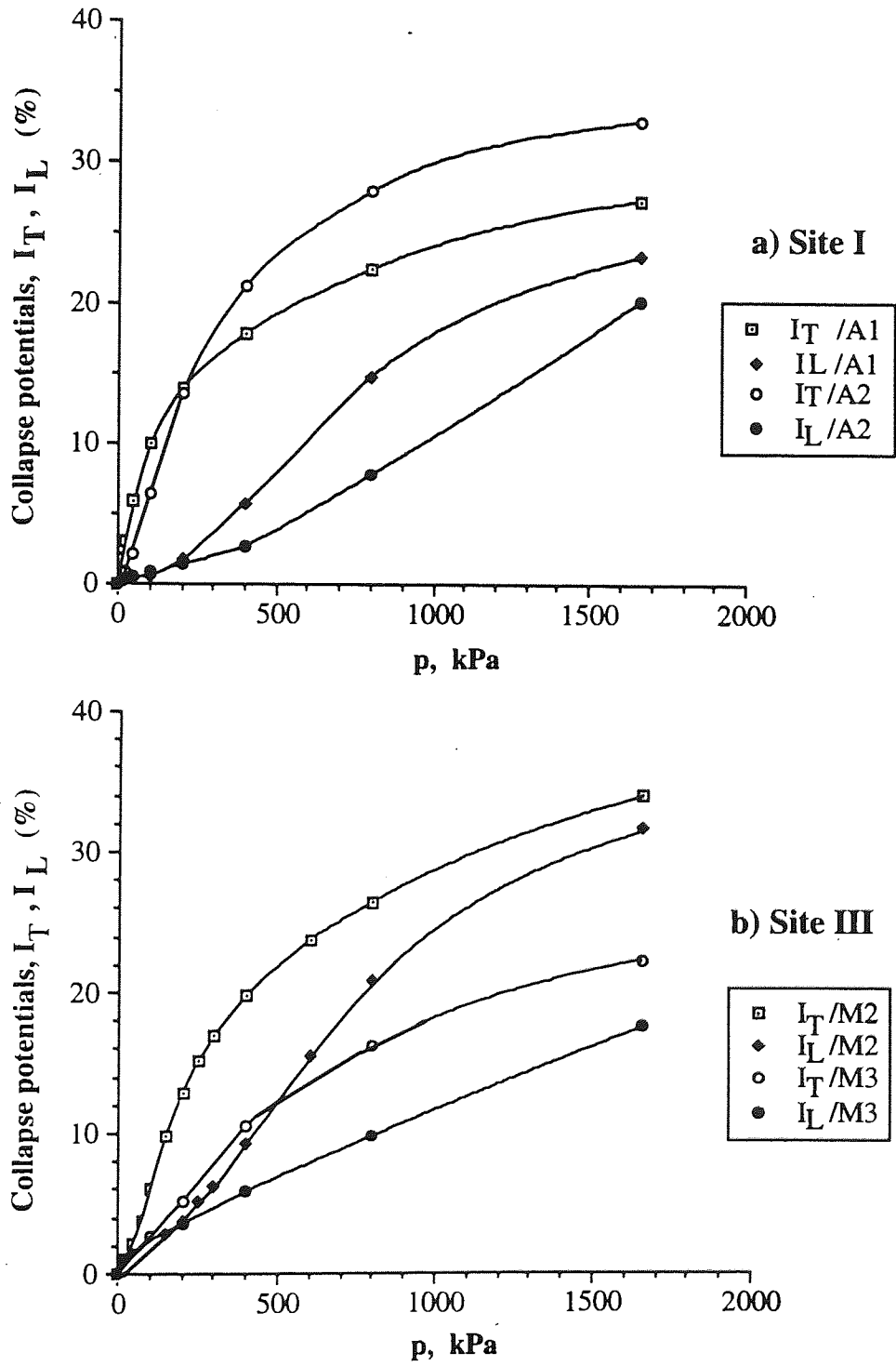
Fig. 5.18 : The total and loading collapse potentials results from the double oedometer test for the soils of sites I and III.
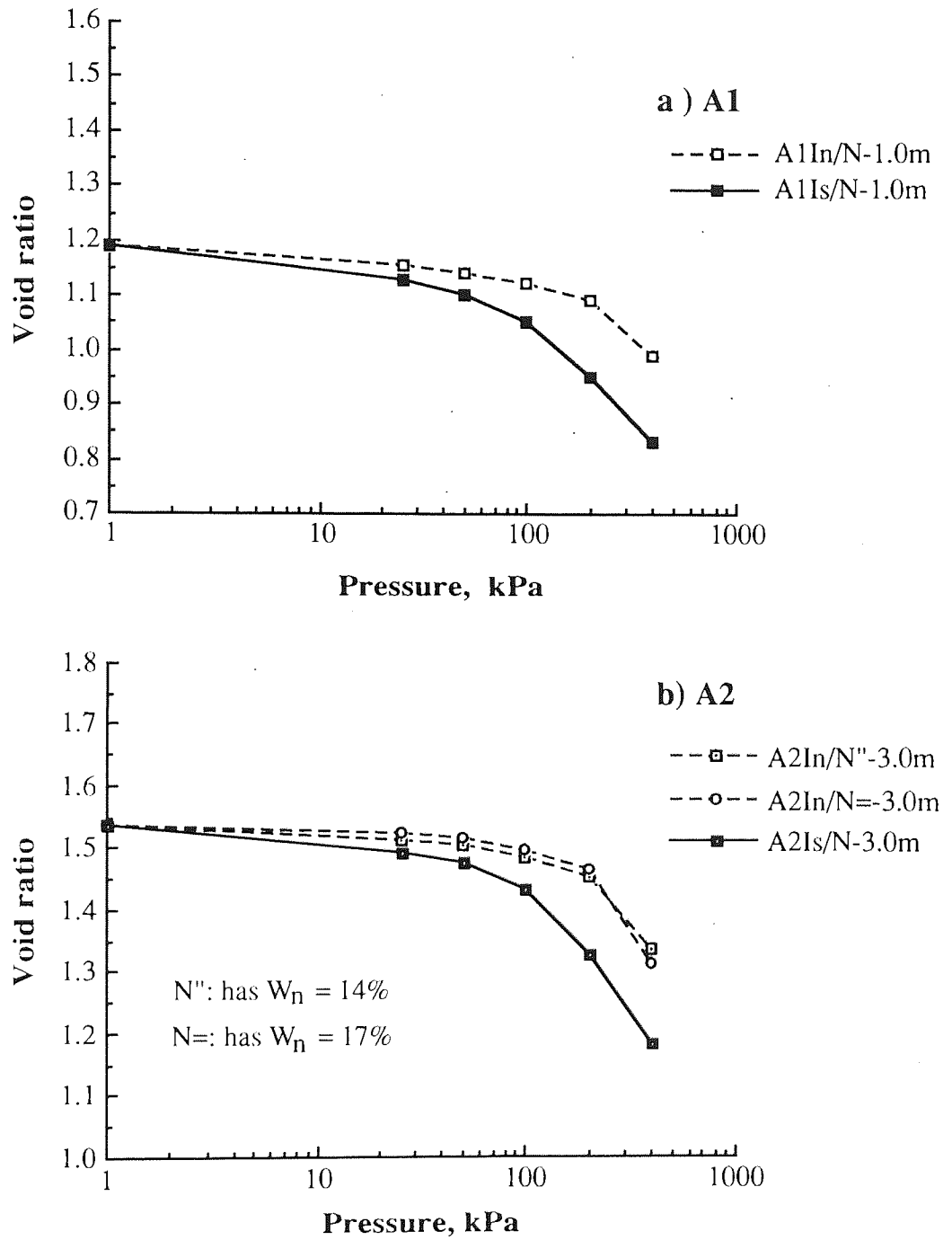
Fig. 5.19 : Isotropic compression results of the natural samples of A1 and A2 tested at the natural and saturated moisture states.
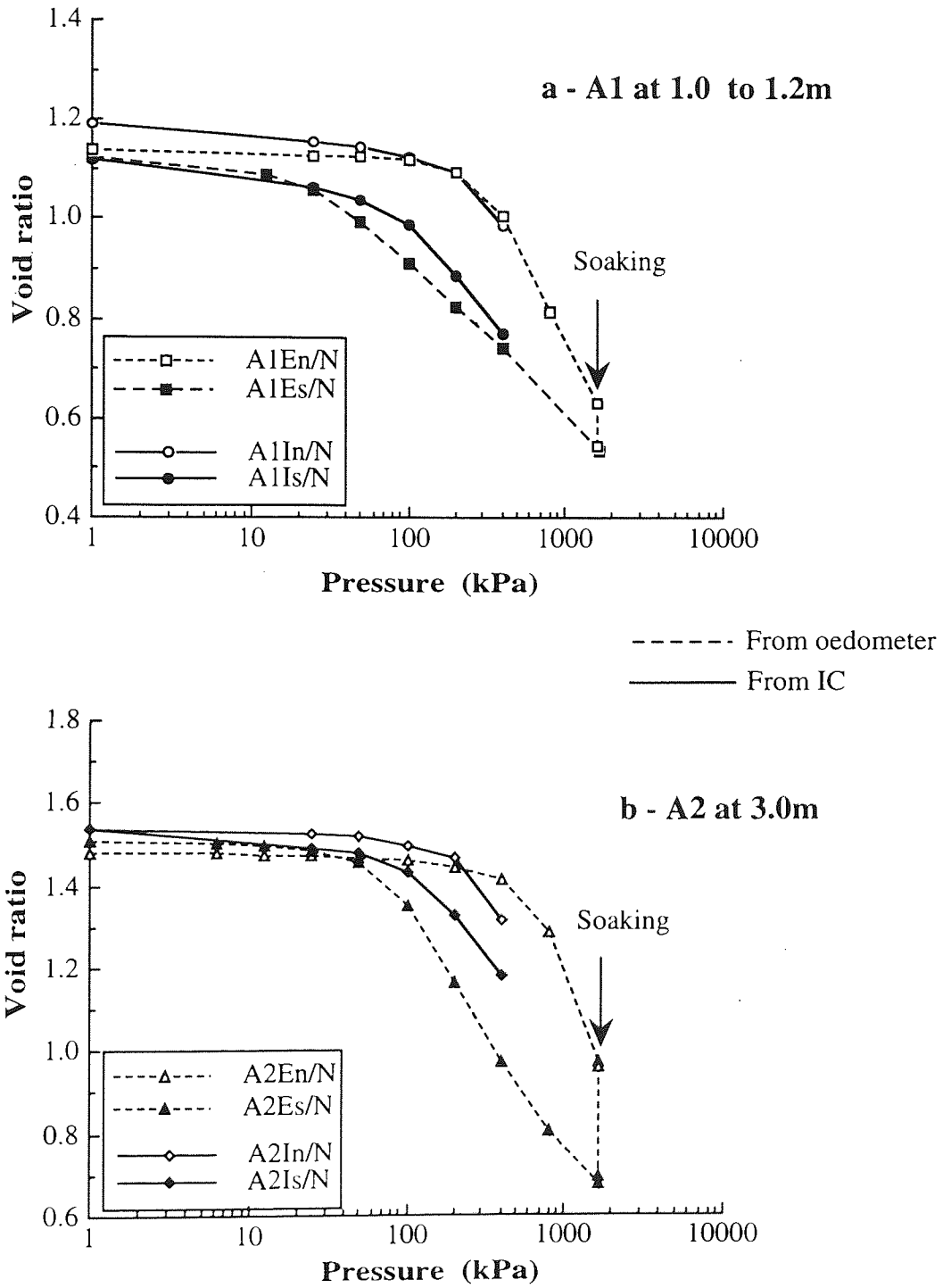
Fig. 5.20 : Results from the double oedometer and isotropic
compression (IC) tests for the natural soils from
site I, tested at both moisture states,
(for IC tests, pressure = cell pressure;
for oedometer tests, pressure = axial stress).
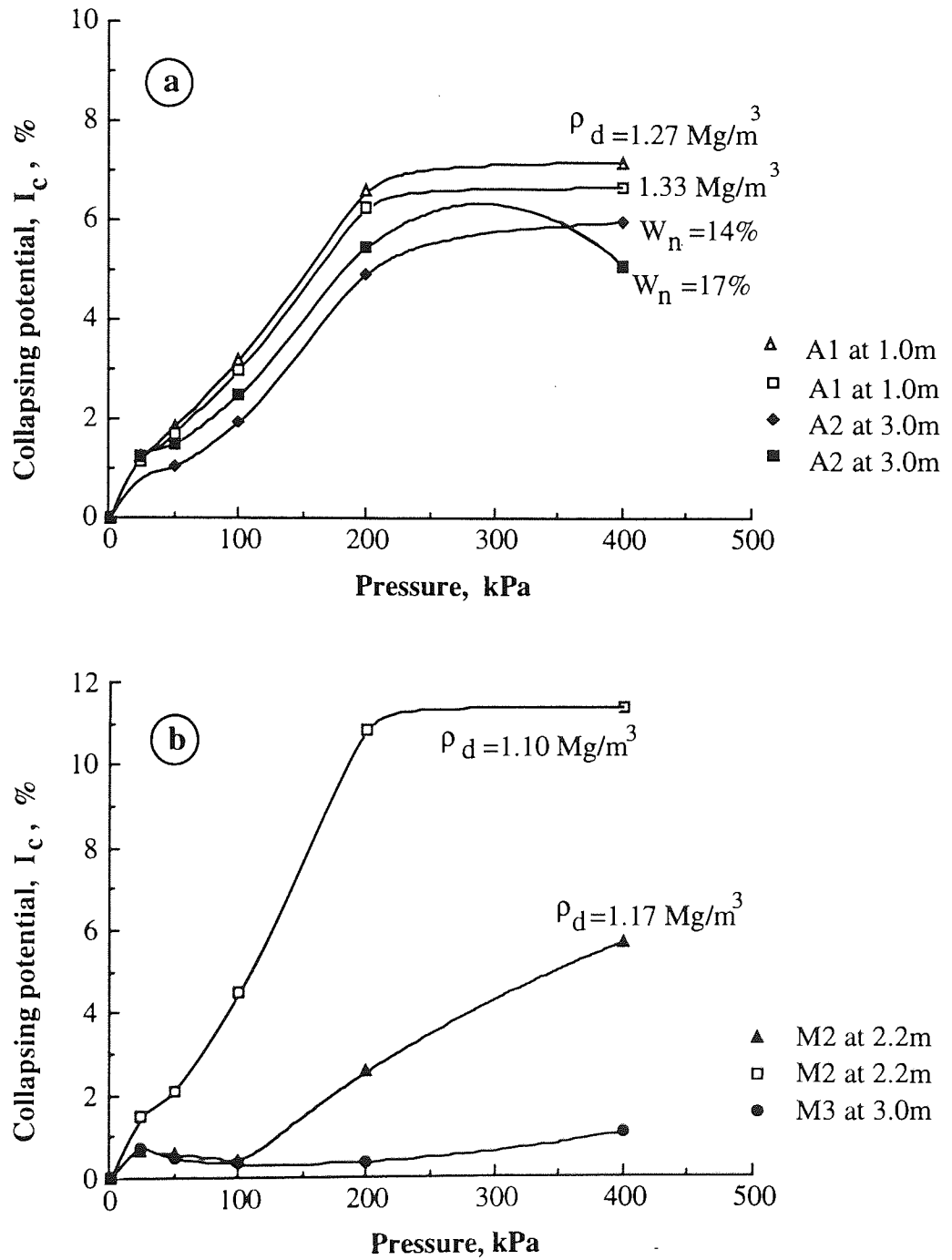
Fig. 5.21 : Collapsing potential from the isotropic compression, IC, tests on the soils; a) A1 and A2, and b) M2 and M3.

CHAPTER SIX

THE DEFORMATION BEHAVIOUR OF THE FIELD TREATED AND DESTRUCTURED SOIL

6.1 INTRODUCTION

An extensive field study has been undertaken to assess the response of the soils to selected treatments. The use of various techniques for modifying the deformation and shear strength characteristics of loess and collapsing soils is well documented, (ASCE, 1978; ASCE, 1987; Evstative, 1988). In this study four major techniques have been applied - ponding, preloading, heavy vibratory compaction and deep compaction, the last three techniques were also used in combination with flooding. Results are presented from field tests to evaluate the depth and the degree of improvement together with the deformation, characteristics determined subsequently in the laboratory. The field treatment tests are described in this Chapter while the field tests, SPT and field density, and laboratory tests, collapsing and double oedometer tests, used to asses the field treatment have been described in Chapters 3 and 5 respectively.

6.2 PONDING - FLOODING WITH WATER

6.2.1 Introduction

The interaction with moisture can greatly affect the performance of a soil, particularly its stability during construction. The natural moisture regime is affected by the depth of the water table and, significantly, by any additional moisture which may be introduced from external sources - irrigation, leaking pipes, rainfall, etc.. Factors which influence the depth of the water table, and consequently the soil moisture, are topography, climate, lithology and structure of the host rock, vegetation and the nature of the soil cover, (Partridge, 1967; Gillott, 1987). The higher the water table, the higher the moisture content of the soil, and vice versa. Changes in the position of the water table and the connected capillary fringe can cause changes in the physical characteristics of the soil, so the position of the water table can exert considerable influence on the shear strength and deformation of the soil, and thereby on foundation stability and the safety of the earthworks (Rethati, 1981).

The study area has experienced a prolonged excess of evaporation over precipitation so that the water table has dropped from 7m to over 30m during the last thirty years. Most of the soils above the water table exist in a relatively dry state and so any change in the soil moisture may jeopardize the stability of existing structures due to the accompanying volume changes. The response of the studied soils to moisture change, without additional loading, was investigated by flooding two locations, MF and KF, at sites III and IV respectively. The field observations included deformation and the extent of infiltration, together with the determination of SPT and field density. This was supported by laboratory assessment of the deformation characteristics of the flooded soils.

6.2.2 Field Testing

6.2.2.1 Ponding Test

Adding water to a collapsing soil before construction can cause it to slump, leading to a densification or hydroconsolidation. The degree of such densification depends mainly on the soil type. Flooding was solely used at two locations, MF and KF, to study the effect of wetting on slump of the soil. An area, 2.5x2.5m, was designated at each location and the top soil removed to produce a level surface for flooding at a depth of 0.6m at location MF and 0.9m at KF.

To monitor the flooded surface, four tiles (25x25x2cm) were placed near the corners and an extra tile was placed in the middle of the flooded area, as shown in Fig. 6.1. The soil underneath each tile was carefully excavated to a depth equal to the tile thickness so the entire flooded surface was level. Each location was frequently flooded with $0.8m^3$ of water, with a water depth equivalent to 12.8cm, each day for a total period of some 42 (at KF) and 50 (at MF) days, with the vertical displacement of the flooded surface being routinely monitored by levelling from two fixed reference points.

To investigate the infiltration of the water in both the vertical and horizontal directions around the flooded area, four auger drilling stations were provided at MF. These four stations were placed at the centre, the edge and 2m and 4m from the edge of the flooded area as shown in Appendix D6-1. The moisture content of each metre, to a depth of 6m, was obtained for each station. Horizontal and vertical undisturbed samples were also taken for both oedometer and falling head permeameter tests to determine the values of the horizontal and vertical coefficients of permeability. At the other location, KF, both auger drilling and SPT tests were carried out at the end of the flooding period at the four stations within and around the flooded area to establish the moisture distribution and the effect of wetting on the SPT values (Ns). The distribution of these stations is shown in Fig. 6.1.

Flooding was used at 10 other locations in combination with the other techniques indicated earlier. Flooding for one day to more than one week was carried out at these locations and the soil response to wetting was monitored before applying the particular technique. The resulting data were used, together with the main results from the two flooded locations, MF and KF, to analyze the response to field wetting.

6.2.2.2 Surface Movement Results and Analysis

Prior to flooding location KF, the levels of the five points (Fig. 6.1) were established and subsequently monitored during flooding, the vertical movements being shown in Fig. 6.2. Initially, the ponded surface moved upwards, recording a maximum expansion of 3.0mm after four days, subsequently it collapsed recording a maximum settlement of 15mm after 12 days of continuous flooding. The average movement of the four measuring points, at edges, was almost the same as that of the central point (E), except that the central point showed an initial collapse of 5mm rather the heave observed elsewhere. With continuous flooding for 42 days, heave in the lower clayey layers possibly limited the overall collapse to a final average of 8mm. At the other flooded location, MF, only heave was recorded with a maximum average value of 9 mm, as shown in Fig. 6.2, so no evidence of collapse was recorded with only flooding. Similar behaviour was recorded for the flooded location GL3 before loading, where a heave of 11mm was measured at 5 days.

Soils above the water table in arid to semi-arid regions exist in an almost dry state and volume increase or swelling upon wetting is common as observed by Holtz (1983), Popescu (1986). Gillott (1987) indicated that there are two types of swelling, interparticle swelling and swelling within the intracrystalline structure. In the former, the almost dry soil particles are held together under tensile (suction) forces by the relic water, so that on wetting the capillary tensions are relaxed and the soil expands. The second type of swelling is related to the presence of appreciable amounts of expanding clay minerals, such as montmorillonite, which were not detected within the particular soils. Thus the final expansion of the flooded soils at MF (Figure 6.3) and the initial expansion at KF (Fig. 6.2) are of the first type. However, reducing the overburden pressure by excavation, typically 10 to 14 kPa, may also account for the observed free swelling, in addition to the low, natural moisture content of these soils. This free swelling was observed in the laboratory with the oedometer specimens exhibiting a free swelling of 2 to 4% when soaked without loading, although under the small setting load this did not occur. The mean collapsing settlement of 12mm, at the flooded location KF (Fig. 6.2) following 9 days of continuous flooding may be related to the downward extension of the wetted zone into the lower layers.

This collapsing is small when compared with that reported for some other flooded collapsing soils. Similar small collapse was observed by Clevenger (1956), who reported that field collapsing settlement of 6.1mm (half of KF collapse) due to flooding loess soils,

demonstrating that saturation would not necessarily cause collapse of the loess. Belese et al (1969) reported that the settlement of loess soil under its own wetted weight had locally reached 2.0m. Similarly a 17m layer of Terkkum loess exhibited a slump of 110cm after two months of surface flooding (Balaev, 1967). Generally, soils which collapse under their own weight upon wetting are considered to be truly collapsing soils, while those which also need loading to produce a considerable collapse are classed as conditional collapsing soils (Reginatto and Ferrero, 1973; Popescu, 1986). Thus the investigated soils would appear to be conditional collapsing soils and this is in agreement with the findings of the laboratory results presented in the preceding Chapter.

6.2.2.3 Water Infiltration Results and Analysis

To provide a better understanding and prediction of volume change requires an accurate knowledge of the extent of infiltration so the moisture content distribution was determined at sites III and IV from the four borings drilled at each site and these are shown in Figs. 6.4(a) and (b), with the location of the various layers also shown. At location MF (Fig 6.4-a), the moisture content of the first layer, sandy silt M1, increased from 16 to 35% at the ponded surface. This increase decreased with depth to reach equalization at a depth of 6.0m, with the moisture content of 18%, being the natural value before flooding. The vertical extension of the wetted zone reached 5.0, 5.0, 4.0 and 3.2 metres at MF1, MF2, MF3 and MF4 respectively, with the water content still being slightly greater than the corresponding natural values. Similarly the moisture content at location KF (Fig.6.4-b) increased from 12 to 28% at 0.6m below the ponded surface within the sandy silty clay K1 and, again, this variation decreased with depth to 2.0m before increasing to record the maximum change of 16 to 36% at 3.0m. Beyond this depth the moisture contents decreased sharply to reach equalization at a depth of 6.0m with the value of 12% corresponding to that before flooding. The changes in the moisture contents beyond depths of 5.0m were small indicating that the vertical extension of the wetted zone reached 5.0m at KF1, KF2, KF3 while, at KF4 no significant differences in the moisture content were produced by flooding. This can be related to the horizontal distance of KF4, 2.5m from the edge of the ponded area, at which the effect of water infiltration was limited compared with the other borings. Similar observations have been reported by Livneh and Shklarsky (1965) and Housten et al (1988). Housten et al reported that the wetted zone in the horizontal direction reached a distance of 1.65 to 2.05m, when a closed loop of 1.8m in diameter was flooded with 800 gal at 12 days. Generally, as the horizontal distance from the ponded area increased, the moisture content clearly decreased with depth.

The infiltration shown in Fig. 6.4 resulted in the formation of a pear-shaped, wetted zone which extended more in the vertical direction (4.0 to 5.0m) than in the horizontal direction (1.8 to 2.2m), as detected from the bores (MF3, MF4, KF3, and KF4) outside the ponded area. This water distribution was influenced by the layering system, the vertical and

horizontal permeability of each layer, the existence of granular pocket or lenses, and the presence of channels such as rootlet holes. The effects of these factors are illustrated in Fig. 6.5, which uses the data in Fig. 6.4 to show the variations in moisture content, at specific levels, in terms of the horizontal extent from the flooded area. In bores MF4 and KF4, at 4.0 and 2.5m from the edge of the flooded areas respectively, the moisture contents were typically below 20%, while in the bores MF3 and KF3, at 2.0 and 1.5m from the edge respectively, the moisture contents were generally above 20% except for soils below 3.8m of site III. Holtz and Gibbs (1962), reported that when the natural moisture content exceeded 20%, the bond between the particles is weakened, and so both differential and total settlement have to be considered. Therefore, a minimum clearance of about 2.0m between structures and any planted or wetted area nearby is desirable to reduce the effect of wetting on bearing soils.

Generally the results in Fig. 6.5 indicate that the increase in the moisture content in the vertical direction was greater than that in the horizontal direction which may be due to both the effect of the gravity and the increased occurrence of vertical bores. Similar observations on the extent of water infiltration underneath a flooded foundation on collapsing soil was reported by Houston et al (1988), while Das (1984) reported that loess deposits are better drained than true silts because of their pattern of vertical root holes, so the coefficient of permeability is appreciably higher in the vertical than in the horizontal direction. Table 6.1 indicates the coefficients of the permeability, before and after flooding, for both directions obtained from the falling head permeameter and the oedometer for samples from various levels at sites III and IV. It is clear that the coefficients of the the permeability for vertical flow (K_v) are greater than these for horizontal flow (K_h). Indeed, it is suggested that the greater the difference in these values, the steeper the slope of the moisture content curves as shown in Fig. 6.5(a) at depths of 0.6 and 4.5m and in Fig. 6.5(b) at depth of 1.5, similarly the flatter slopes in these Figures correspond with those soils, where the differences in the horizontal and vertical permeability were less marked. The permeability coefficients obtained from the falling head tests exceeded those from the oedometer tests (Table 6.1), and this may be due to the stress levels at which the coefficients were calculated in the oedometer tests. The change in the values of K_v and K_h of some soils, such as K1 and M4, after flooding are related to the densifying of the soil by either collapse or filling pore with the migrated fines. The values are compatible with those suggested by Das (1984) and support the field observation of vertical and horizontal infiltration.

6.2.3 Flooding Assessment by Field Testing

Two parameters, the SPT value and the field density, have been used to assess the effect of ponding on the soil, the procedures of these two tests were presented in Chapter 3.

6.2.3.1 The SPT Results and Analysis

This is one of the most economical, field tests for assessing the in situ properties and were conducted at both locations, MF and KF. The SPT values, Ns, with corresponding moisture contents are shown in Figure 6.6 for the natural bore and the flooded bore, MF2, at site III. For the natural bore, the Ns and corresponding W_n values ranged from 6 to 35 and 27 to 15% respectively while, in the flooded bore, they ranged from 3 to 23 and 32 to 14% respectively. Both Figures 6.6 (a) and (b) indicate that the SPT values decreased with increased moisture content in a given layer, and a similar trend was detected from the flooded location KF. This relationship between Ns and moisture content for the layers K1 and K2 is shown in Fig. 6.7 and a quadratic polynomial was found to give the best fit to this curve, regression number 0.95. It is clear that the moisture content has a significant effect on the SPT values and so only when the treated soil returned to its natural moisture content would the possible benefits of flooding become apparent.

As the SPT values of the treated soils are sensitive to the water content correlations are only possible for the same moisture contents. Similar observations have been reported by Clayton (1978) and Reginatto (1971). Reginatto stated that the SPT is not adequate for determining the soil properties which govern the behaviour of collapsing soils, adding that the values are directly related to the moisture content of such soils, and can only be correlated with shear strength values determined at the same moisture content. However, for the treated locations at the NMC, the SPT data can be compared with that before treatment, while those obtained from treated locations, with preflooding, the change in the moisture content has to be considered. Consequently it was decided that an alternative test would be required to assess the effect of ponding and so the measurement of the field density was adopted.

6.2.3.2 Field Density Results and Analysis

These measurements were made at frequent intervals in test pits covering the wetted zone at the flooded locations. Fig. 6.8 shows the variation of the dry density with depth at MF before and after flooding, while Appendix D6-2 shows the same relation for KF. Following flooding slight decreases in dry density are apparent at the surface, 0.6m, and at a depth of 3.0m within the stiff sandy silt M3. At depths between 1.0m and 2.2m no variation was shown while, at 4.2m, a slight increase was measured in the density of the ponded soil. The decrease at the surface reflects the expansion effect (heave) while the decrease at 3.0m may indicate the loss in the fine particles from the sandy silt by leaching to the lower layers which produced the slight increase in their density (Ismael, 1993). At KF there was an increase in density at a depth of 1.2m due to flooding and slight decrease at a depth of 3.0m. The increase reflects the slight measured collapse while, at the lower depth, the slight decrease may reflect fines migration similar to that at MF.

Density has been considered to be useful for assessing both field and laboratory performance (Clevenger, 1956). The calculated Relative Increase in the dry density (RI) of soil M1 was negative, - 5.8%, due to the expansion following flooding, for a negative value means a reduction in dry density, while the RI values for K1 and M4, which collapsed on wetting, were 17.5 and 3.7% respectively, using the data in Fig. 6.8 and D6-2. Overall the effect of flooding on dry density was not marked, except for the sandy silty clay, K1, at 1.2m which exhibited a considerable increase in the density. Indeed, this might be partly due to disturbance of the flooded surface resulting from the operation of the SPT rig before sampling for the field density and laboratory tests. However, the field densities, Fig. 6.8 and Appendix D6-2, were compatible with the other observations, for the changes in density coincided with the swelling or collapsing observations and the loss or gain of fines by infiltration.

6.2.4 Laboratory Deformation Behaviour of the Flooded Soil

The deformation behaviour of the flooded soil was determined by collapsing and double oedometer tests on undisturbed samples removed from test pits of the flooded locations.

6.2.4.1 Single Oedometer Collapsing Results

Typical results are shown in Fig. 6.9, these being for the flooded location KF for soils at a depth of 1.0 and 2.0m. The collapsing potential, I_c, at soaking stresses of 100 and 200 kPa for the samples from 1.0m were 0.2 and 1.2% respectively and for the sample from 2.0m soaked at 200 kPa it was 3.6 %. These values are much smaller than those of the same soil before flooding, (Table 5.3), and a similar trend was apparent with the specimens from MF.

6.2.4.2 Double Oedometer Results

Twelve samples were tested, eight from location MF and four from KF. The results of representative samples from site III, at depths of 1.0, 2.2, 3.0 and 4.2m, are shown in Fig. 6.10. This Figure demonstrates that flooding significantly reduced the collapsing potential, I_c, becoming almost zero at stresses below 100 kPa and remaining very small for stresses up to 800 kPa, compared to the high values (12 to 20%, Fig. 5.17(c)) for the same soils before flooding. The variations in the initial void ratio of the samples from the different depths are simply related to the variations in soil type. The accompanying values of C_c and m_v ranged from 0.391 to 0.694 and 1.2 to 6.22 $\times 10^{-4}$ m^2/kN respectively for the soaked samples (SMC) and from 0.581 to 0.997 and 0.78 to 3.8x10^{-4} m^2/kN for samples tested at their treated moisture content (TMC). The results of the soils from KF exhibited similar trends, as shown in Appendix D6-3.

6.2.4.3 Single and Double Oedometer - Deformation Analysis

The laboratory results for deformation generally indicate that preflooding decreased the collapsing potential (I_c) and increased the compressibility characteristics in comparison with the soils at their natural moisture content. For example, soil K1, at 1.5m below the surface, was ranked as having a moderate to moderately severe collapsing potential, (I_c = 3 to 10.5%, Table 5.8) but, after flooding, it only had a slight potential with I_c between 0.2 to 1.2% as shown in Fig. 6.9. Similar drops in the collapsing potential for the flooded soils, over a wide range of the applied stresses, can be detected from Fig. 6.10. However, despite this considerable decrease in the collapse potential (I_c) due to wetting, a significant increase in the collapse potential due to loading (I_L) occurred, with the total collapse potential (I_T) being the same as before flooding as shown in Fig. 6.11. These variations in the trends of the collapsing potentials are illustrated in Fig. 6.11 for the soils M1 and M2, with similar results being achieved for the other flooded soils. Indeed, these changes in the values of the collapsing potential indicates that flooding had no beneficial effect in terms of the total collapse (the final deformation) unless such collapse takes place predominantly before construction. To achieve such flooding benefit, the design criteria based on the deformation (at wetted condition) rather than the shear strength (at in situ moisture content) should be implemented. Similarly reductions in other characteristics such as, yield stress (σ_{yn}) and yield stress ratio (σ_{yn}/σ_{vo}) at the NMC state can be seen by comparing the values in Table 6.2 with those for the natural soils in Table 5.5. The large reduction in yield stress is related to the increase in the moisture content which led to a relaxation of the water tension and so reduce the capillary bonding forces, in addition to any weakening of the cementation agents. The surviving yield stress, and consequent stress ratio, indicates the continued existence of bonding forces primarily due to the cementation agents, together with some vestigial capillary forces as the degree of saturation after flooding was 67%, still below the complete saturation of M2.

The compression index (C_c) and the coefficient of the volume change (m_v) were also affected by flooding. Overall these values for the different soils tested at the soaked condition (SMC), before (Table 5.4) and after treatment (Table 6.2), are in similar ranges, while those for soils (Table 6.2) tested at their treated moisture contents (TMC), without soaking in the laboratory, are slightly greater than the values for the natural soils (Table 5.5) at the natural moisture content (NMC), this being especially true for the soils M1 and M3. The slight shifting in the deformation curves shown in Fig. 6.10 reflects the previous effects of increasing the moisture content by flooding. The bond forces due to the cementation agents have not suffered a considerable breaking down due to flooding without additional loading as it can be deduced from the high values of the C_c, and σ_y at the soaked state in Table 6.2, compared with the corresponding values before treatment given in Table 5.4.

6.3 PRELOADING AND HYDROCONSOLIDATION

6.3.1 Introduction

Generally it is the collapsing deposits located near the surface that are most likely to produce structural damage and, within the Sana'a area, such deposits are common. When those soils are wetted, considerable damage can be produced in the superstructure of the typical single or two storey buildings located on even shallow foundations due to soil collapse, both wetting and loading contribute to the triggering mechanism for the collapse. This is the major cause of structure damage currently experienced in the Sana'a area. The effects of both wetting and loading on collapsing were investigated by undertaking field collapsing and hydroconsolidation tests at six locations at sites II and III. At each site, two field collapsing tests (one at a soaking stress of 100 and the other at 150 kPa) and one consolidation test (loaded to 50, 100 and 150 kPa) were carried out. In addition, the behaviour of the preloaded soils was investigated both in the field and the laboratory to assess the role of preloading as a technique for improving soil performance.

6.3.2 Field Collapsing and Hydroconsolidation Test

6.3.2.1 Test Procedures

This large scale test was employed to establish the behaviour of the collapsing soil in the field under both loading and wetting. The tests were conducted in a similar manner to the single collapsing and oedometer tests carried out in the laboratory.

The loads were reinforced concrete blocks and in each test, three incremental loads were applied to produce three stresses; 50, 100 and 150 kPa. The first load consisted of one block having a height of 2.0m and a square base of 1.0 by 1.0m. The second load also consisted of one block but with a height of 0.89m and a square base of 1.5 by 1.5m. The last load increment consisted of 4 blocks, each having a height of 0.5m and a rectangular base 0.5 by 2.0m, all the blocks are detailed in Fig. 6.12. Four hooks were cast in each block to simplify handling and placing by crane and so minimise eccentric loading. The block for the second load increment had four groves in the base to prevent conflict with the hooks on the first block and also to help in setting its position on the first load block as shown in Fig. 6.12 and Plate 6.1.

The field loading tests were carried out at three locations at each site - GL1; GL2; and GL3 for site II and ML1; ML2; and ML3 for site III. At each site, the locations were selected sufficiently far apart to ensure that no interference occurred between them. The first and the

second locations were loaded as a collapsing field test, while the last location was loaded as a field consolidation test. At each location, the top soil was removed by hand to expose the loaded surface, 0.8 to 1.5m below the ground surface which, in term, was carefully levelled before loading.

In the collapsing test, the loads were applied while the underlying soil was kept at its natural moisture content until the desired soaking stress was achieved, when the water was added. The first location was loaded as a collapsing field test in which the three incremental loads were applied while the soil remained at its natural moisture content. After reaching equilibrium, when no further settlements were noted under the last incremental load of 150 kPa, the water was added and further settlement due to wetting was recorded. Every 24 hours, approximately 0.3 m^3 of the water was added and the settlement was recorded until equilibrium was reached. The second location was also subjected to a field collapsing test except that the water was added after reaching the equilibrium under the second load increment, 100 kPa. The settlement was recorded every 24 hours with the water continuing to be added each day until equilibrium was achieved, when the last load increment was applied, 150 kPa. The addition of water and the settlement readings were continued till equilibrium when the test considered to have been completed.

In contrast, at the third location the field consolidation test was carried out with the tested soil assumed to be fully saturated. After the loaded surface had been levelled, water was added every day, at a constant rate of 0.5 m^3 per day, for at least 5 days before applying the first increment. The volume change before loading, due to wetting, was monitored. When the vertical movement of the loaded surface had stabilised, the first load was applied and both the immediate settlement and continuing settlement were recorded until equilibrium was achieved. Similarly, the second and the third loads were incrementally applied and the settlement monitored. Plate 6.1 shows the preparation of the loading surface and the field loading at different stress levels. The settlement was monitored by levelling four points marked on the four faces of the first block, as shown also in Plate 6.1. For the various locations the loaded surface levels and the moisture condition at the time of the field loading are tabulated in Table 6.3 together with some good comments.

6.3.2.2 Collapsing Test Results

Typical deformation-time and deformation-stress relationships for the loaded locations, ML1 and ML2, at site III are shown in Figs. 6.13 and 6.14, while Table 6.3 summarises the field collapsing and hydroconsolidation tests for the different locations. The remainder of the field results and graphs are shown in the Appendices D6-4 to D6-6. The immediate settlement due to loading or soaking (Δi), the settlement with time before soaking and/or applying the next load increment (Δt), the summation of settlement under each incremental load or soaking ($\Sigma \Delta$) and the cumulative settlement (Sum Δ) are shown in Table

6.3. Figures 6.13(a) and 6.14(a) show the deformation-time relationships, while 6.13(b) and 6.14(b) show the deformation-stress relationships. The deformation at the NMC condition (Δd) at location ML1 (Figure 6.13(b)), under 150 kPa, reached 9.5mm but, when the location was flooded at the same stress, an additional collapsing deformation (Δc) of 15.5mm was measured. These deformation values, Δd and Δc, were 4.2 and 7.5mm at a soaking stress of 100 kPa for ML2 as shown in Fig. 6.14(b). The total settlement (Sum Δ) after loading to 150 kPa and wetting, reached 26.55 compared with 25.0mm at ML1. The locations GL1 and GL2 exhibited similar behaviour and gave total deformations of 26.0 and 25.5mm respectively, as shown in Table 6.3. At GL1, the loads were adjusted after 20 days for, after soaking for 3 days under 150 kPa, slight tilting started to occur although deformation readings were taken for further 12 days until the test was terminated. The recorded deformation, 26.0mm, just before tilting was taken as the final deformation, the subsequent deformation being considered as a tilting failure as shown in Appendix D6-4 and Table 6.3. It was not possible to establish stiffness values from the field data but crude estimates could be made by dividing the stress (before -K_{bf}- or after -K_{af}- wetting) by the vertical deformation under that particular stress. While this parameter is not the stiffness, it can be used to assess the likely response of wetting on the soil stiffness, and values are given in Table 6.3 together with the average.

6.3.2.3 Collapsing Results Analysis and Interpretation

The field collapsing results indicate the tendency of the soils at both sites to conditionally collapse under both loading and wetting. The particular contributions of loading and wetting to the collapsing deformation (Δc) seemed to be different at each site, although the variation in the final values of Δc (Δc = $\Sigma\Delta$ due to soaking under a specific soaking stress) were small, being 10.5 and 7.5mm under a soaking stress of 100 kPa and 16.8 and 15.5mm under a stress of 150 kPa respectively (Table 6.3). The soil structure, the degree of cementation, the nature of the bonding forces and the degree of saturation are the main factors that affect the influence of wetting and/or loading on the magnitude of the soil collapse. Soaking the soils at ML2 and ML1 under stresses of 100 and 150 kPa (Figs. 6.14 and 6.13) increased the soil deformation ((Δc/Δd)*100)) by 178% and 163% respectively, from 4.2 to 11.7mm and 9.5 to 25.0mm, while increasing the applied stress by 50% from 100 to 150 kPa, at ML2 during soaking, increased the deformation by 127% (Table 6.3). This, clearly, indicates the major influence of both loading and wetting on the collapsing potential, providing that the applied stress exceeds the yield stress. At GL2 and GL1 soaking these soils under stresses of 100 kPa and 150 kPa increased the deformation by 350% and 182% respectively, while increasing the applied stress at the soaked state by 50%, from 100 kPa to 150 kPa, at GL2, increased the deformation by 88% (from 13.5 to 25.5mm). This indicates that the soils at site II were more sensitive to wetting than loading compared to those from site III. These findings are compatible with the observation that the bonding forces within the

soils of site II have primarily been attributed to capillary bonding (suction) whereas the predominant bonding within the soils at site III are cementations. Consequently, at site II the immediate settlement, Δi, exceeded the settlement with time, Δt, which primarily reflects release of the capillary forces due to wetting and the low presence of fines (less cementation), as shown in Fig. 6.15. In contrast, at site III the settlement with time, Δt, exceeded the immediate settlement, Δi, which can be related to the significant cementation forces which required a longer loading period to be ruptured in these soils. These results are also compatible with the laboratory data including the SEM and deformation tests. For both sites the magnitude of Δc increased with soaking stress from 100 to 150 kPa and so these in situ collapsing tests are compatible with the collapsing potential results obtained from the oedometer and the isotropic compression tests (Figs. 5.17 and 5.21). In general, the studied soils at sites II and III are conditionally collapsing soils and the collapse potential (deformation) due to wetting (Δc) is more than that due to loading (Δd), with the soils at site II being more sensitive to wetting than loading compared to those from site III. Such behaviour is compatible with the observations reported by Salas et al (1973).

6.3.2.4 Field Hydroconsolidation Results

Fig. 6.15 and Appendix D6-7 show the field hydroconsolidation results at locations GL3 and ML3 respectively. These field results are summarised in Table 6.3. which show that both locations exhibited free swelling due to soaking. The removal of the overburden and the soil's desiccated nature, due to the low natural moisture content (10-12%), are the main influences on this swelling potential. During the field inspection of site II, surface cracks were observed which resembled the desiccation cracks typical of arid and semi arid climates, as reported by Soultan (1969) and Holtz (1983). The free swelling at locations GL3 and ML3 were 12 and 11mm respectively, while the total compression under 150 kPa, excluding the free swelling values, were 21.5 and 43.12mm for GL3 and ML3 respectively. Unfortunately, the test at ML3 failed by tilting one day after applying the last incremental load and so the last reading of Δt was not measured as indicated in Table 6.3. Under a given stress, the immediate settlement values (Δi) at site III were greater than those at site II, as shown in Table 6.3, apart from those at 50 kPa at site II. The required periods for deformation (Δt) to reach equilibrium, at the soaked state, were longer for the pre-soaked soil at site III than at site II. Similar observations were apparent from the collapsing deformations at ML1 and GL1, about 90% of the deformation was achieved after 7 days at ML1 but after only 3 days at GL1 as shown from the Figures 6.13(a) and D6-4(a). The values of the in situ deformation indicators used to assess the response of wetting on the soil stiffness at the soaked state, K_{af}, were in the range of 5600 to 9090 and 2000 to 9800 kN/m with average values of 6300 and 5000 kN/m for site II and site III respectively while, at the NMC state, the average values of K_{bf} were 24700 and 19800 kN/m for sites II and III respectively as indicated in Table 6.3. The

average values of K_{bf} were about four times those of K_{af} for both sites, indicating the effect of wetting on reducing the soil resistance to deformation.

6.3.2.5 Hydroconsolidation Results Analysis and Interpretation

It is interesting to observe the large increase in deformation when the applied stress exceeded the yield stress. The yield stresses, σ_y, of the soils at site II (G1 and G2) and site III (M1 and M2) were in the range of 43 to 50 kPa and 70 to 82 kPa respectively (see Table 5.4). From Fig. 6.15(b) and Appendix D6-8(b), between 0.0 and 50 kPa the soils at site II showed more deformation than those at site III as the applied stress, 50 kPa, exceeded the average σ_y of G1 and G2. When the applied stress was increased to 100 kPa, the soils at site III deformed sharply, and more than those at site II, as the applied stress exceeded the σ_y range of M1 and M2. Similar behaviour was observed in the oedometer tests with large settlements developed after the yield stress was exceeded. The average, field yield stresses at sites II and III were respectively 45 and 73 kPa, as shown from D6-8, which are compatible with those obtained from the laboratory (Table 5.4).

The final field settlement value (Sum Δ) of GL3 obtained from the hydroconsolidation test (21.5mm) is similar to those values taken, after the last soaked increments, from the field-collapsing tests, GL1 (26mm) and GL3 (25.5mm), while the (Sum Δ) value of ML3 (43.12mm) is greater than those of ML1 (25mm) and ML2 (26.55mm). The high settlement of ML3 can be attributed to the free swelling due to the initial wetting before loading which subsequently weakened the cementation bond of the soils M1 and M2 leading to a greater deformation after loading, the effect of such swelling on the cementation bond being limited in case of the field collapsing tests as wetting was carried out after loading. With GL3 the swelling which can be attributed to the release of the capillary bond of G1, and the low fine content caused a rearrangement of the soil particles. It is suggested that this possibly exercised limited particle rotation and sliding upon loading leading to less settlement for GL3, compared with ML3, and to even less settlement (about 15%) than the same soils produced when loaded before wetting, (GL1 and GL2). Swelling also increased the degree of saturation, leading to more softening of the soil at ML3, which aided internal lubrication leading to further deformation upon loading. Generally, the larger the amount of fine material in the soil (predominant cementation bond), the larger was the difference between the deformation with pre-wetting and that with wetting after loading (partial collapse), and the lower this amount (predominant capillary bond) the lower was the difference in the deformation due to wetting either before or after loading (full collapse). These findings can be illustrated by superimposing the collapsing and hydroconsolidation results for the coarser soils at GL3 and the finer soils at ML3 as shown in Fig. 6.16.

6.3.3 Field Assessment and Testing

The field density was used to assess the effect of preloading the soil, but the SPT was not carried out at any of these loaded locations.

6.3.3.1 The Field Density Results

Fig. 6.17 shows the typical variation of the dry density with depth at selected locations before (solid curves) and after loading. Following loading and wetting the dry density adjacent to the contact surface increased and this increase reduced with depth until it reached the natural density before treatment. Beyond a depth of 0.9 to 1.0m below the loaded area, at both sites, no significant variation was determined indicating that the effect of loading did not extend beyond this depth. An increase in dry density was detected at a depth of 2.0m at ML3 (Fig. 6.17-b), but this was probably due to the local tilting shown in Plate 6.2(a) which produced disturbances in the underlying treated soil. In contrast, wetting extended to 2.2m [1.3m below the loaded surface] as shown in Plate 6.2(b) from the excavated pit dug immediately after terminating the test at ML1. This Plate also shows the failure by tilting at ML3 (Plate 6.2-a) which produced disturbances within the treated soil beneath the applied loads. At depths between 1.0 to 1.3m below the loaded surface, the influence of both loading and wetting was detected and so, within this range it was decided to investigate the mechanical behaviour of the treated soil at three levels (about 0.1, 0.5 and 1.10m below the loaded surface).

6.3.3.2 Results Analysis and Interpretation

Field density has been used to assess both the affected depth and the degree of improvement due to the combined effect of flooding and loading. The calculated Relative Increase in dry density (RI) of soils at different levels below the loaded surfaces are presented in Table 6.5. Overall the effect on dry density of flooding and loading with stresses up to 150 kPa, was only significant just below the area (0.1 to 0.3m) and this effect decreased sharply with depth (Table 6.5).

Immediately beneath the loaded area the RI values at site II are greater than those at site III due to the differences in soil texture (sand-silt at site II and silt-clay at site III). However, the opposite effect occurred 1.0m below the loaded surface due to a slight response in the soft silt/silty clay, M2, at this depth at site III so RI increased while at site II, where soil G1 was still present at this depth, RI continued to decrease. Soils at ML3 responded to treatment more than those at ML1 and this can be attributed to the swelling which weakened the soil structure while at site II, the opposite occurred (RI of GL1 > RI of GL3) due to differences in soil structure and texture. These results are in agreement with the earlier field results and support the presented hypothesis.

The infiltration depth of 1.3m is about one third of that observed at the flooded location MF (Section 6.2) and this can be related to the area of the ponded surface, duration of flooding, the total amount of the added water and the area beneath the applied load. Generally, within this zone, slight to moderate improvement was achieved by this treatment method. The extent of this improvement could be extended by increasing the applied stress and probably the wetting depth.

6.3.4 Laboratory Deformation Behaviour of the Preloaded Soils

6.3.4.1 General

Data from the double oedometer tests were used to identify the collapsing and consolidation characteristics of the preloaded soils. To simplify the understanding of the keys or symbols of the samples, locations, etc., a standard nomenclature is used throughout the thesis so that the indicated depth within the sample code refers to the original ground surface, while the corresponding depths from the loaded or treated surfaces are presented in the appropriate Tables and Figures. In the text, wherever depths are presented between brackets [..m] they refer to depths from the loaded or treated surfaces.

6.3.4.2 Collapsing Results and Analysis

The laboratory results for deformation generally indicate that preloading and flooding caused a moderate improvement in the mechanical behaviour of the soils within 0.5m below the loaded surface, beyond that only a slight effect was achieved. The collapsing potential (I_c) of the soils at site II was greatly reduced at depths to 1.7m [0.5m below the loaded surface] with no effect being achieved at 2.3m [1.1m], when compared with those of the natural soil before loading as represented by the broken-lines in Figure 6.18(a). At site III a similar reduction was achieved at a depth of 0.9m [0.1m] (Fig. 6.18-b, location ML1) while, at 1.4m [0.60m], there was a slight increase in I_c compared with the soil before treatment as shown in Figure 6.18(b). This unexpected increase in I_c, within the low stress range of 0.0 to 200 kPa, was related to the slight destructuring produced both by loading and wetting. This destructuring of the soil bond and structure was partial and resulted in partial stiffening so, when the treated specimen was tested in the laboratory at the treated moisture content, TMC, it sustained the applied stress to a value between the soaked yield stress (σ_y) and the yield stress at NMC (σ_{yn}) of the soil before treatment, when it failed sharply by loading as shown on the e-log p curve of specimen M1Et/NL1-1.4m in Figure 6.19(b). When the other specimen, M1Es/NL1-1.4m, from the same level was soaked in the laboratory (higher degree of saturation), this partial stiffness was released and further destructuring occurred at higher stresses than those applied in the field so, at stresses above 400 kPa, I_c dropped sharply when compared with the curve of the natural soil (Fig. 6.18-b, dot curve). Similar partial

destructuring resulted within the soil at a depth of 1.9m, so a considerable drop in the I_c was detected at stresses above 200 kPa as shown in Fig. 6.18(b). The destructuring achieved at 1.9m (soil M2) was greater than at 1.4m (soil M1) as the reduction in the collapsing potential appeared at a lower stress and this coincides with the field density results (RI at 1.9m was more than at 1.4m). This variation in the soil response is related to the variations in the layering system, the soil type and the soil consistency.

6.3.4.3 Consolidation Results

Twenty samples were tested from the locations GL1, GL3, ML1 and ML3, and the results from representative samples from location GL1, at depths of 1.25 and 1.7m, and location ML1, at depths of 0.9, 1.4 and 1.9m are shown in Fig. 6.19. More extensive data are given in Appendix D6-9. The results in Figure 6.18 have already demonstrated that flooding and loading minimized the collapsing potential, becoming almost zero at stresses below 100 kPa near the contact surface and varying with depth for stresses up to 800 kPa. Variations in the initial void ratio of the samples from the different depths of the same soil reflect the densification effect due to loading as shown in Figure 6.19 (a), while the variation in void ratios shown in Fig. 6.19(b) may also have been affected by the layering system at this location. The values of C_c and m_v for both soaked samples and samples tested at their treated moisture content (TMC) from the four treated locations are summarized in Table 6.4. Fig. 6.20 shows the variation in these values with depth for the location ML1, the results from the other locations exhibiting similar trends.

6.3.4.4 Analysis of the Consolidation Results

The compressibility characteristics, in terms of the coefficient of volume change (m_v) and the compression index (C_c), were only slightly affected by flooding and loading as shown in Fig. 6.20 for location ML1. The m_v values at the TMC condition were greater than those before treatment (at NMC condition) over the treated depth, 1.3m, while those at the SMC condition were lower than those of the natural soil within [0.6m] and at greater depths they were similar (Fig 6.20-a). This suggests that, at the TMC state, the increase in the deformation was mostly related to the increase in the moisture content with only a limited effect due to destructuring while, at the SMC state, the reduction in the deformation produced by loading was only apparent near the contact surface and was possibly due to destructuring. Similarly the values of C_c (Fig. 6.20-b) at the TMC state were higher than those for the natural soil at the NMC state, this was most marked at the loaded surface and decreased with depth to [1.1m] while, at the SMC, these values were slightly lower over the treated depth up to a depth of [1.1m]. Generally, near the contact surface (0.0-0.5m) the deformation at the SMC condition was moderately lower than before treatment (partial destructuring with densification) and almost the same as that before treatment at a greater depth while, at the

TMC condition, it was greater than that of the natural soil at the NMC condition across the entire depth of treatment, mainly due to wetting.

Generally, preloading and wetting resulted in partial wetting and so partial destructuring of the soil structure and bonds to a depth of 1.3m, with the major changes only apparent over a shallow depth. Consequently, this method can be classified as a fair to good improvement technique for these collapsing soils subjected to only low stresses, to 200 kPa.

6.4 VIBRATING ROLLER COMPACTION

6.4.1 General

The use of dynamic compaction has become an increasingly attractive method for treating collapsing soils and two techniques have been studied in this investigation - the use of vibratory or vibrating steel roller (VRC) and Pounding technique or deep compaction (DC) - for comparison with the earlier static methods. This section deals with the vibrating roller while the second method will be presented in the next section. The use of heavy roller compaction for densifying sand and gravelly sand materials is well documented, (Schmertmann, 1970; Whetten and Weaver, 1991). In this study, a heavy vibratory roller was used in combination with flooding to treat the natural collapsing soils at sites I and III. This section includes the compaction process and the field assessment, together with the determination of SPT and the degree of densification achieved with depth. These were supported by laboratory assessments of the deformation characteristics of the compacted soils.

6.4.2 Field Observation and Field Assessment

6.4.2.1 Operation of Steel Roller Compaction

A heavy vibrating steel roller, model SAKAI SV90 with the specified vibration shown in Appendix D6-10 was used to compact and densify the soils at five selected locations. Three of these locations were at site I, AC0, AC1 and AC2, the other two being at site III, MC1 and MC2. At location AC0, the soil was compacted at its natural moisture state while at the other two locations, AC1 and AC2, the surface was flooded for one day and five days respectively before compaction. Similarly, for the locations MC1 and MC2, flooding was applied for one day and three days before compaction. The compacted surfaces at the flooded locations, AC2, MC1 and MC2, were allowed to dry for one to two days before compaction while location AC1 was compacted directly the next day. The compaction effort, forward speed (0.7 m/sec), was constant at all locations as was the weight of the roller (9700kg) and the front wheel was operated at a frequency of 28.3 cycles/sec (Hz).

Each location provided a rectangular area, approximately 3.0 by 7.0m. Along one side, an area 3.0 by 3.0m was prepared for compacting by removing the top 0.4 to 0.8m of soil with the final 0.2 to 0.3m being excavated by hand to minimize disturbance of the prepared surface. On the other side of the rectangle, a gentle slope was formed to enable the steel roller to move forward and backward across the area to be compacted as shown in Fig. 6.21. This compacted area was levelled and three, thin, rectangular, steel plates (150x100x5mm) were placed at different locations on this surface (Fig. 6.21) and these were levelled after every second pass of the roller to monitor the settlement. The individual aspects are shown on Plate 6.3.

6.4.2.2 Ground Surface Depressions -Results and Analysis

The vertical movements of the locations AC0, AC1 and AC2 are shown in Fig. 6.22 and each curve represents the average of three observations. The ground depressions for locations MC1 and MC2 are shown in Appendix D6-11. The maximum vertical depression ($\delta_{v \text{ max}}$), the total number of passes and the suggested economical coverages for each location are given in Table 6.6. Over all the locations, the values of $\delta_{v \text{ max}}$ ranged from 66.3 to 75.0mm, excluding that at AC1 which reached 169mm after 36 passes as shown in Fig. 6.22. After 12 passes at AC1, the soil reached a compacted state after which the soil particles at the surface were seen to slide and produce waves in front of the roller wheel causing sweeping rather than surface depression. This resulted in a continuous soil loss with further coverage after the initial 12 passes so leading to a continuous increase in the measured δ_v value as shown in Fig. 6.22. The using of the heavy vibratory equipment and the high moisture content (31%) of the worked surface at AC1 (wet of Wopt, 21%) contributed to this misleadingly high value of δ_v. The total coverages ranged between 30 and 36 passes with the economical coverages, deemed to give a vertical depression of at least 80% of $\delta_{v \text{ max}}$ (Whetten and Weaver, 1990), being in the range of 8 to 12 passes for all the preflooded locations against 16 passes for location AC0, compacted at the natural moisture, as shown in Fig. 6.22 and Table 6.6, so wetting clearly accelerated compaction and so would make the process more economical.

For depths to 1.5 -1.8m, it has been suggested (ASCE, 1978) that intensive surface compaction can be used as an inexpensive technique for densifying the collapsing soil. The values of $\delta_{v \text{ max}}$ for the different locations in Table 6.6 varied over only a narrow range which did not adequately reflect the effect of wetting at the different locations, the values of δ_v max for the most extensively preflooded locations, AC2 and MC2, were only slightly greater (4-7mm) than at the other locations. The depth of improvement at AC0 (0.5m) was considerably less than those at AC2 and MC2 (0.9 and 1.0m, respectively) although the variations in the $\delta_{v \text{ max}}$ values were only 3-4.5mm. Generally, the value of the ground depression cannot be used to indicate the degree of improvement although it can be used for practical field guidance (Lukas, 1980), and can provide a basis to compare the soil response to

different treatment techniques (see Section 6.7). For instance, the soil improvement by dynamic compaction was better than that achieved by static compaction (preloading, Section 6.3), with the $\delta_{v\ max}$ values for roller compaction being 3 to 6 times greater than those achieved by static compaction.

6.4.2.3 The SPT Field Results and Analysis

Tests were conducted at all locations and the SPT values, Ns, and corresponding moisture contents are shown in Figure 6.23 for the natural and compacted bores at the site 1 locations. For the natural bore to a depth of 3.0m, the Ns and W_n values ranged from 7 to 15 blows and 13% to 15% respectively while, in the compacted bores AC0, AC1 and AC2, the corresponding values ranged from 8 to 17 blows and 5% to 12%, 5 to 11 blows and 13% to 27%, and 3 to 8 blows and 13% to 29% respectively. The data in Figures 6.23 (a) to (d) indicate that the SPT values decreased with increased moisture content, and a similar trend was apparent at the other compacted locations, MC1 and MC2, as shown in Appendix D6-12. It is clear that the moisture content had a significant effect on the SPT values of the compacted soils, despite the densification that was achieved, particularly in the top 0.5m of the treated soils. These results (Fig. 6.23 and D6-12) suggest that the SPT is not a valuable tool for measuring the effectiveness of vibrating roller compaction (VRC) where this treatment is combined with flooding. For the location AC0 (Fig. 6.23(b), at 0.9m), with no flooding, the SPT values after treatment exceeded those before treatment, although this trend was influenced by local decreases in moisture content, and so it is difficult to attribute the change in SPT value solely to the influence of the compaction.

With the passage of time, the treated soil would be expected to return to its natural moisture content so the possible benefits of compaction may be more apparent. This was investigated by retesting at AC1 and AC2 after 27 days and the results are shown by the circular symbols in Figs. 6.23 (c) and (d) respectively. These results indicate that time increased the resistance to penetration, although this was not necessarily due to reduction in the moisture content as the data in Figs. 6.23(d) shows increases in the SPT values despite the moisture contents being higher at the second testing. Lukas (1980) indicated that the pressuremeter modulus 15 days after pounding was lower than before pounding but after 50 days, it exceeded the initial value by 25% and after 70 days it doubled the original value. Mitchell and Solymar (1984) indicated that the in situ densification of a sand deposit may initially lead to a reduced penetration resistance, compared to the value before densification, and so provides a conservative measurement if used as a basis to control densification. However, Schmertmann (1970) reported that caution is advised when relating SPT values to relative density after treatment, specifically if water has been used in combination with other treatments.

6.4.2.4 Field Density Results and Analysis

Fig. 6.24 shows the changes in dry density down to a depth of 1.9m at the site I locations, Fig. 6.24(a), and to a depth of 2.2m at site III locations, Fig. 6.24(b). The appropriate depths of improvement are shown in Fig. 6.24, the values ranging between 0.5 and 1.0m at these locations. The values of the moisture content at the time of compaction (Wcomp) and the local optimum moisture content (Wopt) at specific levels in the various soils at each location, are shown in Table 6.6. The moisture content (31%) at the working surface of AC1 was higher than the optimum moisture content (21%) while, at AC2 and MC1, the moisture content at the working surface was monitored and allowed to approach the optimum value by letting it dry for 1 to 2 days after terminating the flooding. The increases in the dry densities ($\rho_{d\ max}$) of the compacted soils at AC0 and AC1 do not extend to great depths, with depths of improvement of only 0.5 and 0.6m respectively, with these at AC2, MC1 and MC2 being 0.9, 0.8 and 1.0m respectively. The dissipation of improvement was more marked within the top 0.3m and moderate across the rest of the depth of improvement. The values of $\rho_{d\ max}$ at different levels for each location are shown in Table 6.6.

The Relative Increase values (RI) for the soils at different levels below the compacted surface at the different locations are presented in Table 6.6. Overall the effect on dry density of vibratory roller compaction, was only significant just below the surface (0.3 to 0.5m) and this effect decreased rapidly, at AC0 and AC1, and moderately, at AC2, MC1 and MC2, with depth (Table 6.6 and Fig. 6.24). The RI values immediately beneath the compacted area at site I were greater than those at site III, largely due to differences in soil texture and layers as can be seen from comparing the values of RI for AC2 and MC2 in Table 6.6. However, the opposite effect occurred (RI of MC2 > RI of AC2) at 1.7m [1.0m] due to the response of the soft silt/silty clay, M2, present at this depth at site III, while at site I, where the same soil layer, A1, extended beyond this depth.

6.4.2.5 Preflooding Effect on the Degree and Depth of Improvement

Preflooding increased the depth of improvement as shown by the RI values in Figure 6.24. For example, preflooding extended this depth from 0.5m for soils compacted at the natural moisture content, AC0, to 0.9m and 1.0m respectively for soils preflooded for 5 and 3 days before compaction at AC2 and MC2. However, at any given depth, the differences between the moisture content at the compaction time (Wcomp) and the local optimum (Wopt) influenced the particular RI values as indicated in Table 6.6. At depths of 0.1 and 0.5m the Wcomp of MC1 (18-22%) were slightly greater than Wopt while those of MC2 (27-29%) were significantly greater than Wopt, so the RI values at MC1 (9.8-25.8%) were greater than those at MC2 (5.7-22.4%). Similar trends were observed at locations AC1 and AC2. Generally, when Wcomp was marginally greater than Wopt, greater RI values were achieved.

Furthermore, compacting AC0 at the NMC condition, which was below the optimum value, limited the benefits of roller compaction and Hausmann (1990) attributed this inferior compaction to the apparent cohesion mobilised by the surface tension forces which effectively increased the resistance to compaction.

From the inspection of the excavated pits, water infiltration at the preflooded locations reached 0.8 to 1.1m below the treated surface at AC1, AC2 and MC2, but it did not exceed 0.5m at MC1. These infiltration depths are smaller than those produced by the flooding and flooding with loading treatments, and this can be related to the small amount of total water added during preflooding and to the shorter duration of flooding, although within 0.5 to 1.0m below the compacted surface, this treatment achieved a significant improvement. Indeed, in the top 0.1 to 0.2m of the improved depth, excellent improvement is indicated by the very high RI values achieved. Unfortunately, despite these high RI values, crushed particles were observed within the shear planes, due to the high energy that was applied. This phenomenon of creating shear planes at contact points, from trying to maximize the number of passes, was reported by Hausmann (1990). Consequently, he indicated that minimizing the number of passes may have technical as well as economical advantages. Extending the improvement to a greater depth has been reported with granular soils by many investigators (Whetten and Weaver, 1991; Moorhouse and Baker, 1969) but was restricted by the large amount of fine material and the very low moisture content at depth. Whetten and Weaver (1991) indicated that significant fines content, depth of ground water, the presence of a hard underlying layer can have significant impacts on the maximum depth of improvement and the effectiveness of densification. Generally a significant improvement was achieved, in terms of both increased density and depth of improvement, using the VRC treatment technique with preflooding in comparison to compaction at the NMC condition.

6.4.3 Deformation Behaviour of the Roller Compacted Soil

This was determined in the laboratory with undisturbed samples taken from test pits at the treated locations, using single and double oedometer tests. It is necessary to note that, for all locations, the compacted surface levels (C.S.) were 0.7m below the original ground surface (G.S.), apart from at AC1 where it was 1.2m below.

6.4.3.1 Single and Double Oedometer Collapsing Results and Analysis

Typical results together with the collapsing potential (I_c), from the single oedometer test at a soaking stress of 200 kPa, are shown in Figure 6.25 for the treated soils at AC0, MC1 and AC2 for various levels within the improved depth. Generally, the I_c values for specimens taken near the compacted surface were much lower than those of the natural soils (Table 5.3), the values increasing with depth to become equal to those of the natural soils

below the depth of improvement. For example, the I_c values at AC0 for samples from 0.8 and 1.1m [0.1 and 0.4m below the C.S.] were -0.5 (swelling) and 8.7% respectively as shown in Figure 6.25(a) which are less than those of the soil before treatment, (I_c = 10.8% at 1.2m for the soil A1, Table 5.3). Similar trends were apparent for specimens from the other locations, AC1 and MC2.

The collapsing potentials (I_c), detected from the double oedometer test over the applied range of stresses, are shown in Fig. 6.26. Those for the soils at site III were significantly reduced to depths of 1.0m below the compacted surface (1.7m below the G.S.) with a slight effect being achieved down to 1.5m, as shown from the tabulated values for MC2 in Figure 6.26(b). For MC1 considerable reduction in I_c was achieved to a depth of 0.5m below the compacted surface (1.3m below the G.S.) with the effect reducing down to 1.0m and no effect beyond as shown from Figs. 6.25(b) and 6.26(b). However, at stresses below 150 kPa, the values of I_c for MC1 at 0.5 and 1.0m were slightly greater than those of the soil before treatment possibly due to rupturing the bonds, with a limited densification, of the soil at these levels. For the natural condition at site III (Fig. 6.26(b), open symbols), the peak values of I_c of 10% to 17% were reduced to 1% to 7% and to 0.0% to 8% after treatment by VRC with flooding at MC1 and MC2 respectively. Although these peak I_c values for MC1 and MC2 were similar, those for MC2 were achieved at higher stress levels than those for MC1. Similarly, at lower stresses, the rate of increase of I_c for the soils at MC2 was much lower than that for those at MC1. This shows the benefits of a longer period of preflooding in reducing both the collapsing potential and its rate of increase, thereby demonstrating the effectiveness of the treatment. Similar results for the I_c values at a soaking stress of 200 kPa, from the single collapsing test on specimens from the lowest level of the influenced depths, were obtained and these are tabulated and shown in Fig. 6.26. Generally, these results for the different locations are compatible with those of the field density assessment (RI).

6.4.3.2 Double Oedometer - Consolidation - Test Results

Typical results for samples, taken at depths of 0.8, 1.3 and 1.7m, from MC1, and MC2, are shown in Fig. 6.27. These demonstrate that flooding and compaction significantly reduced the collapsing potential. This became almost zero over a range of applied stresses up to 800 kPa for compacted soils within the top 0.3m of the improved depth, and remained small for lower depths, compared to the high values for the same soils before treatment. The changes in the initial void ratio of the samples from different depths reflect the densification effect. Generally the lower the initial void ratio the greater the degree of improvement and, correspondingly, the lower the collapsing potential. Thus, the specimens taken at 1.3 to 1.4m [0.6 to 0.7m], at both locations, indicated more improvement (less deformation and higher stiffness) than the samples from 1.7m [1.0m] as shown from Fig. 6.27. The accompanying values of C_c and m_v for soaked samples and the samples tested at their initial

moisture content, from the different locations at various levels along the treated depth are summarized in Table 6.7.

6.4.3.3 Double Oedometer - Consolidation - Results Analysis and Interpretation

The stiffness of the treated soil was significantly increased by the VRC treatment as indicated by the reduced deformation shown by these soils in Fig. 6.27. The yield stresses, at the SMC (σ_y) condition, were significantly greater than the corresponding values before treatment, and they decreased with depth through the improved zone to reach those of the natural soil beyond the improved depth as summarized in Table 6.7.

The compressibility characteristics, in terms of the coefficient of volume change (m_v) and the compression index (C_c), were significantly affected by VRC with flooding. The variation of these values with depth, for samples from MC1 and MC2 at site III, are shown in Fig. 6.28. The m_v values at the TMC condition were greater than those of the natural soil before treatment over the treated depth, while those at the SMC condition were lower than those of the saturated soil before treatment (Fig. 6.28-a). This indicates that wetting increased the compressibility over the entire wetted depth at the TMC state, compared with that at the NMC state while, at the SMC state, the compaction effect had reduced it across the improved depth. Similarly the values of C_c (Fig. 6.28-b) at the treated moisture content (TMC, 24 to 28%) were higher than those of the natural soil at the NMC, both at the compacted surface (considerable effect) and to a depth of 1.0m below the C.S. (reduced effect) while, at the SMC (16 to 25%), these values were lower both at the surface (considerable effect) and to a depth of 1.0m (less effect), with the exception of the value for MC2 at 0.6m which reached the limit of the natural soil (no effect). Indeed, this indicates water infiltration softened soil layer M2 so that it became more responsive to compaction than the lower part of the medium stiff layer, M1, and this is compatible with the RI assessment. However, the benefits of treatment (low values of m_v and C_c) are apparent when the soil before and after treatment is compared at the same moisture state, SMC, but when these are different in these moisture contents, TMC compared with NMC, the benefits are not reflected. Again, with the passage of time, the treated soil would be expected to return to its natural moisture content when such benefits of compaction may be more apparent. Generally, across the entire depth of treatment (0.0-1.0m), the deformation at the SMC condition was moderately lower than before treatment and almost the same as before treatment at greater depth while, at the TMC, condition it was greater than that of the natural soil at the NMC condition.

Generally, the laboratory results for deformation indicate that VRC with preflooding caused a marked improvement in the deformation behaviour of the soils within 0.5m of the surface and a more moderate improvement for soils between 0.5 and 1.0m below the compacted surface, with only minimal changes at greater depths. Without flooding the benefits of VRC were restricted to the top 0.5m.

6.5 DEEP COMPACTION BY POUNDING

6.5.1 General

Deep compaction by pounding has been selected as a second dynamic method to treat the soils. It has been used widely with success to compact natural silty loess soil in the U.S.S.R. (Abelev,1975) and Bulgaria (Minkov, 1981 and Lutengger, 1986), while Lukas (1980) used pounding to densify natural loose sand deposits. For depths of 1.5 - 1.8m, deep compaction (DC) is considered to be an inexpensive technique for densifying collapsing soil (ASCE, 1978), and a load of 3 to 5 ton dropped from 5 to 8.0m is a traditional method for treating the top 1.5 to 1.8m of the loess soil in Bulgaria (Minkov et al, 1981). The DC was used in combination with flooding to treat the soils at sites I and III. The data includes pounding test, field observations of the ground subsidence during pounding, together with the subsequent SPT and in situ density values. These are supported by laboratory assessments of the deformation characteristics of the impacted soils. As extensive data was obtained, the results from the treated locations at site III are presented in detail, while those from site I are given in Appendix D6 and are only included in the text for correlation and comparison with those from site III.

6.5.2 Field Observation and Field Assessment

6.5.2.1 Deep Compaction 'Pounding' Test

In this technique, a falling weight of 3 metric tons was allowed to fall from a height of 6.0m to dynamically compact the soil. Sites I and III were used for this deep compaction. Each site involved three locations, AD0, AD1 and AD2 at site 1 and MD0, MD1 and MD2 at site III. Two locations, AD1 and MD1 were flooded for one day and another two, AD2 and MD2, were flooded for five days before pounding the final locations, AD0 and MD0, pounding was done without flooding so the soil at these locations was effectively at its natural moisture content.

The falling weight was made of reinforced concrete with a cylindrical shape, 1.5m by 1.0m diameter. A hydraulic releasing system was specially designed and made in the workshop of Aston University and is shown in Fig. 6.29. Once the falling weight had been lifted by crane to the desired height, a hydraulic jack was gently compressed forcing open the release valve, which held the weight from a steel hook at the centre of the top, to allow the load to fall freely and vertically as shown in Plate 6.4. The design of the release system (Fig. 6.29) insured free falling and minimised energy losses between the holding steel wires and the

rolling wheels of the crane (Lukas, 1986). The height of the drop, 6.0m, and the falling weight, 3 ton, were kept constant while the number of blows per location ranged from 6 to 9.

Each location was prepared by excavating the top soil, except at AD0 which was impacted without this removal to assess the effect of this top layer on the depth of treatment. At the other locations a 1.3m diameter hole was manually excavated to depth of 0.7m at site I and 0.34m at site III, and the surface levelled. The vertical displacement was monitored by measuring the level of four points marked on the surface of the falling weight. Generally for all field tests, the tolerance of the measured settlement was ± 0.5mm. The various procedures associated with the pounding treatment are illustrated in Plate 6.4.

6.5.2.2 Ground Surface Depression Results and Analysis

The vertical movements during treatment for MD0 and MD2 are shown in Fig. 6.30, each curve representing the average of the four monitored points at each location, while those for locations AD0 and AD1 are shown in Appendix D6-13. The maximum vertical depression (δ_v), the total number of impacts and the economical impacts, at which no significant further depression was measured (Lukas, 1986), are given for each location in Table 6.8. The values of the soil depression ($\delta_{v\,max}$) in Table 6.8 varied over a wide range from 38.0 to 90.5cm, excluding that at AD2 which reached 130cm after 9 drops, the lowest values generally occurred at the locations not subjected to preflooding, clearly demonstrating the beneficial effect of wetting. The ground depressions produced by this treatment method were significantly greater than those from all the other methods (see Sec. 6.7). At AD2, the high moisture content of the impacted surface at the time of pounding liquefied the soil, due to the development of excessive pore water pressures, and so forced it to flow around the dropping load as shown in Plate 6.5 to produce the misleadingly high value of δ_v. However, the soil depression for such a case cannot be used as a reliable indicator of the depth or degree of improvement, although it does provide field guidance to the number of drops for a specific site (Lukas, 1980). At site I, 7 drops were sufficient for improvement, regardless of the wetting effect, while 6 to 8 drops were required at the preflooded locations at site III against 4 drops for the natural location MD0 as shown in Table 6.8. Clearly wetting did not accelerate the compaction and would not reduce the cost, although it would improve the treatment (increased the degree and depth of improvement) for the same impact energy. The number of drops are compatible with the work of Lukas (1986) and Welsh et al (1987) who reported that normally 10 drops are necessary to produce the required benefit.

6.5.2.3 The SPT Field Results and Analysis

Tests were conducted at both sites and the SPT values, Ns, and corresponding moisture contents are shown in Figure 6.31 for the natural and pounded bores at the site III locations. For the natural bore, to a depth of 4.0m, the Ns and W_n values ranged from 6 to

35 and 12% to 28% respectively while in the three pounded bores, MD0, MD1 and MD2, the corresponding values ranged from 11 to 40 and 14% to 25%, 14 to 36 and 16% to 23%, and 12 to 30 and 14% to 21% respectively. The data in Figures 6.31 (b) to (d) indicate that the SPT values were increased by this treatment. There was a slight drop in the moisture content just below the compacted surfaces and this could contribute to these increases in the SPT values. However at a greater depth where the changes in the moisture contents were minimal, i.e. at 2.8m in Fig.6.31(d) and at 3.0m in the Appendices D5-14 (c) and (d), the increase in the SPT values could not be attributed to such changes, indicating the predominant effect of the treatment by DC, although such small changes in the moisture contents had a major effect on the SPT values detected from the previous treatment methods. A similar trend is apparent with the other pounded locations, AD0, AD1 and AD2 as shown by the data in D6-14.

The SPT results in Fig. 6.31 and D6-14 indicate that SPT is a useful tool for measuring the effectiveness of DC, even when the treatment was combined with flooding, although it failed to evaluate the effectiveness of the other treatments. At site III, to a depth of 4.0m below the ground surface, the SPT values of the treated soils were greater than those before treatment (Fig 6.31), similar behaviour also being apparent at the site I locations (D6-14). Using these SPT values in Fig. 6.31 and D6-13, the depth of improvement (below the C.S.) can be established to range from 2.1 to 2.6m at site I and 2.7 to 3.1m at site III.

6.5.2.4 Field Density Results and Analysis

The values of $\rho_{d\ max}$ at different levels for each location are shown in Table 6.8, while Fig. 6.32(a) shows the changes in dry density to a depth of 4.0m for the locations at site I and Fig. 6.32(b) shows the same to a depth of 4.5m for the locations at site III. The affected depth ranged between 2.0 and 2.2m at site I while, for site III, it ranged between 1.8 and 2.7m. The RI values given in Table 6.8 show that the effect of deep compaction on dry density was considerable to depths of 1.6m to 1.8m below the compacted surface. However, the layering system of the investigated soils and the variations in the soil properties affected both the degree and the depth of improvement as reflected by the sudden changes in the (RI) values shown in Table 6.8. The existence of the stiff layer M3 at site III minimized the effect of the pounding impact beneath it and so restricted the extension of the zone of improvement, with only slight improvement being achieved within layers M3 and M4 as shown in Fig. 6.32(b). The effect of pounding was almost nil (RI = 0.0) in layer M3 at locations MD0 and MD1, with only a slight effect at MD2 (RI = 2.7) which reflected the water infiltration of this soil due to the extended period of flooding, a similar effect was also detected at the lower layer, M4, at the site III locations as shown in Figure 6.32.

In contrast, the action of this stiff layer, M3, as a support to the upper layers, M1 and M2, considerably increased their improvement as the impact energy was partially reflected upwards to further deform these layers rather than being transferred into the lower layer, M4,

as implied by the considerable drop in the RI values between M2 and M3 shown in Table 6.8. As a consequence of the absence of any firm layer within the affected zone at site I, no sudden changes were observed in the RI values shown in Table 6.8. The preflooded locations exhibited greater soil deformation, deeper improved depth and larger degrees of improvement than those treated at the natural moisture content, AD0 and MD0, as can be seen from the increases in ρ_d (RI) in Fig. 6.32 and Table 6.8. The degrees of improvement (RI) at AD1 and MD1 were greater than these at the other locations because the moisture contents at the time of compaction, Wcomp, were marginally greater than the respective optimum values, Wopt, whereas at the other locations, the values of Wcomp were either much less (at AD0 and MD0) or much greater (at AD2 and MD2) than the optimum, as indicated in Table 6.8. At all locations, the top 0.2m of the impacted surface, showed slight surface disturbance and so the maximum dry density was achieved slightly below this level, as shown in Fig. 6.32 and Table 6.8. Welsh et al (1987) indicated that the maximum improvement generally occurs within a zone between one third and one half of the effective depth with less improvement below this level while, above this zone, the improvement was limited due to surface disturbance during impact. However, as the pounded surfaces ended some 0.3 to 0.6m lower than the original ground surface before treatment, this provided some confinement which contributed to the densification and minimized the disturbance at the pounded surfaces. The RI values (Table 6.8) indicate that the degree of improvement at site III was less than that at site I, although the improvement extended to a greater depth at site III. These variations in the soil responses to DC at sites I and III are largely due to differences in soil texture, structure, bonding forces and layering systems (Whetten and Weaver, 1991; Keller et al, 1987; Lukas, 1986).

6.5.2.5 Preflooding Effect on the Degree and Depth of Improvement

Preflooding markedly increased the depth of improvement and the degree of improvement (RI), with the greatest depths of improvement at AD2 and MD2. Preflooding extended the depth of improvement from 1.8m for soils pounded at the natural moisture content (MD0), to 2.7m for soils preflooded for 5 days before pounding, MD2 as shown in Fig. 6.32(b). Indeed, even considering the slight effect on layer M4 at MD0, the depth of improvement of 2.4m is less than that achieved at MD2. In addition, preflooding resulted in considerable soil loss during pounding, for which an appropriate allowance would need to be made during construction. Generally, an excellent improvement was achieved when DC was combined with preflooding, leading to higher densities and greater depths of improvement, compared with those achieved by pounding at the NMC condition.

The primary purpose of DC is to achieve a significant densification at depths greater than those achieved by the other applied methods. Menard and Broise (1975) have proposed the following formula to predict the depth of improvement:

$$D^2 = W \times H \quad\text{------------------------------------}\quad (6.1)$$

where,

> D : Depth of improvement, in metres,
>
> W : Dropping weight, in metric tons, and
>
> H : Falling head, in metres.

Using this equation with the field parameters - dropping weight of 3.0 metric tons from 6.0m, the predicted depth of improvement is 4.24m. The actual depths of improvement at site III from the SPT and field density assessments were 2.7 to 3.1m and 2.4 to 2.7m respectively, which respectively represent 80% and 60% of the predicted depth. Thus the prediction needs to be modified to achieve compatibility with the field values, with different factors necessary for SPT and direct density assessments. Many investigators have reported similar observations with the reduction factor varying from 0.5 for densifying loose sand (Leonards et al, 1980), to 0.65 to 0.8 for sand and clay (Lukas, 1980) and 0.6 for USSR loess (Marinescu, 1986), although the particular value depends upon the actual site conditions, soil type, the equipment utilized (Lukas, 1986; Welsh et al, 1987).

6.5.3 Deformation Behaviour of the Compacted Soil

This was determined in the laboratory on undisturbed samples from test pits at the treated locations, using single and double oedometer tests supported by the SEM observations.

6.5.3.1 Single and Double Oedometer - Collapsing - Results and Analysis

Typical results together with the collapsing potential (I_c), from the single oedometer test at a soaking stress of 200 kPa, are shown in Fig. 6.33 for various levels in the treated soils at MD0, MD1 and MD2. The I_c values of the specimens near the surface were much lower than those of the soils before treatment (Table 5.3) and they increased with depth until they became equal to those of the soils before treatment below the depth of improvement and a similar trend was apparent for specimens from the locations at site I. These I_c values from site III were significantly reduced to depths of 2.6m below the G.S. [1.8m below the C.S.] with a slight effect being achieved down to 4.0m [3.2m] as shown in Figure 6.33, the I_c values for MD0 at 0.2, 1.8, 2.2 and 3.2m below the C.S. were 0.05, 0.9, 1.2 and 4.9% respectively while, before treatment at almost the same levels, they were 7.6, 7.5, 1.3 and 5.6% (Table 5.3). The stiff sandy silt layer, M3, exhibited very similar values before and after treatment, 1.2 and 1.3%, again indicating that pounding had no effect on this layer at MD0, while the underlying layer, M4, exhibited only a minimal effect, I_c being reduced from 5.6 to 4.9%, and these results are compatible with the field density assessment (RI) as shown in Table 6.8.

Reductions in the collapsing potential were achieved, over a wide range of stresses, for the soils from sites I and III in the double oedometer tests as shown in Fig. 6.34 and Appendix D6-15. For the soils at site III (Fig. 6.34) the I_c values were greatly reduced to depths of 2.4 to 2.9m below the C.S (3.7m below the G.S.) at MD0 and MD1, although only a slight effect was recorded down to 2.4m at MD2 as shown in Fig. 6.34(c) and this is similar to the slight increase in the I_c values for this location seen in the results of the single collapsing tests (Fig. 6.33-c). This effect of MD2 may be related to the pore water pressures developed during pounding, due to the higher moisture contents of the soils at this location compared with those of the other locations, reducing the densification at depth. Consequently the RI value at 4.0m, was greater at MD1 (8.9%) than at MD2 (5.7%) and so the I_c values at 3.7m for MD1 (Fig. 6.34(b)) were less than those for MD2 (Fig. 6.34(c)) at the same level, and this indicates the compatibility between the field and the laboratory results. However, despite the variations in the improved depth, the I_c values are still less than those of the soils before treatment.

Figure 6.34 shows that the peak collapsing potential values of 10% to 17% at the natural condition were reduced to 3% and 11% after DC treatment. All these peak I_c values were achieved at high stress levels (800 kPa), at lower stresses the I_c values were smaller and even below zero (Ic/MD2-1.6m in Figure 6.34(c)). These negative values were produced by soaking the highly densified specimens at low stresses, leading to swelling rather than collapsing, although variation in the initial dry density between the two oedometer samples could also lead to these negative values. Interestingly, within the range of the applied stresses, there is no a sharp drop in the l_c values of the treated soils with increasing stress, similar to that exhibited by some of the soils before treatment (Fig. 6.34, open symbol), instead I_c either increased or remained constant with increasing the stress, apart from the silt with sand, A2, as shown in Appendix D6-15. At lower stresses, the rate of increase of I_c for the treated soils at site III was much lower than for the soils before treatment, and similarly a lower rate of increase occurred with those preflooded before pounding than for those pounded at the NMC condition, apart from I_c/MD2-3.7 (Fig. 6.34(c)). At site I, a similar trend was achieved, although the rate of increase of I_c for the treated soils was higher for the soils at site I than for those at site III as shown in D6-15. Overall, the laboratory results from the various pounded locations exhibited an excellent improvement in collapsing potential and they are compatible with the field results.

Having established that Deep Compaction can significantly improve the performance of these Yemeni soils, it is necessary to relate this performance to a practical specification which takes account of the local characteristics. This concept of local specifications has been employed elsewhere for collapsing soils. For example, Minkov and Donchev (1983) have stated that the minimum dry density to be achieved by compacting Bulgarian collapsing soil is 1.55 Mg/m^3 (equivalent to unit weight 15.2 kN/m^3), whereas the natural dry density of these

soils ranged between 1.39 to 1.44 Mg/m^3. However, the Yemeni collapsing soils investigated in this work have very low dry densities ranging between 1.10 and 1.26 Mg/m^3 and, as there is a wide difference between these two ranges for the Bulgarian and Yemeni soils adopting the Bulgarian limit of 1.55 Mg/m^3 may not be an appropriate suggestion. Fig. 6.35 shows the relation between the dry density of the DC treated soils and their collapsing potential at 200 kPa, (Collapsing Index, I_{cx}). This shows that, for a dry density above 1.43 Mg/m^3 (equivalent to unit weight above 14.0 kN/m^3), the collapsing potential is below 2%, and so this value can be selected as an appropriate compaction criterion for the studied soil to minimize the risk of collapse ($I_c \leq 2.0\%$).

6.5.3.2 Double Oedometer - Consolidation - Results Analysis and Interpretation

Typical results for representative samples, taken across the improved depth from MD0, MD1 and MD2 are shown in Fig. 6.36. These demonstrate that pounding, with or without flooding, minimized the collapsing potential, decreased the compressibility and increased the stiffness of the treated soils across the improved depth. The changes in the initial void ratio of the samples from different depths reflect the densification effect. Generally, the lower the initial void ratio of the particular soil, the greater the degree of improvement and, correspondingly, the lower the collapsing potential and soil compressibility and the higher the deformation stiffness. The initial void ratios of the treated specimens from site III at 3.7 to 4.0m below the ground surface within the soil layer M4, were similar to those before treatment and this indicates the minimal effect of pounding at this level, i.e. the lower level of the improved depth. The specimens taken at a depth of 3.0m within the stiff sandy silt, M3, did not show any response, apart from those from MD2 which exhibited slight densification due to wetting by preflooding for five days which weakened the bonding forces before pounding. However, the top two layers, M1 and M2, showed excellent improvement, a minimum collapse and deformation performance. The accompanying values of yield stresses, C_c and m_v for the soaked samples and samples tested at their TMC from various levels in the treated depth at each test location are summarized in Table 6.9.

The deformation of the treated soil was significantly reduced by DC, as shown in Fig. 6.36, leading to an increase in soil stiffness and a decrease in the compressibility characteristics -the coefficient of volume change (m_v) and the compression index (C_c). The yield stress (or the yield stress ratio, σ_y /σ_{vo}) is an indicator of soil stiffness, and the values given in Table 6.9 at both the SMC (σ_y) and TMC (σ_{yn}) conditions were significantly greater than those of the soil before treatment. These decreased with depth through the improved zone to reach those of the natural soil beyond the improved depth, and typical variations for samples from site III are shown in Fig. 6.37 in terms of the yield stress ratio (YSR). At the SMC state the yield stress ratio, YSR, for the soils from MD0 and MD2 -(YSR)s/MD0 and (YSR)s /MD2- at 4.0m below the G.S., reached the value of the natural soil -(YSR)s/MN-, while that for the soil from MD1 -(YSR)s/MD1- was greater. At the same level for the TMC

state, the values for (YSR)t/MD0 and (YSR)t/MD1 reached the value of the natural soil, while that for MD2 -(YSR)t/MD2- was lower due to preflooding for five days which increased the moisture content and so produced less densification. Above this level, at the SMC condition, the yield stresses ratio were greater than those of the natural soils while, at the TMC condition, they were either greater or within the range of the natural soil.

The coefficient of volume change (m_v) and the compression index (C_c), were significantly affected by the DC treatment, as shown by the results for site III in Fig. 6.38. Generally, across the entire depth of treatment (0.0-2.5m), the deformation at both the SMC and TMC conditions was considerably lower than before treatment and almost the same as before treatment at greater depth. The m_v values, at both moisture conditions, were lower than those of the soil before treatment over the treated depth indicating the powerful effect of the pounding in reducing the compressibility at both moisture states so that the associated wetting did not increase the compressibility over the affected depth. With the other treatment techniques, wetting had the predominant effect on compressibility, particularly at the TMC state, but with DC the compaction effect overcame the wetting effect and so the trend of increasing the compressibility with further wetting was not apparent for these treated soils and this is compatible with the field assessment by the SPT. Similarly the values of C_c (Figs. 6.38(b) and (d)) at the both moisture contents, TMC and SMC, were lower than those for the natural soil at the NMC and SMC conditions, ranging from a considerable effect at the impacted surface to a much reduced effect at depths of more than 3.0m. The only exception was the value at the SMC condition for MD2 at 1.4m which reached the limit of the natural soil (minimum effect), which again can be related to the development of excess pore pressures during pounding, which minimized both the collapse of the pores and the rupture of the bonds, so that further loading in the laboratory destroyed the remaining bonds leading to this high value of C_c which is compatible with the RI assessment.

The laboratory results for deformation generally indicate that DC, with or without preflooding, caused a significant improvement in the mechanical behaviour of the soils within 1.5 to 1.8m of the compacted surface (C.S.) and a moderate improvement for soils beyond that up to 2.1 to 2.7m, and only minimal change at greater depths.

6.5.3.3 Scanning Electronic Microscope (SEM) Results and Interpretation

Twelve specimens were selected from various levels in the treated soil at site III to investigate the effect of the treatment on soil structure. Fig. 6.39 shows considerable densification and destructuring of the soils at [0.1 below the treated surface] of MD0 with Fig. 6.39(a) showing some trapped pores possibly due to disturbance within the densified soil at [0.1m] due to the dynamic impact (Lukas, 1986). This high densification includes significant destructuring and even particle crushing (Fig 6.39-b), with the formation of a dense structure that may not involve grain to grain contacts, as the ruptured bonds and fine debris with some

pores have become trapped between the soil grains. Figs. 6.39 (c) and (d) show the SEM results for the soil before treatment, for comparison purpose. As shown in Table 6.8, the RI value at [0.1m] was 23.8% which increased to reach 32.6% at [0.3m] and such values indicate surface disturbance and so are compatible with these SEM results.

Further evidence of the pounding effect is shown in Fig. 6.40 for the treated specimens (Figs. 6.40 (a) - (c)) from the densified zone, [0.7m] at MD1 (RI=27.1%), with the images of the soil before treatment being given in the same figure (Figs. 6.40 (d) - (f)) for comparison. Significant densification throughout the soil mass is apparent from Fig. 6.40(a), with destructuring of the fines and cementation agents shown in Fig. 6.40-(b). This treatment produced a characteristic structure at the contacts involving trapped destructured fines and cementing materials which minimized the grain to grain contacts, as shown in Fig. 6.40(c), a structure that cannot be achieved by static compaction, where grain to grain contact is common as the fine materials have the opportunity (time, slow rate of loading, gradual destructuring, etc.) to slide away allowing the grains to pack. Indeed at this level at MD1 (Fig. 6.40), the soil-water interaction had been markedly affected by preflooding for one day, which increased the moisture content of the upper layers, M1 and M2, to the wet side of the optimum moisture content as indicated in Table 6.8, so significant destructuring and densification were obtained by pounding at this location. At this level, [0.7m], fewer pores were detected, as shown from the structure in Figs. 6.40 (b) and (c), compared to those at surface (Fig. 6.39). In contrast flooding at MD2 for 5 days, led to limited weakening and distortion of the weakly bonding materials, nodules aragonite, at a depth of [1.7m] as shown in Appendix D6-16. This Figure also shows the unaffected buttresses and large pores which possibly indicates slight destructuring and densification (RI=2.7%) of the stiff sandy silt soil, M3, at MD2. Indeed, in the lower part of the influenced depth, some destructuring with less densification is possible and this probably produces a relatively open structure after treatment. Generally, the findings from the SEM are in agreement with the field assessment (RI).

Overall, the results indicate that the soils at site I responded better to the DC treatment than those at site III, particularly at surface, where the soil texture, structure and cementation bonds were more effective in resisting the destructuring and densification of deep compaction. Pounding or deep compaction resulted in variable densification and destructuring to a maximum depth of 2.7m, with the major changes in the top 1.8m. Preflooding slightly extended the depth of improvement and significantly increased the degree of improvement across this depth. The degree of improvement was affected by local factors such as moisture content, layering system and bonding forces, but this method can be classified as a very good to excellent technique for improving the studied soils to a moderate depth.

6.6 STABLIZATION BY CEMENT AND LIME

Two locations were selected at site III, one of these, MSC, was stabilized with cement, while the other, MSL, was stabilized with lime. Each location was excavated to produce an area 1.0 by 1.0m and 0.4m in depth and an auger drill was used to form a central hole at each location 0.1m diameter by 3.0m deep. The hole was filled with the stabilization agent which was also spread over the surface of the excavated location. Approximately 500 litres of water were added to aid the percolation of the agent into the soil mass. Each location was subsequently treated with about 100 litres of water per day for a further 12- 15 days. Sampling and laboratory testing were operated covering soil samples from the top 2.0 to 3.0m of each location. The field assessment and laboratory testing results of the detected samples from both locations exhibited no effect for such treatment. Grouting under high pressure is required and such investigation has been left for future work.

6.7 COMPARISON OF THE FIELD AND LABORATORY RESULTS

This section compares and contrasts the response of those strata which appeared in more than one location and so were subjected to different treatment techniques at different moisture contents. In addition, the field and laboratory data are also used to compare the individual techniques in terms of such factors as ground response and degree of improvement.

6.7.1 Field Results Contrast

6.7.1.1 Ground Displacement

The ground depression is not a reliable indicator of the degree of improvement although it has been used for practical field guidance (Lukas, 1980). However, the ground depression can be used to compare the soil response to different treatment techniques as indicated in Fig. 6.41. This figure indicates that the ground depressions produced by DC treatment method were significantly greater than those from all the other methods - (20 to 30 times) static flooding or loading with flooding and (7 to 10 times) dynamic VRC - demonstrating the effectiveness of the DC method. Fig. 6.41(b) shows minimum variation in the ground depressions between the corresponding treated locations by DC at sites I and III, apart from the excessive depression of AD2, compared with that of MD2, due to the flow of the liquefied soils around the dropping load as indicated earlier. However, at both sites, the ground depressions of the presoaked locations were more than those treated at the in situ

moisture condition. From the previous findings, the degree and depth of improvement was, similarly, greater for the presoaked locations than that for those treated at the in situ moisture condition. This may indicate some qualitative link between the ground depression and the degree and depth of improvement. Further evidence for such link is that, the degree and depth of improvement decreased according to the treatment methods, in the order DC, VRC, preloading and flooding and, again, the ground depression decreased in the same order. Generally, this link seems to be that the greater the ground depression the higher the degree and the greater the depth of improvement. Consequently, the ground depression may be used as a qualitative indicator to compare the effectiveness of treatment (the degree and depth of improvement) by various methods, although this is not totally in agreement with the observation reported by Lukas (1986).

6.7.1.2 Standard Penetration Test (SPT)

Figure 6.42 shows the SPT values plotted against moisture content for the natural soils and those treated by flooding, VRC and DC at site III. This clearly shows for both the natural soils and those treated by flooding that the SPT value decreased with increasing moisture content. This trend was less marked with those treated by VRC and almost non-existent for those treated by DC as can be detected from the slope of the fitted line and the value of the Regression Number (R# or R^2) for the particular treatment. For the DC treatment R# was the smallest, 0.216, as shown in Fig. 6.42(d), while demonstrates that the benefits of this treatment are largely independent of moisture content, and reflects the powerful effect of the DC treatment on improving the particular soils.

6.7.1.3 Field Density

Fig. 6.43(a) provides a comparison between the field density results, in terms of the Relative Increase in the dry density (RI), for two levels below the surfaces of various locations at site III treated by different methods. This indicates the powerful effect of both the DC and VRC treatment methods which increased the density (RI) at the surface [0.05m], within the soil layer M1, while at [1.0m], within M2, the RI values produced by the DC treatment were significantly greater than those from all the other methods demonstrating the effectiveness of this method at this level. In fact, at surface the effectiveness of treatment by VRC slightly exceeded that by DC as indicated from the greater values of RI in Fig. 6.43(a). In contrast, flooding caused a swelling at surface leading to a decrease in the dry density as indicated by the negative value of RI in Fig. 6.43(a).

Fig. 6.43(b) allows comparison between the RI values [at 1.0m below the compacted surface] for the different locations treated by DC at sites I and III. At this level [1.0m], within the soil layer A1 at site I and M2 at site III, the degree of improvement (RI) increased with preflooding (i. e. MD2 >MD1 > MD0) at both sites, although site III showed more

improvement than at site I (i. e. RI at MD2 > AD2 as shown in Fig. 6.43(b)). This slight increase in the RI value of M2 over that of A1 at the same level, particularly for the presoaked locations, indicates the effect of the soil type (sandy silt A1 and silt M2), consistency of the soil (medium to stiff A1 and soft M2), moisture content at tne time of compaction and layering system (the continuity existence of A1 at site I and the existence of the very stiff M3 under M2 which reflected the impact effect) on the effectiveness of the DC treatment. Indeed, at surface where there is a similarity in the soil type (A1 and M1), consistency and layering system, the response of the soils at site 1 to DC treatment was better than that at site III as indicated from the values of RI in Table 6.8.

6.7.2 Laboratory Results Contrast

6.7.2.1 Collapsing Potential

Fig. 6.44 permits the comparison between the collapsing potentials, I_c, of the various treated soils at site III, M1 at the surface and M2 at 1.0m below the compacted surface. At the surface, Fig. 6.44(a) shows the significant effect of both the DC and VRC methods in reducing the magnitude of the collapse over the applied range of stress, with a more moderate effect from both the preloading and flooding methods. These observations are supported by the total collapse potentials, I_T, for the same treated soils at the same level shown in Fig. 6.45(c). Indeed, assessment of the collapsing behaviour of the treated soils using only the I_c values may be misleading as part of the collapse deformation can be exercised under loading alone, I_L, as indicated from the high values of I_L (Fig. 6.45(a)) and I_T (Fig. 6.45(c)) for the soils treated by preloading and flooding. However, the values of I_L for the soils treated by DC and VRC methods are slightly higher than those of the soil before treatment and this is simply due to the low moisture content of the natural stiff sandy silt M1 which exhibited a limited deformation at the NMC state under loads.

At 1.0m below the compacted surfaces, only the DC treatment caused a considerable reduction in the collapsing characteristics (I_c, I_L and I_T) as indicated from the Figs. 6.44(b), 6.45(b) and 6.45(d). At this level, the values of I_L (6.45(b)) of the soils treated by DC are lower than those of the natural soil, M2, before treatment. This soil layer, M2, is soft and has a high moisture content and void ratio and so, at the NMC condition, it deforms moderately under only loads and more than that of the natural soil M1.

6.7.2.2 Consolidation Behaviour

The powerful effect of the DC and VRC methods at surface and of the DC method at [1.0m] is also apparent from the consolidation results, as shown by comparison between the values of volume change coefficient, m_v, at both the SMC and TMC conditions for the soils

treated by different methods at site III, given in Fig. 6.46. At the surface, this figure indicates that with the flooding and preloading treatment techniques, wetting had the predominant effect on compressibility (m_v values), particularly at the TMC state (Fig. 6.46(b)), but with the DC and VRC techniques the compaction effect overcame the wetting effect and so, the trend of increasing the compressibility with further wetting was reduced (Fig. 6.46(a)) for these treated soils and this is compatible with the field assessment by the SPT. In contrast, at 1.0m below the treated surface, the trend of reducing the compressibility with further wetting, due to the effectiveness of the particular treatment, was only apparent from the soils treated by DC method as indicated in Fig. 6.46. Similar findings were observed when the other consolidation characteristics (σ_y, C_c and YSR values) were considered.

6.8 SUMMARY AND GENERAL COMMENTS

From the results of flooding, preloading, VRC and DC treatments specific and general remarks are drawn. These specific remarks for each treatment method are as follows:

6.8.1 Flooding

- The investigated soils would appear to be conditional collapsing soils and surface flooding for a period of 50 days caused only limited volume change, heave and/or collapse. As a result, treatment by flooding has no beneficial effect on the soils of Sana'a area.

_ The infiltration of water resulted in the formation of a pear-shaped, wetted zone which extended more in the vertical direction (4.0 to 5.0m) than in the horizontal direction (1.8 to 2.2m). This water distribution was influenced by the layering system, the vertical and horizontal permeability of each layer, the existence of granular pocket or lenses, and the presence of channels such as root holes. However, a minimum clearance of about 2.0m between structures and any planted or wetted area nearby is desirable to reduce the effect of wetting on bearing soils.

- The SPT values of the studied soils are sensitive to the water content and so, the SPT test is not adequate to assess, correlate or determine the properties of these soils.

6.8.2 Preloading

- In general, the field loading tests indicate that the studied soils are conditionally collapsing soils under both loading and wetting and the collapse potential due to wetting is more than that

due to loading, with the soils at site II being more sensitive to wetting than loading compared to those from site III.

- Preloading and flooding resulted in partial wetting and so partial destructuring of the soil to a depth of 1.3m, with the major changes only apparent over a shallow depth. Near the contact surface (0.0-0.5m) the deformation at the SMC condition was moderately lower than before treatment and almost the same as that before treatment at a greater depth while, at the TMC, condition it was greater than that of the natural soil at the NMC condition across the entire depth of treatment. The field collapsing results are compatible with the laboratory data including the SEM and deformation tests.

- Preloading and flooding caused a moderate improvement in the mechanical behaviour of the soils within 0.5m below the loaded surface, beyond that only a slight effect was achieved. Consequently, this method can be classified as a fair to good improvement technique for these collapsing soils subjected to only low stresses, to 200 kPa.

6.8.3 Roller Compaction

- The economical number of Roller passes was, 8 to 12 for all the preflooded locations against 16 passes for the natural location and so prewetting, to the desirable moisture content (about Wopt), accelerated compaction and would also make the process more economical.

- The SPT is not a valuable tool for measuring the immediate effectiveness of VRC where this treatment was combined with flooding. However, with the passage of time, the treated soil exhibited an increase in the resistance to penetration which was not necessarily due to the reduction in moisture content.

- The effect on dry density of VRC, was only significant just below the surface (0.3 to 0.5m) and decreased rapidly.

- Vibratory roller compaction with flooding resulted in variable densification and destructuring down to 1.0m below the compacted surface. A significant (0.0 to 0.5m) to moderate (0.5 to 1.0m) improvement was achieved using this method with preflooding leading to a higher density and a greater depth of improvement than was achieved at the NMC condition. This treatment method can be classified as a good to very good technique for improving the studied soils to a shallow depth.

6.8.4 Deep Compaction

- The ground depressions produced by DC treatment method were significantly greater than those from all the other methods, and the values of the soil depression varied over a much wider range (38.0 to 90.5cm) than those produced by the other methods.

- Wetting did not accelerate the deep compaction and would not reduce the cost, by reducing the number of drops, although it significantly improved the treatment. With all the tested soils, the sufficient number of drops to produce the required benefit did not exceed 9 drops.

- Just below the compacted surfaces of these treated locations, changes in the moisture content could possibly contribute to the observed increases in the SPT values, while at a greater depth where the change in moisture content was minimal, the increase in the SPT values were attributed to the DC treatment. Consequently, the SPT considered to be a useful tool for measuring the effectiveness of DC, even when combined with flooding, although it failed to evaluate the effectiveness of the other treatments.

- For the studied soils, it was necessary to modify the prediction of the depth of improvement using the formula proposed by Menard and Broise (1975) by applying a reduction factor with an average value of 0.7.

- The dry density of 1.43 Mg/m^3 is recommended as an appropriate value to which the studied soil have to be compacted, to minimize the risk of collapse ($I_c \leq 2.0\%$).

- Generally, the results indicate that the soils at site 1 responded better to the DC treatment than those at site III, where the soil texture, structure and cementation bonds were more effective in resisting the destructuring and densification of deep compaction. Pounding or deep compaction improved the soils to a maximum depth of 2.7m, with the major changes in the top 1.8m. Preflooding slightly extended the depth of improvement and significantly increased the degree of improvement across this depth. The degree of improvement was affected by the moisture content, layering system, age, soil type and bonding forces. This treatment method can be classified as a very good to excellent technique for improving the studied soils to a moderate depth.

6.8.5 Stabilization by Cement and Lime

- Stabilizing a site by flooding the soil with water-lime or cement mixture, without applying pressure, exhibited no effect for such treatment, and grouting under high pressure is required.

6.8.6 Laboratory Study

_ The coefficients of the the permeability for vertical flow (K_v) are greater than these for horizontal flow (K_h), with those obtained from the falling head tests being greater than those from the oedometer tests, and this supports the field observation of vertical and horizontal infiltration.

- The laboratory results, including the SEM analysis, are compatible with the field density assessment (RI).

- Pounding, with or without flooding, minimized the collapsing potential, decreased the compressibility and increased the stiffness of the treated soils across the improved depth.

- The collapsing potentials values, I_c and I_L, of the soils treated by DC were smaller and were achieved at higher stresses, compared to those of the soils treated by the other treatment techniques, apart from those achieved by VRC technique at surface. Similarly, the peak I_c values of the soils treated by DC were smaller and were achieved at higher stresses, compared to those of the soils treated by the other treatment techniques, apart from those achieved by VRC techniques at surface.

- The m_v and C_c values of the soils treated by DC, at both moisture conditions, were lower than those of the soil before treatment over the treated depth indicating the powerful effect of the pounding in reducing the compressibility at both moisture states as the compaction effect overcame the wetting effect. Therefore, the trend of increasing the compressibility with further wetting was less apparent for these treated soils by DC when compared with the other treatment techniques, where wetting had the predominant effect on compressibility, particularly at the TMC state, and this is compatible with the field assessment by the SPT.

Table 6.1: The coefficients of permeability obtained from Oedometer and the Falling Head tests.

| Location | Depth (m) | K_v and K_h from Oedometer test (m/sec) | | | | K_v and K_h from Falling Head test (m/sec) | | | |
| | | Before Flooding | | After Flooding | | Before Flooding | | After Flooding | |
		K_v	K_h	K_v	K_h	K_v	K_h	K_v	K_h
MF	1.0	6.59×10^{-10}	5.53×10^{-10}	5.61×10^{-10}	4.73×10^{-10}	-	-	1.27×10^{-6}	1.87×10^{-7}
	2.0	5.49×10^{-10}	-	7.10×10^{-10}	4.27×10^{-10}	4.54×10^{-6}	3.7×10^{-6}	3.74×10^{-7}	2.71×10^{-7}
	3.0	2.45×10^{-10}	-	7.06×10^{-10}	-	-	-	-	-
	4.2	3.56×10^{-10}	5.92×10^{-10}	2.6×10^{-10}	-	-	-	-	-
KF	1.2	1.37×10^{-9}	—	—	3.31×10^{-9}	-	-	-	-
	2.2	1.20×10^{-9}	—	—	1.69×10^{-9}	-	-	-	-
	3.5	1.16×10^{-9}	—	-	-	-	-	-	-

Table 6.2 : Summary of the engineering characteristics of the soils after flooding at sites III (MF) and IV (KF).

Location	Average initial property			Collapse[a] potential (I_c, %) at stresses		Deformation characteristics					
	Depth (m)	e_o	ρ_d (Mg/m^3)	100 kPa	200 kPa	SMC			TMC		
						σ_y (kPa)	C_c	m_v x10^{-4} (m^2/kN)	σ_{yn} (kPa)	C_c	m_v x10^{-4} (m^2/kN)
KF	1.0	0.822	1.51	0.2	1.2	--	--	--	--	--	--
	2.0	1.035	1.36	--	3.6	220	0.58	2.82	280	0.54	2.18
	3.0	1.258	1.22	--	--	160	0.61	5.41	250	0.76	2.28
MF	1.0	1.122	1.29	--	--	100	0.54	4.9	300	0.99	1.63
	2.2	1.556	1.09	--	--	120	0.69	6.22	170	0.87	3.8
	3.0	0.933	1.42	--	--	240	0.39	1.2	400	0.58	0.78
	4.2	1.192	1.25	--	--	80	0.46	3.91	400	0.67	1.27

a : From the single oedometer test.

Table 6.3 : Summary of the field collapsing and hydroconsolidation tests, carried out at sites II and III.

Location	Depth* m	Applied stress kPa	Loading status	Field settlement in (mm)				Time in days		Deformation Resistance Indicator @ kN/m		General remarks
				Δi	Δt	ΣΔ (Δi+Δt)	Sum Δ	Per load	Total	K_{bf}	K_{af}	
ML1	0.8	50	dry	1.5	1.0	2.5	2.5	7	7	20000	--	
		100	dry	2.5	0.75	3.25	5.75	7	14	15400	--	
		150	dry	3.25	0.5 d	3.75	9.5	4	18	13300	--	d- High settlement with time (Δt) due to soaking, time is needed for deeper water infiltration and so more compression occurs.
		150	soaked	--	15.5	15.5	25.0	17	35	--	--	
ML2	0.8	50	dry	0.6	2.0	2.6	2.6	3	3	19200	--	
		100	dry	1.0	0.6	1.6	4.2	3	6	31250	--	
		100	soaked	-- f	7.5	7.5	11.7	10	16	--	--	f - High immediate settlement (collapse, in few minutes) due to loading after soaking.
		150	soaked	10.1	4.75	14.85	26.55	14	30	--	3400	
ML3	0.8	0.0	soaked	--	--	-11 g	--	5 g	--	--	--	g- Free swelling due to flooding for 5 days, neither the swelling nor the time was add to the compression deformation or corresponding time.
		50	soaked	1.0	4.12	5.12	5.12	6	6	--	9800	
		100	soaked	10.5	14.5	25.0	30.12	11	17	--	2000	
		150	soaked	13.0	h	13.0	43.12	1	18	--	h	h- Failure by tilting took place the next day after applying the last load increment.
										19800	5000	Average

* The indicated depth is the depth of the loaded surface from the ground surface.
@ The deformation resistance indicator is defined as the load over the displacement.

(Table 6.3: Continued).

Location	Depth* m	Applied stress kPa	Loading status	Field settlement in (mm) Δi	Δt	ΣΔ (Δi+Δt)	Sum Δ	Time in days Per load	Total	K_bf kN/m	K_af @ kN/m	General remarks
GL1	1.2	50	dry	0.8	2.4	3.2	3.2	8	8	15625	--	a - After the first 3 days of soaking under 150 kPa a slight tilting started, the last load was adjusted and left for 3 days without soaking after that soaking continued for 9 days more. Extensive settlement occured with slight tilting and then the test stoped. Because off that, the deformation was divided into two sets; the 23 days deformation as the end of the collapsing test (Sum Δ=26mm) and the deformation of the last 9 days as tilting failure deformation (Sum Δ=51.2mm).
		100	dry	2.2	2.0	4.2	7.4	4	12	11900	--	
		150	dry	1.0	0.8	1.8	9.2	5	17	27800	--	
		150	soaked	--	16.8 a	16.8	26	6	23 a	--	--	
					25.2	25.2	51.2	9	32	--	--	
GL2	1.2	50	dry	0.75	0.5	1.25	1.25	6	6	40000	--	b - Load adjusted for7 days before soaking and applying the last load increment, to control failure tilting.
		100	dry	0.75	1.0	1.75	3.0	3	9	28600	--	
		100	soaked	--	10.5	10.5	13.5	14 b	23	--	--	
		150	soaked	9.5	2.5	12	25.5	5	28	--	4200	
GL3	1.5	0.0	soaked	--	--	-12 c	--	5 c	-	--	--	c - Free swelling due to flooding for 5 days, neither the swelling nor the time was added to the compression deformation and the corresponding time.
		50	soaked	2.5	4.5	7.0	7.0	7	7	--	7100	
		100	soaked	7.75	1.25	9.0	16.0	10	17	--	5600	
		150	soaked	4.0	1.5	5.5	21.5	5	22	--	9090	
										24700	6300	← Average

* The indicated depth is the depth of the loaded surface from the ground surface.
@ The deformation resistance indicator is defined as the load over the displacement.

Table 6.4 : Summary of the engineering properties of selected pre-loaded soils at sites I and III.

Location	Average initial property			Collapse potential (I_c , %) at stresses		Deformation characteristics					
						SMC			TMC		
	Depth (m)	e_0	ρ_d (Mg/m^3)	100 kPa	200 kPa	σ_y (kPa)	C_c	$m_v \times 10^{-4}$ (m^2/kN)	σ_{yn} (kPa)	C_c	$m_v \times 10^{-4}$ (m^2/kN)
GL1	1.25	0.964	1.40	--	--	110	0.417	3.17	350	0.296	1.7
	1.7	1.256	1.21	--	--	65	0.375	3.84	130	0.291	2.24
	2.3	1.28	1.20	--	--	35	0.422	4.45	250	0.485	2.25
GL3	1.7	1.258	1.22	--	--	70	0.367	4.1	--	--	--
	1.9	--	--	--	--	--	--	--	--	--	--
	2.4	1.045	1.35	--	--	80	0.298	2.69	100	0.369	3.32
ML1	0.9	1.201	1.26	--	--	120	0.446	2.39	200	0.489	3.24
	1.4	1.306	1.21	--	--	100	0.488	5.1	400	0.68	2.67
	1.9	1.428	1.15	--	--	90	0.541	5.3	200	0.806	3.2
ML3	0.9	1.193	1.27		--	115	0.445	2.21	--	--	--
	1.4	1.377	1.17	--	--	75	0.511	4.67	--	--	--
	1.9	1.307	1.21	--	--	110	0.6	5.25	--	--	--

Taple 6.5 : Summary of the Relative Increase (RI) for the preloaded locations.

Location \ Depth[a] m	0.0-0.1	0.5-0.6	1.0-1.1
GL1	10.8	3.0	0.8
GL3	7.0	2.0	0.7
ML1	4.0	1.0	1.9
ML3	5.6	1.5	2.5

a : The indicated depths are the depths below the loaded surfaces.

Table 6. 6 : Summary of the steel roller compaction at sites I and III.

Location	Depth to the ground surface in (m) [a]	Moisture content (%) Wn	Wopt	Wcomp	State of compaction	δv max (mm)	ρd max (Mg/m³)	Total # of passes	Economical # of passes	RI [b] (%)
AC0	0.7			11	Natural moisture content	70.5	1.79 [c]	32	16	44.7
	1.0	12	21	12			1.35			12.3
	1.2			12			1.21			0.7
AC1	1.2			31 [d]	Preflooded [e] for one day with 1.5 m³	169 [d]	1.71	36	10	42.2
	1.4	12	21	26			1.54			28.1
	1.7	15		20			1.27			1.6
	1.9						1.19			0.0
AC2	0.7			20	Preflooded for five days with 1.5 m³ every day	75	1.78	32	12	48.1
	1.2	12	21	15			1.45			20.6
	1.5						1.31			9.0
	1.7	15		18			1.26			0.8
MC1	0.7			22	Preflooded for one day with 1.5 m³	66.3	1.56	34	10	25.8
	1.1	17	18	18			1.31			9.8
	1.4			16			1.24			2.9
	1.7	25	28	17			1.19			0.8
MC2	0.7			29	Preflooded for three days with 1.5 m³ every day	73.0	1.52	30	8	22.4
	1.1	17	18	27			1.31			9.8
	1.4			26			1.28			5.2
	1.7	25	28	23			1.21			2.5

General field observation:

c- The maximum dry densities, corresponding to the optimum moisture contents, for the soils A1, M1 and M2 are 1.57, 1.53 and 1.52 Mg/m³ respectively.

d- Overcompaction was observed due to the high moisture content at the compacted surface, resulting in δ_v of 66mm after 10 passes and 169mm after 36 passes, with further passes the deformation kept increasing without any equilibrium achievement.

e- For the preflooded locations, a period of 1 to 3 days was given for the wetted surface to loss part of its moisture to reach a moisture content, at surface, allow for operating the roller compaction without any difficulties or causing a state of overcompaction as occurred at the location AC1.

a : The compacted surface of all locations were at a depth of 0.7m below the ground surface, except that of AC1 which existed at 1.2m.

b : Relative Increase in dry density is the percentage of the increase in dry density (compacted - natural) to the natural dry density, (in situ dry density).

Table 6.7 : Summary of the engineering properties of the treated soils after steel roller compaction.

Location	Average initial property			Collapse potential [a] I_c in per cent at stresses		Deformation characteristics					
						SMC			TMC		
	Depth (m)	e_o	ρ_d (Mg/m³)	100 kPa	200 kPa	σ_y (kPa)	C_c	$m_v \times 10^{-4}$ (m²/kN)	σ_{yn} (kPa)	C_c	$m_v \times 10^{-4}$ (m²/kN)
AC0	0.8	1.076	1.35	- -	- 0.5	70	0.312	4.01	- -	- -	- -
	1.1	1.14	1.29	0.9	8.7	- -	- -	- -	- -	- -	- -
AC1	1.3	0.664	1.67	1.3	2.0	250	0.15	1.22	350	0.11	0.9
	1.7	1.32	1.20	- -	6.5	45	0.352	2.98	- -	- -	- -
AC2	0.8	0.767	1.58	2.3	3.3	160	0.232	2.09	400	0.145	0.9
	1.3	0.959	1.43	0.9	0.9	75	0.313	3.41	160	0.306	3.3
	1.7	1.296	1.21	- -	10.3	- -	- -	- -	- -	- -	- -
	2.2	1.06	1.36	- -	- -	- -	- -	- -	- -	- -	- -
MC1	0.8	0.803	1.56	- 0.8	-.04	>800	0.22	1.04	>800	0.187	1.05
	1.3	1.236	1.24	3.3	5.5	60	0.361	4.0	140	0.709	3.60
	1.7	1.412	1.15	- -	- -	100	0.51	5.3	200	0.87	3.94
	2.2	1.30	1.21	- -	6.6	- -	- -	- -	- -	- -	- -
MC2	0.8	0.803	1.56	-1.6	-0.7	>800	0.10	1.79	>800	0.51	1.14
	1.3	1.172	1.28	1.2	2.0	100	0.561	3.30	400	0.56	1.47
	1.7	1.138	1.16	0.3	3.0	110	0.541	4.13	230	0.754	1.92
	2.2	1.474	1.12	- -	4.9	- -	- -	- -	- -	- -	- -

a : From the single oedometer test.

Table 6. 8 : Summary of the Deep Compaction (DC) -Pounding- at sites I and III.

Location	Soil layer	Depth below ground surface (m)	Total soil loss[a] (m)	Wn (%)	Wopt (%)	Wcomp (%)	State of compaction	δv max (cm)	ρd max (Mg/m³)	Total # of drops	Economical # of drops	RI %	General field observation
AD0	A1	0.7	0.45			11	No soil was removed before pounding and compaction was carried out at NMC stste	41	1.73 b	9	7	39.1	b- The maximum dry densities, corresponding to the optimum moisture contents, for the soils A1 and A2 are 1.56 and 1.62 Mg/m³ respectively.
		1.2		12	21	12			1.36			10.9	
		2.2				12			1.31			5.3	
	A2	3.0		18	23	19			1.12			1.7	
AD1	A1	1.4	1.40	14		22	A depth of 0.6m was removed and preflooding for one day with 0.5m³ was under-taken before pounding	77.0	1.61 c	9	7	29.5	c- After pounding, the top surface of the impacted location was slightly loosened or disturbed.
		1.5							1.75			40.6	
		1.7			21	20			1.65			32.6	
		2.0		11		10			1.61			29.4	
		2.7		13					1.3			4.5	
	A2	3.0		21	23	22			1.15			4.4	
	A3	3.6		15	--	14			1.27			0.9	
AD2	A1	2.1	1.90	10	21	31	A depth of 0.6m was removed and preflooding for five days with 0.5m³/day was carried out before pounding	130	1.54	9	7	23.8	d- This measured value was affected by the upward soil displacement around the rammer, due to the high moisture content at compaction, almost at liquid state. A value of only 70cm could be detected from observation of soil in the pit after compaction.
	A2	3.0							1.29 d			17.1	
		3.4		19	23	28			1.35			7.2	
	A3	3.8		15	--	18			1.34			6.4	

a- The total soil loss included both the removed soil before Pounding and the ground depression due to pounding, up to the nearest 0.05 to 0.1m. The depth of removed soil for AD0 was zero and for both AD1 and AD2 was 0.6m.

Table 6. 8 : (Continued).

Location	Soil layer	Depth below ground surface (m)	Total soil loss [d] (m)	Moisture content (%) Wn	Wopt	Wcomp	State of compaction	Field observation δv max (cm)	ρd max (Mg/m³) [b]	Total # of drops	Economical # of drops	RI (%)	General field observation
MD0	M1	0.8				13	A depth of 0.34m was removed and pounding was carried out at the in-situ moisture content		1.54			23.8	b- The maximum dry densities, corresponding to the optimum moisture contents, for the soils M1, M2 and M4, were 1.53, 1.52 and 1.55 Mg/m³ respectively.
		1.0	0.80	16	18	15			1.65			32.6	
		1.5							1.36			9.3	
	M2	2.5		26	28	25		38.0	1.25	6	4	13.5	
	M3	3.0		11	--				1.45			0.0	
	M4	4.0		17	22	18			1.31			5.7	
MD1	M1	1.4		15		26	A depth of 0.34m was removed and preflooding for one day with 0.5m³ were done before pounding		1.49 [c]			19.8	c- After Pounding the top surface of the impacted location was slightly loosened or disturbed.
		1.5	1.30		18	22			1.63			30.8	
		1.6		17					1.52			22.0	
	M2	2.0		25	28	27		90.5	1.40	9	8	27.1	
		2.5							1.27			15.3	
	M3	2.8		10		9			1.45			0.0	
	M4	4.0		18	22	19			1.35			8.9	
MD2	M1	1.3		17		28	A depth of 0.34m was removed and preflooding for five days with 0.5m³ were carried out before pounding		1.51			21.3	
		1.5	1.30		18				1.65			32.6	
		1.7							1.56			25.4	
	M2	2.0		26	28	28		82.0	1.36	9	6	23.5	
	M3	3.1		12	--	13			1.49			2.7	
	M4	4.0		17	22	20			1.31			5.7	
		4.5							1.26			1.6	

d - For all the locations MD0, MD1 and MD2 the depth of removed soil before treatment was 0.34m. After treatment the depth of the compacted surface was taken to the nearest 0.05 to 0.10m to simplify the comparizon.

Table 6.9 : Summary of the engineering characteristics of the soils treated by Deep Compaction at sites I and III.

Location	Depth (m)	e_o	ρ_d (Mg/m³)	Collapse potential (I_c, %) at stresses 100 kPa	200 kPa	SMC σ_y (kPa)	C_c	$m_v \times 10^{-4}$ (m²/kN)	TMC q_n (kPa)	C_c	$m_v \times 10^{-4}$ (m²/kN)
AD0	0.7	0.767	1.58	- -	- -	80	0.276	3.86	- -	- -	- -
	1.4	1.056	1.37	- -	- -	100	0.389	383	>800	0.073	0.44
	2.2	1.192	1.27	- -	4.9	100	0.336	2.54	550	0.197	0.74
	3.0	1.536	1.10	- -	9.1	- -	- -	- -	- -	- -	- -
AD1	1.6	0.598	1.75	- -	- -	>800	1.23	0.8	- -	- -	- -
	2.2	0.694	1.65	- -	- -	>800	0.153	1.15	- -	- -	- -
	2.7	1.22	1.25	- -	- -	- -	- -	- -	- -	- -	- -
	3.0	1.374	1.17	- -	8.1	130	0.176	4.25	200	0.588	4.33
AD2	2.0	0.811	1.55	- -	- -	150	0.249	1.63	- -	- -	- -
	2.8	1.03	1.38	- -	1.9	170	0.339	2.25	- -	- -	- -
	3.2	1.054	1.36	- -	7.0	230	0.535	2.31	200	0.668	2.56
MD0	1.2	0.823	1.53	- -	0.05	>800	0.115	0.76	- -	- -	- -
	1.6	1.136	1.30	- -	0.3	360	0.497	1.73	>400	0.266	0.6
	2.6	1.175	1.28	- -	0.9	260	0.43	1.1	>400	0.05	1.66
	3.0	0.763	1.56	- -	1.2	>400	0.301	1.2	>800	0.034	0.38
	4.0	1.182	1.27	- -	4.0	130	0.466	3.32	- -	- -	- -
MD1	1.6	0.804	1.55	- -	- -	>800	0.156	1.5	>800	0.246	1.74
	2.5	1.256	1.24	- -	0.5	220	0.438	1.35	>800	0.123	0.35
	3.0	0.891	1.48	- -	1.0	200	0.319	1.97	>400	0.103	0.44
	3.7	1.199	1.26	- -	3.9	200	0.561	2.18	400	0.508	0.75
MD2	1.6	0.786	1.56	- -	- -	>800	0.206	1.81	>800	0.096	1.26
	2.3	1.276	1.22	- -	- -	210	0.595	3.13	- -	- -	- -
	3.0	0.726	1.61	- -	3.4	>800	0.169	0.61	>800	0.09	0.52
	3.7	1.223	1.25	- -	2.2	120	0.448	3.54	>800	0.203	0.84
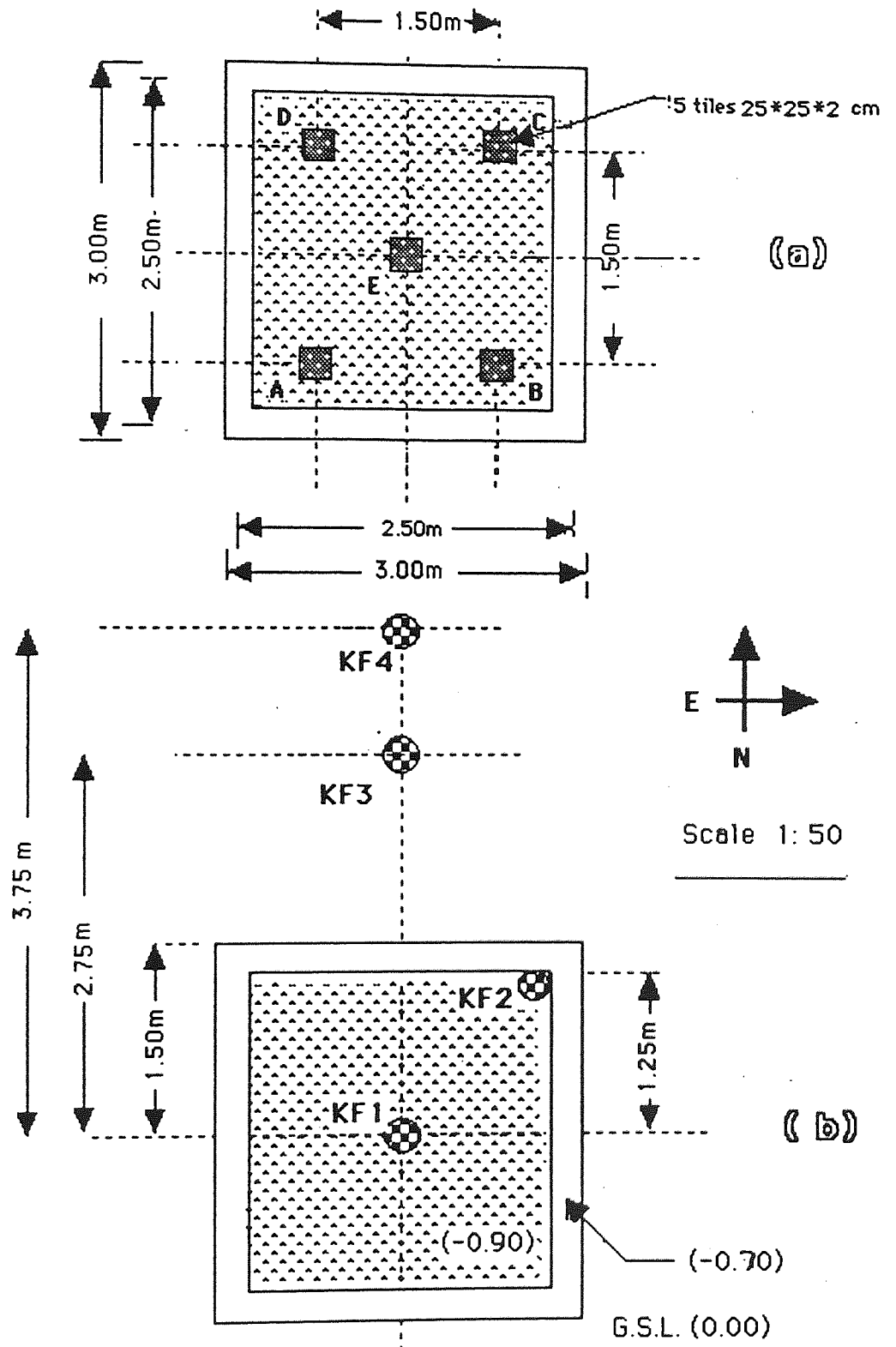
Fig. 6.1 : The flooding location KF.

a) The distribution of the measuring marks, and
b) The distribution of the SPT positions.
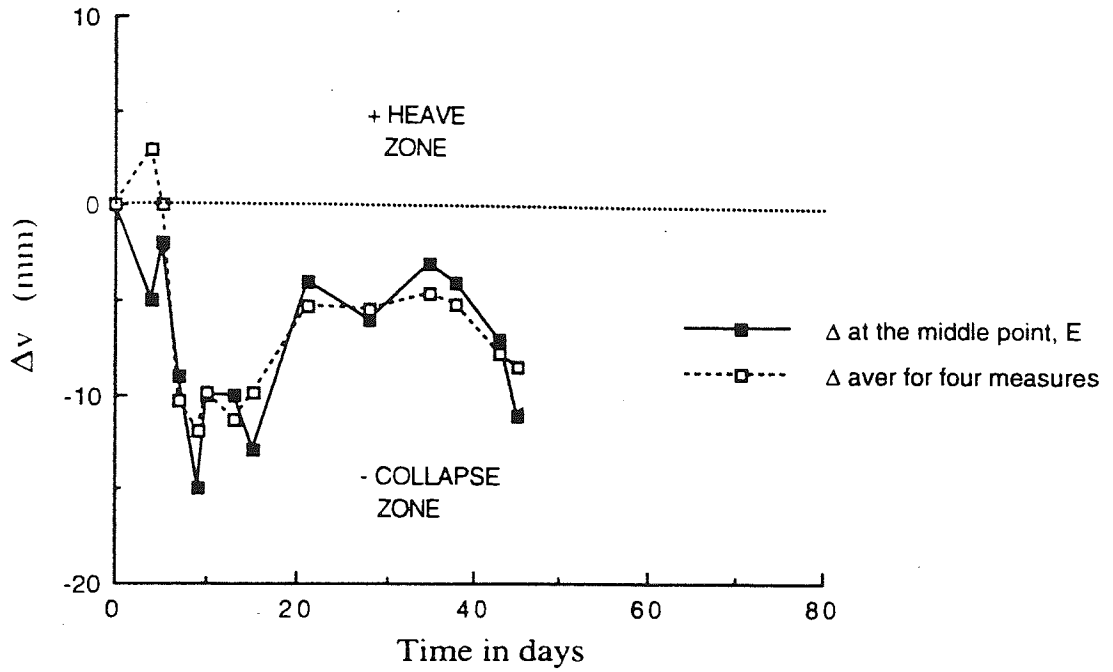
Fig. 6.2 : The vertical displacement of the flooded location, KF, at site IV.
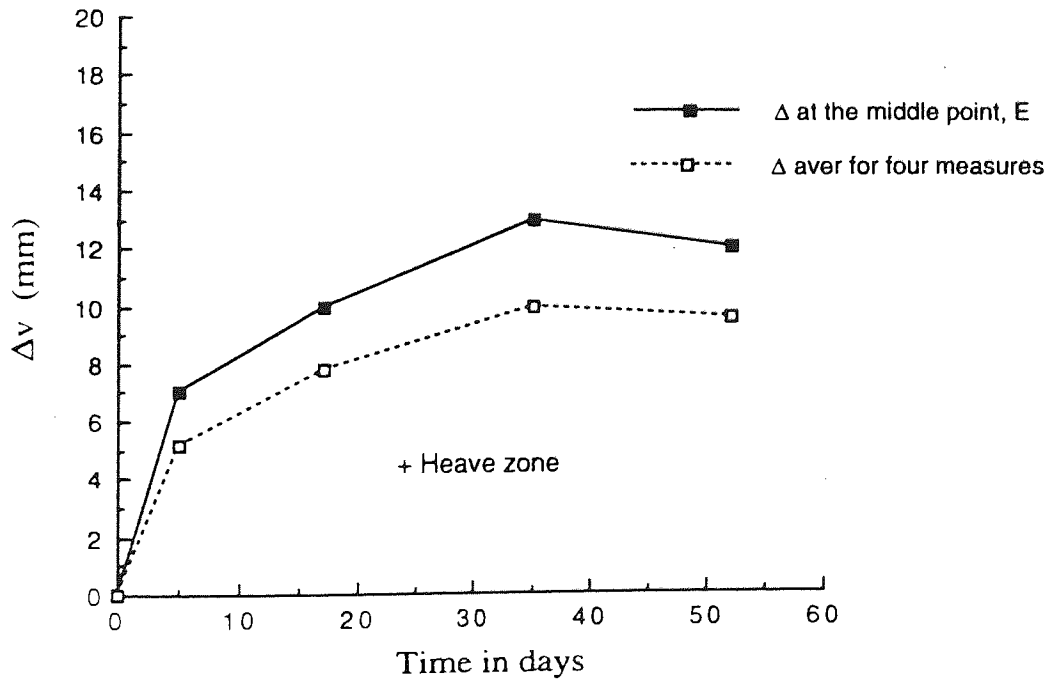
Fig. 6.3 : The vertical displacement of the flooded location,MF, at site III.
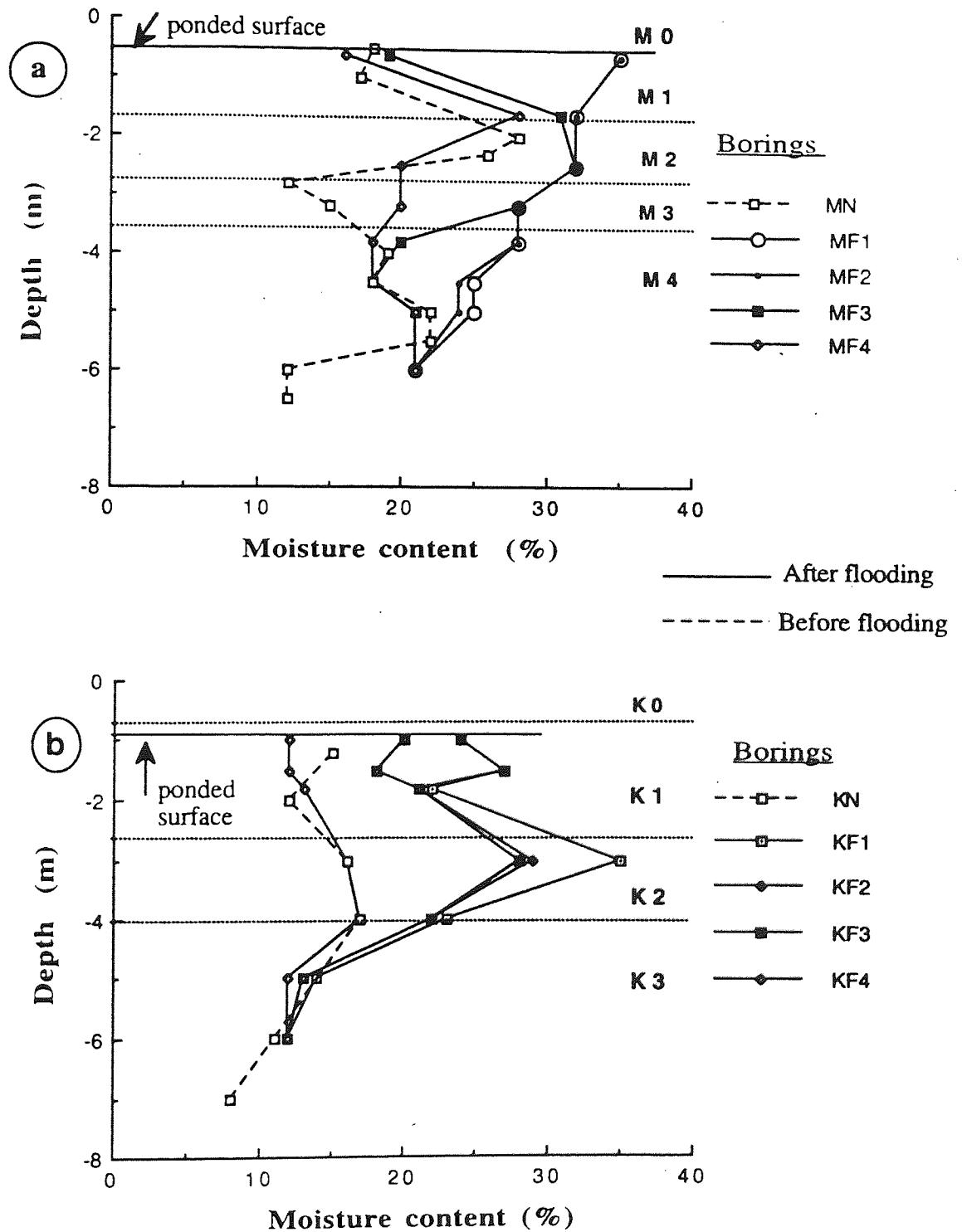
Fig. 6.4 : The variation of the moisture content with depth for each individual boring at the locations; a) MF and b) KF.
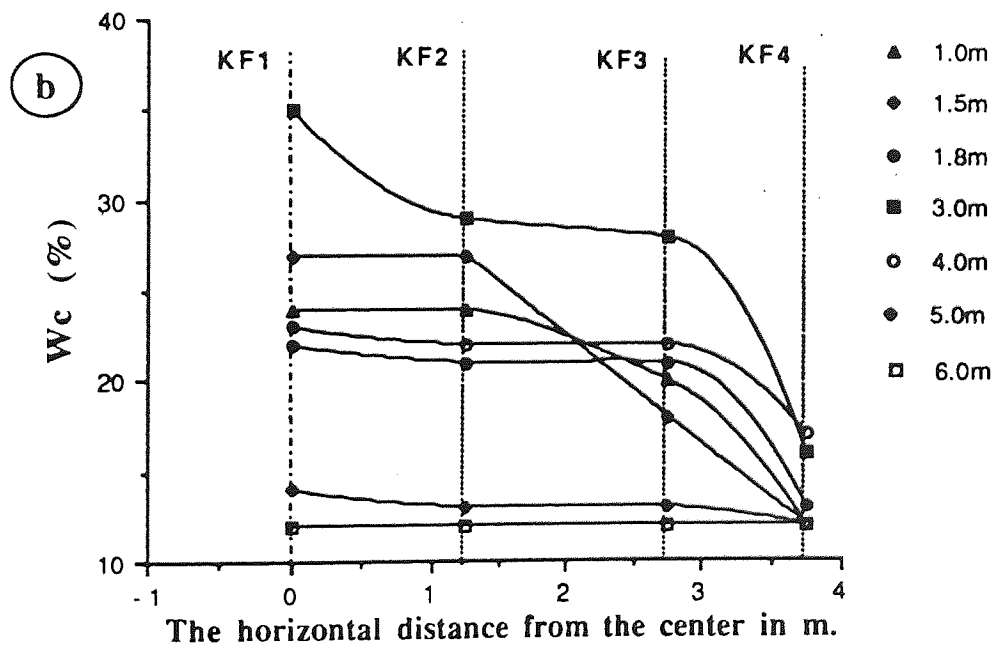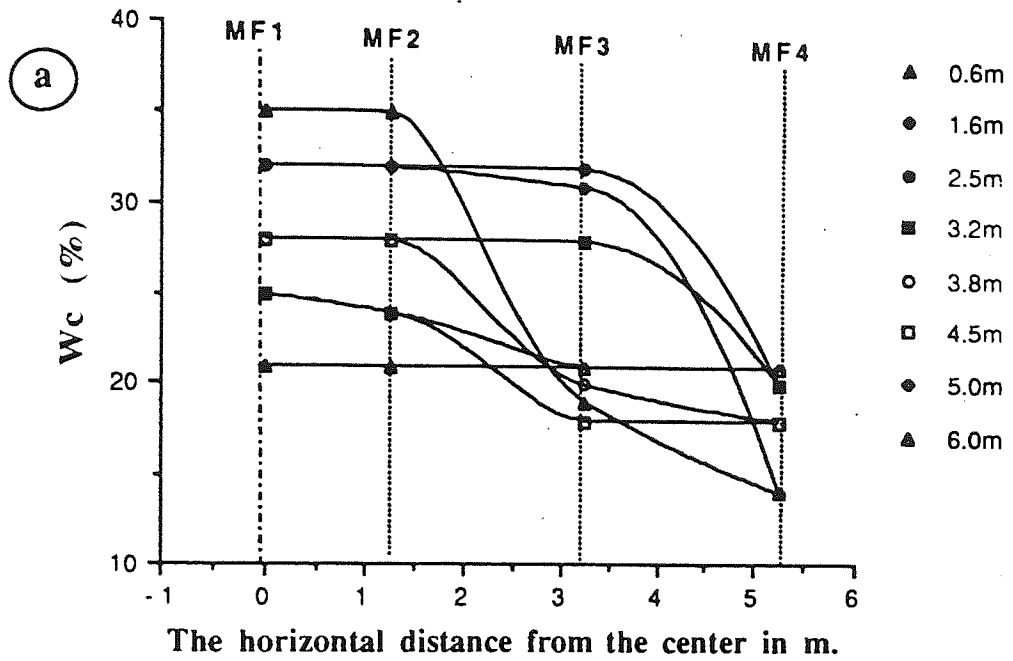
Fig. 6.5 : The depth and extent of moisture distribution beneath the flooded
area at the locations; a) MF and b) KF.
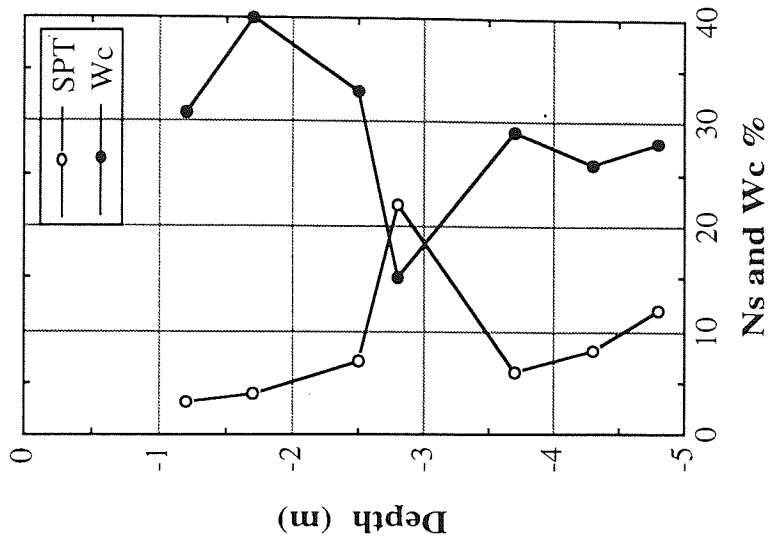
b) The flooded location, MF2.
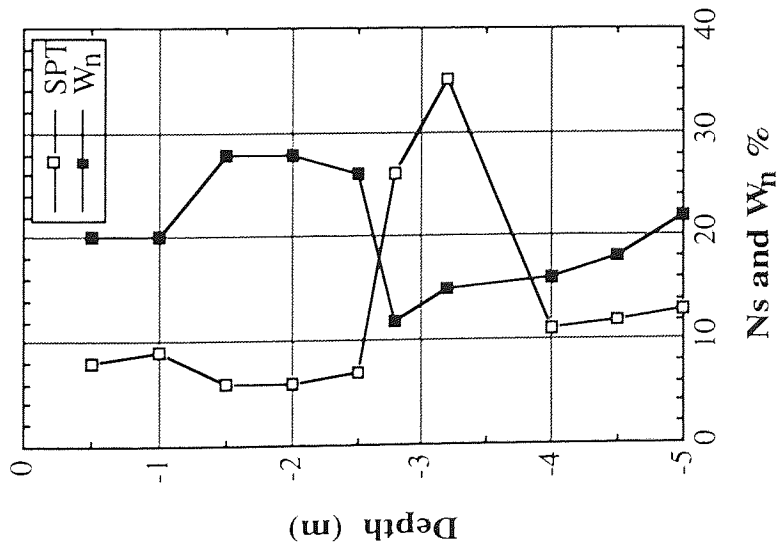
a) The natural location, MN

Fig. 6.6 : The correlations of the SPT values and the corresponding moisture content of the flooded bores MF2 at location MF with those of the location before flooding, MN, at site III.

$$y = 125.21 - 8.4629x + 0.14490x^2 \quad R^2 = 0.946$$
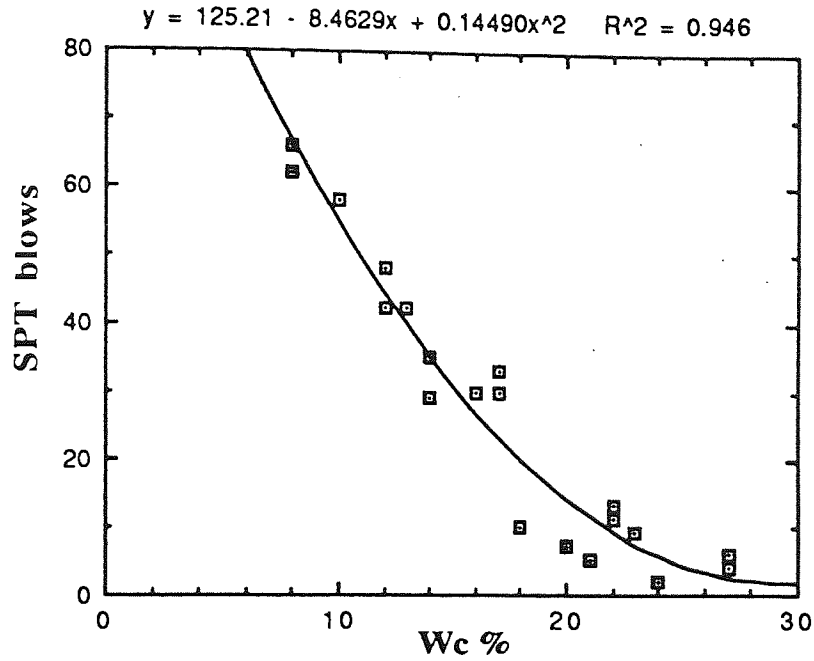
Fig. 6.7 : The variation of SPT values with the moisture content for the flooded location KF at site III, (layers K1 and K2).
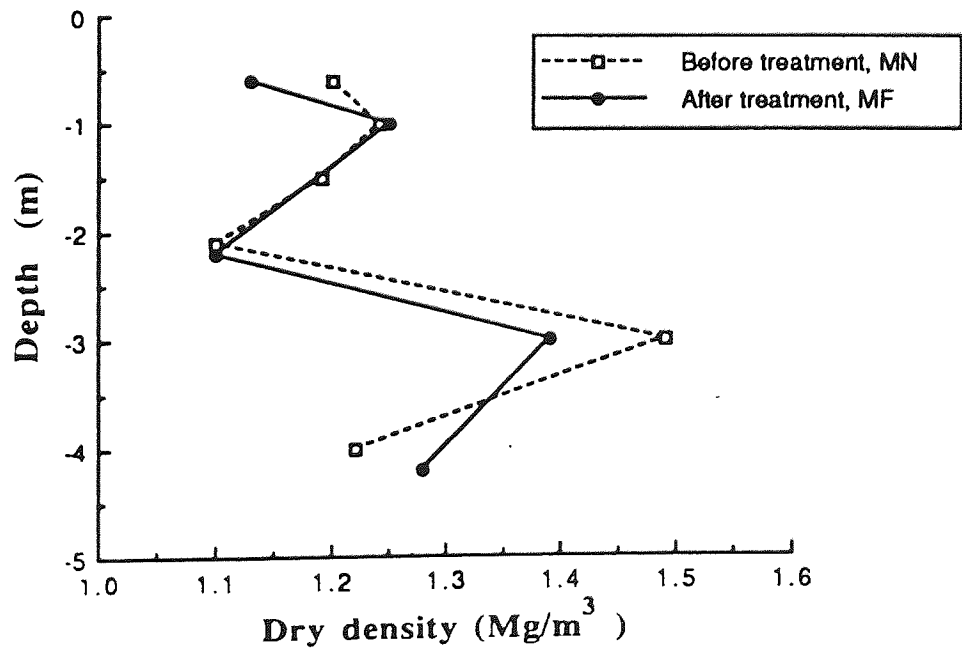
Fig. 6.8 : The variation of the dry density with depth of the location treated by flooding, MF.
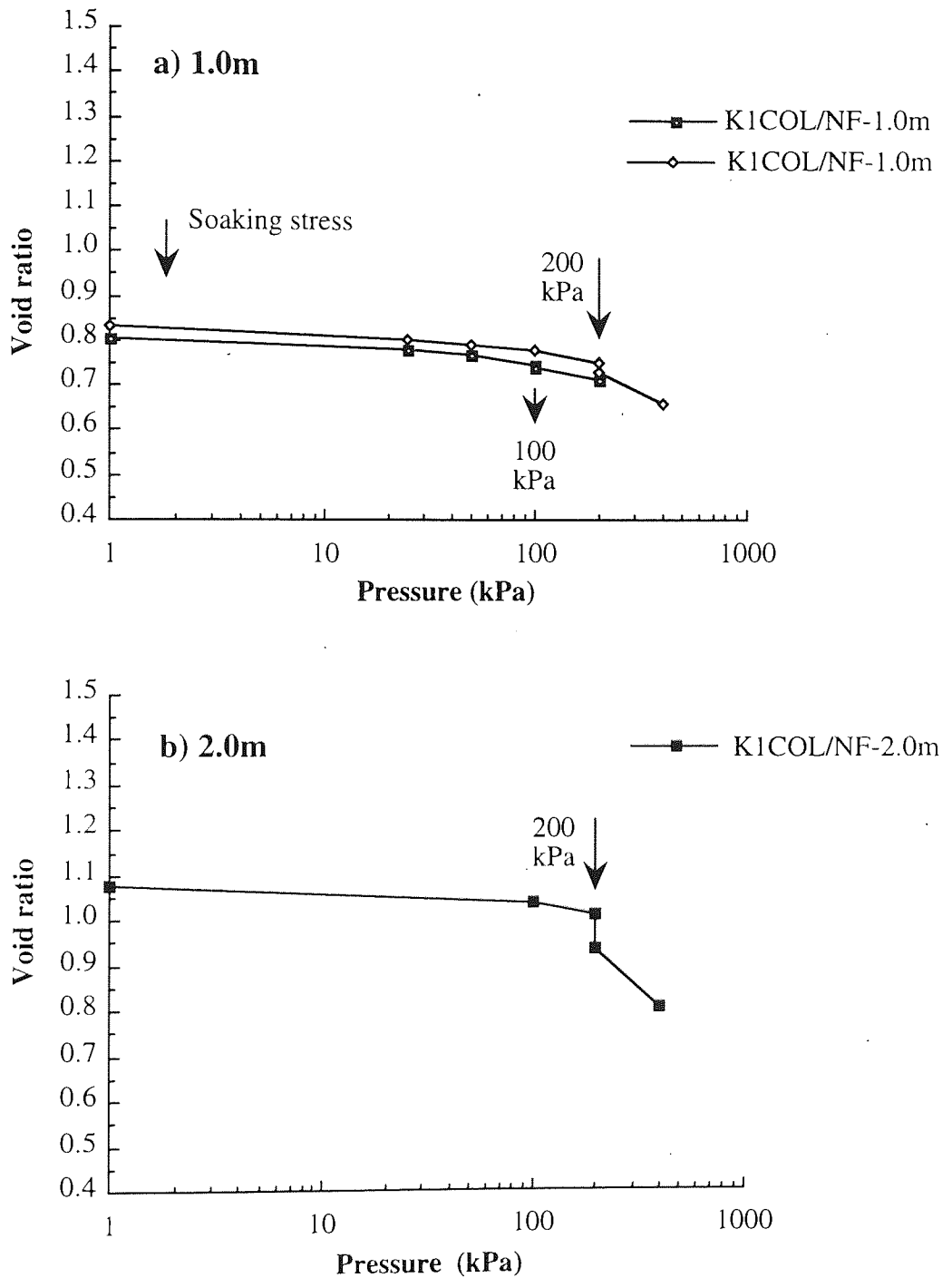
Fig. 6.9 : The collapsing potential results of the flooded soils at location KF.
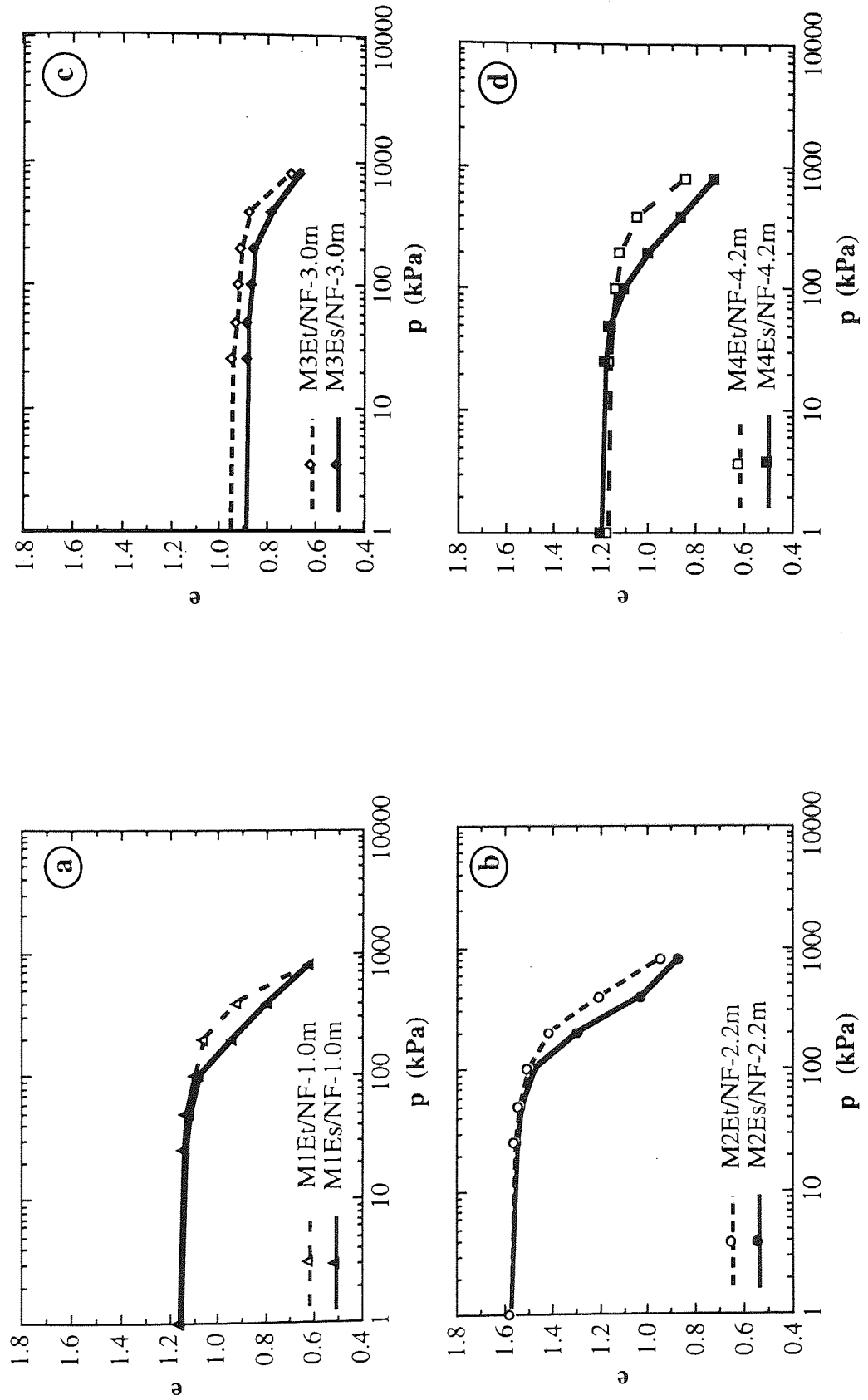
Fig. 6.10 : Double oedometer test results for the samples from the flooded location MF tested at the treated and soaked moisture states, detected from; a) 1.0, b) 2.2, c) 3.0 and d) 4.2 metres.
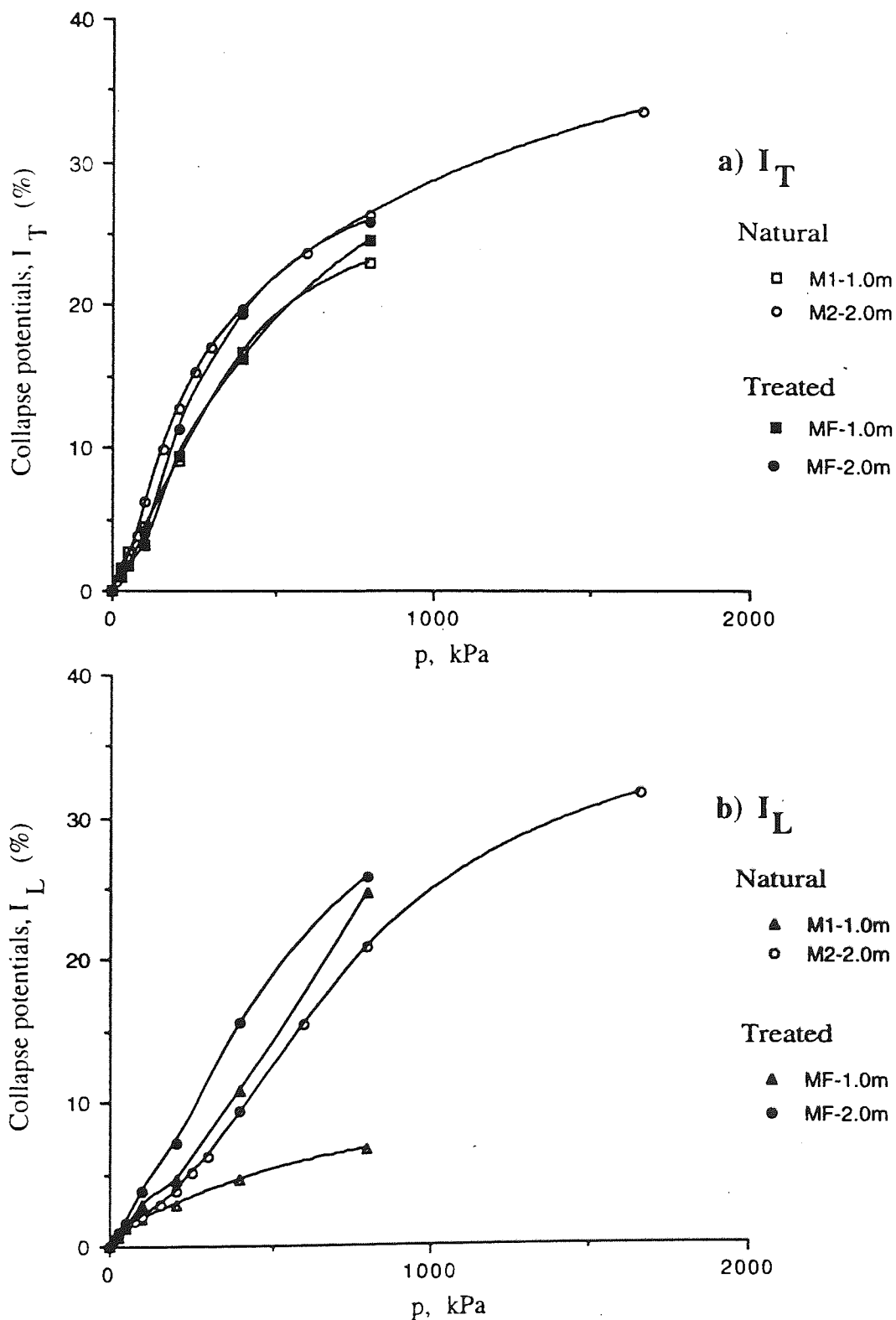
Fig. 6.11 : Variations in the collapsing potentials, I_T and I_L for the natural and flooded soils M1 and M2.
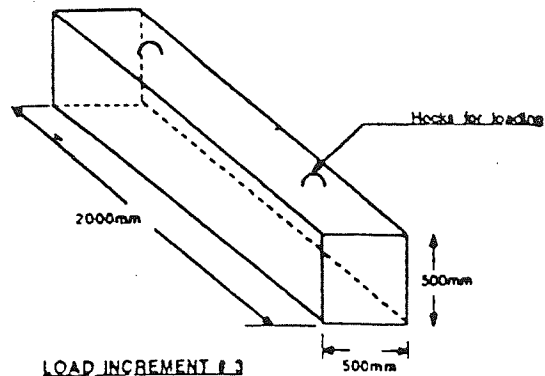
LOAD INCREMENT # 3
4 PICES: 500X2000X500mm
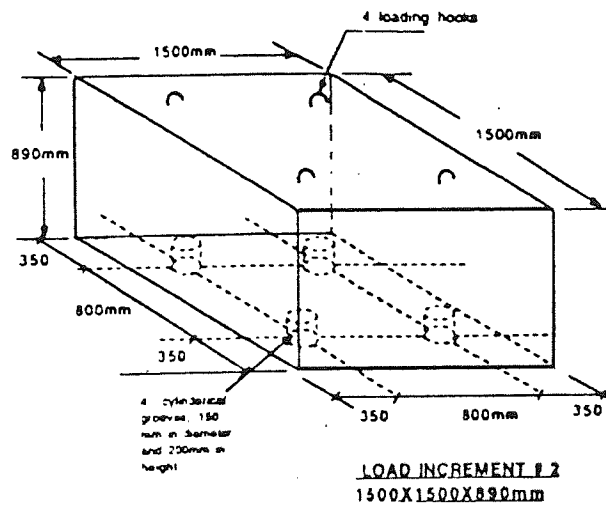
LOAD INCREMENT # 2
1500X1500X890mm
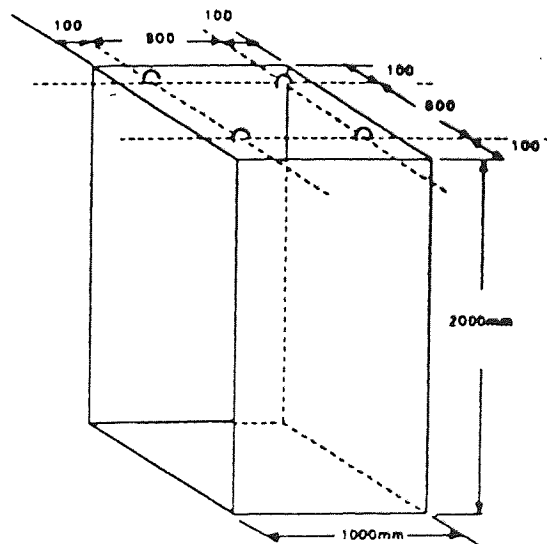
LOAD INCREMENT # 1
1000X1000X2000mm

Fig.6.12: The dimensions of the three concrete, incremental loads
used in the field loading.
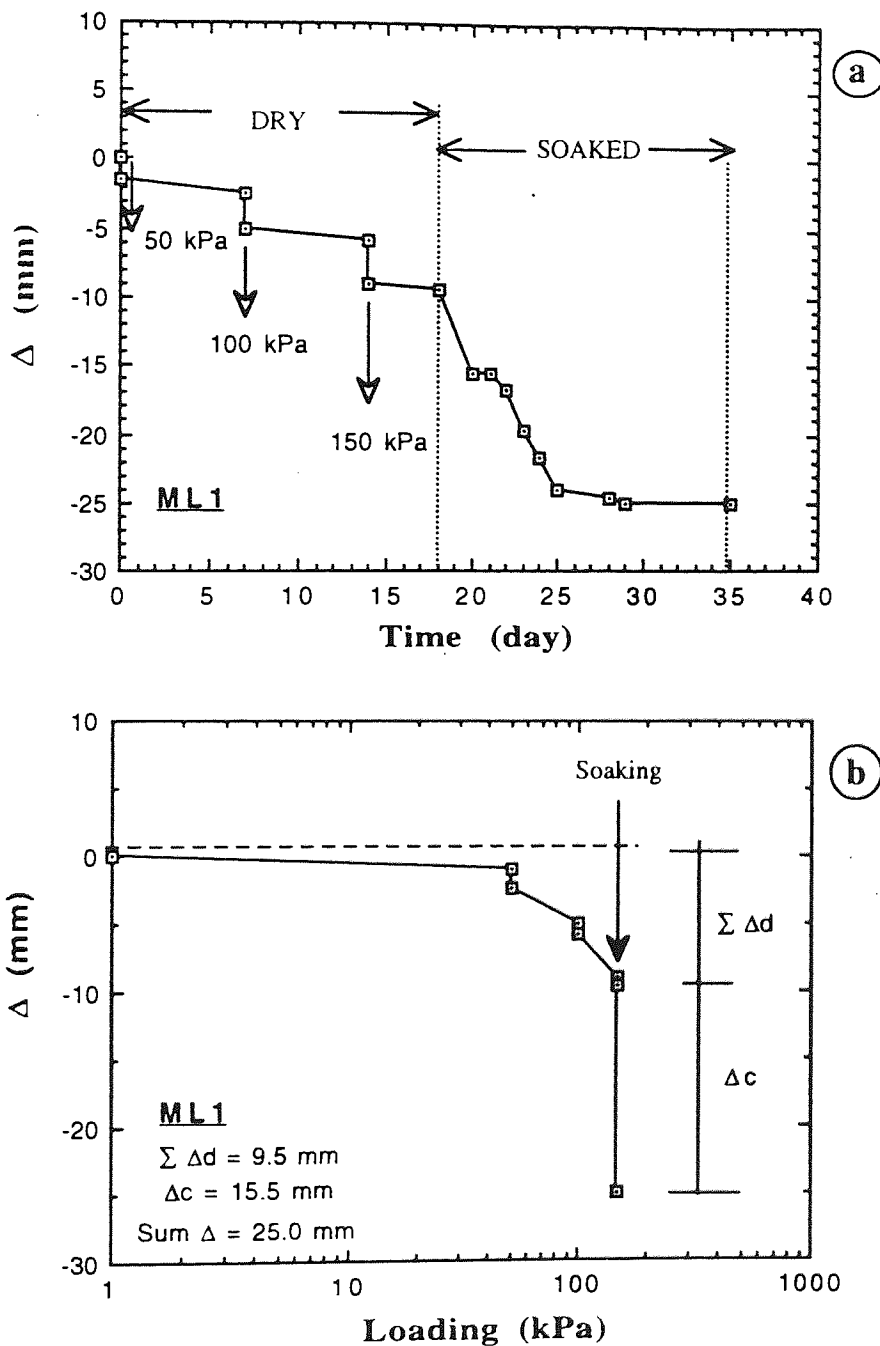
Fig. 6.13 : Field collapsing test under 150 kPa at the location ML1.
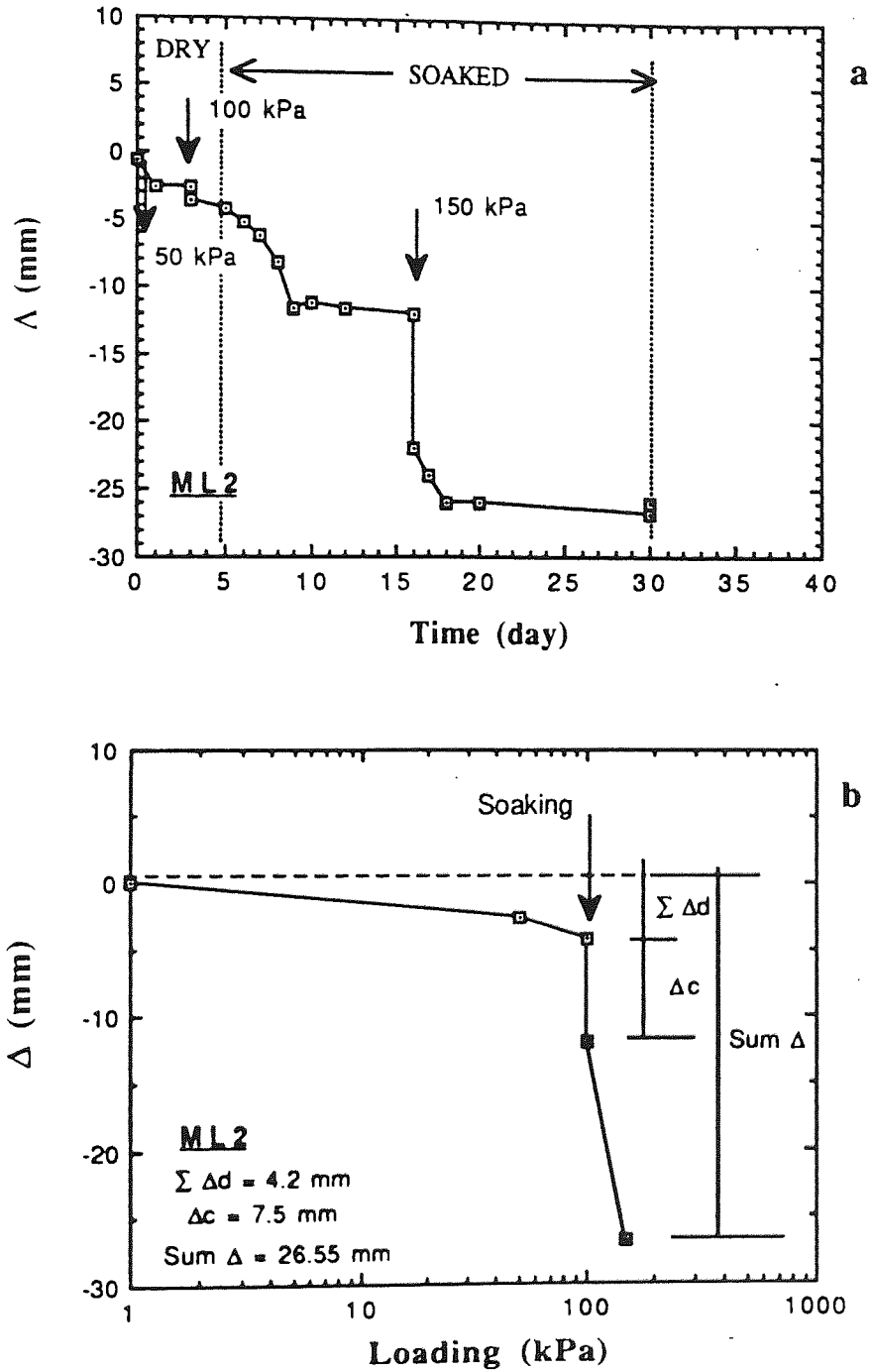
Fig. 6.14 : Field collapsing results under 100 kPa at the location ML2.
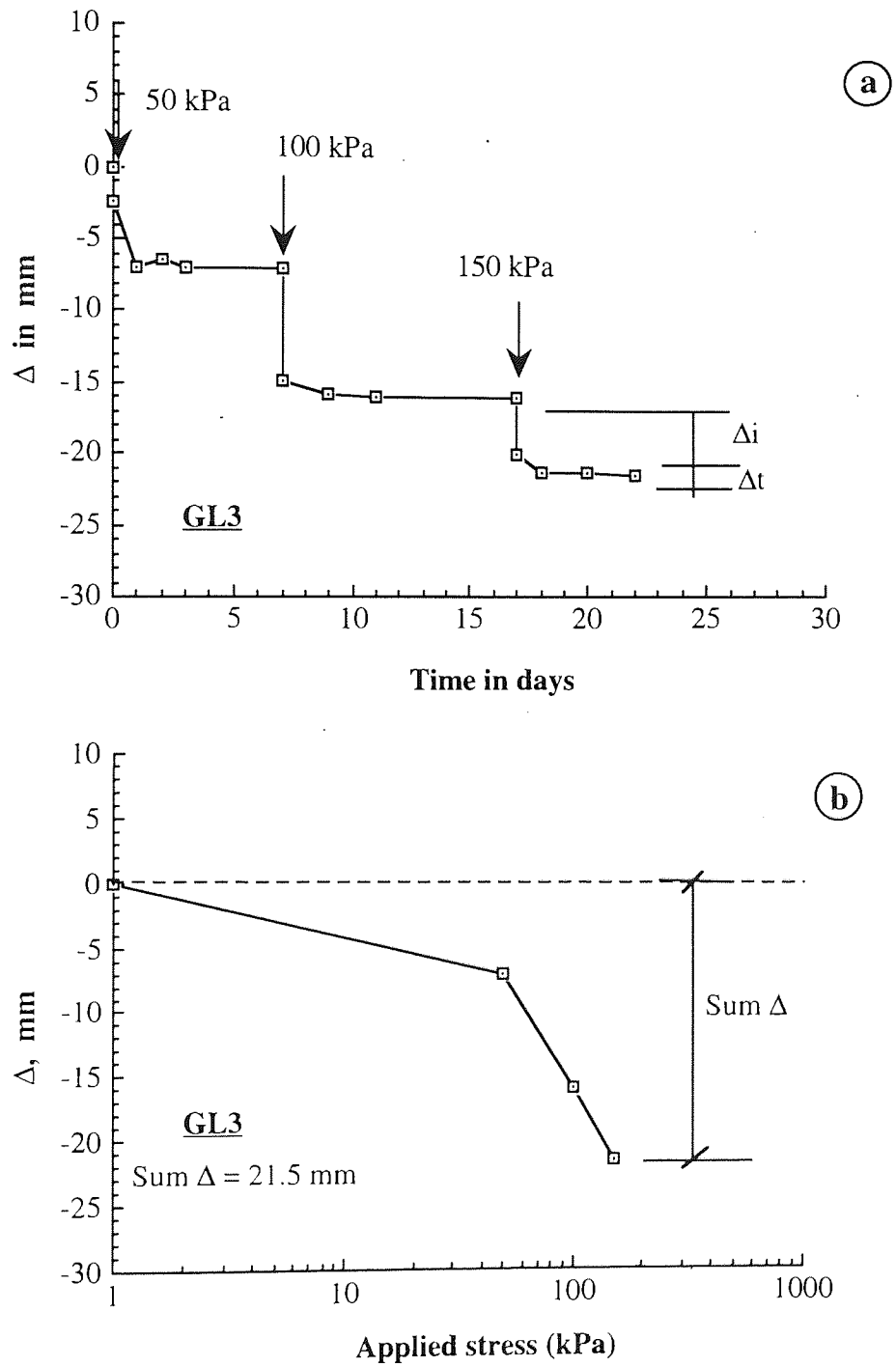
Fig. 6.15 : The results of the field hydroconsolidation test for the location GL3.
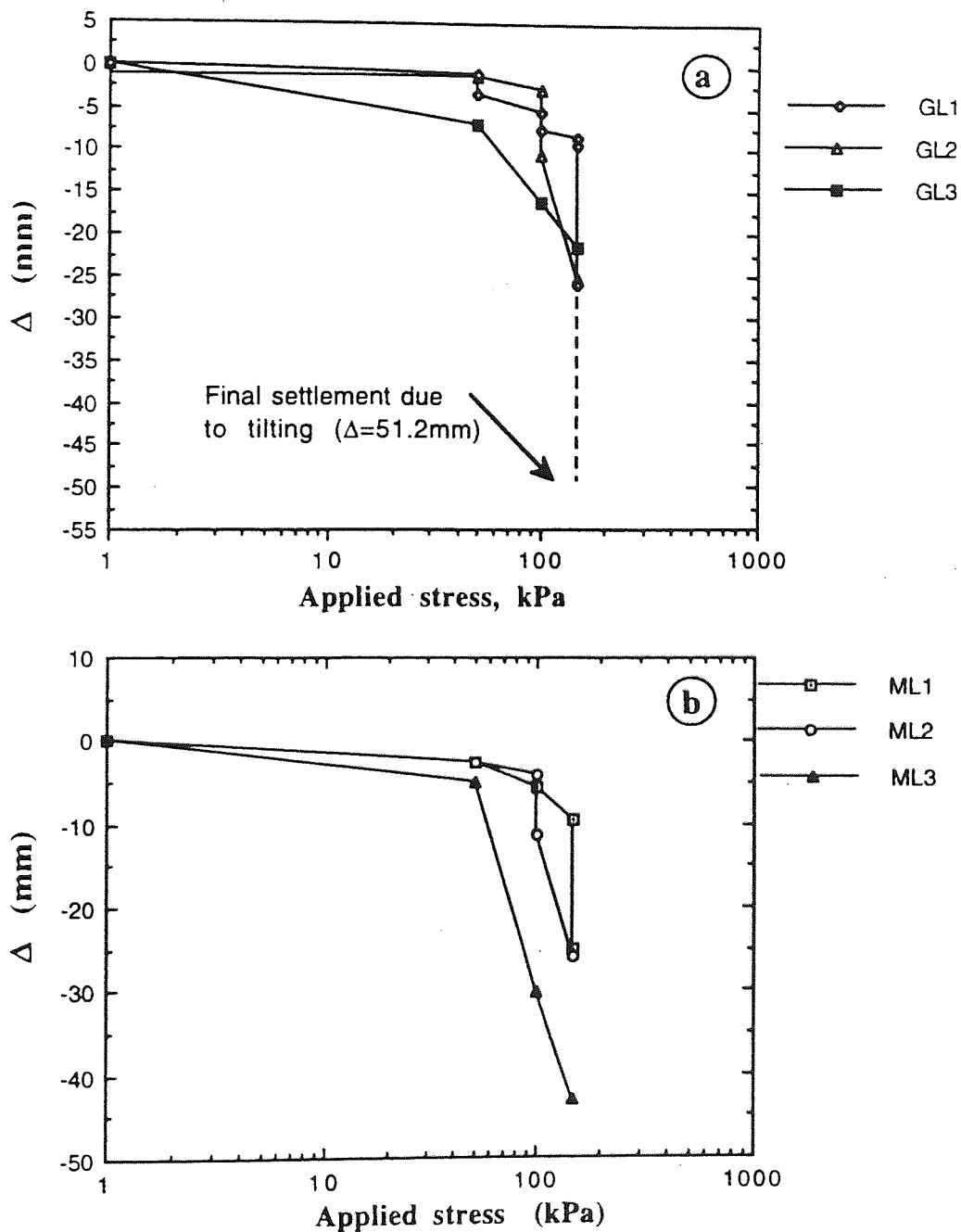
Fig. 6.16 : The superimposed curves of the field loading tests for
the different locations at a) site II and b) site III.
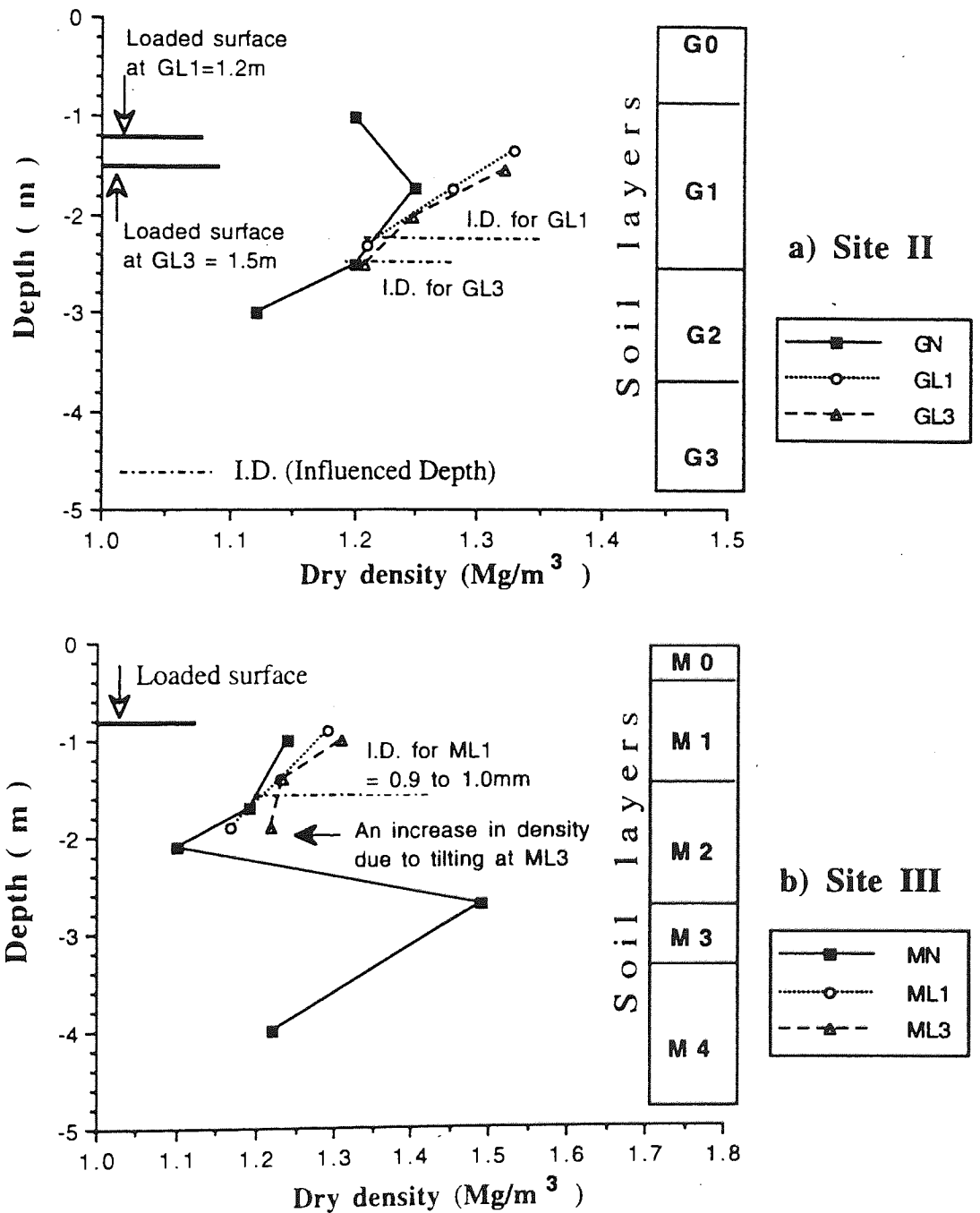
Fig. 6.17 : The variation of dry density with depth for the natural and
preloaded soils from locations;
a) GL1 and GL3 at site II, and b) ML1 and ML3 at site III.
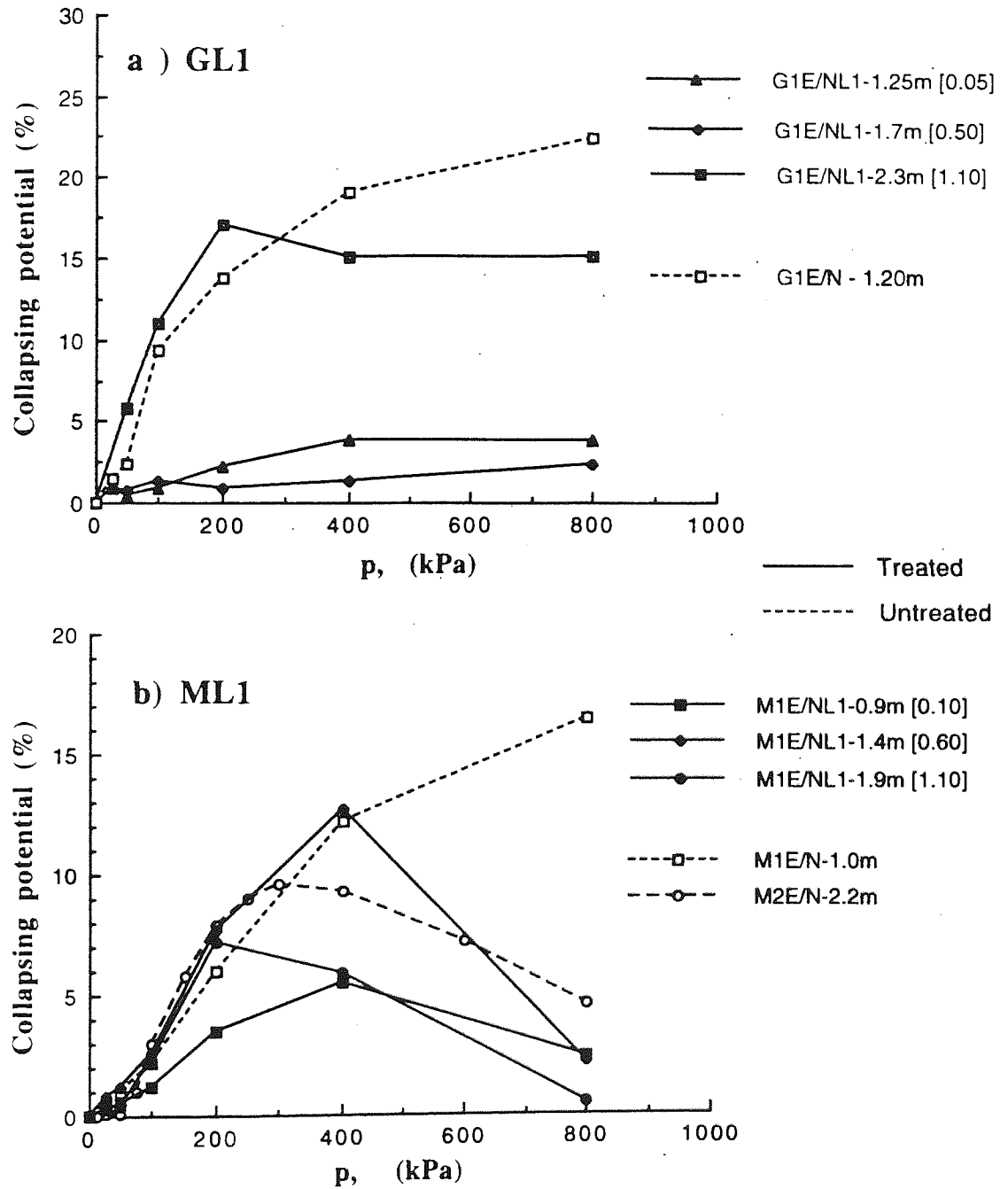
Fig. 6.18 : Collapsing potential of the loaded soils from locations;
a) GL1 at 0.05, 0.5 and 1.1m, and
b) ML1 at 0.1, 0.6 and 1.1m below the loaded surface.
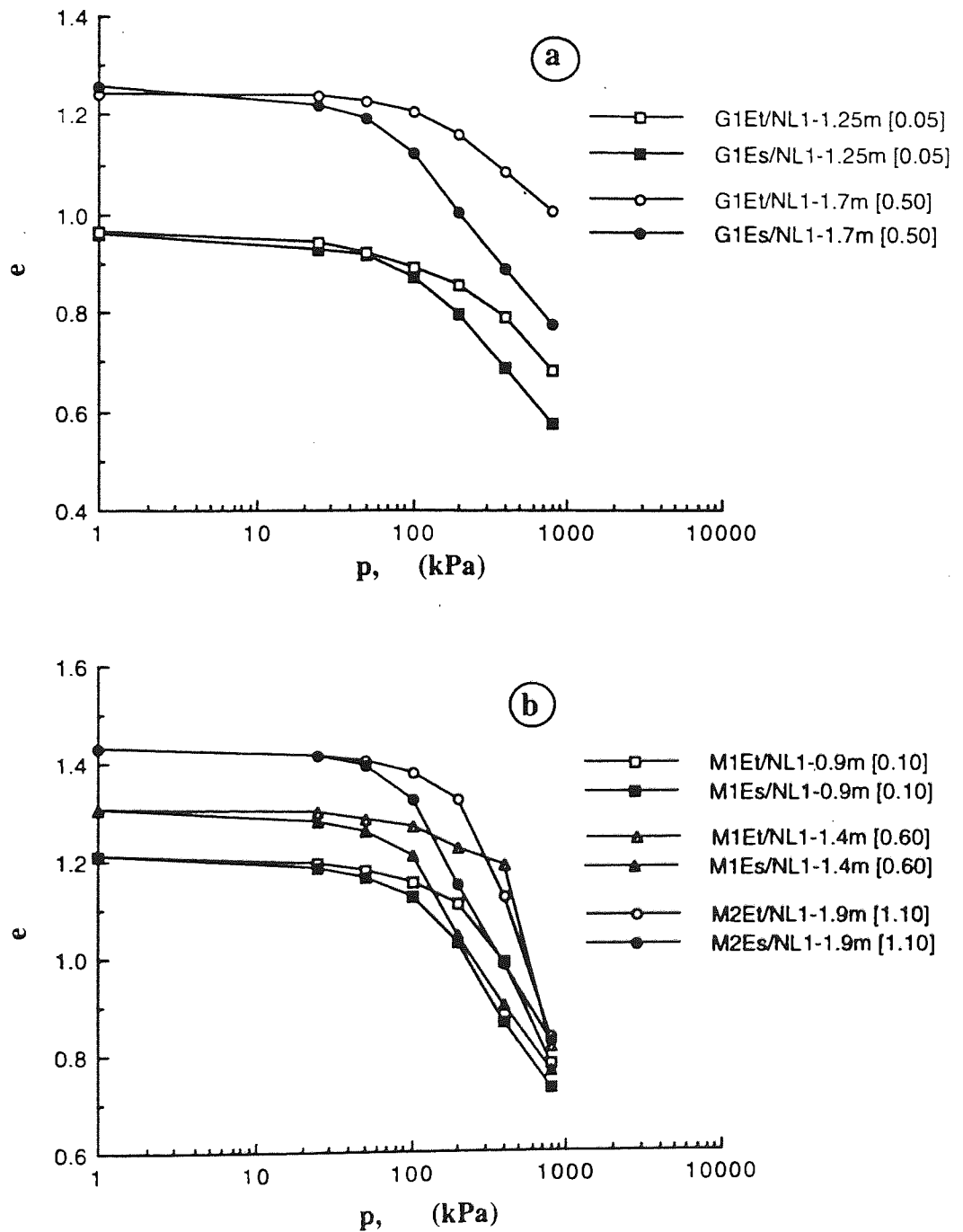
Fig. 6.19 : The double oedometer test results of the pre-loaded soils at;
a) GL1 from 0.05 and 0.5m below loaded surface, and
b) ML1 from 0.1, 0.6 and 1.1m below loaded surface.
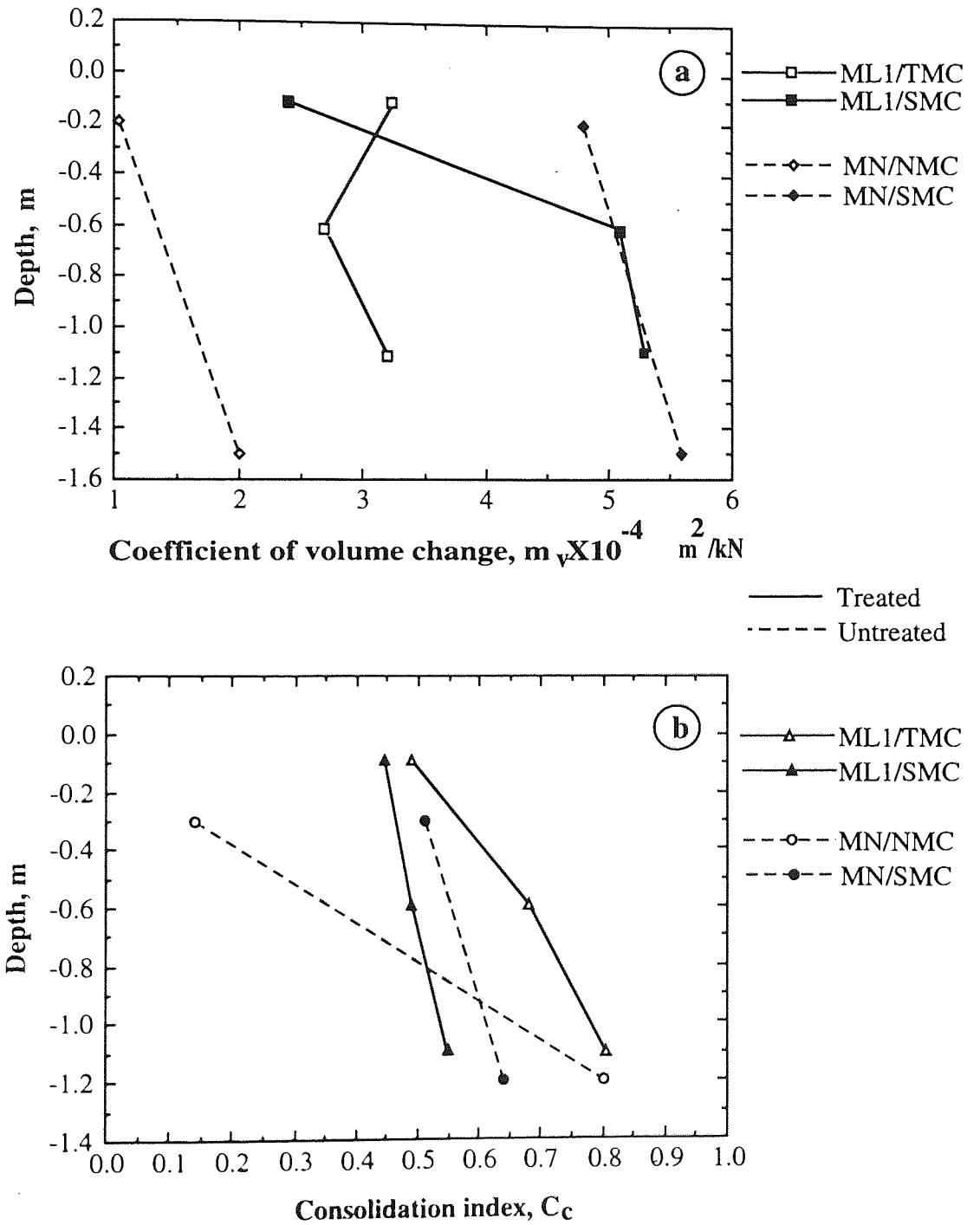
Fig. 6.20 : The effect of flooding and preloading on the C_c and m_v coefficients of the loaded soils at ML1 at site III.
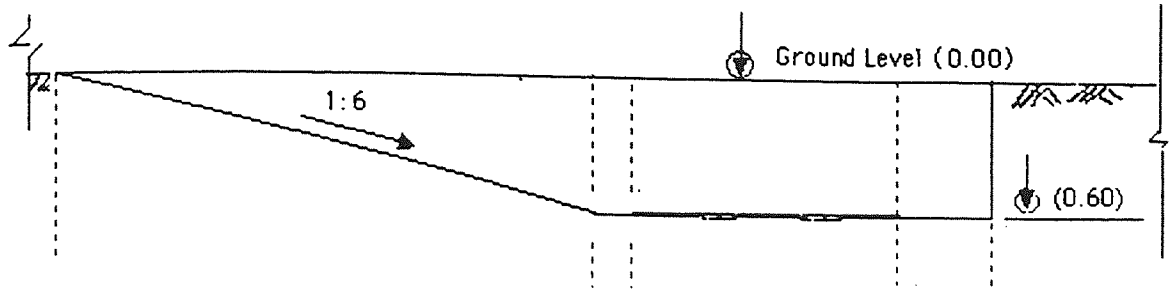
Vertical cross section
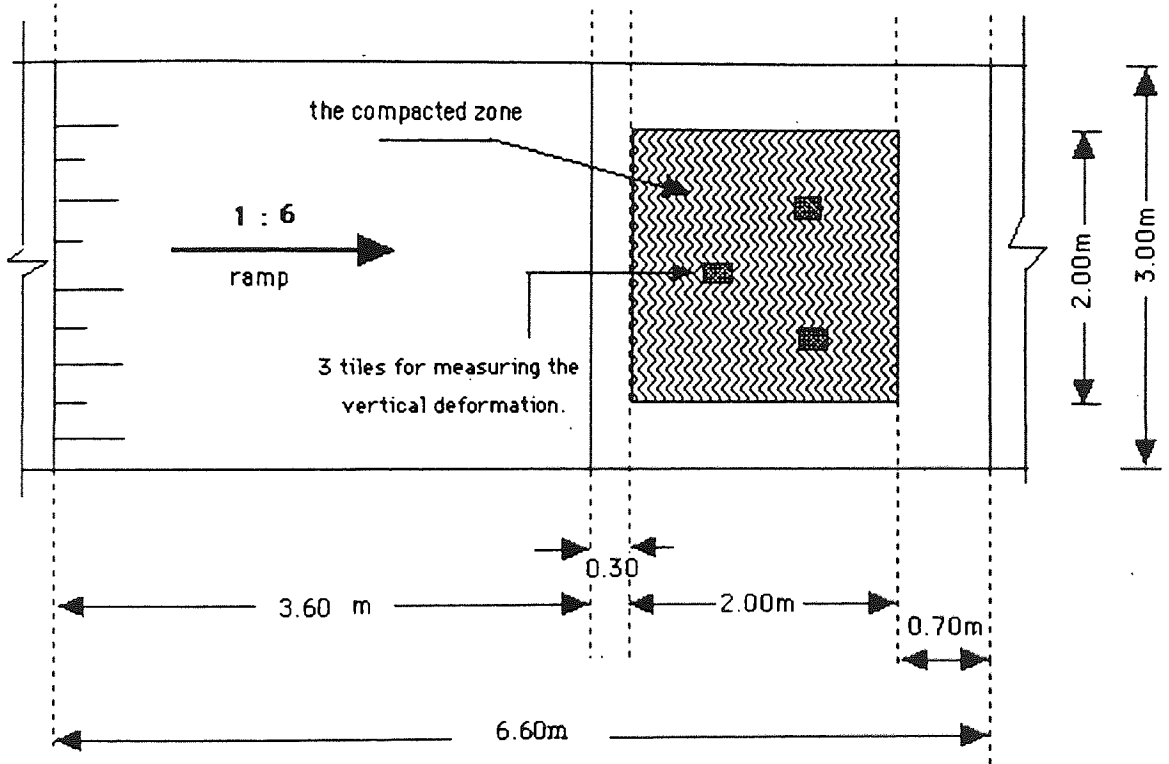
Horizontal plane
Scale 1:50

Fig. 6.21 : The layout of the roller compacted location, MC1.
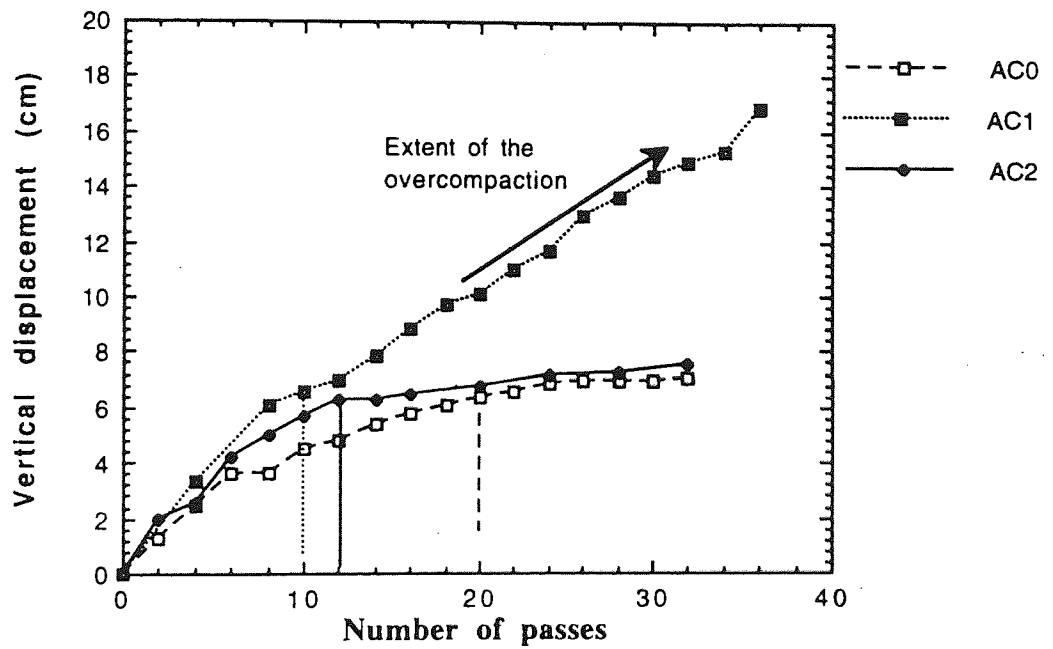
Fig. 6.22 : Vertical displacement and number of roller passes relationship
for site I locations, each curve is the average of three curves.
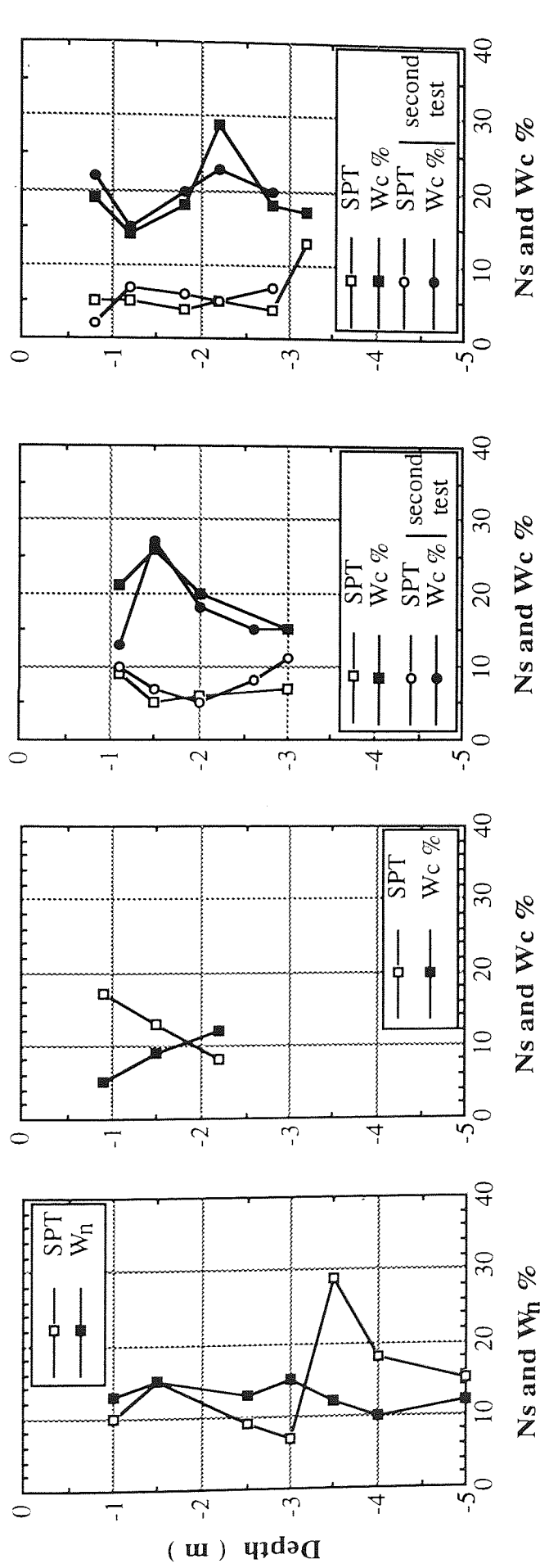
a) Natural location, AN.

b) Compacted location at NMC state, AC0.

c) Compacted location with one day flood, AC1.

d) Compacted location with five days flood, AC2.

Fig. 6.23 : The SPT values and moisture content correlations at the roller compacted locations, AC0, AC1 and AC2, with the corresponding natural values.
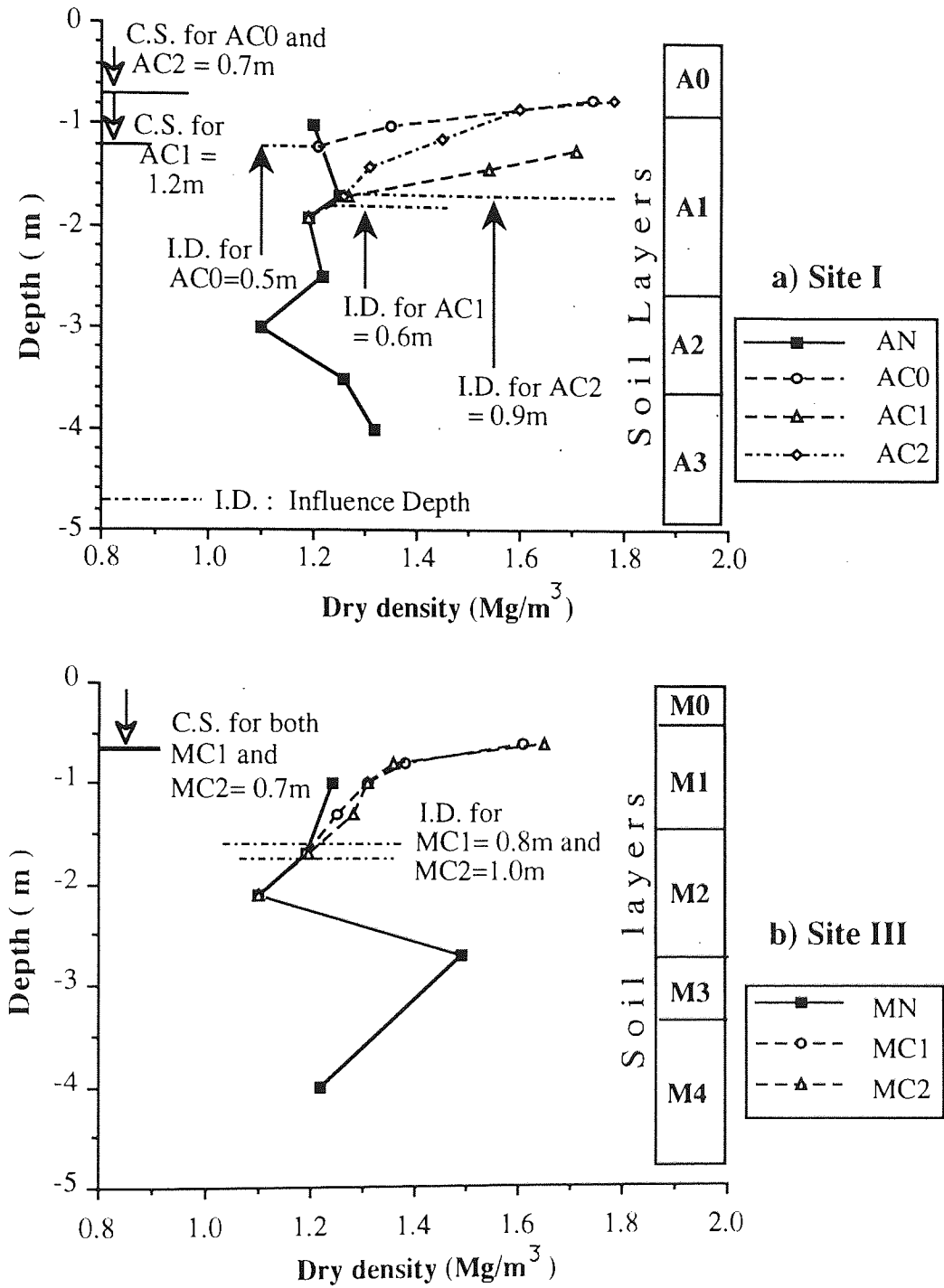
Fig. 6.24 : The variation of dry density with depth for the natural
and VRC soils from locations;
a) AC0, AC1 and AC2 at site I, and
b) MC1 and MC2 at site III.
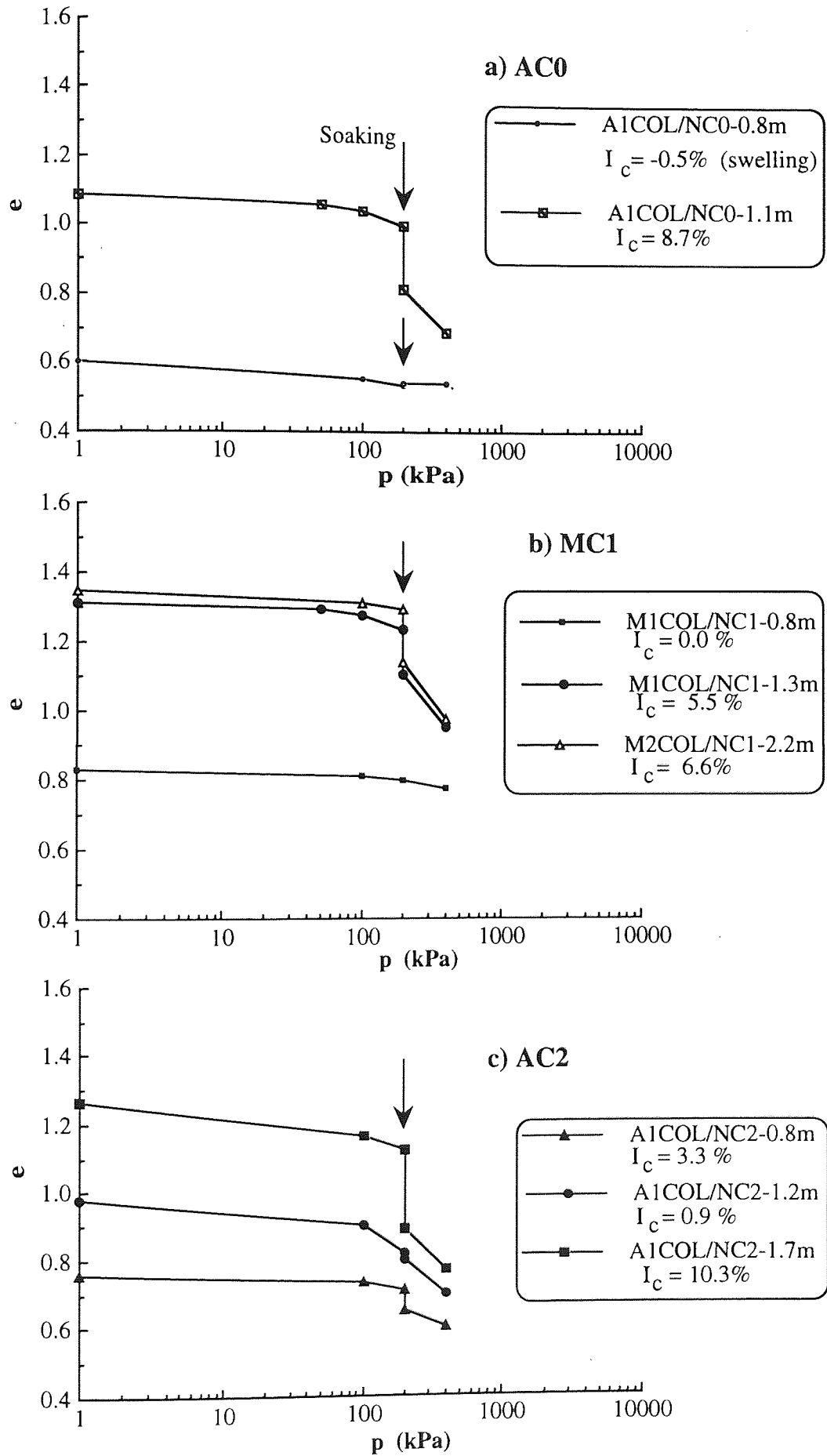
Fig. 6.25 : Single oedometer collapsing results of the soils treated by VRC from locations; a) AC0 compacted at NMC, b) MC1 compacted after one day flooding and c) AC2 compacted after five days flooding.
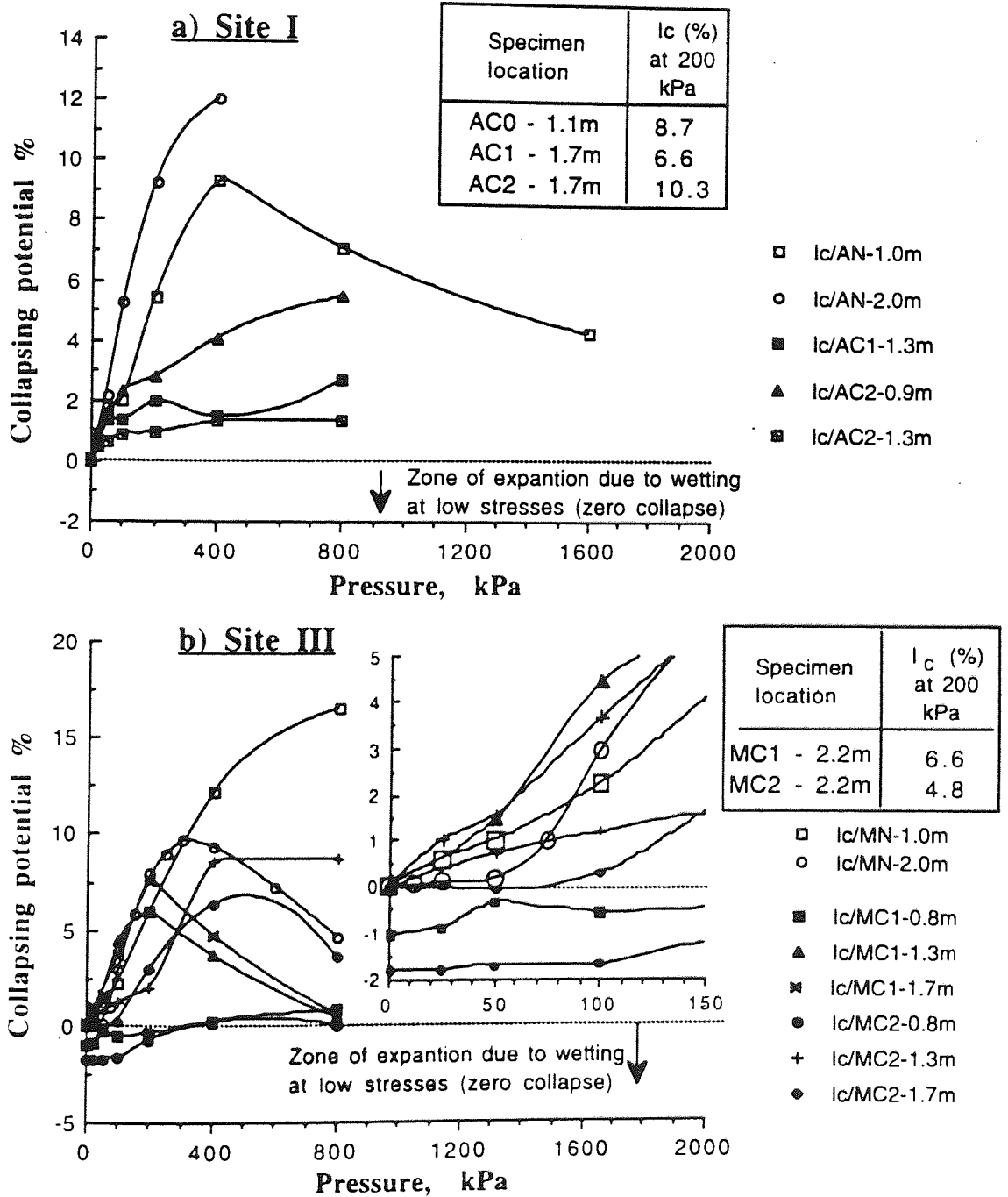
Fig. 6.26 : Collapsing potential, from double oedometer, of the soils treated by VRC at different locations at sites I and III.
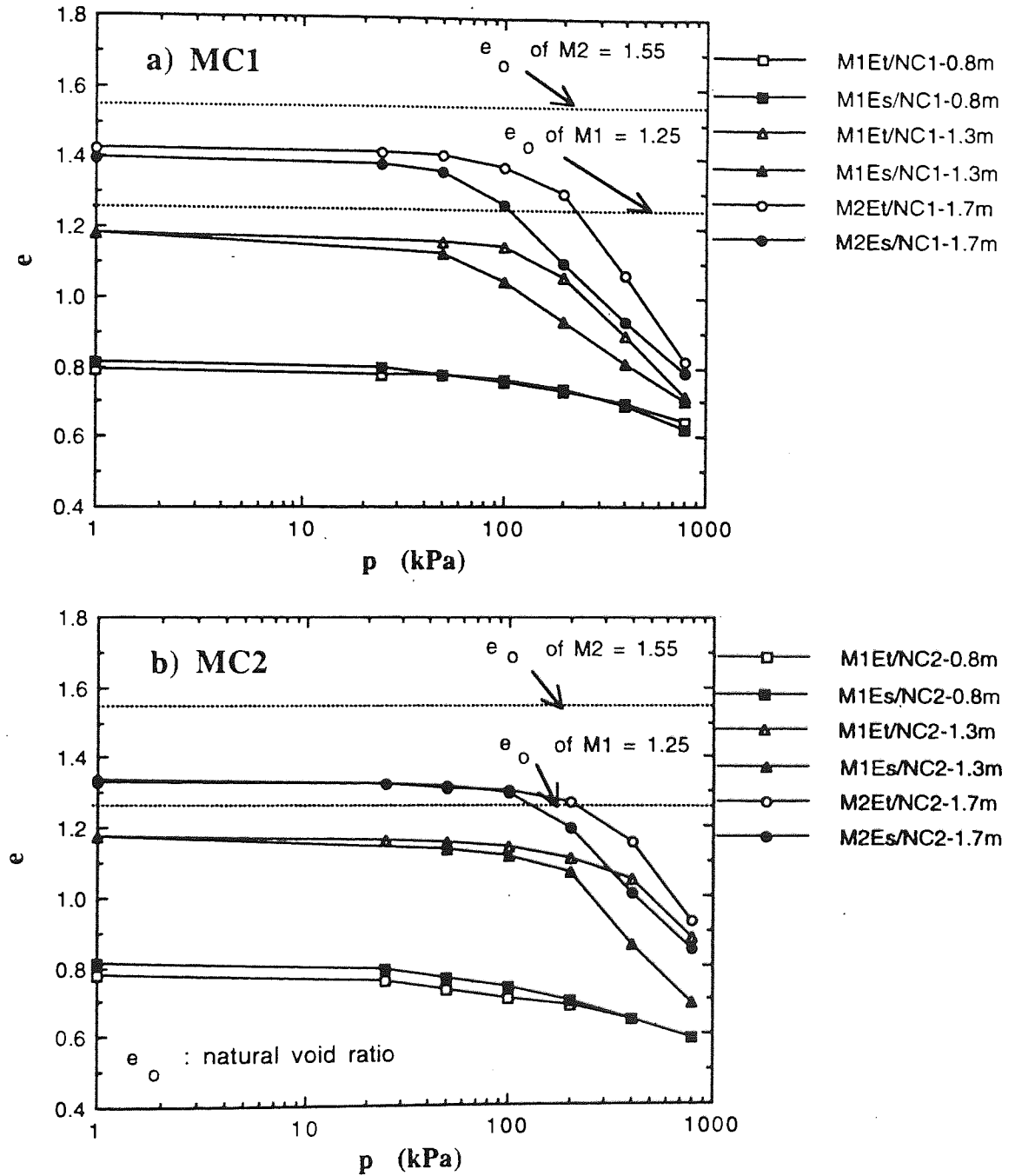
Fig. 6.27 : Double oedometer test results, from different levels at
the roller compacted locations; a) MC1 and b) MC2.
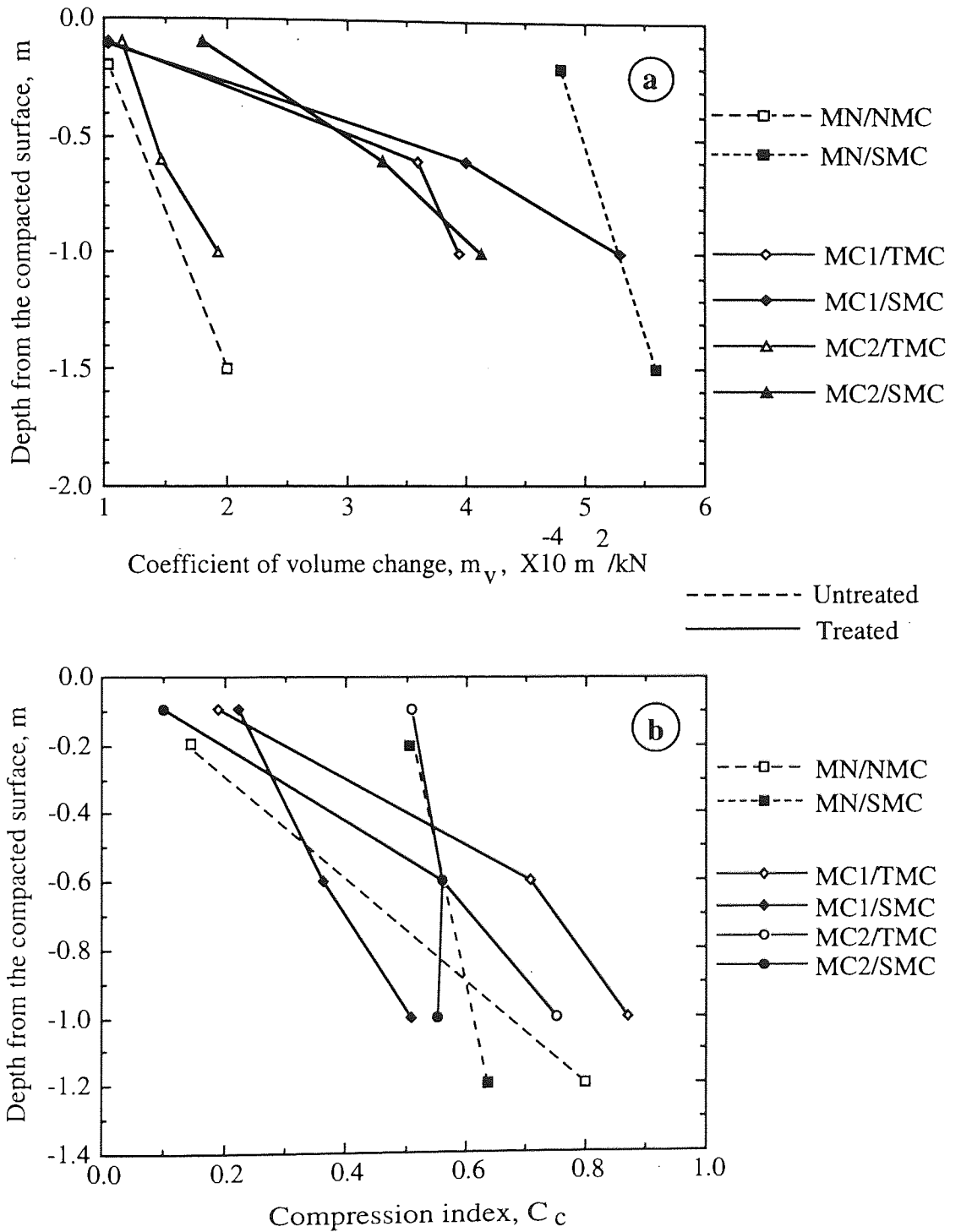
Fig. 6. 28 : The effect of vibratory roller compaction on the C_c and m_v coefficients of the treated soils at site III.
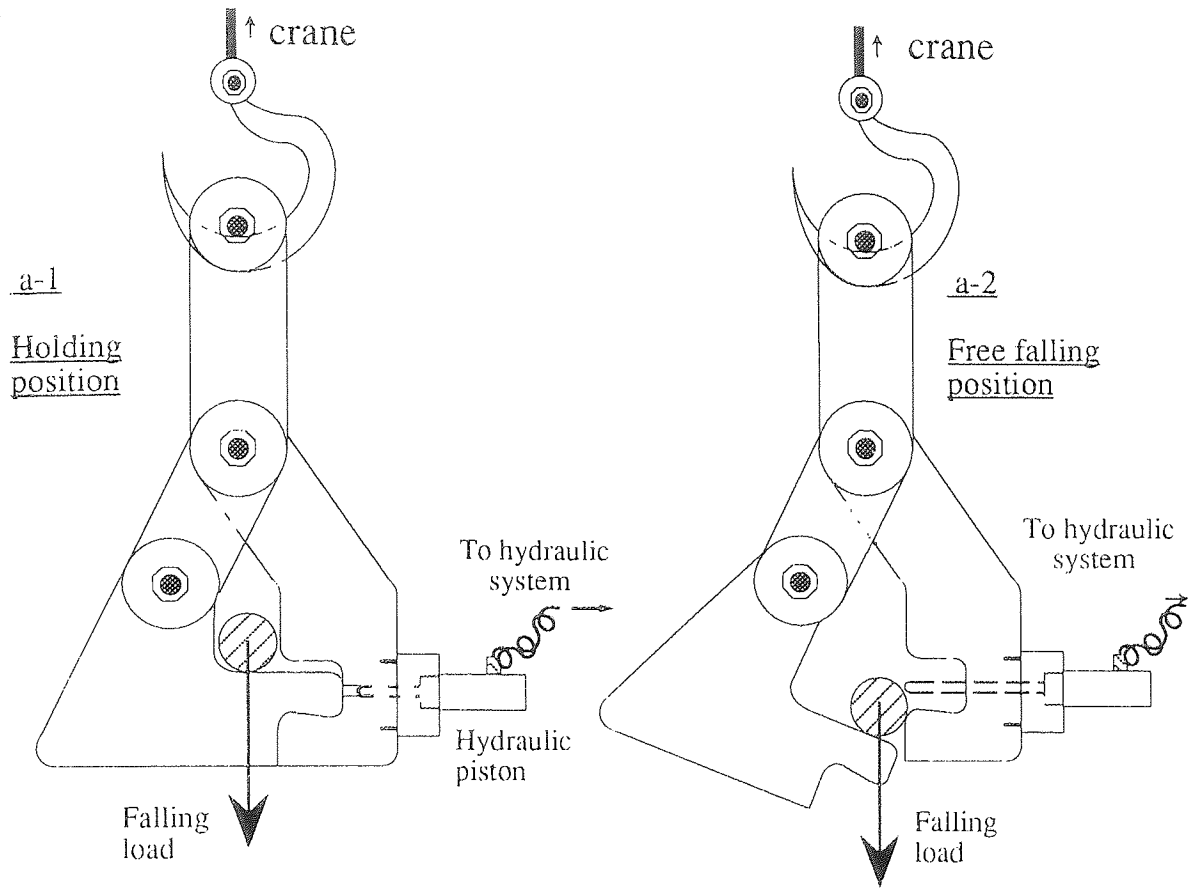
a) Diagramatic sketch of the releasing valve.
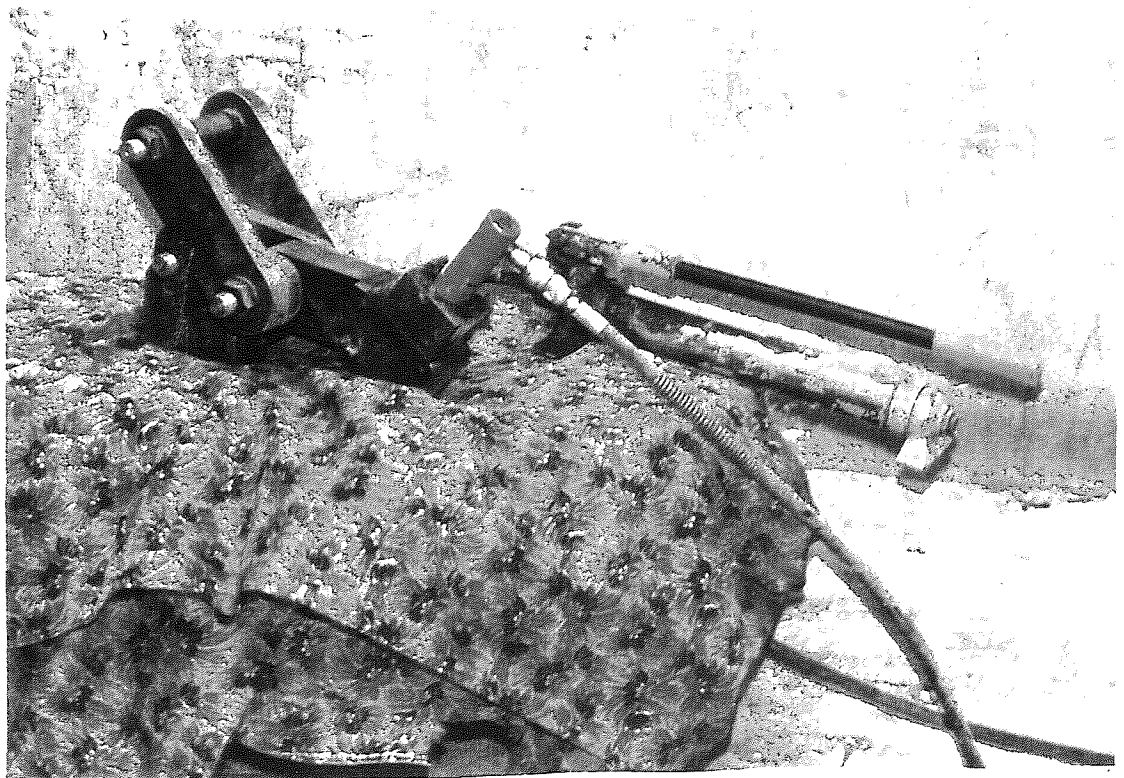
b) Plate of the releasing valve.

Fig. 6.29 : Hydraulic releasing valve.
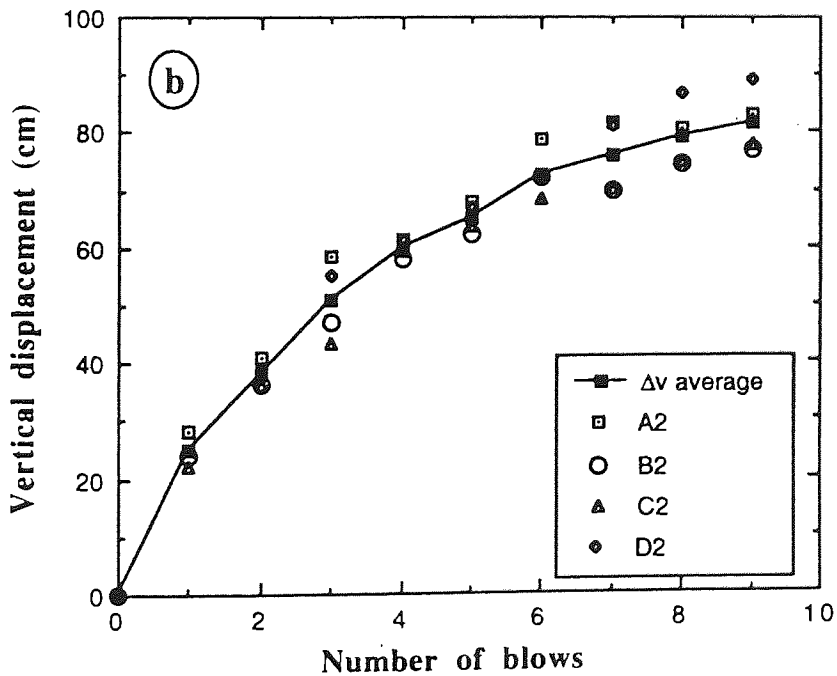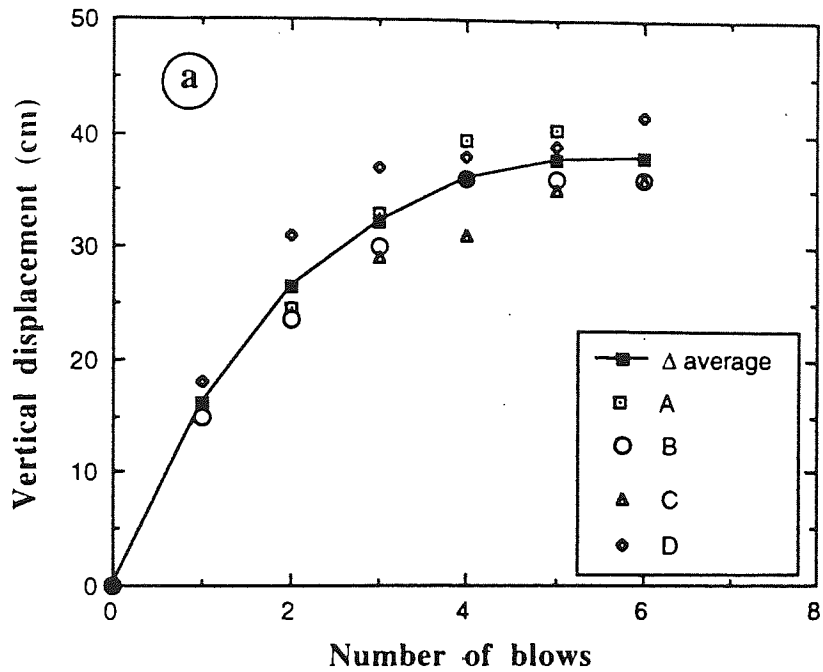
Fig. 6.30 : The vertical displacement of the impacted surface
of the locations; a) MD0 and b) MD2.

a) Natural location, MN.

b) Pounded location at NMC state, MD0.

c)Pounded location with one day flooding , MD1.

d) Pounded location with five days flooding, MD2.
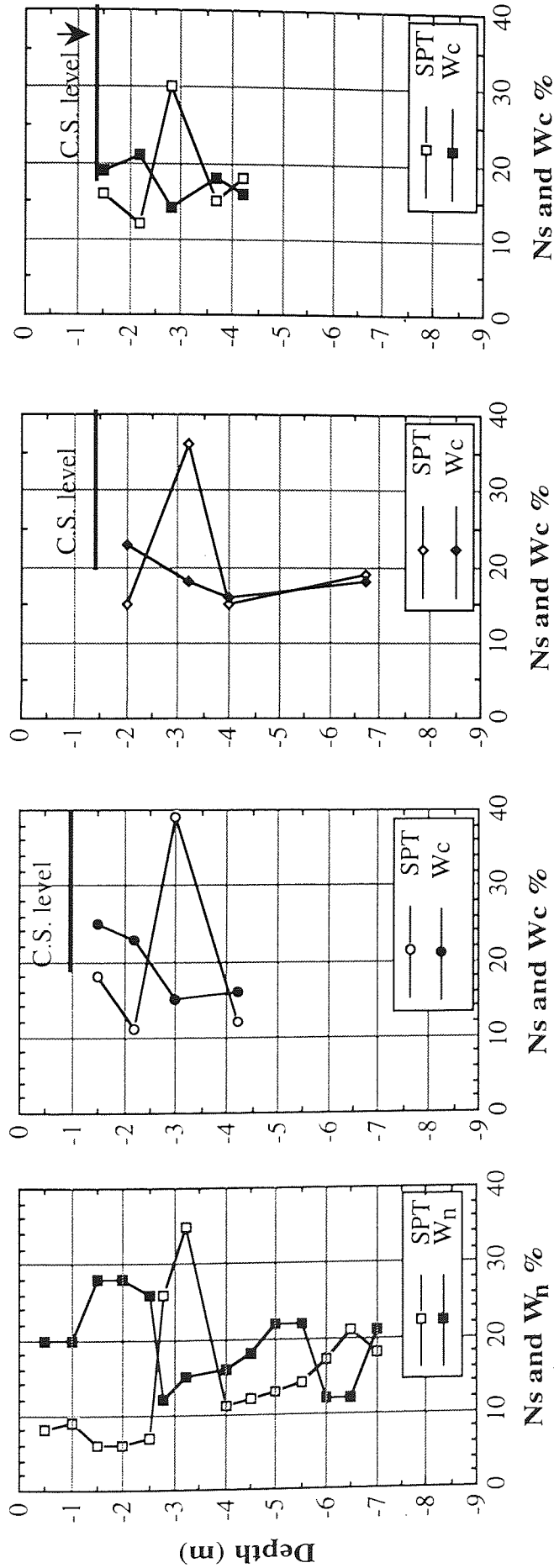
Fig. 6.31 : The SPT values and moisture content correlations at the pounded locations, MD0, MD1 and MD2, with the corresponding natural values.
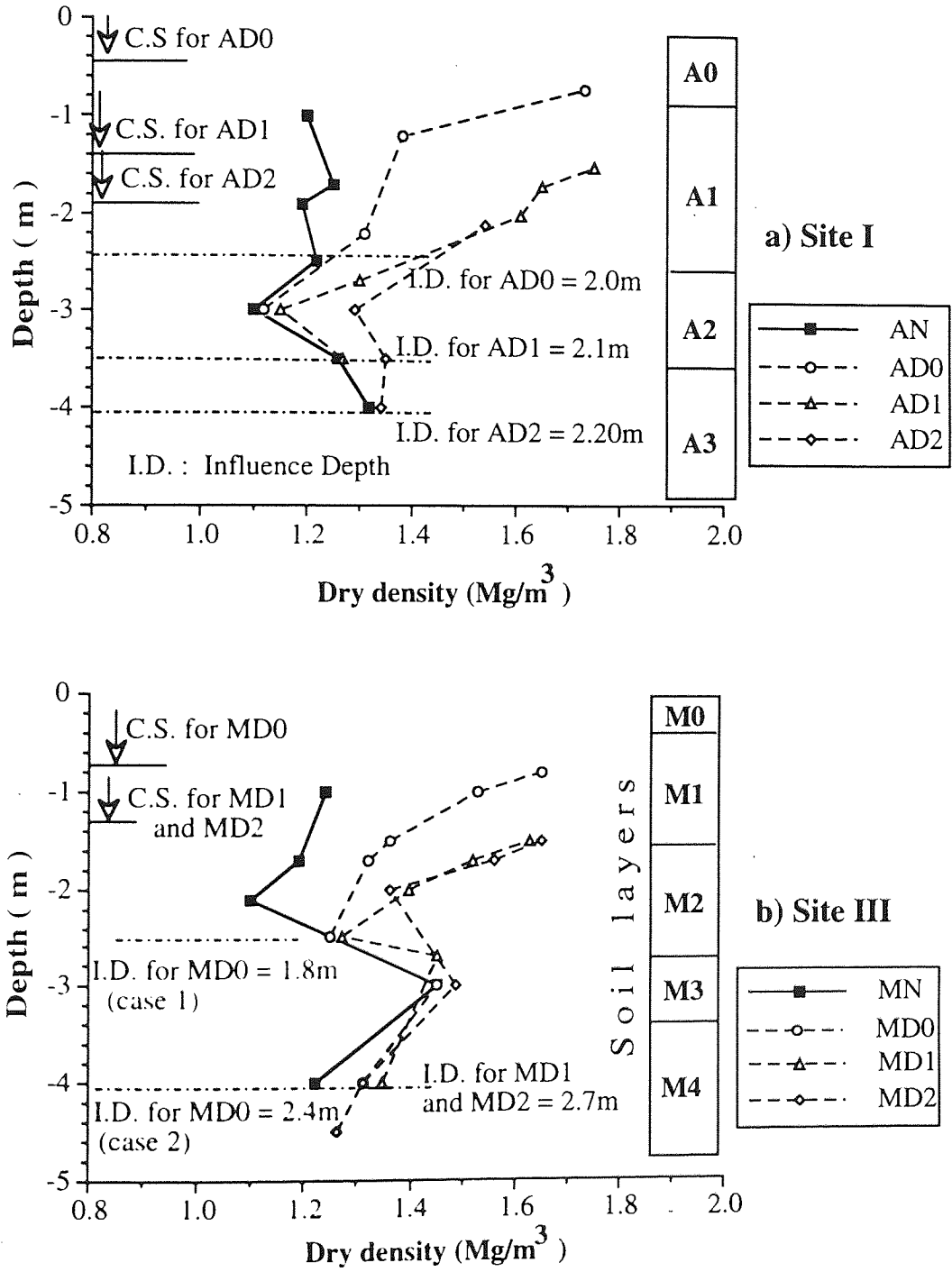
Fig. 6.32 : The variation of dry density with depth at the pounded locations in sites I and III.
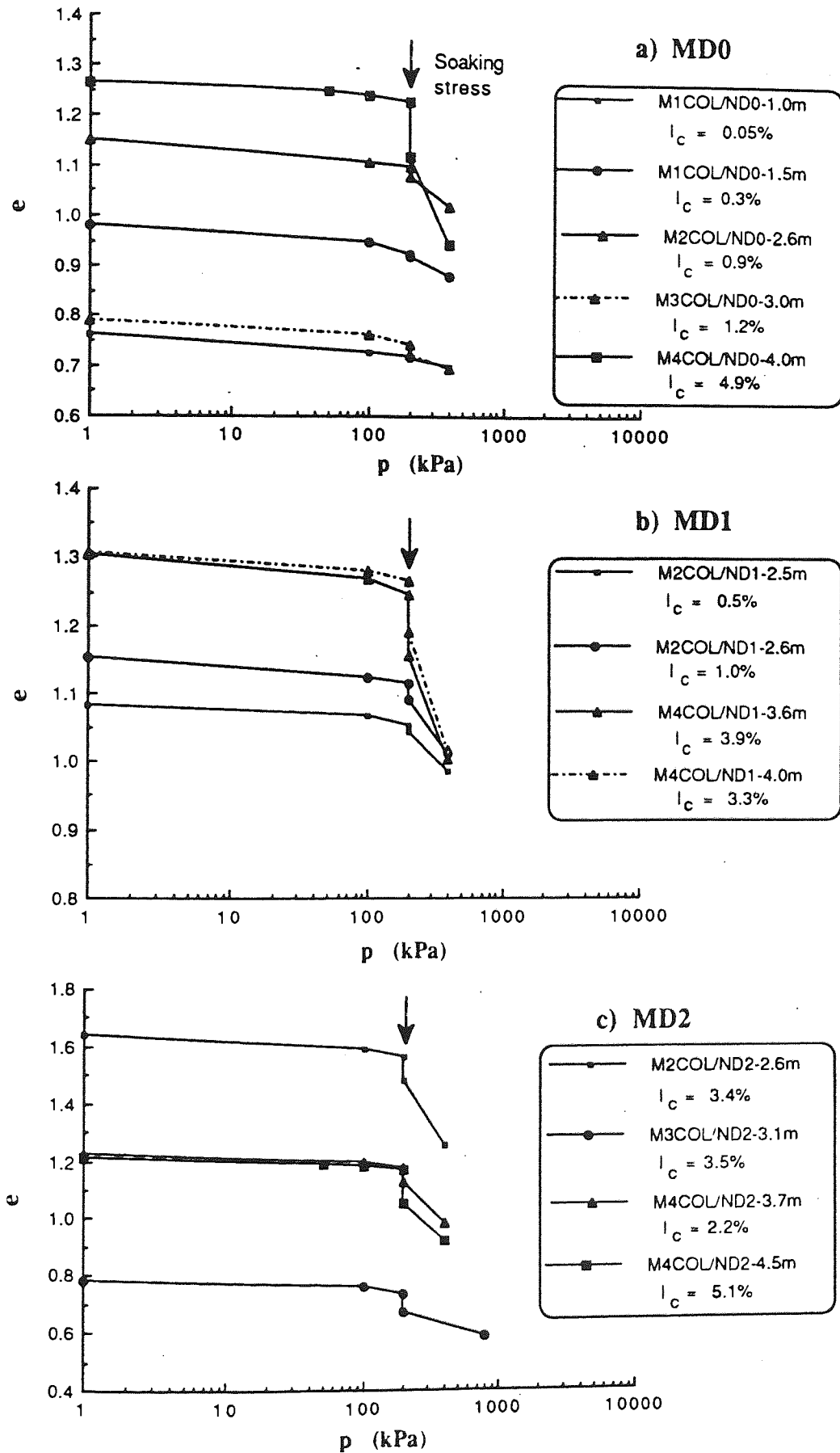
Fig. 6.33 : Single oedometer collapsing results of the soils treated by DC at site III locations, from various levels below the ground surface.
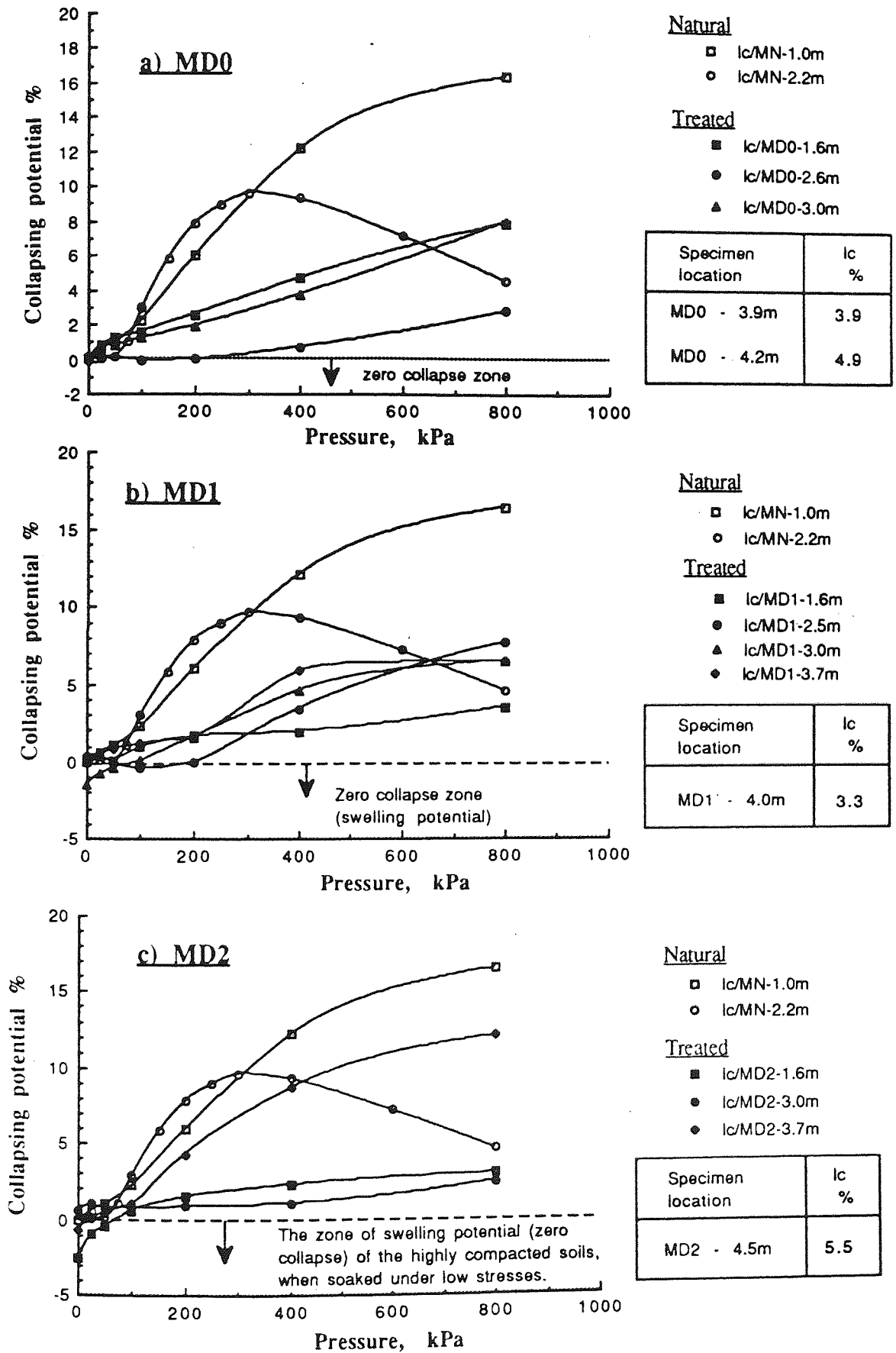
Fig. 6.34 : Collapsing potential I_c of the soils treated by DC at site III.
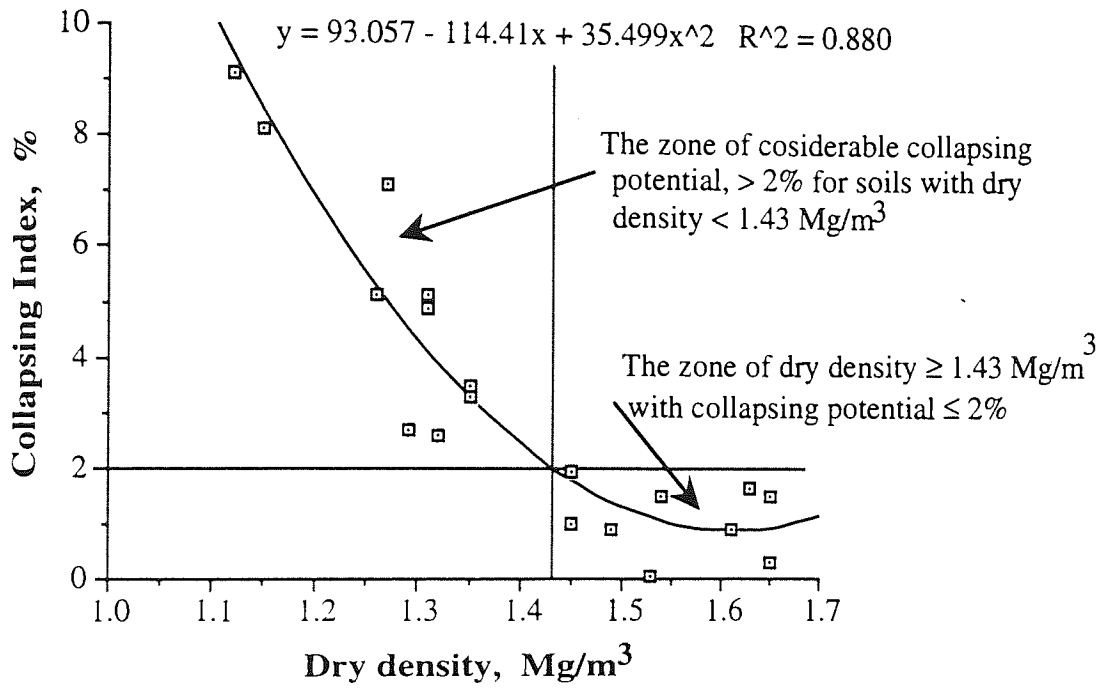
Fig. 6.35 : The collapsing Index-dry density relationship for the soils treated by deep compaction (pounding) at sites I and III, (Collapsing Index = I_c at 200 kPa).
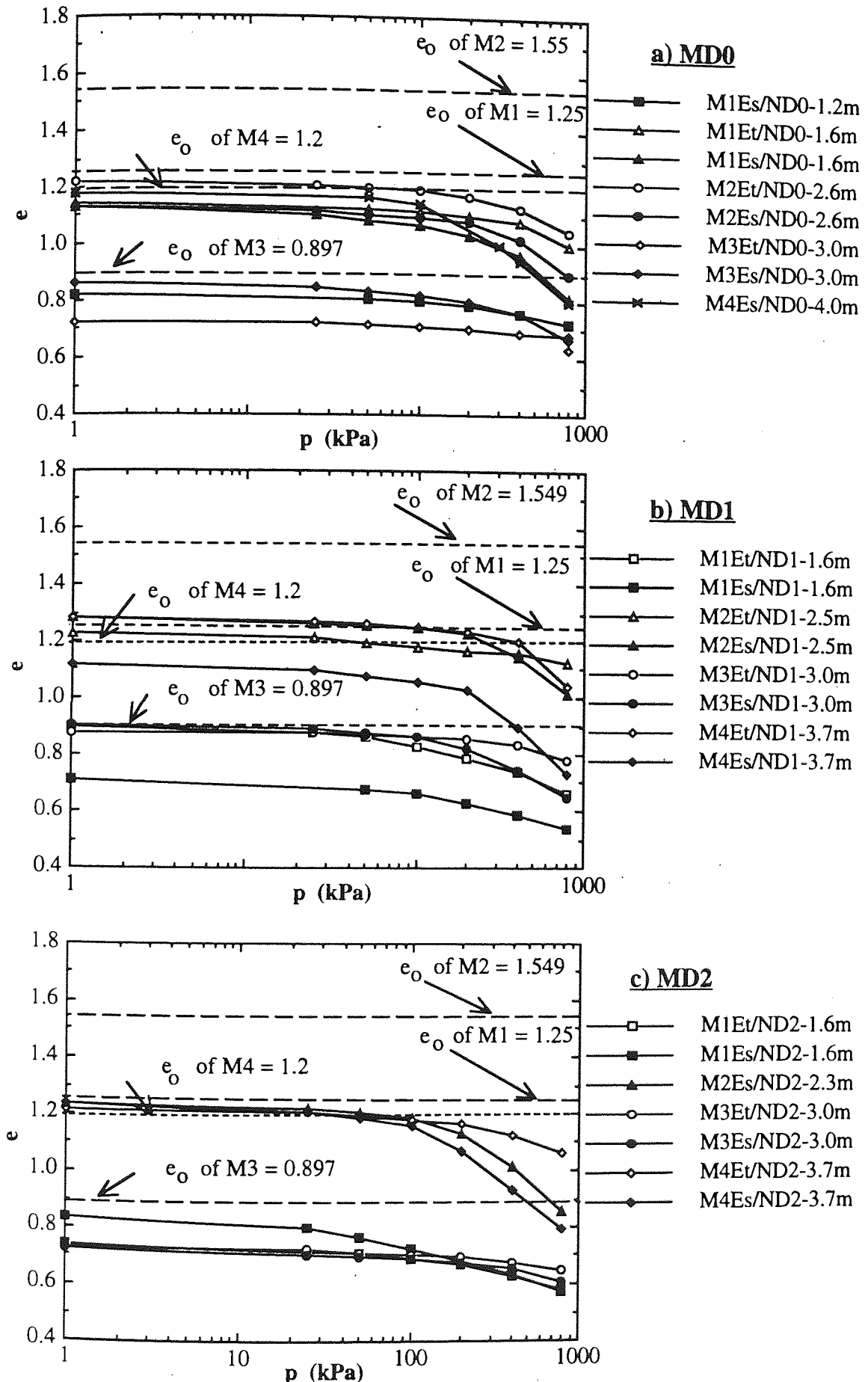
Fig. 6.36 : Oedometer test results of the soils treated by pounding at site III from various depths.
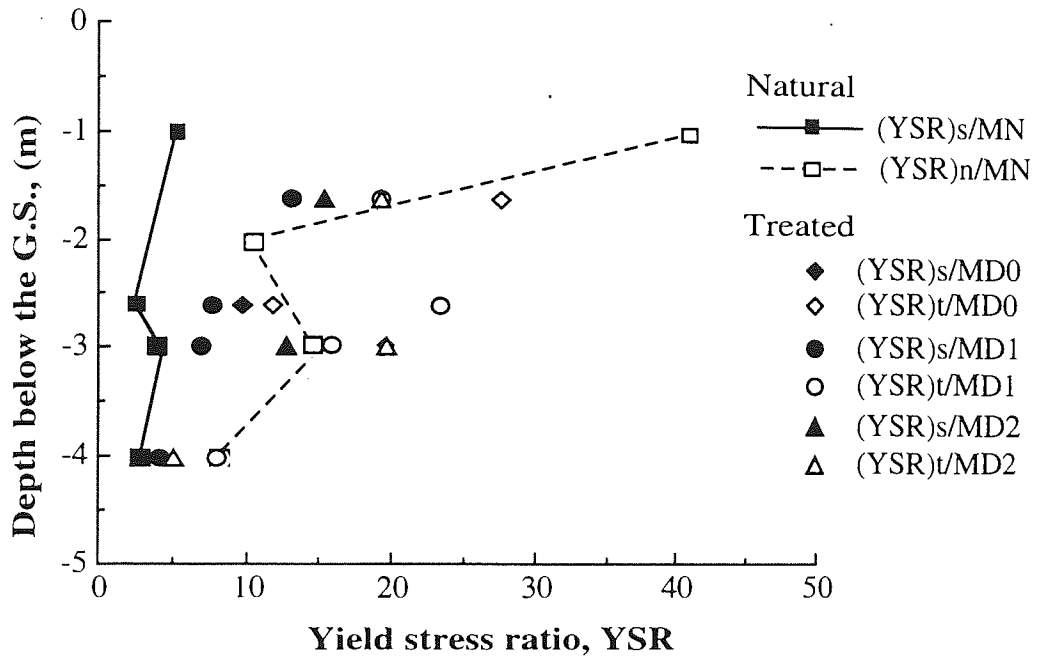
Fig. 6.37 : Oedometer test results showing the variation with depth for the yield stress ratio at SMC -(YSR)s- and TMC -(YSR)t- states.
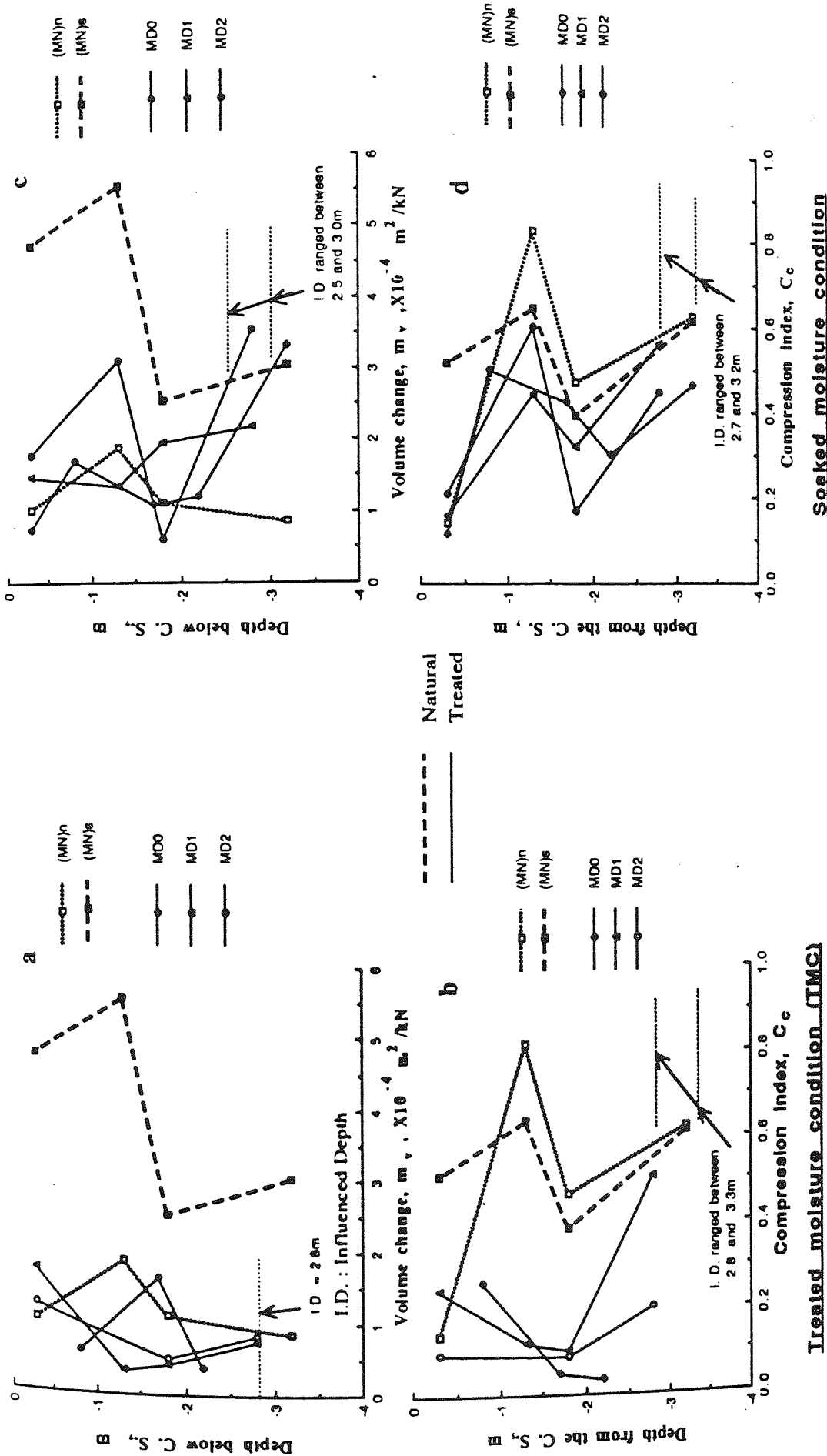
Fig. 6.38 : The variations of the coefficients of volume change and compression index with depth for the soils treated by deep compaction at site III.
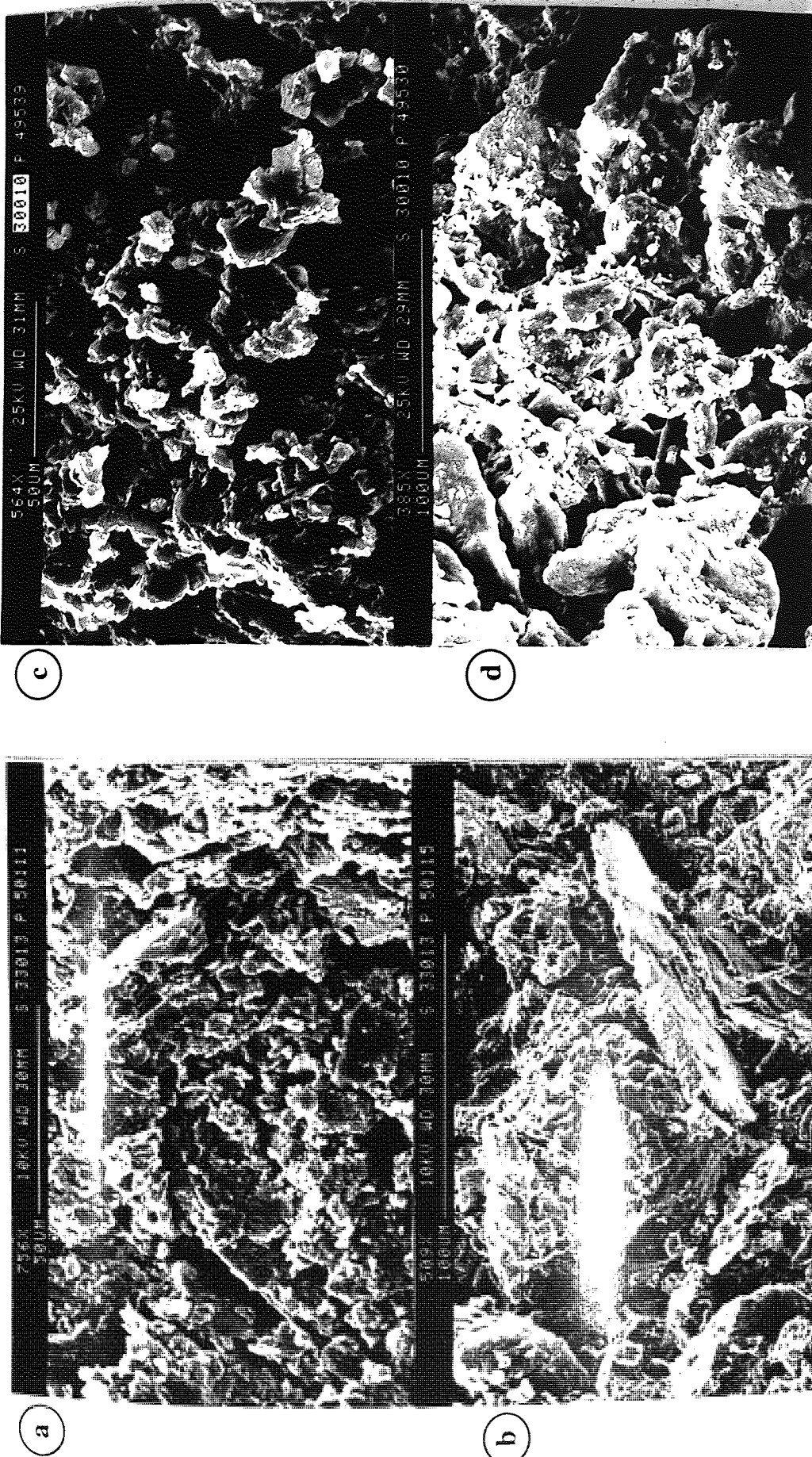
Fig. 6.39: Field destructuring and densification of the sandy silt soil, M1, at MD0 by Pounding, indicating: a) and b) Considerable destructuring and densification by Pounding with some trapped pores (a) and crushed particles (b), c) and d) Images for the same soil, M1, before treatment, for comparison purpose.
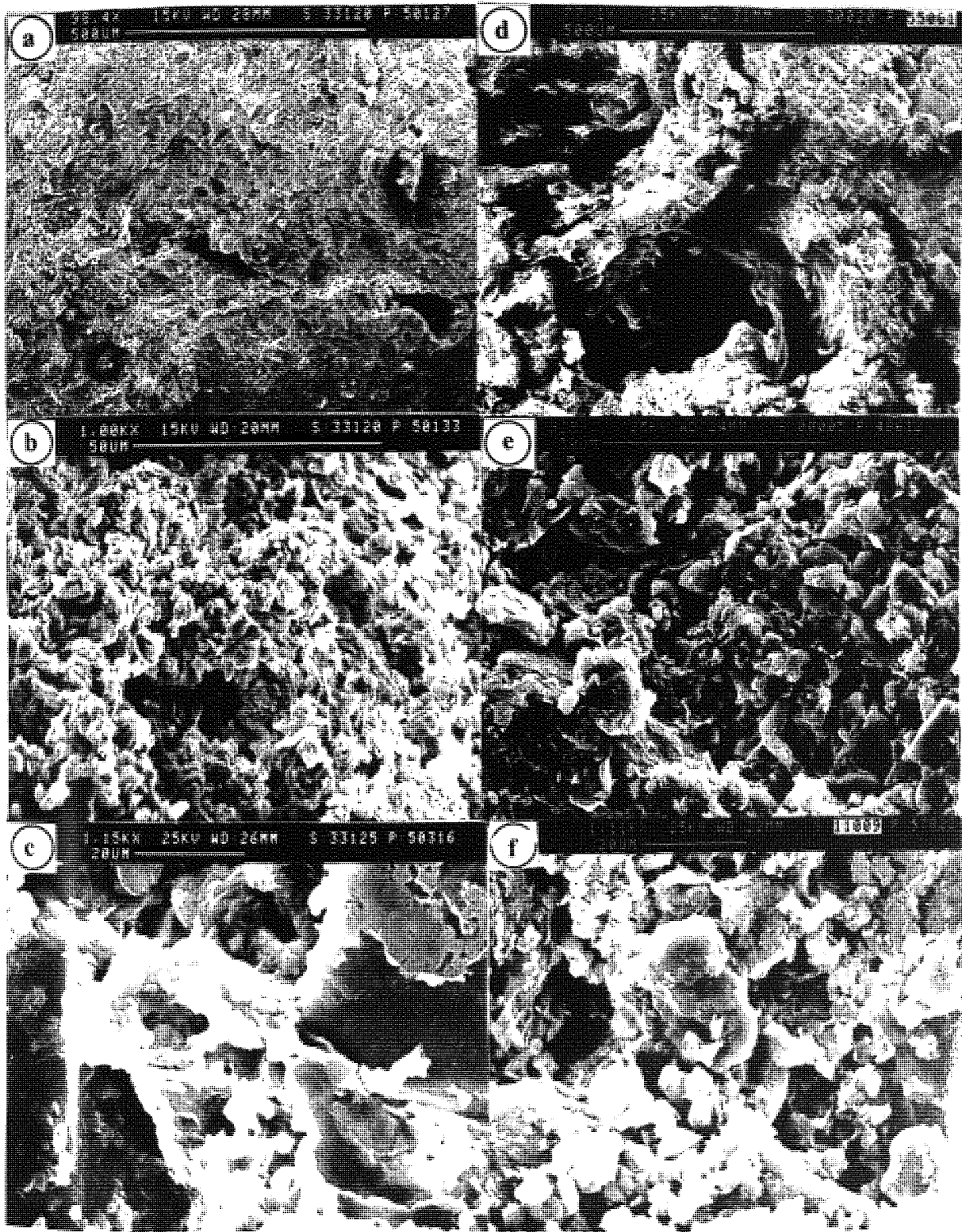
Fig. 6.40 : Field densification and destructuring of the silt/silty clay soil, M2, by Pounding at 2.0m
(0.7m below theimpacted surface of MD1), indicating:

a) Considerable densification at low magnification,
b) Considerable densification and destructuring within the cementation and fine contents,
c) Trapped and destructured fines and cementing agents at contacts, and
d), e) and f) images for the same soil, M2, before treatment, for comparison purpose.

a) Different treatment techniques at site III

Ground displacement, cm (vertical axis: 100, 90, 80, 70, 60, 50, 40, 30, 20, 10, 0, -10)

Legend: MD2, MC2, ML3, MF

Locations: MD2 MC2 ML3 MF

Locations at site III

b) Deep Compaction (DC)

Ground displacement, cm (vertical axis: 140, 130, 120, 110, 100, 90, 80, 70, 60, 50, 40, 30, 20, 10, 0)

Bars: MD0, MD1, MD2, AD0, AD1, AD2

← 130.0 cm
This high depression
was due to the flow
of the liquified soil
around the dropping
load because of the
high moisture content
at the time of pounding.

III   **Site and Location**   I

☐ At in situ moisture   ▨ Preflooded for one day   ▨ Preflooded for five days

Fig. 6.41 : Ground response - depression - to ;

a) different treatment methods at site III and
b) Deep Compaction at sites I and III.

a) SPT values of the natural site, III.

$y = 25.662 - 0.70662x$ $R^2 = 0.697$

b) SPT values of the flooded location, MF2.

$y = 23.067 - 0.53982x$ $R^2 = 0.616$

c) SPT values of roller compacted location, MC1 and MC2.

$y = 35.613 - 0.99990x$ $R^2 = 0.570$

d) SPT values of pounded locations, MDo, MD1 and MD2.

$y = 42.987 - 1.2514x$ $R^2 = 0.216$
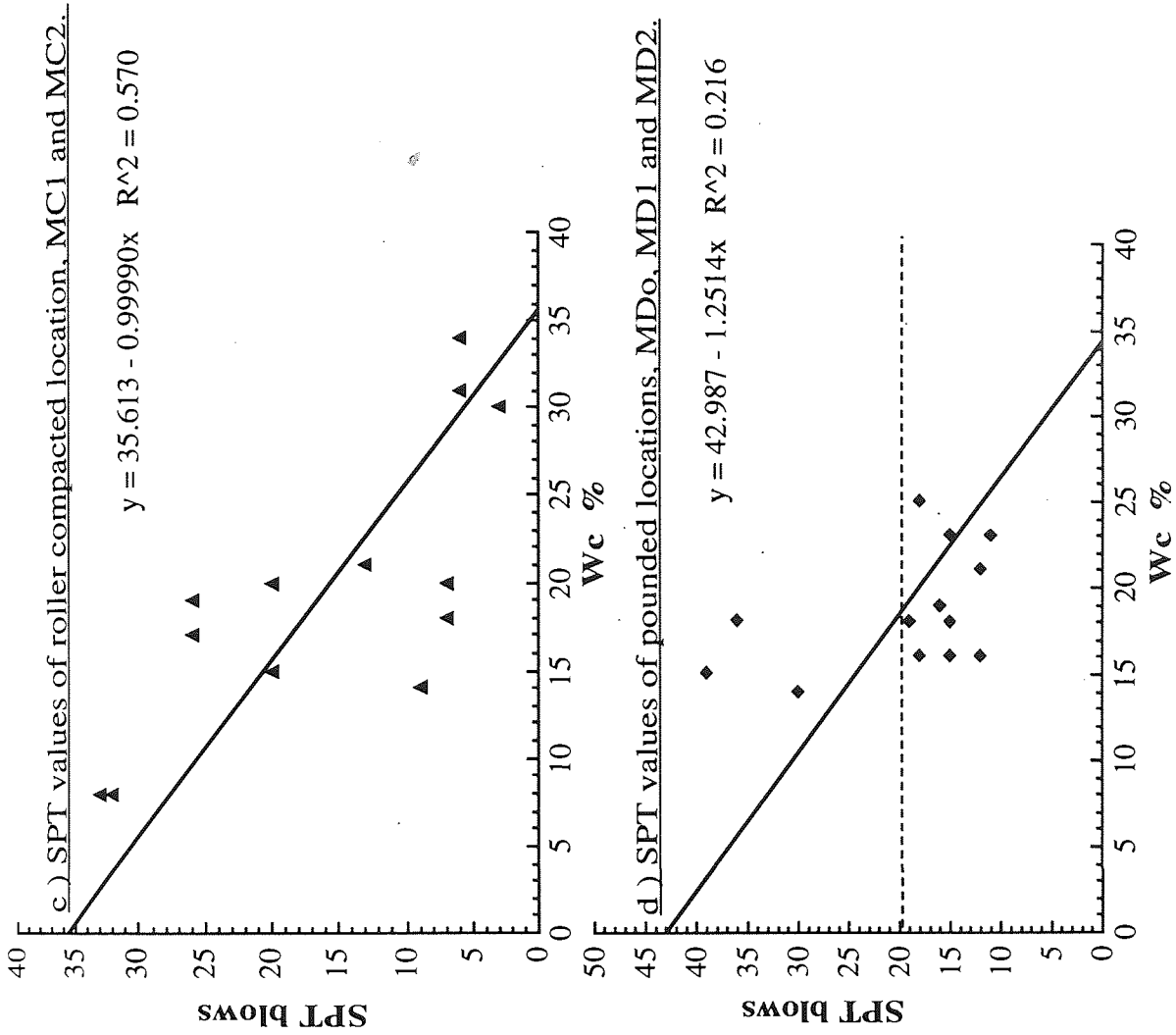
Fig. 6.42 : The patterns of the SPT values versus the moisture content for the natural, flooded, roller compacted and pounded locations at site III.

a) RI at [0.05 and 1.0m] from various locations treated by different methods

Treatment methods -different locations at site III-

b) Deep Compaction (DC)

☐ At in situ moisture ▨ Preflooded for one day ☐ Preflooded for five days
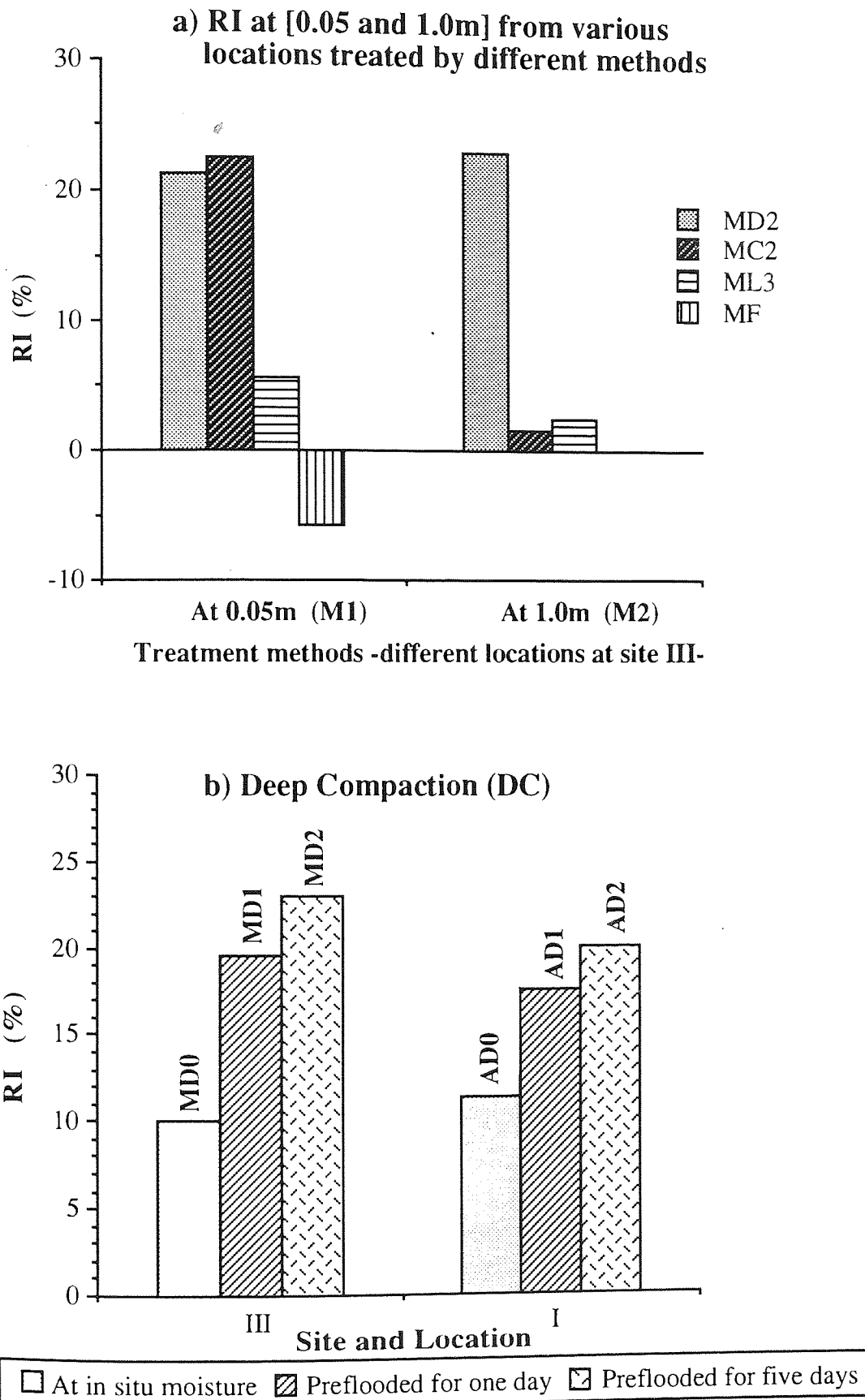
Fig. 6.43 : Comparison of the RI values from;

a) 0.05 and 1.0m below the C.S. of different locations at site III and
b) 1.0m below the pounded surfaces at sites I and III.
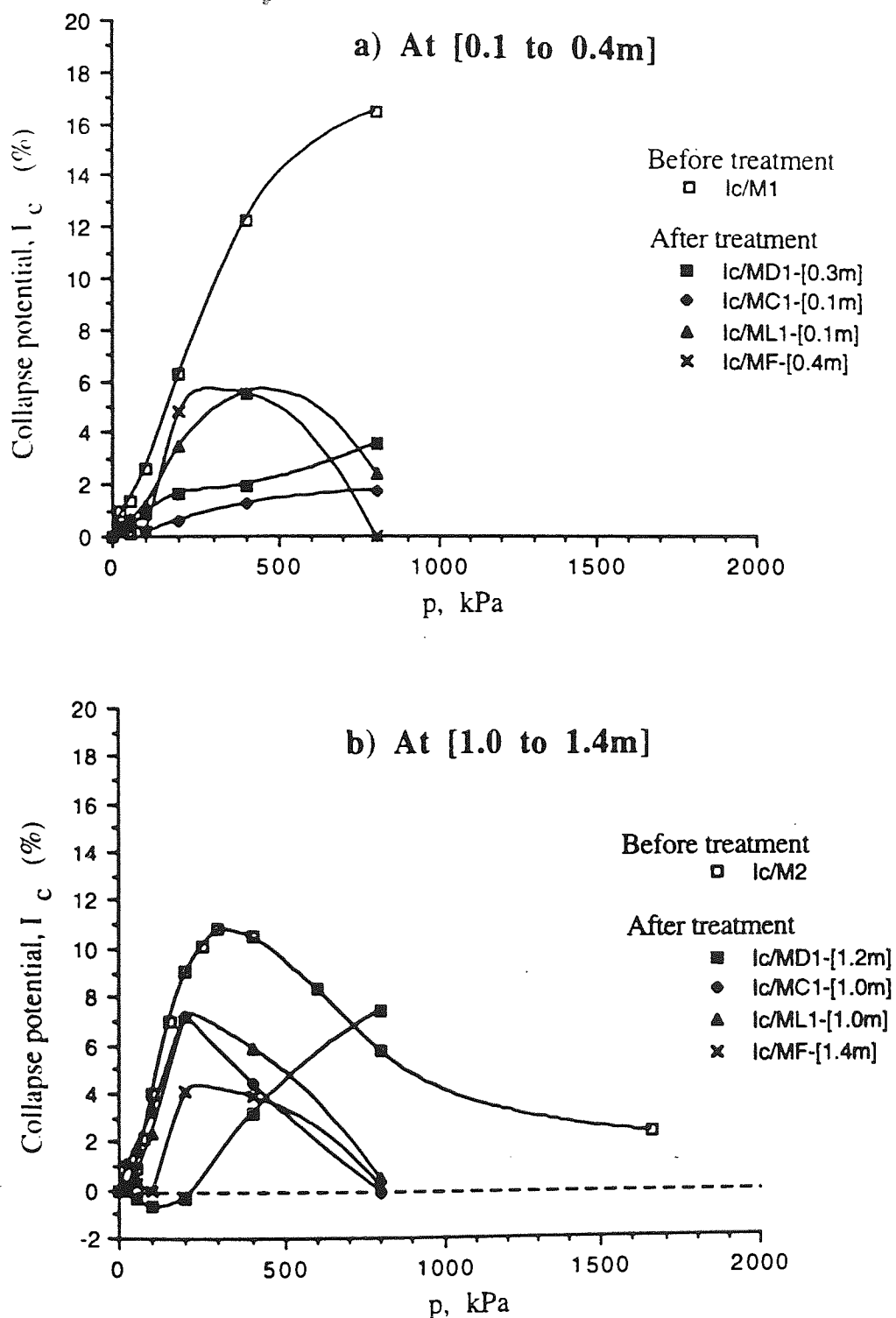
Fig. 6.44 : The comparison between the collapse potentials I_c for locations
at site III treated by different methods, from a) 0.1 to 0.4m and
b) 1.0 to 1.4m below the treated surface.

a) I_L at [0.1 to 0.4m]

[..m] : the depth below the treated surface

Before treatment
□ I_L /M1

After treatment
■ I_L /MD1-[0.3m]
♦ I_L /MC1-[0.1m]
▲ I_L /ML1-[0.1m]
✕ I_L /MF-[0.4m]

b) I_L at [1.0 to 1.4m]

Before treatment
□ I_L /M2

After treatment
■ I_L /MD1-[1.2m]
♦ I_L /MC1-[1.0m]
▲ I_L /ML1-[1.0m]
✕ I_L /MF-[1.4m]

c) I_T at [0.1 to 0.4m]

Before treatment
□ I_T/M1

After treatment
■ I_T/MD1-[0.3m]
♦ I_T/MC1-[0.1m]
▲ I_T/ML1-[0.1m]
✕ I_T/MF-[0.4m]

d) I_T at [1.0 to 1.4m]

Before treatment
□ I_T/M2

After treatment
■ I_T/MD1-[1.2m]
♦ I_T/MC1-[1.0m]
▲ I_T/ML1-[1.0m]
✕ I_T/MF-[1.4m]

Fig. 6.45 : The total and loading collapse potentials of the treated soils by different methods at site III.
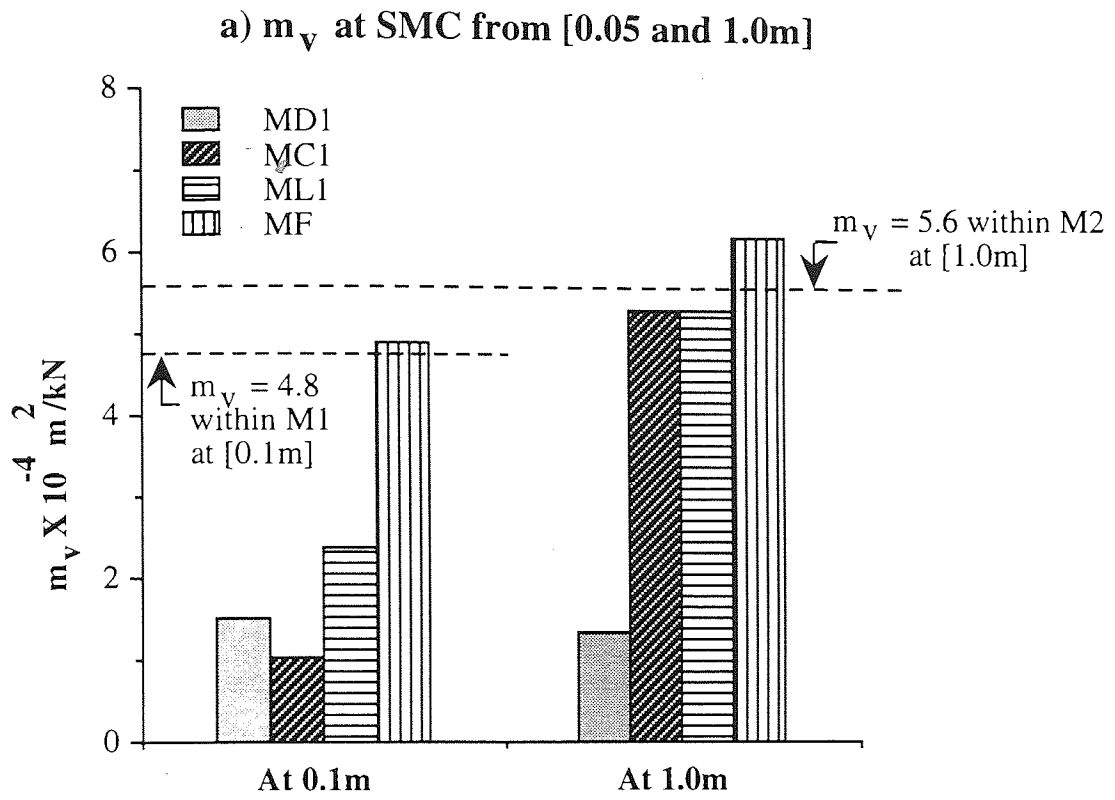
a) m_V at SMC from [0.05 and 1.0m]

Legend:
- MD1
- MC1
- ML1
- MF

m_V X 10^{-4} m^2/kN

m_V = 5.6 within M2 at [1.0m]

m_V = 4.8 within M1 at [0.1m]

At 0.1m   At 1.0m

Treatment methods -different locations at site III-

b) m_V at TMC from [0.1 and 1.0m]

Legend:
- MD1
- MC1
- ML1
- MF

m_V X 10^{-4} m^2/kN

m_V = 2.91 within the M2 layer at [1.0m]

m_V = 1.03 within the M1 layer at [0.1m]

At 0.1m   At 1.0m
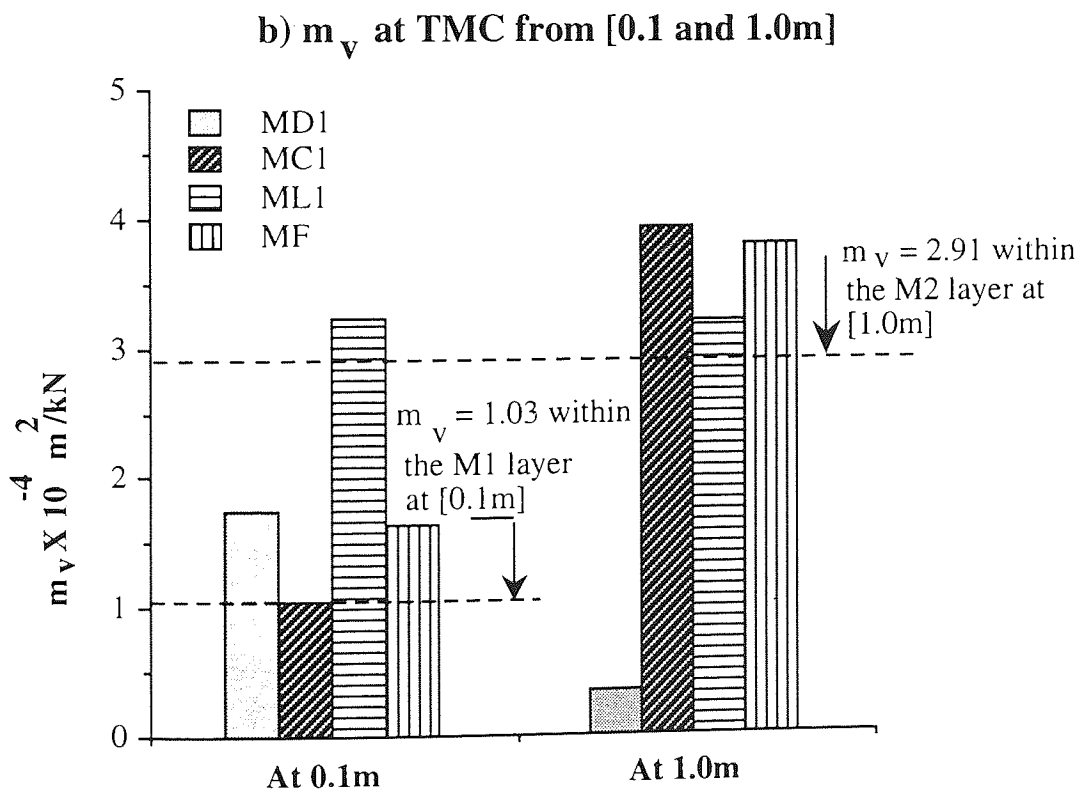
Treatment methods -different locations at site III-

Fig. 6.46 : The comparison of m_V for some locations treated by different methods at both SMC and TMC conditions.

Plate 6.1

Field loading test indicating:-

a) Loaded surface levelling,

b) The measurment of the settlemen under 50 kPa,

c) The full, field loading scale, 150 kPa, and

d) Water level system used in moniterring the field settlement.

a

b
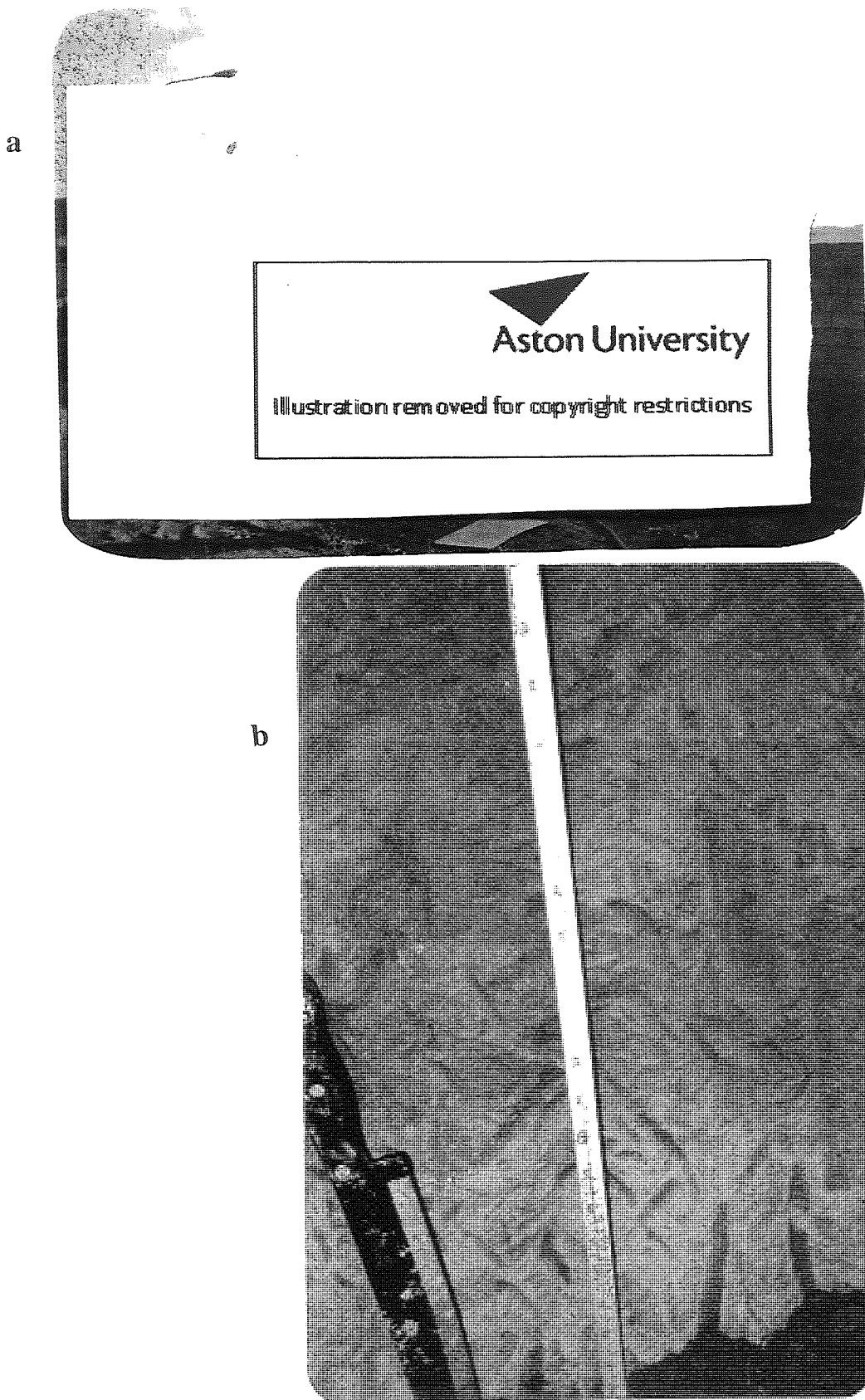
Plate 6.2 : a) Tilting failure of the field loading test at the location ML3.
         b) Detecting the depth of water infiltration after termination of
            the loading test at the location ML1.

a) Location and measuring points preparation
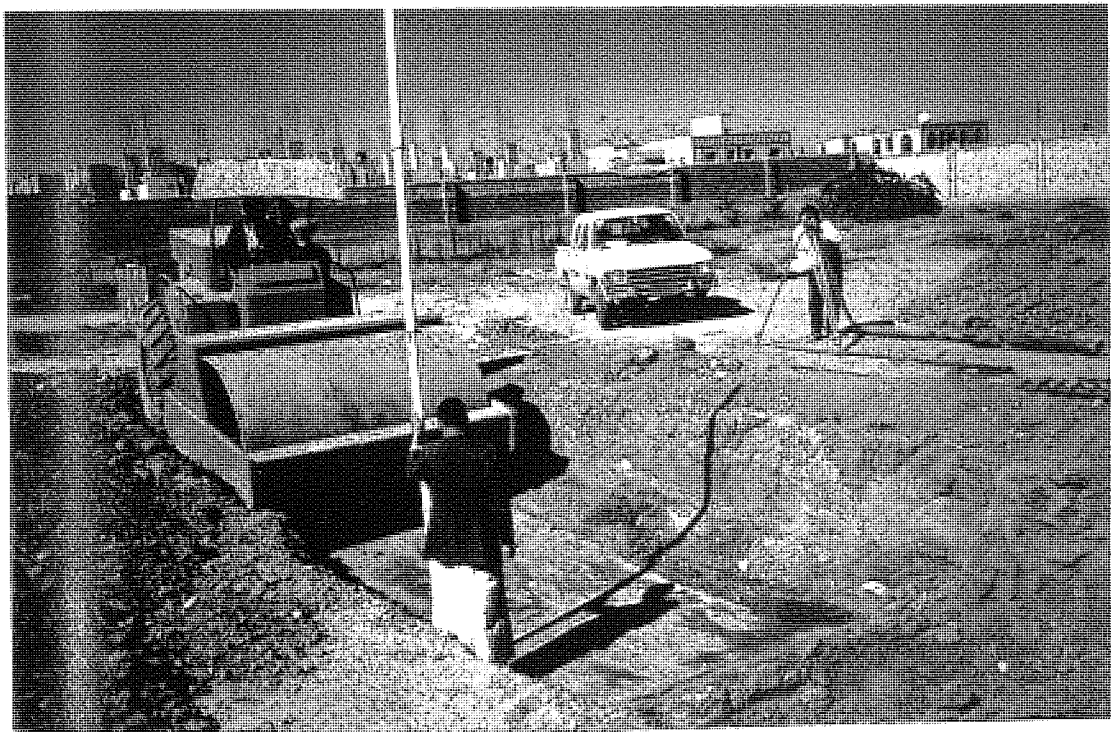
b) Compaction with SAKAI SV 90

Plate 6.3 : Steel Roller Compaction.
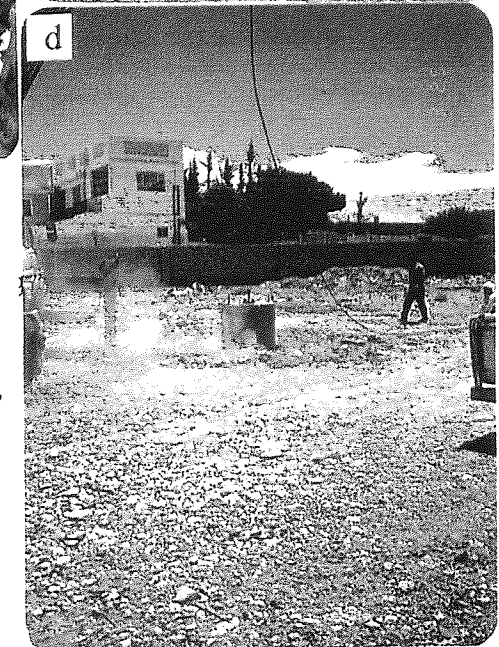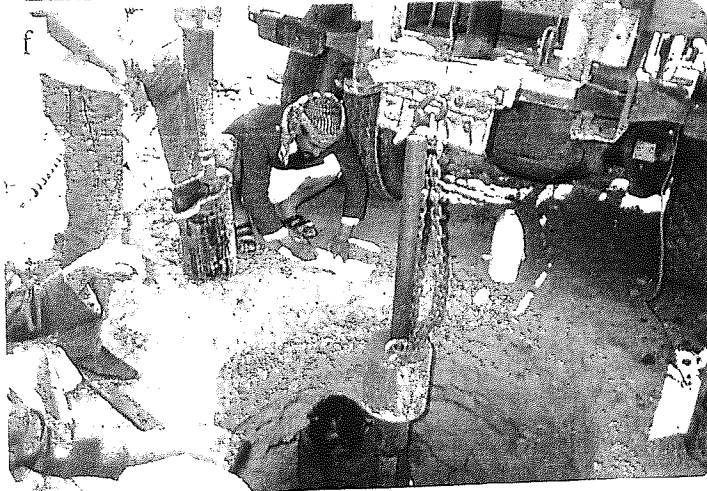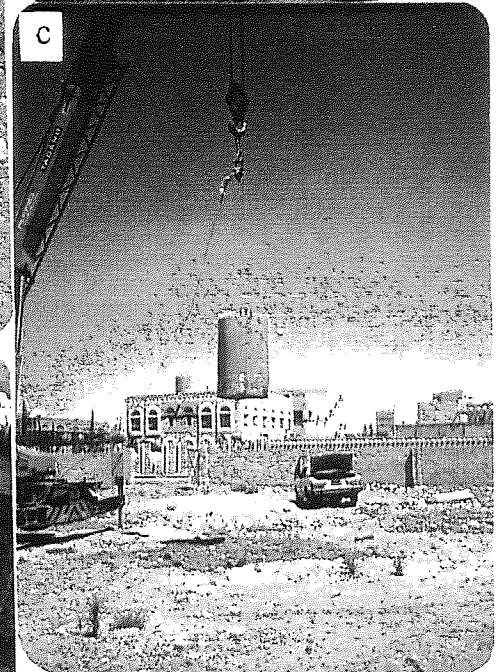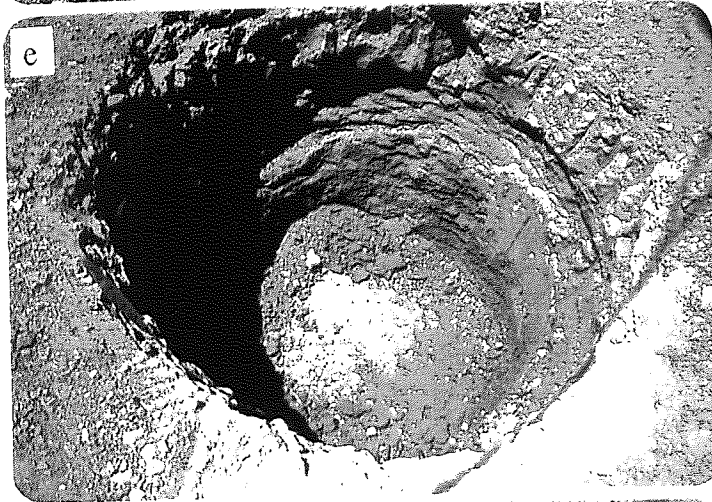
Plate 6.4 :

Deep Compaction "Pounding" procedures.

a) Levelling of location MD1 before pounding,

b) The measurment of the dropping height (6.0m),

c) The vertical free falling of the 3.0 metric ton using hydraulic releasing system,

d) Falling load, at time of contact with ground,

e) Impacted location MD1 after pounding shown the considerable slump (91.0 cm), and

f) Operating of SPT at the treated location MD2.
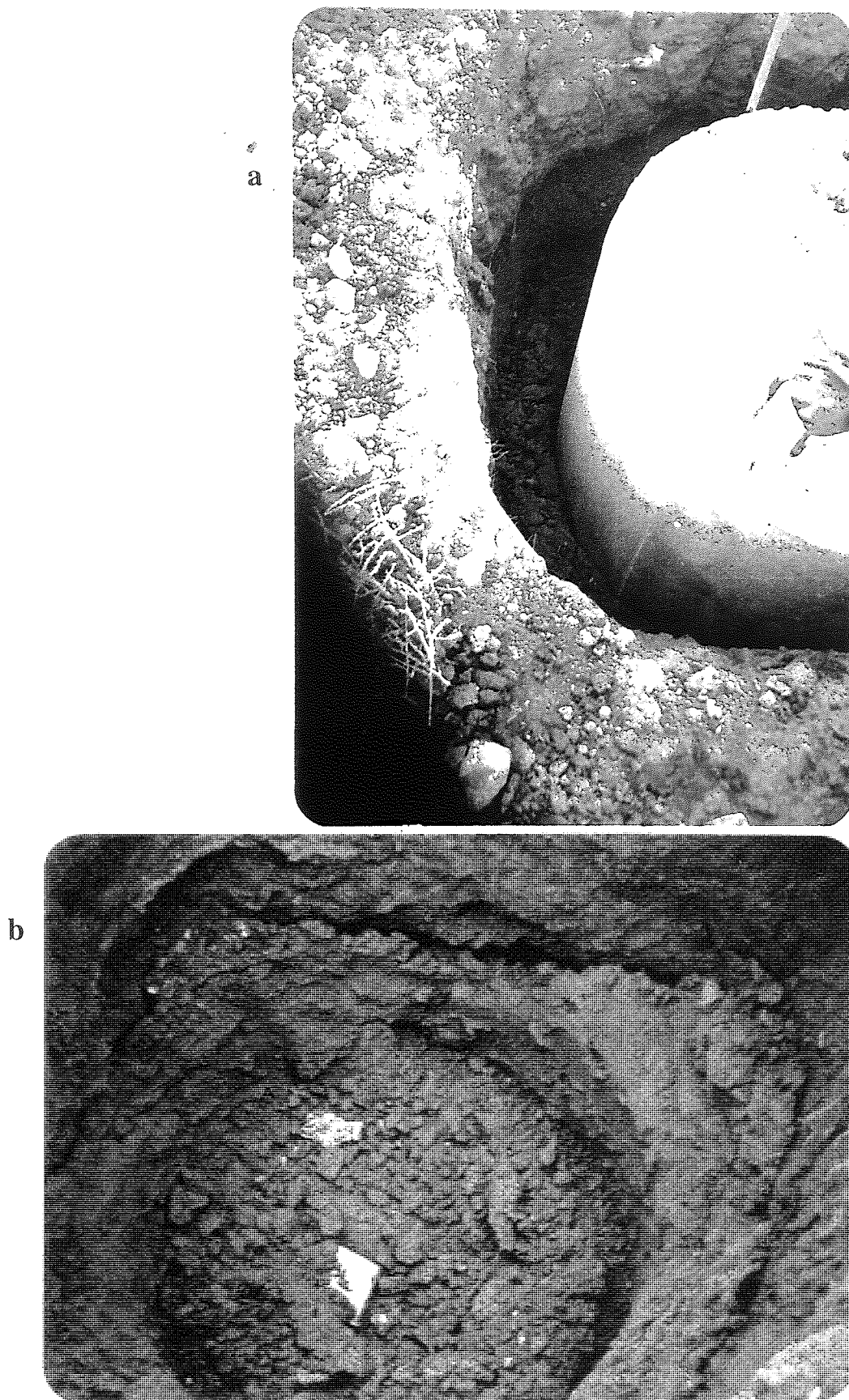
Plate 6.5: The Dynamic Compaction at AD2 following pre-flooding for five
days, indicating;

a) Vertical flow of the highly soaked soil at the time of pounding, and
b) Highly disturbed sides and base of the pounded location AD2.

CHAPTER 7

THE DEFORMATION BEHAVIOUR OF THE LABORATORY COMPACTED AND DESTRUCTURED SOIL

7.1 INTRODUCTION

Compacted fills have been widely used in construction and problems associated with such aspects of their mechanical behaviour as collapse settlement and excessive deformation include both damage to structures placed on fills and distress and/or failure of underground utilities (Lawton et al, 1992). Within the Sana'a region, the use of local soils as compacted fills has led to extensive damage within structures placed on them, particularly structures adjacent to water and sewage pipes, as well as in pavements and subgrade foundations (see Table 1.1). It is, therefore, imperative for engineers to consider and control such damage and so investigation of the mechanical (deformation and collapsing) behaviour of the soils, as compacted materials, is very important. To arrive at a general overview and framework for the mechanical behaviour of these soils, it is necessary to investigate the mechanical behaviour of the compacted soils as destructured material. This term (Leroueil et al, 1979) implies the removal of the bonding forces within the soils.

Selected soils were destructured by both remoulding between the fingers and gentle use of a pestle and mortar (Vaughan et al, 1988), these being A1 and A2 from site I and M2 and M3 from site III. The destructured soils were statically compacted into special moulds, manufactured for preparing the oedometer samples. These soils are termed as destructured/compacted (D/C), the prepared samples being identified by the symbol (Ds) in the standard nomenclature, rather than the (N) used for the natural samples. The deformation and collapsing behaviour of these soils was studied herein.

7.2 DEFORMATION AND COLLAPSING BEHAVIOUR

7.2.1 Deformation Behaviour

The oedometer samples of the natural soils, presented in Chapter 5, were used to produce the D/C samples so as to minimize the variation between the natural and destructured samples of the same soil. After testing and subsequent oven-drying, each natural sample was

destructured and prepared to the same initial moisture content and dry density as the corresponding natural sample by statically compacting the destructured material into the same oedometer ring and tested in the same equipment. Typical oedometer results are shown in Fig. 7.1 for the D/C samples of the soil A2 at both the compacted moisture content, CMC, (Fig. 7.1(a)) and soaked moisture content, SMC, (Fig. 7.1(b)). The corresponding results for the natural samples, at both moisture states, are represented by the dotted lines. X1, X2 and X3 refer to termination points at which SEM specimens were detected (see Sec. 7.2.4).

Natural cementation and bonding forces increase the resistance of the soil to deformation. When the cementation is broken down, the magnitude and rate of subsequent deformation are large, especially when accompanied by an increase in pore water pressure (Sangrey, 1972). Although the corresponding pairs of A2 samples were produced at the same water content and dry density, the total deformation of the destructured samples was significantly greater than that of the intact samples at same moisture conditions, this was particularly marked at the SMC state. An analysis of the data indicated that the soil stiffness was also reduced by destructuring, 5000 to 2080 kPa for the NMC samples and from 760 to 300 kPa for the SMC samples, and similar behaviour was observed in both the yield stress values, σ_{yn} and σ_y, and the compression index C_c. The reduction in C_c demonstrates the effect of the rupture of the cementing bonds which, in the intact soils, had resisted deformation at stresses up to the yield value although at higher stresses excessive deformation occurred due to the break down of these bonds. This excessive deformation represents the unstable state of the cemented soils and so, subsequently, greater C_c values were obtained from the intact than from the destructured soils. However, at low stresses, the D/C samples exhibited more deformation than the intact soils, and this was also true for the total deformation. Generally destructuring the soil, at the SMC state, softened it so that its stiffness and yield stress were reduced while the compressibility and deformation increased but, at the CMC state, some stiffness and deformation resistance was mobilised due to the capillary or suction bonds.

In the e-log p space, for the SMC condition, the curve for the destructured soil is almost linear, except at very low stresses, and it lies below the normal consolidation line of the intact soil (Fig. 7.1(b)) with both tending towards a limiting state relation at high stresses. In contrast, at the CMC and NMC conditions, the progressive changes in the void ratio with increasing stress follow curvature trends which are mainly a function of the residual capillary bond, which was recaptured after compacting the destructured material. When each of these samples was wetted, at the end of the tests, the void ratio was reduced to the same value as the corresponding presoaked sample (intact or undisturbed) as shown in Fig. 7.1, such reduction being termed the collapsing potential. Similar behaviour was achieved with the other soils with some exceptions for the soils A1 and M3. For the D/C sandy silt (A1), over the applied range of stresses, the differences in the void ratio between the two destructured curves , at the CMC and SMC conditions, were very small due to the soil texture (high sand and low fine contents). In the case of the stiff sandy silt, M3, a slight increase was observed in the stiffness and yield

stress at the SMC condition, due to its higher dry density compared with the other soils as shown in Appendix E7-1. Generally, at both moisture conditions the D/C soils exhibited greater deformation and lower stiffness and yielding stresses than those of the corresponding natural soils, particularly when tested at the SMC condition. The different values of the soil stiffness, yield stress and the compression index for the destructured/compacted soils at both moisture states are summarised in Table 7.1.

7.2.2   Collapsing Behaviour

Collapsing settlement due to wetting within compacted fill is a common problem which has led to many failures (Lawton et al, 1992). The collapsing potential, I_c, of the D/C soils were determined from the double oedometer results as shown in Figs. 7.2(a) and (b) for the soils from sites I and III respectively, together with those for the natural soils. The collapsing potential, at any stress level up to 200 kPa, for the D/C soils at site III was greater than that for the intact samples (Fig. 7.2(b)) while, at site I, it was greater for the soil A2 but minimal for A1 (Fig. 7.2(a)). The collapsing potential at stresses of 50, 100 and 200 kPa, for the D/C soils are summarized in Table 7.1. The maximum values (I_c max) occurred at lower stresses with the D/C soils than for the intact soils, apart from the sandy silt soil, A1, where the collapsing potentials were extremely small over the entire range of applied stresses as shown in Fig. 7.2. Generally, the results indicate that destructuring soils characterised by having significant fines and cementation (soils A2, M2 and M3) did not reduce the collapsing potential (I_c), when compacted to the natural dry density at the in situ moisture content. However, for the sandy to sandy silt soil, A1, which was characterized by having a low fines content (clay and colloidal) and high coarse (sand) content, the collapsing potential was virtually eliminated when it was similarly treated. Lawton et al (1992) indicated that compacted silt-clay became more susceptible to collapse when a clay content was between 10% and 20%, and at clay contents below 10%, the silty soils collapsed more than sandy soils. Similar observations on the effects of soil texture and composition on the collapse potential were reported by Al-Waili (1990) and Basma and Tuncer (1993).

The nature and type of the cementation bonds significantly affects the collapsing potential of soil. For the destructured/compacted soils, the physical bonds due to the cementation were removed and so all the D/C soils, at the SMC state, exhibited very similar deformation trends while, at the CMC state, different trends were observed due to variations in the residual bonding forces of the capillary or suction type. The response of the different soils to wetting at the end of the tests (Fig. 7.1(a)) supports the concept of residual capillary bonds, and so such bonds were not as markedly affected by destructuring as those due to cementation. Houston and El-Ehwany (1991) stated that cementation caused by negative pore pressure is relatively insensitive to disturbance and probably recaptured when the specimen is recompacted to the same dry density and moisture content. Although this concept of regaining the suction

bonds seems to be valid for the soils A2, M2 and M3, this was not so for soil A1. While structure is a predominant factor influencing the deformation and collapsing behaviour, destructuring and preparing the soils to the dry density and moisture states of the corresponding natural soils does not guarantee improved deformation and collapsing behaviour. Furthermore, variations in the initial moisture content or the dry density of the soil can influence the deformation and collapsing potential (Booth, 1975-a; Lawton, 1986) and so it was considered necessary to investigate the effects of such variations and sample preparation on soil behaviour.

Fig. 7.3 shows the collapsing potentials due to loading alone, I_L, for the D/C soils from both sites I and III. It indicates that the collapsing potential I_L, over the applied range of stress (to 1660 kPa), for the D/C soils (dark symbol) was greater than that for the intact samples (open symbol). This is simply due to the lower resistance to deformation under loads arising from the loss of cementation bonds by destructuring. At low to moderate stresses, the rate of increase in I_L was higher for the D/C soils than for the intact soils and, furthermore, for the D/C soils the rate of increase becomes more marked for these soils in the order A1, M2, A2 and M3 as shown in Fig. 7.3. This change in behaviour can again possibly be attributed to variations in soil texture. Similar results were obtained for the total collapsing potential I_T, under both loading and wetting, with the I_T for the D/C soils being greater than that for the intact soils, again due to the loss of bonds by both destructuring (cementation bond) and wetting (suction bond). Generally, as expected, destructuring and compacting the soils to the in situ dry density at the natural moisture content increased both their total and loading collapsing potentials.

7.2.3 The Effects of Moulding Moisture, Dry Density and Sample Preparation

7.2.3.1 Effect of Moulding Moisture Content

For this task, three or four samples from each soil type, were destructured after oven drying and compacted to the same dry density, at moisture contents ranging from 10% to 30%, into a specific mould including the oedometer ring (Booth, 1975-b). They were loaded up to 1660 kPa at their prepared moisture content (CMC) and water was subsequently added after equilibrium had been reached under the last load increment. Typical results for A2 are shown in Fig. 7.4, while Appendix E7-2 shows the results for M2. The data in Fig. 7.4 show that all the curves reached the same lower boundary corresponding to the presoaked, destructured curve (A2Es/Ds), either by wetting at the end of the test for samples at low moisture content or by increasing the stress during the test for those with high moisture contents so, as the moulding moisture content increased, the soil stiffness decreased and the deformation increased. Generally, the role of the water was vital in destroying the bonded structure with the deformation curves being translated to the lowest boundary in the stress-strain domain. Similar

results were obtained from the other soils, with the exceptions of A1 which exhibited less sensitivity to the moisture variations as indicated earlier.

The effect of moisture content on the collapsing potential (I_c) for M2 and M3 is shown in Fig. 7.5, indicating that as the moisture content decreased the collapsing potential increased exceed that of the natural soil represented by the open symbol in Fig. 7.5. The initial rate of increase in the collapsing potential of these samples was considerably greater than that for the corresponding natural samples so that their maximum values of I_c were achieved at lower stresses than those for the natural soils, due to the loss of the bonding resistance of the D/C soils to deformation - particularly at the SMC state. This indicates the role of cementation in controlling the collapse at low stresses, but when the cementation is broken down the yield stress is reduced and the collapse under low stresses increases.

An interesting feature is the significant collapsing potential of those samples prepared at moisture contents on the wet side of the optimum, Wopt. Many investigators (Barden et al, 1973; Hausmann, 1990) have suggested that soils compacted at a water content wetter than Wopt do not collapse. Booth (1975-a) and Lawton et al (1992) have stated that this concept cannot be strictly valid as it does not consider either the effect of the prewetting density and moisture content of the soil. They indicated that significant collapse can occur in samples compacted wetter than Wopt if low density and/or postcompaction drying are provided. For soil M2, sample I_c-M2/Ds,Wc=30% in Fig. 7.5(a) was prepared at a moisture content of 30 %, which was 2% higher than Wopt (28%), yet a maximum collapsing potential of 10.5% was achieved at stress 100 kPa, and similar behaviour was observed for soil A2. This indicates that the D/C samples of A2 and M2 prepared at Wc > Wopt still exhibited significant collapse, due to their low dry density and this is in agreement with the observations reported by Booth (1975-a) and Lawton et al (1992).

For a set of samples, a plot of collapsing potential against moisture content could reveal a critical moisture content above which collapse would not occur, and such data is shown in Fig. 7.6 for the soils of site I. Generally, as the moulding moisture content increased the collapsing potential decreased until it reached a minimal or zero value at the critical moisture content. This shows that for stresses greater than 25 kPa the critical moisture contents for the soils A1 and A2 were 20% and 25% respectively, the values for all the soils are shown in Table 7.1. Similar observations, but in terms of the critical degree of saturation were reported by Booth (1975-a) who indicated that the critical values were proportional to the optimum moisture content.

7.2.3.2 Effect of Dry Density

To study the effect of variations in dry density on the deformation behaviour of the D/C soils, five destructured, oven dried samples of each soil were prepared at the same in situ moisture content but to different initial dry densities (including two below and two above the in

situ value), and tested in the soaked condition. In this investigation no tests were carried out at the moulding moisture content, CMC, to assess the effect of dry density on the collapsing potential. However, many investigators have indicated that, for similar collapsing soils, the collapsing potential decreases as the dry density increases (Booth, 1975-a; Lawton et al, 1992), and so similar effects could be expected with the studied soils.

Typical deformation behaviour is shown in Fig. 7.7 and Appendix E7-3 for the soil A2 and M2 respectively. These results exhibit a convergence towards a limiting line, with increasing the stress. Similar convergence was also apparent from the samples prepared to same dry density, but at different initial moisture contents. This limit line is denoted as the "destructured line" to which the behaviour of all the samples of a given soil converge under loading. Figure 7.7 indicates that when the dry density (ρ_d) exceeded the in situ value (1.10 Mg/m^3), the soil exhibited higher stiffness, higher yielding (overconsolidation) stress and more deformation resistance than at the in situ ρ_d, and converged to the destructured line at higher stress. In contrast at dry density values below the in situ value, the soil deformed easily and the behaviour followed a concave curve with low yielding stress and stiffness, as shown by the curves in Fig. 7.7 for samples prepared at 0.75 Mg/m^3 and 0.9 Mg/m^3. At a stress equivalent to that of the overburden pressure, 38.4 kPa on A2, the curves for the loose ($\rho_d < 0.75$ Mg/m^3), in situ ($\rho_d = 1.10$ Mg/m^3) and the medium dense states ($\rho_d = 1.29$ Mg/m^3) converge to the destructured line on Fig. 7.7, and similar results were obtained with the other soils. For these soils, an applied stress of about 200 kPa was sufficient for each to deform according to the particular destructured line in the e-log p space, as shown in Fig. 7.7 and Appendix E7-3. Generally, for the destructured/compacted soil the deformation and collapsing behaviour decreased with increased dry density and decreased vertical stress. With decreased moisture content the deformation (loading collapse, I_L) decreased and the collapse (I_c) increased. For each soil a limit destructured line was established as the lower boundary line in the e-log p space to predict the deformation behaviour of the soil in its destructured state, particularly under stresses greater than the overburden pressure.

7.2.3.3 Effect of Sample Preparation

Specimens can be compacted by several methods, including static, kneading, impact and vibratory, but work on the behaviour of the compacted cohesive soils (Hausmann, 1990; Lawton et al, 1989) has indicated that these methods had only a minor influence on the collapse behaviour of clayey sand. Booth (1975-b) reported that sets of virtually identical specimens could be obtained using static compaction and so this method was adopted for the compaction of the oedometer specimens to achieve uniform samples.

Destructuring procedures have not been standardised and several techniques have been considered by Leroueil and Vaughan (1990). The basic requirement for a destructured soil is that all the particles should be separated so that each individual particle will be able to act as a solid particle during shearing without further rupture. The soils were destructured by

remoulding between the fingers and by gentle use of a pestle and mortar as suggested by Vaughan et al (1988). However, it is impossible to guarantee both the total separation of all the fines, particularly the colloidal aggregations, and the stability of individual particles by carefully employing these simple techniques, although a significant degree of destructuring was achieved. Johnson and Moston (1975) reported that agitation by ultrasonic energy, produced high quality, disaggregated and dispersed samples using less time and effort than that was required for the mechanical techniques. In addition, this method appeared to cause no deleterious effect on the primary particle sizes. However, due to the need for water in this method, it may only be appropriate for preparing reconstituted samples from slurries unlike the samples in this study which were mainly prepared at a specified initial moisture state. However, the use of the ultrasonic method for destructuring could be suggested for future work on destructured samples.

Oven-dried samples were used to obtain the raw material for the specimens in this study. For residual soils, Vaughan et al (1988) reported that irreversible changes may occur within remoulded, destructured samples if subjected to drying and so it should be avoided. Such effects were investigated by testing specimens from soils A2 and M3 destructured in the wet and oven-dried conditions. Fig. 7.8 shows the results of these tests and it is clear that negligible variations occurred between the two samples of each soil. Similar observations have been reported for samples at Alaskan silt investigated at different moisture conditions (Fleming and Duncan, 1990). Consequently, oven-dried specimens can be used without materially effecting the deformation behaviour. In addition, destructuring dry soil is easier to perform since part of the wet soil sticks between the fingers and on the pestle or mortar, particularly when the fines content is high.

An interesting point to be considered is the use of soil in either a moist state as a slurry or as a reconstituted material to provide the destructured sample. Fig. 7.9 shows the destructured lines achieved for samples from soils A2 and M3 produced from oven-dried material either compacted at the in situ conditions or reconstituted from a slurry. Generally, the destructured line obtained from the slurry (reconstituted) sample tends to lie above that obtained from the destructured sample prepared at the in situ moisture condition. In addition, the destructured curves obtained from slurry samples did not converge to the limiting line, particularly when the samples had differences in the initial void ratios (dry densities). Moreover, the slurry samples exhibited high sensitivity to setting and loading in such a semi-liquid state and so samples prepared to have almost the same dry density (1.04 to 1.09 Mg/m^3), exhibited different converging trends. This is illustrated by the results in Fig. 7.10 for six samples of M2 prepared at different moisture contents greater than the LL and different dry densities where no specific deformation trend is apparent from the six curves. Similar observations were found by testing disturbed remoulded and slurry samples of Chemususu Dam soil (Bressani, 1990). In contrast, six samples from soil A2 prepared from oven-dried (2 specimens), air-dried (2) and natural wet (2) material, but to the same dry density, displayed

similar behaviour as shown in Fig. 7.11. This indicates that some form of bond exists within the slurry samples, or those prepared at high initial moisture contents, and this may be related to the occurrence of irreversible changes or bonds in the destructured slurry soil due to soil water interaction (Mitchell, 1976), aging and growth in the bonding agents (Mitchell and Solymar, 1983). The latter stated that solution, precipitation reactions and the formation of cementation bonds at interparticle contacts must be considered when evaluating the results of laboratory tests on reconstituted samples. The development of a time dependent bond was reported by Nagaraj et al (1990), who stated that, " Soil suspensions subjected to consolidation pressures less than 5-6 kPa would not be stable so long as to result in the development of bonds. However, it is possible that the cementation bonds are developed at higher pressures when the soil has equilibrated to water contents less than liquid limits". Furthermore, from the practical point of view, the use of destructured soil in the slurry form to predict the field behaviour of destructured soil does not seem to be compatible with the in situ conditions for most civil engineering applications. As a conclusion, producing reconstituted samples from the slurry state may not fully simulate the destructured state and so the production of a limiting destructured curve as a boundary line from such samples was not pursued.

7.2.4 The Microstructure of the Oedometer Destructured Samples

Numerous images (photomicrographs) were taken to show objects of special interest to the study such as collapsed pores distributions, contact points, cementation agents. Although only a few representative images are presented, the general discussion and conclusions are based on all the observations. Microscopic observations were made of both natural samples destructured by loading (oedometer testing, Fig. 7.12 and Appendix E7-4) and destructured/compacted samples that were subjected to similar loading (Fig. 7.13). For this investigation, the results of the silt to silt with sand soil, A2, have been selected as representative.

In the open structure of the natural soils (Chapter 5), the arrangement of the grains is maintained by cementing agents in the form of bridges, buttresses and/or coatings. These produce high pore volume and few grain to grain contacts. Such a structure for soil A2 was shown in Fig. 4.15, the soil having a very high void ratio of 1.55.

Fig. 7.12(a) shows the natural sample from soil A2 which has been loaded at the natural moisture content (NMC) in the oedometer to a stress of 1660 kPa with a final void ratio of 0.985 before soaking (similar to point X1 in Fig. 7.1(a)). This densification was characterized by limited particle rearrangement, sliding and rotation as shown from the unaffected clothed assemblages and pores (Fig.7.12(a)) but, at very high magnification, partial distortion of the bonding agents at contacts (connectors) was observed which led to partial packing of the large grains, as shown in E7-4(a). The absence of wetting of the fines and

cementation agent, due to the low moisture content, contributed to this partial packing. Generally, only partial destructuring was achieved by loading the natural soil at the NMC state in the oedometer.

Two images of a similarly loaded sample which had been wetted before loading (point X2 in Fig. 7.1(b)) are shown in Figs. 7.12 (b) and (c) so any changes in the soil structure, in comparison with Fig. 7.12(a), can be attributed to prewetting. Compression under wetting considerably reduced the visible voids with a final void ratio of 0.676 at X2. As Barden et al (1973) and Gillott (1987) have observed, the softening produced by soaking can result in the close packing of the soil grains shown in Fig. 7.12 (b), which in term led to breakage of the weakened bonds around the particles (coating) and at contacts as shown in Fig. 7.12 (c). The applied stress was sufficient to crush the cement bonds at the contacts and so push the debris into the vacant pores, but it was not sufficient either to crush the large grains or to force them to slide across each other and so lead to further destructuring. Thus, the destructuring by loading to 1660 kPa at the SMC state was partial since the soil still appeared to retain some natural bonds that had not been significantly affected. Further evidence for this partial destructuring is the presence of pores within the destructured sample as shown in E7-4 (b) and (c). These SEM results are compatible with the oedometer results in Fig. 7.1 as the destructuring (poit X2) did not sufficiently compress the sample to reach the destructured line (poit X3) on Fig. 7.1, and so some further loading would be required.

The microstructure of the destructured/compacted (D/C) sample, loaded to 1660 kPa at SMC (point X3 in Fig. 7.1) is shown in Fig. 7.13. The compression of the D/C soil under wetting reduced the visible voids so that the final void ratio was 0.605. The most visible sign of modification, though, was the distortion of the cement coatings, which reflects the mechanical rearrangement of the large particles. Compacting the D/C soil to its in situ density (high voids) permitted the particles, both large and small, to slide and turn upon each other without bond restrictions. With increasing load, continuous rearrangement enabled the particles to achieve the closest packing characterized by an increase in the grain to grain contacts (Fig. 7.13(a)). In addition, most of the trapped pores were filled with the chipped or softened cementing agents, which had acted as lubricating agents for coarse grains, (Fig. 7.13(b)) leading to a significant degree of interlocking of the large grains (Fig. 7.13(c)). The reorientation and destructuring also resulted in a significant crushing of the needle form of calcium carbonate and to limited crushing of the large particles. Damage to the coarse grains can be seen at the upper centre of Fig. 7.13(a). Generally, a significant loss of both the intra- and inter-particles voids is apparent in Fig. 7.13 indicating that extensive destructuring was achieved by loading the D/C soil in the SMC state. For a naturally cemented soil, a fully destructured state can be achieved when the deformation trend of the soil in the e-log p space reaches the destructured line.

288

Table 7.1 : Summary of the deformation and collapsing characteristics of the destructured soils.

Site	Soil	Depth m	Sand %	Silt %	Clay %	Wc %	ρ_d Mg/m³	E_b kN/m²	σ_{yn} kN/m²	C_c	E_a kN/m²	σ_y kN/m²	C_c	50 kN/m²	100 kN/m²	200 kN/m²	I_c max %	p_{cc} kN/m²	Critical moisture %	Wopt [d] %
I	A1	1.5	56 [c]	31	7	10	1.24	337	12.5	0.25	362	6.25	0.141	0.6	0.0	0.0	1.0	25	20	21
	A2	3.0	21	58	19	17	1.10	2080	140	0.686	300	6.25	0.42	11.8	14.6	14.5	14.9	120	25	23
III	M2	2.2	10	66	24	25	1.10	630	80	0.836	180	12.5	0.488	10.3	14.6	13.3	14.6	100	33	28
	M3	3.0	29	43	21	12	1.45	2600	200	0.343	409	35	0.24	0.7	6.0	9.4	10	260	24	--

a - CMC : Compacted or moulding moisture content
b - SMC : Soaked moisture content
c - Average gradation for the soil A1, obtained at 1.2 and 1.8 m
d - Optimum moisture content (Table 4.7)
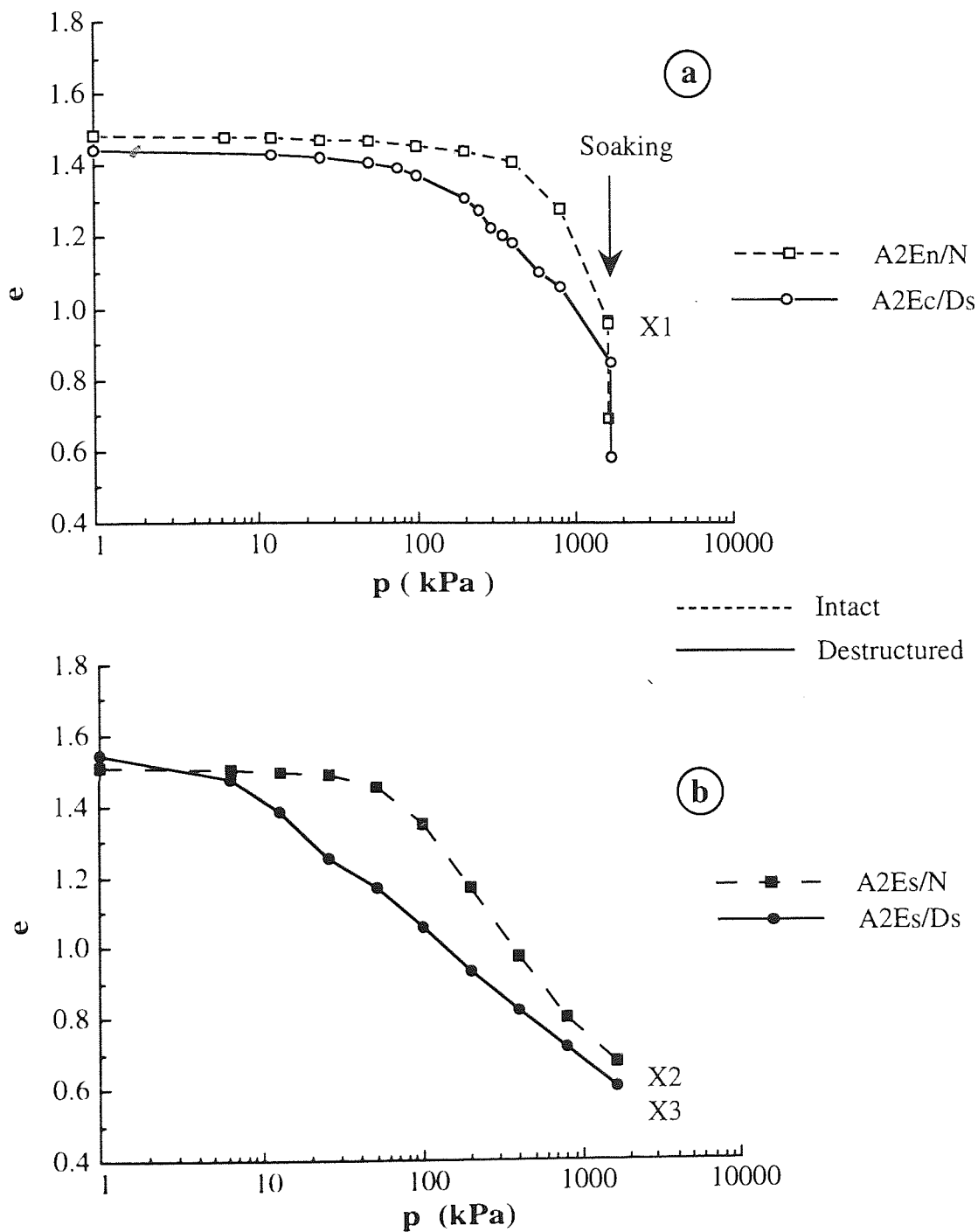
Fig. 7.1 : Oedometer test results of the destructured and intact soil A2 at the a) partially saturated, and b) soaked conditions.
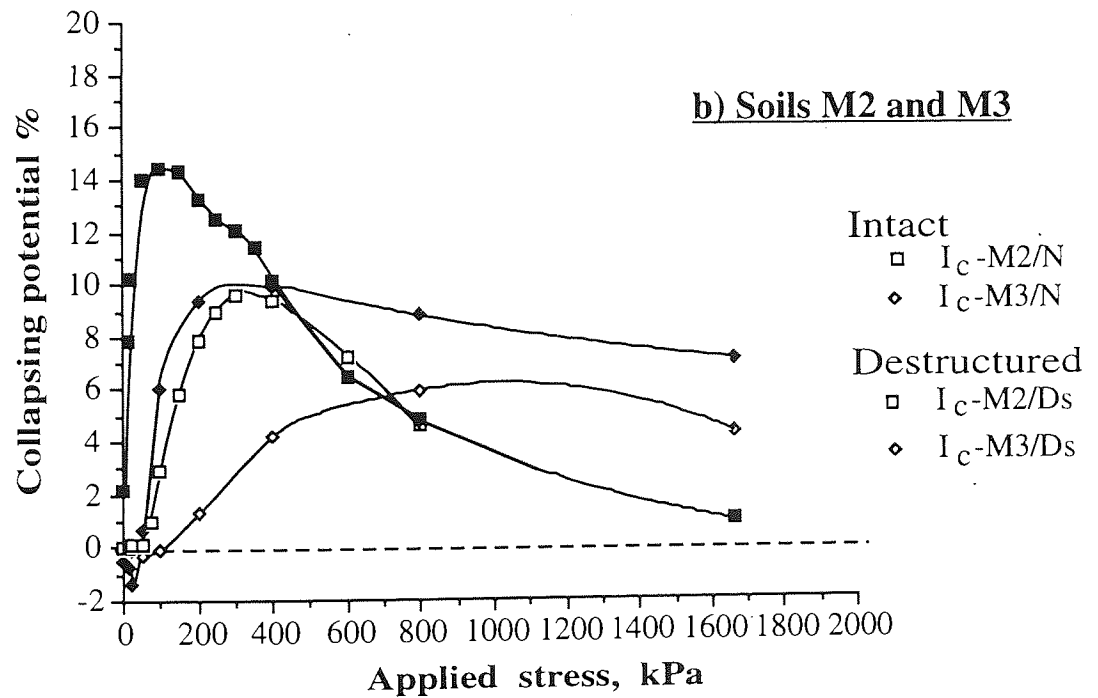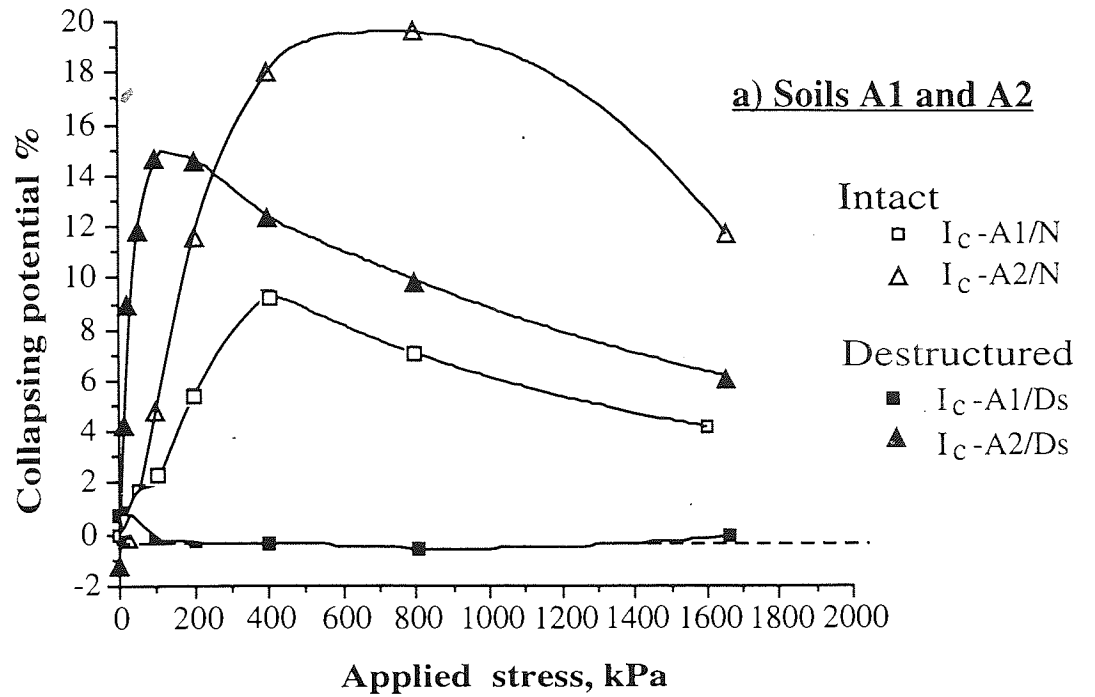
Fig. 7.2 : Collapsing potential of the destructured/compacted
and natural soils from sites I and III.
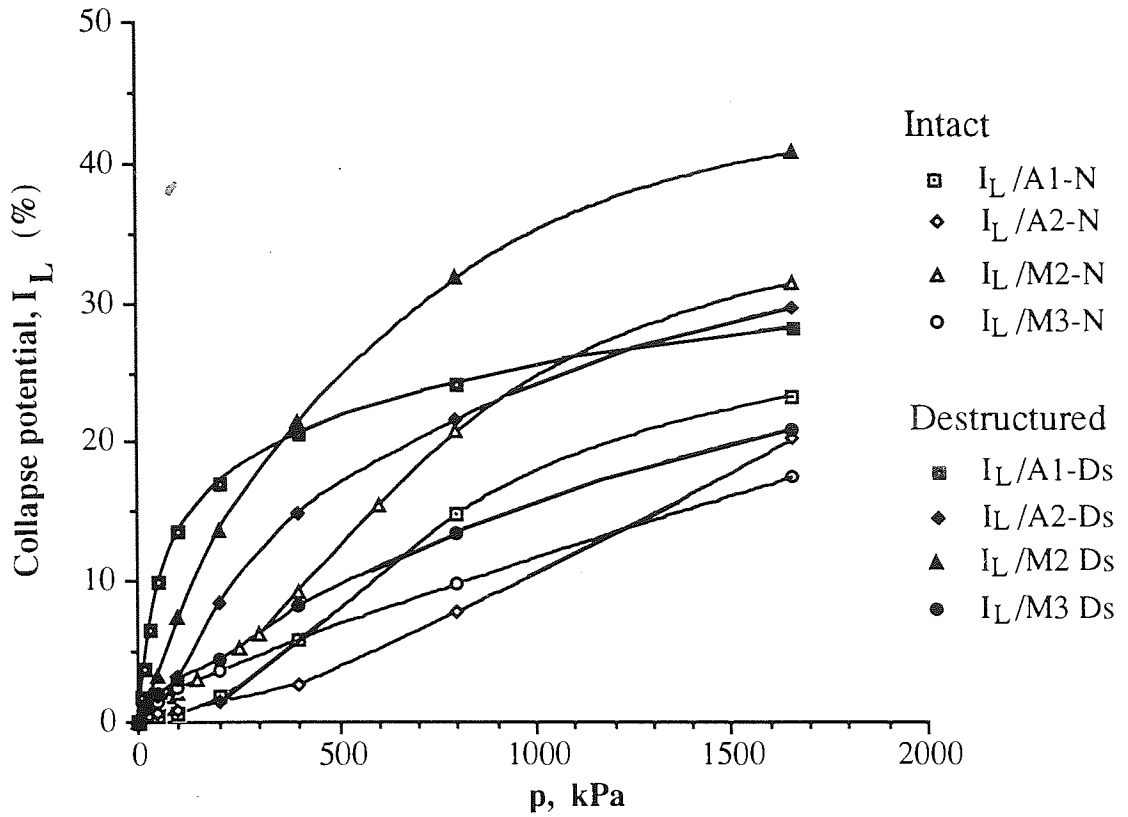
Fig. 7.3 : The collapsing potential due to loading alone for the D/C
soils from sites I and III.
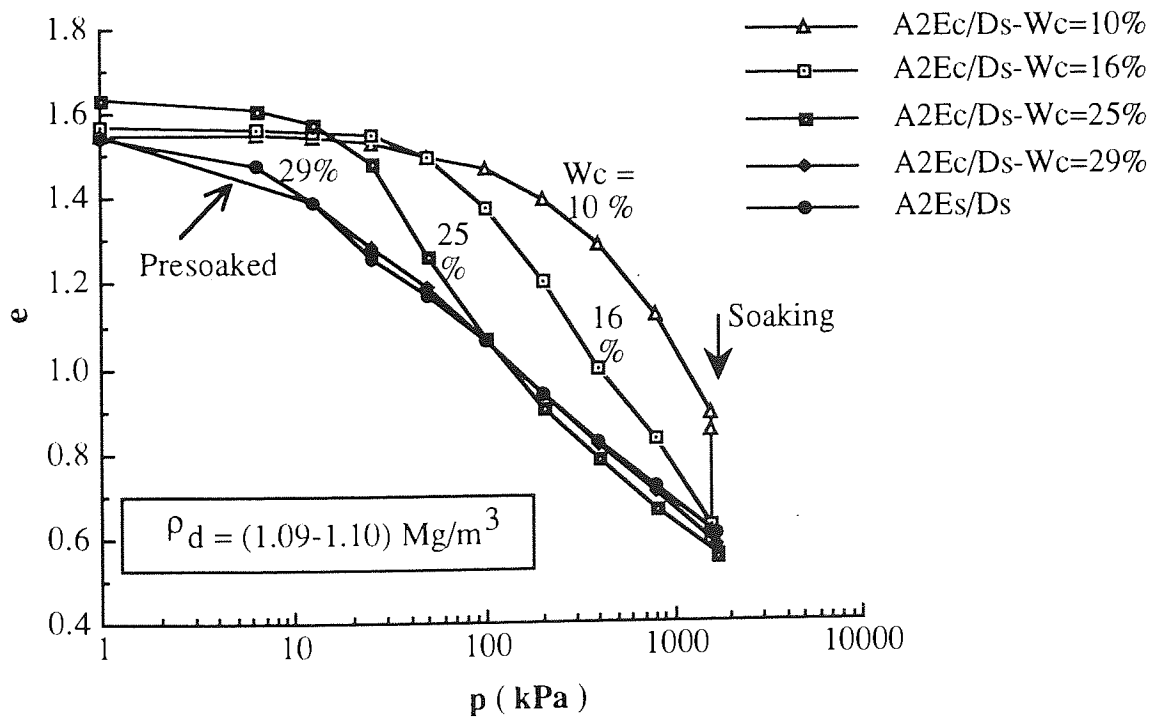
Fig. 7.4 : The compressibility results for the destructured/compacted
(D/C) samples of soil A2, prepared at different compacted
moisture contents (CMC).
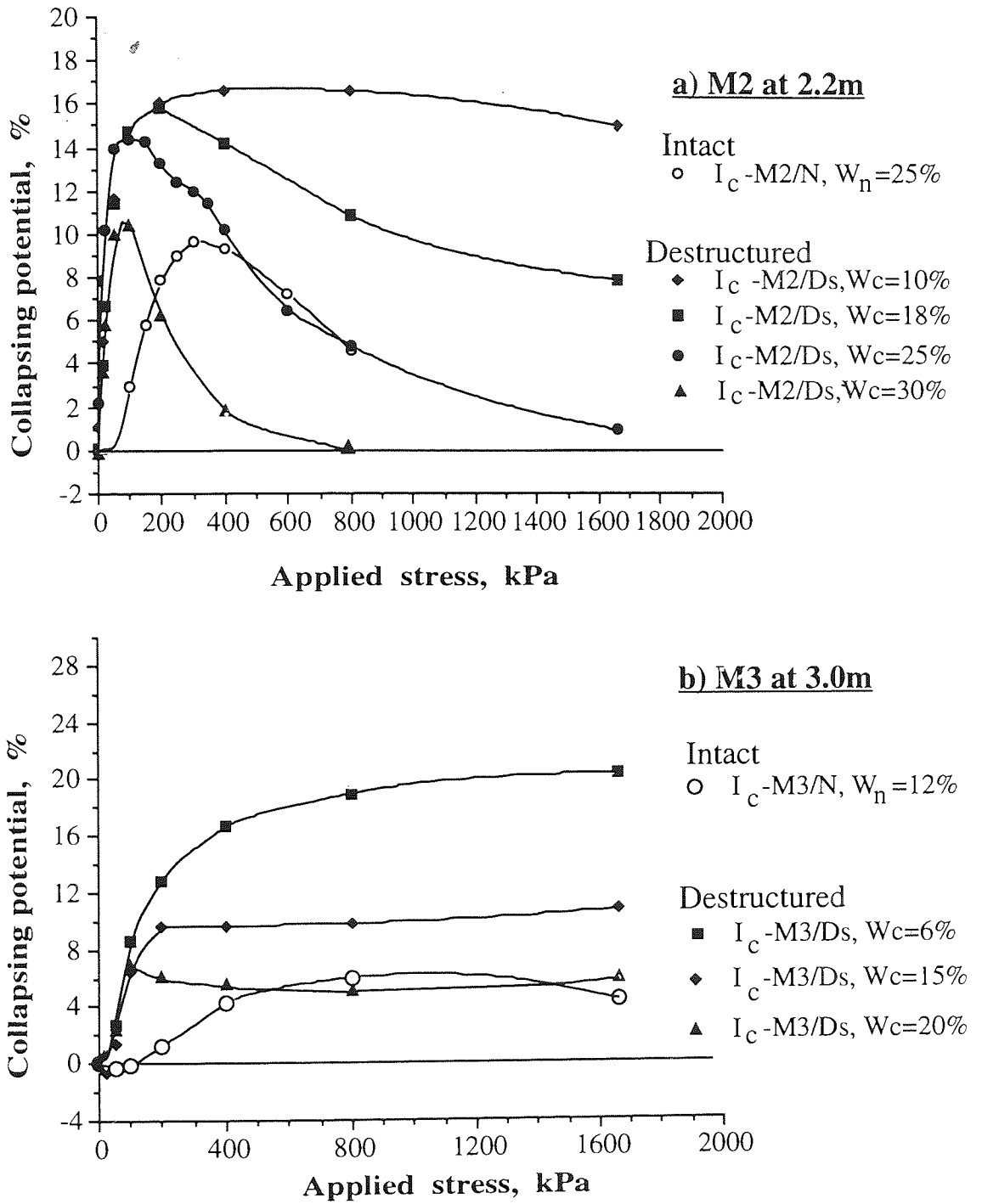
Fig. 7.5 : Collapsing potential of the destructured/compacted
soils, M2 and M3 from site III, at different compacted
moisture contents.
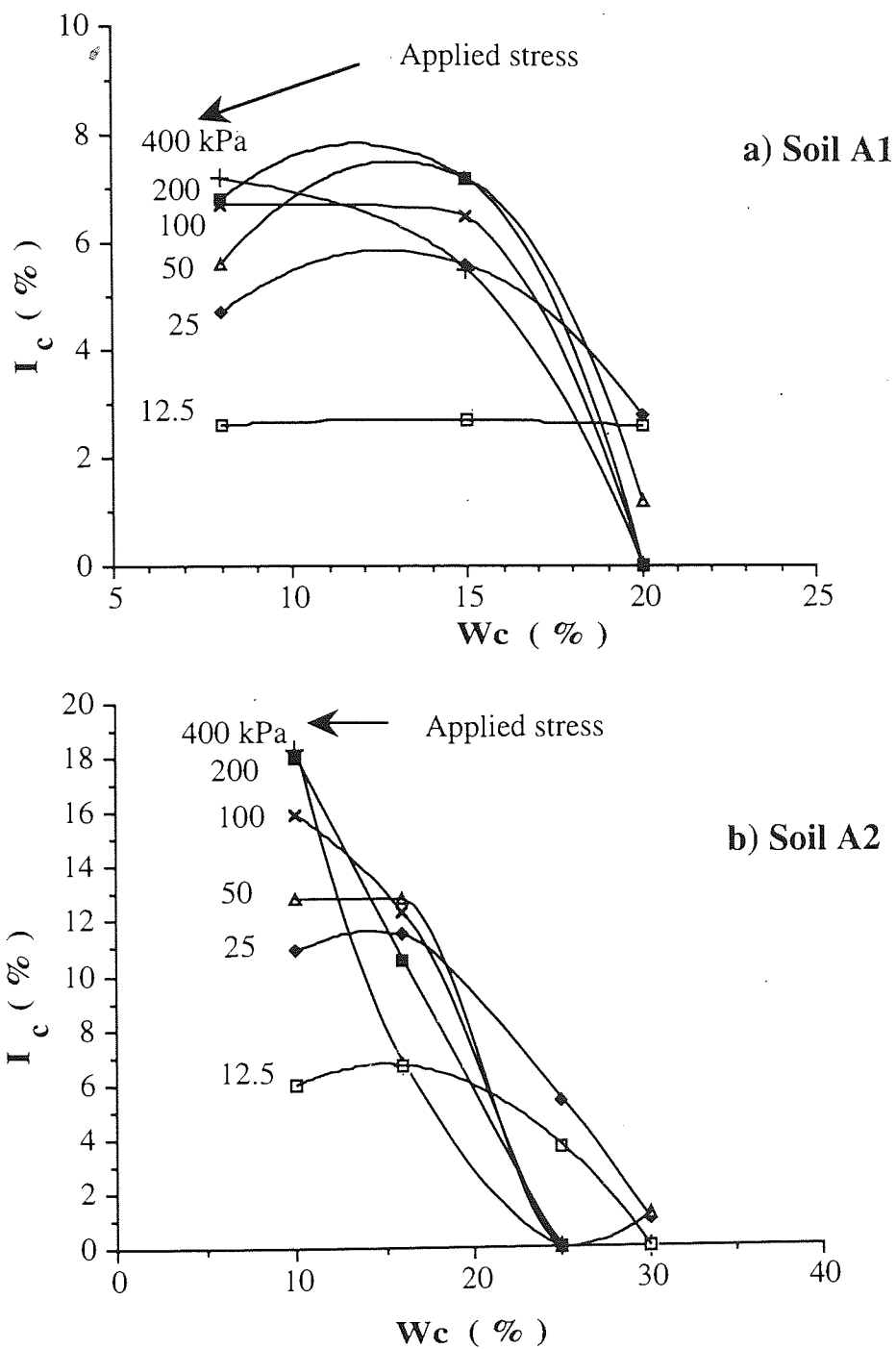
Fig. 7.6 : Collapsing potential-moisture content relationship
under different stresses for the destructured/compacted
soils at site I.
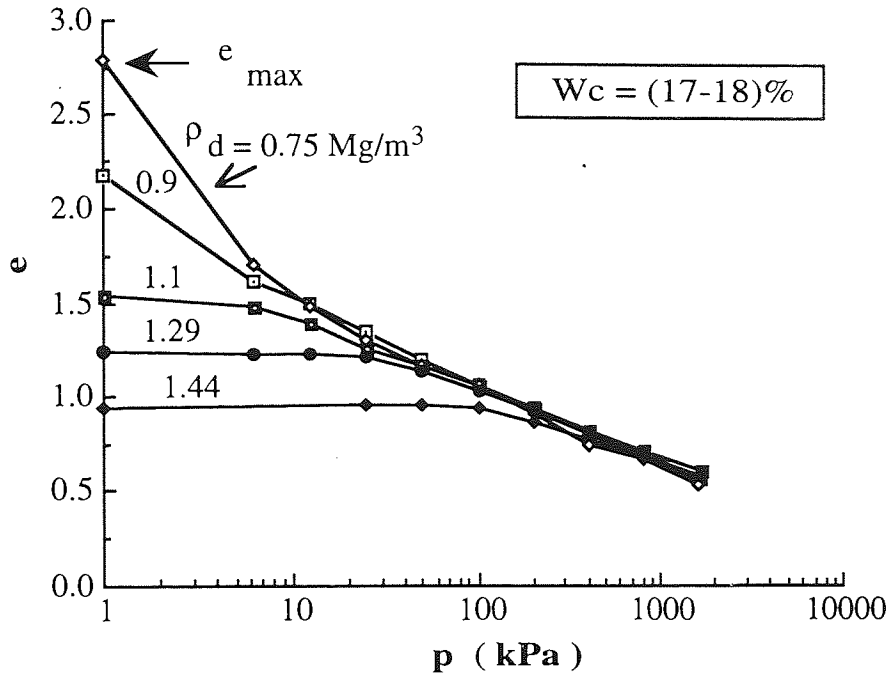
Fig. 7.7 : The compressibility of destructured/compacted samples of A2, tested at different initial dry densities.
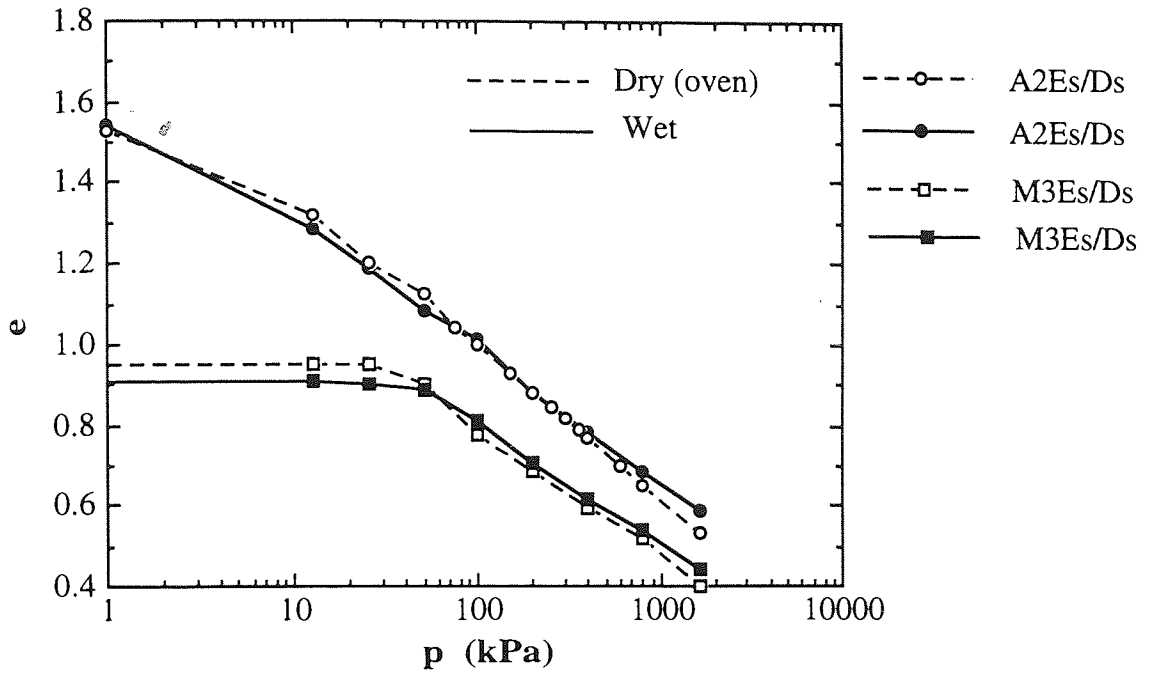
Fig. 7.8 : Oedometer results for the destructured samples prepared
from oven-dried and wet samples of both soils A2 and M3.
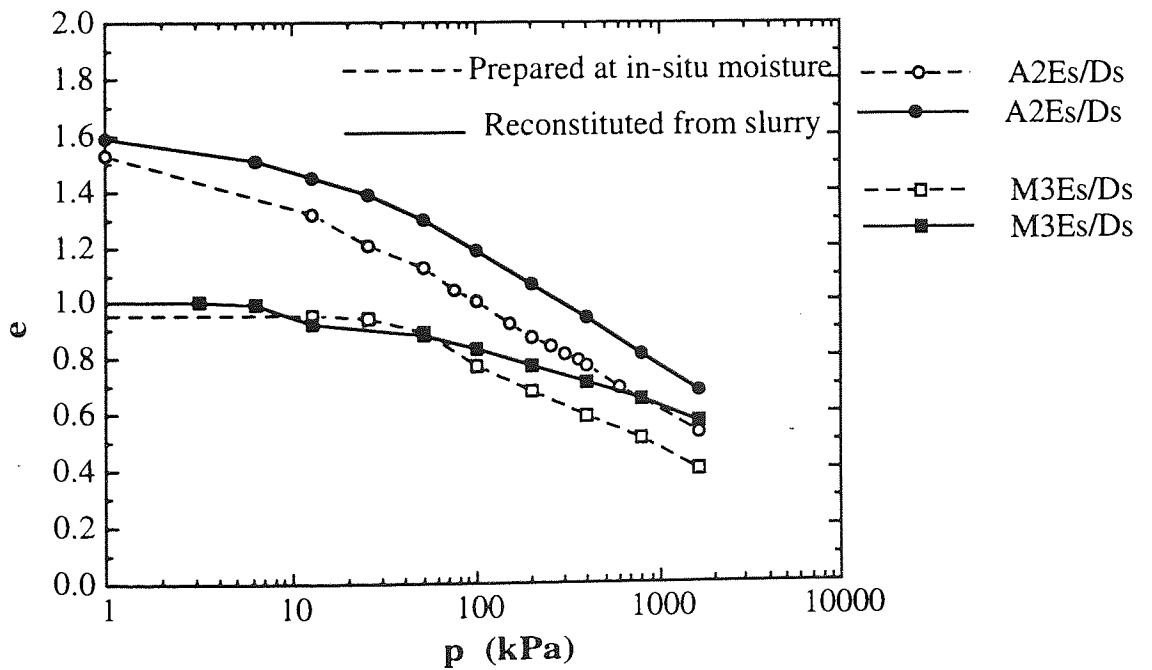
Fig. 7.9 : Oedometer results for the destructured samples prepared
from oven-dried samples at in-situ moisture contents and
from slurries for both soils A2 and M3.

Symbol	Moisture cont. in %	ρ_d in Mg/m³
◆	Wc=1.05LL	1.25
○	Wc=1.35LL	1.09
◇	Wc=1.4LL	1.08
■	Wc=1.44LL	1.04
□	Wc=1.6LL	0.98
▲	Wc=1.69LL	0.90
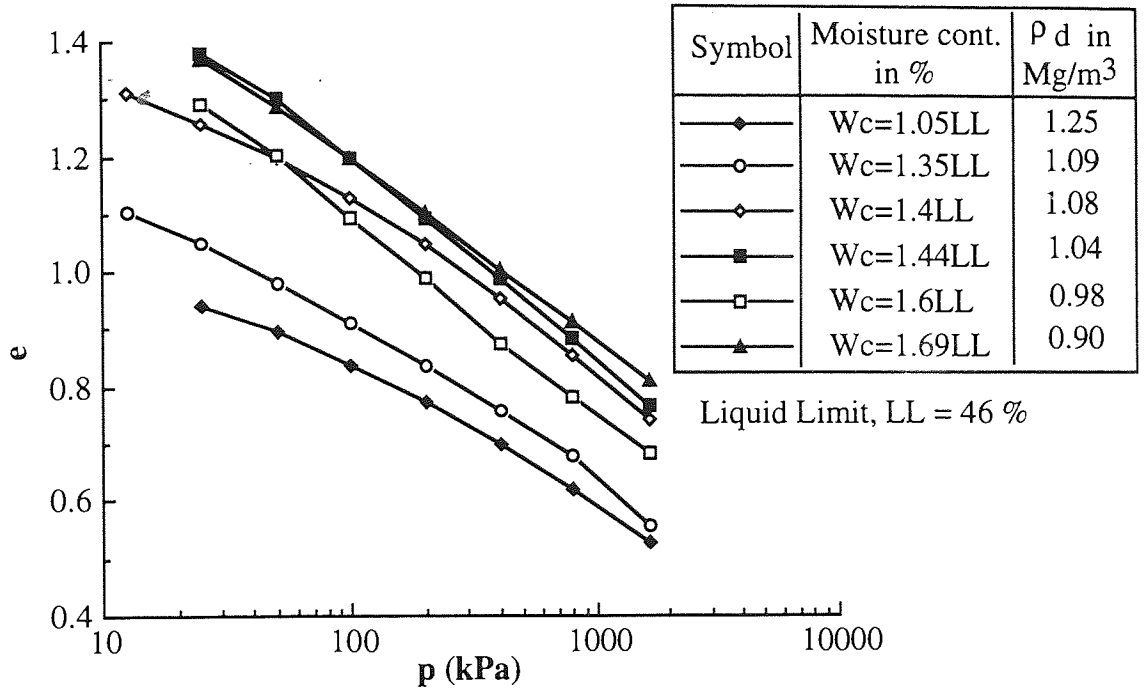
Liquid Limit, LL = 46 %

Fig. 7.10 : Oedometer results for reconstituted samples of M2 prepared at different moisture contents, proportional to the liquid limit, and different dry densities.

$W_n = 25\%$, $\rho_d = 1.10$ Mg/m³

Wet at W_n
Wet at W_n
Air-dried
Air-dried
Oven-dried
Oven-dried
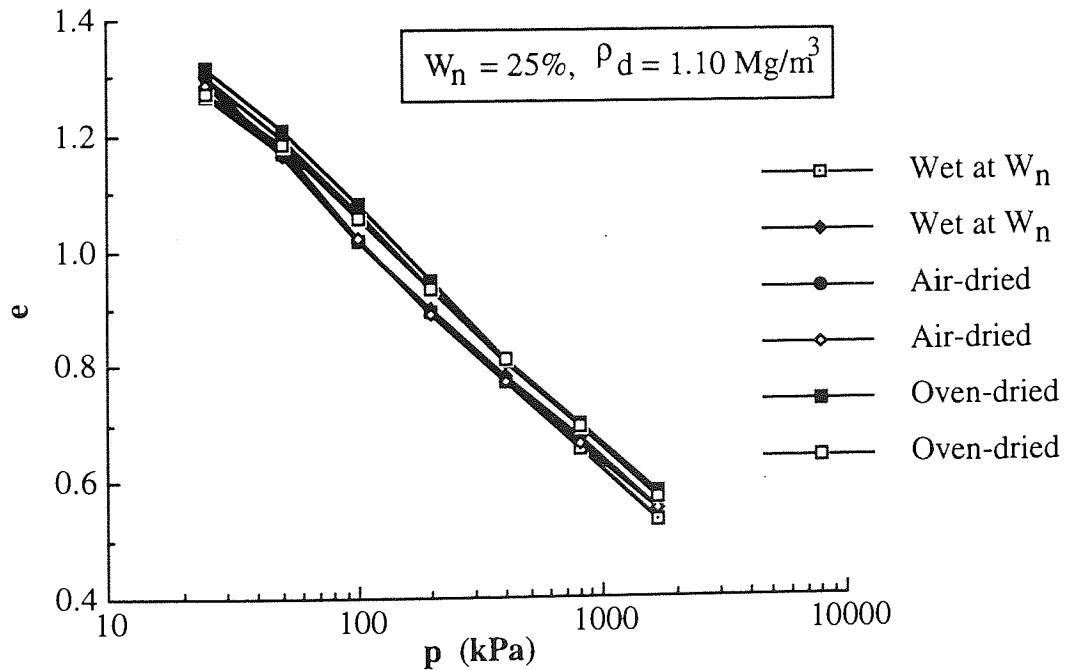
Fig. 7.11 : The effect of sample preparation at different moisture conditions on the oedometer behaviour of the destructured/compacted soil, M2.

292
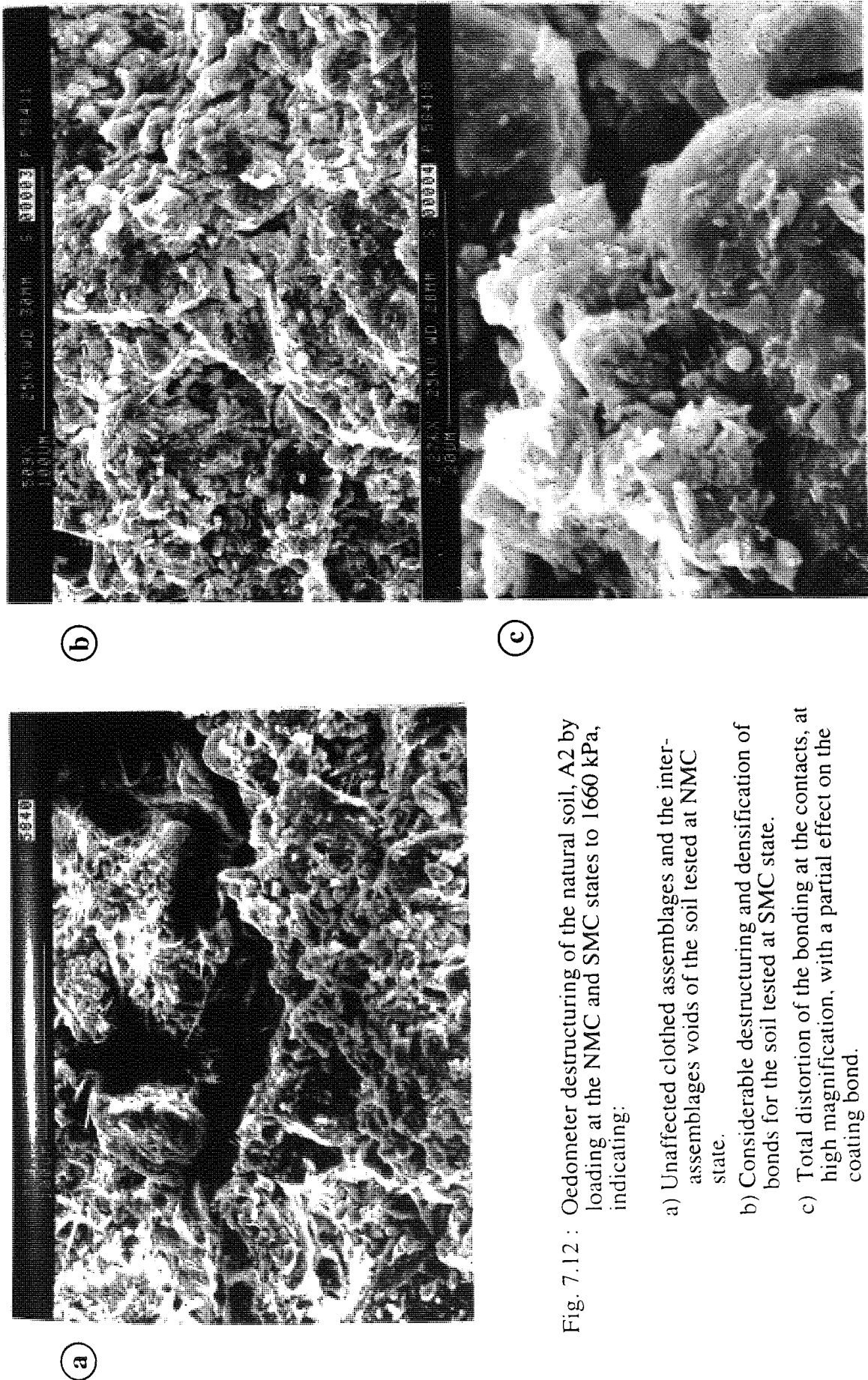
Fig. 7.12 : Oedometer destructuring of the natural soil, A2 by loading at the NMC and SMC states to 1660 kPa, indicating:

a) Unaffected clothed assemblages and the inter-assemblages voids of the soil tested at NMC state.

b) Considerable destructuring and densification of bonds for the soil tested at SMC state.

c) Total distortion of the bonding at the contacts, at high magnification, with a partial effect on the coating bond.
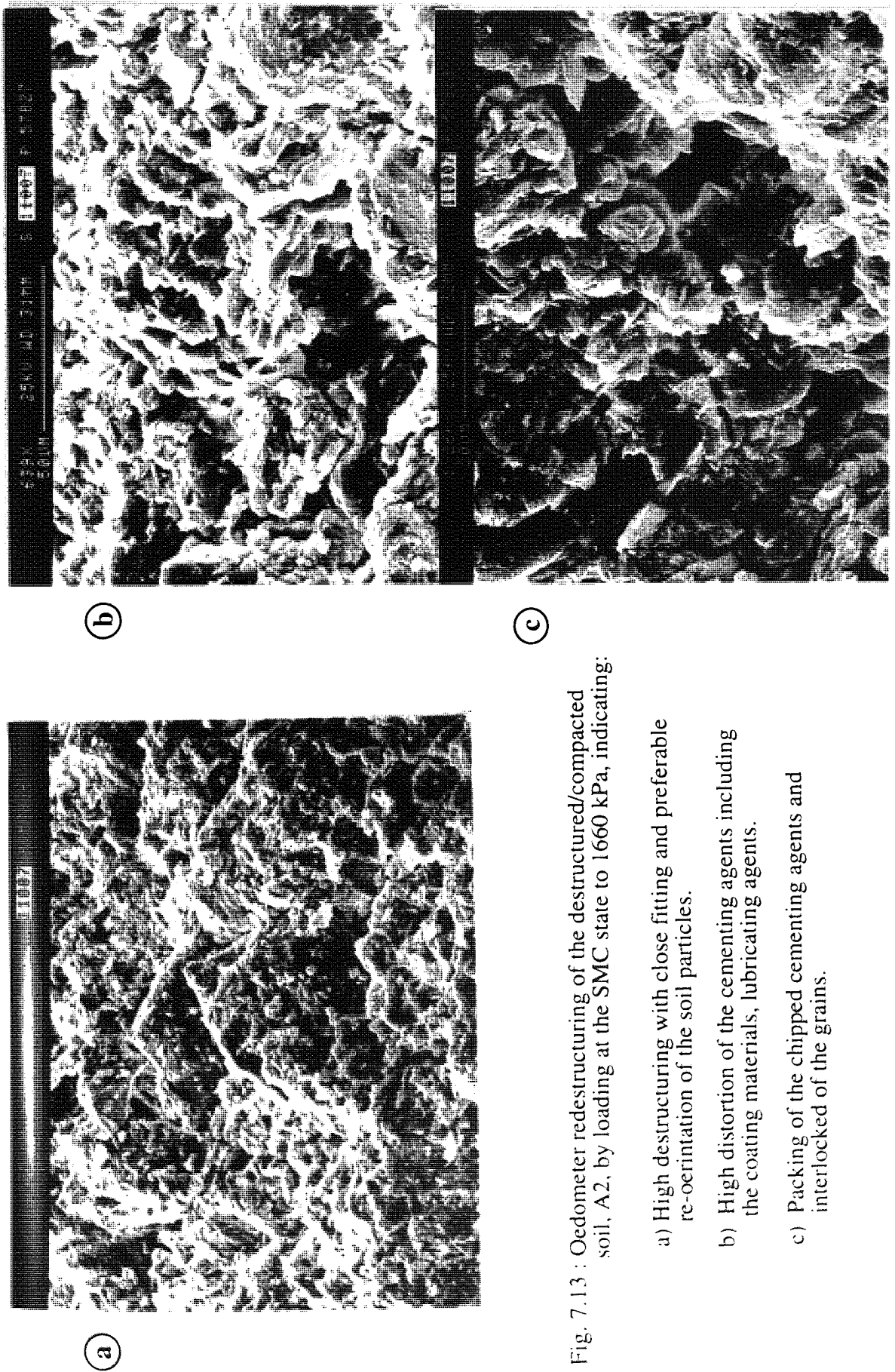
Fig. 7.13 : Oedometer redestructuring of the destructured/compacted soil, A2, by loading at the SMC state to 1660 kPa, indicating:

a) High destructuring with close fitting and preferable re-oerintation of the soil particles.

b) High distortion of the cementing agents including the coating materials, lubricating agents.

c) Packing of the chipped cementing agents and interlocked of the grains.

CHAPTER 8

THE FRAMEWORK FOR THE DEFORMATION BEHAVIOUR OF THE COLLAPSING AND DESTRUCTURED SOILS

8.1   INTRODUCTION

In studying the deformation behaviour of structured, or collapsing, soils in either the remoulded/destructured or natural state, many investigators have established conceptual and mathematical models to provide frameworks for describing such behaviour. The most common frameworks for the collapsing soils (Jennings and Knight, 1975; Houston et al 1988; ATSM, 1992) were presented in detail in Chapter 2 together with others developed for structured soils (Vargas, 1953; Leroueil et al 1979; Maccarini, 1987; Bressani, 1990). Pandian et al (1990) established a generalized parameter for analyzing the shear strength and compressibility of tropical, uncemented, partially saturated soils, by relating them to the void ratio and the degree of saturation. Burland (1990) introduced the term "intrinsic" to describe the behaviour of reconstituted soils from which the effect of the structure and bonding have been removed. He showed that a unique normalized intrinsic compression curve, in the void ratio-log p' space, exists for widely varying clays, and referred to this as the "intrinsic compression line" (ICL). Natural soils having a bonded structure usually exist above or on the ICL. Den Haan (1993) developed a generalized power formulation which described the virgin compression of a wide range of soils, including granular soils, remoulded and reconstituted clays and naturally cemented clays. Similar frameworks and models, using different approaches, have been reported to describe the behaviour of cemented structured and destructured soils (Vaughan et al, 1988; Nagaraj, 1990; Coop and Atkinson, 1993).

However, despite the availability of several frameworks to describe the individual behaviour of collapsing and destructured soils, the link between them has not been established. Consequently there is interest in combining the collapsing and destructuring criteria to develop a generalized framework which both represents and satisfies the general definition of the bonded structure, by involving the cementation (cementing agents, chemical, clay) and apparent (suction or capillary tension) bonds at both the natural and soaked moisture conditions. To undertake this task, the approach presented by Vaughan et al (1988) has been adopted and developed in an attempt to provide a generalized framework to account for the deformation and collapsing behaviour of these soils. This has involved the development of a generalized laboratory framework for the particular soils, with their collapsing and destructuring mechanisms being described in terms of the established framework. All the

established frameworks have been developed from laboratory results and so their applicability to field situations has yet to be demonstrated. Consequently examples are presented to demonstrate how the proposed laboratory framework can be used to assess the response of the soil to field treatment and destructuring, together with the limitations on its applicability.

8.2 PARTICULAR FRAMEWORK

8.2.1 Laboratory Framework Approach

Vaughan et al (1988) presented a laboratory framework to describe the deformation behaviour of structured and destructured soils which described appropriate zones for structured and destructured soils (see Fig. 2.17). This approach considered the upper consolidation curve of the soaked, structured soil, as the upper boundary in the void ratio-log p space, while the lower boundary was provided by testing a destructured, reconstituted specimen, starting from a high void ratio in the slurry state. However, in the modified framework the following approaches were adopted:

(1) The lower boundary limit is provided by the deformation curve obtained by re-testing the soil at the soaked condition after destructuring and compacting it to the original dry density (same initial void ratio) at the natural moisture content. Consequently, the variations in the degree of saturation during testing and the initial conditions of the specimens (structured and destructured) were minimised if not eliminated. In addition, the possibility of bonding, due to the high moisture state and very low stresses in the slurry sample (Mitchell, 1976; Mitchell and Solymar, 1983; Nagaraj et al, 1990), did not exist and so the destructured state along and below this limit was represented in the most extreme condition.

(2) Testing the natural soil at the NMC was introduced to permit description of the collapsing of the natural soil.

This modified approach attempts to cover the general case for the deformation behaviour of bonded structured soil, involving both the open metastable structure (predominantly suction bond) of the collapsing soil and the structure (predominantly cementation bond) of the bonded soil, and the effects of variation in the moisture condition. Without the inclusion of all these effects, the framework terms would not have broad application. For instance some of the field treatments described in Chapter 6, even when combined with flooding, produced only partial destructuring due to the presence of a residual, capillary (suction) and cementation bond resistance. Such partial destructuring and residual bonding cannot be predicted from a laboratory framework which only considers the extreme condition associated with highly soaked soils with limited suction bond. Consequently, the

effects of suction have to be considered essentially similar to those of physical bonding (Leroueil and Vaughan, 1990) in defining the term structure in its general application to all structured soils.

8.2.2. Laboratory Framework for the Investigated Soils

The ideal framework should account for the deformation behaviour of both the intact and destructured soils at any expected moisture state. Such an ideal framework is suggested for future work in Chapter 9, this study has lead to the development of a simplified framework. However, due to the interference of the bonding forces involved in the interactions between both soil particles and water, it was not possible to precisely define the relations between the deformation trends of the natural and destructured soils in both the partially saturated and soaked states, particularly for the destructured soils in the partially saturated state (DC). The results indicate that volume changes due to soaking intact (Δe_c) and destructured (Δc_{ds}) soils were different and similarly those due to destructuring were different in samples at NMC (Δe_{dn}) and after soaking (Δe_d) as summarised in Fig. 8.1 (see G9-3, for further indication of these volume changes). These variations are probably related to variations in the nature of the bonding mechanisms. To investigate the interactions of the bonds, particularly for partially saturated soils, further work is required beyond the scope of this investigation.

Generally, by limiting the consideration to the deformation behaviour of the natural soils at the soaked and in situ conditions and the destructured soils at the soaked conditions, the collapsing potential, the destructuring potential and the degree of destructuring of the natural soils can be identified. The framework in the void ratio-log p space, at the simplest level, consists of two main regions, those of the stable structure and the metastable structure for specimens having the same initial void ratio (dry density). These two regions are separated by the deformation curve of the destructured soil tested at the SMC state (DS) as shown in Fig. 8.2. All saturated soils, having higher or the same dry density, without cementation bonds exist within the stable space below the DS curve, and they cannot be placed above the DS curve in the metastable space. In contrast, soils with a bonded structure exist in the metastable state, above the DS curve, and it has been suggested that their remoteness from this curve is related to the degree of bond (Vaughan et al, 1988; Leroueil and Vaughan, 1990). Within the metastable space an infinite number of deformation curves can be plotted according to the moisture content, degree of saturation, the type and degree of the bonds and the degree of destructuring. When changes in the (initial) dry density are added to these variations, the framework becomes even more complicated. However, from the previous analysis for a given soil at the same initial dry density, three curves are sufficient to define the limits and scope of the framework. These are the deformation curves for the intact natural soil tested at the NMC state (NN), the intact natural soil tested at the SMC state (NS)

and the destructured soil tested at the SMC state (DS). The horizontal line passing through the initial in situ void ratio is used as an upper limit in the metastable state to simulate the soil at rest or at in situ conditions with zero collapse deformation (OCD). This general framework is illustrated in Fig. 8.2, while Fig. 8.3 shows the particular frameworks for the soils at site I, the sandy silt to silty sand (A1) and the silt with sand (A2), with those for the soils at site III, M2 and M3, being given in Appendix F8-1. The associated soil structures for A2 in the intact (OCD) and oedometer destructured (ending points of the curves NN, NS and DS) states are shown in Fig. 8.4. The deformation curve for the D/C soil at the CMC state (DC), shown by the dotted line in Fig. 8.3, is not a part of the developed framework although its function will be discussed later. The developed framework is termed the Collapsing-Destructuring Framework and is referred to as the CDFW.

Three main zones can be identified within the e-log p space in Fig. 8.2. The unstable space covers two zones, a collapse zone (between OCD and NS), where the capillary or suction bond is the critical bonding force (total collapsing potential, I_T, zone), and a destructured or cemented structure zone (between NS and DS), where cementation and particle arrangement dominate the bonding (destructuring potential zone). However, the NN limit can be considered as a sub-limit in this zone, by which both the collapse due to loading and that due to wetting are distinguished within the collapse zone, zone 2. The third zone lies below the DS curve and is the fully destructured zone, third zone, which represents the stable structure space. In fact, the overall collapse zone involves both the domain of the collapsing potential, I_L, due to loading alone (between the OCD and the NN lines) and the domain of the collapsing potential, I_c, due to wetting under loads (between the NN and NS lines). As demonstrated in Chapter 5, the summation of the collapsing potential due to wetting, I_c, and that due to loading, I_L, defines the total collapse potential, I_T. Generally, the partial loss of bonds shifts the particular deformation curve, NN or NS, towards the DS line in proportion to the loss of bonding associated with particle rearrangement until the curves coincide when all the bonding has been eliminated and the most preferable particle arrangement has been achieved. The loss of bonding due to both wetting and loading, expressed in terms of the vertical volume reduction between the OCD and NS states (Σe_c), defines the collapsing deformation of the natural soils due to both loading and wetting. In contrast, the volume reductions, due to the loss of cementation bonds (i. e. repeated short-term events such as loading and reloading, earthquake), between the NS and DS states define the destructuring deformation (Δe_d). The summation of Σe_c and Δe_d defines the extreme volume reductions or the total deformation ($\Sigma \Delta e$) that the natural soil may exhibit under any events of loading and at any moisture states.

The variations of Σe_c, Δe_d and $\Sigma \Delta e$ with stress level are shown in Fig. 8.5 for the soils A1, A2, M2 and M3. Fig. 8.5(a) suggests an inverse relationship between the collapsing and destructuring deformations for the different soils. The collapse deformation

increased with the continuous increase in the stresses and the terminal values ranked the soils in the order A2, M2, A1 and M3. This order reflects the respective dry density values, 1.1, 1.1, 1.25 and 1.45 Mg/m^3, of these soils. The soils A2 and M2 exhibited very similar behaviour as they have the same dry density, 1.1 Mg/m^3, and it is suggested that there is a correlation between the collapse deformation and the initial dry density, so that the lower the dry density the greater the collapse deformation. While the destructuring deformation increased with stresses up to 50, 75, 100 and 200 kPa for the soils A1, A2, M2 and M3 respectively, with further increase in stress these deformations decreased. The existence of a correlation between the destructuring deformation and the initial dry density is not apparent from the results in Fig. 8.5(a). The stresses, at which the destructuring deformation trends started to change, represent the stress levels at which the cementation bonds started to fail and are comparable to the respective yield stresses shown in Table 5.4 in Chapter 5, namely 50, 70, 82 and 160 kPa. Indeed as the stress level increases beyond the yield stress, the destructuring deformation decreases until it reaches zero when the NS curve coincides with the DS curve indicating the total loss of bonds, this represents the fully destructured state.

Fig. 8.5(b) shows the collapse deformation together with the total deformation for the different soils. It is clear that the total deformations ($\Sigma \Delta e$), for all the soils, exhibited a similar correlation with the dry density, to that of the collapsing deformation, with the $\Sigma \Delta e$ values being arranged in descending order for the soils M2, A2, A1 and M3. It is suggested that these curves could be used to predict the collapse under both wetting and loading and also the total deformation under the extreme conditions of loading and at any moisture states. Although these predictions could be expected to be conservative, they may provide a safe value for the design criteria for long term stability especially for regions, such as the Sana'a area, where the risk of carelessness, low labour skills, lack of design specifications and unpredictable events are high. Before using these curves to estimate the deformations, it would be necessary to establish the extent of underlying soil that would be affected under the particular design stress.

8.3. COLLAPSING AND DESTRUCTURING MECHANISMS

As a result of this study, analysis of the collapsing mechanisms in the natural and destructured/compacted (D/C) soils, including both collapse due to loading alone at the natural moisture state and collapse upon loading and wetting, are presented for inclusion in the framework (CDFW). The mechanism for the loss of the suction and probably the weak chemical bonds was reviewed when considering collapsing soils in Chapter 2. However, the destructuring mechanism of the cementation bond in the natural soils has not been reviewed earlier, and so it is necessary to present details, including the progressive distortion of these

bonds and the resultant particle rearrangements as detected from the oedometer and SEM tests.

8.3.1 Collapsing Mechanism

Since the first recognition of the collapse phenomenon, great effort has been made to thoroughly understand the mechanism of collapse and the behaviour of collapsing soils. The task was difficult due to the widely differing origins of the soils, together with the complexity of the intergranular bonding mechanism. Many hypotheses have been suggested, as presented in Chapter 2, and they confirm that many factors are involved in the collapse process such as soil type, density, moisture content, plasticity, mineralogy, fabric and nature of grain to grain contact. In general, collapsing criteria are widely documented to be related to large reductions in the void ratio upon wetting, with or without loading. However, the studied soils are termed conditionally collapsing soils as loading is essential for wetting collapse and so the mechanisms of both collapse due to loading alone and that due to wetting under loads have to be considered for incorporation in the CDFW.

When the natural soil was moderately loaded at the relatively low natural moisture state, it compressed only slightly (elastic deformation, Burland (1965)) - within zone 1 between the OCD and NN states as shown in Fig. 8.2, possibly with no or relatively limited movement of the soil grains. With increasing the stress level, beyond 400 kPa, this movement slightly increased (Fig. 8.3) possibly due to the reduction of the bonding strength. At high stress level, 1660 kPa, the reduction of bonding strength may be due to partial loss of the clay bonding and distortion of cementation agents, although it is difficult to know how much is due to each. However, at this stress level, when the natural soil was wetted it collapsed to the same corresponding void ratio of the same soil soaked before testing and loaded to the same stress level, as indicated earlier in Fig. 7.1 (points X1 and X2). This suggests that when the natural soil is loaded at low moisture content up to a high stress level, it compresses slightly as a result of a considerable distortion of the cementation bond at grains and assemblages contacts and, possibly, a limited loss of the suction bond, due to the limited relative movements of the soil grains (as shown in Fig. 8.4(b)) associated with slight increase in the degree of saturation . With wetting, the residual suction bond is lost and the frictional resistance at contacts is reduced and so further volume reduction or collapse occurs leading to close packing of the grains possibly with further distortion of the cementation and clay bonds as shown in Fig. 8.4(c).

When the natural soil was allowed free access to water, soaking or wetting, under loads the bonding forces (suction, clay and cementation bonds) that provided the stability of the soil structure were reduced. This reduction in the soil strength resulted either in swell or collapse of the soil structure according to the magnitude of the applied stress, initial moisture

content, density, clay contents, amount of the income water during wetting and mineralogy of the particular soil (Burland, 1965; Al-Alfi, 1984). The interference between the effects of these factors makes prediction of the volume change difficult.

Soaking the intact soil at a stress which cannot be resisted by the residual bonding strength, results in a partial destructuring due to a partial loss of the bonding forces, leading to a reduction in the void ratio from point Y1 on the NN line to Y2 on the NS line as shown in Fig.8.3 (a), while some residual cementation bonds exist within the soil matrix as represented by the space between the NS and DS lines. This soaking stress, however, for the conditionally collapsing soils has to be greater than the yield stress of the intact soil at the SMC state, σ_y, for considerable collapse to take place (Popescu, 1986; Bell, 1992). At stresses slightly above this value, the collapse started to increase as the cementation bond began to rupture, initially at weakly bonded contacts, in addition to the loss of suction bond. With further increase in the stress level, extensive breakdown in the cementation bond took place leading to packing of the grains, as shown in Fig. 8.4(c), and further collapse occurred until the total destructured state was achieved when the NN and NS states reached the DS state. At a soaking stress lower than σ_y the natural soils exhibited a slight collapse (see Fig. 5.8 and Table 5.3) which is mainly due to the cementation bond sustaining the soil structure, despite the significant loss of suction bond. However, when the natural soils were wetted at zero stress in the oedometer cell, they exhibited a free swelling potential due to the relaxation of suction bond similar to that observed during field flooding. Indeed, swelling was observed when the soil M2 was soaked under 50 kPa, which was probably due to the high clay content (24%) of M2 and its low initial moisture content (18.5%), as indicated earlier in Table 5.3.

The collapsing mechanisms of the destructured/compacted soils (D/C) were expected to differ from those of the intact soils due to variations in the particle arrangement and the degree and type of bonding. For the D/C soil, prepared to the in situ moisture content and dry density, some suction was recaptured but the chemical cementation was lost (Houston and El-Ehwany, 1991), although some secondary or weak bonding could develop (Nagaraj et al, 1990; Mitchell and Solymar, 1983). The magnitude of the recaptured suction affects the deformation of the D/C soil at the compacted moisture content and it depends on the soil gradation and the degree of saturation with it being high in clay, less marked in silt and minimal with sandy soil, for the same degree of saturation (Walsh et al, 1987).

At the compacted moisture content (CMC), a relatively low moisture state, some of the soils such as A1 when destructured and compacted, deformed easily even under low stresses as shown in Fig. 8.3(a), and so its deformation curve, DC, did not lie between the NN and NS lines as shown by the dotted line in Fig. 8.3(a), as had been expected. In contrast, soils A2, M2 and M3 considerably resisted deformation at the CMC state and so their deformation curves lie between the NN and NS lines, as shown for A2 in Fig. 8.3(b). This is probably

due to variations in the recaptured suction bond which can probably be related to variations in the soil gradation, compacted moisture content, dry density and degree of saturation. However, the interference between the effects of these factors on the deformation resistance at 'the CMC state made the problem complex. However, the soil gradation seemed to have the predominant effect as shown by comparing the results of the different soils. Soil A1 has a higher coarse content and a lower fine content than the soils A2, M2, and M3. Its deformation curve (DC) was much closer to DS curve, due to the small difference in void ratios between the DC and DS states at a given stress, than those of A2, M2, and M3, despite of the lower moisture content, higher dry density and lower degree of saturation of A1 compared to those of A2 and M2. This suggests that the recaptured bond of the D/C soil A1 was significantly lower than that of the other soils with higher fine contents. The effect of increasing the fine content in increasing the deformation resistance has been recently reported by Coop and Atkinson (1993) and Huang and Airey (1994).

Generally, when the D/C soil was loaded at the in situ moisture content and dry density, it compressed slightly under low to moderate stresses but the collapse increased considerably with further increase in the stress. This collapse, due to loading, was greater than that of the natural soil, at the same conditions, and is simply due to the reduction of the bonding from the loss of the cementation bond. The recaptured suction provided the apparent strength of the D/C soils at the CMC state. The large collapse deformation of A1 due to loading was probably due to its weak bonding strength.

However, when the water was added under light stresses (< 25 kPa), the D/C soils exhibited slight swelling due to the relaxation of the suction bond. With the exception of the stiff sandy silt M3 which exhibited swelling even under a stress of 50 kPa, at stresses equal or greater than 25 kPa, the suction was lost and the soils exhibited rapid collapse. This suggest that the collapse of the D/C soils involved slipping and rolling of the soil grains over each other and even a distortion and crushing of the soil particles under high stresses as shown from the Figure 8.4(d). The rate of collapse was high at low to moderate stresses and decreased at high stresses. Generally, at low stresses, the D/C soils exhibited higher collapsing potential upon wetting under loading than the intact soils (Fig. 7.2), apart from the D/C soil A1, and this is again attributed to variations in soil gradation. Similar observations for the compacted soils have been reported by Basma and Tuncer (1992) who indicated that the collapse potential increased with increasing clay content relative to the sand content. For the D/C soils A1, A2, M2 and M3 the differences between the amounts of sand and clay (S-C), in per cent, were found to be 65, 2, - 14 and 8% respectively, and so, in the D/C condition, soil A1 would be expected to have a comparatively low collapsing potential due to its S-C value and this is in agreement with the earlier laboratory observations.

8.3.2 Destructuring Mechanism

The partial or total loss of the cementation bonds of an intact soil can occur through a gradual destructuring process so that loading in an oedometer test can produce destructuring leading to a partial or total removal of these bonds, although partial loss can also result from other factors such as sample disturbance (Houston and El-Ehawany, 1991), liquefaction, earthquake and cyclic loading (Holtz et al, 1986; Fleming and Duncan, 1990). The total loss of bond, or destructuring, is primarily achieved by mechanical modification and remoulding of the natural soil as presented in this study. Generally, the alteration of the cemented structure from the intact to the fully destructured state, passes through a series of partially destructured stages and this progressive distortion in the cementation bonds has been recognized by many investigators (Delage and Lefebvre, 1984; Clayton et al, 1992).

In this study, the destructuring of the natural structure at the SMC state has been investigated by subjecting the natural intact soils M2 (6 samples), A2 (6 samples) and A1(1 sample, for comparison only) to a series oedometer tests, including conventional testing to various stress levels and cyclic tests involving unloading and reloading. After each test, SEM samples were taken to study the progressive changes in the soil structure and the cementation bonds. To cover the proposed framework in Fig. 8.2 three samples of A2 and five samples of M2 were subjected to different stress levels along the soaked deformation curve (NS) and, for each soil type, one of the stress levels was selected just below the yield stress while the others were in excess of the yield value. Table 8.1 summarizes the initial properties, stress levels (P_L), yield stress for each specimen, the average value of the yield stress for each soil type and the range of cyclic loading for the various samples tested in this series.

Fig. 8.6 summarises the consolidation results for the five samples of M2, loaded to 100, 150, 200, 400 and 1660 kPa. The yield stress, σ_y, is in the range of 90 to 120 kPa with an average value of 110 kPa as shown in Fig. 8.6. The termination points for each of the five stress levels are shown as S1 to S5 in Fig. 8.6. The final deformation strain (ε_L) for each test is given in Table 8.1. For the sample consolidated at 100 kPa, just below the average σ_y, no significant changes were observed in the intact structure, as shown by the SEM results in Fig. 8.7 (a,c,e and g). This indicates that, at this stress level, no major breakdown was achieved in the cementation bonds, as would be expected with the applied stress being lower than the yield stress. The measured strain (ε_L) at this stress level was small, 1.9%, indicating only limited deformation with little scope for internal breakdown.

For the sample consolidated at 150 kPa, just above σ_y (S2 in Fig. 8.6), slight changes were observed in the soil structure, particularly around the large pores as shown in Fig. 8.7 (b,d,f and h). These images are placed adjacent to those for the sample consolidated at 100 kPa to enable comparison and to trace the progress of the distortion of the cementation

bonds. The measured strain (ε_L) was 4.8% (Table 8.1), indicating that some destructuring had occurred and, from the comparisons in Fig. 8.7, this can be identified, as follows:

1) When the soil was loaded to 150 kPa, distortion the cementation bonds can be seen to start at the large pores, i.e. rootlet and channels, by comparing Fig. 8.7(b) with 8.7(a).

2) This slight distortion developed to produce limited change in the soil structure in the vicinity of the affected pores, as can be seen by comparing Fig. 8.7(d) with 8.7(c). This is particularly emphasised at the contacts between the fine aggregations and the large particle grains as shown by comparing Fig. 8.7 (f) with 8.7 (e).

3) The micropores and the fine aggregations were not significantly affected at these stress levels as shown from Figs. 8.7 (g) and (h).

Increasing the stress beyond the yield value extended the deterioration structure and this was characterised by rapid change in the void ratios as shown in Fig. 8.6. At a stress of 200 kPa, Fig. 8.8 shows considerable structural collapse in both the large pores (Fig. 8.8 (a)) and the surrounding structure (Fig. 8.8 (b)) which directly contributed to the marked changes in the void ratio. However, no deterioration was observed of the fine cementation bonds at the connectors, present as buttress (Fig. 8.8 (c)) and bridge (Fig. 8.8 (d)) bonds. The large measured strain (ε_L) of 13.8 % is a further indication of the extensive collapse in the pore structure with the rapid increase from 4.8% at 150 kPa to 13.8% at 200 kPa indicating the sensitivity of destructuring to loads above the yield stress.

For the sample consolidated at 400 kPa, significant collapse was observed in the large pores, associated with the developing distortion of the clothed coating and bridge bonds as shown in Figs. 8.9 (a) and (b). Up to this stress level, most of the microstructural components, pores and aggregations, had not been significantly affected and so the destructuring was concentrated at the large pores, the arching structure around the affected pores and the weak bridge and cloth coating bonds. The large pores arose from residual channels or rootlet holes and trapped pores between the assemblages or aggregations. Progressive destructuring was reported by Delage and Lefebvre (1984) to start in the largest pores and, as consolidation proceeded, smaller and smaller pores became affected.

At the highest stress level, 1660 kPa, significant loss was observed in the cementation bonds. The large pores had extensively collapsed (8.9 (c)), with the bridge and buttress connectors and the coating bonds largely broken down (8.9 (d)), and so some of the cementation particles, micropores and even the fine aggregations started to suffer distortion and failure as shown in Figs. 8.9 (e) and (f). These fine aggregations and cementation particles were mainly composed of calcium carbonate (calcite) and were clay sized due to the weathering processes during deposition. Natural carbonate aggregations are weaker than the clay aggregations (Sheeler, 1968) and they significantly breakdown at high stresses (Coop,

1990). Indeed at 1660 kPa, they had broken down to produce smaller aggregations, with the existence of micropores in the distorted structure, as shown in Figs. 8.9 (e) and (f), and so some limited bonding structure was still present. Despite the high strain ($\varepsilon_L = 29.3\%$) at this stress level, full destructuring had not been achieved, and higher levels would be required to cause complete destructuring of the residual bonds so that the deformation shown by the destructured curve (DS) could be achieved. The SEM results for soil M2 are compatible with the trends of the consolidation curves from oedometer tests since the NS lines is above the DS line at the stress level of 1660 kPa, which can be demonstrated by superimposing Figure F8-1(a) and Figure 8.6. The differences in the void ratios between the NS and DS define the destructuring deformation (Δe_d), which has to be zero in case of complete destructuring.

Soil M2 suffered partial destructuring when loaded to 1660 kPa in the oedometer in the soaked moisture state. This included the collapse of the large pores, deterioration of the linking bonds at the connectors and between the assemblages, distortion of the clothing coating bonds, and some breakage of the cementation particles and aggregations with minor destructuring of the microfabric. Residual bonds were still present and higher stresses and further straining would be required to reach the fully destructured state. The progression in destructuring is in agreement with the observations reported by Delage and Lefebvre (1984) and Clayton et al (1992), apart from the slight distortion of the carbonate aggregations at the highest applied stress.

Similar results were observed when the silt with sand, A2, was similarly tested. The consolidation curves for these samples, at 75, 200 and 1660 kPa are shown in Appendix F8-2 and the initial properties and results are summarized in Table 8.1. The unaffected soil structure of the sample consolidated below the yield stress at 75 kPa is shown in F8-3 together, for comparison, with the slight to moderate destructuring of the cloth coating and bridge bonds at 200 kPa. The results for sample consolidated at 1660 kPa were presented in Figs. 7.12 and E7-4. Generally, the destructuring of this soil was similar to that of M2, with slight variations in the degree of destructuring at each specific stress level. It was slightly higher within the structure of soil A2 than that of M2, which can be related to variations in the bonding of those two soils. Soil M2 had a higher clay content (24%) and exhibited a greater average yield stress (110 kPa) than A2 with values of 16% and 95 kPa respectively, so destructuring by wetting and loading was slower in M2 than in A2, i.e. at a stress of 200 kPa the bridge bonds of A2 were ruptured (F8-3(d)) while those in M2 were not (Fig. 8.8(d)).

The repetition of short-term events can have a significant effect leading to progressive destructuring. Such events can involve cyclic loading by many agencies and, although the effect of each event on the progressive destructuring may be small, over hundreds or thousands of cycles the bonds in the soil may be extensively broken down if not totally destructured. It was decided to investigate such effects by cyclically loading and unloading natural samples from soils A2 (3 samples), M2(1) and A1 (1). The three samples of A2 were

subjected to cyclic oedometer loading between, 12.5 and 75, 12.5 and 200, and 50 and 400 kPa for, respectively, 7, 9 and 4 cycles, and typical results are shown in Fig. 8.10. The initial properties, the loading range, the number of cycles, the destructuring potential ($I_{d\ max}$ and I_d) and the ratio of $I_d / I_{d\ max}$ for all the samples are summarized in Table 8.1. Generally, cyclic loading increased the degree of destructuring by extending the breakdown of the bonds. This increase in the degree of destructuring has been interpreted and evaluated from the results of both the oedometer and the subsequent SEM tests.

The destructuring deformation, Δe_d and the destructuring potential, I_d, are introduced in this study. In this investigation, destructuring deformation is defined as 'the reduction in void ratio at a specific stress due to loss of the cementation bonds associated with particle rearrangement under the effect of short events' ; i. e. earthquake, liquefaction, cyclic loading to the given stress, and is similar in concept to the collapsing deformation, Δe_c. The reduction in the void ratio between the NN and NS states, shown in Fig. 8.2, is primarily due to the loss of capillary bonds and the weakening of the cementation bonds and relates to the collapsing deformation, while the reduction in the void ratio between the NS and DS states is primarily due to the loss of cementation bonds associated with particle rearrangement and so relates to the destructuring deformation. The destructuring potential, I_d, can be similarly defined as the collapsing potential, I_c. At a specific stress, the value of I_d is defined as:

$$I_d = [(e_1 - e_2) / (1 + e_0)] \ X \ 100 \quad \text{..............................(8.1)}$$

where, I_d :   The destructuring potential in (%), at a specific stress.

$e_1 - e_2$: Change in void ratio, at a specific stress, produced by short events effect as cyclic loading; where e_1 = void ratio on the NS line and e_2 = void ratio after the last cycle of the repeated loading on any destructured state, at the same stress of e_1.

e_0 :   Initial void ratio.

At any specific stress, the reduction in the void ratio between the NS and the lower limit DS state defines the total destructuring deformation Δe_d, total destructuring is achieved with the complete loss of bond leading to the most preferable arrangement of the soil particles under that stress, and so I_d becomes the maximum destructuring potential, $I_{d\ max}$.

The values of $I_{d\ max}$, I_d and the ratio of ($I_d / I_{d\ max}$) for A2, due to cyclic loading are illustrated in Fig. 8.10 for the upper limits, 75, 200 and 400 kPa. These values indicate that the degree of destructuring was limited when the maximum stress was lower than the yield stress, i.e. at 75 kPa the destructuring potential, I_d, after 7 cycles was 0.6%, representing only 3.9% of $I_{d\ max}$ at the same stress. In contrast, these values increased considerably when the cyclic stressing was greater than the yield stress. For a maximum cyclic stress of 200

kPa, Fig. 8.10 (b), the value of I_d was 2.3% being 17% of $I_{d\ max}$ at the same stress, and similarly at 400 kPa, these values became 4.0% and 26.5% respectively. Similar results were obtained from the other soils, A1 and M2, as illustrated by their I_d and $I_{d\ max}$ in Table 8.1.

Fig. 8.11 shows the SEM results for the sample of A2, A2/200-R, consolidated to 200 kPa and subjected to 9 cycles of loading between 12.5 and 200 kPa. This Figure indicates the extent of the deterioration in the clothing and bridge bonds compared with that observed within the same soil consolidated at 200 kPa without load repetitions (F8-3). The extent of this destructuring is compatible with the destructured potential, I_d, of 2.3% given in Fig. 8.10(b). Generally, cyclic loading had a considerable effect by extending the breakdown of the bonds associated with further particles packing and so increased the degree of destructuring, particularly at stresses beyond the yield stress. However, it is suggested that under the effects of the short event stresses at a specific stress, the particle packing and rearrangement contribute to the reduction in the void ratio together with that arising from the breakdown of bonds. It is difficult to predict how much of the reduction is related to each effect, although it can be seen from the trend of the reduction in the void ratio with increasing the cycles of the repeated loading as shown in Appendix F8-4 for the soils A2 and M2, subjected to cyclic loading up to 200 kPa.

8.4 ASSESSMENT OF FIELD TREATMENT USING THE LABORATORY FRAMEWORK (CDFW)

In Chapter 6, assessment of the field treatment was carried out directly by field testing - dry density and SPT data - and indirectly by using laboratory data from samples taken from the different treated locations. Some correlations were established by comparing the results from the treated soils with those of the same soils before treatment. In this section, the laboratory framework is examined as a technique for evaluating the field treatment as it has the advantage of including a lower boundary limit (DS) to which the degree of densification and destructuring can be precisely referred. For a specific soil, it involves most of the common states to which the soil can be subjected and so it can be used to evaluate or represent the likely behaviour of the soil. The following representative examples indicate its applicability and validity for such a task.

Fig. 8.12 shows the complete framework for soil A2, consisting of the family of compression curves for the natural soil, tested intact at the NMC and SMC conditions, and for the D/C samples tested both at a range of different moisture contents with a constant dry density (in situ density) and at a constant moisture content (in situ moisture) for different dry densities. These curves represent the laboratory compression results which can be used to

simulate the compression behaviour of the same soil in the field. Fig. 8.12 also includes the deformation curves of pounded samples from a depth of 3.0m at the location AD2, from the laboratory compression curves. These destructured field samples had an improved dry density of 1.36 Mg/m^3 (in situ dry density, ρ_d = 1.1 Mg/m^3) and plotted between the laboratory destructured samples with compacted dry densities of 1.24 and 1.45 Mg/m^3. The trend of these field samples was similar to those of the laboratory destructured samples, and they all converged towards a narrow band represented by destructured deformation curve (DS) which is represented by the dark circular symbols in Fig. 8.12. Indeed, the field improved samples in Fig. 8.12 start to converge towards the DS line at stresses lower than those of the densest laboratory sample (ρ_d = 1.45 Mg/m^3) but greater than those of the moderately dense laboratory sample (ρ_d = 1.24 Mg/m^3). A total destructuring and a significant densification had been achieved within these field samples (Fig. 8.12, light dotted lines), as their deformation relationships do not traverse across the DS line into the unstable space. Instead, they lie in the stable (destructured) space and join the DS line at stresses depending on the degree of destructuring and densification, as indicated by the in situ dry density of 1.36 Mg/m^3 and the corresponding relative increase (RI) of 23%.

These observations suggest that there may be some correlation between the dry density (void ratio) and the deformation behaviour below the DS line (stable structure space). In previous studies indexing, between the overburden pressures and the void ratios, has been suggested as a procedure to represent the behaviour of destructured soils (Vaughan et al, 1988). Further examples of this simulation above the DS line are given in Appendices F8-6(a) and (b) for the collapsing deformation of a sample from the pounded location AD0 at a depth of 3.0m, which indicates no improvement, and the compression deformation of two samples, at the TMC and SMC conditions, from the pounded location AD1 at 3.0m which indicate limited improvement. These results demonstrate that laboratory compression curves can be used to simulate and evaluate the deformation behaviour of the field treated soils. However, this method requires many samples to establish the family of curves which would increase the testing costs. In addition, considerable confusion arises from using such a framework as it has many curves.

An alternative approach is to use the deformation curves of the CDFW, namely the OCD line, the NN limit, the DS as a lower limit separating the stable and metastable spaces and the NS line. This last boundary acts as a limit to define the partial destructuring of the cementation bonds between the NS and DS lines, and that of the capillary bonds due to partial wetting and collapse between the NN and NS lines. By adopting these four limits in evaluating the field destructuring, the scope for confusion between the curves is reduced.

Fig. 8.13 shows this evaluation for the flooding location at MF, for soils M1, M2 and M3 at three different levels. It suggests that no destructuring of the cementation bond was achieved at any of the levels as demonstrated by the coincidence of the NS line and the

various curves for the soaked, treated samples shown as dotted lines with dark symbols. However, it is clear that the partial wetting produced by flooding led to a partial loss of the capillary bonds. This is demonstrated by the lateral shift of the curves for the field samples tested at the treated moisture content, shown as dotted lines with open symbols, towards the NS line (reducing the collapse potential due to wetting, I_c) and away from the NN line (increasing the collapse potential due to loading alone, I_L) in these graphs. The magnitude of this shift decreased with increasing depth below the flooded surface, demonstrating that flooding became less effective at greater depths. This partial wetting resulted in some weakening in the bonding agents causing an increase in I_L, a decrease in I_c and a reduction in the yield stresses of the treated soils compared to those of the intact soils at the NMC state. However, the curves of the treated samples at 3.0m (Fig. 8.13(c)) exhibit limited stiff behaviour which could be due to the fine leaching and particle migration, although there was also the possibility of sample variation, particularly for the soil at this level. The flooded soils were still located in the metastable region and so no considerable improvement or destructuring had been achieved, although there was a reduction in the I_c due to the partial wetting effect. Those results are compatible with those presented in Chapter 6, Section 6.2.

Fig. 8.14 shows another example of the method to evaluate the preloading treatment for soil G1, from site II. Fig. 8.14(a) shows the deformation trends, as dotted lines, for samples of this treated soil taken from the loaded surface which was 1.2m below the original ground surface (G.S.). One sample was tested at the treated moisture content (TMC) state, shown by the open circular symbol, while the other was tested at the soaked moisture (SMC) state, shown by the solid circular symbol. Both samples exhibited partial destructuring since their deformation trends crossed the DS limit into the semi-destructured zone (between the NS and DS). The difference between the trends of the two treated samples indicates the role of soaking which resulted in partial loss of the capillary suction and cementation bonds. The residual cementation bonds of the soaked sample were broken down with further loading to 800 kPa as shown by the change in its deformation trend which converged towards the DS line, unlike that of the sample tested at the TMC state.

The soaked sample exhibited stiff behaviour up to 100 kPa, between this value and 200 kPa its deformation curve was parallel to the DS line, after which it became steeper than the DS and at 500 kPa the two lines converged and continued together thereafter. Indeed, the increase in stiffness up to 100 kPa, the partial densification and destructuring and the residual cementation bonds which started to breakdown beyond 100 kPa are all compatible with the stress history (field loading) of this treated sample from 1.2m below the G.S.. At this level, the soil in the field was subjected to an applied net stress of $q_{net} = 136$ kPa which resulted in partial destructuring and densification. When the treated sample was reloaded in the laboratory to stress below 136 kPa, stiff behaviour was observed, but when the stress level exceeded 136 kPa (200 kPa) more deformation occurred with further breakdown in the

residual bonds, which demonstrates the compatibility between the field and laboratory results. The sample tested at the TMC state exhibited a reduction in stiffness and yield stress compared to the limit NN, established at the in situ moisture content, due to the effect of wetting. This indicates the increase in the collapse due to loading alone, despite of the decrease in both the collapse due to wetting and the total collapse deformation. Audric (1976) indicated that wetting, for partially saturated soils, reduced the yield stress and, as the moisture content increased and the clay content decreased, the yield stress decreased. Destructuring occurs after reaching the yield stress, and as increasing the moisture content decreased this value, it subsequently accelerated destructuring so, further wetting in the laboratory, resulted in a lower stiffness and yield stress and more destructuring occurred within the soaked treated sample than in that tested at the TMC state.

At 1.7m below the G.S. [0.5m below the loaded surface], no significant change was detected in the deformation behaviour, as shown in Fig. 8.14(b), apart from the limited effect of wetting on the sample at the TMC state. At this level a relative increase in the dry density (RI) of only 3% was achieved (see, Table 6.5) which may not have been sufficient to influence the deformation behaviour, particularly as this soil is characterised by a low content of fine material and very weak cementation bonds.

A further application of the CDFW is shown in Fig. 8.15 where it used to evaluate the field response to the roller compactor. At 0.8 to 0.9m below the ground surface [0.1 to 0.2m below the compacted surface], the soil experienced significant destructuring and densification, including particle crushing, causing a considerable displacement of the deformation curves as shown in Fig. 8.15(a). These indicate that total destructuring was achieved leading to a major improvement with a dense and very stiff soil produced immediately beneath the wheel of the roller. A significant degree of destructuring and improvement was also detected from the deformation curves for the samples taken 1.2 to 1.3m below the G.S. [0.5 to 0.6m below the compacted surface], as shown in Fig. 8.15(b). At this location the soil exhibited partial destructuring (a partial loss of the cementation bonds) with the residual bonds being destroyed by further loading as shown in Fig. 8.15(b), also shown are the increases in stiffness and yield stress due to the densification accompanying the destructuring. There are no differences between the curves for the samples from [0.5m] at the two moisture states, since preflooding had been part of the treatment at this location, AC2. However, a slight difference is apparent between the two curves for the top layer (Fig. 8.15(a)) and it suggested that this could be due to the loss in the moisture through evaporation during field testing and sampling which was less marked at greater depths. At 1.7m below the G.S. [1.0m] no effect was apparent as shown from the collapsing behaviour of this treated sample, as shown in Fig. 8.15(c) and, again, these results are compatible with those in Chapter 6 for this location.

The final examples are given in Figs. 8.16 and 8.17 and these relate to the deep compaction treatment at AD0 and AD1. At the first location the soil was compacted at the in

situ moisture content and the impacted surface was the natural ground where the top layer was a stiff lean clay (A0). In contrast, AD1 was preflooded for one day before the treatment and the compacted surface was 0.7m below the original G.S for soil A1. Due to the extensive layering system at site I and the need to ensure coverage of the expected depth of improvement, a more extensive framework was needed, covering soils A1, A2 and, possibly, A3, to evaluate the deformation behaviour and the degree of improvement of the treated soils.

There are some interesting points on Fig 8.16 that merit further consideration. The deformation curve for the compacted stiff lean clay, A0, at 0.7m below the G.S, plotted in Figure 8.16(a), is significantly displaced below the DS line thereby indicating significant destructuring and densification. However, this soil is different from the underlying sandy silt, A1, and so use of the framework for A1 is not appropriate as shown by the divergency of its deformation curve from the DS line for A1. This demonstrates the necessity of using the appropriate framework to evaluate each soil. Secondly, this stiff surface layer, A0, severely restricted the benefits of the treatment extending into the underlying soils as is shown in Figure 8.16(a) by the limited partial destructuring and the collapsing potential of soil A1 from 1.4m below G.S. [1.0m]. Thirdly, the treated soil at 2.4m below G.S. was within the transitional zone between soils A1 and A2 and its deformation curves shown in Fig. 8.16(b) almost coincide above the OCD and NS lines of the framework for A1, reflecting not only that the treatment had no effect at this level but also that there were some variations in the soil type. Fig. 8.16(b) was replotted together with the CDFW for soil A2, as shown in Appendix F8-7, to indicate the effect of the soil variations at the transition zone as will discussed subsequently. Finally, at 3.0m below G.S. [2.6m] no effects were detected as shown in Fig. 8.16(c) by the coincidence of the two parts of the collapsing deformation curve, that before wetting with the NN curve and that after wetting with the NS curve, indicating that the collapsing potential was the same before and after treatment.

The results of the second example of deep compaction, at AD1, exhibited a more consistence response to treatment as shown in Fig. 8.17. This indicates that the improvement extended to a depth beyond 3.0m below the G.S. [1.7m] as shown by the partial effect on the deformation and the collapsing behaviour in Figs. 8.17(b) and 8.17(c). At 1.6 and 2.1m [0.3 and 0.8m] a high degree of improvement was achieved as is evidence in Figure 8.17(a).

Generally, all these examples indicate the validity of using the developed collapsing and destructuring framework CDFW to evaluate the deformation behaviour, degrees of destructuring and improvement and the extent of the treatment in the soils. The results of this method are compatible with those obtained from the other methods presented in Chapter 6, with the advantages that it provides a general view of the deformation behaviour while recognising, and explaining, misleading results due to soil variation, sample disturbance, particularly at the transition zones.

8.5 FACTORS AFFECTING THE DEVELOPED FRAMEWORK AND ITS LIMITS

This framework is a tentative attempt to present, in the e-log p space, the deformation behaviour of collapsing and destructured soils in both the partially saturated and soaked states. Its accuracy in predicting the deformation behaviour may be affected by many factors, such as moisture content, type of test and loading system, the degree and manner of destructuring, layering system and homogeneity of the particularly soil. It is, therefore, necessary to consider the effect of these factors on the developed framework.

The deformation limit (NN) presents the behaviour of the natural soil at the in situ moisture content and so any variation in this moisture content affects the locus of this limit. A decrease in the moisture content below the in situ value will shift the NN line in the unstable structure space, towards the 0CD line, to reach a boundary limit when the moisture content is almost zero, dry state. Such a case seems unreal as soil with zero moisture content will give a very low dry density in the moisture content-dry density relationship and this will never exist in the field. As most of the work in this research has reflected field conditions, from the practical stand-point the in situ moisture content is considered to be the most appropriate moisture content for the upper limit as a practical guide-line. However the role of this moisture content has been investigated and Figure 8.18 shows the shift of the limit, NN, for the silty clay, M2, further into the unstable space towards the 0CD line when this in situ moisture content is reduced from 26% to 18%, and this is attributed to the more effective suction bond in the drier sample. This also produced a greater yield stress and higher collapsing potential I_c, despite the reduction in the collapse potential I_L (between 0CD and the new extended NN), for the sample with the lower moisture content. Generally, for a specific soil, it might be preferable to define the possible range of the in situ moisture content over the various seasons so that a range can be defined for the position of this upper limit.

Crawford (1964) and Holtz et al (1986) indicated that the rate of loading and the type and manner of testing can affect the configuration of the consolidation curve and the characteristics of deformation, i. e. the yield stress, the compression index and the collapsing and destructuring potentials. However, in this study the type of testing (oedometer consolidation and the isotropic compression tests) with the same loading system (constant ratio increment) produced some variations in the deformation results, as indicated earlier in Chapter 5 (Table 5.8 and Fig. 5.20). In contrast, variations in the loading system for the same type of test did not produce significant variations in the deformation trends as shown by the consolidation results for samples of the soil A2 in Fig. 8.19. Similar results were also obtained for the soil M2. Generally, the influence of the type of test on the deformation trend

of the studied soils was in agreement with the observations reported by Crawford (1964) and Holtz et al (1986), but the effects of the loading system did not show the same agreement.

Leroueil and Vaughan (1991) stated that "If the properties of the destructured soil are used as a reference framework to determine the contribution of structure to the behaviour of structured soil, the degree and manner of destructuring need to be selected with care". The degree and manner of destructuring clearly effect the locus of the destructured deformation curve, DS, which represents the boundary between the stable and metastable spaces and also provides the reference line for the destructuring potential. Consequently, defining the locus of this curve to a high degree of accuracy is of a great importance, since identification of both the degree of bond in the structured, intact soils and the degree of destructuring of destructured soils are based on the DS locus. The manner of destructuring, the type of material and the sample preparation were investigated in the section 7.2.3. In this study the most appropriate DS curve was established from destructured samples produced to the in situ void ratio (same in situ dry density) at the same moisture content, as this curve was found to provide the lowest boundary including those from slurry or reconstituted samples at the loosest state (maximum possible void ratio), as discussed in sub-section 7.2.3.3. It was considered that the development of any possible bond, due to any irreversible changes in a destructured slurry soil (Mitchell, 1976; Mitchell and Solymar, 1983; Nagaraj et al, 1990), would not be reflected in this lowest DS. Moreover, the field samples destructured by the various mechanical methods were found to converge to the DS curve as indicated in the previous section, which supports the reliability of using this curve to describe the deformation behaviour of the bonded structured and destructured soils. It can therefore be concluded that the degree and manner of destructuring adopted in this study were satisfactory and reliable for establishing the DS boundary in the particular framework for these soils. For other types of soil, the effects of such factors would need to be considered.

The interference of the different bonds effects (suction, clay and cementation) made the establishment of the ideal generalized framework more complicated as discussed earlier, particularly when the deformation curve of the D/C soil at the partially saturated state (DC) was included . The investigation of such task is beyond the scope of this study and was left for future work.

The Sana'a region is characterized by complex soil profiles with various soil layers. This variation, which was observed in both the vertical and horizontal directions, can restrict the applicability of any specific framework since it would require many individual models to match the number of soil layers, particularly when there is considerable variation in the soil characteristics at the transition layers. In this study, a separate framework was established for each soil type. Accuracy was achieved when the framework for a specific soil was used to describe the behaviour of the same soil, although some approximation could be involved in describing the behaviour of soils in the transition zone between layers, especially when the

variation in the soil type between the adjacent layers was significant and the thickness of these layers and the transitional zone was small. An example for the approximation and misleading evaluation of such case has been illustrated in Fig. 8.16(b), where the framework for A1 was used to evaluate the field destructuring by deep compaction at a depth of 2.4m. The soil at this level was transitional, between A1 and A2, and its intact consolidation trend is compared with that of A1 and A2 in Fig. 8.20. The soil at this level experienced some destructuring with some improvement being achieved by deep compaction, but this effect was not correctly reflected when the framework of the upper soil layer, A1, was used (Fig. 8.16(b)) and, of course, it is not logical to use the framework for the lower layer to evaluate upper soils unless they are the same. The data in Fig. 8.20 clearly show that the behaviour of the soil in the transition zone was between that of A1 and A2 so, for an accurate assessment, it would be necessary to establish a specific framework for this transition zone.

A further example of the wrong evaluation that could occur when the framework for a specific soil is used to evaluate another soil type is shown in Fig. 8.21. The framework for A1 was initially used to evaluate field destructuring by deep compaction at depths of 2.8 and 3.0m at AD2, although the soil at these depths is of the A2 type. Figure 8.21(a) shows the curve for the destructured samples extending into the metastable space of the framework of soil A1 which is impossible for the destructured soils. This implies that an evaluation using the A1 framework was not appropriate and, in contrast, a more appropriate evaluation became apparent when the framework for A2 was used as shown in Fig. 8.21(b). This clearly shows the destructuring behaviour and indicates that the evaluation depends on the selection of the correct framework, as was also shown for the A0 soil in Fig. 8.16(a). For a given soil layer, its homogenity can affect the reliability of the results, with homogeneous soils expected to provide the highest degree of accuracy. Variation of the soil within the same layer can result in a variation in the initial conditions (moisture content and void ratio) which may affect the deformation behaviour and hence the applicability to the framework of the particular soil. It is clear that the established framework for a particular soil should only be used to present and evaluate that soil. The normalizing of the different frameworks to a generalized unique framework is outside the scope of this study and it is suggested for future work.

Generally, it can be concluded that, using the laboratory framework method to evaluate the field treatment has given an improved explanation and correlation for the deformation behaviour and destructuring degree of the field treated soils compared to the methods discussed in Chapter 6. In addition, the uncertainty of predicting the stability of the treated soils using the previous methods, especially in the lower half of the influenced depth, can be overcome by using the CDFW. Moreover, the trend of the behaviour of the treated destructured soils can be predicted, while the deformation behaviour, including the collapsing and destructuring potentials, of the intact structured soils can be satisfactory presented and described with the CDFW.

Table 8.1 : Summary of the oedometer and Scanning Electronic Microscope results to identify the progression of destructuring.

Sample name	Depth (m)	Wn %	e₀	Type of loading	PL kPa	eL %	σy kPa	σy aver. kPa	range of cyclic loading kPa	No. of cycles	Id max %	Id %	Id / Id max	General features of the SEM results (effects on the cementation bonds)
M2/100	2.2	28.7	1.481	Conv.[a]	100	1.9	--		-	-	16.7	-	-	Softening and dilution
M2/150	2.2	27.0	1.518	Conv.	150	4.8	100		-	-	17.6	-	-	Limited collapse in the large pores and surrounding fabrics
M2/200	2.2	25.0	1.536	Conv.	200	13.8	130	110	-	-	12.0	-	-	Remarkable collapse in pores and the vicinity structure
M2/400	2.2	26.2	1.507	Conv.	400	16.0	125		-	-	12.9	-	-	Considerable destructuring included bridge connectors
M2/1660	2.2	24.6	1.543	Conv.	1660	29.3	105		-	-	13.6	-	-	Significant destructuring of coating, bridges buttresses, with slight at the aggregations and cemetation particles.
M2/200-R	2.2	25.5	1.508	Repe.[b]	200	12.5	105		12.5-200	7	14.9	2.4	0.161	
A2/75	3.0	21.9	1.525	Conv.	75	2.5	--		-	-	16.9	-	-	Softening and dilution of bonds
A2/200	3.0	18.0	1.52	Conv.	200	9.9	100		-	-	16.0	-	-	Slight collapse in large pores and coating and bridge bonds
A2/1660	3.0	17.4	1.52	Conv.	1660	34.7	65	95	-	-	5.0	-	-	Significant destructuring of coating, bridges buttresses, with considerable distress at cemen-ted particles and aggregations
A2/75-R	3.0	18.0	1.526	Repe.	75	3.1	--		12.5-75	7	14.5	0.6	0.039	No further effect at 75kPa for cyclic loading and re-loading
A2/200-R	3.0	17.3	1.52	Repe.	200	14.7	70		12.5-200	9	13.5	2.3	0.17	Extending the distortion of the clothed coating and bridge bonds
A2/400-R	3.0	21.5	1.464	Repe.	400	17.4	170		50-400	4	15.1	4.0	0.265	Further distortion at buttresses
A1/50-R	1.8	9.5	1.209	Repe.	50	6.6	~40		12.5-50	6	6.5	0.86	0.13	Considerable distortion in coating and bridge bonds

a- Conventional consolidation test   b- Repeated cyclic loading and unloading test
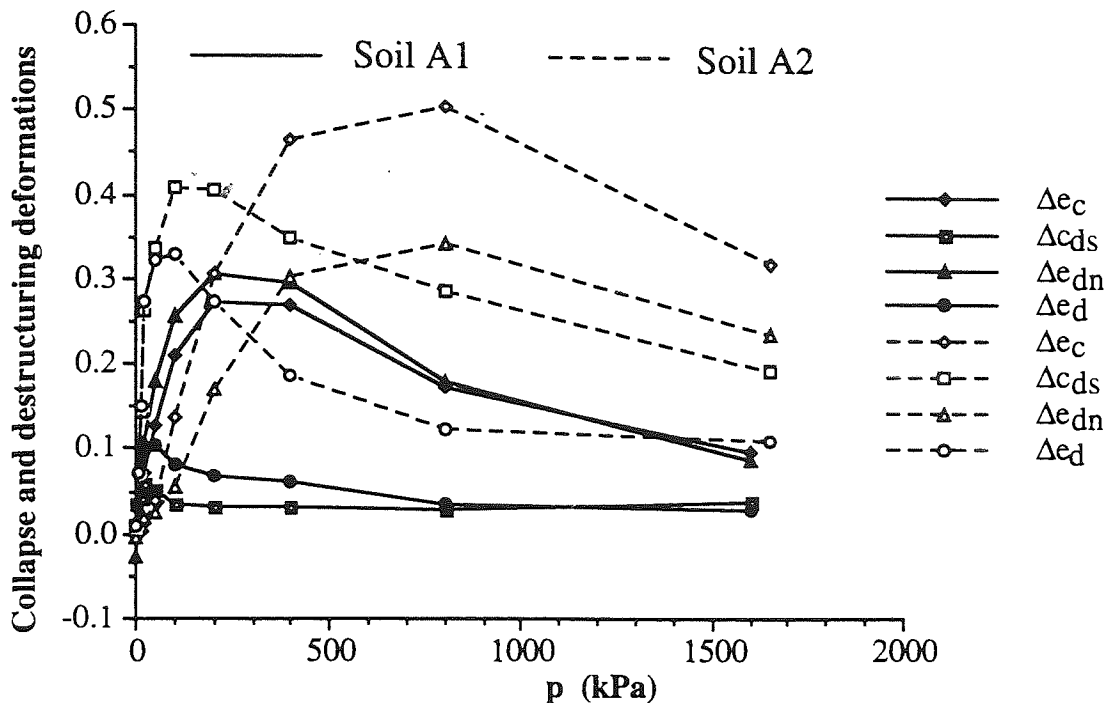
Fig. 8.1:Variation of the collapsing and destructuring deformation for the intact and D/C soils at both the saturated and partially saturated states.
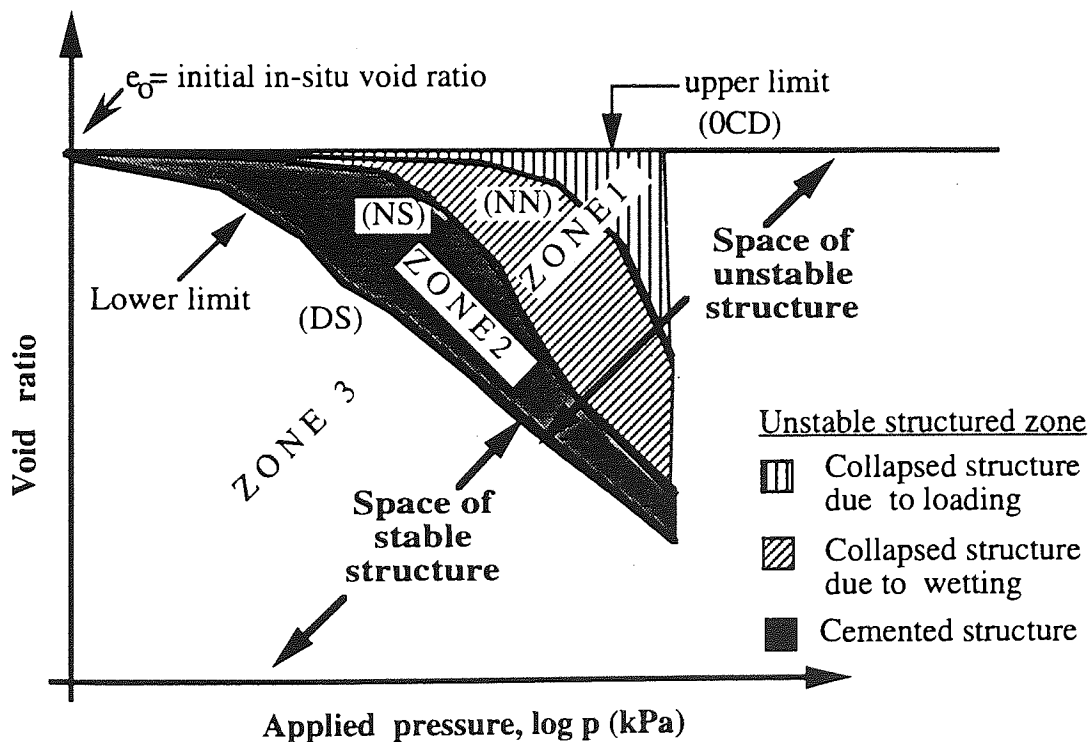
Fig. 8.2 : Developed laboratory framework for representing the deformation behaviour of the collapsing, structured and destructured, natural soils, with the four deformation boundaries defined as:
OCD : Intact unloaded at natural moisture content
NN : Natural loaded at natural moisture content
NS : Natural loaded at soaked moisture content
DS : Destructured loaded at soaked moisture content.
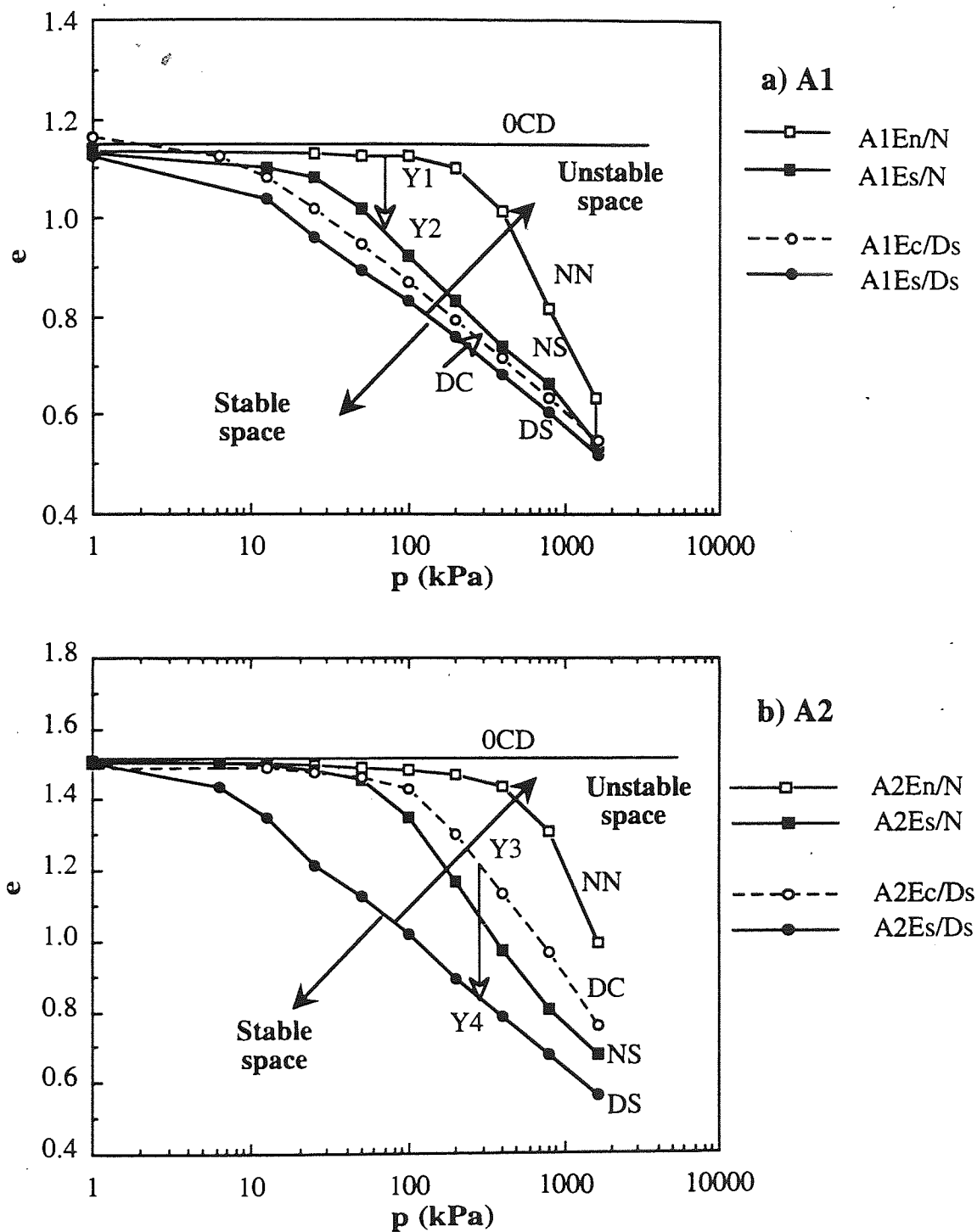
Fig. 8.3 : The deformation framework of the intact and destructured/
compacted (D/C) soils from site I, A1 and A2.

317
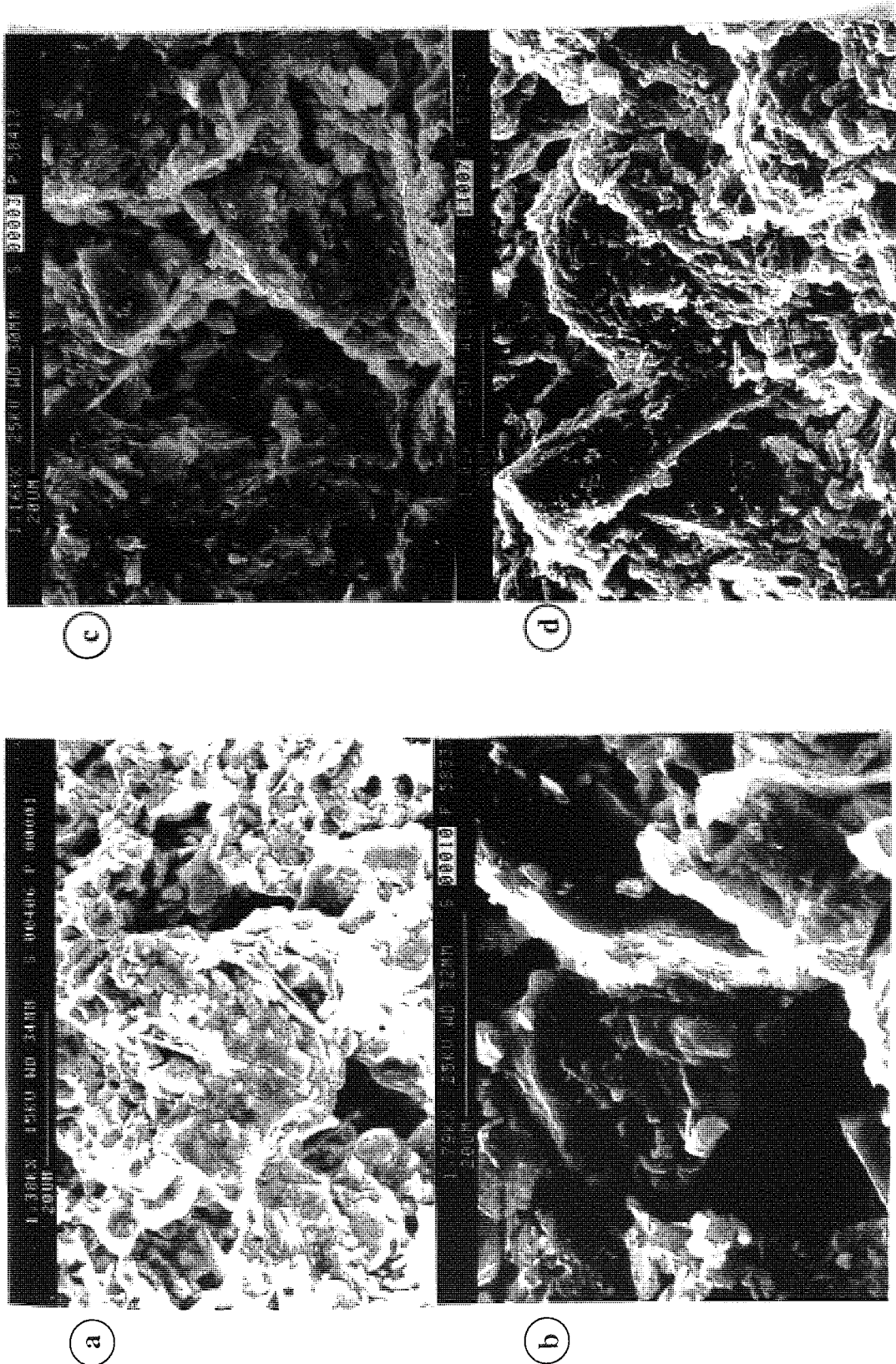
Fig. 8. 4 : Comparison of the A2 soil structure at the different states of the CDFW, showing; a) Intact structure (OCD), b) Limited distortion and grains packing by loading to 1660 kPa at NMC state (NN), c) Significant distortion and grains packing by loading to 1660 at SMC state (NS) and d) Total distortion of fines with grains slipping, rolling and dense packing of the D/C soil at 1660 kPa (DS).
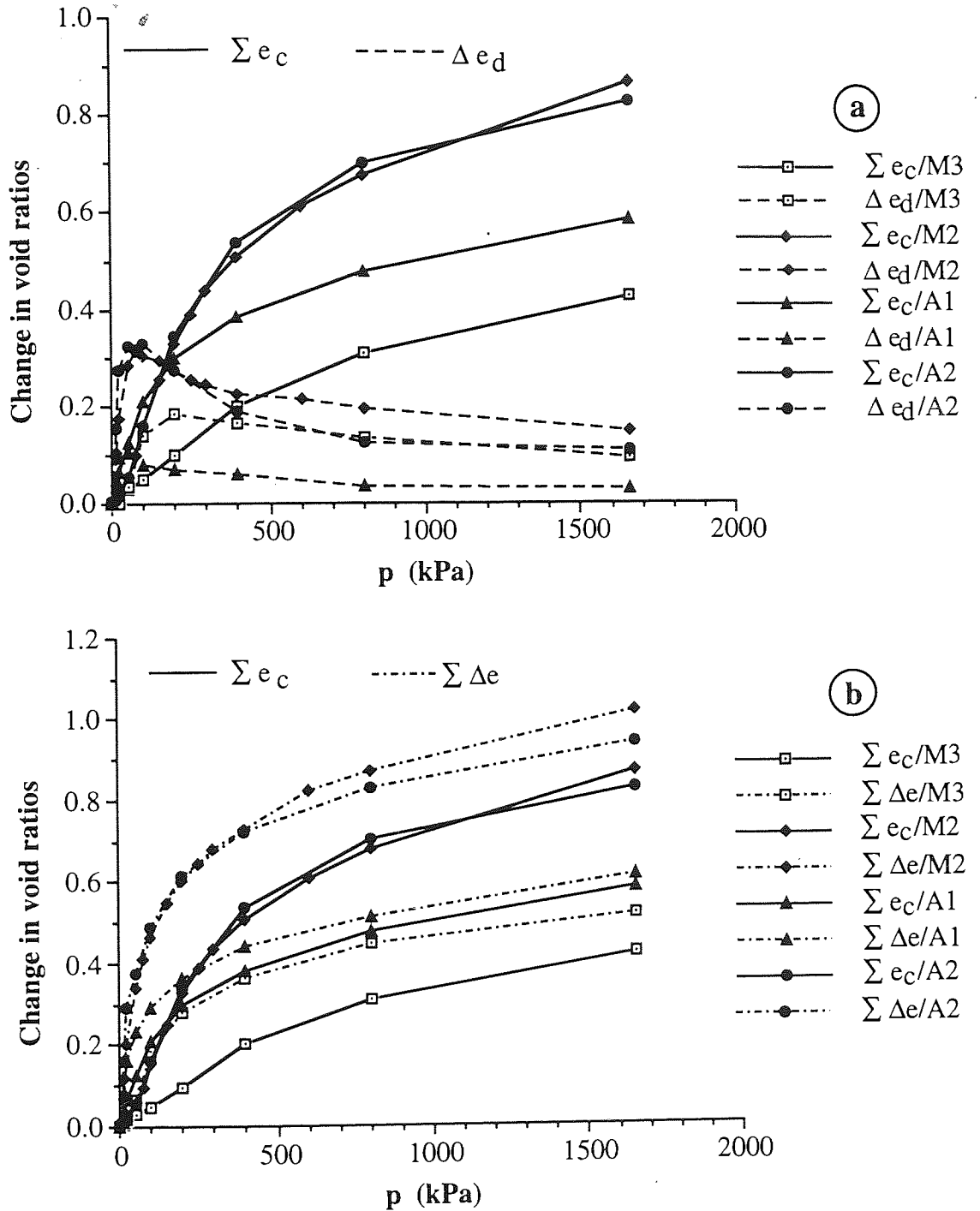
Fig. 8.5 : The changes in void ratios of the collapse, destructuring and total deformations with stresses for the different soils.
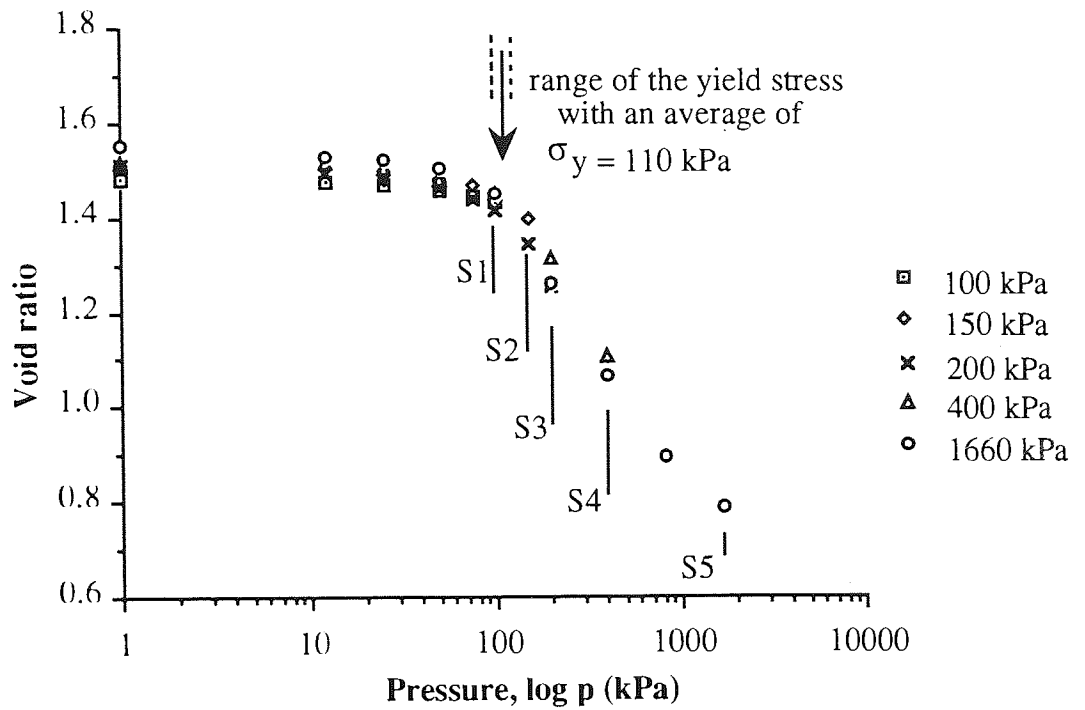
Fig. 8.6 : Consolidation curves of five samples of the silty clay soil, M2, up to 100, 150, 200, 400, and 1660 kPa.
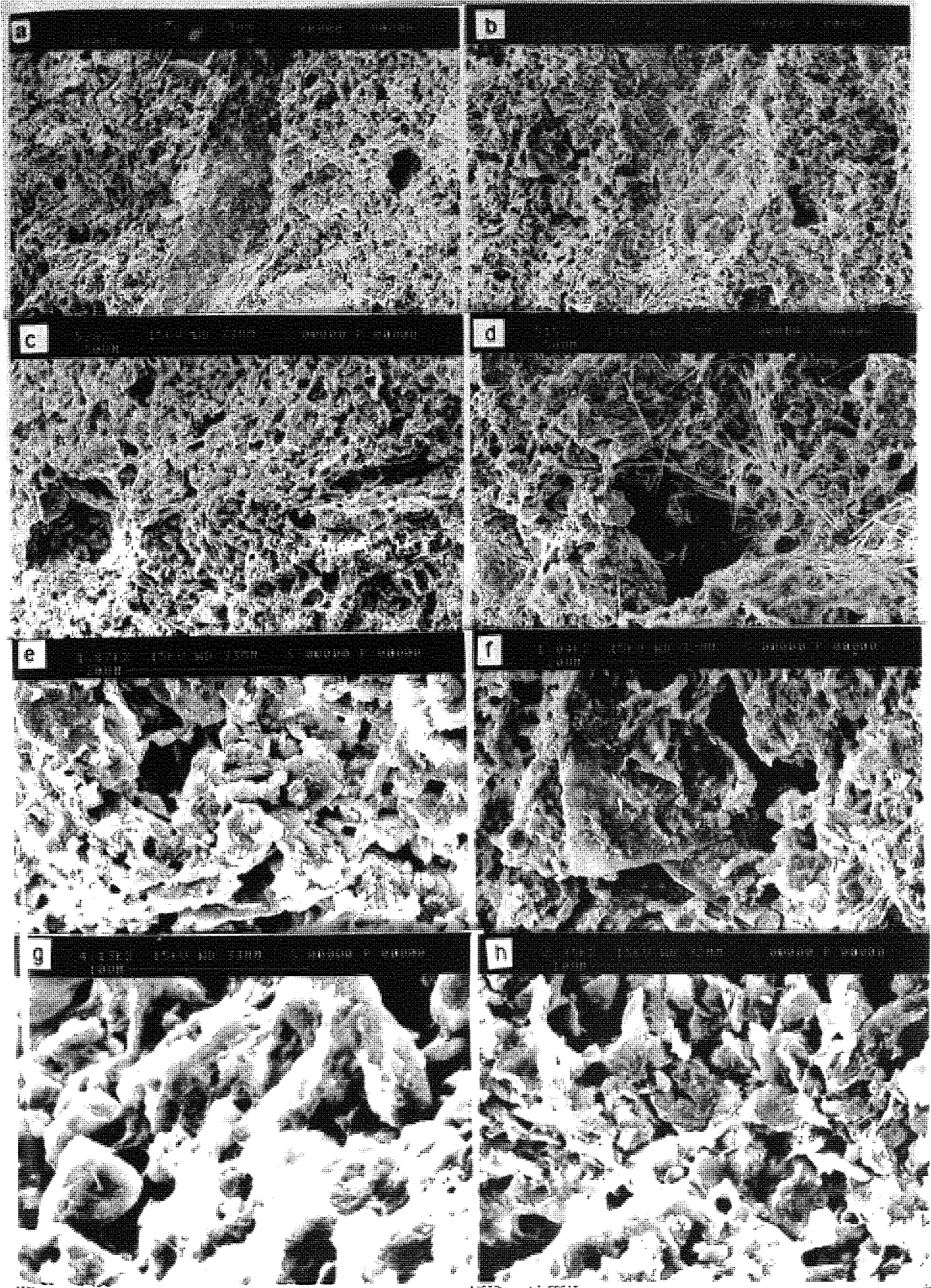
Fig. 8.7 : The progressive failure of the soil M2 in the oedometer at 100 (a, c, e, g) and 150 (b, d, f, h) kPa indicating failures at the pores (a, b), structures around the pores (c, d), assemblages and aggregations (e, f) and at microstructure (g, h).
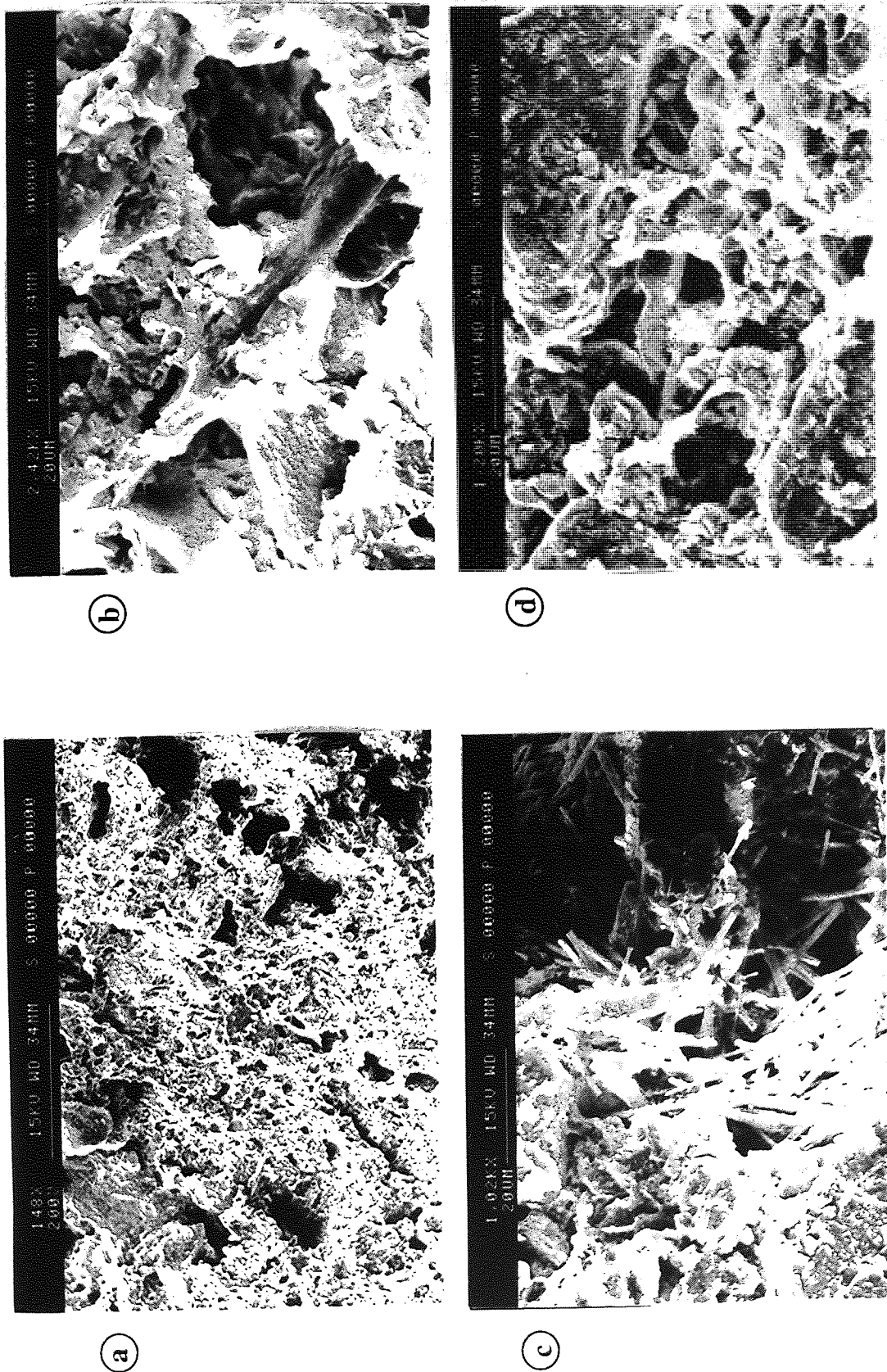
Fig. 8.8 : Progressive failure of M2 in the oedometer sample loaded to 200 kPa, showing ; a and b) considerable collapse of the large pores and the surrounding structure, c) no effect on the buttresses, and d) limited effect on the bridge connectors.
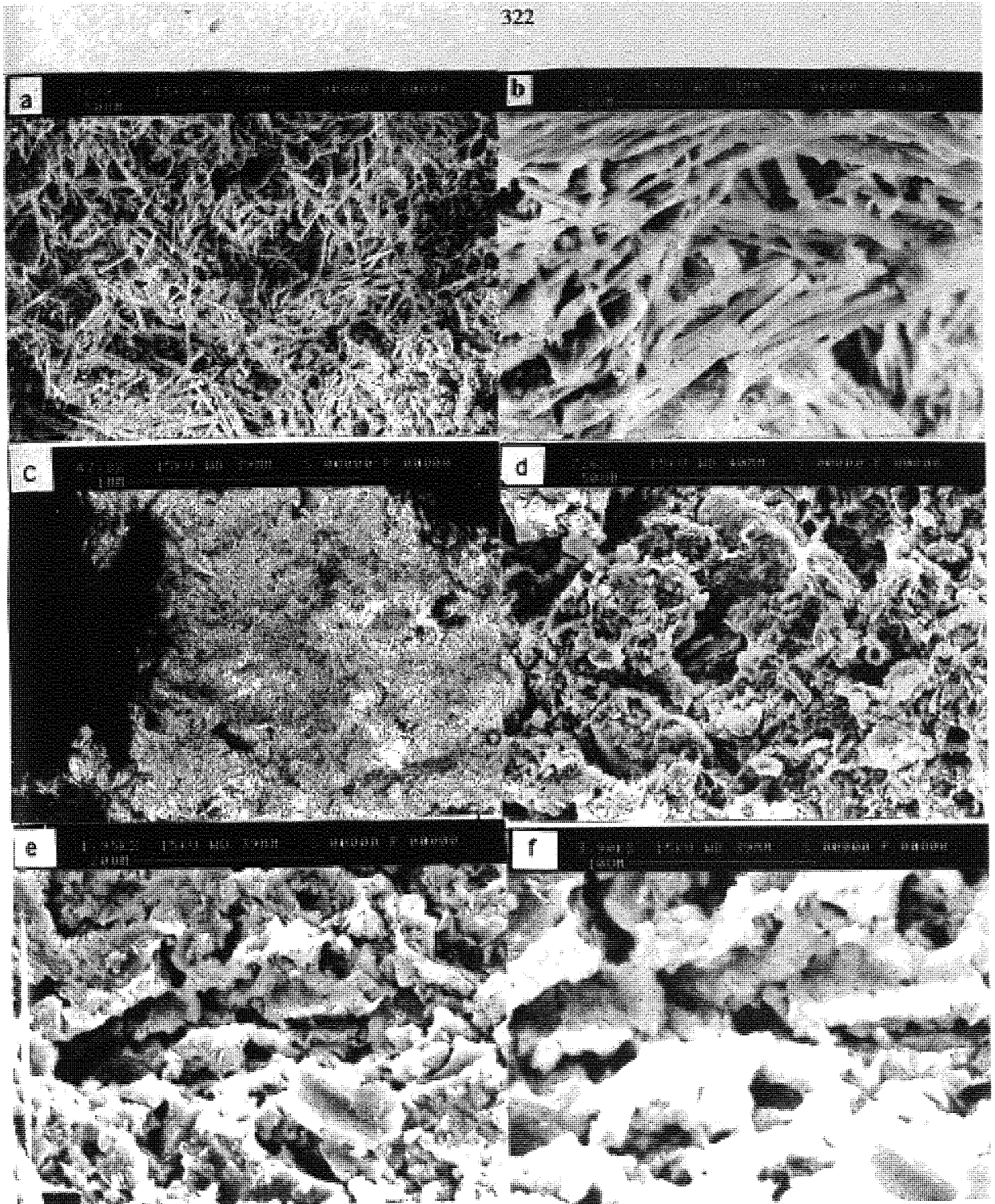
Fig. 8.9 : The progression of destructuring of M2 in the oedometer, loaded
to 400 kPa (a and b) and to 1660 kPa (c to f).
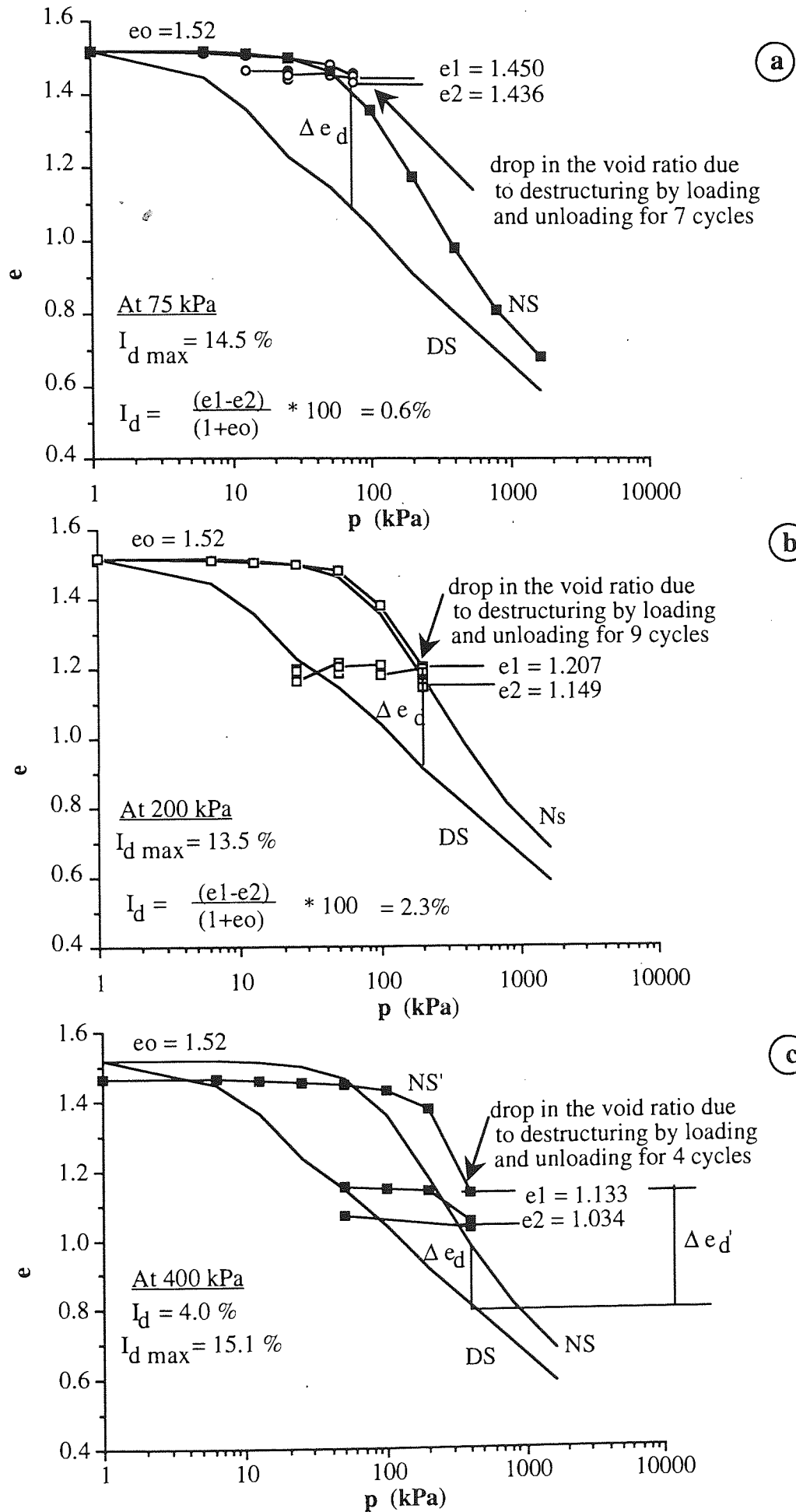
Fig. 8.10 : Consolidation results of A2 samples destructured by
cyclic of loading and unloading between:
a) 12.5-75, b) 12.5-200, and c) 50-400 kPa.
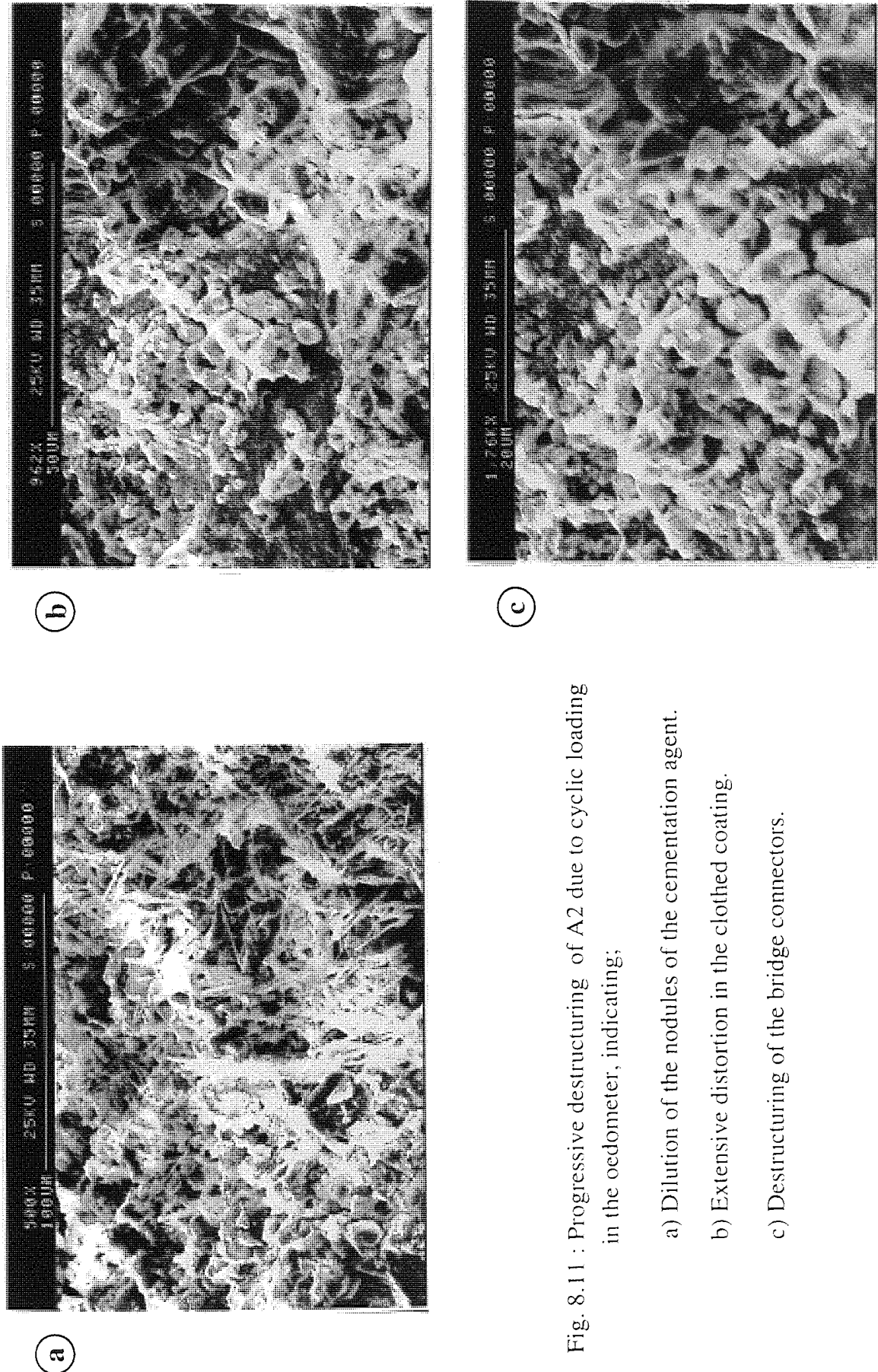
Fig. 8.11 : Progressive destructuring of A2 due to cyclic loading
in the oedometer, indicating;

a) Dilution of the nodules of the cementation agent.

b) Extensive distortion in the clothed coating.

c) Destructuring of the bridge connectors.
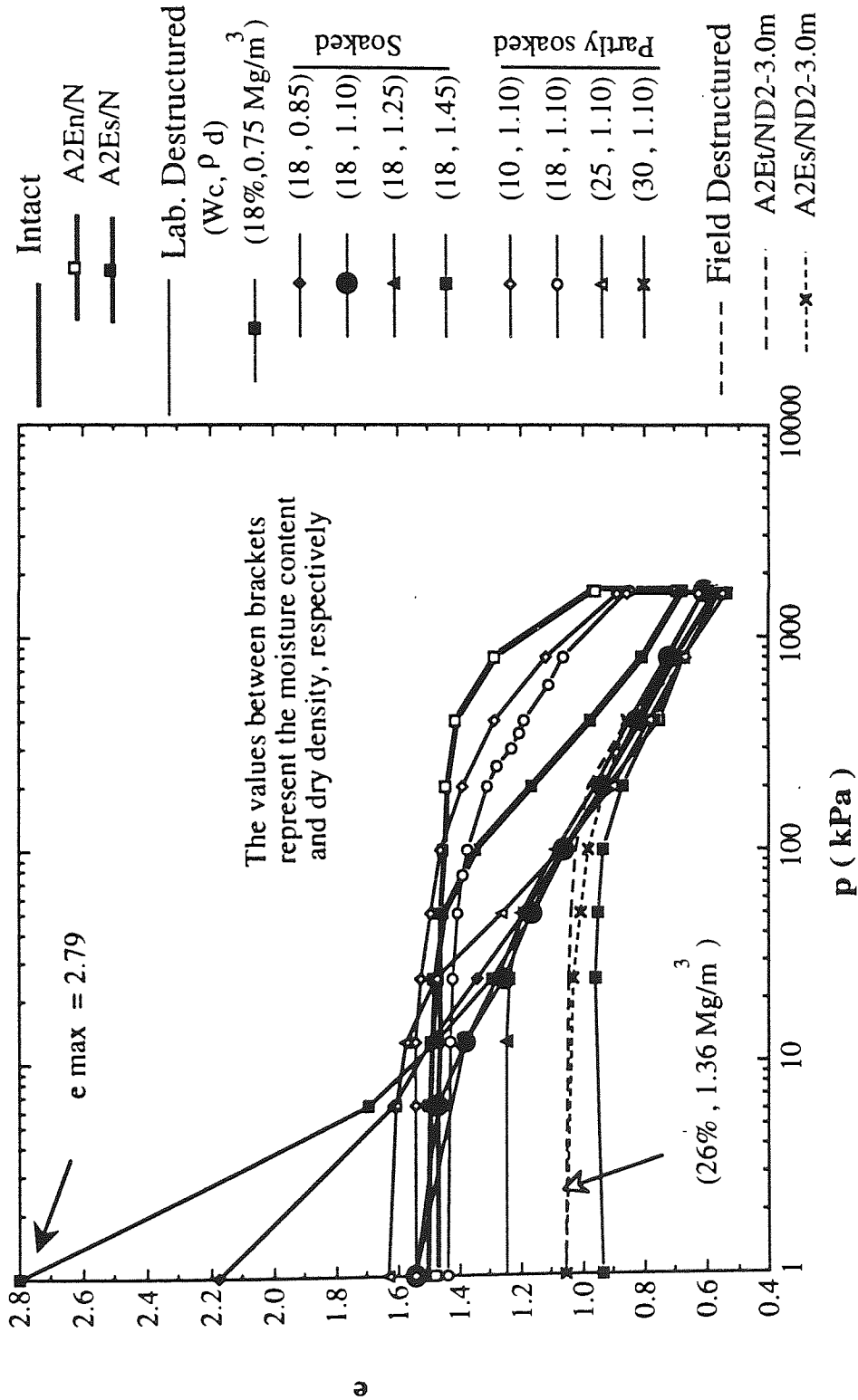
Fig. 8.12 : Complete laboratory framework for soil A2 for simulating the field destructuring at AD2, the variable values between brackets are the moisture content and dry density, repectively.
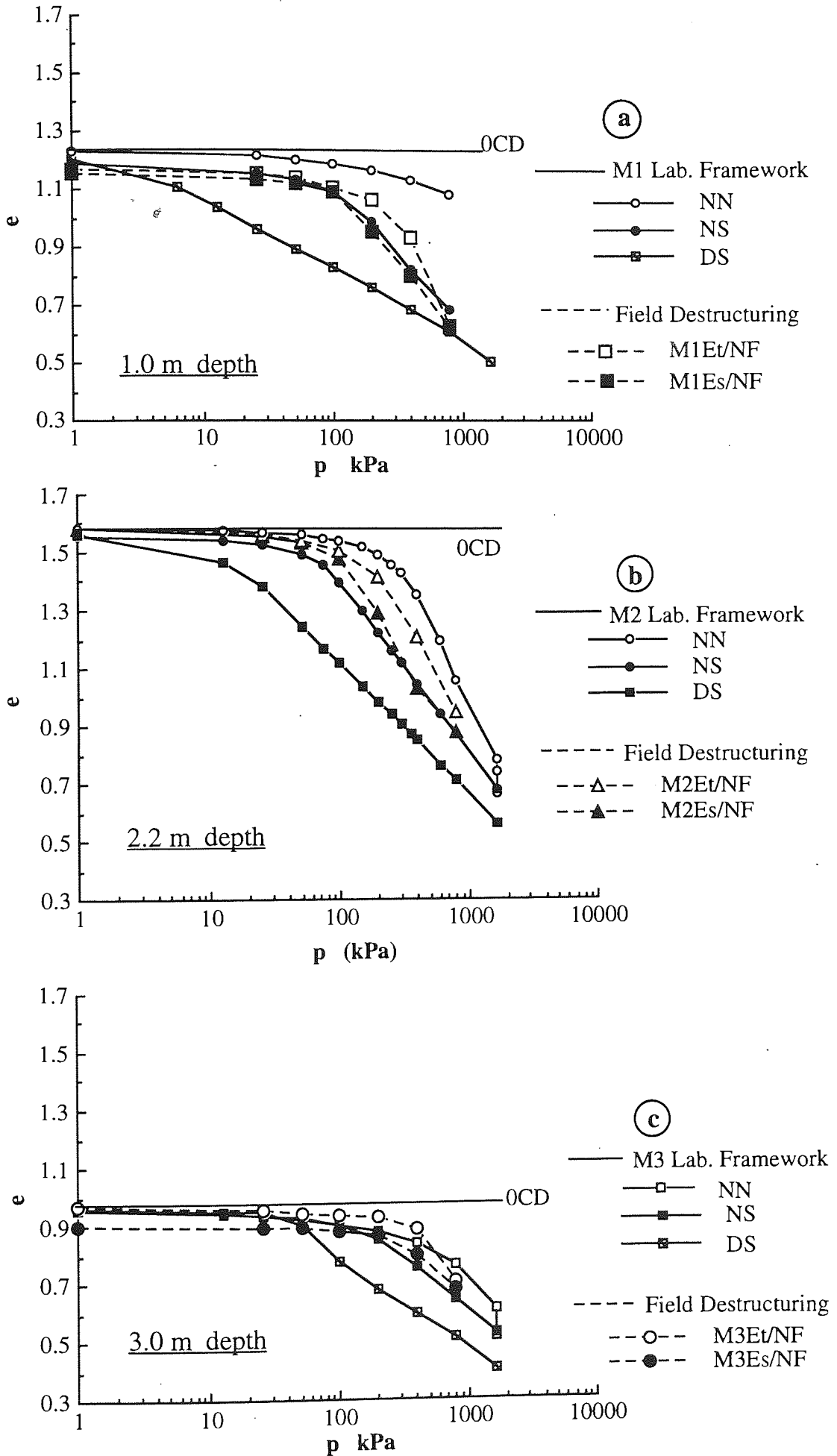
Fig. 8.13 : Evaluation of field destructuring by flooding at the
location MF using the laboratory frameworks for the
soils, a) M1, b) M2 and c) M3.
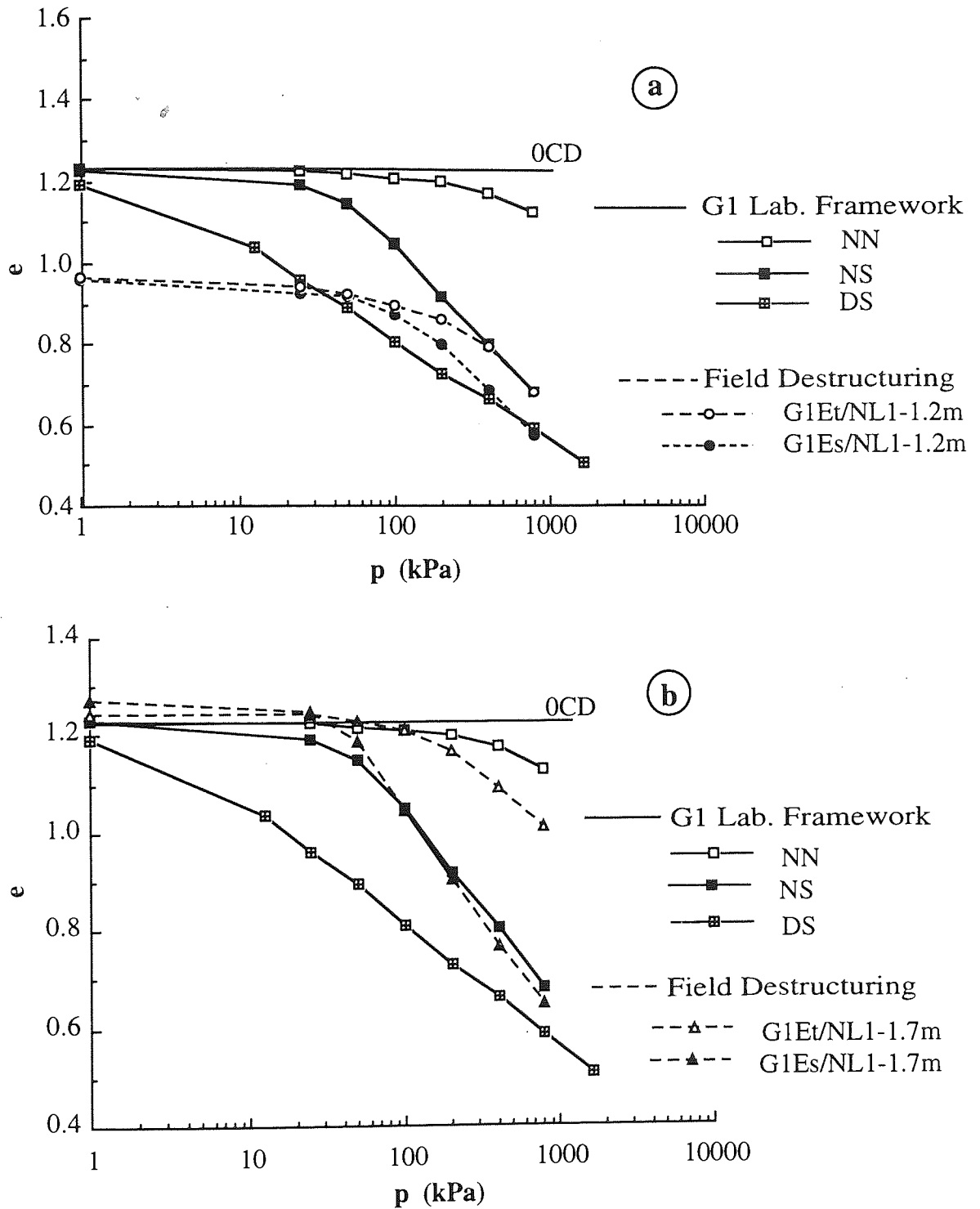
Fig. 8.14: Evaluation of the field destructuring by Preloading at the
location GL1 using the laboratory framework of soil G1
at depths of, a)1.2 and b)1.7m.
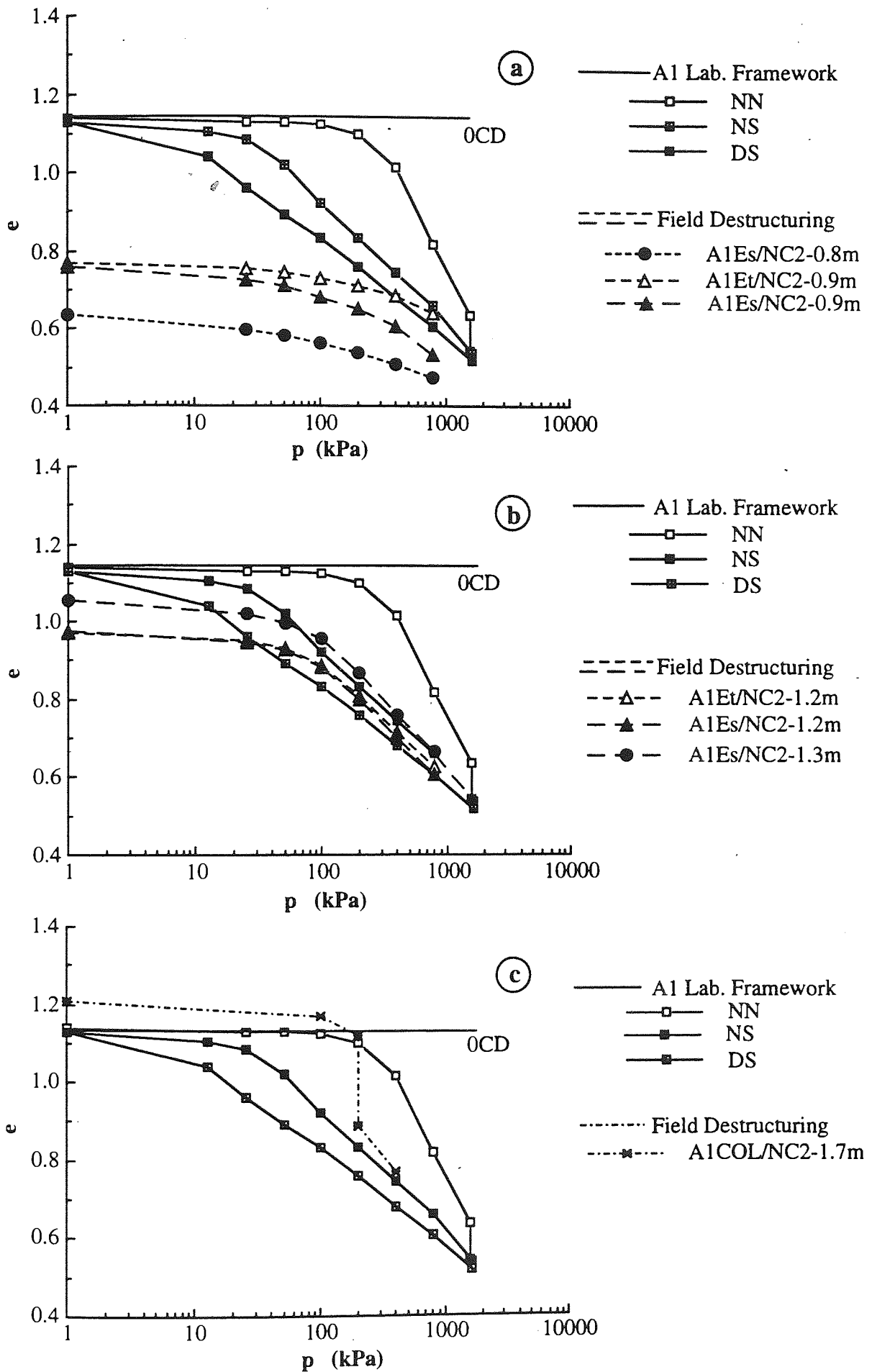
Fig. 8.15 : Evaluation of field destructuring by Roller compactor at the location AC2 using the laboratory framework of the soil A1 at various depths.
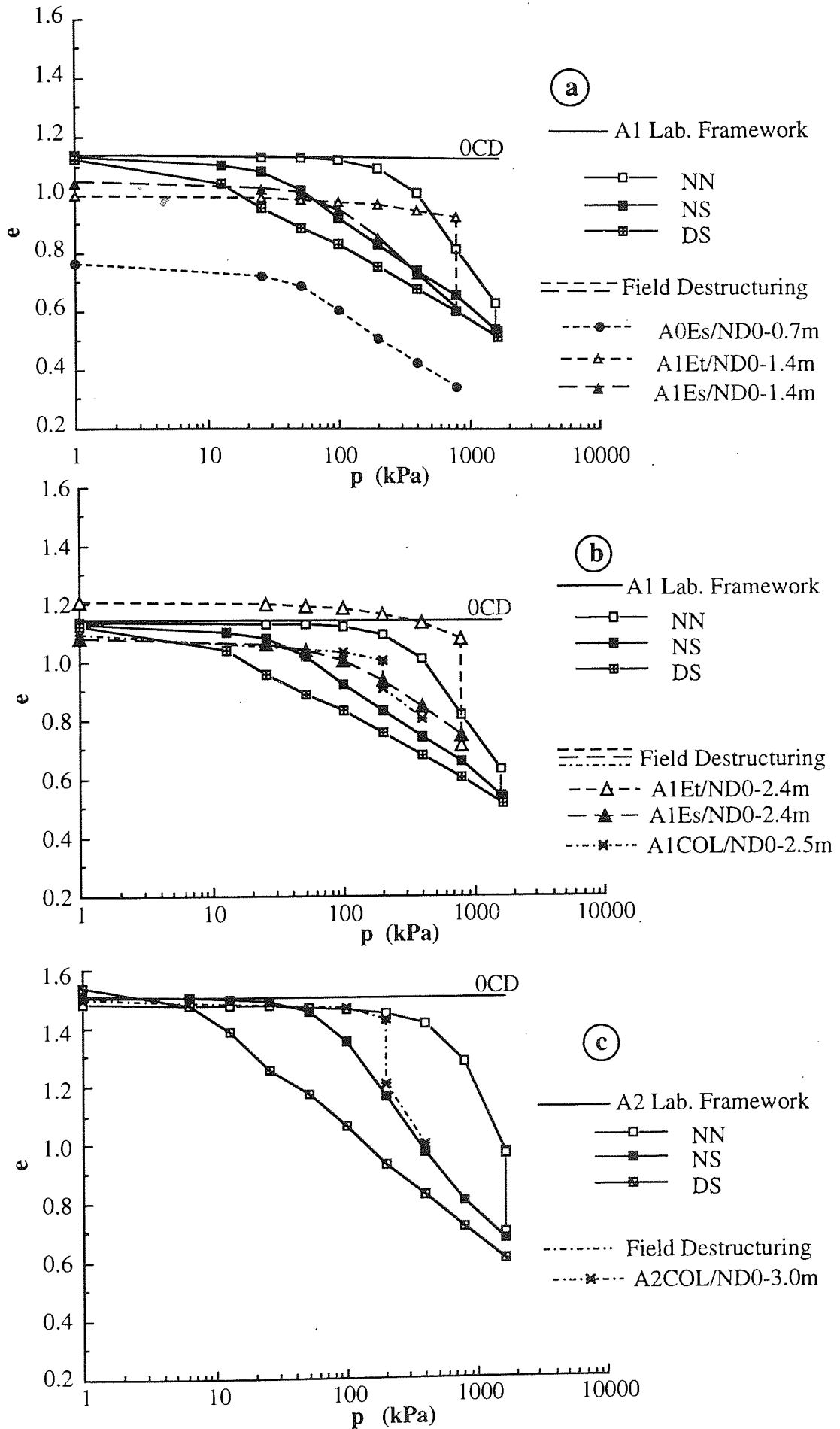
Fig. 8.16 : The use of the laboratory frameworks of A1 and A2
to evaluate the field destructuring by deep compaction
at various depths at the location AD0.
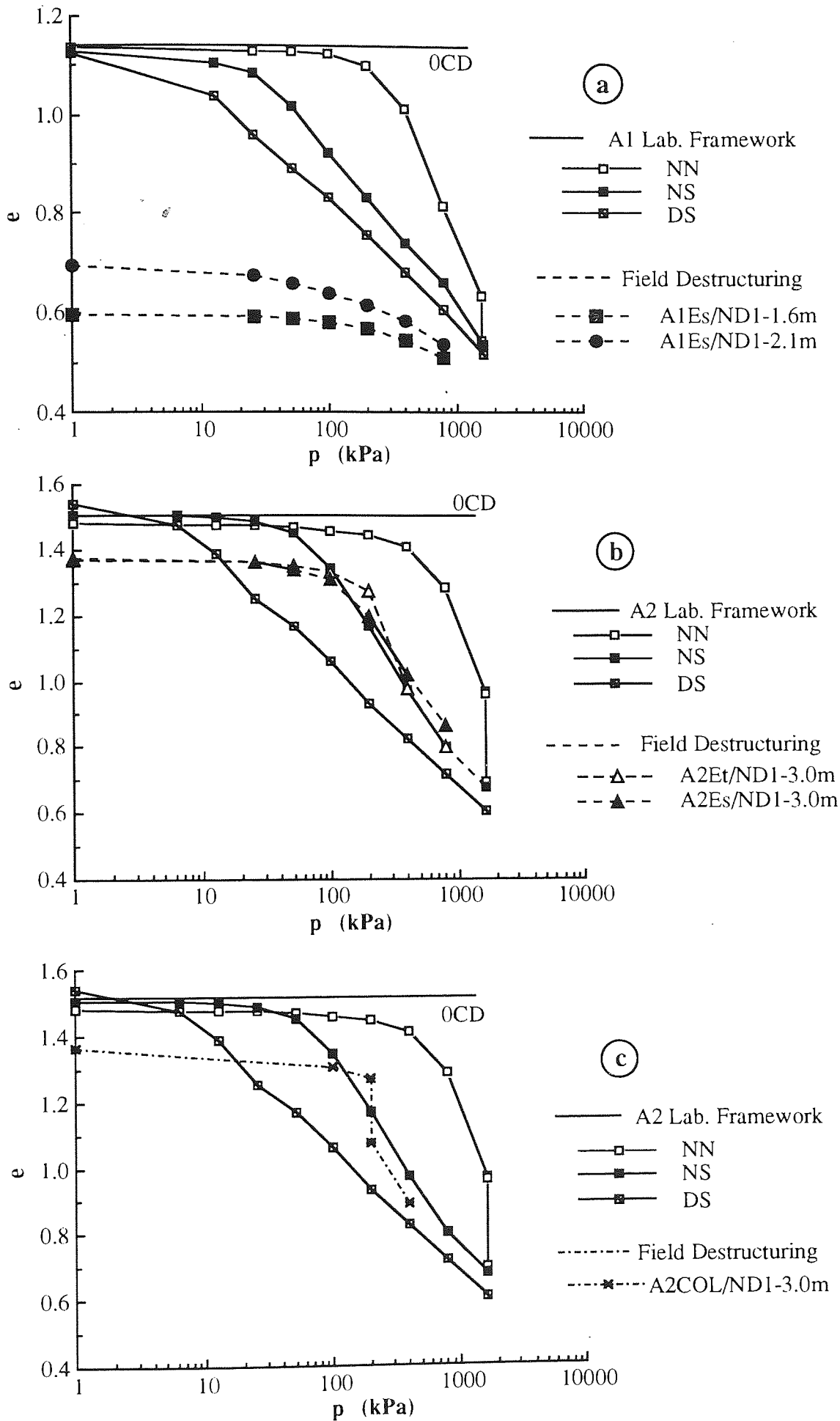
Fig. 8.17 : The use of the laboratory frameworks for A1 and A2 to evaluate the field destructuring by deep compaction at various depths at the location AD1.
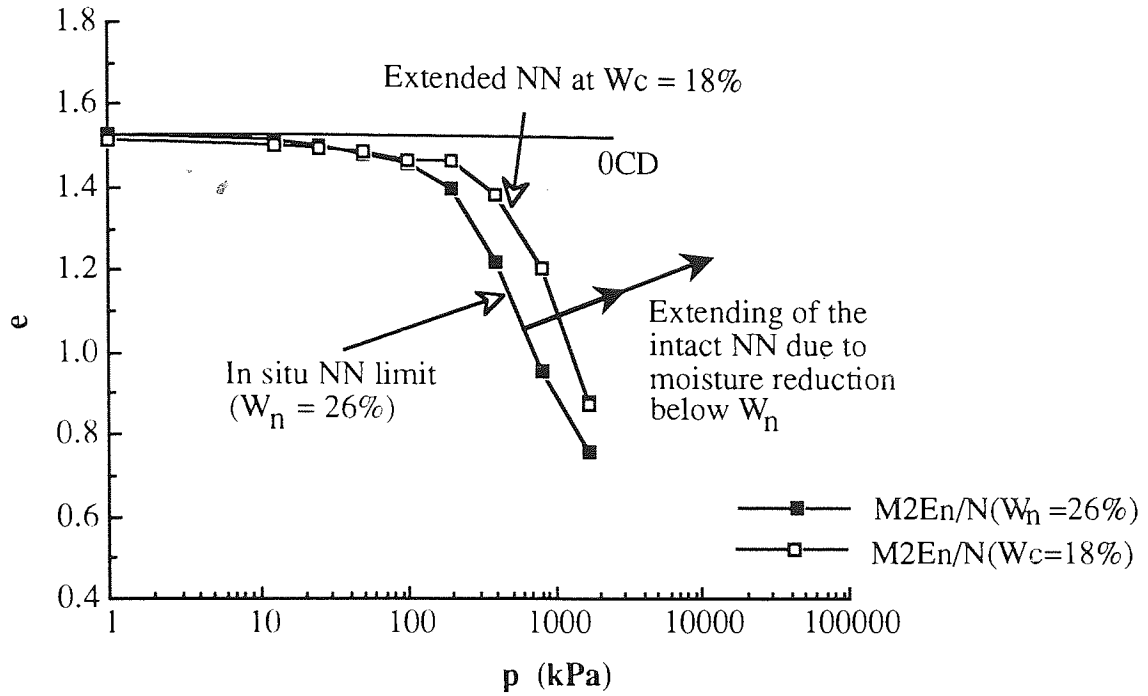
Fig. 8.18 : The effect of a reduction in moisture content, below the in situ value, on the behaviour of soil M2.
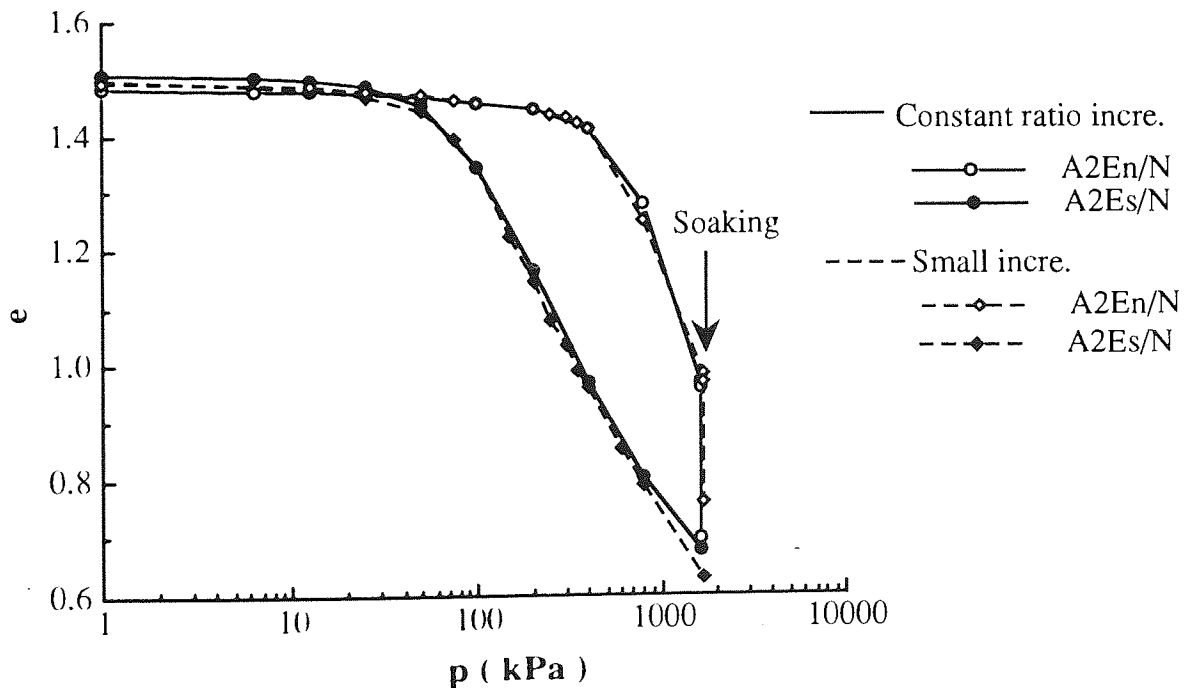
Fig. 8.19 : The effect of the loading system on the NN and NS limits of the natural soil A2.
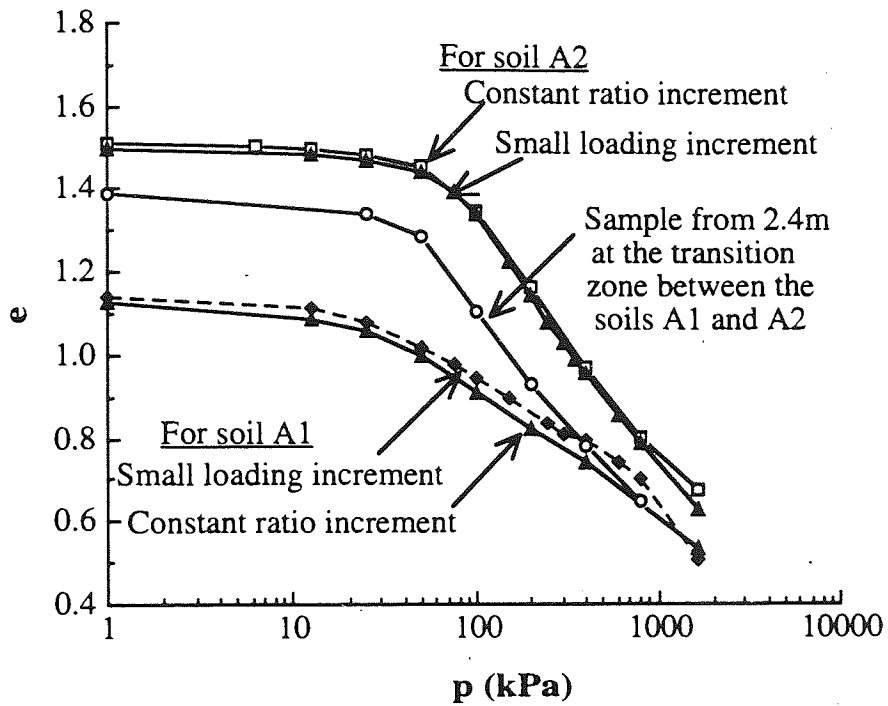
Fig. 8.20 : The effect of layering at the transition zone and loading system on the NS limit of the natural soils A1 and A2.
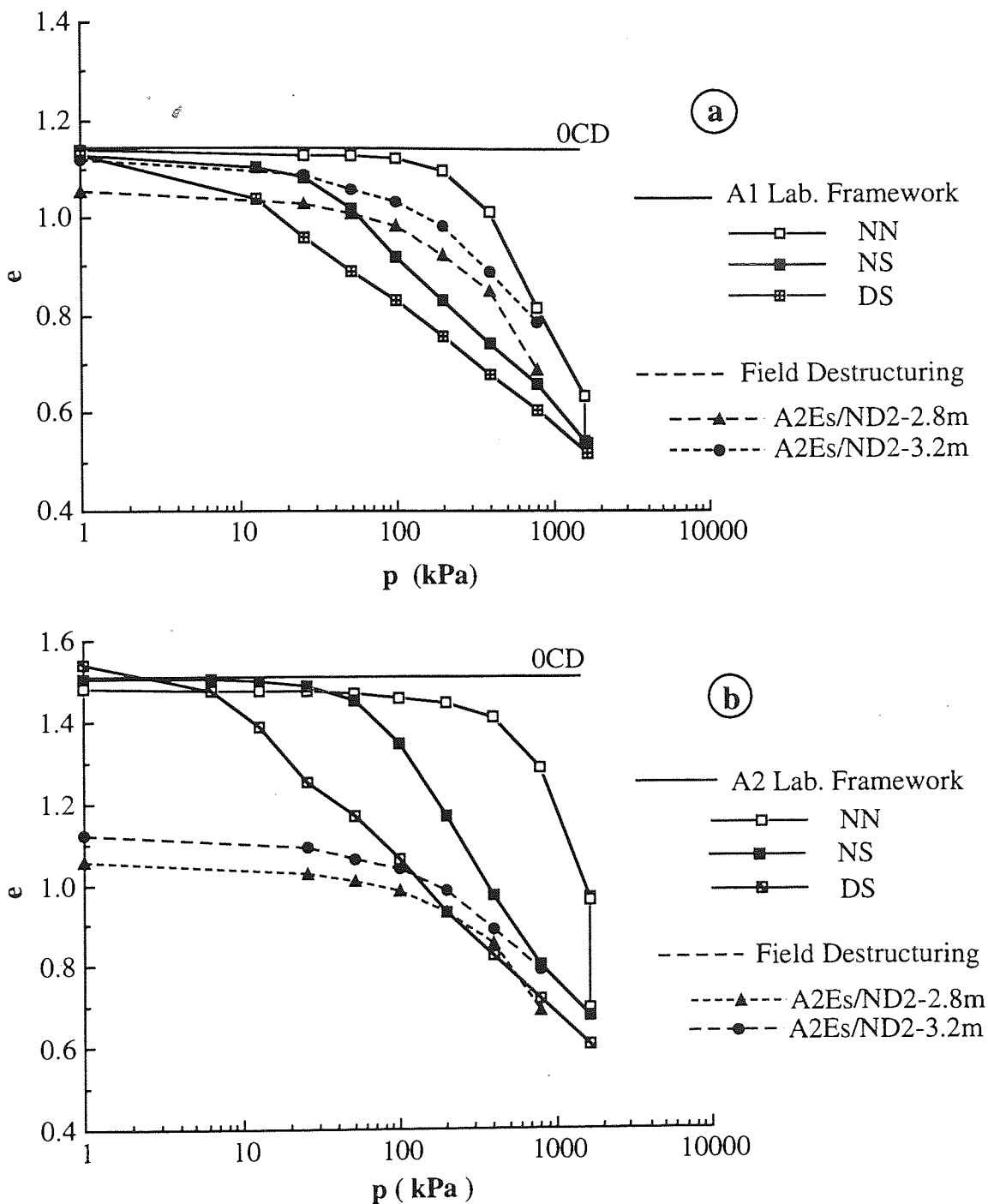
Fig. 8.21 : Evaluation of field destructuring by deep compaction
at the location AD2 using;
a) the inappropriate A1 framework, and
b) the appropriate A2 framework.

CHAPTER 9

SUMMARY AND CONCLUSION

9.1 GENERAL SUMMARY AND CONCLUSION

Based on the field and laboratory programmes carried out at Sana'a and Aston universities on soils from Sana'a, the capital of the Yemen Republic, the following conclusions can be drawn:

1) Structures within the Sana'a area, a highland plain with an arid to semi arid climate, are founded on troublesome soils which have led to a wide variety of failure cracks within these structures and this evidence is documented to show the engineering problems associated with the studied soils. These soils are mostly fine sediments resulting from both alluvial deposition, in form of water-laid deposits, and aeolian deposition, in form of wind-laid deposits. These two depositional systems have produced a repetitive layering system, with the thicker layers being the wind-laid formations, mainly primary loess (top horizon) and secondary or modified loess (lower horizon). These two horizons are sometimes separated by a thinner layer of water-laid deposits.

2) The fine soils are characterized by having high silt contents, with some clay, coated with considerable amounts of calcium carbonate and iron oxide as cementation agents leading to very low to moderate dry densities, characterized by high void ratios. These soils have two types of structure; an open metastable structure characterized by a granular disperse phase of sand and silt accumulations with low clay contents in the forms of coated particles, bridges and buttresses with the root holes which are features of the loess soils, and a cemented metastable structure characterised by having silt accumulation with high clay contents in the forms of aggregated assemblages with highly clothed interactions and trapped pores (lenses), which are features of weakly cemented soils. These soil have been greatly affected by environmental effects, such as drying and wetting, leaching and evaporation as revealed by the weathering effects, particularly at the top of the soil horizon. In the natural state, the soils have low moisture contents and so the role of suction contributes significantly to their bonding forces.

3) The thorough investigation of their collapsing behaviour, using data from SEM, oedometer and isotropic compression tests indicated compatibility between the results of these tests and the collapsing susceptibility of the soils. The collapse potential due to wetting, I_c, under loads was found to be the most reliable indicator to identify and classify the collapsing

potential of these soils which, varied from nil to severe collapse. The top horizons of the soils were susceptible to collapse when wetted at low stresses, 50 to 100 kPa, while the lower horizons only became susceptible when the wetting stress exceeded 100 kPa. Generally the soils were identified to be conditionally collapsing soils where both loading and wetting are essential for collapse to occur, with the collapse potential due to wetting under loads, I_c, being greater than that due to loading alone, I_L. The consequences of collapsing upon wetting were also shown by variations in the mechanical behaviour of the natural soils at both the NMC and SMC states: -

- The reduction in both the stiffness and yield stresses.

- The reduction in the volume change upon wetting under loads.

- The increase in compressibility.

4) The natural soils at the natural moisture content (NMC) exhibited less compressibility and a higher yield stresses than at the soaked condition (SMC). The deformation behaviour of the natural soils at the NMC state implies a framework of the weakly to strongly bonded soils, with a significant loss of this bond due to wetting indicating the role of capillary suction in such bonding. In contrast, the deformation behaviour of the natural soils at the SMC state implies a framework of weakly bonded soils, mainly due to the presence of clay bonds and cementation agents, this bonding effect being recognized from:

- The high stiffness and low compressibility as the applied pressure was raised to the yield stress, followed by a reduction in stiffness and considerable compressibility (high compression index, C_c) with further increase in the applied pressure.

- The cementation bonds which reflect the apparent slightly overconsolidated trend.

- The continuous volume decrease, which is possibly due to the loss of cementation bond and particles rearrangements, under the effect of the short events produced by cyclic loading.

- The SEM and EDS results which indicated the presence of cementation agents, primarily calcium carbonate and iron oxide.

The values of the compression index, swelling index and the coefficient of consolidation were in the range for kaolinite, with the results from both the oedometer and isotropic compression tests being compatible.

5) Flooding treatment produced a reduction in the collapsing potential, I_c, due to increased the moisture content. This reduction in the I_c upon wetting was compensated by an increase in the collapse potential due to loading alone, I_L, with the total collapse potential, I_T, being the same before and after flooding. A drastic increase in the compressibility and reduction in the soil stiffness were associated with increasing the NMC. The water infiltration

in the soils was appreciably higher in the vertical direction than in the horizontal direction, so the wetted zone extended vertically to 5.0m at the centre and to 3.0m at 1.0 to 1.5m away from the edge of the flooded area, while at 2.5m away from the edge no significant variation was detected in the moisture content.

6) Field preloading and wetting resulted in partial wetting and so partial destructuring of the soil structure and bonds to a depth of 1.3m, with the major changes only being apparent over a much shallower depth. However, within the range of the applied field stress of 50 to 150 kPa, a limited improvement was achieved. Field loading tests at the NMC state caused a limited volume change, but upon wetting under loads a further marked volume change, collapse, was observed indicating that the collapse potential at the field conditions was conditional, with that due to wetting being more than that due to only loading, these field results being compatible with the laboratory results.

7) Vibratory roller compaction with flooding resulted in a moderate improvement to a maximum depth of 1.0m, but the major changes were only apparent over a depth of 0.5m. Preflooding extended the improved depth achieved by compaction and increased the degree of improvement across this depth. In addition, it accelerated the treatment, with the economical number of passes varing from 8 to 12 with preflooding against 16 passes at the in situ condition.

8) Pounding or deep compaction resulted in moderate to excellent improvement to a maximum depth of 2.7m, with the major changes in the top 1.8m. Preflooding slightly extended this depth of improvement but significantly increased the degree of improvement across this depth. This treatment can be classified as a very good to excellent technique for improving the soils to a moderate depth. A clear relationship was found between the dry density of the soils treated by deep compaction and the collapsing potential. For a dry density above 1.43 Mg/m^3 the resulting collapsing potential (I_c) was below 2%, and so this value of the dry density can be recommended as an appropriate criterion to minimize the collapsing potential of these soils. The prediction of the depth of improvement by deep compaction followed the relation suggested by Menard and Broise (1975), Eq. (6.1), although with the particular soils, an average correction factor of 0.7 was appropriate.

9) For all the treatment techniques, the degree of improvement was influenced by the degrees of densification and destructuring, moisture content, layering system, age, soil type and bonding forces. The soil texture, structure and cementation bonds were effective in resisting the field destructuring and densification and so restricted the depth of improvement. Field improvement, destructuring and densification, increased the stiffness and yield stress and decreased the collapsing potentials and compressibility.

10) The use of the Standard Penetration Test to assess the benefits of field treatment was unrelible whenever the treatment produced a variation in the moisture content, apart from

some exceptions for deep compaction. In contrast, field density assessment of the field improvement gave results compatible with those obtained from the laboratory testing of field treated samples, and so it was shown to be a powerful tool for assessing the degree and extent of improvement regardless of the moisture content variations.

11) Laboratory destructuring and compacting the soils to the in situ conditions resulted in a considerable reduction in their stiffness and yield stresses and an increase in their compressibility, particularly at stresses below the yield stress of the natural soil. Destructuring soils characterised by having significant fines and cementation did not reduce the collapsing potential (I_c), when they were compacted to the natural dry density at the in situ moisture content, this was particularly apparent at low to moderate stresses. The deformation behaviour of the destructured soils in the e-log p space converged to a limit representing the lower boundary state (DS). This boundary limit which is provided by the destructured condition, indicates the degree of bonding in the natural soil as demonstrated by the offset of the SMC consolidation curve above this destructured line in the e-log p space. Developing such a limit using slurry or reconstituted samples may involve some approximation, possibly due to the effect of aging which may have lead to cementation growth, particularly at low stresses.

12) The mechanism of destructuring was a progressive failure starting with the largest pores, and increasing with applied stress beyond the yield value to include smaller and smaller pores, deterioration of the linking bonds at the connectors and between the assemblages (bridges, buttresses and clothing coating bonds), and some breakage of the cementation particles and aggregations with minor destructuring of the microfabric. The destructuring under the effects of short events resulted in a reduction in the void ratio, between the natural soil loaded at soaked moisture (NS) state and the destructured soil loaded at soaked moisture (DS) state, due to both loss of cementation and particles rearrangement. The destructuring potential, I_d, was introduced to describe such effects in a similar manner to the collapse potential, I_c, which describes the collapsing behaviour.

13) A laboratory framework has been developed to present the collapsing, destructuring and deformation behaviour, CDFW, of the intact soil at both the partially soaked and soaked states and the laboratory destructured soils at the soaked state and it produced satisfactory results for predicting such behaviour. The field destructured soils were also satisfactory evaluated using the CDFW and it provided an improved explanation of the deformation behaviour and destructuring degree of the field treated soils. Moreover, the uncertainty of predicting the stability of the treated soils using the established methods, especially over the lower half of the influenced depth, can be overcome by using the CDFW. At this stage, the framework for a particular soil should only be used to present and evaluate that soil. The degree and manner of destructuring adopted in this study were satisfactory and reliable for establishing the DS boundary in the particular framework for these soils.

9.2 GENERAL REMARKS AND RECOMMENDATIONS

Based on the prior conclusions the following remarks, suggestions and recommendations are raised:-

1-   For the natural collapsing soils of the Sana'a region, the design criteria has to be selected with great caution, considering the effect of wetting on the bearing layers. Therefore, two design approaches can be followed:

a)   If the design of the foundation is based on the shear strength criterion, the moisture content of the bearing soil should not exceed the average in situ moisture content and protection of the underlying soil is essential to avoid the risk of collapsing and differential settlement.

b)   If wetting is allowed, a settlement criterion should be considered and special foundation systems must be designed to safeguard the superstructure against differential settlement. The continuous strip foundation, as a shallow foundation system, is an alternative recommendation for such soils and this type of foundation is either in one direction (Appendix G9-1, after Clemence and Finbarr, 1981) or in two directions as recommended after Zeevaret (1983) and shown in Appendix G9-2. However, for the settlement criterion to provide a safe design for long term stability especially for regions such as the Sana'a area, where the risk of carelessness, lack of design specifications and unpredictable events are high, it is suggested that the curves in Fig. 8.5 could be used to predict the collapse under both wetting and loading and also the total deformation under the extreme conditions of loading and at any moisture states. Another alternative is the use of deep foundations and furthermore the soil should be treated before construction as demonstrated in this work. However, the selection of any design depends on many factors such as the type of structure, the factor of safety, the costs, the site and the surrounding structure conditions.

Generally, in selecting a specific design criterion , the designer has to keep in mind the safety of the structure resting on a collapsing soil and the cost of the safe foundation system.

2-   Soil collapsibility cannot be classified in terms of either the collapsing potential due to loading, I_L, or the total collapse potential, I_T, the collapsing potential upon wetting, I_c, represents the most appropriate term for a collapsing classification system.

3-   When the studied soils are compacted to a minimum dry density of 1.43 Mg/m^3 (equivalent dry unit weight, 14.0 kN/m^3), the risk of collapse is desirably reduced ($I_c \leq$ 2.0%).

4-   The use of the Standard Penetration Test to investigate the Sana'a soil to obtain design data or even correlation parameters is not recommended.

5-   When there is the possibility of the development of a moist or wetted zone adjacent to an existing structure, such as from the surface wetting of a planted area, a horizontal distance of at least 2.0m should be left between the structure and the wetted zone.

6-   Removal the upper 1.0 to 1.5m of the top horizon is recommended so as to provide a foundation base possibly with reduced collapse. For special structures, deep investigation is essential and if similar soils to those investigated are found, deep compaction or other equivalent technique will be needed to provide a satisfactory foundation.

9.3   SUGGESETIONS FOR FUTURE WORK

The following works are suggested for future.

- Other treatment techniques such as grouting need to be considered for treating these soils to a greater depths, particularly where deep compaction is not applicable, such as in a restricted area.

- The effect of wetting with sewage water from septic tanks, or any other polluted water, on the deterioration of the cementation agents and the subsequent collapsing and destructuring potentials.

- The effect of the destructuring procedure on the degree of destructuring and, hence, the lower boundary DS curve, covering such techniques as agitating with ultrasonic method.

- The development of the suggested ideal generalized framework (Appendix G9-3) for presenting the deformation behaviour of the intact and D/C soils at both the partially and soaked states and the effects of the bond interferences on the deformation trends.

- The development of an ideal, normalized and generalized framework that includes the variations in the soil type (layering system), moisture content and dry density for presenting the deformation behaviour of the intact and D/C soils.

- Finally, consideration of whether the developed (CDFW) and the suggested frameworks, presented the deformation behaviour, can be extended to present the shear strength behaviour.

REFERENCES

Abelev, M. Y. (1975). Compaction of loess in the U.S.S.R., Geotechnique, 25: 79-82.

Abduljauwad, S. & Al-Gasous, K. (1991). Soil deformation and shear strength characteristics of the Sana'a soil, The Yemen Arab Republic. Eng. Geol.,31: 291-314.

Abduljauwad, S., Al-Mana, A. & Al-Gasous, K. (1991). Engineering properties of the soil of Sana'a, The Yemen Arab Republic. Eng. Geol., 30: 171-194.

Agha Shaher, G. (1984). Geography of natural Yemen, North Yemen. Al Anwar Publisher, Damascus, Syria.

Aitchison, G. & Donald, I. (1956). Effective stresses in unsaturated soils. Proc. 2nd. Australia-New Zealand Conf. on SMFE: 1-8

Al-Alfi, A. (1984). Mechanical and electron optical properties of a stabilized collapsable soil in Tucson, Arizona. PhD. thesis, The University of Arizona, Arizona.

Al-Gasous, K. (1988). Geotechnical properties of the surficial soils of Sana'a, The Yemen Arab Republic. MSc. thesis, King Fahd University, Dhahran, Saudi Arabia.

Al-Waili, T. (1990). Mechanism and effect of fines on the collapse of compacted sandy soils. PhD. thesis, Washington State University, Pullman Washington.

Anderson, P. (1968). Collapsing soils and their basic parameters in an area in the Tucson Arizona Vicinity. MSc. thesis, University of Arizona, Tucson, Arizona.

ASCE (1987). Soil improvement - A ten year update. Geotechnical special publication No. 12, Joseph P. Welsh, New York, USA.

ASCE (1978). Soil improvement, history, capability and outlook. Geotechnical special publication by ASCE, February, New York, USA.

ASTM (1992). Standard method for measurement of collapse potential of soils, Annual book of ASTM standards, 04.0R: 34-40.

ASTM (1985). Soils and rock, Annual book of ASTM standards, Building Stones, Philadelphia, Vol. 4.

Audric, T. & Bouquier, L. (1976). Collapsing behaviour of some loess soils from Normandy Eng. Geol, 9: 265-277.

Balaev, L. (1967). Prognosis of slumping deformation of loess soils, Jor. of SMFE, 3: 195-197.

Barden, L. (1973). Macro- and microstructure of soils. Appendix to the Proc. of the Int. Symp. on Soil Structure, Gothenburg, Sweden: 21-26.

Barden, L. , Madedor, A. & Sides, G. (1969). Volume change characteristics of unsaturated clay. Jor. of Soil Mech. and Found. Div., ASCE, 95, SM1 : 33-49.

Barden, L. , McGown, A. & Collins, K. (1973). The Collapse mechanism in partly saturated soil. Eng. Geol., 7: 49-60.

Basma, A. & Tuncer, R. (1993). Evaluation and control of collapsable soils. Jor. of Geo. Div., ASCE, 118, 10: 1491-1504.

Beles, A. A., Stanculescu, I. I. & Schally, V.R. (1969). Prewetting of loess-soil foundation for hydraulic structures. Proc. 7th ICSMFE, 2: 17-26.

Bell, F. G. (1992). Engineering properties of soils and rocks. 3rd edition. Butterworth Heinemann Ltd., Great Britain.

Benites, L. A. (1968). Geotechnical properties of the soils affected by piping near the Benson Area, Cochise County, Arizona. MSc. thesis, University of Arizona, Tucson, Arizona.

Beer, F. E. (1964). Chemistry of the soil. 2nd Edition. Reinhold Publishing Corporation, New York.

Bishop, A. W.& Blight, G. E. (1963). Some aspects of effective stress in saturated and partly saturated soils. Geotechnique, 13, 3: 101-109.

Bjerrum, L. (1967). Engineering geology of Norwegian normally consolidated clays as related to settlements of buildings. Geotechnique, 17: 81-118.

Bjerrum, L. & Wu, T. H. (1960). Fundamental shear strength properties of the Lilla Edit clay. Geotechnique, X, 2: 101-109.

Booth, A. R. (1975-a). The factors influencing collapse settlement in compacted soils, Sixth Regional Conference of Africa on SMFE, Durban, South Africa : 57-63.

Booth, A. R. (1975-b). Compaction and preparation of soil specimens for oedometer testing, Symp. on Soil Specimen Preparation for Laboratory Testing, ASTM STP599, Montreal : 216-228.

Bowles, J. E. (1984). Physical and geotechnical properties of soil. McGraw-Hill Book Co, New York.

Bowles, J. E. (1988). Engineering properties of soils and their measurement. McGraw-Hill Book Co, New York.

Bradford, J. M. & Norton, L. D. (1983). Stress-deformation properties of loess and loess-derived alluvium in Western Iowa. Proc. Symp. on Geological Environment and Soil Properties, ASCE, Houston: 99-122.

Bressani, L.A. (1990). Experimental properties of bonded soils. PhD. thesis, Imperial College, London.

Bressani, L.A. & Vaughan, P.R. (1989). Damage to soil structure during triaxial testing. Proc. 12th ICSMFE, Rio de Janeiro, 1: 17-20.

British Standards Institution. (1975). Methods of test for soils for civil engineering purposes, BS 1377. London: BSI.

Bull, W. B. (1964). Alluvial fans and near-surface subsidence in Western Fresno County, California. Geological Survey, Washington, D.C. Professional Paper 437-A.

Bull, W. B. (1972). Recognition of alluvial-fan deposits in the stratigraphic record, recognition of ancient sedimentary environment. Soc. Econ. Planotologistsand Mineralogists, Special publication No. 16, Tulsa, Okla: 68-83.

Buraczynski, J. (1988). Lithological, mineralogical and geochemical characteristics of loesses in the Rhinegraben. Eng. Geol., 25, 2-4: 201-208.

Burland, J. B. (1965). Some aspects of the mechanical behaviour of partly saturated soils, Moisture equilibrium and moisture changes in soils beneath covered areas, G. D. Aitchison, Ed., Butterworths, Australia : 270-278.

Burland, J. B. (1990). On the compressibility and shear strength of natural clays. Geotechnique 40, 3: 329-378.

Casagrande, A. (1932). The structure of clay and its importance in foundation engineering. Jor. of the Boston Society of Civil Engineerings,19, 4: 168-208 .

Chaney, S., Slontim, S. M. & Slontim, S. S. (1981). Determination of calcium carbonate content in soils. Symp. on Geotechnical Properties, Behaviour, and Performance of Calcareous Soils, ASTM STP 777: 3-15.

Clayton, R. (1978). A note on the effect of density. on the results of standard penetration tests in chalk. Technical note. Geotechnique 28: 119-122.

Clayton, C., Hight, D. & Hopper, R. (1992). Progressive destructuring of Bothkennar clay: implications for sampling and reconsolidation procedures. Geotechnique 42, 2: 219-239.

Clemence, S.P. & Finbarr, A. O. (1981). Design considerations for collapsible soils. Jor. of Geo. Div., ASCE, 107, GT3 : 305-317.

Clevenger, W. A. (1956). Experience with loess as a foundation material. Jor. of Soil Mech. and Found. Div., ASCE, 82, SM3 : 1-26.

Clough, G. W., Sitra, N. , Bachus, R. C. & Rad, N. S. (1981). Cemented sand under static loading. Jor. of Geo. Div. , ASCE, 107, GT6: 799-817.

Collins, K. & McGown, A . (1974). The form and function of microfabric features in a variety of natural soils. Geotechnique 24, 2: 151-180.

Coop, M. R. & Atkinson, J. H. (1993). The mechanics of cemented carbonate sands. Geotechnique 43, 1: 53-67.

Crawford, C. B. (1964). Interpretation of the consolidation test. Jor. of Soil Mech. and Found. Div., ASCE, 90, SM5: 87-101.

Das, B. (1984). Principles of foundation engineering. Wadsworth, Inco., Belmont, California.

Day, R. W. (1994). Discusion of Walsh et al (1993). Jor. of Geo. Eng., 120, 9: 1648-1649.

Den Haan, E. J. (1993). The formulation of virgin compression of soils. Geotechnique, 42, 3: 465-483.

Denisov, N., Y. (1951). The engineering properties of loess and loess loams. Gosstroiizdat, Moscow.[In Russian].

Derbyshire, E.& Mellors, T.W. (1988). Geological and geotechnical characteristics of some loess and loessic soils from China and Britain: a comparison. Eng. Geol., 25, 2-4 :135-176.

Douglas, J. (1983). The standard penetration test. Proc. of an extension course on In-situ Testing for Geotechnical Investigation. Edited by Ervin, M. C. , Sydney: 21-31.

Dudley, J. H. (1970). Review of collapsing soils. Jor. of Soil Mech. and Found. Div., ASCE, 97: 925-947.

El-Anbaawy, M. I. (1985). Geology of Yemen Arab Republic, Sana'a University, Sana'a.

El-Ehwany, M. & Houston, S.L. (1990). Settlement and moisture movement in collapsable soils. Jor. of Geo. Div., ASCE, 116,10: 1521-1535.

Evstatiev, D. (1988). Loess improvement methods. Eng. Geol., 25, 2-4: 341-366.

Feda, J. (1964). Colloidal activity, shrinking and swelling of some clays. Proc. of the Soil Mech. Seminar, Loda : 531- 546.

Feda, J. (1966). Structural stability of subsident loesses from Praha-Dejvice. Eng. Geol., 1, 3: 201- 219.

Feda, J. (1988). Collapsing of loess upon wetting. Eng. Geol., 25, 2-4: 263-269.

Fleming, L. N. & Duncan, J. M. (1990). Stress-deformation characteristics of Alaskan silt. Jor. of Geo. Div., ASCE, 116, 3: 377-393.

Foss, I. (1973). Red soil from Kenya as a foundation material. Proc. 8th ICSMFE, Moscow, 2.2: 73-80

Gao, G. (1988). Formation and development of the structure of collapsing loess in China. Eng. Geol., 25, 2-4: 235-245.

Gibbs, H. J.& Bara, J. P. (1962). Predicating surface subsidence from basic soil tests. U.S. Bureau of Reclamation Soil Engineering, Report EM-658.

Gibbs, H. J., Hilf, j. W., Holtz, W. G. & Walker, F. C. (1960). Shear strength of cohesive soils. Proc. Research Conference on Shear Strength of Cohesive Soil, ASCE, Boulder, Colorado: 33-162 .

Gillott, J. E. (1987). Clay in engineering geology. Elsevier Science Publishers, Amsterdam.

Gillott, J. E. (1976). Importance of specimen preparation in microscopy, Soil Specimen Preparation for Laboratory Testing, ASTM STP599: 289-307.

Goldshtein, M. N. (1969). Principles of building design on soils prone to slump-type settlement owing to wetting. Jor. of SMFE, 6: 420-423.

Grolier, M. J. & Overstreet, W. C. (1983). Geotechnical map of Yemen Arab Republic, U. S. Geological Survey, Reston,Virginia, U. S. A.

Handy, R. L. (1973). Collapsable loess in Iowa. Soil Science Society of America Proc., 37: 281-284.

Hausmann, M. R. (1990). Engineering principles of ground modification, McGraw-Hill Inc, New York.

Holtz, R. D., Jamiolkowski, M. B. & Lancellota, R. (1986). Lessons from oedometer test on high quality samples. Jor. of Geo. Div., ASCE, 112, GT8: 768-776.

Holtz, W. G. (1983). The influence of vegetation on the swelling and shrinking of clays in the United States of America. Geotechnique, XXXIII, 2:159-163.

Holtz, W. G.& Gibbs, H. G. (1951). Consolidation and related properties of loessial soils. Symp. on Consolidation Testing of Soils, SSTM SPT126, Philadelphia: 9-33.

Holtz, W. G.& Hilf, J. W. (1961). Settlement of soil foundations due to saturation. Proc. 5th ICSMFE, 1: 673-679.

Houston, S. & El-Ehwany, M. (1991). Sample disturbance of cemented collapsable soils. Jor. of Geo. Div., ASCE, 117,5: 731-752.

Houston, S., Houston, W. & Spadola, D. (1988). Prediction of field collapse of soils due to wetting. Jor. of Geo. Div., ASCE, 114, 1: 40-58.

Houston, W. N.& Mitchell, J. K. (1969). Property interrelationships in sensitive clays. Jor. of Geo. Div., ASCE, 95, SM4: 1037-1062.

Huang, J. T. & Airey, D. W. (1994). Discussion of Coop and Atkinson (1992). Geotechnique 44, 3: 533-537.

Hvorslev, M. J. (1948). Subsurface exploration and sampling of soil for civil engineering purposes. Waterways Exp. Sta., Vicksburg.

International Society for Soil Mech. and Foundation Engineering. (1981). The international manual for the sampling of soft cohesive soil, Tokyo University Press, Tokyo Japan.

Ismael, N. F. (1993). Laboratory and field leaching tests on costal salt-bearing soils. Jor. of Geo. Div., ASCE, 119, SM3: 453-470.

Italconsult. (1973). Water supply for Sana'a and Hoddidah, Report of 3 Vol. Rome.

Jennings, J. E.& Burland, J. B. (1962). Limitations to the use of effective stresses in partly saturated soil. Geotechnique, 12, 2: 125-144.

Jennings, J. E. & Knight, K. (1957). The additional settlement of foundations due to a collapse of structure of sandy subsoils on wetting. Proc. 4th ICSMFE, 1: 316-319.

Jennings, J. E.& Knight, K. (1975). A guide to construction on or with materials exhibiting additional settlement due to collapse of grain structure. Proc. 6th. Regional Conf. for Africa on SMFE, Durban, South Africa : 99-105.

Johnson, A. I.& Moston, R. P. (1975). Use of ultrasonic energy for dissaggregation of soil samples. Symp. on Soil Specimen Preparation for Laboratory Testing, ASTM STP599, Montreal: 308-319.

Kantey, B. (1967). Collapsing soils. Proc. 4th. Regional Conf. on SMFE, Cape Town, South Africa, Vol 1: 394.

Keller, T. T. , Castro, G. & Rogers, J. H. (1987). Steel creek dam foundation densification. Soil improvement - A ten year update, ASCE Geotechnical special publication No. 12, Joseph P. Welsh, New York, USA: 136-165.

Kenney, T. C., Moum, J. & Berre, T. (1967). An experimental study of bonds in a natural clay. Proc. of the Geo. Conference, Shear Strength Properties of National Soils and Rocks, 1: 65-69.

Knight, K. (1963). The origin and occurrence of collapsing soils. Proc. 3rd. Regonal Conf. on SMFE, Vol 1: 127-130.

Kruck, W. (1983). Geological Map of the Yemen Arab Republic, Federal Institute for Geosciences and Natural Resources, Hanover, Federal Republic of Germany.

Krynine, D. P. (1957). Principles of engineering geology and geotechnics, McGraw-Hill Book Company.

Lambe, T. W. (1951). Soil testing for engineering, John Wiley & Sons, Inc., New York.

Lambe, T. W. & Martin, R. T. (1953). Composition and engineering properties of soils. Highway Research Board Proc., I.

Lawton, E.C. (1986). Wetting-induced collapse in compacted soil. PhD. thesis, Washington State University, Pullman Washington.

Lawton, E.C., Fragaszy , R. J. & Hardcastle, J. H. (1989). Collapse of compacted clayey sand. Jor. of Geo. Div., ASCE, 115, 9: 1252-1267.

Lawton, E.C., Fragaszy, R. J. & Hetherington, M. D. (1992). Review of wetting-induced collapse in compacted soil, Jor. of Geo. Div., ASCE, 118, 9: 1376-1394.

Leach, J. A. (1974). Soil structures preserved in carbonate concretions in Loess. Technical Note, Qua. Jor. of Eng. Geol., 7: 311- 314.

Leonard, G. , Cutter, W. & Holtz, R. (1980). Dynamic compaction of granular soils. Jor. of Geo. Div., ASCE, 106, GT1: 35-44.

Leroueil, S., Tavenase, F , Brucy, F., La Rochelle, P. & Roy, M. (1979). Behaviour of de-structured natural clay. Jor.of Geo. Div., ASCE, 106, GT6: 759-778.

Leroueil, S. & Vaughan P.R. (1990). The general and congruent effects of structure in natural soils and weak rocks. Geotechnique, 40, 3: 467-488.

Lin, Z. G. & Wang, S. J. (1988). Collapsibility and deformation characteristics of deep-seated loess in China. Eng. Geol., 25, 2-4: 271-282.

Livneh, M. & Shklarsky, E. (1965). Saturation criteria in pavement design for semi-arid zones. Moisture in Soil Beneath Covered Area, Australia, Butterworth: 237-242.

Lukas, R. G. (1980). Densification of loess by pounding. Jor. of Geo. Div., ASCE, 106, GT4: 435-446.

Lukas, R. G. (1986). Dynamic compaction for highway construction, Design and construction guide-lines. Federal Highway Administration, Office of Research and Development, U.S. D.O.T., Washington, D.C., Vol. 1, Report No. FHWA/RD-86/133..

Lutengger, A. J. (1986). Dynamic compaction in friable loess, Jor. of Geo. Eng., ASCE, 112, 6: 663-667.

Lutengger, A.J.& Hallberg, G. (1988). Stability of loess. Eng. Geol., 25, 2-4 :247-261.

Lutengger, A. J. & Saber, R. T. (1988). Determination of collapse potential of soils. Geotechnical Testing Jor., 11, 3: 173-178.

Maccarini, M. (1987) . Laboratory studies of a weakly bonded artificial soil. PhD thesis, University of London.

Manye, P. W., Jones, J. S. & Dumas, J. C. (1984). Ground response to dynamic compaction. Jor. of Geo. Eng., ASCE, 110, GT6: 757-774.

Marinescu, K. (1986). Modified methods for intensive dynamic compaction of weak soils. Jor. SMFE, Plenum Publishing Corporation: 73-78.

Maswoswe, J. (1985). Stress paths for a compacted soil during collapse due to wetting. PhD. thesis, Imperial College, London.

Mc Gowen, J. H. & Garner, L. H. (1970). Physographic features and stratification types of coarse-grained point bars modern and ancient examples. Sedimentology, 14: 77-112.

Menerd, L. & Broise, Y. (1975). Theoretical and practical aspects of dynamic consolidation. Geotechnique, 15, 1: 757-774.

Ministry of Public Works. (1985). Unpublished report about investigated bores within Sana'a Area, Sana'a.

Minkov, M. & Donchev, P. (1983). Development of heavy tamping of loess bases. Proc. 8th ICSMFE, Helsinki, 7: 797-800.

Minkov, M., Evstatiev, D., Donchev, P.& Steffanoff, G. (1981). Compaction and stabilization of Loess in Bulgaria. Proc. 10th ICSMFE, Stockholm, 3: 745-748.

Mitchell, J. (1976). Fundamentals of soil behaviour. Wiley, New York.

Mitchell, J. & Sitra, N. (1982). Engineering properties of tropical residual soils. Proc. Eng. and Construction in Tropical and Residual Soils, ASCE, Honolulu, Hawaii: 30-57.

Mitchell, J. & Solymar, Z. (1984). Time-dependent strength gain in freshly deposited or densified sand. Jor. of Geo. Eng., ASCE, 110, 11:1559-1576.

Moorhouse, D. C. & Baker, G. L. (1969). Sand densification by heavy vibratory compactor. Jor. of Geo. and Found. Div., ASCE, 95, 4: 985-994.

Mustafa, I. A. (1985). Geographical study of Sana'a Region. MSc. thesis, Sana'a University, Sana'a.

Nagaraj, T. S., Srinivasa Murthy, B. R., Vatsala, A. & Joshi, R. C. (1990). Analysis of compressibility of sensitive soils. Jor. Geo. Eng., ASCE, 116, 1, 105-118.

Northey, R. D. (1969). Engineering properties of loess and other collapsible soils. Proc. 7th ICSMFE, 1: 445-452.

Pandian, N. S., Nagaraj, T. S. & Siva Kumar Babu, G. L. (1992). Generalized state parameter for partly saturated soils. Jor. of Geo. Eng., ASCE, 118, 4: 622-627.

Partridge, T. C. (1967). Some aspects of the water table in South Africa. Proc. 4th Regional Conf. on SMFE, Cap Town, South Africa, 1: 41-44.

Peck, R. B., Hanson, W. E. and Thorburn, T. B. (1974). Foundation engineering. Wiley, New York.

Phien-wej, N., Pientog, T. & Balasubramaniam, A. S. (1992). Collapse and strength characteristics of loess in Thailand. Eng. Geol., 32: 59-72.

Popescu, M. E. (1986). A comparison between the behaviour of swelling and collapsing soils. Eng. Geol., 23: 145-163.

Priklonski, V. A. (1952). Gruntovedenie-Vtoraic Chast., Gosgeolzdat, Moscow, USSR. [in Russian].

Quigley, R. M. & Thompson, C. D. (1966). The fabric of anisotropically consolidated sensitive marine clay. Canadian Geotechniqual Jor., 3, 2: 61-73.

Rethati, A. (1981). Geotechnical effects of changes in ground water level. Proc. 10th ICSMFE, 1: 471-476.

Reginatto, A. R. (1971). Standard penetration tests in collapsable soils. Proc. 4th Panamerican Conf. on SMFE, Puerto Rico, II: 77-85.

Reginatto, A. R. & Ferrero, J. C. (1973). Collapsing potential of soils and soil water chemistry. Proc. 8th ICSMFE, 2.2: 177-183.

Riani, H. C. & Barbosa, M. C. (1989). Collapsable sand and its treatment by compaction. Proc. 12th ICSMFE, Rio de Janeiro, 1: 643-646.

Richard, D. D. (1983). Depositional systems. Prentice-Hall, U.S.A.

Rizkallah, V. & Keese, K. (1989). Geotechnical properties of collapsable soils. Proc. 12th ICSMFE, Rio de Janeiro, 1: 101-104

Sam Wan. (1982). Unpublished report about Sana'a Sewage Project. Italconsult , Sana'a.

Salas, J., Justo, J., Romana, M. & Fraco, C. (1973). The collapse of gypseous silts and clays of low plasticity in arid and semi arid climates. Proc. 8th ICSMFE, Moscow, 2.2: 193-199.

Sangrey, D. A. (1972). Natural cemented sensitive soils. Geotechnique, 22, 1: 139-152.

Saxena, S. K. & Lastrico, R. M. (1978). Static properties of light cemented sand. Jor.of Geo. Eng., ASCE, 104, 12: 1449-1464.

Schmermann, J. H. (1970). Sand densification by heavy vibratory compactor. Jor. of Soil Mech. and Found. Div., ASCE, 69, 1: 363-365.

Sergeyev, Y. M., Budin, D. Y., Osipov, V. I. & Shibakova, V. S. (1973). The importance of the fabrics of clay in estimating their engineering-geological properties. Int. Symp. on Soil Structure, Gothenburg: 243-251.

Skvaletskii, E. N. (1967). Compaction of slumping soil after flooding under conditions of Tadzhikistan, Jor. of SMFE, 3:191-194.

Sheeler, J. B. (1968). Summarization and comparison of engineering properties of loess in the United States. Highway Res. Rec., 212:1-9.

Smart, P. (1975). Soil microstructure. Soil Science, 119: 385-393.

Sultan, H. A. (1969). Foundation failures on collapsing soils in the Tucson area, Arizona. Proc. of the Second Conference on Expansive and Collapsing Soils, Texas A& M Press, College Station: 394-398.

Tavenas, F. & Leroueil, S. (1985). Discussion. Proc. 11th ICSMFE, San Francisco, 5: 2693-2694.

Terzaghi, K. (1925). Simplified soil tests for subgrades and their physical significance. Public road, October.

Terzaghi, K.& Peck, R. B. (1967). Soil mechanics in engineering practice. 1st edition. John Wiley, New York.

Tomlinson, M. J. (1980). Foundation design and construction. 4th Edition. Pitman Publishing, London.

Uriel, R. & Serrano, A. (1973). Geotechnical properties of two collapsing volcanic soils of low bulk density at the site of two dams in Canary Island (Spain). Proc. 8th ICSMFE, Moscow, 2.2: 257-264.

Vargas, M. (1953). Some engineering properties of residual clay soils occurring in Southern Brasil. Proc. 3rd ICSMFE, Zurich, 1: 67-71.

Vaughan, P.R. (1985). Mechanical and hydraulic properties of tropical lateritic and saprolitic soils, particularly as related to their structure and mineral components. Proc. 1st Int. Conf. Geomech. Trop. Lateritic and Saprolitic Soils. Brasilia, 3:231-263.

Vaughan, P.R. (1988). Characterising the mechanical properties of in-situ residual soil. Proc. 2nd Int. Conf. on Geomech. in Trop. Soils. Singapore, 2: 469-487.

Vaughan, P.R., Maccarini, M.& Mokhtar, S.M. (1988). Indexing the engineering properties of residual soil. Qua. Jor. of Eng. Geol., 21: 69-84.

Welsh, J., Anderson, R., Barkesdale, R., Satyapriya, C., Tumay, M. & Wahls, H. (1987). Densification. soil improvement - A ten year update, ASCE Geotechnical special publication No. 12, Joseph P. Welsh, New York, USA: 67-75

Wesley, L. D. (1974). Discussion of Wallace (1973). Geotechnique, 24, 1: 101-105.

Wesley, L. D. (1990). Influence of structure and composition on residual soils. Jor. of Geo. Eng., ASCE, 116, 4: 589-603.

Whetten, N. L. & Weaver, J. W. (1991). Densification of gravelly sand fill using intensive surface compaction. Jor. of Geo. Eng., ASCE, 117, 7: 1089-1094.

Wilson, S. D. (1960). Effect of compaction on soil properties. Symp. on Soil Compaction: 148-161.

Wray, W. K. (1986). Measuring engineering properties of soil. Prentice-Hall. A division of Simon and Schuster, Inc., Englewood Cliffs, U.S.A..

Zeevaret, L. (1983). Foundation Engineering for difficult subsoil condotions. Van Nostrand Reinhold Publishing Co., New York.

Zur, A. & Wiseman, G. (1973). A study of collapse phenomena of an undisturbed loess. Proc. of the 8th ICSMFE., Moscow, 2.2: 265-269.

APPENDIX   A2

APPENDIX   B4

B4-1 : Location layout at site II.

B4-2 : Location layout at site IV.

B4-3

Description of the Selected Soils

Soils of Sites I and II

On the soil profile, Figure 4.9, four soil horizons are shown and the grading of these four soils are shown in Figure 4.10. The top lean clay layer was not included in this study and so is only described briefly while the others are covered in detail.

A0) The Top Dark Stiff Fissured Lean Clay 'Merriah': This occurs only as a surfacial soil layer across the Sana'a area and its thickness varies from zero to 1.8m. At sites I and II, its thickness was found to vary from 0.5 to 1.3m. It was not included in this study for several reasons. Firstly, as this is a stiff soil of very low permeability, it seals the collapsible soils beneath it against weathering and the effects of surface loading. Consequently, the effects of mechanical improvement could be limited if this layer is not removed. Secondly, as this is a surfacial soil it is usually removed before construction, so it is not sensible to include it in this study. Furthermore, preliminary identification has shown that it does not have a collapsing tendency, the main concern of this thesis.

A1) Medium to Stiff Reddish to Light Brown Sandy Silt Soil 'Suffrri': This sandy silt covers most of the middle part of the Wadi area and is locally known as "Suffrri" due to its yellowish to reddish brown colour although it becomes pale when dry. It was found within the four studied sites. Typically it occurs about 1.0m below the ground surface extending downward to 3.0m and, in some cases, with a relatively large thickness (3.0 to 4.0m) as shown in plate 4.2-b, together with lenses or pockets of coarse particles. In many locations the vertical continuity of this soil is interrupted by a 0.2m -0.8m layer of silty clayey sand with gravel as shown in Plate 4.2-a. Within the two sites this layer was found typically 0.5 to 1.3m below the surface overlaid by the stiff fissured lean clay layer although, in few locations, it was found at the surface. The thickness varied from 1.5 to 2.2m with some discontinuity due to the random scattering of the sandy-gravel sheets, pockets or lenses. This soil is known as wind deposit loess. By neglecting the top lean clay layer this layer is identified by A1, G1, M1 and K1 at the first, second, third and the fourth sites respectively.

In reality this soil layer is a normally consolidated soil with a high void ratio and low unit weight, although it exhibited limited overconsolidation behaviour. The dry density ranged from 1.18 to 1.31 Mg/m^3 (dry unit weight, 11.6 - 12.8 kN/m^3), the slight increase with depth being attributed to the overburden pressure and the cyclic wetting and drying. These factors produced leaching of the fine contents from the top layers into the bottom layer of this soil.

In some locations the gradation of the top of the sandy silt has been affected by this fine leaching so that the soil classification may be shifted, either from one group to another or within the same group. At the top this may shift a sandy silt (ML group) to silty sand (SM group) or from a silt or silt with sand to a sandy silt in the lower part of the same layer, and may even affect the lower layers depending on the duration and extent of the leaching.

Fig. 4.9 gives the SPT values (Ns) obtained at 15cm intervals, at each level, down the borehole, and the discontinuous layering system of the soils at this site is indicated by the large change in values of the last 15cm at 3.0m and 5.0m depths. The values of SPT for all sites were evaluated with great care, due to the random distribution of sand and gravel particles within some layers, in addition to the possible disturbance due to the auger drilling, particularly at the first 15cm interval. Therefore, at each level, the sum of the readings of the last two intervals (30cm) provided the SPT values in Fig. 4.9. The Ns values of the upper layer, A1, vary from 8-13 and according to these values the consistency of this layer varies from medium to stiff (Terzaghi and Peck, 1967; Bowles, 1984).

Evidence of very thin roots and great number of small holes were visible, specially in the lower part of this layer (1.8 to 2.8m). White traces of calcium carbonate were visible within and around these thin holes, although at a low content with respect to the lower layer, A3. The grain size analysis on three selected samples obtained from 1.2m, 1.5m and 1.8m below the ground surface are shown in Fig. 4.10. Comparing curve A1-1.2m with A1-1.8m, it is notable that, the deeper soil had the higher clay content due to the leaching process. The liquid limits and plastic limits of this soil are 27%-35% and 20%- 29%, respectively. The water content, at 13% - 15%, is below the plastic limit, which may cause this soil to be sensitive to wetting.

A2) Soft to Medium Brown Silt with Sand "Suffrri":   This third layer occurs at both sites I, (A2), and II, (G2), at 2.6 to 2.8m below the ground surface with the thickness varying from 0.6 to 0.8m (see Plate 4.2). At other locations within the Wadi Area (Bier Al Dar and Near Arwa School), its thickness exceeded 2.0m. In contrast, this layer was not observed at sites III and IV. The main visible features of this layer are the brown colour, its homogeneity with the near absence of gravel particles and the very thin root-holes or tubes lined with white traces of calcium carbonate. The maximum visible diameter of these tubes was about 1mm.

It is very easy to cut and obtain undisturbed samples, when compared with the other selected soils, because of its softness, homogeneity and low gravel content, as shown by its gradation curve in Figure 4.10. It has higher clay and silt contents, and less sand and almost no gravel when compared with the other soils at the same site. Its natural moisture was below the plastic limit. The SPT value (Ns) for this soil was about 8 at a moisture content of 15% as indicated in Fig. 4.9. According to the SPT values, its consistency is medium to stiff after Terzaghi and Peck, (1967) and medium after Bowles (1984).

A3) Medium to Stiff, Light to Reddish Brown Sandy Silt to Sandy Silt with Gravel

'Zanjabili':   This soil was found at all the sites as (A3), (G3), (M4) and (K3). It was found at 3.3 to 3.9m below the ground surface and extended downward below 5.0m at all the sites. This soil resembles the "Suffrri" soil although there are some differences in the soil texture as it has a larger coarse fraction, with well cemented particles of sandstone and/or limestone in the size of gravel grains, and less fines than "Suffrri" soils. Such variations led to variations in the plasticity index and consistency.

The cemented particles were calcareous gravel and may reach up to 18% of the soil. Across the Sana'a Plain, their presence is common to this soil layer, known locally as "Zangabili" which refers to the shape and form of these particles. They have rough, yellowish surfaces with sharp edges and give a subangular to subrounded shape to the particle which ranged in diameter from 1.0mm to over 15mm. They exist in the form of solid veins extending downwards, the length varying from 5mm to more than 100mm (Appendix B4-8/6 -a). In some locations, AD2 and MN0, these particles accumulated near each other to form a vertical sheet or membrane of highly cemented calcareous gravel extending downwards in discontinuous form. Their concentration within a single layer varied from very high, which made it very difficult to obtain undisturbed samples, to lower concentrations from where most of the samples were obtained for identifying the engineering properties. This selection of the samples may have resulted in some bias with respect to the soil texture.

Generally, this soil can be classified as sandy silt, sandy silt with gravel, to sandy silty clay with gravel, according to the texture variation mentioned above and this needs to be borne in mind when considering the results for this particular layer. Fig. 4.13 shows the gradation curves for this soil from the various sites with their different gravel concentrations. The gravel varied from 6-7% at sites I and III, Fig. 4.13(a,b), to 18% at site IV, 4.13(c), while the clay content varies from 6 to 17%. As a result of these variations, the consistency of this soil varies from medium to stiff, with the plastic limit ranging from 20 to 27% and the liquid limit from 30 to 35%. The SPT values are high with respect to the upper layers in Fig. 4.9, and range from 17 to 20 in the sandy silt with low gravel content to 35 in the sandy silt with a higher gravel content.

Soil of Site III

Fig. 4.12(a) indicates the soil profile of this site which consisted of five layers to 6.0m below the ground surface. These layers are described briefly herein with a concentration on the variations as compared with the soils at site I.

M0) - Stiff Brown to Mixed Material Fill: The top layer is a fill and is unlike the stiff lean clay in site I. This fill is simply the result of man-made activities in this site, and it varies in thickness from 0.3 to 0.6m. There is no interest in such fill for this research.

M1) - Medium to Stiff Light Brown Sandy Silt (Suffrri):   This soil is similar to K1 but it varied in both appearance and profile with respect to A1. Its thickness varied from 0.8 to 1.2m and it contained traces of very small, hollow tubular particles, 7 to 15mm in length and 3 to 5mm in diameter. Unlike A1, no gravel particles were observed and so this soil has higher clay (16%) and silt (58%) contents, but a lower sand (20%) content with respect to the other sandy silts A1 and K1. Fig. 4.11 shows the gradation curves for the soils from this site. This sandy silt was relatively homogeneous and so its gradation did not show significant change with depth.

The SPT value was about 9 at a moisture content of 20% as indicated in Fig. 4.12(a) and is similar to the values of A1 and K1, and so the consistency of this layer is rated medium after Bowles (1984) and stiff after Terzaghi and Peck (1967).

M2) - Soft to Medium Dark Grey to Blackish Brown Silty Soil " Soft Carab :   This soil is recognizable by its unique dark grey colour. It exists 1.6 to 1.9m below the ground surface with an average thickness of 1.0m. Fig. 4.11 indicates the very high silt (66%) and clay (24%) contents of this soil. To some extent, this soil is similar to the A2 for they both have the same consistency with high silt and clay contents and low sand and gravel contents, although M2 has a higher fines and lower coarse contents than A2. In contrast, they differ in both colour and general appearance for the thin roots with the white traces present in A2 are absent in M2 and, while M2 contains small, sharp-edged particles in very low concentrations, A2 does have any such particles. The intraparticle pores are less homogeneous in M2 than in A2 and these trapped pores have given rise to the local name "Carab".

The Ns values are very low, 6 at a moisture content of 28%, this moisture content being the highest present within any of the selected soils. The SPT values in Fig. 4.12(a) for the entire profile do not show any sudden change in the values of each 15cm penetration within the same layer which indicates its relative homogeneity at this site, unlike site, I.

M3) - Stiff to Very Stiff Greenish to Yellowish Sandy Silt Soil (Stiff Carab):   This soil has only been detected at this site and its consistency and general appearance are different from all the other soils despite its classification as a sandy-silt. It exists at a depth of 2.7 to 2.9m although at one location, MD2, it was found at 3.1m, with a thickness between 0.3 to 0.7m. The soil is characterized by obvious root holes and pores, reaching 3mm in diameter, even so this soil exhibited high stiffness due to its well graded texture shown in Fig.4.11(c) and the significant adhesion between the different soil grains. Typically, it consisted of 7% gravel, 29% sand, 44% silt and 20% clay. The coarse particles are subrounded sandstone and limestone, generally well cemented within the soil matrix. In some areas "Zangabili" type

gravel particles, up to 20mm in diameter were found, but in other areas no gravel was found. As a consequence of these variable gravel contents, cementation and non-uniform pore distribution, sampling was very difficult leading to some disturbance.

Compared to all the other soils, the Ns value was very high, 25 blows at a moisture content of 12%, as shown in Fig. 4.12(a), so the layer was classified as stiff to very stiff.

M4) Medium to Stiff, Light to Reddish Brown Sandy Silt to Sandy Silt with Gravel 'Zanjabili':   This soil resembled A3 and was found at almost the same depth as A3, 3.8m although, compared with A3, it had less gravel (4%) and clay (4%) but more silt (54%) and sand (34%) as indicated in Fig. 4.11(d). It did not have a high gravel content or any calcareous concentrations as is clear from the similarity of the Ns values at different levels, apart from the high values between 3.7 and 4.1m. Here there was a transition zone of dense medium to fine sand with low gravel content between the layers, M3 and M4, as shown by the high Ns value (35) in Fig. 4.12(a). Below 4.1m and up to 5.5m the Ns value varied in the range of 13 to 16 with no sudden changes, indicating the absence gravel and sand pockets or concentration present at site I.

The soils M2 and M3 were not identified in the previous investigations carried out by Al-Gasous (1988) and Abduljauwad et al (1991), therefore they should be added to those common seven units which covered the Sana'a area.

c) M1 at 1.0m

a) A1 at 1.5m

d) K1 at 2.2m

b) A2 at 3.0m
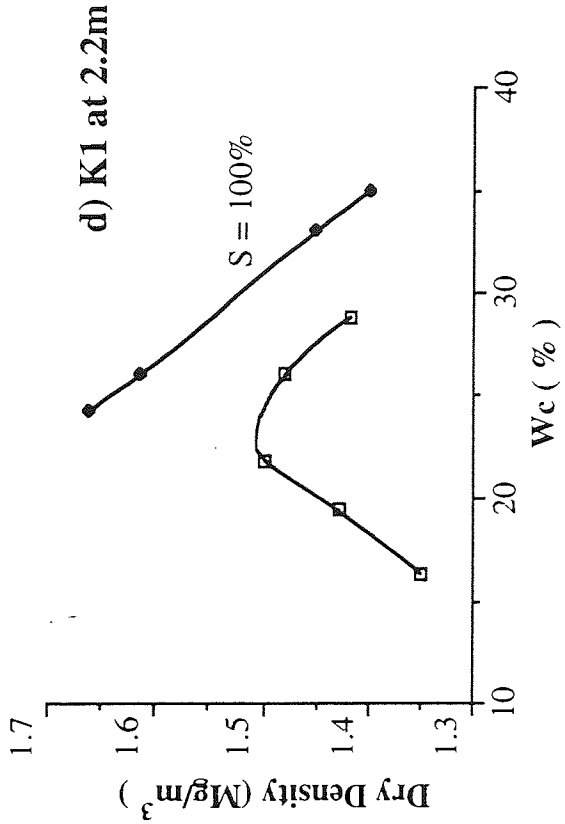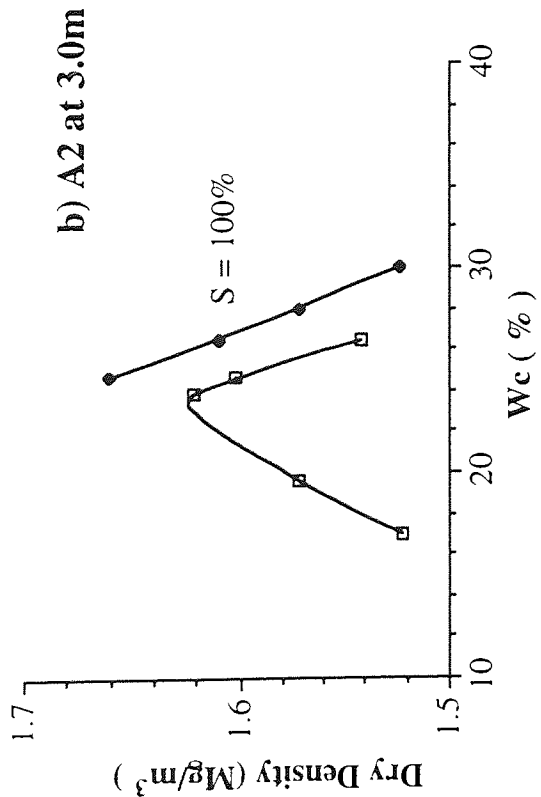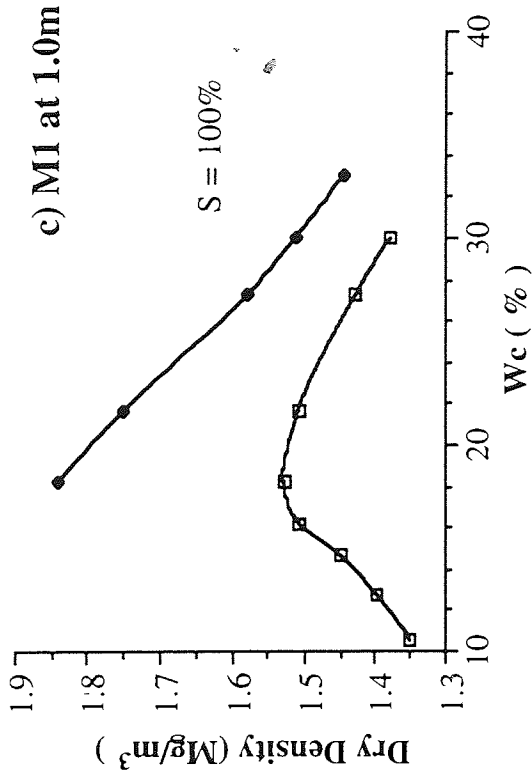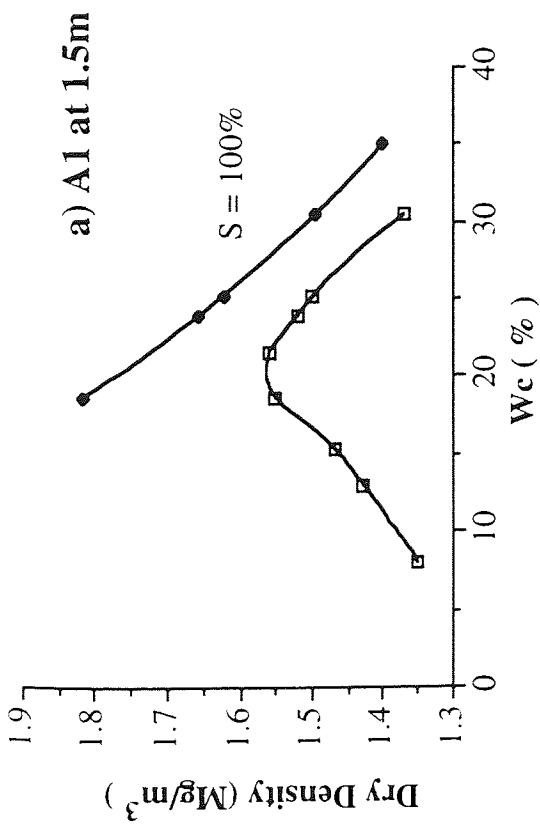
B4-4 : Typical moisture-density relationship for soils from various sites.
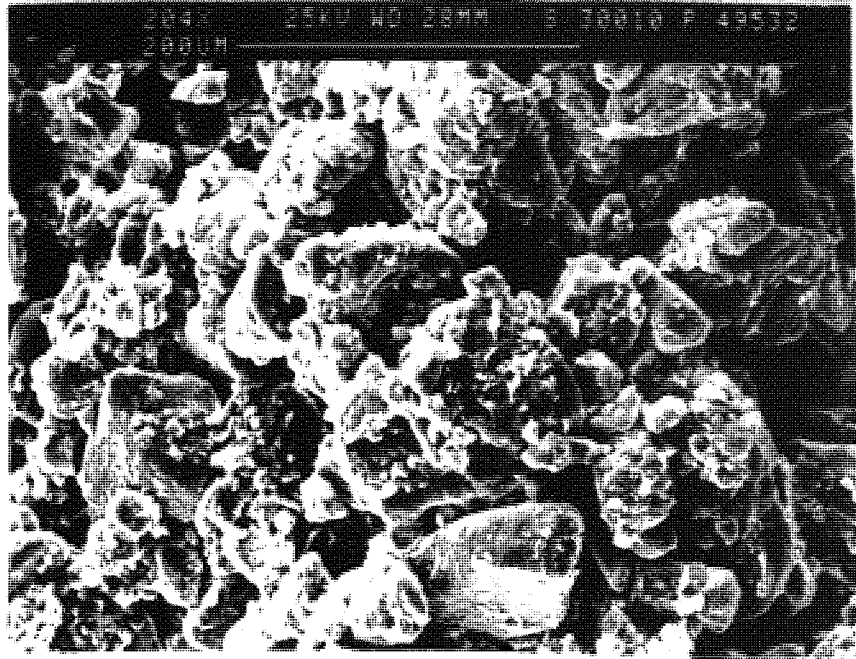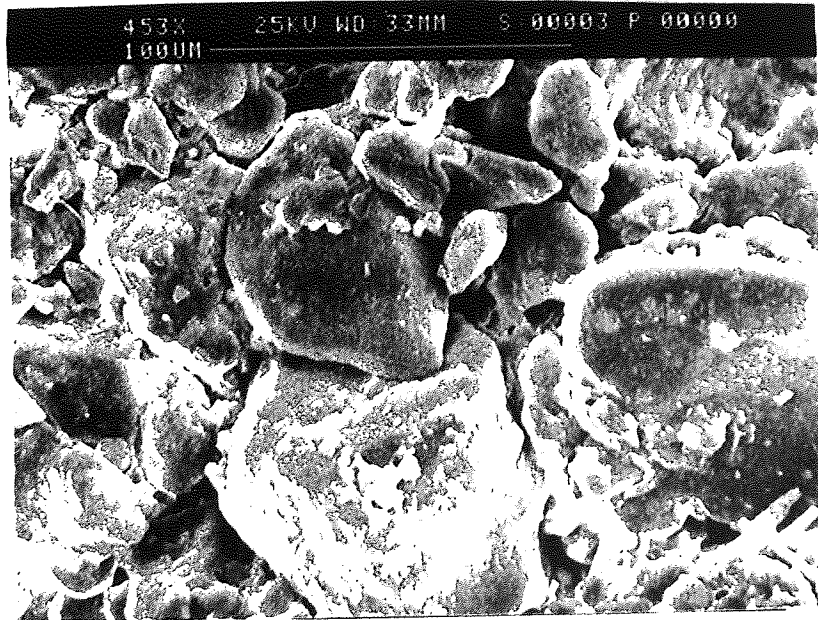
B4-5 : Open soil fabric of the sandy silt.

a) Very open fabric of soil M1 at 1.2m.

b) Moderately open fabric of soil A1 at 1.8m.
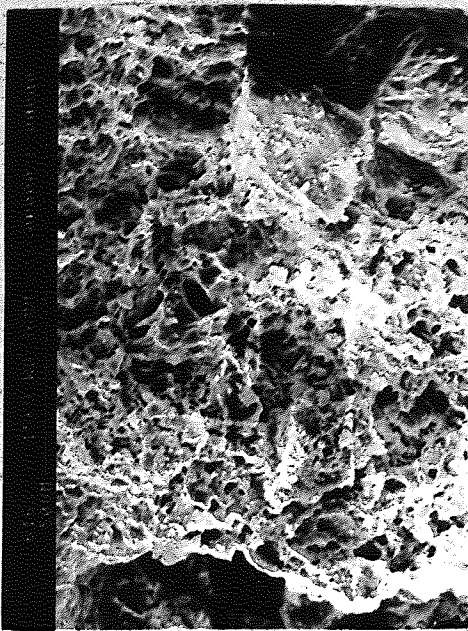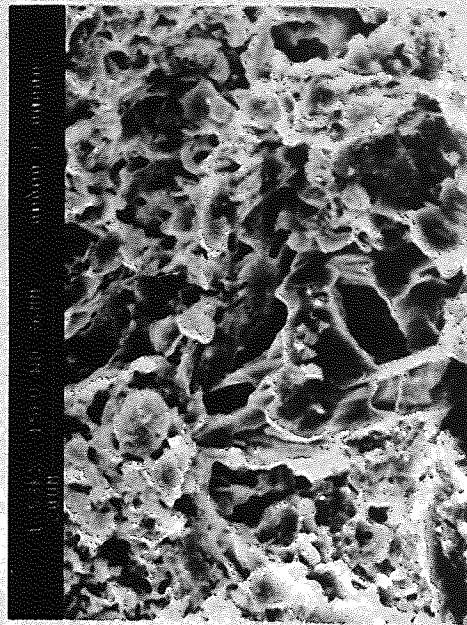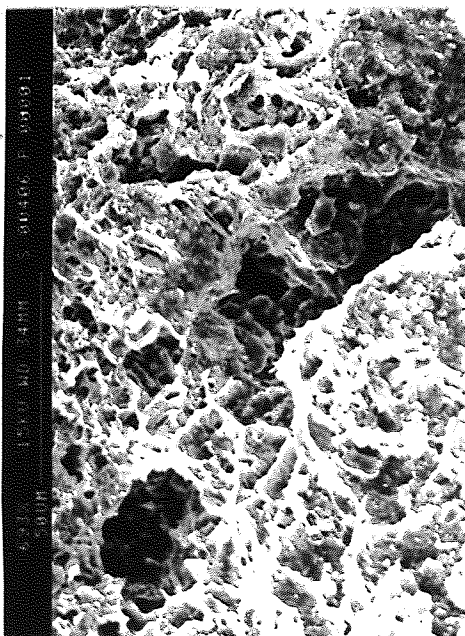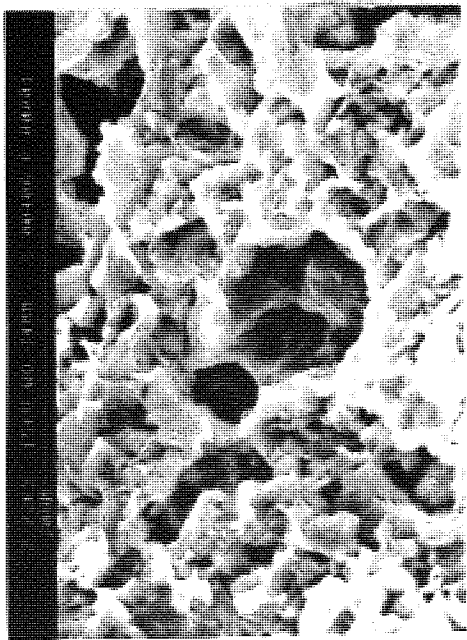
B4-6 : SEM of the high aggregations and coated assemblages with cementation agents including the interparticle and assemblage pores of, the silt with sand, A2 (a,b), and silt, M2 (c,d), soils.
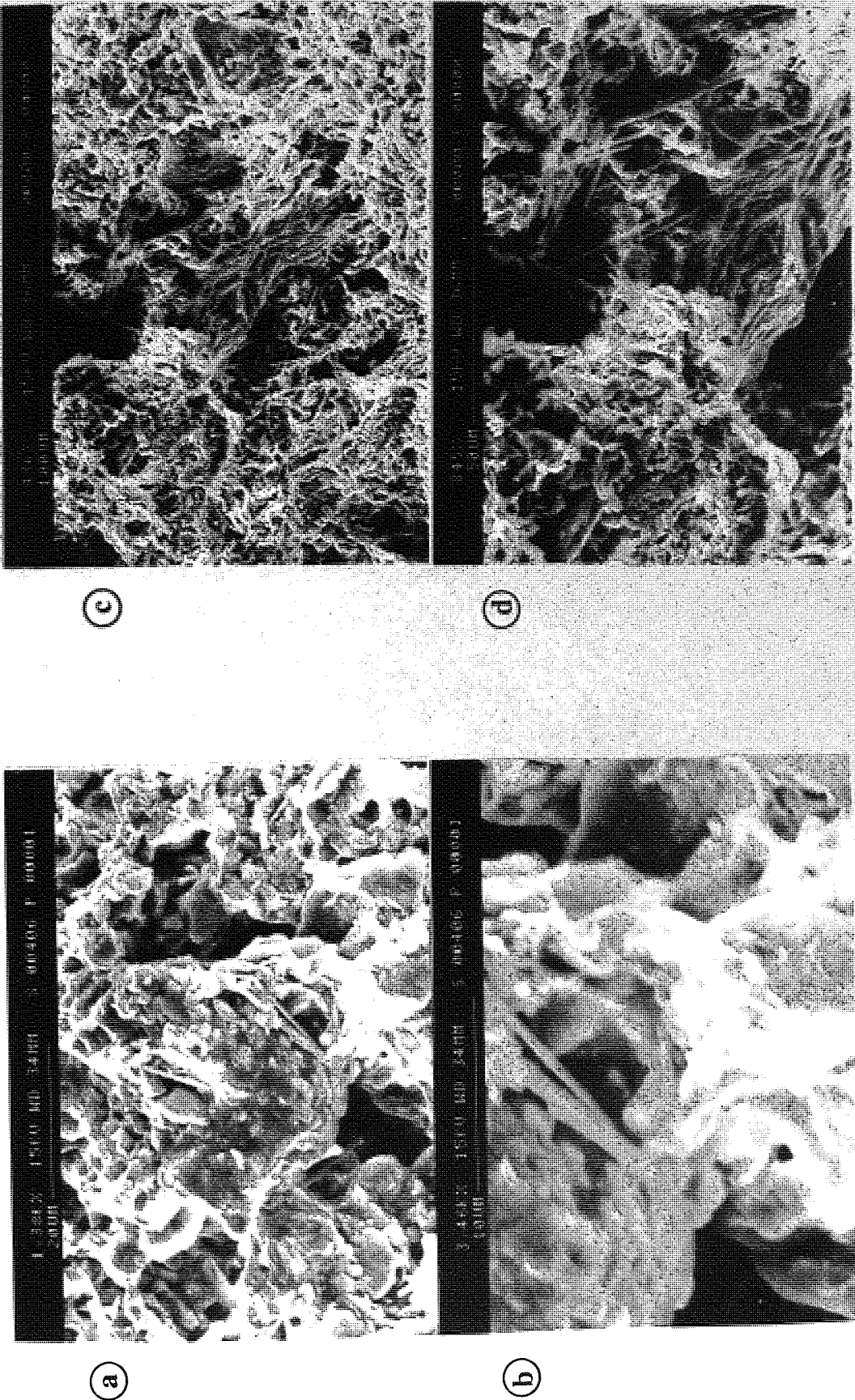
B4-7 : Assemblages and assemblage connectors of silt with sand, A2 (a, b), and silt/silty clay, M2,(c,d). (b) and (d) were taken with a higher magnification than (a) and (c).

B4-8

Depositional Effects on Soil Fabric

Soil fabric is influenced by the depositional processes and environmental conditions. The soil formations of Sana'a Plain have yet to be classified with respect to the effect of the depositional and environmental conditions but the general features of the selected soils are considered below.

Derbyshire and Mellors (1988) reported that there is little information available about the unweathered fabric of freshly sedimented aeolian silt but young, unweathered loess from the semi-arid Lanzhour region may provide a preliminary model. This consists of a clean angular to sub-angular silt skeleton, with abundant face-to face contacts, with widely scattered clay particles. Weathering has affected this young fabric so that through repeated wetting and drying, the clays have become aggregated and flocculated. The leaching process has led to accumulations of fine clay forming bridges and buttresses and/or to coating the larger sand-silt grains with fine clays. These processes produced weathered formations in the upper leached horizons and precipitation in the lower horizons so that the soil fabric across the entire soil profile has been reformed.

The consequences of weathering can be identified by studying the texture, composition and fabric of the soil. Derbyshire and Mellors (1988) indicated that clay, in the form of bridges and coatings may be locally abundant in weathered soil horizons. Weathered brickearth soils from Kent and China showed etching of feldspars and calcite grains. In loess samples that have not been decalcified, calcium carbonate is found to be distributed throughout the specimens both as discernible grains and as tubular lining to rootlet holes. In the oldest loess, silica and iron can also become concentrated as a cement at grain contacts, particularly at the silt-size quartz and feldspar grains.

The chemical and mineral composition and textural features can be used to classify loess soil. Buraczynski (1988) adopted four basic groups for this lithological description of loess as shown in Table 4.11, and both this system and the prior description provided by Derbyshire and Mellors (1988) have been used to classify the selected soils.

The first soil, A1 has been greatly affected by the depositional and environmental factors with evidence of water transformed sediments at different levels within this layer. The effect of leaching is highly pronounced with examples of clay coating (Fig. 4.18-a), clay bridges and eroded aragonite around the rootlet holes (Fig. 4.14-b). These effects were more prevalent in the upper zone of this layer, 1.1 to 1.5m, than the lower zone, 1.8 to 2.8m. In

the third layer, silt with sand - A2, calcium carbonate in the form of aragonite needles was detected around the walls of the channel and rootlet holes, B4-8/1. Aragonite and calcite have the same chemical composition but, due to difference in their molecular structure, aragonite is more soluble (Chaney et al, 1982). The aragonite of A2 does not show any evidence of erosion or dissolution which suggests that this layer is unweathered. The general features of this soil layer, including fabric, chemical and mineral composition and the physical properties, are typical of loess or aeolian deposits (Sergeyv et al, 1973). It did not show the bridge systems or the particle coating as the other soils, A1, M1, M3, although the assemblages were coated with clay and cement. The coating and cementing of the silt grains and assemblages and the contacts between these assemblages may be produced from the chemical precipitations leached from the top layers, A1 and the lean clay -A0, rather than being due to the weathering of this layer, A2. However, the presence of the top layer of impermeable lean clay probably acted as a protection against such further weathering.

Weathering of the soil at site III was obvious in terms of leaching, precipitation and oxidation. The light brown sandy silt of the top layer had a clay content within the range of weathered loess as shown in Table 4.11 and many of the features of such weathered soil were observed. The consequences of leaching and precipitation are apparent in B4-8/2 which show the erosion of aragonite in the upper layer, M1, and its precipitation in the lower layers as calcite, such processes represent the transformation process of aragonite to calcite.

The structure around the rootlet holes and channels in the silty soil, M2, shown in B4-8/3 indicate that most of the aragonite had been transformed to calcite due to the leaching, for only arching structures of aragonite were found around channels. This can be defined as the "intermediate stage" in the transformation of aragonite to calcite since the dissolving of aragonite and its regrouping to form calcite had not been completed.

Buraczynski (1988) indicated that weathered loess typically has a silicon content between 65-72%, compared to only 50% for unweathered loess. The silt contents of the M2 soil is very high, 66%, and this is indicative of a high silicon content (Derbyshire and Mellors,1988). In addition, its high clay content, 24%, is typical for weathered loess shown in Table 4.11. Moreover, both this soil and the underlying layer, M3, had very high iron oxide contents of 32 and 38% respectively, as shown by the EDS plot in B4-8/4. The dark grey to blackish area in the photomicrographs is an indicator of iron oxide. Generally the darker the colour of the soil the higher its iron oxide content, and so the blackish brown colour of M2 indicates the presence of iron oxide which was not significant in the reddish to yellowish brown silt with sand, A2. This silty soil, M2, is classified as a weathered aeolian formation and may be described as a moderately weathered.

The third layer at site three is the greenish yellow to beige, very stiff, sandy silt, M3, which exhibited extensive weathering. B4-8/5 shows the presence of calcite in this soil,

produced from the highly eroded aragonite. The calcite occurs as bulky particles, or shells, (Mitchell, 1976), with some etching calcite grains similar to the weathered brickearth loess from Kent and China (Derbyshire and Mellors, 1988), as shown in B4-8/5 (a,b). This layer, M3, was the most stable of those investigated and this may be due to its relatively high clay, 20%, and sand, 29%, contents together with the concentrations of both calcite and iron oxide as cementing agents. Weathering and decomposition of this layer resulted in reforming it in a state that it could be classified as a modified or secondary loess (Terzaghi and Peck, 1967). The calcite accumulated either in the trapped pores, to form gravel particles as white limestone grains, or with aggregations of quartz and sand-silt grains, to form fine to coarse gravel (7-10%) as light yellowish sandstone. Such particles resembled the gravel particles of the lower layers (A3, M4 and K3) but were much smaller, 2-7mm in diameter, than the particles in these layers. B4-8/6 indicates the particles with sharp-edges in M4 together with highly concentrated structure of calcite.

The final soil is the sandy silt with gravel (A3, M4 and K3), which may represent the top layer of a second repetitive layered system. It was found at virtually all the selected sites, despite some variations in the gravel and clay contents. It was very similar to the top sandy silt layers (A1, M1 and K1) in its general features apart from the presence of highly cemented gravel particles with sharp edges (B4-8/6). It was characterized by having clay contents below 9%, together with high sand and gravel contents at 28 and 12% respectively. In some locations the gravel content exceeded of 17% and this made it difficult to obtain undisturbed samples. This soil was unlikely to be affected by mechanical destructuring or improvement as it was likely to lie beyond the affected depth and so it was not investigated in detail. Table 4.12 summarizes the general structural and weathering features of the different soils.
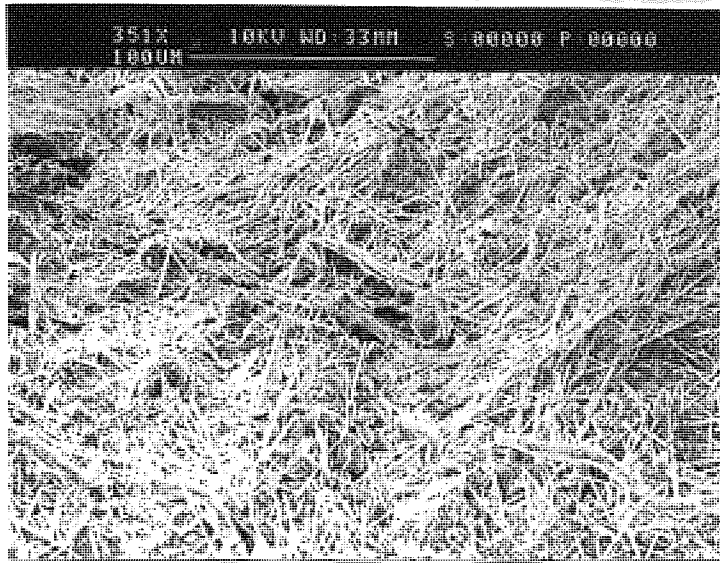
B4-8/1 : Rich, unweathered, aragonite needle structure found as;

    a) Calcareous tubular linings to rootlet holes, and

    b) Around the pores as arching structures.
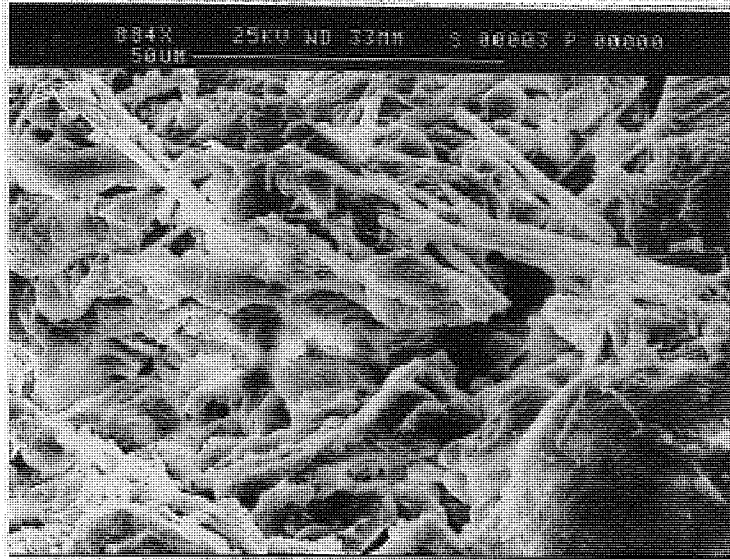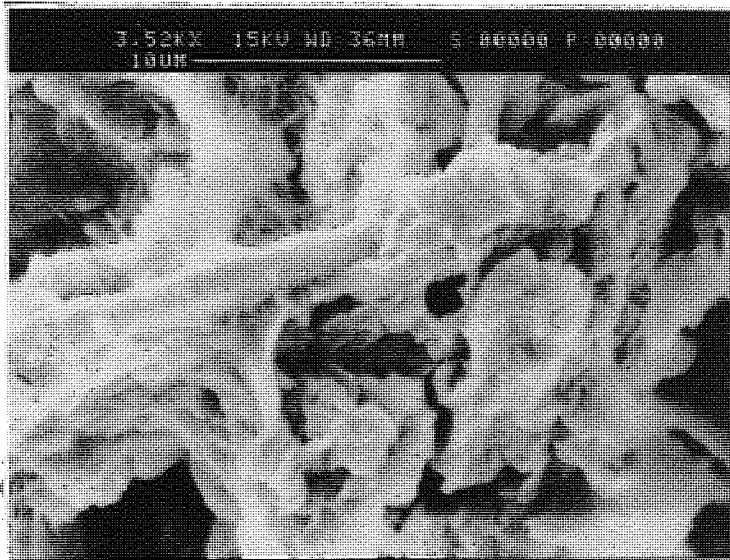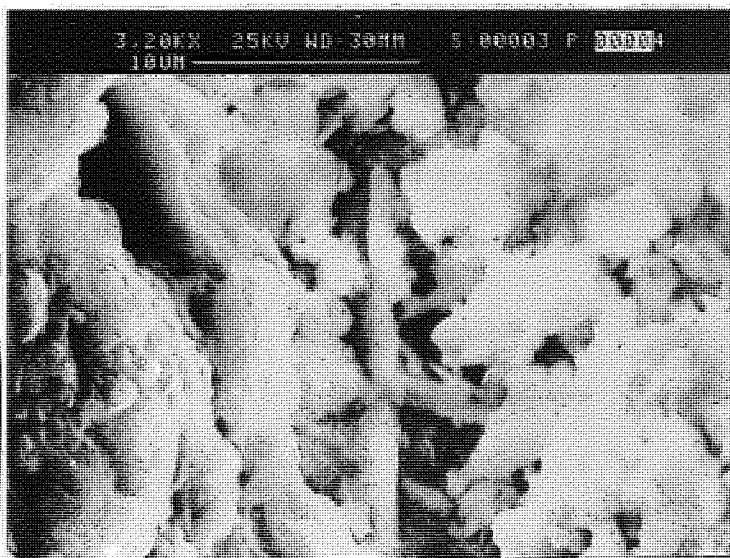
B4-8/2 : Leaching of aragonite from the top horizon, sandy silt M1 (a), to the lower horizons, M2 (b) and M3 (c).
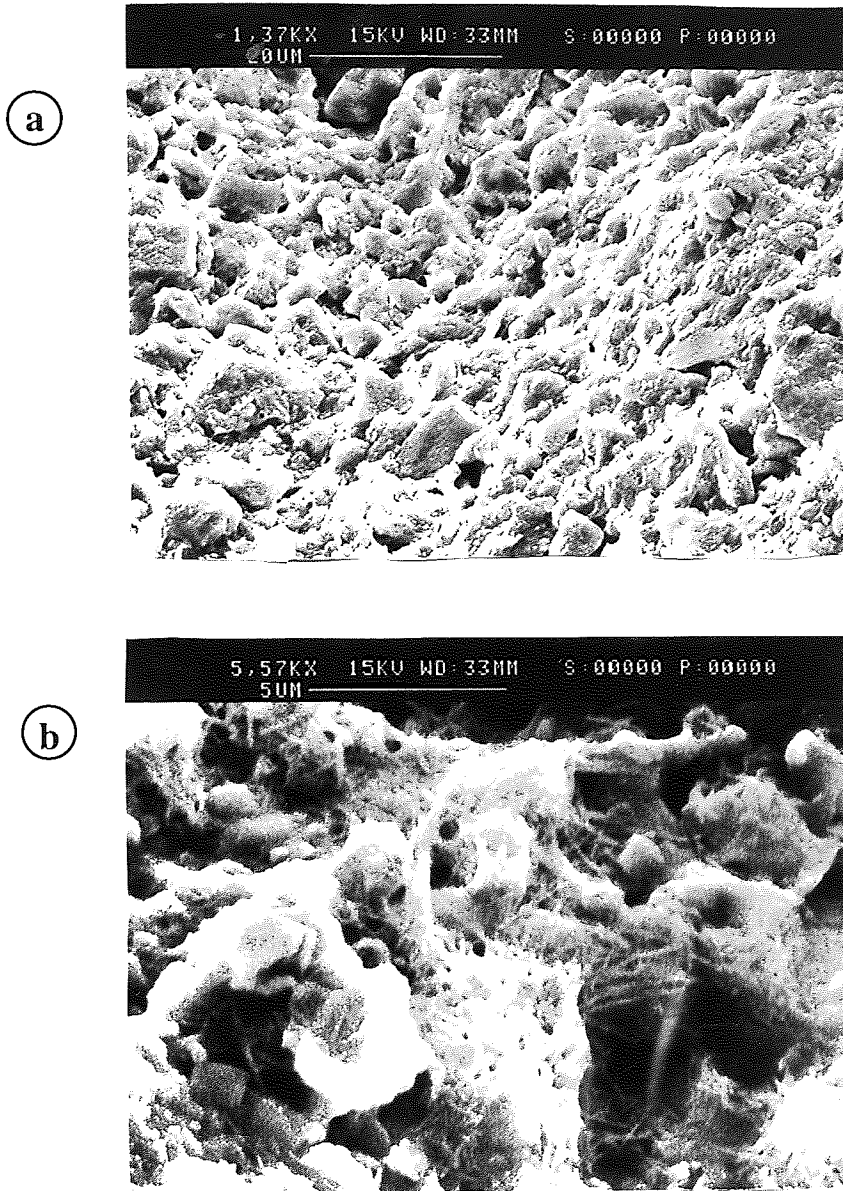
B4-8/3 : Intermediate stage of aragonite leaching and transformation, within the upper horizon (M2) indicating;

a) Concentration of calcite-aragonite within the channels, and

b) The microfabric of the partially transformed aragonite.
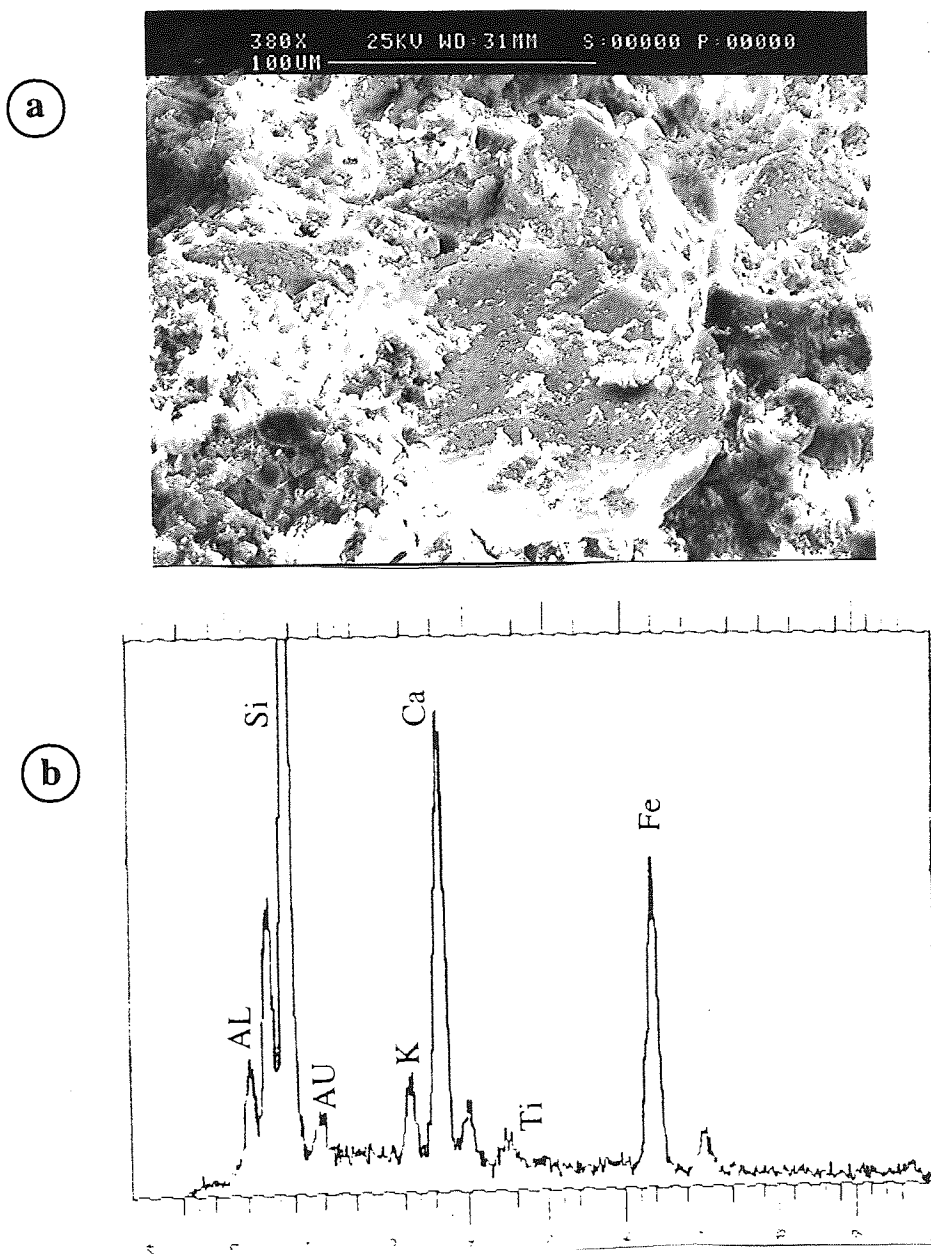
B4-8/4 : High iron oxide occurrance detected in M2;

a) SEM of the coated grain with iron oxide content of 32%, and

b) EDS of the view in (a).

369
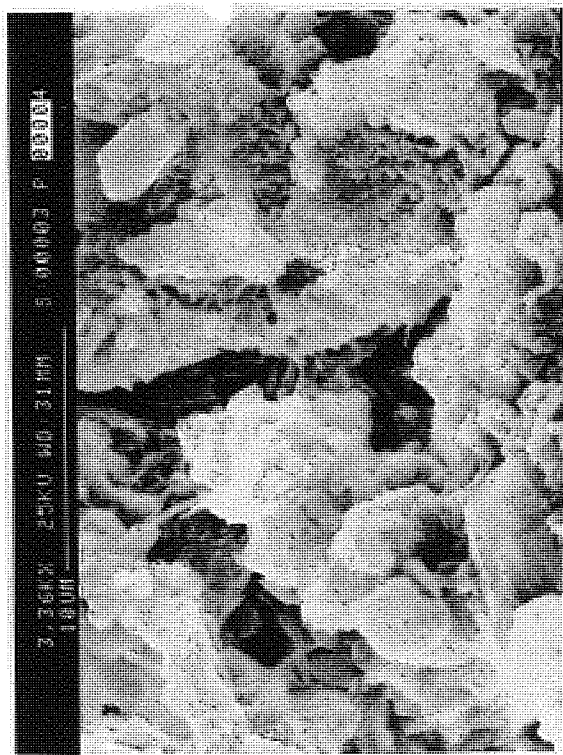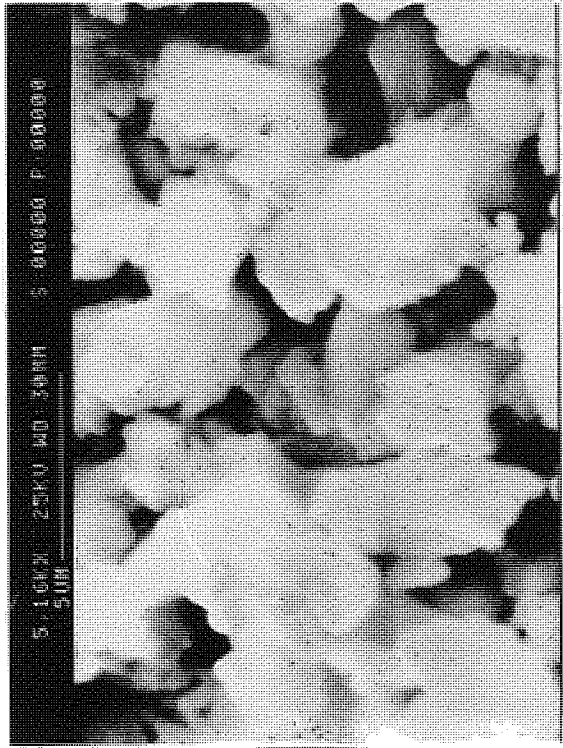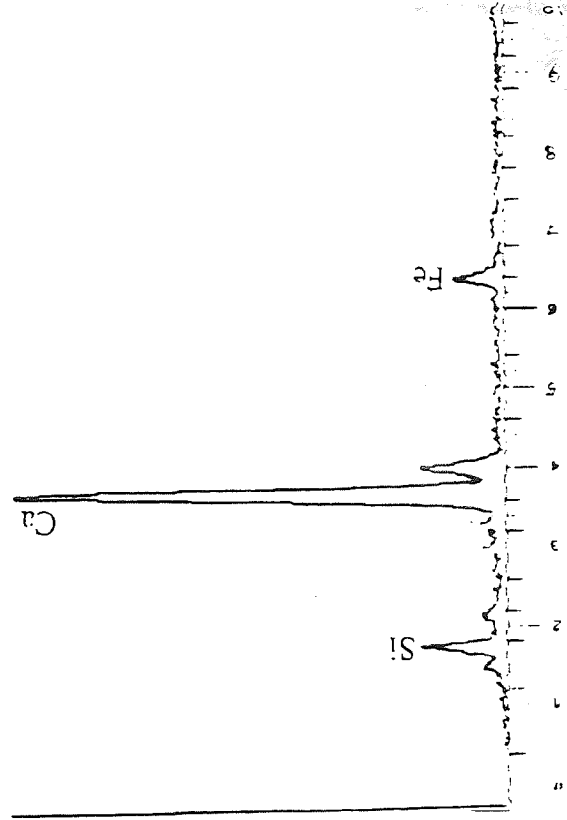
B4-8/5 : Calcite structure derived from the leached aragonite, penultimate stage into the lower horizon, sandy silt-M3, indicating;

a) High calcite concentrations, 38%, with etching grains, bottom left;

b) Crystal structure of calcite, and

c) EDS of calcite shown in (b).
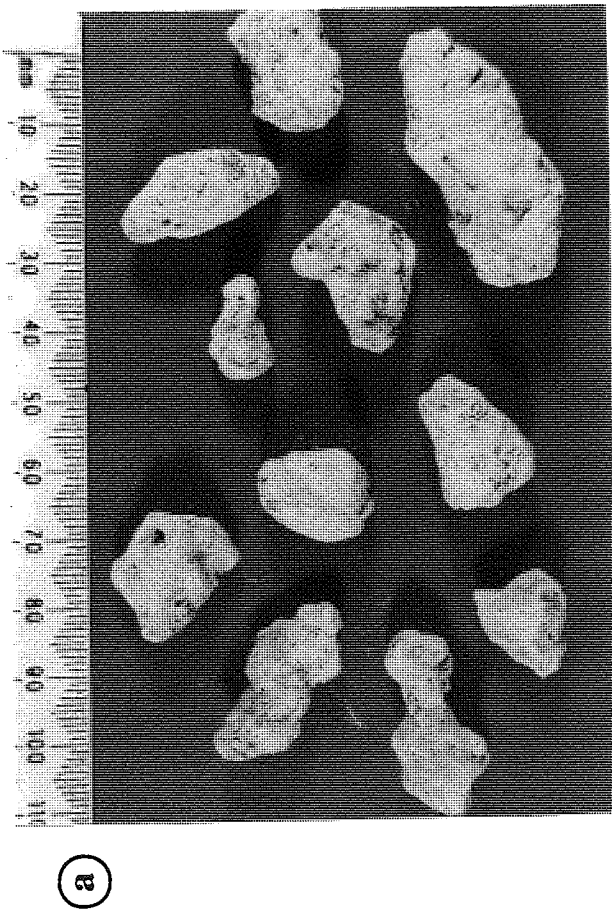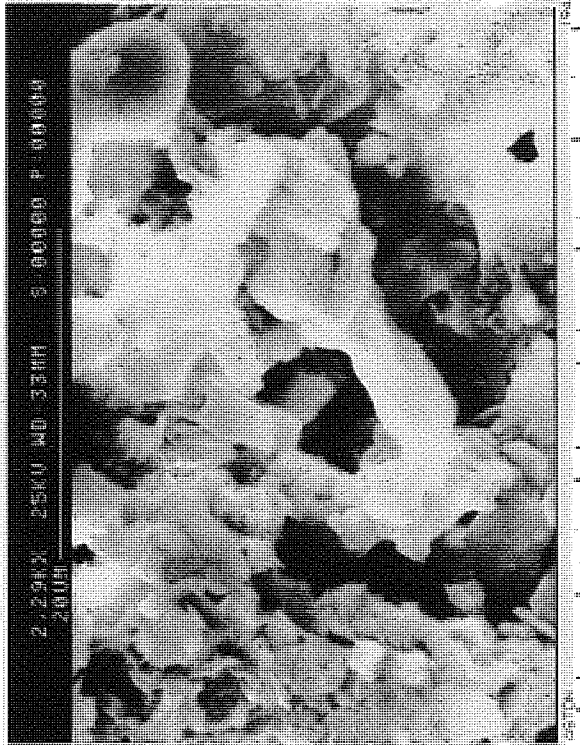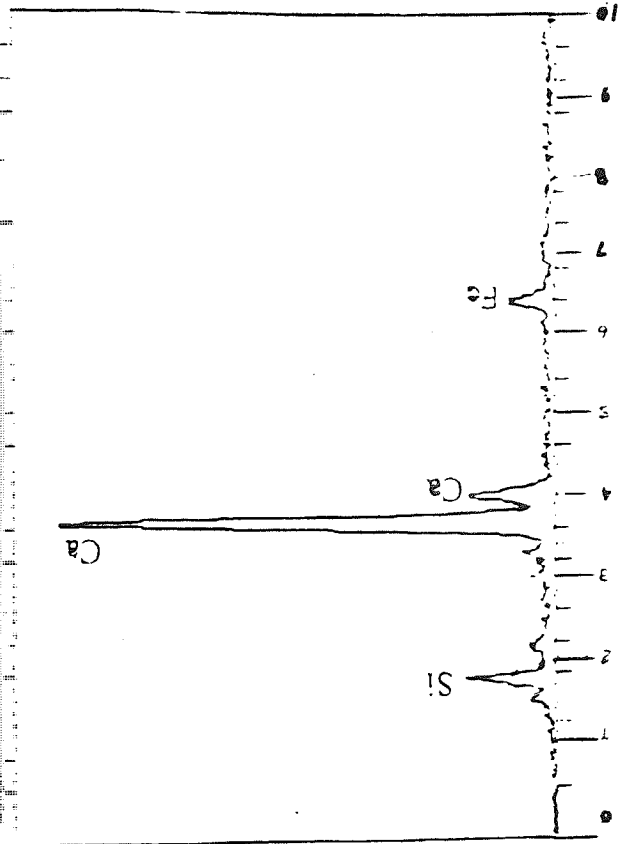
B4-8/6 : SEM of the limestone gravel with sharp edges from the sandy silt with gravel indicating;

a) Low magnification of the structure;.

b) Microstracture of the high calcite concentrations with clay particles and presence of micropores; and

c) EDS of the view in (b).

APPENDIX   C5

A2 at 3.0m

C5-1 : Collapsing potential of A2 from 3.0m below the surface.

C5-2 : Collapsing potential of the natural soils, G1 and G2 from site II.
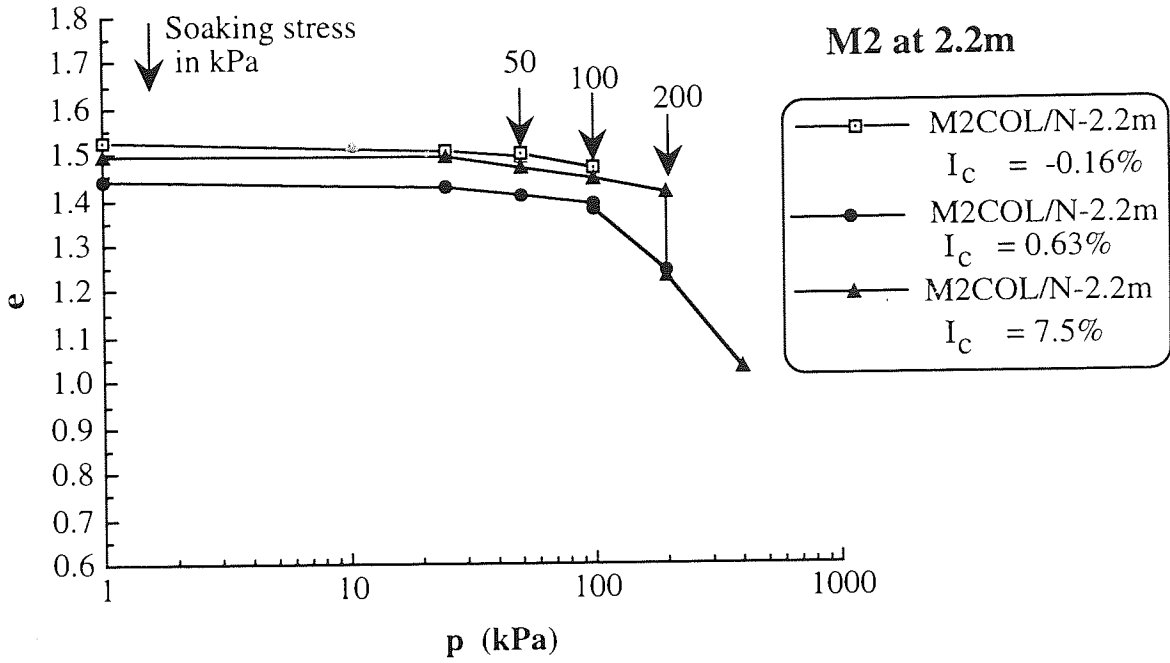
C5-3 : Collapsing potential of M2 from 2.2m below the surface.
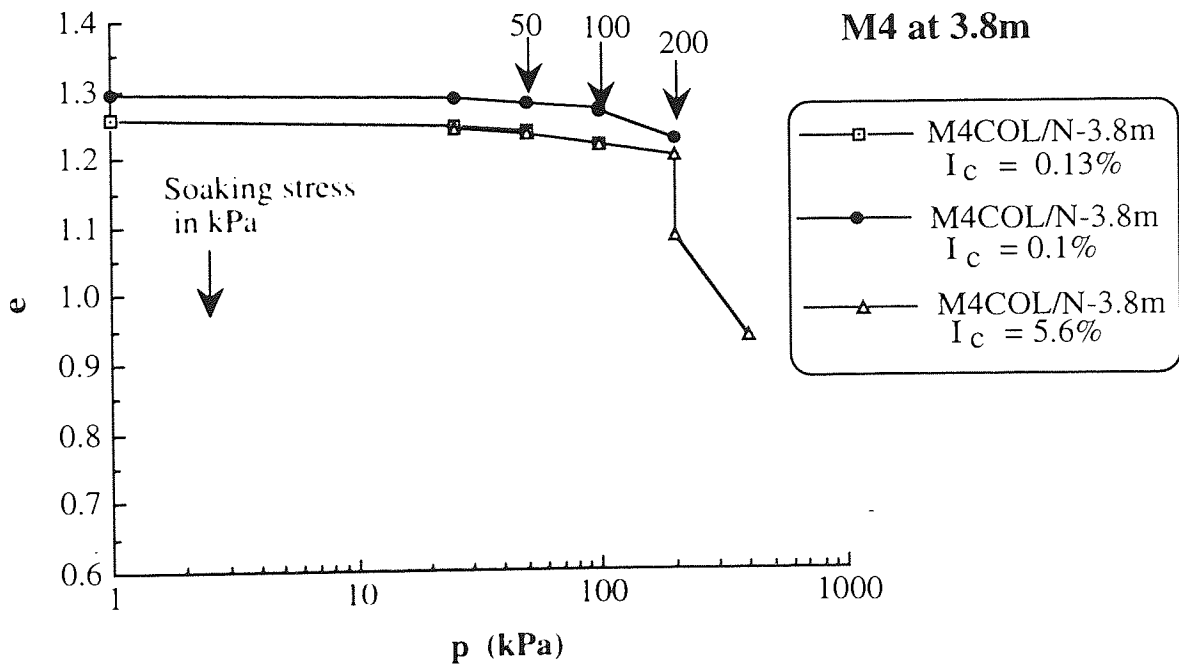
C5-4 : Collapsing potential of M4 from 3.8m below the surface.
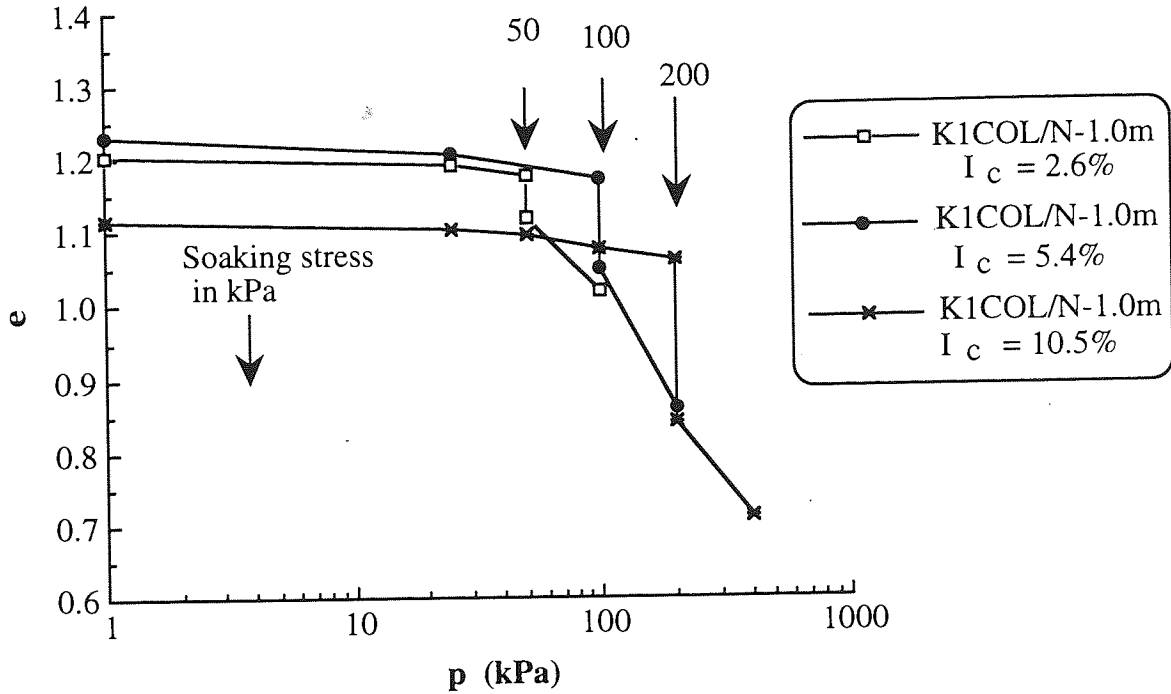
C5-5 : Collapsing potential of K1 from 1.0m below the surface.
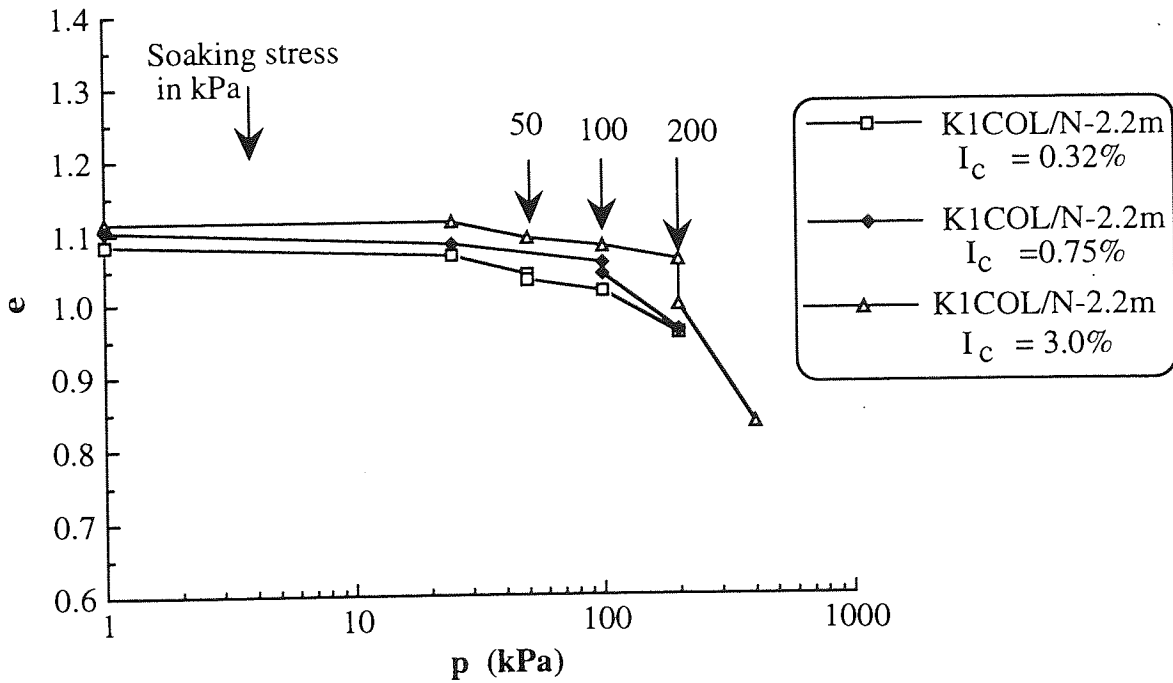
C5-6 : Collapsing potential of K1 from 2.2m below the surface.

C5-7

Procedures For The Consolidation Test

1) The empty ring was weighed and its internal diameter and height were measured.

2) The specimen was cut, trimmed into the ring, and levelled and the ring and specimen (sample) were weighed. The trimmed soil was used to determine the moisture content.

3) A filter paper was placed over the bottom porous stone and the sample was placed in the consolidation cell over the filter paper.

4) The beam was adjusted and the dial gauge set under a seating load of 0.5 to 1.0 kPa.

5) The specimen was saturated by adding the distilled water into the cell, before applying any further stress to the specimen.

6) The specimen was loaded incrementally, starting either from 6.25 or 12.5 kPa, and continued up to 800 or 1660 kPa followed by unloading to 200 or 100 kPa. The period of consolidation under each load increment was 24 hours and the load increment was unity (i.e. every load except the first one was double the previous load.

7) During consolidation under loads of 100, 200 and 400 kPa, dial reading were taken at the following times 0.25, 0.5, 1, 2, 4, 8, 15, 30, 60, 120, 240, 480 and 1440 minutes.

8) After the final unloading, the cell was drained and the specimen was removed and weighed.

9) Finally, the specimen was dried in the oven under 110 °C then its dry weight, and hence moisture content, determined.
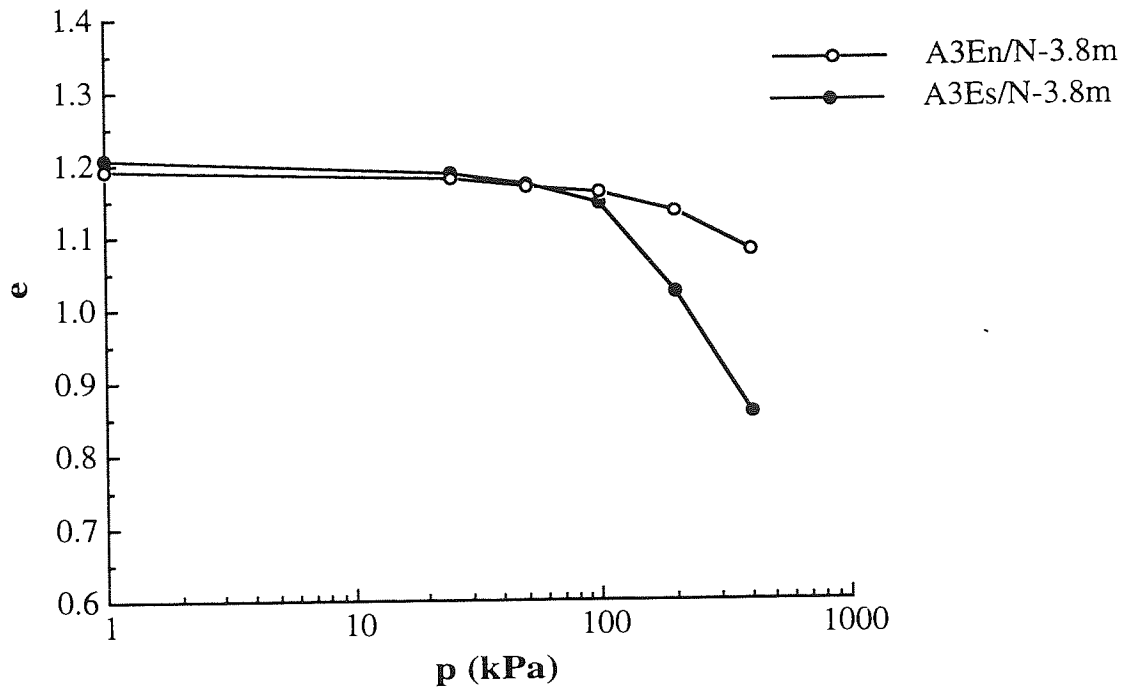
C5-8 : Oedometer test results for the natural samples of A3 tested at the natural and soaked moisture conditions.
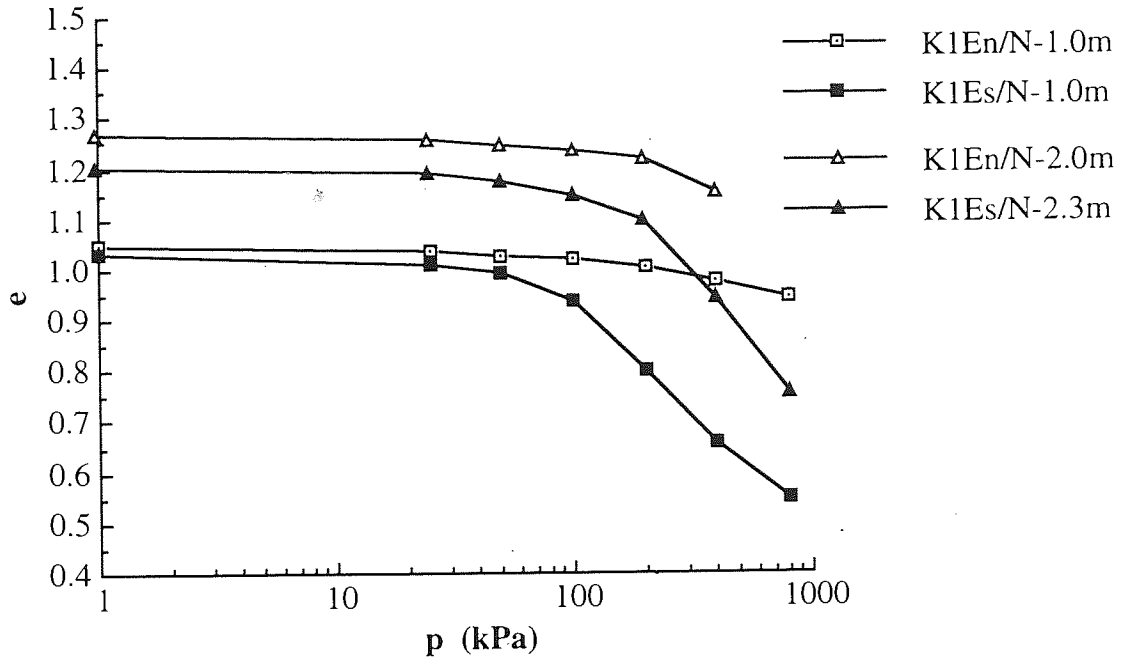
C5-9 : Oedometer test results for the natural samples of K1
tested at the natural and soaked moisture conditions.
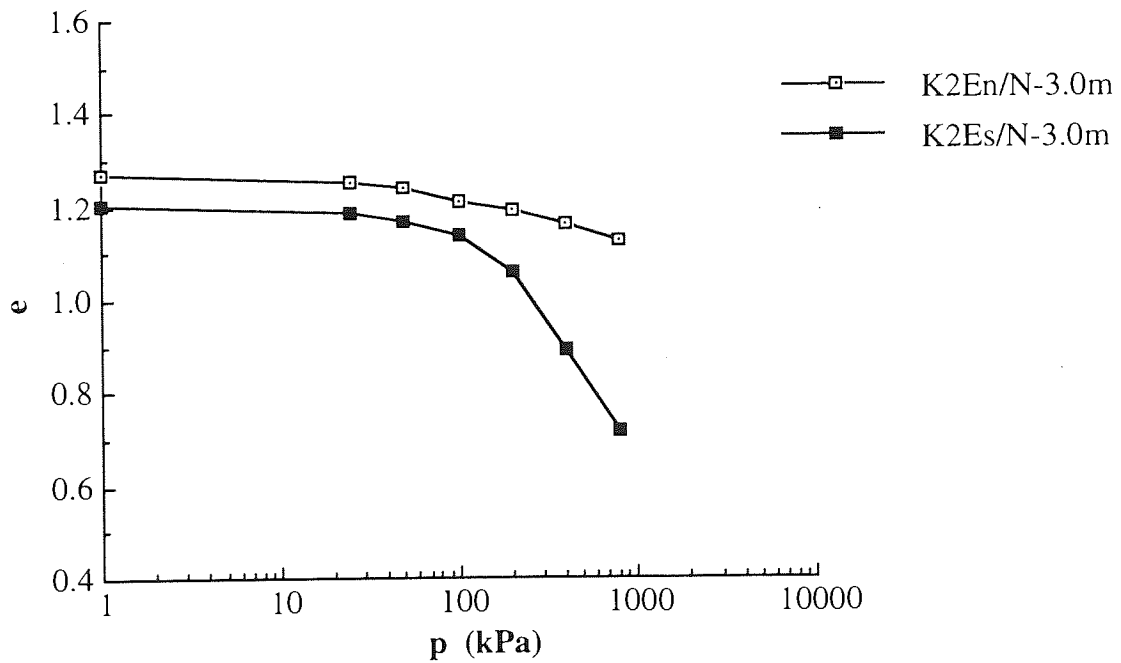
C5-10 : Oedometer test results for the natural samples for K2
tested at the natural and soaked moisture conditions.

C5-12 : Values of C_c , C_v , C_s of clay minerals (Adopted from Mitchell, 1976).

Clay mineral	C_c	C_v $\times 10^{-4}$ cm^2/ sec	C_s
Kaolinite	0.19 - 0.28	12 - 90	0.05 - 0.08
Montmorillonite	0.5 - 1.1	0.03 - 2.4	0.11 - 0.37
Illite	1.0 - 2.6	0.06 - 0.3	0.34 - 1.53
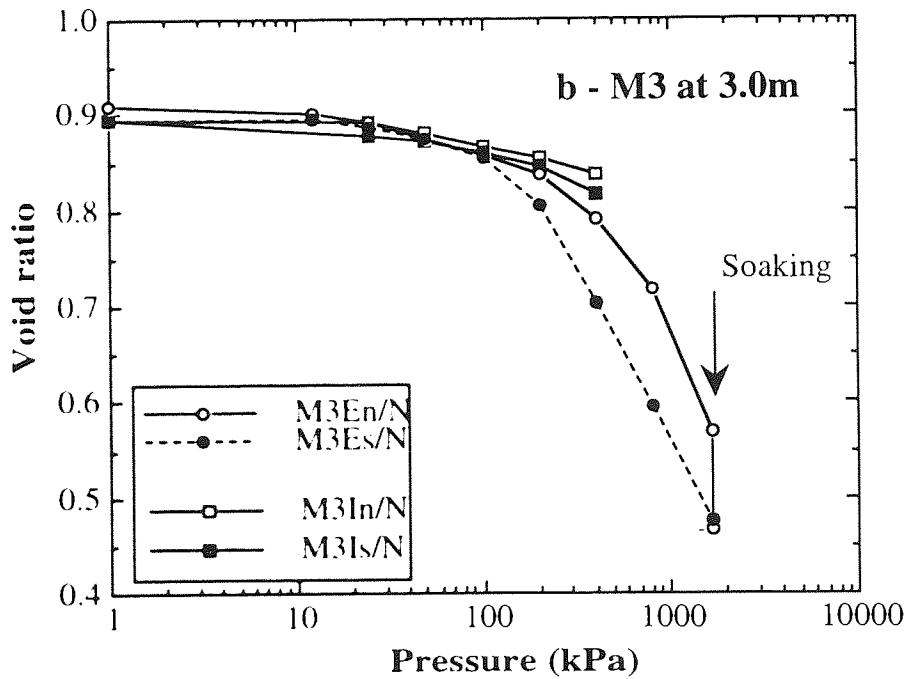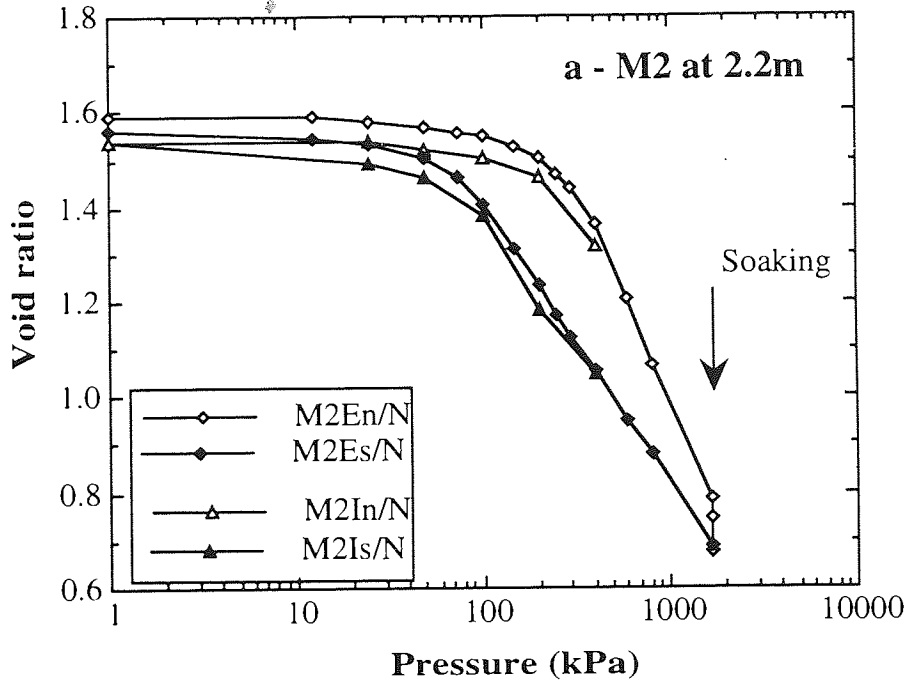
C5-13 : Results from the double oedometer and isotropic
compression tests for the natural soils from site
III, tested at the NMC and SMC conditions.

APPENDIX   D6

1.50m

5 tiles 25*25*2 cm

D

C

3.00m

2.50m

1.50m

E

a

A

B

2.50m

3.0m

MF4

N

E

Scale 1:50

MF3

5.25m

3.25m

MF2

1.50m

1.25m

b

MF1

(− 0.60)

(−0.50)

G.S.L. (0.00)

D6-1 : The flooding location MF, shown;
    a) The distribution of the measuring marks, and
    b) The distribution of the SPT locations, MF1 to MF4.

D6-2 : The variation of dry density with depth for the flooded soils from the location KF at site IV.
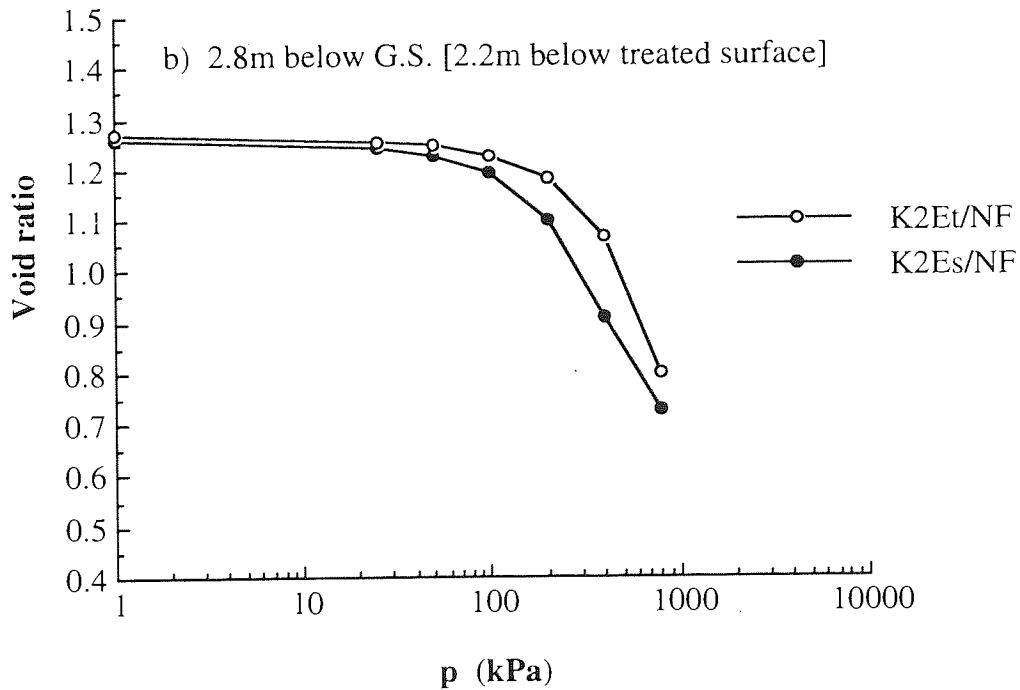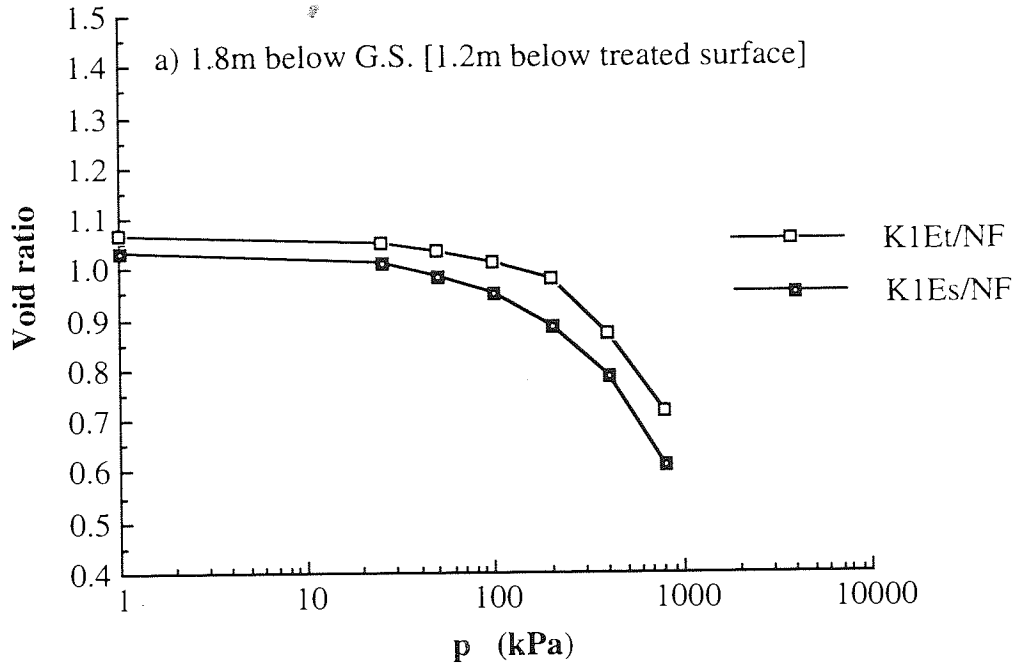
D6-3 : Oedometer results for the flooded soils at KF,
tested at both moisture states -TMC and SMC.
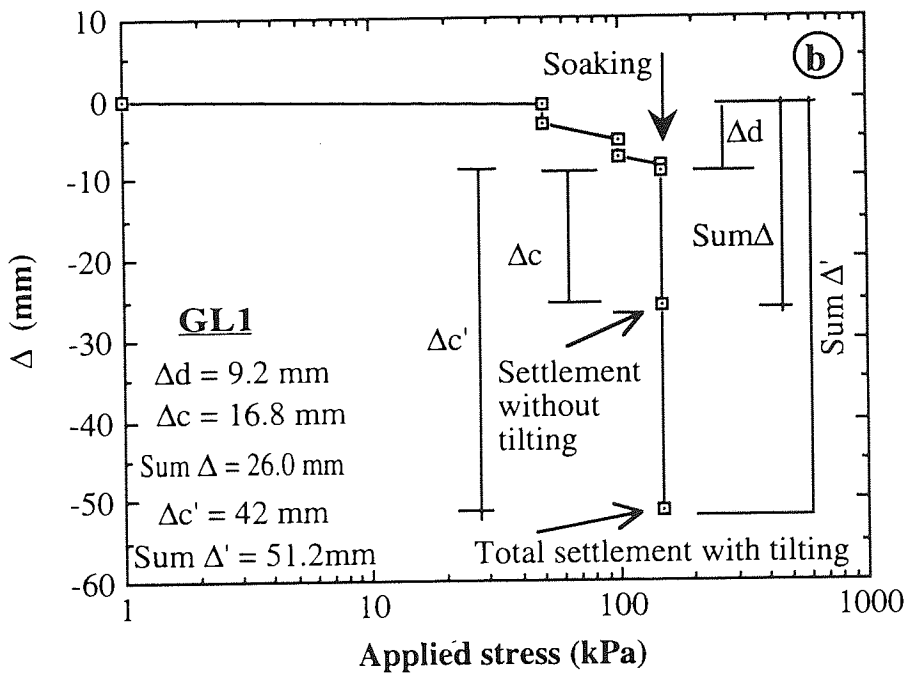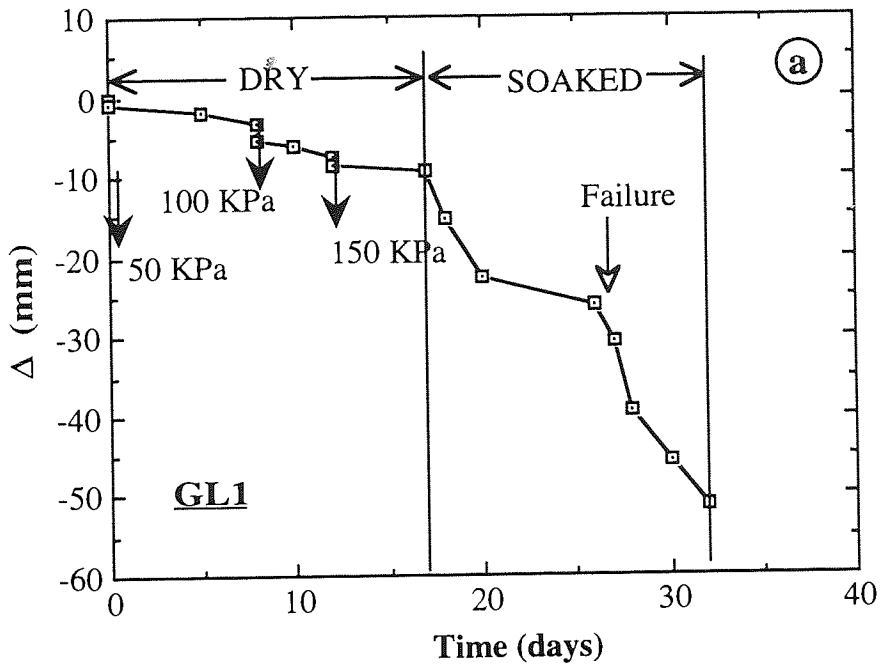
D6-4 : Field collapsing test results at location GL1 under a total load of 150 kPa.
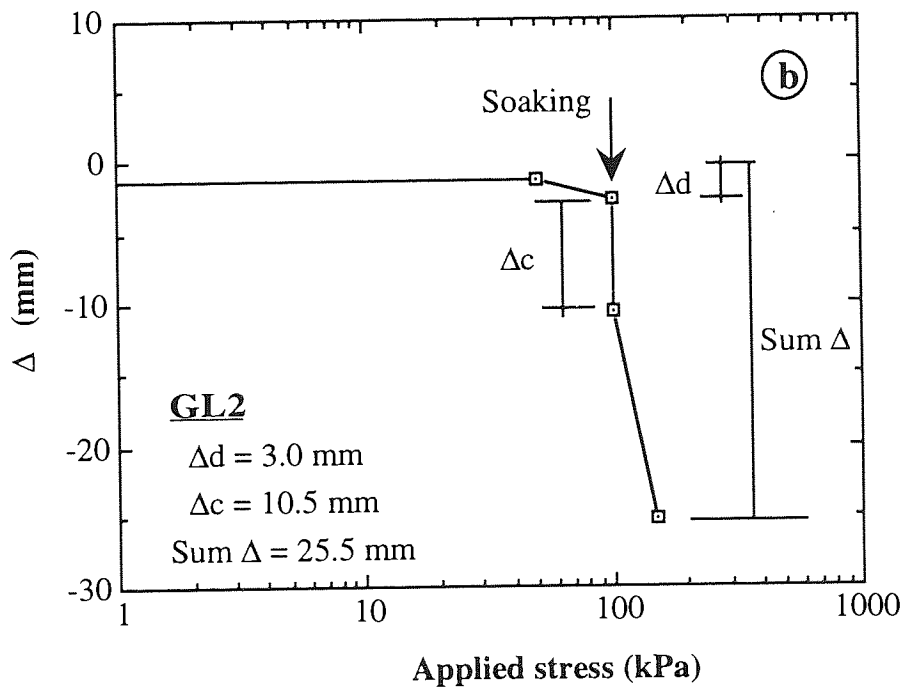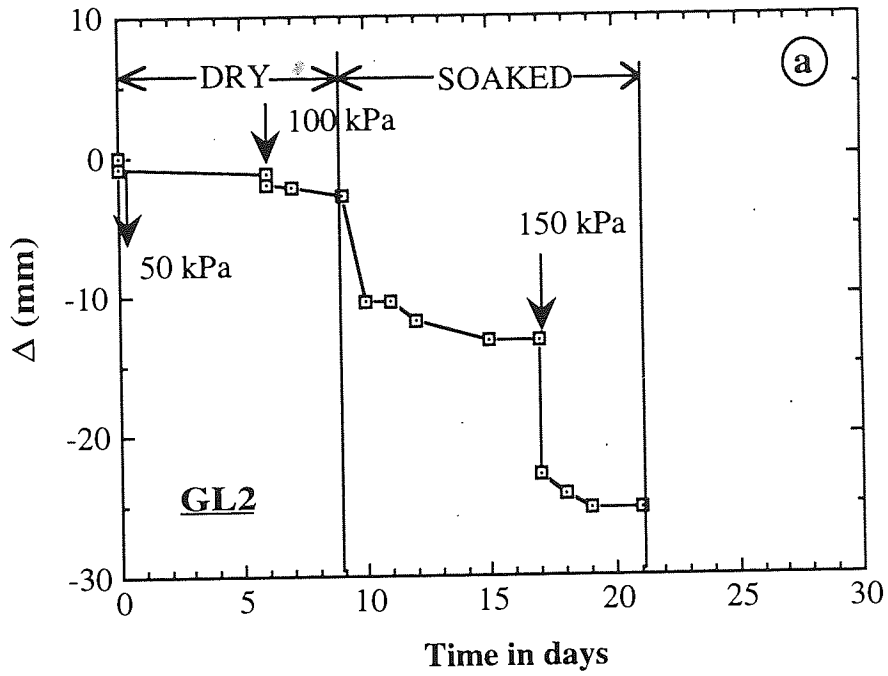
D6-5 : Field collapsing test results at location GL2 under
a total load of 100 kPa.

D6-6 : Typical field loading data sheet of the location ML1.

DATE	Time (Days)	Sum time (days)	State	Loading (KPa)	a	b	c	d	(Δi) ave mm	Σ (Δt) ave mm	Σ Δ mm	SUM Σ Δ mm
31570	0	0			0	0	0	0	0	0	0	0
	0	0	Dry	50	-1	-2	-2	-1	-1.5	-1		
31577	7	7	=	50	-1.5	-0.5	-1	-1	-1.5	-1	-2.5	-2.5
SUM		7		50								
31577	0	7	=	100	-2.5	-2.5	-3	-2	-2.5	-2.4		
31585	7	14	=	100	-2	0	0	-1	-2.5	-0.75	-3.25	-5.75
SUM		14		100						-0.75		
31585	0	14	Dry	150	-5	-3	-2	-3	-3.25	-0.5		
31589	4	18	=	150	-1	0	0	-1	-3.25	-0.5	-3.75	-9.5
SUM		18		150						-0.5		
31589	0	18	Soaked	150	-3	-4	-12	-5		-6		
31591	2	20	=	150	-3	-5	-9	-6		-5.75		
31592	1	21	Soaked	150	-2	-5	-12	-10		-7.2		
32324	1	22	=	150	-2	-5	-19	-17		-10.3		
31594	1	23	=	150	-2	-6	-22	-19		-12.2		
31595	1	24	=	150	-3	-6	-27	-22		-14.5		
31596	1	25	=	150	-2	-6	-28	-25		-15.2		
31599	3	28	=	150	-3	-6	-28	-25		-15.5		
31600	1	29	=	150						-15.5	-15.5	-25
SUM		29		150					-7.25	-17.75		
TOTAL		35		150							-25	

D6-7 : Field hydroconsolidation results from location ML3.

a) Site II

$\sigma_{y_{ave}} = 45$ kPa

31   59

b) Site III

$\sigma_y = 73$ kPa
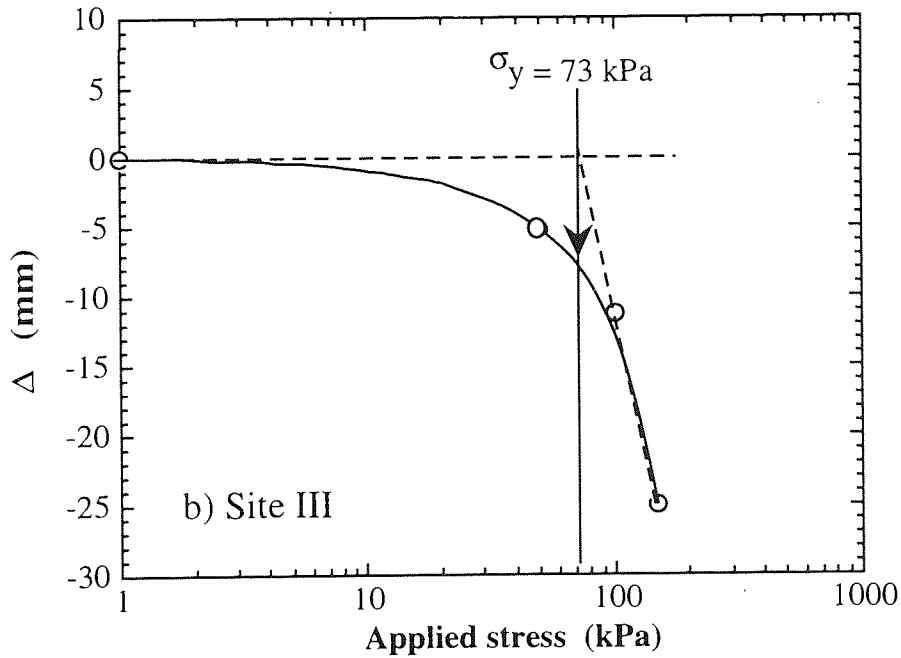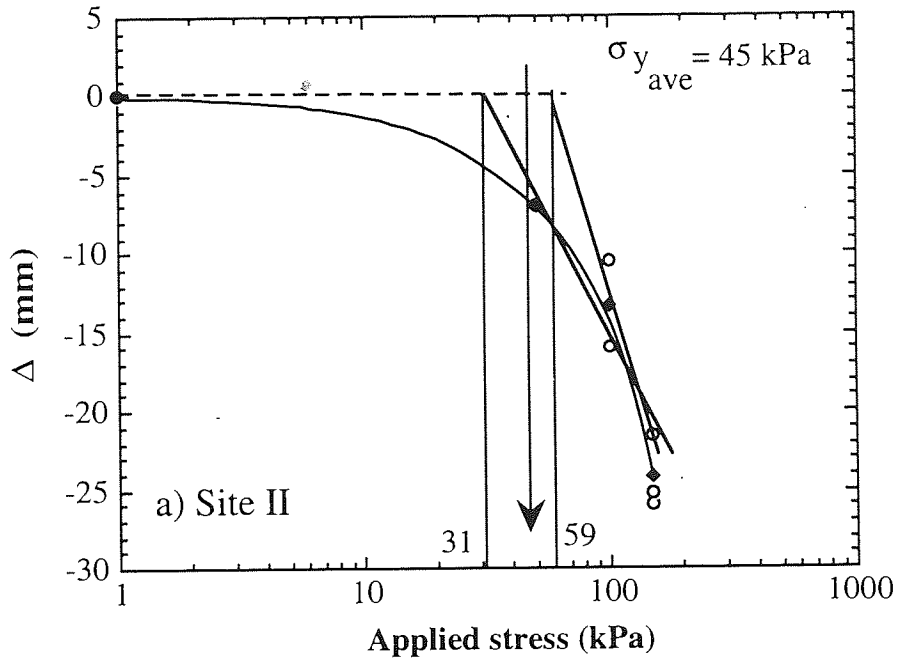
D6-8 : The yield stresses interpolated from the termination of the field hydroconsolidation and collapsing tests for sites II and III.
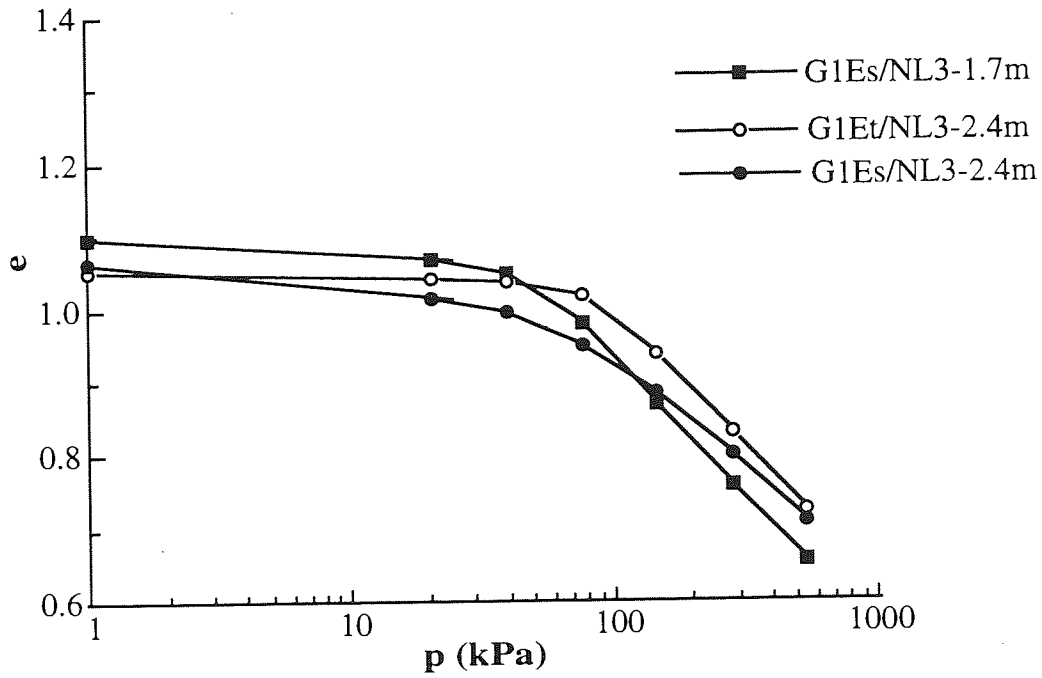
D6-9 : Oedometer results for the preloaded soils from location GL3 taken 0.2 and 0.9m below the loaded surface.

D6-10 : Specification of the steel roller compactor, SAKAI SV 90.

SPECIFICATIONS

Weight

Gross weight	9,700kg
Front wheel	5,200kg
Rear wheel	4,500kg

Dimension

Overall length	5,280mm
Overall width	2,250mm
Overall height	· 2,790mm
Wheelbase	2,800mm

Performance

Speed (km/h)

		1st	2nd	3rd
Forward and	Low	0 ~ 5	0 ~ 7	0 ~ 10
Reverse	High	0 ~ 14	0 ~ 21	0 ~ 28

Vibrating Power	Low Amplitude		High Amplitude	
	1	2	1	2
Frequency (vpm)	1,700	2,400	1,300	1,700
Centrifugal force (kg)	8,500	17,000	10,000	17,000

Gradability	20°
Turning radius	5.6m
Rolling width	2,100mm

Engine

Model	ISUZU DA640 Diesel Engine (with turbo charger)
type	4-cycle, water-cooled, vertical mounted precombusion chamber type
Total displacement	6,373cc

Performance

Rated output	133ps/2200rpm
Fuel consumption	207g/psh
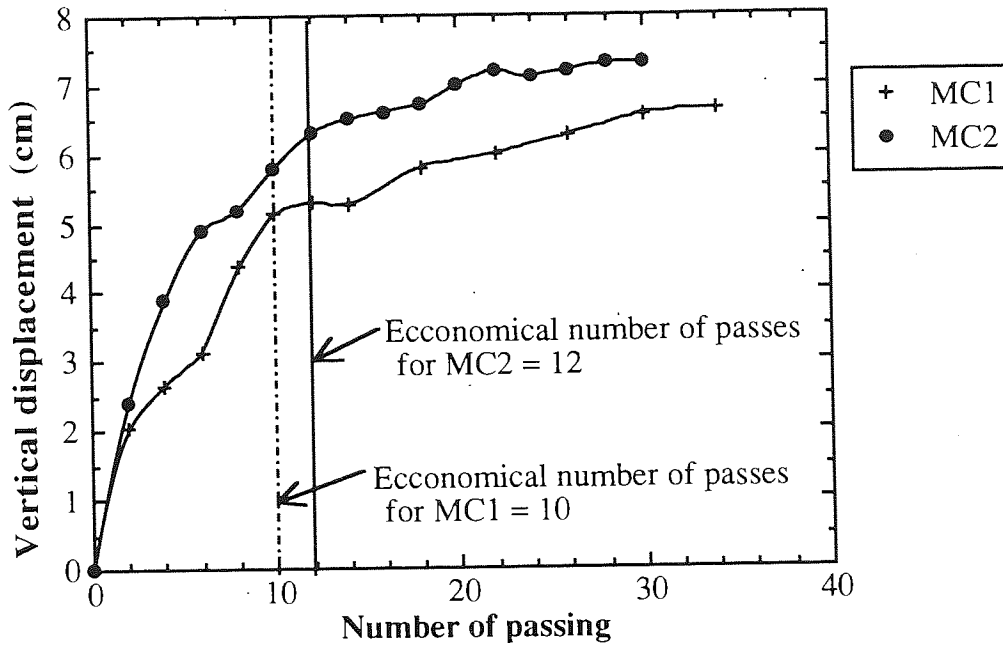
D6-11 : The relationship between the number of passes and the
average ground settlement at MC1 and MC2 for site III.
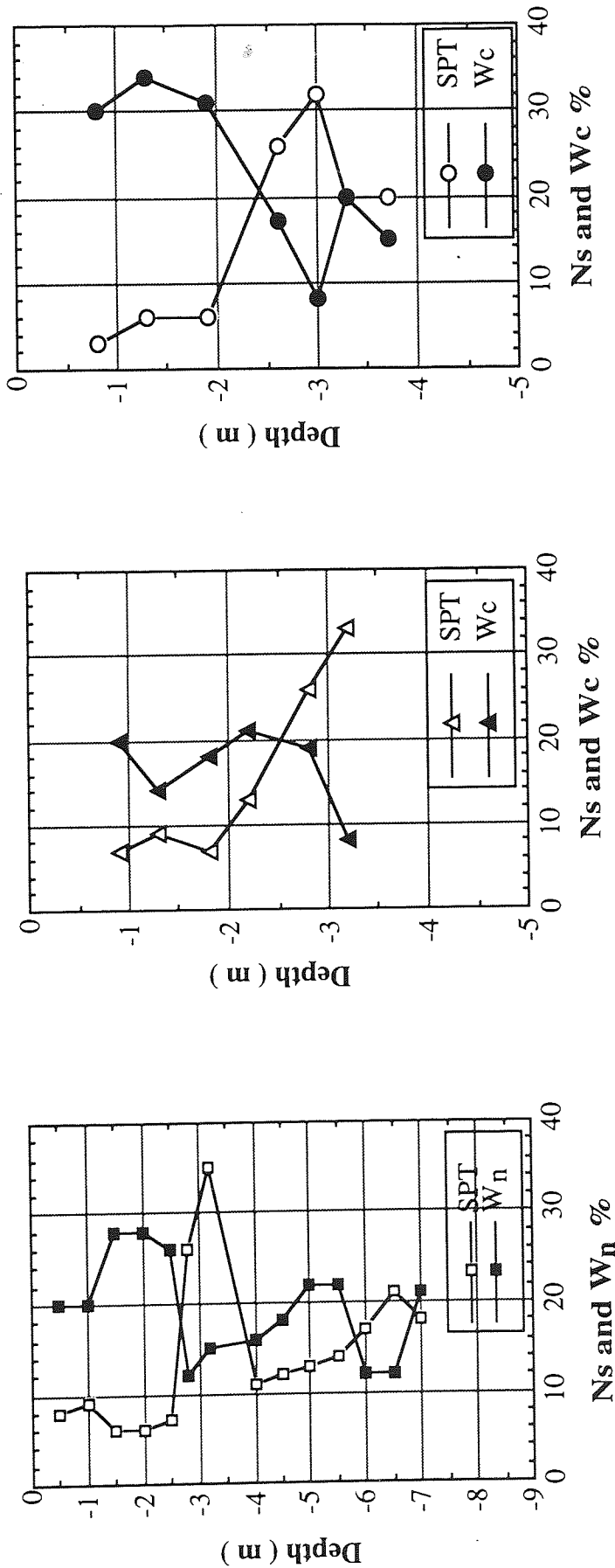
a) Natural location, MN.

b) Roller compacted location with one day flooding, MC1.

c) Roller compacted location with three days flooding, MC2.

D6-12 : The SPT and moisture content correlations for the roller compacted locations, MC1 and MC2, together with the corresponding natural values.

The change in the deformation trend due to the extend of the improvement beyond the top stiff lean clay layer, A0.

Legend (chart b):
- ▬■▬ Δ average
- ▫ A
- ○ B
- △ C
- ◇ D
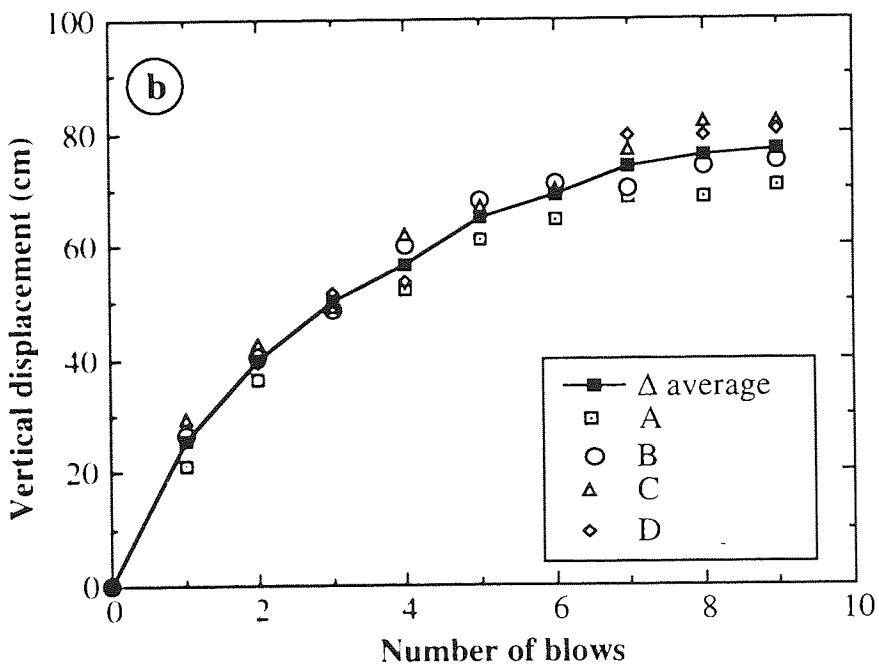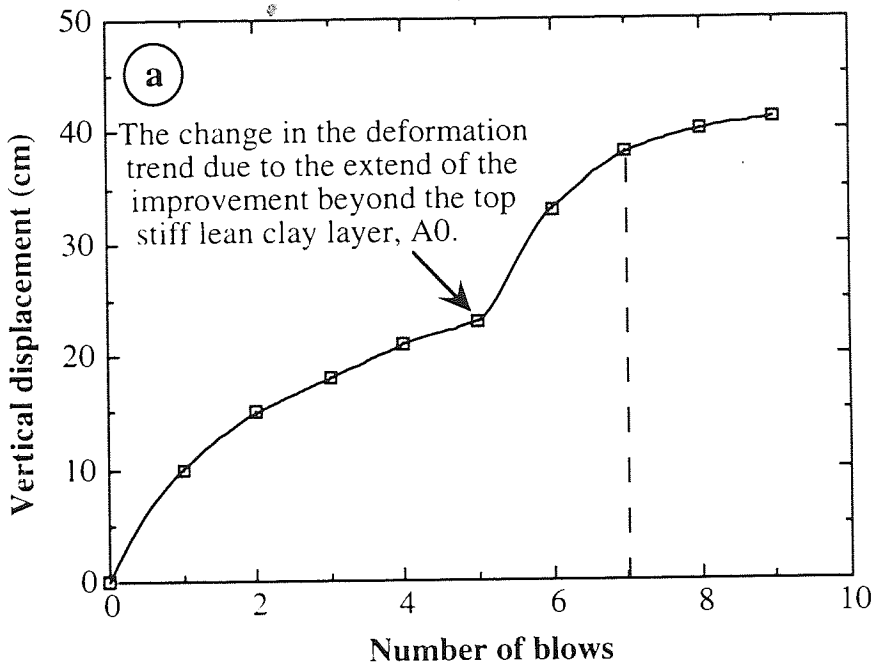
D6-13 : The vertical displacement of the pounded surface at locations; a) AD0 and b) AD1 at site I.

D6-14 : The SPT and moisture content correlations for the pounded locations, AD0, AD1 and AD2, together with the corresponding natural values.
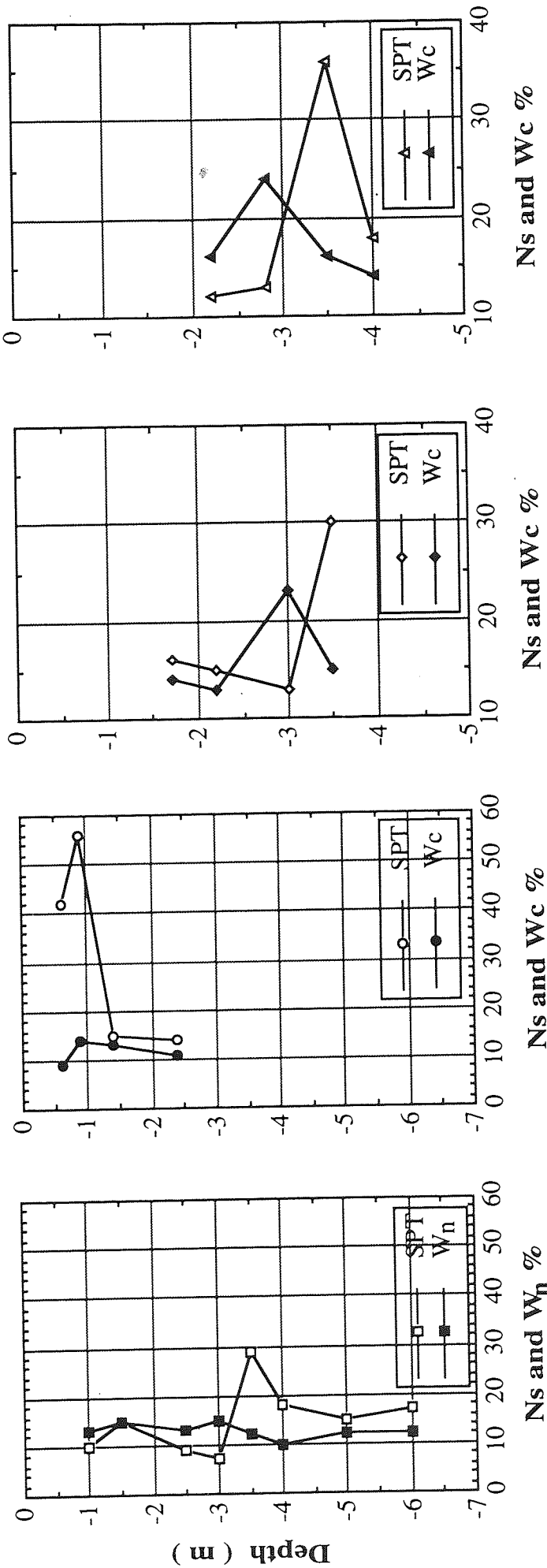
a) Natural location, AN.

b) Pounded location at natural moisture, AD0.

c) Pounded location with one day flooding, AD1.

d) Pounded location with five days flooding, AD2.

a) AD0

Natural
- □ I_C /A1-1.0m
- ◇ I_C /A1-2.0m
- ○ I_C /A2-3.0m.

Treated
- ▲ I_C /AD0-1.4m
- ◆ I_C /AD0-2.2m

Specimen location	I_C %
AD0 - 2.2m	4.9
AD0 - 3.0m	9.1

b) AD1

Natural
- □ I_C /A1-1.0m
- ◇ I_C /A1-2.0m
- ○ I_C /A2-3.0m.

Treated
- ▲ I_C /AD1-3.0m

Specimen location	I_C %
AD1 - 3.0m	8.1

c) AD2
Natural
- □ I_C /A1-1.0m
- ◇ I_C /A1-2.0m
- ○ I_C /A2-3.0m.

Treated
- ● I_C /AD2-3.2m

Specimen location	I_C %
AD2 - 3.2m	1.9
AD2 - 3.5m	7.0

D6-15 : The collapsing potential of the soils treated by pounding at site I.
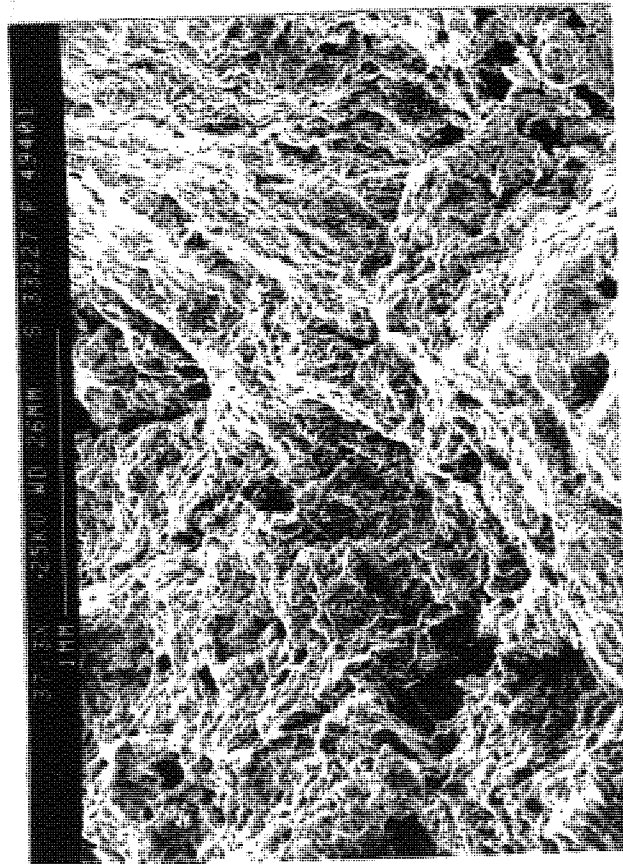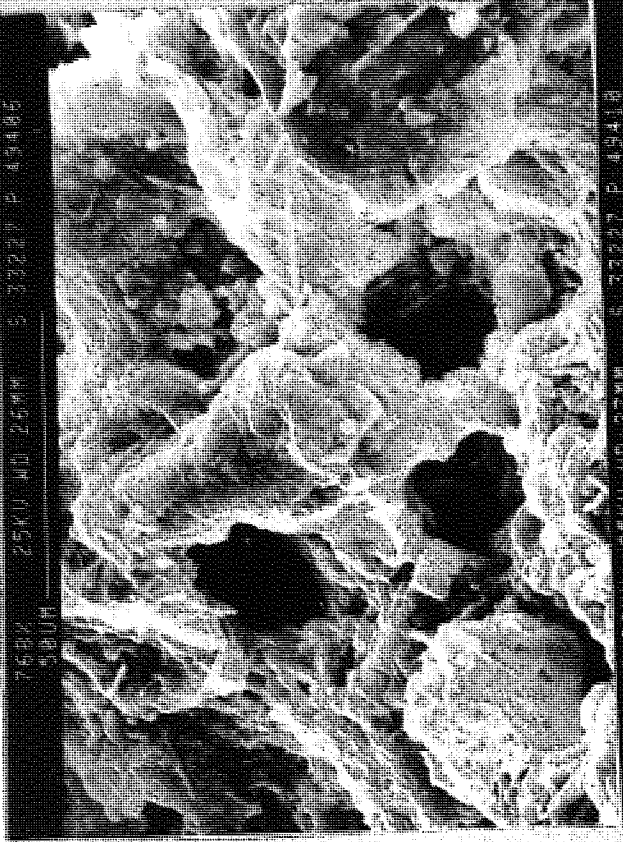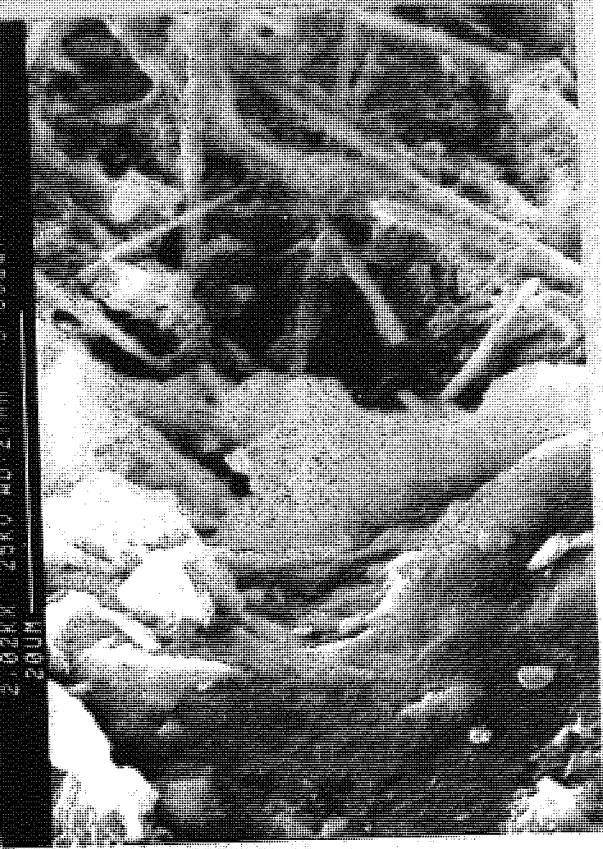
D6-16 : Field densification and destructuring of the stiff sandy silt soil, M3, by pounding at 3.0m (1.7m below the impacted surface) of MD2, indicating:

    a) Limited effect of Pounding at low magnification.

    b) Unaffected pores and buttress structures.

    c) Wetting effect on weakening bonds with no considerable destructuring for fines.

APPENDIX   E7

E7-1 : Oedometer results of the destructured and intact soil M3 at the, a) partially saturated, and b) soaked conditions.
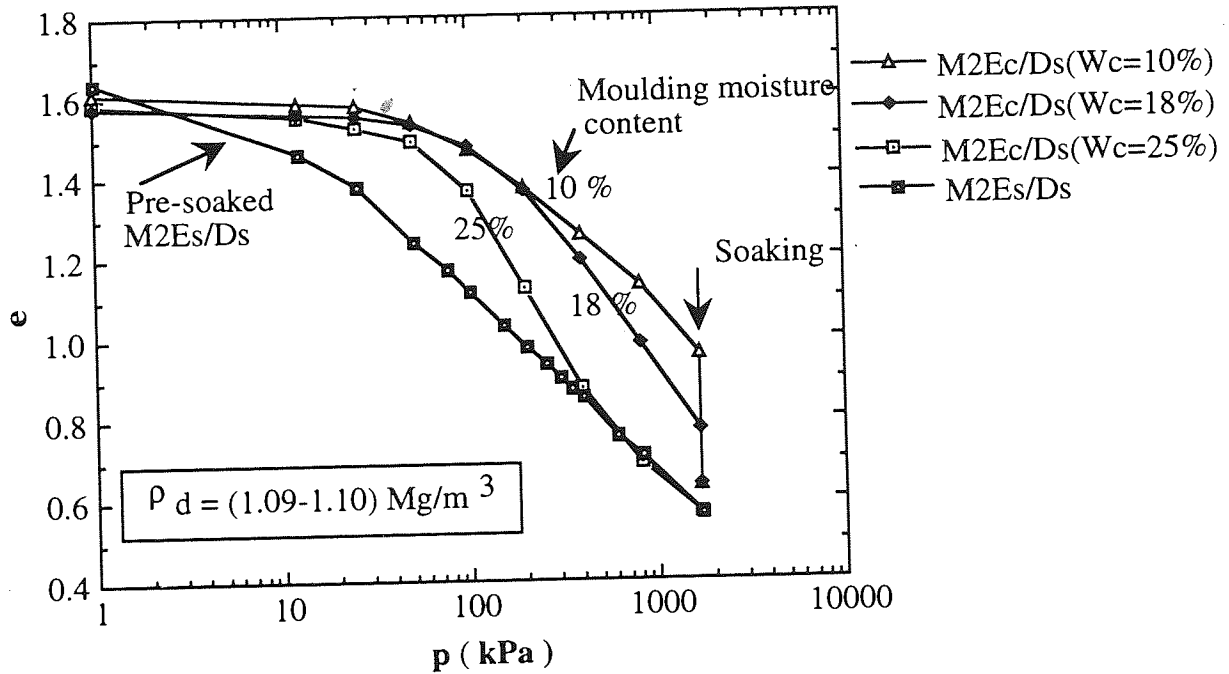
E7-2 : The compressibility results for destructured samples of M2, compacted at different moulding moisture contents.
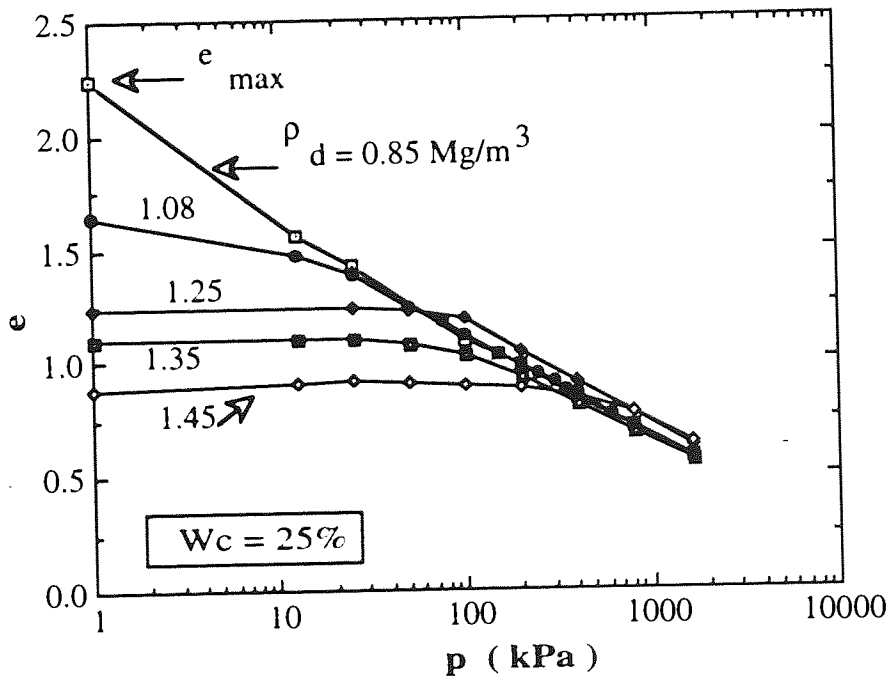
E7-3 : The compressibility results for destructured samples of M2, tested at different initial dry densities.
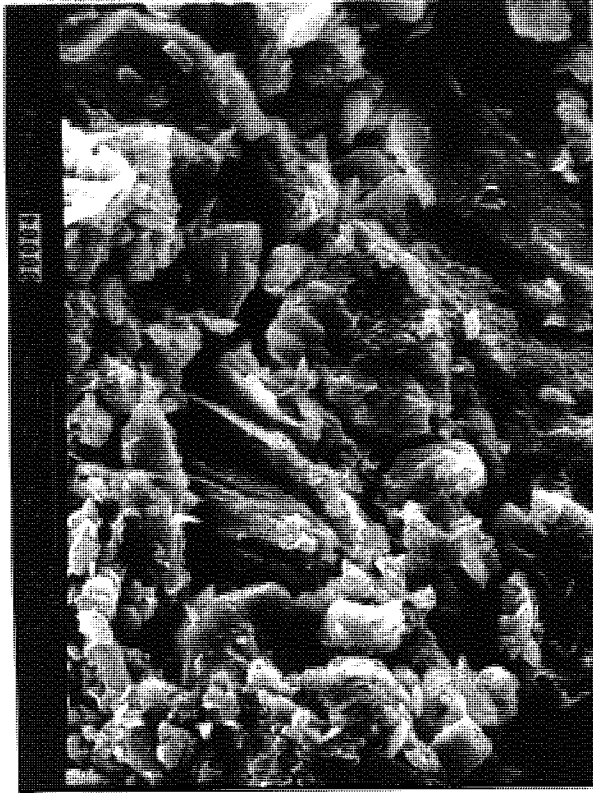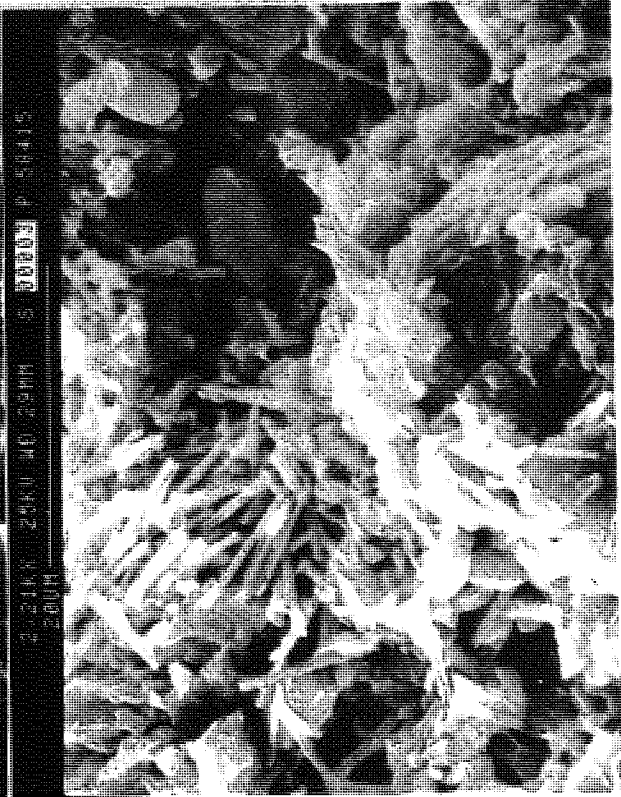
E7-4 : Oedometer destructuring of the natural soil, A2, by loading at the NMC (a) and SMC (b and c) states to 1660 kPa, indicating:

a) Localized distortion of the bonds at the contact points with limited effect on the coating bonds.

b) Partial grain to grain contacts inside the trapped pores of (a).

c) Partial destructuring of the arching structure around the rootlet pores together with the remaining trapped micropores.

APPENDIX   F8

F8-1 : The generalized Collapsing-Destructuring Frameworks of M2 and M3 from site III.
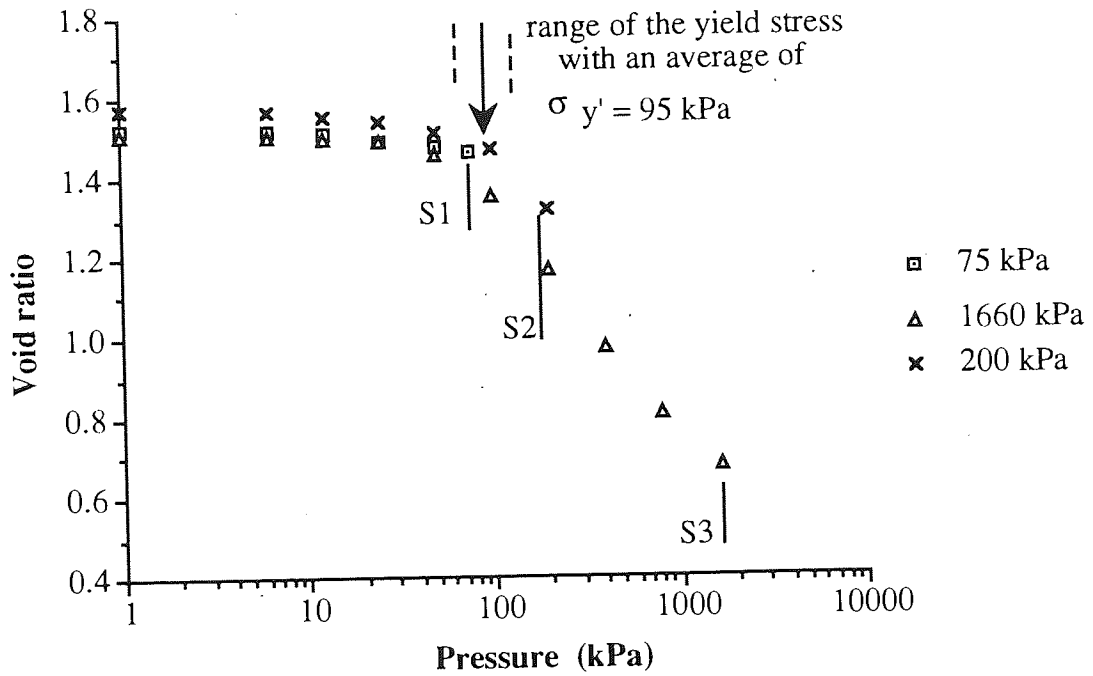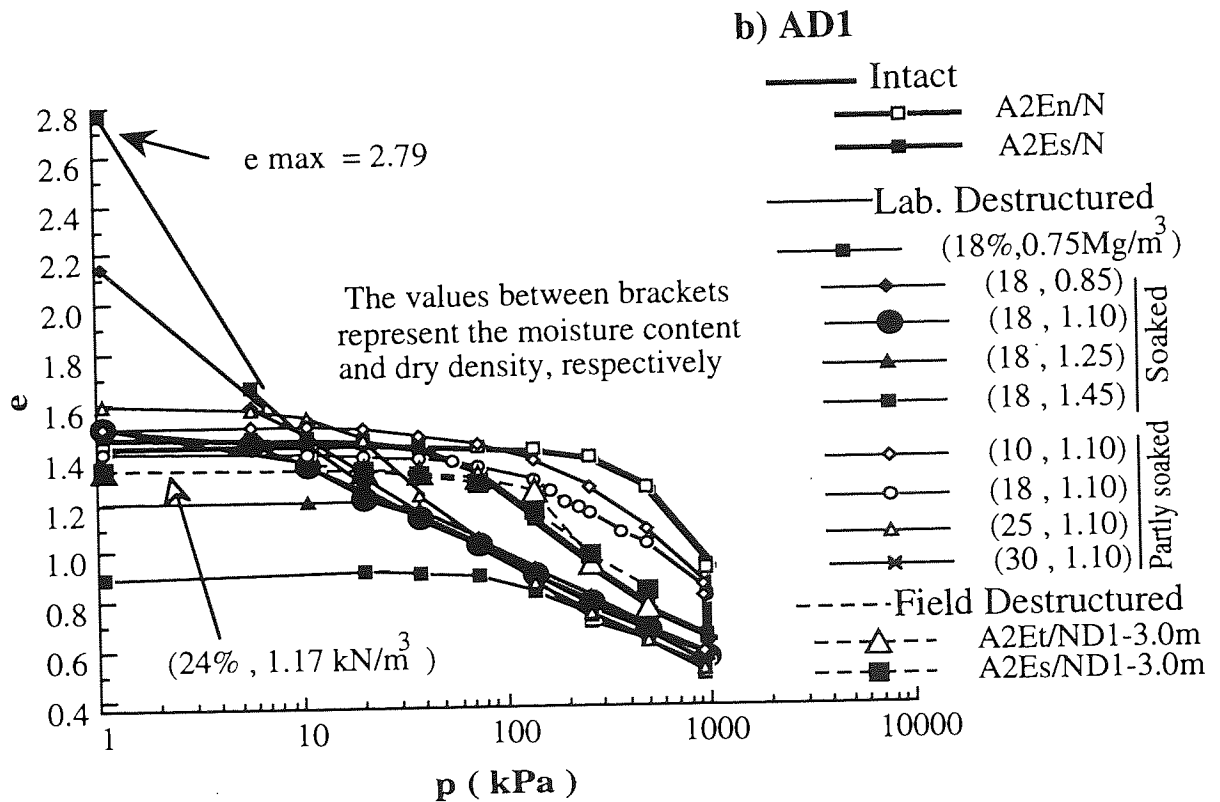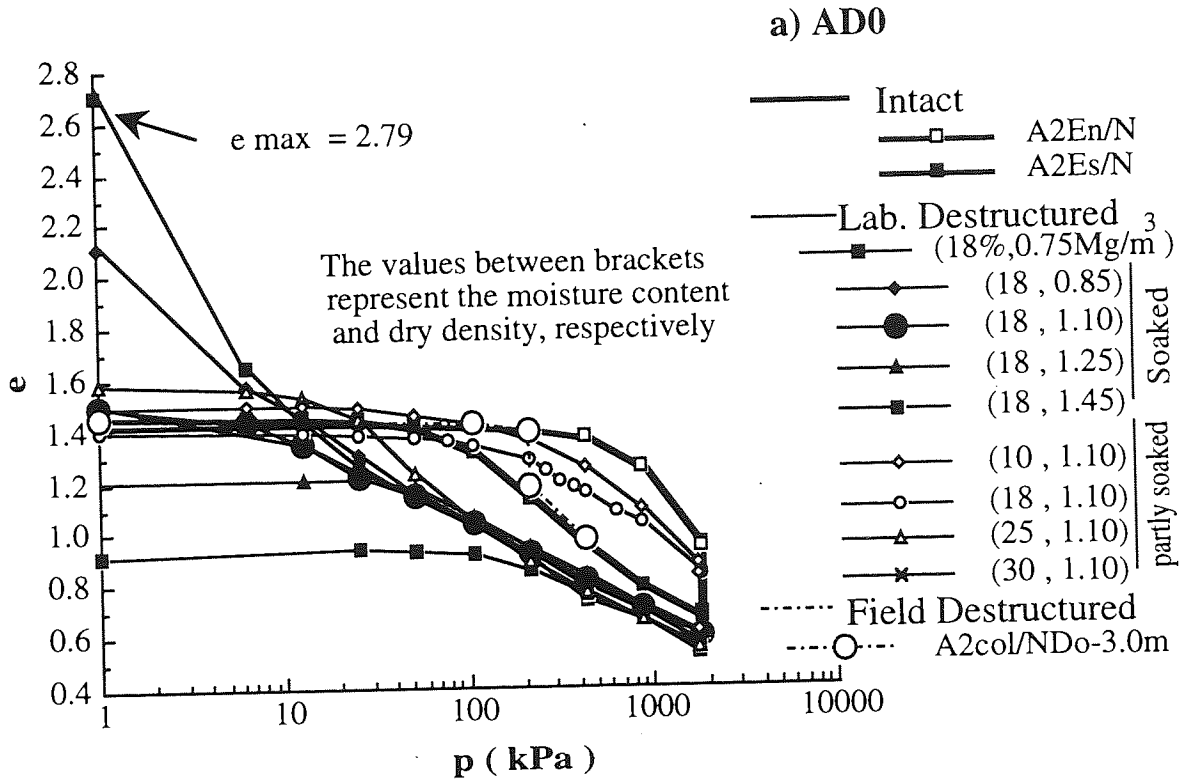
F8-2 : Consolidation curves of three samples A2 loaded up to 75, 200, and 1660 kPa.
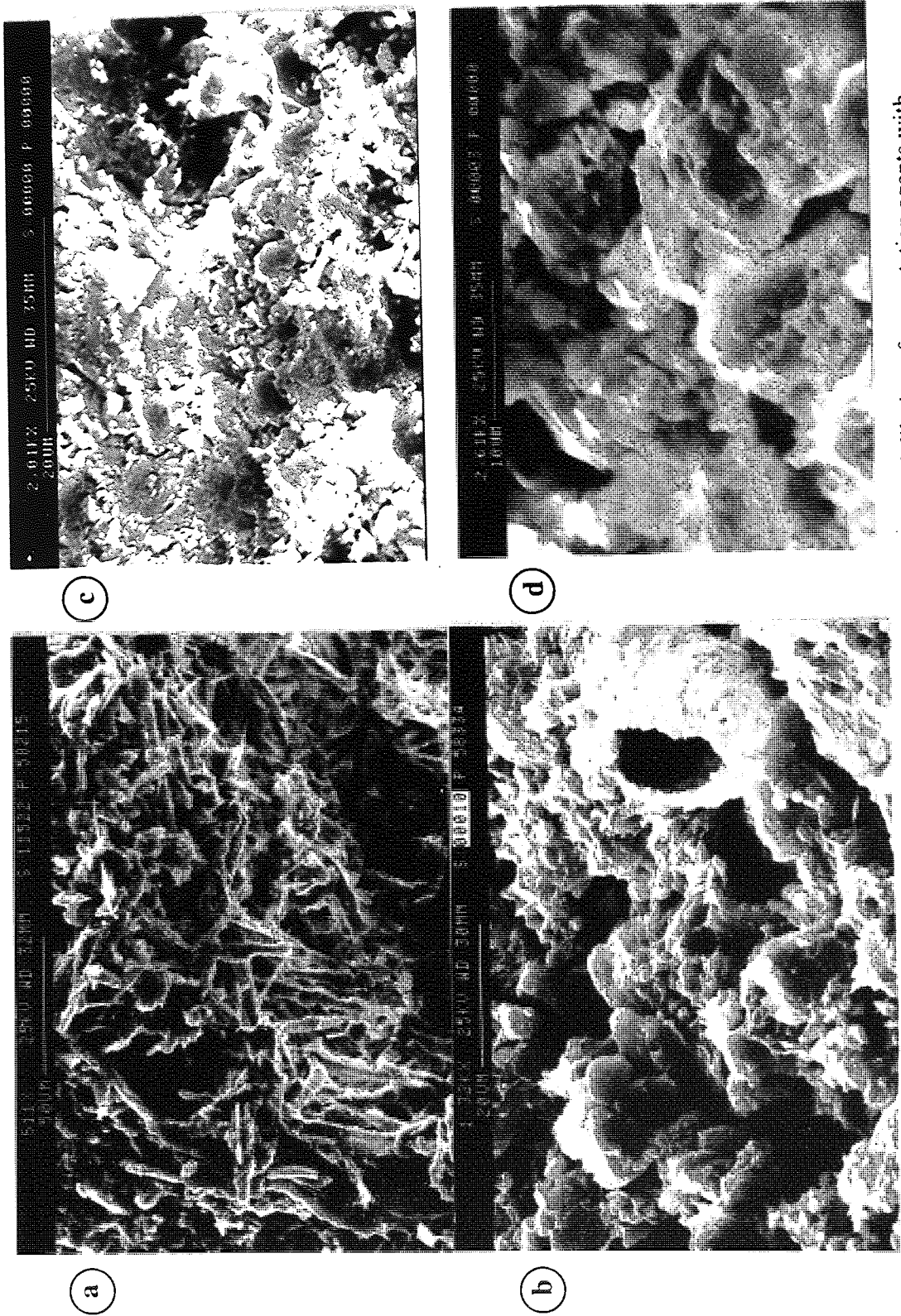
F8-3 : Destructuring progression of the samples of A2, showing; a and b) limited dilution of cementation agents with unaffected connectors at 75 kPa, c) initial breakdown in the clothed coating at 200 kPa , and d) considerable effect on the bridge connectors at 200 kPa.
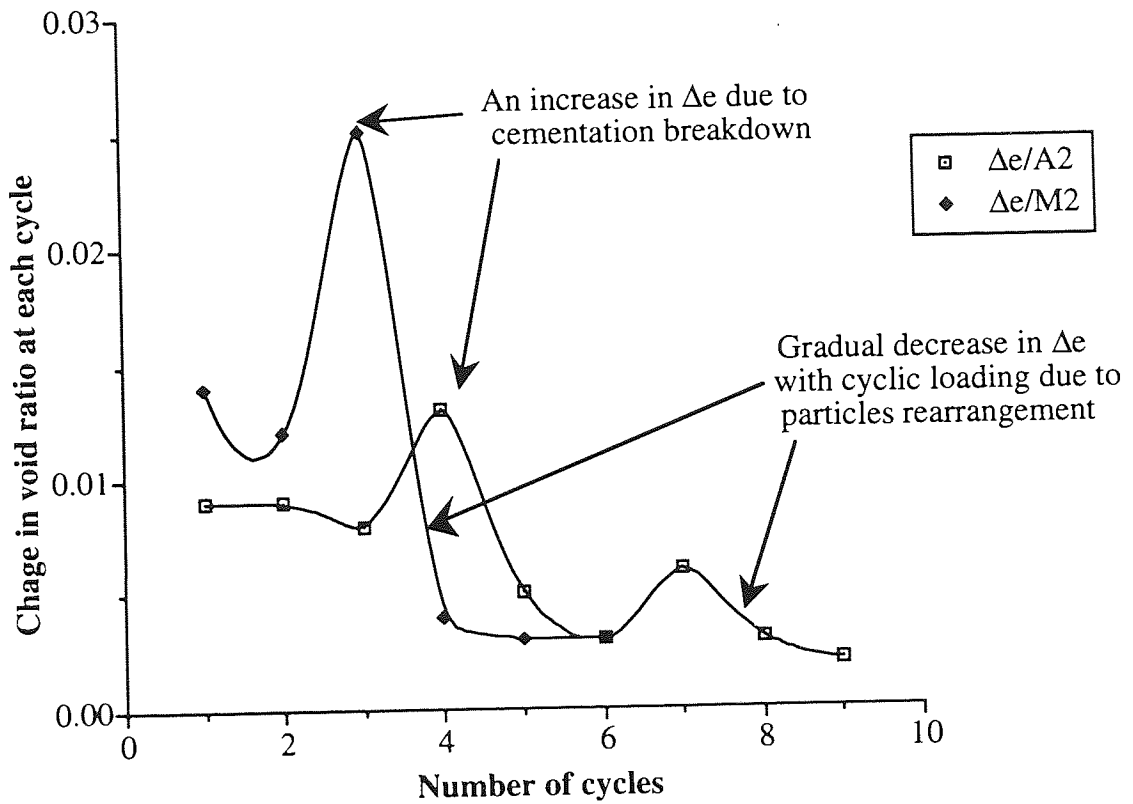
F8-4 : The assessment of the change in the void ratio
due to the effects of cementation breakdown
and particles rearrangement.

a) AD0

e max = 2.79

The values between brackets
represent the moisture content
and dry density, respectively

Legend:
- ——— Intact
- ——□—— A2En/N
- ——■—— A2Es/N
- ——— Lab. Destructured
- ——■—— (18%,0.75Mg/m³)
- ——♦—— (18 , 0.85) ⎤
- ——●—— (18 , 1.10) ⎥ Soaked
- ——▲—— (18 , 1.25) ⎥
- ——■—— (18 , 1.45) ⎦
- ——◇—— (10 , 1.10) ⎤
- ——○—— (18 , 1.10) ⎥ partly soaked
- ——△—— (25 , 1.10) ⎥
- ——✕—— (30 , 1.10) ⎦
- ------ Field Destructured
- ----○--- A2col/NDo-3.0m

p (kPa)

b) AD1

e max = 2.79

The values between brackets
represent the moisture content
and dry density, respectively

(24% , 1.17 kN/m³)

Legend:
- ——— Intact
- ——□—— A2En/N
- ——■—— A2Es/N
- ——— Lab. Destructured
- ——■—— (18%,0.75Mg/m³)
- ——♦—— (18 , 0.85) ⎤
- ——●—— (18 , 1.10) ⎥ Soaked
- ——▲—— (18 , 1.25) ⎥
- ——■—— (18 , 1.45) ⎦
- ——◇—— (10 , 1.10) ⎤
- ——○—— (18 , 1.10) ⎥ Partly soaked
- ——△—— (25 , 1.10) ⎥
- ——✕—— (30 , 1.10) ⎦
- ----- Field Destructured
- --△-- A2Et/ND1-3.0m
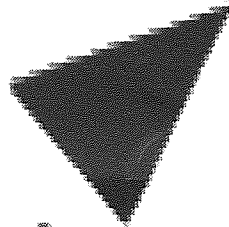- --■-- A2Es/ND1-3.0m

p (kPa)

F8-5 : Complete laboratory framework for soil A2 to evaluate
field destructuring at AD0 and AD1.
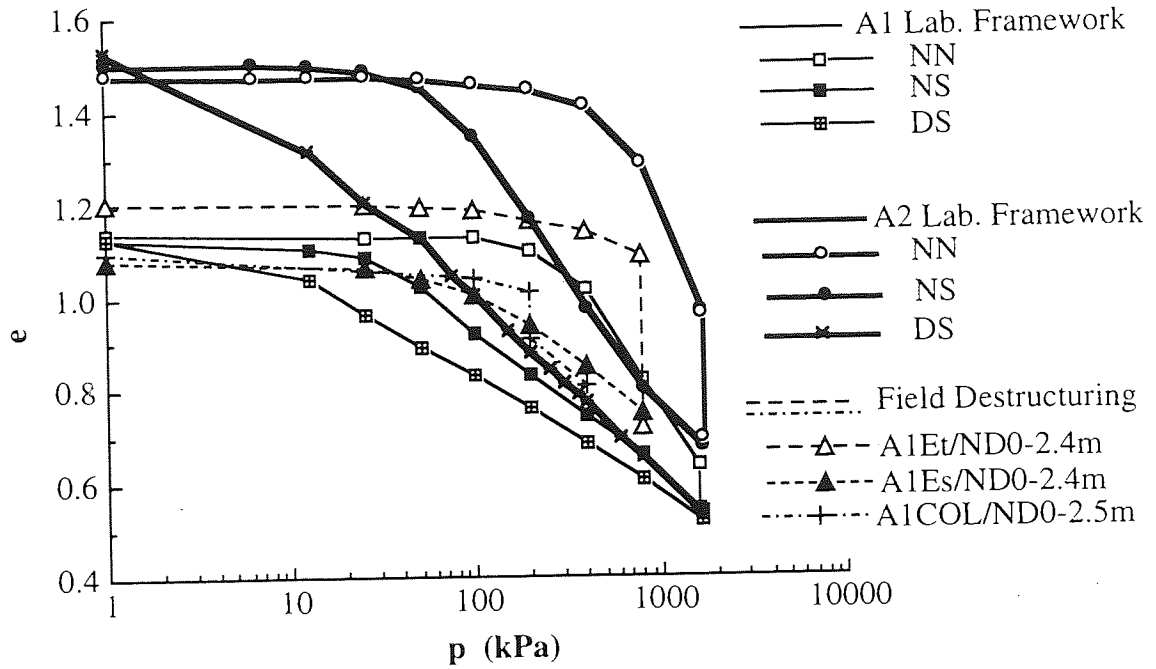
F8-6 : Evaluation of field destructuring by deep compaction at AD0, at the transition zone, using the laboratory framework for soils A1 and A2.
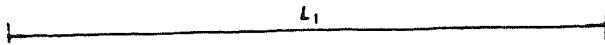
APPENDIX   G9

G9-1 : Continuous strip footing in one direction (Clemence and Finbarr, 1981).

L_1

G9-2 : Continuous strip footing in two directions (Zeevaret, 1983).
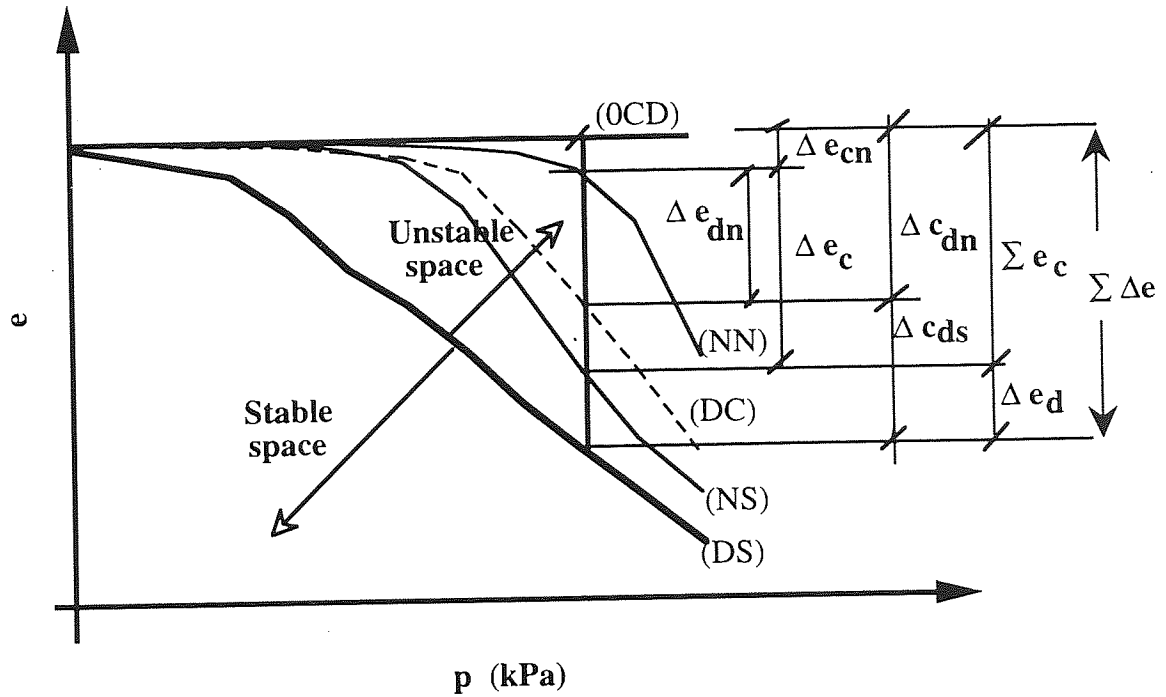
G9-3 : Ideal generalized framework, with five boundray
limits, for presenting the natural and destructured
soils at both moisture states.

Δe_{dn} = Destructuring of natural soil at the in situ moisture content

Δe_{d} = Destructuring of natural soil at SMC state

Δe_{c} = Collapse upon wetting of natural soils

Δc_{ds} = Collapse upon wetting of D/C soils

Δe_{cn} = Collapse upon loading alone of natural soils

Σe_{c} = Collapse upon both wetting and loading of natural soils

$\Sigma \Delta e$ = Total deformation due to both collapse and destructuring